

Developing Chemical Tools to Study Ribitol-5-Phosphate within Cell- Surface Glycans

Kathryn Emma Huxley

PhD

University of York

Chemistry

September 2022

Abstract

α -dystroglycan is a cell-surface protein which provides essential links between the extracellular matrix and the cytoskeleton through interactions between *O*-linked glycans on α -dystroglycan, and extracellular proteins involved in regulating tissue architecture and signalling pathways. Some of these binding interactions are essential for maintaining muscle integrity and loss of these binding interactions causes a subset of muscular dystrophies named dystroglycanopathies.¹⁻³ In recent years, the glycan responsible for these essential interactions has been shown to possess a unique tandem D-ribitol-5-phosphate linker which was not previously known to exist within mammalian cells. The possibility remains for this unique monosaccharide to be present elsewhere within mammalian cell glycans. Detailed in this Thesis is the synthesis of a panel of 1-azido-analogues of D-ribitol-5-phosphate as metabolic labelling probes, carrying different levels of protection suitable for *in vitro* enzyme assays and *in vivo* glycan labelling studies. A 12-step synthetic route to the fully-protected 1-azido probe has been developed from the starting sugar D-ribose, and the method development and protecting group manipulations explored in this route have aided the development of synthetic routes to 2- and 3-azido-D-ribitol-5-phosphate probes. A key challenge in the synthesis of the cell-permeable probes was the incorporation of a *bis*(*S*-acetyl-2-thioethyl) phosphate group onto the ribitol scaffold. This was overcome by the development of new methodology that introduces the protected phosphotriester *via* a two-step process that utilises an easy-to-synthesise *tris*(2-bromoethyl) phosphate starting material. The synthesised probes enable the development of a highly specific labelling technique to target α -dystroglycan, which if metabolised provide a powerful tool to study this protein, enabling the monitoring of levels of glycosylated α -dystroglycan, changes to protein glycosylation in response to cellular stimuli and differences between healthy and disease models. Additionally, with successful metabolic labelling, these probes possess the ability to uncover new sites of ribitol-5-phosphate incorporation, enhancing our understanding of the cellular use and significance of this uncommon sugar.

1. M. Kanagawa and T. Toda, *J. Neuromuscul. Dis.*, 2017, **4**, 259-267.
2. L. Wells, *J. Biol. Chem.*, 2013, **288**, 6930-6935.
3. H. Manya and T. Endo, *Biochim. Biophys. Acta Gen. Subj.*, 2017, **1861**, 2462-2472.

Table of Contents

Abstract.....	2
List of Tables	7
Table of Figures.....	8
Table of Schemes	11
Acknowledgements.....	18
Declaration.....	19
Chapter 1: Introduction	20
1.1 <i>O</i> -Mannosylation in Mammals.....	20
1.2 α -Dystroglycan	21
1.3 α -Dystroglycan Biosynthesis	23
Core M1 and M2 Glycan Biosynthesis	23
Core M3 Glycan Biosynthesis.....	24
Matriglycan	25
1.4 The Tandem D-Ribitol-5-Phosphate Linker	26
Identification.....	26
<i>2-C-methyl-D-erythritol-4-phosphate cytidyltransferase</i> (ISPD).....	28
<i>Fukutin</i> (FKTN) and <i>Fukutin Related Protein</i> (FKRP)	29
1.5 Muscular Dystrophies	32
1.6 Questions Still to be Answered.....	33
1.7 Project Aims	33
1.8 References	36
Chapter 2: Chemical Reporters to Study Mammalian <i>O</i> -glycosylation	40
2.1 Abstract.....	40
2.2 Introduction	40
2.3 Oxidation of Cell Surface Glycans	42
2.4 Metabolic Oligosaccharide Engineering (MOE)	43
2.5 Chemoenzymatic Glycan Labelling (CeGL).....	47

Bump-and-Hole Strategies	49
2.6 References	51
Chapter 3: Synthesis of 1-Azido-D-Ribitol-5-Phosphate Probes	55
3.1 Abstract	55
3.2 Introduction	55
Structure	56
Bioorthogonal Handle	56
Protecting Group Strategy	57
3.3 Aims	57
3.4 Results and Discussion	58
Retrosynthesis Design	58
Route 1	62
Route 2	64
Route 3a	65
Route 3b	69
Route 4a	73
Route 4b	76
Incorporation of a Deprotected Phosphate Monoester for the Synthesis of 1-Az-OH- Phos.....	79
Synthesis of Probes from Commercially Available Starting Sugar 5-Allyl-2,3,4- <i>tri-O</i> - Benzyl-D-Ribitol	84
3.5 Conclusion	85
3.6 Experimental	86
3.7 References	104
Chapter 4: Development of Novel Methodology for Synthesis of <i>S</i> -Acetyl-2-Thioethyl- Protected Phosphates.....	107
4.1 Abstract	107
4.2 Introduction	107

4.3 Aims	110
4.4 Results and Discussion	111
Methods A and B: Discussion.....	111
Method C: Addition of a Phosphodiester	113
Method D: Triflic Anhydride Activation of a Phosphotriester	115
4.5 Conclusion.....	119
4.6 Experimental.....	121
4.7 References	128
Chapter 5: Optimisation and Substrate Scope of the New <i>S</i> -Acetyl-2-Thioethyl-Protected Phosphate Synthesis Methodology	130
5.1 Abstract.....	130
5.2 Introduction	130
Huang's Method.....	131
Adler's Method	133
5.3 Aims	135
5.4 Results and Discussion	135
Optimisation Summary	140
Phosphate Addition Side Product	141
SATE Phosphate Formation.....	143
Substrate Synthesis and Testing	144
Glucose Sugar Derivatives.....	144
Tyrosine Derivatives.....	150
GlcNAc Derivatives.....	152
5.5 Conclusion.....	153
5.6 Experimental	155
Substrates	159
SATE Compounds	171
5.7 References	182

Chapter 6: Towards the Synthesis of 2-Azido- and 3-Azido-D-Ribitol-5-Phosphate Probes..	185
6.1 Abstract.....	185
6.2 Introduction	186
6.3 Aims	186
6.4 Results and Discussion	187
2-Azido Ribitol-5-Phosphate Probe.....	187
3-Azido Ribitol-5-Phosphate Probe.....	191
Alternatively protected probes.....	194
6.5 Conclusions	195
6.6 Experimental	196
6.7 References	200
Chapter 7: Summary and Future Work.....	201
7.1 Summary	201
7.2 Future Work.....	203
Biological Testing: <i>in vivo</i> Analysis	203
Biological Testing: <i>in vitro</i> Analysis	204
Future Probe Generations	205
Phosphate Future Work.....	207
7.3 References	209
Appendix: NMR Spectra	210
Chapter 3.....	210
Chapter 4.....	248
Chapter 5.....	262
List of Abbreviations	296
References	300

List of Tables

Table 1: Reagents and conditions for acid catalysed trityl deprotection	67
Table 2: Approximate pKa values for the acetate-carbonyl and trityl-ether conjugate acids and acid catalysts ²²¹⁻²²³	68
Table 3: Optimisation of the synthesis of 3-phenyl-propyl-diethyl-phosphate through the distillation of triflic anhydride and adding 3-phenyl-propanol as a solution in DCM.....	136
Table 4: Optimisation of the synthesis of 3-phenyl-propyl-diethyl phosphate through changing the order of reagent addition and the number of equivalents of pyridine	137
Table 5: Optimisation of the synthesis of 3-phenyl-propyl- <i>bis</i> (2-bromoethyl) phosphate by inserting a pre-activation time after the addition of triflic anhydride, and before the addition of pyridine	138
Table 6: Optimisation of the synthesis of 3-phenyl-propyl- <i>bis</i> (2-bromoethyl) phosphate by investigating the effect of increasing the pre-activation time after pyridine addition to the reaction	139
Table 7: Optimisation of the synthesis of 1,2,3,4-tetra- <i>O</i> -benzyl-glucose-6- <i>bis</i> (2-bromoethyl)phosphate by the investigation of the effect of reaction length on yields	140
Table 8: Comparison of the original, and optimised procedure for the formation of 2-bromoethyl phosphates by the Huang et al methodology.....	141
Table 9: Yields for the phosphorylation of C6 unprotected glucose derivatives.....	147
Table 10: Yields for the Phosphorylation of C1 unprotected glucose derivatives.....	149
Table 11: Yields for the phosphorylation of Thr derivatives.....	151
Table 12: Yields for the phosphorylation of GlcNAc derivatives	152

Table of Figures

Figure 1: Glycan formation results in a wide diversity of potential carbohydrate structures. Overview presenting an array of possible donors, sugars, glycosidic bond configurations and schematic glycan structures representing a variety of chain lengths and branches.	20
Figure 2: Overall Structure of the DGC, showing the position of the α - and β -dystroglycan (DG) subunits and the three types of <i>O</i> -mannosyl glycans that are all found on α -DG.	22
Figure 3: Schematic representation of the biosynthesis of the core glycans of α -DG, showing linkage types and the enzymes responsible for the formation of each glycosidic bond. Shown is just the unextended M1 and M2 glycan structures, further modification to these glycans can occur through the addition of <i>N</i> -acetylneuraminic acid (Neu5Ac), <i>N</i> -glycolylneuraminic acid (Neu5Gc) or fucose (Fuc) residues. ²¹	24
Figure 4: The full structure of the core M3 glycan, including the two uncommon phosphodiester linkages and the matriglycan structure which is unique to this glycan.....	25
Figure 5: Potential cleavage sites of the phosphodiester linkages in the core M3 <i>O</i> -mannosyl glycan by HF and NaIO ₄ (top) and periodate cis-diol oxidation products for both furanose and linear sugar structures presenting both the intact and split glycan products (bottom).	27
Figure 6: Schematic structure of the Core M3 Glycan of α -DG with the biosynthetic enzymes responsible for each glycosidic bond or phosphoester bond formation indicated in orange.....	28
Figure 7: Azide-tagged analogues of ribitol-5-phosphate this project aims to synthesise A) phosphate containing probes for <i>in vivo</i> labelling studies with protection of both hydroxyl (R ₁) and phosphate (R ₂) groups B) Ribitol probes for <i>in vivo</i> cell studies with protected hydroxyl groups (R ₁) C) Unprotected probes for <i>in vitro</i> studies.	35
Figure 8: Chemical reporter strategies to study glycans. A) Chemical or enzymatic oxidation of glycans enables the labelling of specific monosaccharide residues by reaction with amine-functionalised reporter groups. B) Metabolic oligosaccharide engineering makes use of the cell's endogenous glycan biosynthetic machinery to install unnatural monosaccharide derivatives into glycans. The introduced tags can be further labelled by bioorthogonal 'click' reactions. C) Chemoenzymatic glycan labelling exploits the activity of recombinant glycosyltransferases to transfer unnatural monosaccharides onto specific glycans.	42
Figure 9: Chemical oxidation of cell surface glycans. Monosaccharides that carry a cis diol motif, such as sialic acids, are sensitive to oxidation by periodate treatment. The aldehyde generated upon oxidative cleavage can react with an amine nucleophile such as hydrazide for conjugation to a desired reporter group.	43

Figure 10: Metabolic oligosaccharide engineering. Cells are fed with unnatural, tagged derivatives of naturally occurring monosaccharides, such as the peracetylated azide-tagged derivatives of ManNAc and GlcNAc shown. After uptake and deprotection of the acetyl groups (bottom left), the metabolic precursors enter the cellular pathways for conversion into the corresponding CMP- or UDP-activated donors which are then used for glycan biosynthesis. ManNAc derivatives are incorporated as sialic acids into cell surface glycans (A) while GlcNAc derivatives label intracellular proteins that are targets for O-GlcNAc modification (B). The azide-tagged glycans can be labelled by bioorthogonal ligation reactions such as the strain-promoted (A) or the copper(I)-catalysed (B) azide-alkyne cycloaddition. 44

Figure 11: Tandem chemoenzymatic glycan engineering. In CeGL, recombinant glycosyltransferases are used to transfer unnatural monosaccharides from appropriate donors onto glycan acceptors. A double labelling strategy was designed with successive reactions catalysed by ST3Gal1 and ST6Gal1, installing the same alkyne-tagged CMP-sialic acid derivative onto unextended Gal-GalNAc disaccharides present on O-glycans or uncapped Gal-GlcNAc disaccharides at the non-reducing end of N-glycans, respectively. Tagged glycans were labelled via two separate azide-alkyne cycloaddition reactions for the simultaneous visualisation of both glycan types at the cell surface with different fluorophores. 48

Figure 12: Structure of 1-azido-2,3,4-*tri-O*-acetyl-D-ribitol-5-bis(*S*-acetyl-thioethyl)phosphate (1-Az-OAc-SATE) and related probes 58

Figure 13: Ring opening side products **8** and **9** formed by the reaction of compound **1** with DIBAL-H, in respective yields of 45% and 55%..... 63

Figure 14: Fully acetylated major side product **25** formed in the synthesis of compound **19** from **21**..... 70

Figure 15: Side product **45** formed by the deprotection of **44**..... 83

Figure 16: Structure of bis(diisopropylamino-chlorophosphine **52**..... 109

Figure 17: Test substrate to prove the mechanism of substitution for the Huang *et al* method 131

Figure 18: Migration side product 1,2,3,6-tetra-*O*-acetyl glucose **81** 145

Figure 19: Furanoside side product formed from Fischer glycosylation and benzylation..... 146

Figure 20: Tyrosine mimics for testing the SATE phosphate reaction 150

Figure 21: GlcNAc substrates for the testing of the SATE phosphate methodology 152

Figure 22: Structures of the fully protected 2-azido and 3-azido-D-ribitol-5-phosphate probes carrying acetate and SATE protection for the purpose of in vivo metabolic labelling. 186

Figure 23: 1-methoxy-3-benzyl-D-arabinose side product 189

Figure 24: Overview of *in vivo* metabolic incorporation of 1-azido-ribitol-5-phosphate: 1) upon uptake of the probe into cells, the protecting groups are cleaved by non-specific esterase and lipase activity releasing the free probe for incorporation into enzymatic pathways, 2) cell lysis is conducted breaking down the cell membrane, 3) copper(I) catalysed azide-alkyne cycloaddition (CuAAC) labelling allows the conjugation of a fluorescent or biotin tag, 4) labelled biomolecules can be characterised by either SDS-PAGE or MS/MS analysis following the conjugation of a fluorescent or biotin tag respectively. Cat. = catalyst, THPTA = tris(benzyltriazolylmethyl)amine 203

Figure 25: Schematic representation of the *in vitro* studies of modified ribitol-5-phosphate, showing the conversion of ribitol-5-phosphate into CDP-ribitol by ISPD and B) the modification of a core M3 trisaccharide with ribitol-5-phosphate by FKTN, using the ISPD reaction product CDP-ribitol as a donor. 205

Figure 26: Proposed structures for additional panels of ribitol-5-phosphate metabolic labelling probes: A) alkyne labelled probes B) propargyl ether labelled probes, including alternative site of label incorporation on the phosphate. For *in vivo* probes $R_1 = \text{OAc}$ and $R_2 = \text{SATE}$, for *in vitro* probes $R_1 = R_2 = \text{OH}$ 206

Figure 27: Proposed activity-based probes and inhibitors of FKTN and FKRP utilising A) phosphonate, B) phosphothionate C) vinyl sulphone and D) acrylate groups. For *in vivo* probes $R_1 = \text{OAc}$ $R_2 = \text{SATE}$, for *in vitro* $R_1 = R_2 = \text{OH}$ 207

Figure 28: NAc-tyramine on which the compatibility of NAc groups within the SATE methodology can be tested 207

Figure 29: Examples of cytidine structures of interest for the testing of the SATE phosphate synthesis on nucleotides. R = Fmoc or CBz 208

Figure 30: Commercially available *tris*(2-chloroethyl)phosphate on which the SATE methodology can be tested 208

Table of Schemes

Scheme 1: Schematic representation of the formation of CDP-ribitol by ISPD.....	29
Scheme 2: Schematic representation of the enzymatic function of FKTN and FKR in the formation of the tandem ribitol-5-phosphate modification of the Core M3 Glycan	31
Scheme 3: Enzymatic cleavage of SATE protected phosphates.....	57
Scheme 4: Protecting group strategies for the synthesis of 1-Az probes: A) protecting group strategies for pentose (ring closed) and pentitol (ring-opened) sugars; B) structures of protecting groups discussed within this thesis; C) proposed retrosynthetic pathway from the fully protected 1-Az-OAc-SATE probe to ribose starting materials. R = protecting group. D) Compound numbering for D- and L-ribose and D-ribitol.....	59
Scheme 5: Retrosynthetic pathway of 1-Az Probes from Key Intermediate 2	61
Scheme 6: Route 1 from L-Ribose to the 1-Az-OAc-SATE probe. Reagents and Conditions: a) i) HCl, MeOH, r.t., 2 hr, ii) TBDPS-Cl, pyridine, r.t., 24 hrs, (55%), b) BnBr, NaH, TBAI, DMF, r.t. 2 hrs, (67%) c) DIBAL-H, toluene, 10 min, 60°C (0%) Proposed Conditions: d) BnBr, TBAI, DMF, e) TBAF, THF, f) i) TsCl, pyridine, ii) NaN ₃ , DMF, g) AcOH, 80°C, h) i) PO(OEt-2Br) ₃ , Tf ₂ O, pyridine, DCM, ii) KSAC, acetone, i) i) BCl ₃ , DCM, ii) Ac ₂ O, pyridine	62
Scheme 7: Route 2 for the synthesis of the 1-Az-OAc-SATE Probe. Reagents and Conditions a) TrCl, pyridine, r.t., 24 h, (48%) b) NaBH ₄ , EtOH, r.t., 2 h, (0%) Proposed Conditions c) TBDPS-Cl, pyridine, d) BnBr, TBAI, DMF, e) p-TsOH, MeOH, f) i) TsCl, pyridine, ii) NaN ₃ , DMF, 60°C, g) TBAF, DMF, h) PO(OEt-2Br) ₃ , Tf ₂ O, pyridine, DCM, ii) KSAC, acetone, i) Ac ₂ O, H ₂ SO ₄ ,.....	64
Scheme 8: Route 3 for the synthesis of 1-Az-OAc-SATE Reagents and Conditions a) TBDPS-Cl, pyridine, r.t. 48 h, (60%) b) NaBH ₄ , EtOH, r.t., 2 h (43%), c) TrCl, pyridine, 60°C, 48 h, (60%) d) Ac ₂ O, pyridine, r.t., 48 h, (78%), e) HCl, AcOH, DCM, r.t., 1 h, (22%) Proposed Conditions f) i) TsCl, pyridine, ii) NaN ₃ , DMF, 60°C, g) TBAF, DMF, h) PO(OEt-2Br) ₃ , Tf ₂ O, pyridine, DCM, ii) KSAC, acetone	65
Scheme 9: Acid catalysed acetate migration mechanism	67
Scheme 10: Alternative route to the synthesis of compound 19 , Reagents and Conditions a) TsCl, pyridine, 0°C, 3 h, then Ac ₂ O, 0°C, 4 h (27%) b) NaN ₃ , DMF, 60°C, 24 h (25%)	70
Scheme 11: A) Formation of elimination product compound 26 , B) Mechanism for the formation of alternative possible elimination products 27 or 28	71
Scheme 12: Attempted synthesis of 1,2,3,4-tetra-O-acetyl ribitol 29 and side products formed 30 and 31 Reagents and Conditions: TBAF, THF, 0°C-r.t. 18 h (44% 2:3 mixture of 30 and 31)	71
Scheme 13: Synthesis of the 1-Az-OAc probe Reagents and Conditions: a) TBAF, THF, 3 h, 0°C-r.t. b) Ac ₂ O, pyridine, DMAP cat., r.t., 20 h, (91% over 2 steps).....	72

Scheme 14: Route 4a for the synthesis of the 1-Az-OAc-SATE probe **Reagents and Conditions:** a) TBDPS-Cl, DMAP cat., pyridine, r.t., 72 h, (60%) b) NaBH₄, EtOH, r.t., 5 h, (43%) c) TrCl, NEt₃, DCM, r.t., 72 h, (60%) d) BnBr, NaH, TBAI, DMF, 0°C-r.t., 2 h, (25%) **Proposed Conditions:** e) p-TsOH, MeOH, r.t., 4.5 h, f) MsCl, NEt₃, DCM, r.t., 24 h, then, NaN₃, DMF, 60°C, 24 h, g) TBAF, THF, 0°C-r.t., 2 h, h) PO(OEt-2Br)₃, Tf₂O, pyridine, DCM, ii) KSAc, acetone, i) BCl₃, DCM, -78°C, 2 h, j) Ac₂O, pyridine, DMAP, r.t, 24 h. 73

Scheme 15: Benzylation of compound **12 Reagents and Conditions:** NaH, BnBr, TBAI, DMF, 0°C – r.t., 4 h (**13** = 25%, **32** = 20%)..... 74

Scheme 16: General mechanism of the ZnCl₂-mediated site-selective acetolysis of benzylated sugars 75

Scheme 17: Selective debenzylation test with fully benzylated ribitol **33 Reagents and Conditions:** a) BnBr, NaH, TBAI, DMF, 0°C-r.t., 24 h, (67%) b) ZnCl, Ac₂O, AcOH, r.t., 3 h, (92%) 75

Scheme 18: Route 4b for the synthesis of **1-Az-OAc-SATE Reagents and Conditions:** a) TBDPS-Cl, DMAP cat., pyridine, r.t., 72 h, (60%) b) NaBH₄, EtOH, r.t., 5 h, (43%) c) TrCl, NEt₃, DCM, r.t., 72 h, (60%) d) TBAF, THF, 0°C-r.t., 2 h, (75%) e) BnBr, NaH, TBAI cat., DMF, 0°C-r.t., 2 h, (82%) f) p-TsOH, MeOH, r.t., 4.5 h, (75%) g) MsCl, NEt₃, DCM, r.t., 24 h, then, NaN₃, DMF, 60°C, 24 h, (46%) h) i) ZnCl, Ac₂O, AcOH, r.t., 2 h, ii) NaOMe, MeOH, r.t., 2 h, (69% over 2 steps) i) PO(OEt-2Br)₃, Tf₂O, pyridine, DCM, (42%) ii) KSAc, acetone, (quant.) j) BCl₃, DCM, -78°C, 2 h, (quant.) k) Ac₂O, pyridine, DMAP, r.t, 24 h (quant.)..... 76

Scheme 19: Synthesis of **36** via OMs and OTs intermediates **Reagents and Conditions:** a) MsCl, pyridine, DCM, 0°C-r.t., 3 h, b) TsCl, pyridine, DCM, 0°C-r.t., 24 h c) NaN₃, DMF, 80°C, 24 h, (46% via OMs, 28% via OTs)..... 77

Scheme 20: Two-step selective debenzylation of the primary benzyl group of **36** to form **6** a) ZnCl, Ac₂O, AcOH, r.t., 2 h (93%) b) NaOMe, MeOH, r.t., 3.5 h, (73%) 77

Scheme 21: Synthesis of final ribitol and ribitol-5-phosphate probes from Key Intermediate compound **6: Reagents and Conditions** a) i) PO(OEt-2Br)₃, Tf₂O, pyridine, DCM ii) KSAc, acetone, (42%) b) BCl₃, DCM, -78°C, 4h, (quant.) c) Ac₂O, pyridine, DMAP r.t., 24h, (quant.) d) BCl₃, DCM, -78°C, 4h, (quant.) e) Ac₂O, pyridine, DMAP, r.t., 24h, (quant.) f) EtO₃PO, Tf₂O, pyridine, r.t., 1.5 h, (55%) g) i) TMSBr, DCM, r.t., 16 h, ii) BCl₃, DCM, -78°C, 4 h, (56% over two steps) 78

Scheme 22: Investigated methodologies for the synthesis of the free-phosphate containing probe utilising the simple alcohol 3-phenyl-propanol as a model substrate **Reagent and Conditions** a) POCl₃, pyridine, THF, H₂O (0%), b: via Mistunobu) DIAD, PPh₃, NEt₃, THF, r.t., 16 h (0%), via DCC coupling) DCC, NEt₃, DCM, r.t., 18 h (16%) via dibenzyl-chlorophosphate) oxalyl chloride, NaH, DCM,

r.t., 3 h, (32%) d) triethyl phosphate, Tf ₂ O, pyridine, DCM, (39%) Proposed Reagents and Conditions	
c) BCl ₃ , DCM, e) TMSBr.....	79
Scheme 23: Mechanism for the Mitsunobu reaction between dibenzyl phosphate and 3-phenyl-propanol 40	81
Scheme 24: Mechanism for the DCC coupling reaction between dibenzyl phosphate and 3-phenyl-propanol 40	81
Scheme 25: Mechanism for the oxalyl chloride activated reaction between dibenzyl phosphate and 3-phenyl-propanol 40	82
Scheme 26: Formation of the 1-Az-OH-Phos probe from compound 6 Reagents and Conditions a) tri-ethyl phosphate, Tf ₂ O, pyridine, DCM, r.t., 1h, (55%) b) TMSBr, c) BCl ₃ , DCM, -78°C, 3 h, (56% over 2 steps).....	83
Scheme 27: Synthesis of compound 6 from commercially available 5-allyl-2,3,4-tri-O-benzyl-ribitol Reagents and Conditions a) i) MsCl, pyridine, r.t., 3 h ii) NaN ₃ , DMF, 100°C, 72 h, (57%) b) PdCl ₂ , MeOH, r.t., 18 h (63%).....	84
Scheme 28: Proposed mechanism for the selective allyl deprotection with PdCl ₂ based on literature observations reported by Barbier et al ²⁴⁷	84
Scheme 29: Enzymatic cleavage of SATE protected phosphates.....	108
Scheme 30: Traditional synthesis route towards bis(SATE) protected phosphoprobosc, first presented by Lefebvre and co-workers in 1995. Reagents and Conditions: a) S-Acetyl-2-thioethanol, NEt ₃ , THF, -78°C-r.t, b) Probe-OH, 1H-tetrazole, THF, c) mCPBA, DCM, -40°C-r.t.....	109
Scheme 31: Modified phosphoramidite approach to SATE-protected phosphates published by Kohler and colleagues in 2021 ²⁵⁹ Reagents and Conditions a) bis(diisopropylamino)chlorophosphine 52 , DBU, DCM, r.t., 1 h, b) S-acetyl-2-thioethanol, 1H-tetrazole, DCM, r.t., 12 h, c) m-CPBA, DCM, -40°C to r.t., 3 h	109
Scheme 32: Reported methodologies for the synthesis of protected phosphates A) Chlorine substitution methods, here illustrated by tri-substitution of POCl ₃ , B) Protection of a phosphate monoester, C) Coupling of a probe to a protected phosphate, D) Synthesis of mixed phosphates by activation of phosphotriesters with triflic anhydride and pyridine Reagents and Conditions: a) NEt ₃ , DCM b) MSNT, pyridine, or accessed via varied coupling conditions including via DCC coupling) DCC, NEt ₃ , DCM, c) varied coupling conditions including via Mitsunobu) DIAD, PPh ₃ , NEt ₃ , THF, via DCC coupling) DCC, NEt ₃ , DCM, via dichlorophosphate formation) oxalyl chloride, NaH, DCM d) Tf ₂ O, pyridine, DCM	110

Scheme 33: Attempted synthesis of phosphoramidite 56 through an adapted phosphoramidite methodology published by Bhat and colleagues ²⁶² Reagents and Conditions a) DBU, toluene, 0°C-r.t, b) NEt ₃ , THF, 0°C-r.t (0%).....	111
Scheme 34: Synthesis of protected phosphates through the reaction of alcohols selectively with POCl ₃ Reagents and Conditions a) NEt ₃ , DCM, r.t., 3 h, b) allyl alcohol, NEt ₃ , DCM, r.t., 16 h, (70%) c) S-acetyl-2-thioethanol 53 , NEt ₃ , DCM, r.t., 16 h, (46%).....	112
Scheme 35: General synthesis strategy to SATE protected Phosphates utilising a bis(SATE)phosphate starting material Proposed reagents and Conditions: varied coupling conditions including via Mistunobu) DIAD, PPh ₃ , NEt ₃ , THF, via DCC coupling) DCC, NEt ₃ , DCM, via dichlorophosphate formation) oxalyl chloride, NaH, DCM d) Tf ₂ O, pyridine, DCM	113
Scheme 36: Proposed synthesis and deprotection strategies for the synthesis of bis(SATE)phosphate from phenyl-dichlorophosphate Reagents and Conditions a) 2-bromoethanol, NEt ₃ , DCM, r.t., 16 h, (64%) b) KSAC, acetone, r.t., 16 h, (74%) c) S-acetyl-2-thioethanol, NEt ₃ , DCM, r.t., 16 h, (9%), Proposed Reagents and Conditions d) NaOH, e) BnOH, NaH, THF, f) BCl ₃ , DCM	114
Scheme 37: Decomposition pathway of the 2-bromoethyl compound 62 following ESI-MS evidence of both compounds 63 and 64 and the proposed decomposition of the SATE compound 60	115
Scheme 38: Attempted synthesis of benzyl-bis(SATE)phosphate through A) transesterification of phenyl-bis(SATE)phosphate B) the POCl ₃ methodology Reagents and Conditions a) BnOH, NaH, THF, 0°C-r.t. (0%) b) BnOH, NEt ₃ , DCM, r.t., 3 h, c) S-acetyl-2-thioethanol 53 , NEt ₃ , DCM, r.t., 18 h (0%).....	115
Scheme 39: Synthesis of tris(SATE)phosphate Reagents and Conditions a) i) 2-bromoethanol, NEt ₃ , DCM, r.t., 16 h, (50%) b) KSAC, acetone, r.t., 18 h, (60%, 30% over two steps).....	116
Scheme 40: Test Reactions for the synthesis of SATE-protected phosphates with triflic anhydride and pyridine utilising tris(SATE)phosphate Reagents and Conditions a) i) Tf ₂ O, pyridine, DCM, r.t., 10 min, ii) 3-phenyl-propanol, DCM, r.t., 30 min, (33%) d) i) Tf ₂ O, pyridine, DCM, r.t., 10 min, then 2,3,4,6-tetra-O-benzyl-ribitol, r.t., 30 min (0%)	116
Scheme 41: Test Reactions for the synthesis of ethyl phosphates with triflic anhydride and pyridine utilising triethyl phosphate Reagents and Conditions a) i) Tf ₂ O, pyridine, DCM, r.t., 10 min, ii) 3-phenyl-propanol, DCM, r.t. 30 min, (45%) b) i) Tf ₂ O, pyridine, DCM, r.t. 10 min, then 2,3,4,6-tetra-O-benzyl-ribitol, r.t., 30 min, (14%)	117
Scheme 42: Attempted synthesis of bis(SATE) phosphate products Reagents and Conditions: a) i) Tf ₂ O, pyridine, DCM, r.t. 10 min then ii) 21 , DCM, r.t., 1 h. (0%) b) i) TfO ₂ , pyridine, DCM, r.t. 10	

min then ii) **11**, DCM, r.t., 1 h. (0%) c) i) Tf₂O, pyridine, CDCl₃, r.t. 10 min then ii) **40**, 2,3,4-tri-O-benzyl-5-TBDPS-1-trityl ribitol, CDCl₃, r.t., 1 h. (sugar shown to have degraded by crude NMR) 118

Scheme 43: Test Reactions for the synthesis of SATE Phosphates with triflic anhydride and pyridine utilising tris(SATE) phosphate **Reagents and Conditions** a) i) Tf₂O, pyridine DCM, r.t. 10 min, ii) 3-phenyl-propanol, DCM, r.t. 30 min (17%) b) i) Tf₂O, pyridine, DCM, r.t. 10 min then 2,3,4,6-tetra-O-benzyl-ribose, r.t., 30 min (11%), c) KSAc, acetone, r.t., 24 h, (72%) 119

Scheme 44: Comparison of the Adler et al and Huang et al methodologies for the synthesis of mixed phosphonates. Unique elements of the Huang et al method are shown in blue, and of the Adler et al method in red 131

Scheme 45: Mechanism proposed by Huang and co-workers for their method of synthesising mixed phosphonates 132

Scheme 46: Mechanism proposed by Alder and co-workers for their method of synthesising mixed phosphonates 134

Scheme 47: Attempted synthesis of **70** via the Adler method for mixed phosphonate synthesis **Reagents and Conditions** i) Tf₂O, pyridine, DCM, ii) TBAI ii) 3-phenyl-propanol **40**, NaH, THF (0%) 136

Scheme 48: Reactions attempted to recover the free alcohols from the triflated side product. **Reagents and Conditions:** a) TBAF, THF, r.t., 16 h, (**73**: 51%) b) NaOH, MeOH, THF, r.t., 16 h, (**73**: 59%) 142

Scheme 49: SATE phosphate formation of 1,2,3,4-tetra-O-benzyl-D-glucose-6-bis(2-bromoethyl)phosphate **Reagents and Conditions a)** KSAc, acetone, r.t., 24 h, (quant.) b) i) Tf₂O, DCM, r.t., 10 mins,, then pyridine, 10 min, then 1,2,3,4-tetra-O-benzyl-D-glucose, r.t., 1.5 h, ii) KSAc, acetone, r.t., 24 h, (51% over 2 steps) 143

Scheme 50: Glucose substrate structures and general methods of synthesis. **Reagents and Conditions:** a) TrCl, pyridine, r.t., 72 h (50%) b) OAc) Ac₂O, pyridine, DMAP cat., r.t., 56 h, (70%) OAllyl) AllylBr, NaH, DMF, 0°C-r.t., 18 h (70%) OBn) BnBr, NaH, DMF, 0°C-r.t., 18 h, (71%) OBz) BzCl, pyridine, DMAP cat., r.t., 56 h, (80%) c) HBr, AcOH, DCM, 10°C, 5 min, (55-70%) d) OBn) i) AcCl, MeOH, 60°C, ii) BnBr, NaH, DMF, (94%) OAllyl) i) AcCl, MeOH, 60°C, ii) AllylBr, NaH, DMF, (45%) e) H₂SO₄, AcOH, 100°C, 2.5 h, (50-57%) f) OBz) BzCl, pyridine, DMAP cat., 18 h, (72%) g) BnNH₂, THF, r.t., 18 h, (72-90%) 145

Scheme 51: Initial attempted synthesis of compound **87** **Reagents and Conditions** a) i) (2BrEtO)₃PO, Tf₂O (1.5 equiv.), DCM, r.t., 10 mins ii) pyridine (2 equiv.), DCM, r.t., 10 mins. iii) 2,3,4,6-tetra-O-benzyl-D-glucose (2 equiv. in DCM), DCM, r.t., 1.5 h., (26%) b) KSAc, acetone, r.t., 18 h, (0%) 148

Scheme 52: Synthesis of serine and threonine analogues for SATE phosphate testing	
Reagents and Conditions a) Boc anhydride, NaHCO ₃ , THF, H ₂ O, r.t., 4 h, (50%) b) Fmoc chloride, NaHCO ₃ , THF, H ₂ O, r.t., 4 h, (30%) c) benzyl chloroformate, NaHCO ₃ , THF, H ₂ O, r.t., 4 h, (64%).....	151
Scheme 53: Difference in stereochemical outcome of azide substitution reactions using A) two- and B) three-step conversion of alcohols to azides through mesylated intermediates.	187
Scheme 54: Proposed retrosynthetic pathway from the fully protected 2-azido-ribitol probe to pentose starting materials D-arabinose and D-lyxose, R = protecting group. Compound numbering for ring closed and ring-open structures shown, with the sites of azide incorporation shown in red, and the sites for phosphate incorporation in blue.	188
Scheme 55: Proposed synthesis of 2-azido-1,3,4-tri-O-acetyl-ribitol-5-(bis(SATE)phosphate)	
Reagents and Conditions a) TBDPSCl, dry pyridine, DMAP, r.t., 18 h, (72%) b) DMP, CSA, DCM, r.t., 16 h, (72%) c) BnBr, NaH, TBAI, THF, r.t., 16 h (90%) d) 1% HCl in MeOH, r.t., 45 min (16%) Proposed Reagents and Conditions: e) BzCl, pyridine, r.t. f) DIBAL-H, THF, g) BnBr, NaH, DMF, TBAI cat., h) NaOMe, MeOH, i) i) MsCl, pyridine, ii) NaN ₃ , DMF, j) TBAF, THF, k) PO(OEt-2Br) ₃ , Tf ₂ O, pyridine, DCM, l) KSAc, acetone, m) 1M HCl, n) BCl ₃ , MeOH, o) Ac ₂ O, pyridine, DMAP cat.	188
Scheme 56: Revised synthesis of 2-azido-1,3,4-tri-O-acetyl-ribitol-5-(bis(SATE)phosphate)	
Reagents and Conditions a) TBDPS-Cl, pyridine, DMAP, r.t., 18 h (72%) b) DMP, CSA, DCM, r.t., 16 h (72%) c) BnBr, NaH, TBAI, THF, r.t., 16 h (90%) d) 1% HCl in MeOH, r.t., 45 min e) BzCl, DMAP, pyridine, r.t., 72hr, f) 50% TFA, 50°C, 3hr; g) NaBH ₄ , EtOH, 0°C, 30min (2.5% over four steps) Proposed Reagents and Conditions h) BnBr, NaH, DMF, TBAI cat. i) NaOMe, MeOH, j) TBDPS-Cl, pyridine, r.t., 24 h, k) i) MsCl, pyridine, ii) NaN ₃ , DMF, 100°C, l) TBAF, THF, m) PO(OEt-2Br) ₃ , Tf ₂ O, pyridine, DCM, n) KSAc, acetone, o) BCl ₃ MeOH, p) Ac ₂ O, pyridine, DMAP cat.	189
Scheme 57: New route to 2-azido-1,3,4-tri-O-acetyl-ribitol-5-(bis(SATE)phosphate) from D-lyxose Reagents and Conditions a) i) AcCl, MeOH, 18 h, 0°C-r.t., ii) BnBr, NaH, DMF, 0°C-r.t., 2 h (50%) b) H ₂ SO ₄ , AcOH, 100°C, 1 h, c) NaBH ₄ , EtOH, r.t., 5 h (8.3% over 2 steps) Proposed Reagents and Conditions d) TBDPS-Cl, pyridine, e) i) MsCl, pyridine, ii) NaN ₃ , DMF, 100°C, f) TBAF, THF g) PO(OEt-2Br) ₃ , Tf ₂ O, pyridine, DCM h) KSAc, acetone.....	190
Scheme 58: Schematic representation of the formation of both furanose and pyranose forms of D-lyxose and the corresponding ring-opened products after the reaction sequence shown in Scheme 57 (steps a-c).	191
Scheme 59: Proposed Retrosynthetic pathway from the fully protected 3-azido-ribitol probe to pentose starting materials D-and L-xylose, R = protecting group. Compound numbering for ring closed and ring-open structures shown, with the sites of azide incorporation shown in red, and the sites for phosphate in blue.	192

Scheme 60: Synthesis of the 3-azido probes from D-xylose Reagents and Conditions a) TBDPSCI, pyridine, r.t., 72 h (36%) b) 2,2-DMP, p-TSOH, acetone, r.t. 72 h (45%) c) Ac₂O, pyridine, r.t. 24 h (86%) **Proposed Reagents and Conditions** d) HCl, DCM, e) NaBH₄ EtOH, f) BnBr, NaH, DMF, g) NaOMe, MeOH, h) i) MsCl, pyridine ii) NaN₃, DMF, 100°C, j) TBAF, THF, 0°C-r.t., k) PO(OEt-2Br)₃, Tf₂O, pyridine, DCM l) KSAc, acetone, m) BCl₃ DCM, n) Ac₂O pyridine 192

Scheme 61: **Proposed reagents and conditions** a) i) Tf₂O, pyridine, 0 °C, ii) NaN₃, DMF, r.t., b) 75% AcOH, 55 °C, 1.5 h, c) NaIO₄/H₂O, EtOH, 0 °C, 20 min then NaBH₄, d) AllylBr, NaH, DMF, e) p-TsOH, DCM, f) NaBH₄, EtOH, g) BnBr, NaH, DMF, h) PdCl₂ MeOH, i) PO(OEt-2Br)₃, Tf₂O, pyridine, DCM, j) KSAc, acetone, k) BCl₃, DCM, l) Ac₂O, pyridine 193

Scheme 62: Synthesis of final ribitol and ribitol-5-phosphate probes from key intermediate compound 6: **Reagents and Conditions** a) i) PO(OEt-2Br)₃, Tf₂O, pyridine, DCM, ii) KSAc, acetone, (42%) b) BCl₃, DCM, -78°C, 4h, (quant.) c) Ac₂O, Pyridine, DMAP, r.t., 24h, (quant.) d) BCl₃, DCM, -78°C, 4h, (quant.) e) Ac₂O, pyridine, DMAP, r.t., 24h (quant.) f) EtO₃PO, Tf₂O, pyridine, r.t., 1.5 h, (55%) g) i) TMSBr, DCM, r.t., 16 h ii) BCl₃, DCM, -78°C, 4 h, (56% over two steps) 194

Acknowledgements

None of this would be possible without the help and support of my amazing supervisor Dr Lianne Willems. No thanks is enough for all your support and guidance both inside and out of lab. Thank you for steering me out of my chemistry rabbit-holes, and for helping me see the positives when yields were in single digits.

The Willems group, you have all been great in your own ways. What an awesome group of people, it has been wild watching the group grow and seeing all the fun and personality you all bring! Tom (W), we started this wild ride together and you've been a great friend from day one. Lloyd, so many thanks - and some apologies - for continuing on our ribitol/SATE mission, I know you'll smash it! To the rest of the gang, Quentin, Mia, Angelo and Tom (R), and past MChems Amy, Ava and Oliver, thank you all for being the best workmates/friends I could ask for, and I look forward to what you all go on to achieve. The same goes for the rest of the B Block ~~babes~~ professionals. Both students and staff, you've all become such great friends, and I cannot wait to see what the future holds for you all. Special shout out to Tasha, my original carbohydrate buddy! Without you I would probably still be scared to use the column machine and the lab felt so empty after you left.

To my gin fuelled Chemistry/COVID support group, Ros, Ryan and Catherine, without our weekly catch-ups PhD life would have been much less fun, your friendship was a saviour when gin night turned virtual during the pandemic!

So many thanks go to my amazing parents inspiring me with tales of science and their PhDs. As much as it pains me to admit, you were always right and things did work out in the end! Last but not least, Ant. I'm sorry for the bundle of stress you agreed to move in with, and no thanks are enough for the meals and cups of tea you've made me along the way. Thank you for all your endless support, and putting up with all my chemistry grumbles.

Declaration

I declare that this thesis is a presentation of original work and that I am the sole author. This work has not been presented for an award at this, or any other, University. All sources are acknowledged as references. Chapter 2, '*Chemical Reporters to Study Mammalian O-glycosylation*' has been previously published as a mini-review as indicated at the start of this chapter. Reference: K. E. Huxley, L. I. Willems, *Biochem. Soc. Trans.* 2021, **49**, 903–913.

This Thesis was supported by work conducted by other Willems group members. This is further referenced in footnotes at the appropriate results; PhD student Tom Ward conducted preliminary CMP-Glo kinetic assays mentioned in Chapter 3; PhD student Lloyd Murphy has tested benzyl sugar tolerance in a phosphate reaction detailed in Chapter 4, and tested an additional substrate for the optimisation detailed in Chapter 5, Post-Doc Quentin Foucart synthesised GlcNAc substrates for testing of the phosphate methodology detailed in Chapter 5; and MChem student Henrietta Amy McIntosh conducted the synthesis from arabinose detailed in Chapter 6.

Chapter 1: Introduction

1.1 O-Mannosylation in Mammals

Glycosylation is a common, highly diverse post-translational protein modification within eukaryotic cells. Though only 10 different monosaccharides are found in mammals, these can be assembled through numerous possible glycosidic linkages differing in both regio- and stereochemistry, since the anomeric position of one sugar is, in principle, able to link to any unmodified hydroxyl group on the other, with either an α - or β - configuration. Additionally, the ability to form linkages with any free hydroxyl group allows for the formation of branching glycan chains, which produces further diversity in chain structure (Figure 1). This is in contrast to DNA and peptides which have a linear structure. The vast diversity in the structure of glycans allows for a wide range of functions. These biological functions can be split into three main classes, (1) to maintain protein structure and stability; (2) to store nutrients; (3) to allow for recognition by glycan-binding proteins, allowing for communication between cells and the extracellular matrix.⁴ Not only do these varying functions highlight glycan diversity but also their optimised structures for different roles.

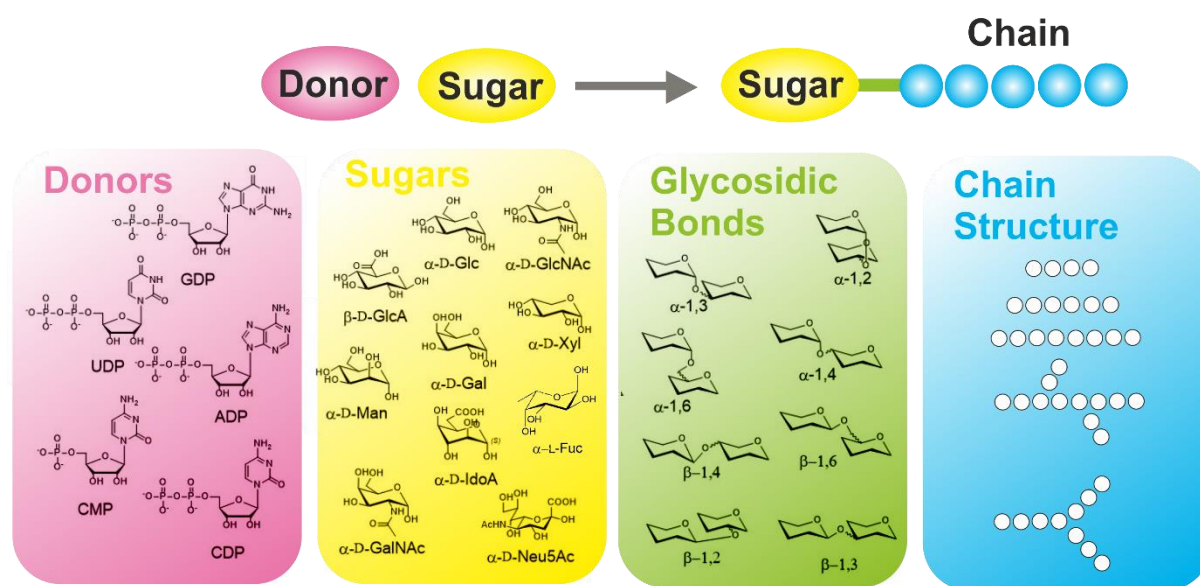


Figure 1: Glycan formation results in a wide diversity of potential carbohydrate structures. Overview presenting an array of possible donors, sugars, glycosidic bond configurations and schematic glycan structures representing a variety of chain lengths and branches.

Within eukaryotes, five different classes of glycans exist. These are classified as *N*-glycosylation, *O*-glycosylation, *C*-glycosylation, phosphoglycosylation and glypiation.⁵ *N*-, *O*- and *C*-glycosylation is defined by the atom linking the amino acid to the glycan chain. Phosphoglycosylation is defined by the binding of the glycan to a phosphate of a serine residue, and in the case of glypiation, glycoposphatidylinositol (a lipid anchor) is added to the C-terminus of a protein. *N*-glycosylation is the most common and widely understood of the classes.⁶⁻⁹ *N*-glycans are

covalently linked to the nitrogen of asparagine residues and all *N*-glycans share a common core structure, GlcNAc₂Man₃. Contrastingly, *O*-glycosylation is a lot more varied, with *O*-glycans extending from serine and threonine residues. Though they are initiated by many sugars, the most common in mammals are *O*-*N*-acetylglucosamine (*O*-GlcNAc), *O*-*N*-acetylgalactosamine (*O*-GalNAc), *O*-mannose (*O*-Man), and *O*-xylose (*O*-Xyl). Glycosylation can occur in multiple organelles; the cytoplasm for cytosolic proteins, and the endoplasmic reticulum (ER) or Golgi apparatus for extracellular and secreted proteins. The monosaccharide building blocks are provided by activated nucleotide- and dolichol-linked donors which are synthesised within the cytosol of cells. The most common nucleotide for activation is uridine-*di*-phosphate (UDP).¹⁰

O-mannosylation is a sub-category of *O*-glycosylation, with the first residue being mannose, and is an essential sub-class of glycosylation conserved between fungi, mammals and humans. *O*-mannosyl glycans were first identified within Baker's yeast in 1968,¹¹ where they are frequent modifications of secreted cell wall proteins and consist of repeated mannose residues.¹² In mammals, the initial mannose can be elongated into three core structures, which unlike the yeast glycan do not contain further mannose residues (See Section 1.3 α -Dystroglycan Biosynthesis, pg. 23). It has been shown that *O*-mannosyl glycans make up around 30% of *O*-glycans in the brain.^{13, 14}

1.2 α -Dystroglycan

It was not until 1997 that *O*-mannosyl glycans were identified in mammals,³ in the basement membrane protein α -dystroglycan (α -DG).^{15,13 12} α -DG is a highly glycosylated glycoprotein and is a major component of the dystrophin-glycoprotein complex (DGC), which acts across the cell membrane and is responsible for maintaining skeletal muscle integrity and the functionality of the central nervous system.^{1, 15-17} The DGC, shown in Figure 2, is a multi-component complex that possesses both stabilising and signalling roles between the intracellular cytoskeleton, cell membrane and the extracellular matrix. Mutations within components of the DGC have been shown to cause muscular dystrophy so understanding the key components, as well as their assembly, is of great biological interest.

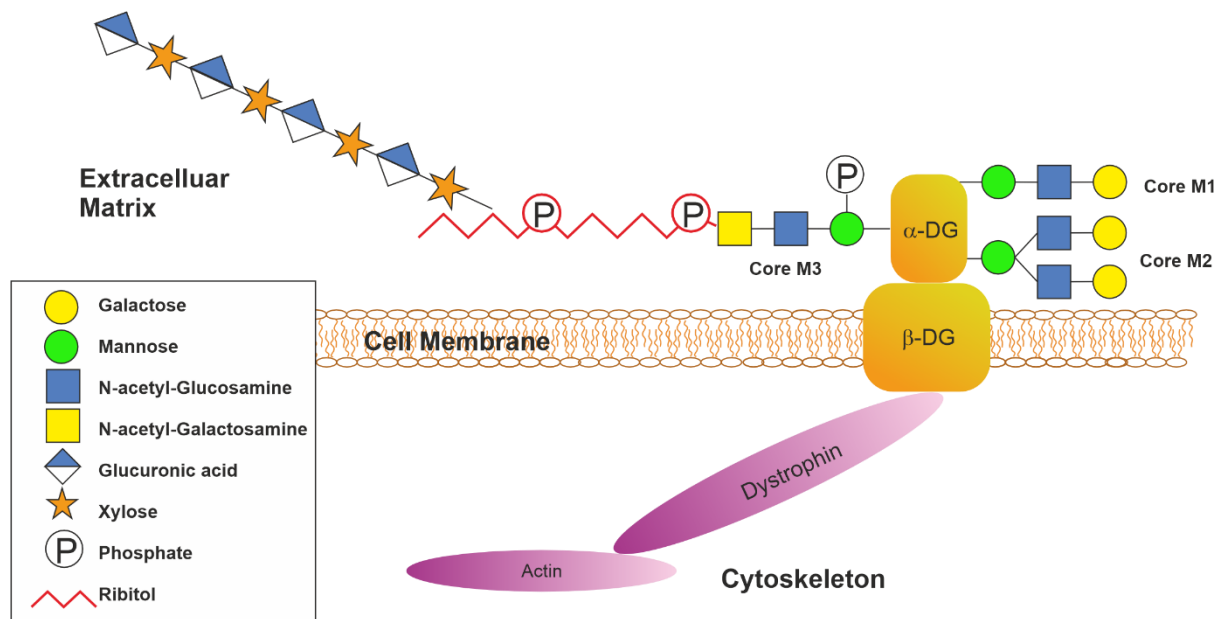


Figure 2: Overall Structure of the DGC, showing the position of the α - and β -dystroglycan (DG) subunits and the three types of *O*-mannosyl glycans that are all found on α -DG.

α -DG is encoded by the DAG1¹³ gene and was first isolated from skeletal muscle.¹⁸ It is translated as a single peptide that is post-translationally cleaved into two subunits, alpha and beta.¹⁹ Evidence of this α/β -peptide was first reported in 2000 by Campbell and co-workers.¹⁹ Following cleavage of this peptide, the beta subunit forms a transmembrane protein that binds to both dystrophin,^{15, 20} and the highly glycosylated extracellular alpha subunit. α -DG is composed of three domains: an *N*-terminal domain, a serine-threonine-rich mucin-like domain, and a *C*-terminal domain.¹⁸ The serine-threonine rich domain contains approximately 40 Ser/Thr residues, and this mucin-like domain carries all three types of *O*-Man glycans including the core M3 glycan responsible for binding extracellular matrix proteins.

α -DG has a predicted mass of 74 kDa, though when purified from native tissues appears at a much higher mass of 156 kDa in muscle, and 120 kDa within the brain. This is due to the great amount of post-translational modification with several types of glycans expressed on α -DG. α -DG contains three different classes of *O*-mannosyl glycans, named Core M1, M2 and M3. Core M1 glycans are formed by extension of the initial Man residue with GlcNAc and Gal and further modification to this glycan can occur through the addition of *N*-acetylneuraminic acid (Neu5Ac) or fucose (Fuc) residues.²¹ By the addition of another GlcNAc-Gal branch to the Man residue branched Core M2 glycans are formed (Figure 3), which again can be extended by further modification. The Core M3 glycan is also formed by the addition of a GlcNAc residue, though this is linked through 1,4-linkage to mannose instead of the 1,2- and 1,6-linkages found in core M1 and core M2 glycans, followed by a GalNAc residue. The Core M3 structure further differs from the Core M1 and M2

through the phosphorylation of the O6 site of mannose. The Core M3 glycan is often termed 'the functional glycan' as this Core M3 structure is further extended with a large glycan of repeating GlcA-Xyl disaccharide units, named matriglycan (see section '*Matriglycan*', pg. 25), which gives the glycan its ligand-binding capabilities. The functions of Core M1 and Core M2 are currently unknown, though the majority of O-mannosyl glycans within cells are Core M1 and M2 types, with only a small number of Core M3 glycans known to exist solely on α -DG.

Many extracellular matrix proteins with varying functions bind to the matriglycan of α -DG. These include; agrin, a large proteoglycan that is released at muscle fibres to stimulate receptor aggregation;²² perlecan, a key component of the vascular matrix;²³ neurexin, a transmembrane protein that functions on the cell surface of neurons;²⁴ pikachurin, a protein with an essential role in interactions between the photoreceptor ribbon synapse and bipolar dendrites (the branched extensions of nerve cells);²⁵ slit, a protein with important roles for axonal guidance in the mammalian nervous system;²⁶ and laminin. Laminins are the best characterised extracellular proteins found to bind to α -DG and play a central role in establishing networks among other extracellular matrix proteins as well as connecting the membrane to the surfaces of adjacent cells.¹⁵ This ligand binding is crucial for the proper function of the DGC so further understanding the structure and biosynthesis of the glycans on α -DG is of great importance. In addition, a lack of functional matriglycan at the cell surface, due to malfunctioning of the glycan's biosynthetic pathway, can lead to a subset of congenital muscular dystrophies (see 1.5 *Muscular Dystrophies* page 32).

1.3 α -Dystroglycan Biosynthesis

Core M1 and M2 Glycan Biosynthesis

The Core M1 glycan was initially identified in the early '90s by Endo and colleagues from purified bovine α -DG.²⁷ Attachment of the initial mannose unit onto the Ser and Thr residues in α -DG is catalysed by the *Protein O-Mannosyltransferase 1 and 2* (POMT1/POMT2) complex (Figure 3).²⁸ This complex is localised in the ER and catalyses the transfer of mannose from dolichol phosphate mannose (Dol-P-Man) onto α -DG.²⁹ The function of POMT1 and 2 in humans was identified in 2004, based on yeast homologues whose same role was already identified.³⁰ Following mannose addition, *protein O-mannose β -1,2-N-acetylglucosaminyltransferase* (POMGnT1) transfers a GlcNAc residue from UDP-GlcNAc to the O-mannosyl proteins, forming a GlcNAc β 1-2Man linkage. POMGnT1 was first characterised by Yoshida-Moriguchi and co-workers in 2001 and was shown to be a 660 amino acid sequence, 71.5 kDa type II membrane protein with activity in the brain.³¹ Knockout of POMGnT1 has been shown to cause the loss of laminin-binding, despite this enzyme not being

present in the biosynthetic pathway of the functional Core M3 glycan. This indicates a link between Core M1 and 2 with the biosynthetic pathway of Core M3. Modification of the Core M1 glycan is achieved by the addition of a β -1,6-GlcNAc branch. This modification is conducted by α -1,6-Mannosylglycoprotein 6- β -N-Acetylglucosaminyltransferase B (GnT-IX) and leads to the formation of the Core M2 glycan. GnT-X1 is expressed only in the brain,^{32,33} therefore, the Core M2 is found primarily in the brain and has a very minor population in skeletal muscle.¹⁸ Extension of both the core M1 and M2 glycans is conducted by the addition of a β -1,4-galactose residue by a β -1,4-galactosyltransferase (GalT), with extension of the core M2 glycan occurring after the branched structure has formed.¹⁴

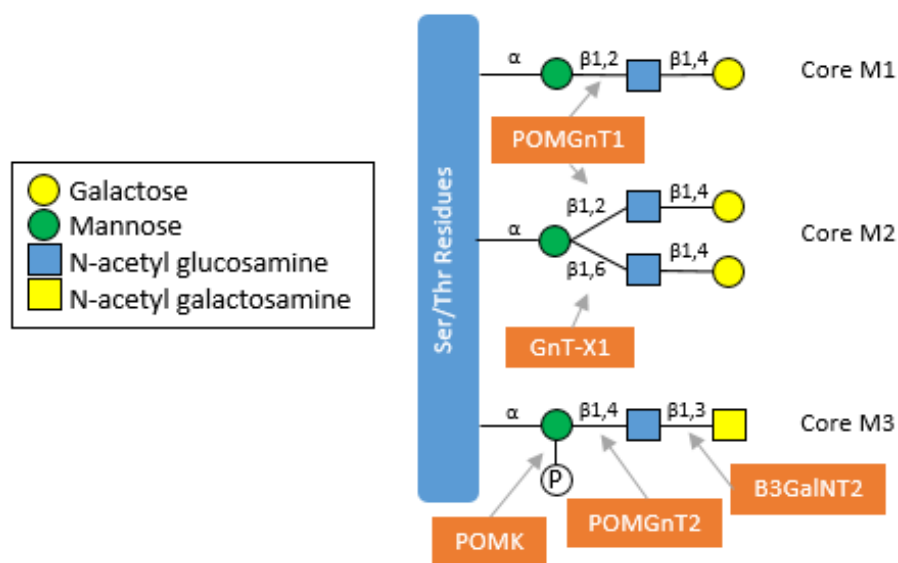


Figure 3: Schematic representation of the biosynthesis of the core glycans of α -DG, showing linkage types and the enzymes responsible for the formation of each glycosidic bond. Shown is just the unextended M1 and M2 glycan structures, further modification to these glycans can occur through the addition of N-acetylneuraminic acid (Neu5Ac), N-glycolylneuraminic acid (Neu5Gc) or fucose (Fuc) residues.²¹

Core M3 Glycan Biosynthesis

It was not until after the discovery of Core M1 and M2 glycans that glycans with C6 phosphorylated mannose units were discovered. These were termed Core M3 glycans and the full structure of the Core M3 glycan is shown below in Figure 4. This glycan contains three distinct units; the core M3 phosphorylated trisaccharide (labelled in blue), the ribitol-5-phosphate linking region (shown in red) and the extended matriglycan chain (labelled in green) which directly binds extracellular matrix ligands. The biosynthesis of each of these units will be explained further.

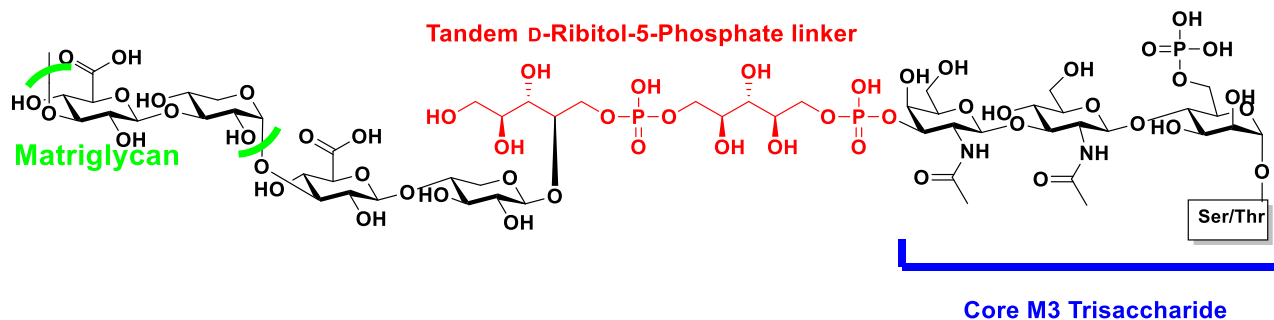


Figure 4: The full structure of the core M3 glycan, including the two uncommon phosphodiester linkages and the matriglycan structure which is unique to this glycan.

Matriglycan

In 2004, the enzyme *LARGE xylosyl- and glucuronyltransferase 1* (LARGE) was found to restore laminin-binding of α -DG within mice with muscular dystrophy.³⁴ The highest expression of LARGE is found in the brain, heart and skeletal muscle, much like the distribution of functional α -DG.³⁵ This led to further investigation of the role of LARGE, and in 2012, its ability to form a polysaccharide of xylose-glucuronic acid repeat units extending the Core M3 glycan of α -DG was discovered.³⁶ This extending polysaccharide unit has since been termed 'matriglycan'¹⁵ and is responsible for the physical link between extracellular species and α -DG. As well as synthesising the matriglycan chain, it is believed that LARGE is also responsible for determining the length of the formed polysaccharide, potentially through competition with the sulfotransferase Human Natural Killer 1 (HNK-1) which has recently been shown to modulate glucuronic acid residues in matriglycan.³⁷ The brain form of α -DG has a higher affinity for laminin than within muscle, which indicates LARGE's ability to vary the affinity of the glycan for ECM ligands in different contexts.¹⁵ Different chain lengths of matriglycan are found in different distributions around the body, though the minimum length of repeat units needed to bind to a sufficient number of laminin units for proper function remains unknown.³⁸ Over-expression of LARGE in cells containing fully formed α -DG has been shown to lead to further glycosylation and extension of matriglycan.³⁴ Though this is key evidence in the hypothesis that matriglycan length is determined by the amount of LARGE expression, further research is required for it to be fully established.

After the discovery of matriglycan and the Core M3 trisaccharide, a linking region between these units was identified (see 1.4 *The Tandem D-Ribitol-5-Phosphate Linker*, pg. 26). Once identified as a tandem ribitol-5-phosphate unit, it was found that LARGE was unable to directly add the matriglycan chain to ribitol-5-phosphate. Instead, two priming enzymes add the initial xylose and glucuronic acid residues. These were identified as *Ribitol Xylosyltransferase 1* (TMEM5), and *Beta-1,4-Glucuronyltransferase 1* (B4GAT1) respectively.³⁹ TMEM5 shows sequence similarity with other glycosyltransferases and was initially identified in screenings of genes uncovered in loss of anti-

dystroglycan antibody (IIH6) binding activity.³⁹⁻⁴¹ In 2016, Praissman and co-workers were able to identify TMEM5 as a xylosyltransferase, able to transfer xylose from UDP-xylose onto CDP-ribitol, but not ribitol or ribitol-5-phosphate, suggesting the need for ribitol-5-phosphate to be linked through a phosphodiester linkage to act as an acceptor.⁴² Further evidence for the involvement of TMEM5 came from knockdown of TMEM5 in zebrafish causing muscular dystrophy symptoms, specifically those matching Walker-Warburg-Syndrome (See 1.5 *Muscular Dystrophies*, pg. 32).³⁹ The function of B4GAT1 (also known as B3GNT1) was identified before TMEM5 by Willer and colleagues in 2014.⁴²

1.4 The Tandem D-Ribitol-5-Phosphate Linker

Identification

In 2010 Yoshida-Moriguchi and co-workers identified the presence of a phosphate diester moiety on the Core M3 glycan of α -DG. They achieved this by treatment of α -DG with aqueous HF, which specifically cleaves phosphate esters. The loss of both immunoreactivity activity with an IIH6 antibody, as well as loss of laminin-binding activity in treated α -DG samples proved the presence of phosphate esters linking matriglycan to the Core M3 glycan.⁴³ Immobilized metal affinity chromatography (IMAC) beads, which bind monoester and not diester moieties, were able to bind α -DG in congenital muscular dystrophy muscle tissue, but not fully glycosylated α -DG from control cell extracts. This proved that the phosphate in functional α -DG was in a phosphodiester linkage, though lead to the hypothesis that matriglycan was linked to the C6 phosphate of mannose within the Core M3 trisaccharide.

It was later in 2016 that the linking region was fully elucidated as a tandem D-ribitol-5-phosphate linkage between the Core M3 trisaccharide and matriglycan.^{39, 44, 45} The identification of the phosphodiester linkage location and the carbohydrate residues involved proceeded by varied methods, conducted by three separate groups.^{3, 39, 44-46} Both Praissman and co-workers³⁹ and Kanagawa's group⁴⁷ utilised mass spectrometry studies alongside treatment of recombinant α -DG fragments with HF. The sites of possible cleavage are shown within Figure 5. Kanagawa's group utilised this method to identify the presence of a cleaved ring-open pentitol phosphate unit which was proven to be ribitol by GC-MS analysis.⁴⁴ Praissman's group utilised HF treatment to identify the presence of a linear pentitol on a Xyl-GlcA fragment among further extended matriglycan fragments.³⁹ Searching for evidence of the other half of the phosphodiester linkage, they discovered that mild periodate treatment, which cleaves vicinal diols (Figure 5), led to the formation of a phosphoribitol fragment linked to the Core M3 trisaccharide. This oxidative cleavage also proved the ring-open formation of the ribitol sugar. As periodate does not affect glycosidic bonds, cleavage of

vicinal diols within furanose (ring closed) sugars leaves the chain intact, whereas cleavage of pentitol (ring open) sugars leads to the formation of two separate fragments (Figure 5). Comparatively, Bommer and co-workers identified the phosphodiester linking moiety following the identification of the roles of the key enzymes, *2-C-methyl-D-erythritol-4-phosphate cytidyltransferase* (ISPD), *Fukutin* (FKTN) and *Fukutin Related Protein* (FKRP) in its formation.⁴⁵ Their findings are detailed in sections *ISPD*, pg. 28, and *FKTN and FKRP*, pg. 29, respectively.

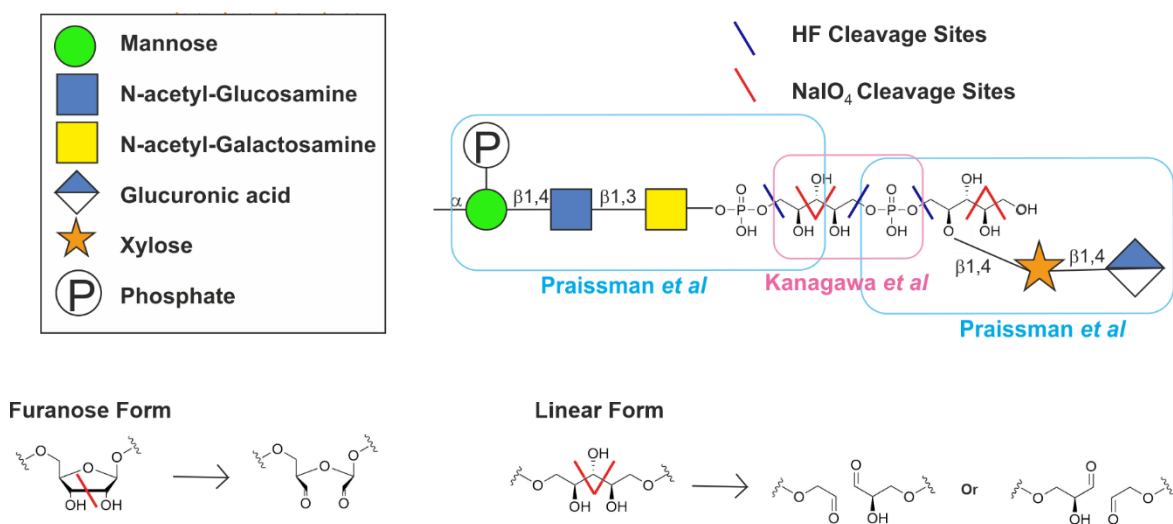


Figure 5: Potential cleavage sites of the phosphodiester linkages in the core M3 O-mannosyl glycan by HF and NaIO₄ (top) and periodate cis-diol oxidation products for both furanose and linear sugar structures presenting both the intact and split glycan products (bottom).

Previous studies had identified phosphorylation at the C6 position of mannose within the Core M3 trisaccharide (see Figure 4 pg. 25) and it had been initially hypothesised that functional extension occurred at this phosphate.⁴³ However, utilising NMR analysis, Kanagawa and colleagues were able to identify the site of addition of the phosphate diester at the third carbon of the GalNAc residue of the core M3 trisaccharide.⁴⁴ At the same time, the Praissman group's periodate cleavage experiments also detected the presence of phosphate, in addition to the C6 mannose phosphorylation, on the obtained Core M3 fragments, further reinforcing that ribitol was not bound to the C6 phosphate of mannose, and that two phosphates were attached to the Core M3 trisaccharide unit.³⁹ Since the discovery of the phosphodiester linkage, the knowledge of the biosynthesis of the Core M3 glycan has grown significantly. Multiple genes with previously unknown functions have been found to play a role in the formation of this moiety. These genes have since been found to encode enzymes responsible for the addition of ribitol-5-phosphate onto the core M3 glycan (FKTN and FKRP) as well as the enzyme that produces the CDP-activated donor that is needed for the phosphoribitol transfer reactions (ISPD). All of these findings lead to the full biosynthetic pathway of the Core M3 glycan detailed below in Figure 6.

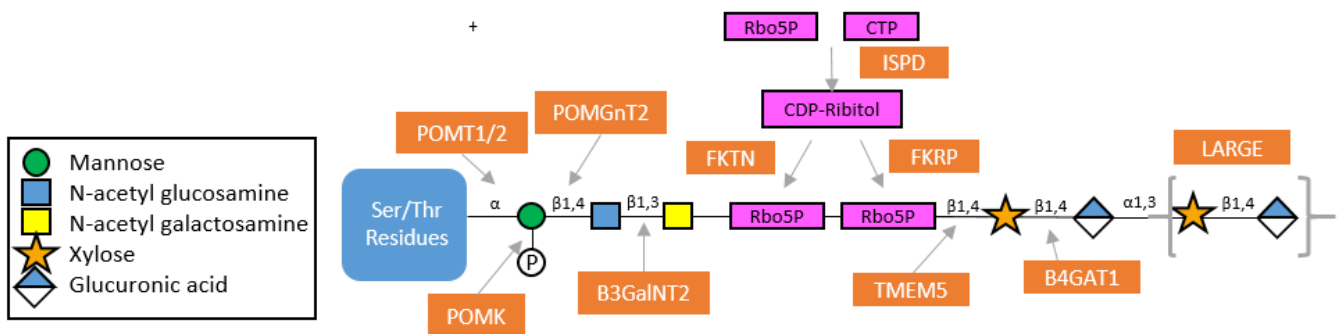
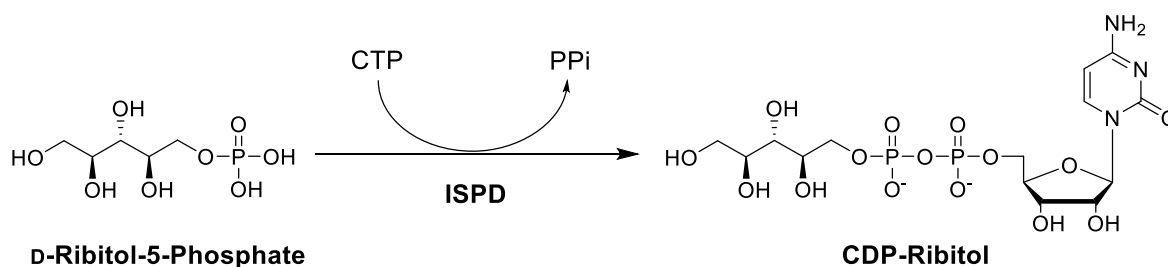


Figure 6: Schematic structure of the Core M3 Glycan of α -DG with the biosynthetic enzymes responsible for each glycosidic bond or phosphoester bond formation indicated in orange.

2-C-methyl-D-erythritol-4-phosphate cytidyltransferase (ISPD)

2-C-methyl-D-erythritol-4-phosphate cytidyltransferase (ISPD) is an enzyme with homologs in other organisms including plants and bacteria, where it is a major component of the non-mevalonate pathway (MEP pathway).^{48, 49} Within this pathway, ISPD functions in converting methylerythritol phosphate and CTP into 4-Diphosphocytidyl-2-C-methylerythritol (CDP-Me), releasing pyrophosphate (PPI). ISPD in humans (hISPD), was first linked to muscular dystrophy and improper laminin-binding of α -DG in 2012.^{40, 50, 51} In mammals, however, the MEP pathway is absent, indicating the presence of a different ISPD function that is essential for the proper function of α -DG.

The function of ISPD in mammalian cells was first identified by Riemersma and colleagues in 2015, following their determination of a crystal structure of ISPD, which showed strong homology to other cytidyltransferases.¹⁰ Immune cytochemical staining showed a staining pattern consistent with ISPD being expressed in the cytosol. Assays with malachite green, to monitor the release of PPI representing cytidyltransferase activity, against several hexose and pentose phosphate substrates was attempted. The activity with pentose-5-phosphate was found to be considerably higher than for hexose sugars, with the highest levels recorded for ribose-5-phosphate and ribulose-5-phosphate. Ribitol-5-phosphate was then shown to be converted into CDP-ribitol (Scheme 1), with a conversion rate that was higher than reactions using ribulose- and ribose-5-phosphate as the substrates. This cytidyltransferase activity of mammalian ISPD has been further confirmed in two separate studies published the following year, by Kanagawa⁴⁴ and Praissman³⁹ who both confirmed the formation of CDP-ribitol from ribitol-5-phosphate and CTP. More recently, Toda *et al* have demonstrated the ability to restore abnormal glycosylation of α -DG within ISPD-deficient muscular dystrophy exhibiting mice by the administration of cell permeable CDP-Rbo derivatives in which the sugar and nucleotide base were partially, or fully, acetylated.⁵² Not only does this indicate a potential for CDP-ribitol-based pro-drug therapies for the treatment of muscular dystrophies caused by mutations in ISPD, but this also further enforces the role of ISPD in the formation of functional α -DG.



Scheme 1: Schematic representation of the formation of CDP-ribose by ISPD

It is currently not known how mammalian cells produce D-ribose-5-phosphate, the substrate used by ISPD to generate CDP-ribose. In certain gram-positive bacteria, which use ribitol-5-phosphate as a prominent building block of cell wall teichoic acids,^{53, 54} the formation of CDP-ribose has been shown to proceed *via* two different enzymatic pathways. *H. Influenzae* contains the gene *BCS1*, which encodes an enzyme able to reduce ribulose-5-phosphate to ribitol-5-phosphate with NADPH, and its subsequent reaction with CTP to form CDP-ribose.⁵³⁻⁵⁵ Alternatively, other bacteria, such as *Streptococcus pneumoniae*, rely on separate enzymes, TarJ and TarI which catalyse the reduction of ribulose-5-phosphate, and cytidyl transfer to ribitol-5-phosphate separately.⁵⁶ To be able to verify whether ISPD was able to reduce ribulose-5-phosphate to ribitol-5-phosphate and consequently generate CDP-ribose, the Riemersma group incubated ribulose-5-phosphate and ISPD in the presence of CTP alongside reducing agents NADH and NADPH.¹⁰ Neither reaction generated CDP-ribose, showing that human ISPD does not exhibit additional ribulose-5-phosphate reducing activity, and acts only as a cytidyltransferase for ribitol-5-phosphate.

There are currently two hypotheses for the biosynthesis of ribitol-5-phosphate within mammalian cells. Treatment of cells with Sorbinil, an aldose reductase inhibitor, has been shown to decrease cellular levels of CDP-ribose, indicating the reduction of ribose or ribose-phosphate to ribitol(-phosphate) by an unknown enzyme may be involved in CDP-ribose formation.⁴⁵ On the other hand, supplementing cells with ribitol has been shown to increase the levels of CDP-ribose irrespective of treatment with Sorbinil, indicating that a kinase might be able to directly phosphorylate ribitol to generate ribitol-phosphate that is needed as a substrate by ISPD. This kinase is hypothesised to be the D-ribulokinase FGGY,^{45, 57} knockdowns of which have been shown to prevent increased levels of CDP-ribose on the addition of ribitol to cells, though this effect is not detected in the absence of ribitol supplementation.

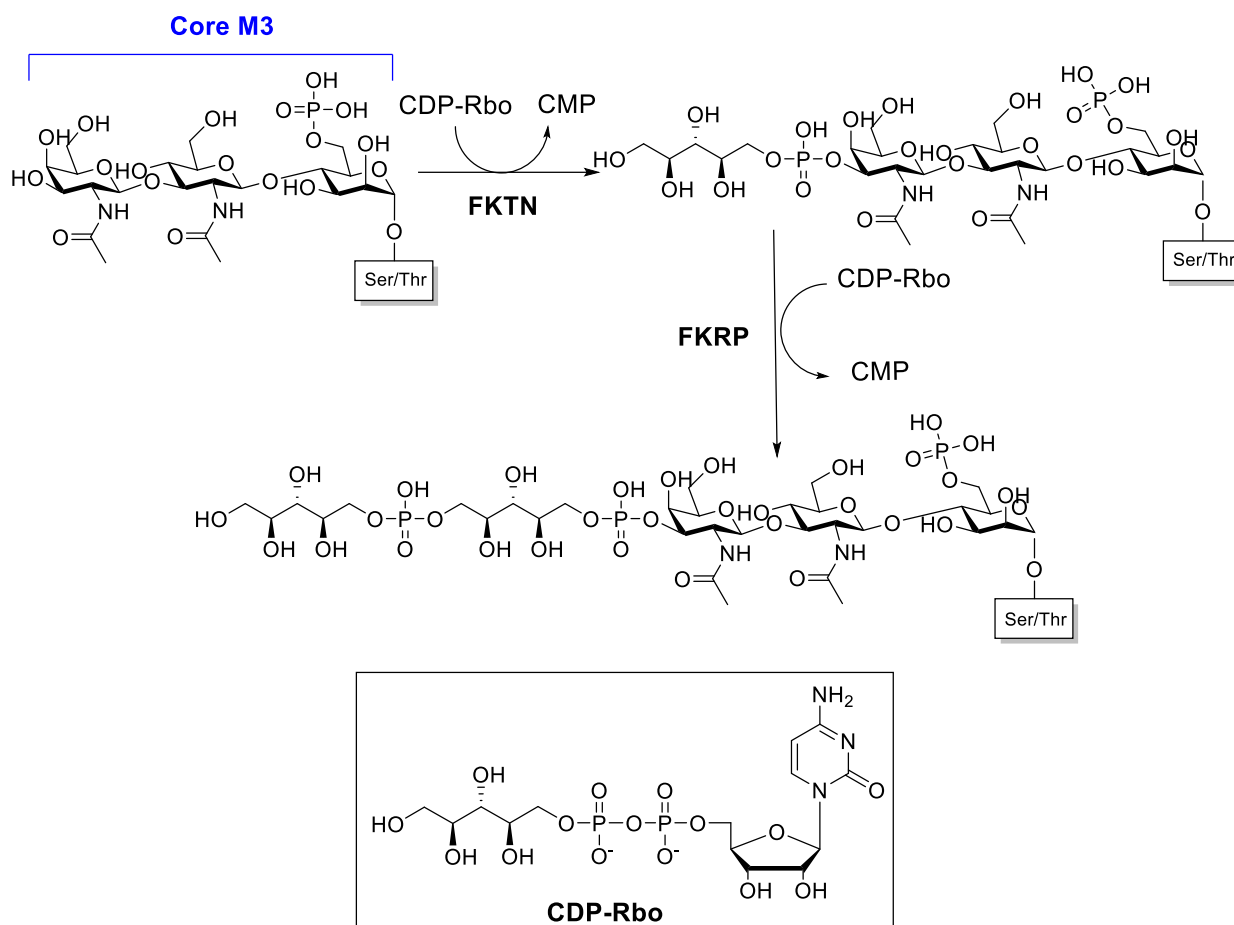
Fukutin (FKTN) and Fukutin Related Protein (FKRP)

Mutations within the *Fukutin* (FKTN) gene were identified as causative for Fukuyama type muscular dystrophy in 1998 by Toda and co-workers.⁵⁸ In 2001, *Fukutin Related Protein* (FKRP) was found to be causative for muscular dystrophy as well.⁵⁹ Despite their function remaining unknown

until 2016, as early as 1999, the study of other Fukutin family genes, as well as a computational study of FKTN's sequence indicated it worked as a cell surface modifier, capable of transferring phospholigands to glycoproteins expressed on the cell-surface.^{60, 61} Site-specific monoclonal antibody studies showed FKTN to be a very low abundance protein, localised to the Golgi, with certain disease-causing mutations shown to lead to a mislocalisation to the ER.⁶² A first indication of the involvement of FKTN in the functional glycosylation of α -DG was reported in 2006, in a study that found FKTN to localise and interact with glycosylated α -DG.⁶³ Similar enzymes within bacteria have been proven to transfer both choline phosphate and ribitol-5-phosphate onto cell surface glycoproteins.^{56, 64, 65} The discovery of a tandem D-ribitol-5-phosphate unit, alongside the presence of the highly similar proteins FKTN and FKRP with unknown functions was an important indicator of the functions of the enzymes in the formation of the phosphodiester linkage.

The link between the function of ISPD and FKTN and FKRP was first noted in 2012 by Roscolli and colleagues,^{40, 51} and, following the identification of the phosphodiester linkage and the function of ISPD, this link was further explored. The role of FKTN and FKRP in the synthesis of α -DG was confirmed by two groups in 2016.^{44, 45} Gerin and co-workers were able to confirm the function of FKTN and FKRP utilising isotopically labelled CDP-ribitol derivatives with either the phosphate attached to ribitol (³²P) or the adjacent ribitol unit (³H at C1) labelled. These were incubated with either FKTN or FKRP with purified α -DG fragments, and subsequently radioactivity was detected. Significant incorporation of these probes was seen in the presence of catalytically active FKTN and FKRP. The incorporation of the ³²P label suggested that the ribitol residue was transferred as ribitol-5-phosphate from CDP-ribitol. In separate cell studies, knockout of FKTN lead to complete loss of ribitol-5-phosphate incorporation, whereas knockout of FKRP still showed evidence of ribitol-5-phosphate incorporation. Therefore, the sequential addition of two ribitol-5-phosphate units by FKTN and FKRP was hypothesised. This was confirmed in a parallel study conducted by Kanagawa and colleagues in 2016,⁴⁴ who hypothesised the function of FKTN and FKRP as ribitol-5-phosphate transferases and modified a synthetic α -DG peptide with the Core M3 trisaccharide. This was utilised as an acceptor substrate and underwent incubation with FKTN and CDP-ribitol. HPLC analysis alongside MS showed the addition of a ribitol-5-phosphate unit to the Core M3 trisaccharide. The same experiment was conducted with FKRP, incubating with CDP-ribitol and either the Core M3 trisaccharide-modified peptide or the ribitol-5-phosphate modified peptide generated by FKTN. Only the ribitol-5-phosphate modified peptide was altered by the addition of a second ribitol-5-phosphate unit to form the tandem phosphodiester linkage, with the non-modified Core M3 trisaccharide unchanged by FKRP. A schematic representation of this reaction sequence is presented in Scheme 2. Further confirming the formation of the tandem ribitol-5-phosphate linker by the actions of FKTN

and FKRP, a 2022 publication by Toda *et al* has also been able to show *in vitro* the subsequent elongation of this linker by the action of TMEM5, B4GAT1 and LARGE respectively.⁶⁶



Scheme 2: Schematic representation of the enzymatic function of FKTN and FKRP in the formation of the tandem ribitol-5-phosphate modification of the Core M3 Glycan

The catalytic mechanisms for FKTN and FKRP are yet to be elucidated. The structure of FKTN is still unknown, although a crystal structure for FKRP has recently been published by Kuwabara and colleagues.⁶⁷ The group were able to obtain crystal structures of FKRP alongside structures in complex with CDP-ribitol, CMP, and the Core M3 trisaccharide plus ribitol-5-phosphate. FKRP had previously been shown, in 2011, to exist as homodimers, coordinated by disulphide linkages through cysteine residues that exhibit two-fold symmetry,⁶⁸ and this was corroborated by this work. Their structure also showed the recognition of the ribitol-5-phosphate moiety by the catalytic domain as well as the *O*-mannose C6 phosphorylation being recognised by the stem domain of another subunit. The structure of the region of the catalytic domain is similar to the catalytic domain of the nucleotidyltransferase (NTase) family. The similar metal coordination at two sites, alongside co-ordination of asparagine residues in a similar pattern, indicates that their mechanism may be shared, though this is yet to be confirmed. A CDP-ribitol soak with FKRP crystals containing two Mg²⁺ ions showed degradation of CDP-ribitol to CMP and ribitol-5-phosphate. This shows that at least one of

the Mg²⁺ ions has a catalytic function. The authors also note that the catalytic domain of FKR and FKTN have sequence similarities, with the sugar donor site expected to be the same, and the sugar acceptor site expected to be different due to the specificity of the tandem addition of FKR and FKTN. A crystal structure is still yet to be obtained for FKTN, and additional studies are needed to elucidate mechanisms for these enzymes.

1.5 Muscular Dystrophies

The identification of POMGnT mutations within Muscle Eye Brain disease (MEB) patients was the first indication of a link between the glycosylation of α -DG and muscular dystrophies. Since then 17 different genes have been shown to be causative for dystroglycanopathies, though for around half of the patients diagnosed with dystroglycanopathies the causative gene is unknown.⁶⁹ This highlights the diverse range of dystroglycanopathies and the difficulties in finding a 'one size fits all' cure.

Of the over 40 different known congenital muscular dystrophies (CMDs) predominantly only the dystrophies associated with O-mannose glycosylation defects have a significant neurological component. This includes symptoms such as cobblestone lissencephaly - disorganisation of the neurons within the cortex due to increased migration, which produces a characteristic nodularity on the brain surface as the folds within the brain muscle become less distinguished;³ muscle weakness and delayed motor function development; atrophy to the optic nerve and other ocular abnormalities causing a reduction in sight;⁷⁰ and in many cases severe retardation of the affected individual.^{15, 71, 72} These are key characteristics for patients suffering from Fukuyama CMD which is the second most common form of muscular dystrophy and is a common genetic disease in Japan.^{2, 73} This disease is caused by mutations within FKTN, so further understanding this enzyme and having ways to effectively target it is of great importance to being able to treat this disease and similar conditions. Mutations within FKR have also been shown as causative for muscular dystrophy, more specifically Limb-girdle muscular dystrophy type 2I. Limb-girdle muscular dystrophy is a term used to describe a group of diseases that cause muscle weakness and wastage. Early stages of these diseases show a characteristic walking gait and inability to run, with the disease progressing to a stage where wheelchair assistance is required for mobility. Unlike Fukuyama CMD, occurrences of Limb-girdle muscular dystrophy are less specific to a single country, and cases are spread more equally worldwide.⁷⁴

Mutations in ISPD are the second most common cause of Walker-Warburg syndrome.^{2, 10} Walker-Warburg syndrome sufferers display symptoms similar to those with Fukuyama CMD and other FKTN caused muscular dystrophies with decreased muscle function, eye abnormalities and

brain lissencephaly. This is explained by the newly understood biosynthetic pathway from ribitol-5-phosphate to functionally glycosylated α -dystroglycan, as without conversion of ribitol-5-phosphate to CDP conducted by ISPD, FKTN and FKRP are unable to transfer ribitol-5-phosphate units to the dystroglycan chain, which ultimately leads to loss of laminin-binding and α -dystroglycan malfunction similar to that caused by FKTN and FKRP mutations. Like limb-girdle muscular dystrophy, Walker-Warburg syndrome is widely spread worldwide, and is estimated to affect 1 in 60,500 newborns worldwide.⁷⁵ It should be noted that Walker-Warburg syndrome can be caused by mutations in at least a dozen genes including FKTN and FKRP,⁷⁶ and cases are not limited to ISPD mutations.

1.6 Questions Still to be Answered

Though great advancements in the understanding of the formation of the phosphate linking moiety, as well as the formation of CDP-ribitol, have been achieved there are still numerous questions still to be answered. Previously mentioned was the still unidentified mechanism for both FKTN and FKRP, as well as an FKTN crystal structure. Many aspects of core M3 glycan structure and function remain unclear, such as the regulation of matriglycan length, its possible presence on other, as yet unidentified, cell surface proteins, and the dynamics of glycan levels and structure in response to various stimuli and pathological conditions.

Also unclear is the biosynthesis of ribitol-5-phosphate within cells.²⁸ ISPD has been shown to have no ribitol-5-phosphate dehydrogenase activity and it is possible that, in a similar way to TarI and TarJ, there is a further ISPD-related, unidentified enzyme able to catalyse this transformation within humans, which could be one of the as-of-yet unidentified CMD causing genes. More interestingly, identification of D-ribitol-5-phosphate within the core M3 glycan represented its first, and currently only, identification within mammalian cells, and there is a possibility that this moiety is also present in other (unidentified) glycan structures.

1.7 Project Aims

This project aims to metabolically label D-ribitol-5-phosphate containing glycans through the use of azide-containing D-ribitol-5-phosphate (RbOP) analogues. These labelling studies hold the potential to reveal new sites or new glycoconjugates in which this sugar moiety is present. If unsuccessful in uncovering new sites of ribitol-5-phosphate incorporation, the azide-tagged probes possess the ability to act as specific labelling tools in the study of core-M3 modified dystroglycan. At present, specific imaging and quantification of fully functional α -DG is highly challenging, relying on the use of low-affinity antibodies or complex mass spectrometry techniques (the latter of which has not yet been performed on the native glycoprotein). Therefore, the development of a highly specific labelling technique will provide a great tool for the study of α -DG, enabling the monitoring of levels

of glycosylated protein, changes to protein glycosylation in response to cellular stimuli, as well as study of the differences between healthy and disease models. The developed probes will also provide insight into ISPD and FKTN's tolerance to modified ribitol-5-phosphate, which will influence future generations of metabolic labelling probes.

Utilising metabolic labelling with modified monosaccharides is a commonplace technique to gain insight into biological systems (Chapter 2, pg. 40). As the biosynthetic pathway of D-ribitol-5-phosphate within mammalian cells is unknown, and the metabolic pathway from D-ribitol-5-phosphate onto the Core M3 glycan *via* the enzymes ISPD, FKTN and FKRK has been previously proven, our probe design is based on this phospho-pentitol structure (Figure 7A). The bioorthogonal labelling strategy for these probes utilises azide as a tag because of its small size, and high prevalence as a metabolic labelling tool. It can be reacted with a desired reporter group through either Staudinger-Bertozzi ligations or through the use of copper(I)-catalysed or copper-free azide-alkyne cycloadditions. In order to transport the chemical probes across the cell-membrane for *in vivo* analysis, cell-permeable protecting groups will be utilised for protection of both hydroxyl (R_1) and phosphate (R_2).

Parallel to the synthesis of these phosphate containing probes will be the synthesis of non-phosphorylated reporters (Figure 7B). Though the biosynthetic pathways is unknown for D-ribitol-5-phosphate, a number of reports suggest it may be biosynthesised from ribitol.^{45, 57} These simpler probes not only allow us to gain insight into to the possible biosynthetic pathway of D-ribitol-5-phosphate, they also avoid the more complex synthetic steps for incorporation of the phosphate triester. Additionally, synthesis of the unprotected azido-RboP probes (Figure 7C), will allow for *in vitro* testing on purified ISPD and FKTN enzymes. This will not only give insight into the kinetics of probe turnover and the positions along the ribitol backbone at which these enzymes are more tolerant towards modification, it will also aid in troubleshooting should *in vivo* metabolic labelling studies be unsuccessful.

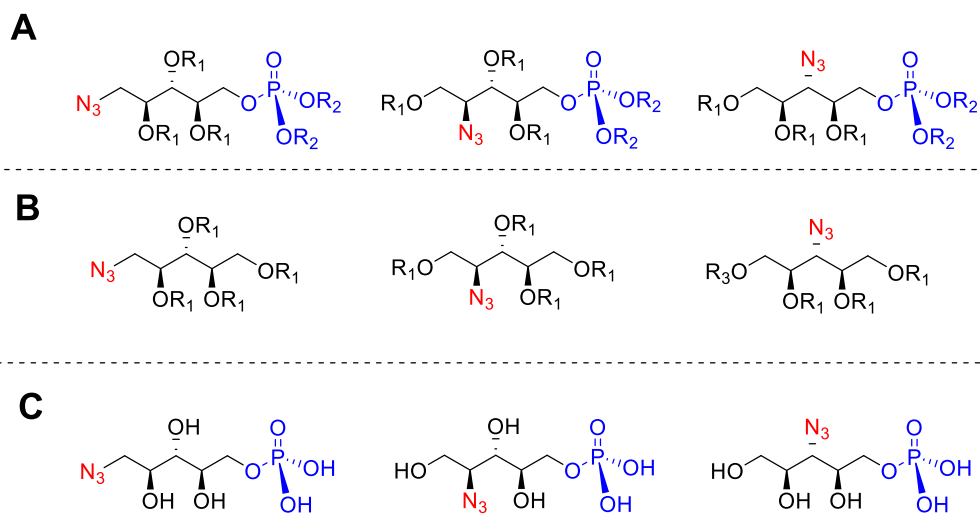


Figure 7: Azide-tagged analogues of ribitol-5-phosphate this project aims to synthesise A) phosphate containing probes for *in vivo* labelling studies with protection of both hydroxyl (R_1) and phosphate (R_2) groups B) Ribitol probes for *in vivo* cell studies with protected hydroxyl groups (R_1) C) Unprotected probes for *in vitro* studies.

1.8 References

1. M. Kanagawa and T. Toda, *J. Neuromuscul. Dis.*, 2017, **4**, 259-267.
2. L. Wells, *J. Biol. Chem.*, 2013, **288**, 6930-6935.
3. H. Manyá and T. Endo, *Biochim. Biophys. Acta Gen. Subj.*, 2017, **1861**, 2462-2472.
4. A. Varki and P. Gagneux, *Glycobiology*, 2017, **27**, 77-88.
5. R. G. Spiro, *Glycobiology*, 2002, **12**, 43R-56R.
6. C. Reily, T. J. Stewart, M. B. Renfrow and J. Novak, *Nat. Rev. Nephrol.*, 2019, **15**, 346-366.
7. E. Bieberich, *Adv. Neurobiol.*, 2014, **9**, 47-70.
8. N. Lannoo and E. J. Van Damme, *Plant Sci.*, 2015, **239**, 67-83.
9. S. Esmail and M. F. Manolson, *Eur. J. Cell. Biol.*, 2021, **100**, 151186.
10. M. Riemersma, D. S. Froese, W. van Tol, U. F. Engelke, J. Kopec, M. van Scherpenzeel, A. Ashikov, T. Krojer, F. von Delft, M. Tessari, A. Buczkowska, E. Swiezewska, L. T. Jae, T. R. Brummelkamp, H. Manyá, T. Endo, H. van Bokhoven, W. W. Yue and D. J. Lefeber, *Chem. Biol.*, 2015, **22**, 1643-1652.
11. R. Sentandreu and D. H. Northcote, *Biochem. J.*, 1968, **109**, 419-432.
12. M. Loibl and S. Strahl, *Biochim. Biophys. Acta*, 2013, **1833**, 2438-2446.
13. S. H. Stalnakar, R. Stuart and L. Wells, *Curr. Opin. Struct. Biol.*, 2011, **21**, 603-609.
14. J. L. Praissman and L. Wells, *Biochemistry*, 2014, **53**, 3066-3078.
15. T. Yoshida-Moriguchi and K. P. Campbell, *Glycobiology*, 2015, **25**, 702-713.
16. K.-I. Inamori, Y. Hara, T. Willer, M. E. Anderson, Z. Zhu, T. Yoshida-Moriguchi and K. P. Campbell, *Glycobiology*, 2013, **23**, 295-302.
17. H. Xiong, K. Kobayashi, M. Tachikawa, H. Manyá, S. Takeda, T. Chiyonobu, N. Fujikake, F. Wang, A. Nishimoto, G. E. Morris, Y. Nagai, M. Kanagawa, T. Endo and T. Toda, *Biochem. Biophys. Res. Commun.*, 2006, **350**, 935-941.
18. M. Taniguchi-Ikeda, I. Morioka, K. Iijima and T. Toda, *Mol. Aspects Med.*, 2016, **51**, 115-124.
19. K. H. Holt, R. H. Crosbie, D. P. Venzke and K. P. Campbell, *FEBS Lett.*, 2000, **468**, 79-83.
20. C. M. Dobson, S. J. Hempel, S. H. Stalnakar, R. Stuart and L. Wells, *Cell. Mol. Life Sci.*, 2013, **70**, 2849-2857.
21. Y. Zhang, C. Meng, L. Jin, X. Chen, F. Wang and H. Cao, *Chem. Commun.*, 2015, **51**, 11654-11657.
22. S. H. Gee, F. Montanaro, M. H. Lindenbaum and S. Carbonetto, *Cell*, 1994, **77**, 675-686.
23. H. B. Peng, A. A. Ali, D. F. Daggett, H. Rauvala, J. R. Hassell and N. R. Smalheiser, *Cell Adhes. Commun.*, 1998, **5**, 475-489.
24. S. Sugita, F. Saito, J. Tang, J. Satz, K. Campbell and T. C. Südhof, *J. Cell Biol.*, 2001, **154**, 435-445.
25. S. Sato, Y. Omori, K. Katoh, M. Kondo, M. Kanagawa, K. Miyata, K. Funabiki, T. Koyasu, N. Kajimura, T. Miyoshi, H. Sawai, K. Kobayashi, A. Tani, T. Toda, J. Usukura, Y. Tano, T. Fujikado and T. Furukawa, *Nat. Neurosci.*, 2008, **11**, 923-931.
26. K. M. Wright, K. A. Lyon, H. Leung, D. J. Leahy, L. Ma and D. D. Ginty, *Neuron*, 2012, **76**, 931-944.
27. A. Chiba, K. Matsumura, H. Yamada, T. Inazu, T. Shimizu, S. Kusunoki, I. Kanazawa, A. Kobata and T. Endo, *J. Biol. Chem.*, 1997, **272**, 2156-2162.
28. M. Kanagawa and T. Toda, *J. Biochem.*, 2018, **163**, 359-369.
29. H. Manyá, A. Chiba, A. Yoshida, X. Wang, Y. Chiba, Y. Jigami, R. U. Margolis and T. Endo, *Proc. Natl. Acad. Sci. U. S. A.*, 2004, **101**, 500-505.
30. K. Akasaka-Manyá, H. Manyá and T. Endo, *Biochem. Biophys. Res. Commun.*, 2004, **325**, 75-79.
31. A. Yoshida, K. Kobayashi, H. Manyá, K. Taniguchi, H. Kano, M. Mizuno, T. Inazu, H. Mitsuhashi, S. Takahashi, M. Takeuchi, R. Herrmann, V. Straub, B. Talim, T. Voit, H. Topaloglu, T. Toda and T. Endo, *Dev. Cell*, 2001, **1**, 717-724.

32. K.-I. Inamori, T. Endo, Y. Ide, S. Fujii, J. Gu, K. Honke and N. Taniguchi, *J. Biol. Chem.*, 2003, **278**, 43102-43109.
33. M. Kaneko, G. Alvarez-Manilla, M. Kamar, I. Lee, J.-K. Lee, K. Troupe, W.-J. Zhang, M. Osawa and M. Pierce, *FEBS Lett.*, 2003, **554**, 515-519.
34. R. Barresi, D. E. Michele, M. Kanagawa, H. A. Harper, S. A. Dovico, J. S. Satz, S. A. Moore, W. Zhang, H. Schachter, J. P. Dumanski, R. D. Cohn, I. Nishino and K. P. Campbell, *Nat. Med.*, 2004, **10**, 696-703.
35. T. Endo, *J. Biochem.*, 2015, **157**, 1-12.
36. K.-I. Inamori, T. Yoshida-Moriguchi, Y. Hara, M. E. Anderson, L. Yu and K. P. Campbell, *Science*, 2012, **335**, 93-96.
37. M. O. Sheikh, D. Venzke, M. E. Anderson, T. Yoshida-Moriguchi, J. N. Glushka, A. V. Nairn, M. Galizzi, K. W. Moremen, K. P. Campbell and L. Wells, *Glycobiology*, 2020, **30**, 817-829.
38. M. M. Goddeeris, B. Wu, D. Venzke, T. Yoshida-Moriguchi, F. Saito, K. Matsumura, S. A. Moore and K. P. Campbell, *Nature*, 2013, **503**, 136-140.
39. J. L. Praissman, T. Willer, M. O. Sheikh, A. Toi, D. Chitayat, Y.-Y. Lin, H. Lee, S. H. Stalnaker, S. Wang, P. K. Prabhakar, S. F. Nelson, D. L. Stemple, S. A. Moore, K. W. Moremen, K. P. Campbell and L. Wells, *Elife*, 2016, **5**, 1-18.
40. S. Vuillaumier-Barrot, C. Bouchet-Séraphin, M. Chelbi, L. Devisme, S. Quentin, S. Gazal, A. Laquerrière, C. Fallet-Bianco, P. Loget, S. Odent, D. Carles, A. Bazin, J. Aziza, A. Clemenson, F. Guimiot, M. Bonnière, S. Monnot, C. Bole-Feysot, J.-P. Bernard, L. Loeuillet, M. Gonzales, K. Socha, B. Grandchamp, T. Attié-Bitach, F. Encha-Razavi and N. Seta, *Am. J. Hum. Genet.*, 2012, **91**, 1135-1143.
41. L. T. Jae, M. Raaben, M. Riemersma, E. van Beusekom, V. A. Blomen, A. Velds, R. M. Kerkhoven, J. E. Carette, H. Topaloglu, P. Meinecke, M. W. Wessels, D. J. Lefeber, S. P. Whelan, H. van Bokhoven and T. R. Brummelkamp, *Science*, 2013, **340**, 479-483.
42. T. Willer, K.-I. Inamori, D. Venzke, C. Harvey, G. Morgensen, Y. Hara, D. Beltrán Valero de Bernabé, L. Yu, K. M. Wright and K. P. Campbell, *Elife*, 2014, **3**, 1-24.
43. T. Yoshida-Moriguchi, L. Yu, S. H. Stalnaker, S. Davis, S. Kunz, M. Madson, M. B. A. Oldstone, H. Schachter, L. Wells and K. P. Campbell, *Science*, 2010, **327**, 88-92.
44. M. Kanagawa, K. Kobayashi, M. Tajiri, H. Manya, A. Kuga, Y. Yamaguchi, K. Akasaka-Manyá, J.-I. Furukawa, M. Mizuno, H. Kawakami, Y. Shinohara, Y. Wada, T. Endo and T. Toda, *Cell Rep.*, 2016, **14**, 2209-2223.
45. I. Gerin, B. Ury, I. Breloy, C. Bouchet-Seraphin, J. Bolsée, M. Halbout, J. Graff, D. Vertommen, G. G. Muccioli, N. Seta, J.-M. Cuisset, I. Dabaj, S. Quijano-Roy, A. Grahn, E. Van Schaftingen and G. T. Bommer, *Nat. Commun.*, 2016, **7**, 11534.
46. H. Manya, Y. Yamaguchi, M. Kanagawa, K. Kobayashi, M. Tajiri, K. Akasaka-Manyá, H. Kawakami, M. Mizuno, Y. Wada, T. Toda and T. Endo, *J. Biol. Chem.*, 2016, **291**, 24618-24627.
47. N. Kuwabara, H. Manya, T. Yamada, H. Tateno, M. Kanagawa, K. Kobayashi, K. Akasaka-Manyá, Y. Hirose, M. Mizuno, M. Ikeguchi, T. Toda, J. Hirabayashi, T. Senda, T. Endo and R. Kato, *Proc. Natl. Acad. Sci. U. S. A.*, 2016, **113**, 9280-9285.
48. S. B. Richard, M. E. Bowman, W. Kwiatkowski, I. Kang, C. Chow, A. M. Lillo, D. E. Cane and J. P. Noel, *Nat. Struct. Biol.*, 2001, **8**, 641-648.
49. W. N. Hunter, *J. Biol. Chem.*, 2007, **282**, 21573-21577.
50. T. Willer, H. Lee, M. Lommel, T. Yoshida-Moriguchi, D. B. V. de Bernabe, D. Venzke, S. Cirak, H. Schachter, J. Vajsar, T. Voit, F. Muntoni, A. S. Loder, W. B. Dobyns, T. L. Winder, S. Strahl, K. D. Mathews, S. F. Nelson, S. A. Moore and K. P. Campbell, *Nat. Genet.*, 2012, **44**, 575-580.
51. T. Roscioli, E.-J. Kamsteeg, K. Buysse, I. Maystadt, J. van Reeuwijk, C. van den Elzen, E. van Beusekom, M. Riemersma, R. Pfundt, L. E. L. M. Vissers, M. Schraders, U. Altunoglu, M. F. Buckley, H. G. Brunner, B. Grisart, H. Zhou, J. A. Veltman, C. Gilissen, G. M. S. Mancini, P. Delrée, M. A. Willemsen, D. P. Ramadža, D. Chitayat, C. Bennett, E. Sheridan, E. A. J. Peeters, G. M. B. Tan-Sindhunata, C. E. de Die-Smulders, K. Devriendt, H. Kayserili, O. A. E.-F. El-

- Hashash, D. L. Stemple, D. J. Lefeber, Y.-Y. Lin and H. van Bokhoven, *Nat. Genet.*, 2012, **44**, 581-585.
52. H. Tokuoka, R. Imae, H. Nakashima, H. Many, C. Masuda, S. Hoshino, K. Kobayashi, D. J. Lefeber, R. Matsumoto, T. Okada, T. Endo, M. Kanagawa and T. Toda, *Nat. Commun.*, 2022, **13**, 1847.
 53. M. P. Pereira and E. D. Brown, *Biochemistry*, 2004, **43**, 11802-11812.
 54. M. Zolli, D. J. Kobric and E. D. Brown, *Biochemistry*, 2001, **40**, 5041-5048.
 55. A. Follens, M. Veiga-da-Cunha, R. Merckx, E. van Schaftingen and J. van Eldere, *J. Bacteriol.*, 1999, **181**, 2001-2007.
 56. S. Baur, J. Maries-Wright, S. Buckenmaier, R. J. Lewis and W. Vollmer, *J. Bacteriol.*, 2009, **191**, 1200-1210.
 57. C. Singh, E. Glaab and C. L. Linster, *J. Biol. Chem.*, 2017, **292**, 1005-1028.
 58. K. Kobayashi, Y. Nakahori, M. Miyake, K. Matsumura, E. Kondo-Iida, Y. Nomura, M. Segawa, M. Yoshioka, K. Saito, M. Osawa, K. Hamano, Y. Sakakihara, I. Nonaka, Y. Nakagome, I. Kanazawa, Y. Nakamura, K. Tokunaga and T. Toda, *Nature*, 1998, **394**, 388-392.
 59. M. Brockington, D. J. Blake, P. Prandini, S. C. Brown, S. Torelli, M. A. Benson, C. P. Ponting, B. Estournet, N. B. Romero, E. Mercuri, T. Voit, C. A. Sewry, P. Guicheney and F. Muntoni, *Am. J. Hum. Genet.*, 2001, **69**, 1198-1209.
 60. L. Aravind and E. V. Koonin, *Curr. Biol.*, 1999, **9**, R836-837.
 61. K. Kuchta, L. Knizewski, L. S. Wyrwicz, L. Rychlewski and K. Ginalski, *Nucleic Acids Res.*, 2009, **37**, 7701-7714.
 62. T. A. Lynch, L. T. Lam, N. T. Man, K. Kobayashi, T. Toda and G. E. Morris, *Biochem. Biophys. Res. Commun.*, 2012, **424**, 354-357.
 63. T. Yamamoto, M. Kawaguchi, N. Sakayori, F. Muramatsu, S. Morikawa, Y. Kato, N. Shibata and M. Kobayashi, *Neurosci. Res.*, 2006, **56**, 391-399.
 64. J. N. Weiser, M. Shchepetov and S. T. Chong, *Infect. Immun.*, 1997, **65**, 943-950.
 65. J. R. Zhang, I. Idanpaan-Heikkila, W. Fischer and E. I. Tuomanen, *Mol. Microbiol.*, 1999, **31**, 1477-1488.
 66. J. I. Tamura, T. Tamura, S. Hoshino, R. Imae, R. Kato, M. Yokono, M. Nagase, S. Ohno, N. Manabe, Y. Yamaguchi, H. Many and T. Endo, *ACS Chem. Biol.*, 2022, **17**, 1513-1523.
 67. N. Kuwabara, R. Imae, H. Many, T. Tanaka, M. Mizuno, H. Tsumoto, M. Kanagawa, K. Kobayashi, T. Toda, T. Senda, T. Endo and R. Kato, *Nat. Commun.*, 2020, **11**, 303.
 68. M. Alhamidi, E. Kjeldsen Buvang, T. Fagerheim, V. Brox, S. Lindal, M. Van Ghelue and Ø. Nilssen, *PLoS One*, 2011, **6**, e22968.
 69. K. Johnson, M. Bertoli, L. Phillips, A. Topf, P. Van den Bergh, J. Vissing, N. Witting, S. Nafissi, S. Jamal-Omidi, A. Lusakowska, A. Kostera-Pruszczyk, A. Potulska-Chromik, N. Deconinck, C. Wallgren-Pettersson, S. Strang-Karlsson, J. Colomer, K. G. Claeys, W. De Ridder, J. Baets, M. von der Hagen, R. Fernandez-Torron, M. Zulaica Ijurco, J. B. Espinal Valencia, A. Hahn, H. Durmus, T. Willis, L. Xu, E. Valkanas, T. E. Mullen, M. Lek, D. G. MacArthur and V. Straub, *Skelet. Muscle*, 2018, **8**, 23.
 70. K. M. Fumiaki Saito, *Skelet. Muscle*, 2011, **1**, 22.
 71. S. H. Stalnaker, K. Aoki, J.-M. Lim, M. Porterfield, M. Liu, J. S. Satz, S. Buskirk, Y. Xiong, P. Zhang, K. P. Campbell, H. Hu, D. Live, M. Tiemeyer and L. Wells, *J. Biol. Chem.*, 2011, **286**, 21180-21190.
 72. H. Topaloğlu and B. Talim, *Handb. Clin. Neurol.*, 2008, **87**, 219-234.
 73. J. Sasaki, K. Ishikawa, K. Kobayashi, E. Kondo-Iida, M. Fukayama, H. Mizusawa, S. Takashima, Y. Sakakihara, Y. Nakamura and T. Toda, *Hum. Mol. Genet.*, 2000, **9**, 3083-3090.
 74. Muscular Dystrophies U. K. Charity The limb girdle muscular dystrophies (LGMDs) Factsheet, <https://www.muscular dystrophyuk.org/wp-content/uploads/2015/09/LGMD-general.pdf> (accessed 13/04/2022).

75. Genetics Home Walker-Warburg syndrome, <https://ghr.nlm.nih.gov/condition/walker-warburg-syndrome>, (accessed 25/07/2019).
76. National Institute of Health - MedlinePlus, Walker-Warburg syndrome, <https://medlineplus.gov/genetics/condition/walker-warburg-syndrome/#causes>, (accessed 10/9/2022).

Chapter 2: Chemical Reporters to Study Mammalian *O*-glycosylation

2.1 Abstract

Glycans play essential roles in a range of cellular processes and have been shown to contribute to various pathologies. The diversity and dynamic nature of glycan structures and the complexities of glycan biosynthetic pathways make it challenging to study the roles of specific glycans in normal cellular function and in disease. Chemical reporters have emerged as powerful tools to characterise glycan structures and monitor dynamic changes in glycan levels in a native context. A variety of tags can be introduced onto specific monosaccharides *via* the chemical modification of endogenous glycan structures, or by metabolic or enzymatic incorporation of unnatural monosaccharides into cellular glycans. These chemical reporter strategies offer unique opportunities to study and manipulate glycan functions in living cells or whole organisms. Herein is discussed the recent advances in metabolic oligosaccharide engineering and chemoenzymatic glycan labelling, focusing on their application to the study of mammalian *O*-linked glycans. Described within are the current barriers to achieving glycan labelling specificity, and the innovations that have started to pave the way to overcome these challenges.

2.2 Introduction

Glycans play crucial roles in a diversity of cellular processes. Glycoproteins are essential mediators of cell-cell and cell-matrix interactions, they are involved in cell recognition and signalling events, and they control the stability, localisation and function of proteins.^{77, 78} Glycans are also key in a range of pathological processes, including host-pathogen interactions,⁷⁹ neurodegenerative disorders,⁸⁰ and cancer metastasis.⁸¹ The major types of vertebrate glycans are *N*-linked and *O*-linked glycans, which are attached to the side chain nitrogen atom of asparagine residues or the hydroxyl group of an amino acid side chain (usually serine or threonine), respectively. *N*-linked glycans consist of a universal core structure that starts with an *N*-acetylglucosamine (GlcNAc) and is further extended and edited by networks of glycosyltransferases and other glycan-modifying enzymes, resulting in a large diversity of mature *N*-glycan structures.⁷⁸

Contrastingly, *O*-glycans do not have a common core structure and are classified by the nature of the first monosaccharide residue that is linked to the protein. The most common type of cell surface *O*-glycosylation is mucin type glycosylation, in which the first monosaccharide is an *N*-acetylgalactosamine (GalNAc).⁸² Other types of *O*-glycosylation include glycans initiated by GlcNAc, mannose, fucose, glucose or xylose residues.⁷⁸ A unique form of glycosylation found on nuclear, cytosolic and mitochondrial proteins of eukaryotic cells is the *O*-GlcNAc modification, in which a single GlcNAc residue is attached to serine or threonine hydroxyl groups. The *O*-GlcNAc modification is not further extended and is a highly dynamic regulator of diverse cellular processes.⁸³

The immense structural diversity of glycans, their non-genetically encoded nature and the complexity of glycan biosynthesis make it difficult to unravel the biological function and structures of individual glycan species. At the same time, a cell's glycome - the total set of glycans that is present in a cell at any given time - is dynamic and will vary in response to changes in the physiological state of the cell. Tools and techniques that help to characterise glycans and modulate their function in a native cellular context offer great opportunities to advance our understanding of glycobiology and can provide avenues for therapeutic intervention. Chemical reporters enable the visualisation, enrichment and/or modulation of glycan structures by the introduction of unnatural tags into specific monosaccharide residues within native glycans of live cells or organisms. In some cases, the introduced tag is a fluorophore or other reporter group, but more commonly, it is a small group with unique chemical reactivity that serves as a handle for further conjugation to a second reagent through what is known as 'bioorthogonal chemistry'.^{84, 85} Bioorthogonal reactions involve reagents that can react selectively and efficiently with each other in a biological environment but are inert towards functionalities present in biomolecules, a classic example being the 'click' cycloaddition reaction between azides and alkynes.^{86, 87}

Early approaches for the covalent tagging and enrichment of cell surface glycans relied on the chemical or enzymatic oxidation of specific carbohydrate residues, leading to the formation of aldehydes that can be conjugated to an amine-linked reporter group (Figure 8A).^{88, 89} While these methods are still used today, they are limited to the labelling of sialic acid and galactose- or GalNAc-containing glycans and offer little flexibility in the choice of labelling chemistry. Over the past decades, various chemical reporters have been developed that enable the labelling of endogenous glycans through metabolic and chemoenzymatic glycan engineering strategies.⁹⁰⁻⁹⁵ In these approaches, termed metabolic oligosaccharide engineering (MOE, Figure 8B) and chemoenzymatic glycan labelling (CeGL, Figure 8C), unnatural carbohydrate derivatives are incorporated into glycans either by the cell's own metabolic machinery or by the action of recombinant glycosyltransferases,

respectively. Advances made in these areas, in combination with a growing number of bioorthogonal ligation reactions,^{84,96} have greatly expanded the available glycan labelling toolkit.

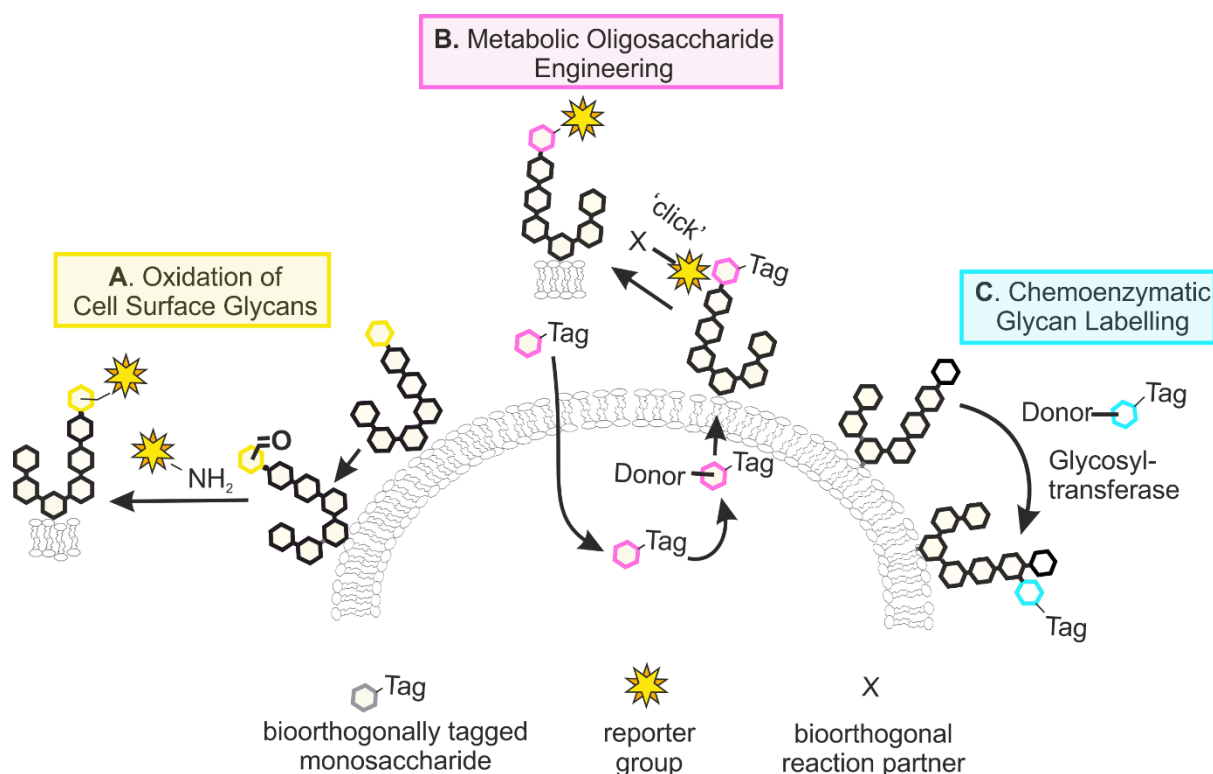


Figure 8: Chemical reporter strategies to study glycans. A) Chemical or enzymatic oxidation of glycans enables the labelling of specific monosaccharide residues by reaction with amine-functionalised reporter groups. B) Metabolic oligosaccharide engineering makes use of the cell's endogenous glycan biosynthetic machinery to install unnatural monosaccharide derivatives into glycans. The introduced tags can be further labelled by bioorthogonal 'click' reactions. C) Chemoenzymatic glycan labelling exploits the activity of recombinant glycosyltransferases to transfer unnatural monosaccharides onto specific glycans.

2.3 Oxidation of Cell Surface Glycans

A subset of natural monosaccharides, including sialic acids and galactose, display a *cis* diol motif that is susceptible to oxidative cleavage by reagents such as sodium periodate. This unique property forms the basis of a chemical tagging strategy based on the chemical oxidation of glycans, which specifically targets monosaccharides with *cis* diol containing monosaccharides (Figure 9).⁸⁸ The resulting aldehyde intermediates provide handles for further reaction with amine nucleophiles such as hydrazine or aminoxy reagents. The utility of this approach, especially in the context of live cell imaging, has been limited due to the slow kinetics of the oxime ligation step, and its optimal reaction pH of 5-6. A considerable advancement to this methodology was made by the Paulson group, who introduced an aniline catalyst that drastically enhanced labelling efficiency at neutral pH.⁹⁷ Termed periodate oxidation and aniline catalysed oxime ligation (PAL), this approach allows the labelling of glycans on the surface of living cells without affecting cell viability.

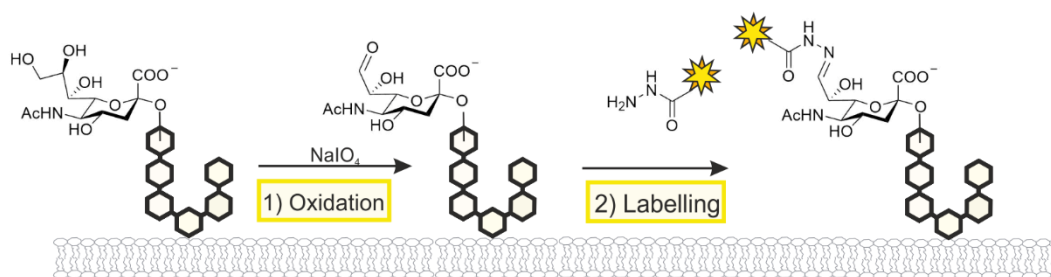


Figure 9: Chemical oxidation of cell surface glycans. Monosaccharides that carry a cis diol motif, such as sialic acids, are sensitive to oxidation by periodate treatment. The aldehyde generated upon oxidative cleavage can react with an amine nucleophile such as hydrazide for conjugation to a desired reporter group.

Selectivity for the labelling of certain glycan types can be achieved by careful tuning of the oxidation conditions. Mild periodate oxidation leads to the selective oxidation of cell surface sialic acids, a strategy that was used to enrich sialylated *N*- and *O*-glycans,⁹⁸ while harsher oxidation conditions can be used to oxidise *trans* diols in carbohydrates such as GlcNAc. This approach permits the isolation and characterisation of *O*-GlcNAc modified proteins.⁹⁹ Alternatively, cell surface glycans can be oxidised by enzymatic oxidation using a specific galactose oxidase that targets terminal galactose- and GalNAc-containing glycans.⁸⁸ As for PAL, oxidation is followed by an oxime ligation step accelerated by the use of an aniline catalyst.¹⁰⁰ Specificity for other types of monosaccharides has been achieved by the generation of engineered variants of galactose oxidase that target, for example *N*-glycolylneuraminic acid (NeuAc).¹⁰¹

The main limitation of the chemical oxidation approaches is the potential for off-target reactivity, which can occur during either the ligation step, due to the presence of naturally occurring carbonyl groups, or periodate oxidation step through oxidation of 2-amino alcohols found in *N*-terminal serine and threonine amino acids of proteins.⁹⁹ One solution to this problem is the protection of the *N*-terminus *via* dimethyl labelling, which inhibits oxidation at these sites.¹⁰² Despite these drawbacks, both chemical and enzymatic oxidation strategies are useful methods to monitor changes in glycosylation status, which are often a hallmark of disease.¹⁰³ Kohler and co-workers used both sialic acid labelling with PAL and labelling with galactose oxidase to identify host glycoproteins that are desialylated by pneumococcal neuraminidases.¹⁰⁴ Neuraminidase substrates were identified by detecting either a loss in PAL-mediated labelling or a gain in galactose oxidase-mediated labelling due to the exposure of galactose residues upon the loss of sialic acids.

2.4 Metabolic Oligosaccharide Engineering (MOE)

As an alternative to the direct chemical modification of native glycan structures, MOE exploits the flexibility in the cell's own metabolic machinery for the introduction of tagged monosaccharides into desired glycans (Figure 3). This approach was pioneered by Reutter and co-workers who showed that cells fed with unnatural derivatives of *N*-acetylmannosamine (ManNAc)

are able to convert them into the corresponding cytidine monophosphate (CMP)-sialic acid donors and incorporate the unnatural substrates into cell surface glycans.¹⁰⁵ Although the strategy was not used to install tags for detection, it demonstrated that the cellular machinery for glycan biosynthesis tolerates structurally modified analogues of ManNAc and sialic acid with larger *N*-acyl substituents than their natural counterparts. The Bertozzi group then showed that the same principle can be applied to the introduction of ketone- or azide-tagged sialic acids into cell surface glycans (the azide strategy is shown in Figure 10A).^{106, 107} The azide is one of the most popular bioorthogonal tags and is typically labelled through azide-alkyne cycloadditions, which are catalysed by the use of either a copper(I) catalyst (Figure 10B) or a ring strained cyclooctyne reagent (Figure 10A).^{108, 109} Following these initial reports, the scope of MOE has expanded to include derivatives of a wide variety of different monosaccharides and diverse types of bioorthogonal tags, which are not covered here. Instead, for comprehensive overviews of the various chemical reporters and bioorthogonal chemistries that have been developed to date, consult these recent reviews.^{84, 85, 91-96}

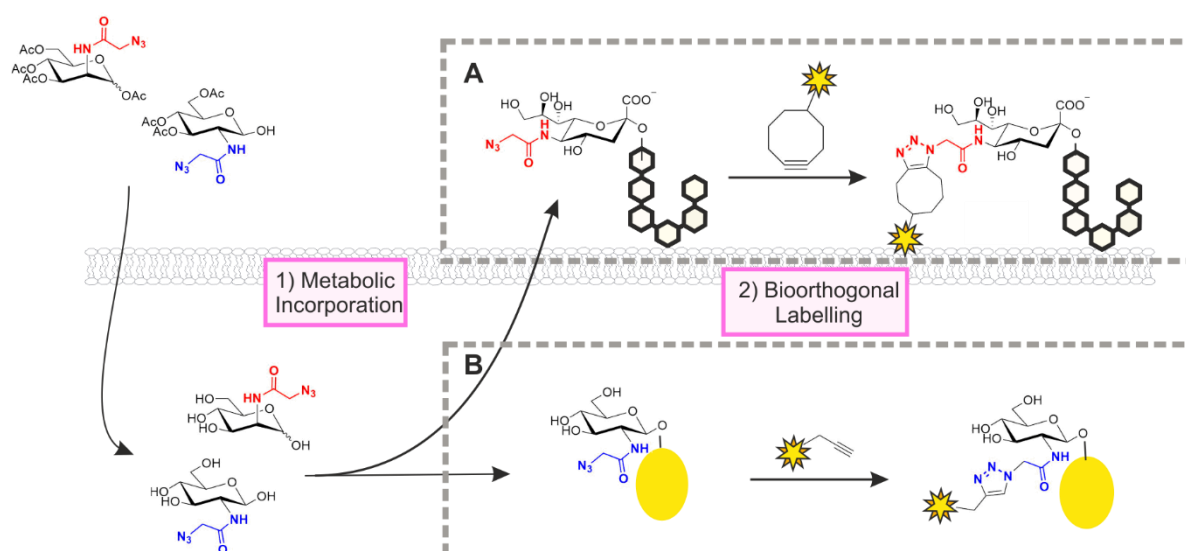


Figure 10: Metabolic oligosaccharide engineering. Cells are fed with unnatural, tagged derivatives of naturally occurring monosaccharides, such as the peracetylated azide-tagged derivatives of ManNAc and GlcNAc shown. After uptake and deprotection of the acetyl groups (bottom left), the metabolic precursors enter the cellular pathways for conversion into the corresponding CMP- or UDP-activated donors which are then used for glycan biosynthesis. ManNAc derivatives are incorporated as sialic acids into cell surface glycans (A) while GlcNAc derivatives label intracellular proteins that are targets for *O*-GlcNAc modification (B). The azide-tagged glycans can be labelled by bioorthogonal ligation reactions such as the strain-promoted (A) or the copper(I)-catalysed (B) azide-alkyne cycloaddition.

One of the key considerations for the design and evaluation of MOE probes is glycan specificity. As most monosaccharides enter multiple glycan biosynthetic pathways, tagged derivatives of these carbohydrates will similarly be incorporated into various glycan structures. For example, while *N*-azidoacetylglucosamine (GlcNAz) labels primarily intracellular proteins that are *O*-GlcNAc modified (Figure 10B),¹¹⁰ it can also be installed in both *N*-glycans and mucin type *O*-glycans on the cell surface.^{111, 112} A study by Boyce *et al.* revealed that the *N*-acetylgalactosamine derivative

GalNAz also provides access to *O*-GlcNAc modified proteins through an endogenous cellular pathway that interconverts uridine diphosphate (UDP)-GlcNAc and UDP-GalNAc donors.¹¹³ While this discovery made it possible to label *O*-GlcNAcylated proteins with higher efficiency than that observed for GlcNAz itself, it also highlights the potential complication of MOE experiments due to crosstalk between metabolic pathways.

The type of bioorthogonal tag and its position on a monosaccharide can have an impact on both the incorporation efficiency of chemical reporters and their selectivity for certain glycan types.^{112, 114, 115} Pratt and co-workers demonstrated the dramatic effects that an apparently small change in tag, going from an azide to an alkyne, can have on the overall labelling efficiency of MOE as well as on the set of glycans that is labelled.¹¹² This effect was shown to be dependent on cell type and the type of monosaccharide used. While initial MOE approaches relied on attachment of the unnatural tag at the *N*-acyl group of hexosamines, several more recent studies have explored the substitution of hydroxyl groups,¹¹⁶⁻¹²⁰ or the *N*-acyl group in GlcNAc¹²¹ with a bioorthogonal tag. In many cases, this strategy has led to the development of chemical reporters with enhanced selectivity towards specific classes of glycans. For instance, 6-azido-6-deoxy-GlcNAc is selectively installed onto *O*-GlcNAc modified proteins but not on cell surface glycans.¹¹⁶ Strikingly, selectivity within a glycan class was reported for a neuraminic acid derivative carrying a sydnone ligation handle at C9.¹¹⁸ In contrast to its C9-azide-tagged analogue, the sydnone probe selectively labels a subpopulation of sialylated glycoproteins in a glycosidic linkage-specific manner.

The overall success of MOE approaches relies on both the efficiency of unnatural carbohydrate incorporation into glycans and the efficiency of the ensuing bioorthogonal labelling reaction. Comparative studies by Dold et al. revealed that incorporation efficiency can vary widely, even for structurally closely related probes, from less than 1% to more than 60%.^{122, 123} Advances in bioorthogonal ligation kinetics have been shown to enable efficient glycan labelling even if incorporation rates of the MOE probes are as low as 1%.¹²⁴ At the same time, other studies have demonstrated that improved reaction kinetics do not always lead to improvements in glycan labelling, suggesting that the efficiency of metabolic conversion is equally important for the success of MOE probes.¹²⁵ Quantification of cellular levels of monosaccharides and the corresponding nucleotide-activated glycosyl donors can provide additional insights into the effects of specific structural changes on the efficiency with which unnatural carbohydrate derivatives are taken up and metabolised by cells.^{122, 126, 127}

The hydroxyl groups in chemical reporters are often protected with acetyl groups to reduce polarity and thereby enhance cell permeability of the molecules. In a cautionary report, however,

Chen and co-workers demonstrated that peracetylated monosaccharides can cause non-enzymatic labelling of cysteine residues, which leads to misidentification of endogenous glycosylation sites.¹²⁸ It was later reported that the extent of *S*-glycosylation is dependent on the reporter used,¹²⁹ and that partial protection of azide-tagged *N*-acyl hexosamines at the C1 and C3 positions alleviates the problem.¹³⁰ It has also been shown that acetyl groups can also enhance the cytotoxicity of chemical reporters, especially when installed at C6,^{121, 131} although these effects appear to depend on other structural properties of the reporters as well.^{115, 132} In light of the potentially harmful properties of acetyl groups, it is interesting to note that not all chemical reporters will need to cross the cell membrane. Gilormini *et al.* studied the cellular uptake mechanisms of unprotected alkyne-tagged ManNAc and sialic acid derivatives and concluded that these are internalised by an as yet unidentified transporter and endocytosis, respectively.¹³³ A GLUT1 transporter was shown to be responsible for the cellular uptake of peracetylated galactose-derived probes.¹¹⁹

Moving beyond the metabolic labelling of single types of monosaccharides, several groups have explored combinations of multiple bioorthogonal ligations for the simultaneous labelling of two glycan populations on the same cells.^{124, 132, 134} Building on the latest advances in bioorthogonal chemistry, a triple labelling of cell surface glycans using ManNAc derivatives with three different tags has also been described.¹³⁵ The Vocadlo group used a dual bioorthogonal strategy to verify the existence of co-translational *O*-GlcNAcylation, a modification that had thus far been believed to occur only post-translationally.¹³⁶ Two other innovations in MOE-based glycan labelling involved the imaging of protein-specific *O*-GlcNAcylation,¹³⁷ and the use of a directly fluorescently labelled MOE probe.¹³⁸ Doll *et al.* used FLIM-FRET (Fluorescence lifetime imaging microscopy - Förster resonance energy transfer) imaging to monitor the glycosylation status of individual proteins in living cells by combining genetically encoded fluorescent tags (EGFP) with a chemical reporter for *O*-GlcNAc that was reacted with a cell-permeable fluorophore.¹³⁷ Vocadlo and co-workers developed a fluorescently labelled metabolic precursor for UDP-GlcNAc that is tolerated by *O*-GlcNAc transferase (OGT) and allows the direct visualisation of *O*-GlcNAcylated proteins in cells without the need for bioorthogonal ligation.¹³⁸ Approaches such as these hold great potential for studying the dynamics of protein-specific glycosylation and glycosyltransferase activity in living cells.

The developments in MOE made over the past decade have made a great impact on our ability to visualise, characterise and/or modulate glycan structures in live cells and even in whole organisms.^{91, 139, 140} Even though exogenous monosaccharides can impact metabolic pathways and glycan structures,¹⁴¹ the direct incorporation of tags into endogenous glycans nonetheless provides great opportunities for monitoring cellular glycans and dynamic changes that occur, for example, during cell maturation and development.^{109, 120, 142} A key challenge remains labelling selectivity,

which is limited by the incorporation of monosaccharides into multiple glycan types and the cellular interconversion of monosaccharide metabolites. Recent advances in the targeted delivery of MOE probes enable the labelling or engineering of glycans on specific cell types only. Examples include the use of liposomes for targeted delivery,^{117, 143} and methods that exploit enzymatic 'uncaging' of inactive MOE precursors at a target site.¹⁴⁴ Cell type specific MOE can in turn serve as a targeting strategy for the selective delivery of nanoparticles carrying, for example, imaging agents or therapeutics.^{145, 146}

2.5 Chemoenzymatic Glycan Labelling (CeGL)

To address the glycan specificity issues of MOE, an alternative labelling strategy has been developed termed chemoenzymatic glycan labelling (CeGL).⁹⁴ This method exploits the specialised activity of specific recombinant glycosyltransferases to transfer a modified monosaccharide analogue from a suitable glycosyl donor onto a specific glycan acceptor. First described in 1979 for the transfer of radiolabelled [¹⁴C]-sialic acid onto cell surface glycans,¹⁴⁷ the field of CeGL has since grown in parallel to the fields of MOE and bioorthogonal chemistry. It now encompasses many different bioorthogonal tags and reporter groups and offers the ability to target a variety of monosaccharide acceptor and donor specificities.^{94, 140, 148, 149}

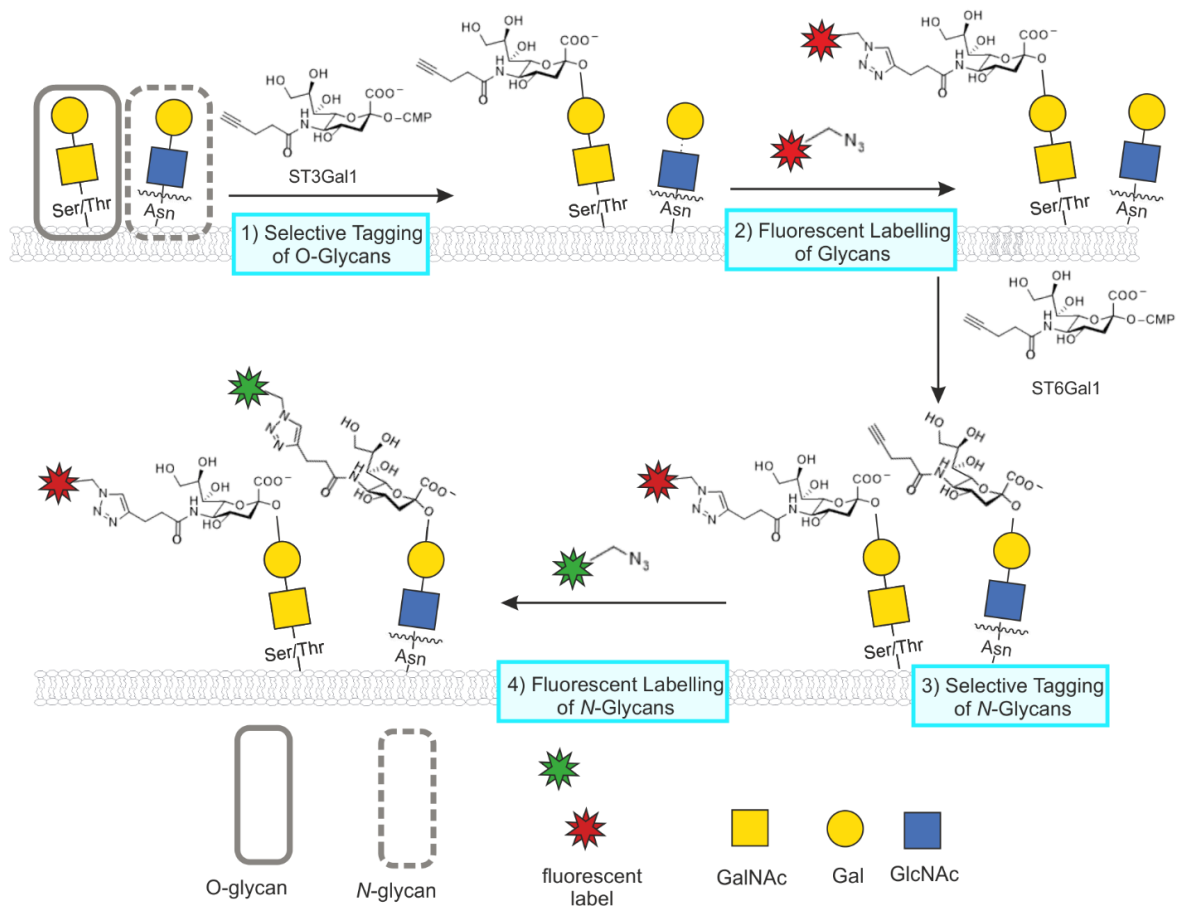


Figure 11: Tandem chemoenzymatic glycan engineering. In CeGL, recombinant glycosyltransferases are used to transfer unnatural monosaccharides from appropriate donors onto glycan acceptors. A double labelling strategy was designed with successive reactions catalysed by ST3Gal1 and ST6Gal1, installing the same alkyne-tagged CMP-sialic acid derivative onto unextended Gal-GalNAc disaccharides present on O-glycans or uncapped Gal-GlcNAc disaccharides at the non-reducing end of N-glycans, respectively. Tagged glycans were labelled via two separate azide-alkyne cycloaddition reactions for the simultaneous visualisation of both glycan types at the cell surface with different fluorophores.

CeGL facilitates the selective targeting of *N*- or *O*-glycans by exploiting the substrate specificity of the sialyltransferases ST6Gal1 and ST3Gal1, respectively.¹⁵⁰⁻¹⁵³ The approach was first demonstrated in 2013 for the specific labelling of *N*-glycans with C9 azido- tagged CMP-sialic acid (CMP-Neu5Ac9N₃) by ST6Gal1.¹⁵⁴ In a comparative study, *O*- and *N*-glycans were labelled with either MOE using the chemical reporter Ac₄ManNAz or CeGL (referred to as SEEL) using ST3Gal1 and ST6Gal1.¹⁵² Metabolic labelling occurred almost exclusively in *O*-glycans, while the spectral count from MS analysis was significantly higher for CeGL tagged glycans. Building on the selective labelling profiles of ST3Gal1 and ST6Gal1, Wu and co-workers utilised a double labelling approach with both enzymes in their study of human cancers.¹⁵³ This approach allowed differential visualisation of both *N*- and *O*-glycans in the same tissue by utilising successive labelling with ST3Gal1 and ST6Gal1. While both enzymes transferred an alkyne-tagged CMP-sialic acid donor onto their target glycans, differential fluorescent labelling was achieved through two sequential ligation steps (Figure 11).

In addition to specificity towards the broader classes of *O*- and *N*- glycans, selectivity of the CeGL methodology has been narrowed down to the identification and labelling of specific glycan structures. In 2011, Zheng *et al* developed an effective method for labelling *N*-acetyllactosamine (LacNAc), a galactose(Gal)- β 1,4-GlcNAc disaccharide, by utilising a recombinant *H. pylori* α (1,3)fucosyltransferase.¹⁵⁵ Other groups have applied similar strategies, using azido and alkynyl derivatives of GalNAc for selective labelling of Gal β 1,3-GalNAc disaccharides – also known as the Thomsen–Friedenreich antigen,¹⁵⁶ fucose(Fuc)- α (1-2)-Gal glycan biomarkers,¹⁵⁷ and the NeuAc- α (2-3)-Gal linkage.¹⁵⁸ Zhu and co-workers developed a strategy to distinguish between α 2,3- and α 2,6- linkages within Neu5Ac-Gal disaccharides.¹⁵⁹

Another attractive aspect of CeGL is the ability to employ enzymes with higher tolerance towards donor modifications. This allows for incorporation of larger reporters than what is generally possible for MOE, where structural flexibility is restricted by tolerance of the cell's endogenous metabolic machinery restricts promiscuity towards bulky substrates. The direct incorporation of fluorophores or affinity tags has been reported to improve the efficiency of cell surface labelling of glycoconjugates compared to both two-step CeGL and MOE.¹⁶⁰ One-step CeGL with fluorescent donors has vastly grown in popularity and scope. Recent applications include the labelling of fucosyltransferase substrates with multiple fluorescent Fuc derivatives,¹⁶¹ *O*-GlcNAc modified proteins via a tandem labelling strategy with a fluorescent glucuronic acid (GlcA) derivative,¹⁶² and terminal galactose on *N*- and *O*-glycans with BODIPY-tagged sialic acid derivatives.¹⁶³ These studies reveal efficient labelling that demonstrates the high tolerance of glycosyltransferases to functional group modification, as well as the ability of CeGL to allow for direct functionalisation of target glycans.

With the aim of further advancing the scope of CeGL, Wen *et al.* chemoenzymatically synthesised a library of UDP-GlcNAc and UDP-GalNAc derivatives, which they screened against multiple enzymes reported to label Fuc α 1,2-Gal and Neu5Ac α 2,3-Gal epitopes.¹⁶⁴ The new derivatives covered a range of functionalities that broadened the scope of glycosyl donor structures. Additionally, Hong *et al.* have recently screened for bacterial glycosyltransferases able to directly incorporate Cy3-fluorophore and Biotin containing sugars.¹⁶⁵ These additions to the CeGL toolkit will facilitate further discoveries in this field.

Bump-and-Hole Strategies

Bump-and-hole methodology is an approach that relies on the engineering of enzyme active sites, forming a 'hole' able to accommodate unnaturally modified, or 'bumped' substrates. The power of this approach to augment the scope of MOE was demonstrated by Yu *et al.* in a strategy

designed to overcome the cell's poor tolerance towards a photocrosslinker-tagged GlcNAc derivative.¹⁶⁶ Though technically not considered true bump-and-hole, this work demonstrated that overexpression of a mutant of AGX1, the enzyme responsible for the final step in the biosynthesis of UDP-GlcNAc, led to successful metabolic labelling of *O*-GlcNAcylated proteins.¹⁶⁶ Specific engineering of glycosyltransferases to accommodate non-natural, bioorthogonally tagged sugars was first reported by Qasba and Ramakrishnan in 2002.¹⁶⁷ Over recent years, bump-and-hole strategies have been used to label glycans in a cellular context. Bertozzi and co-workers used bump-and-hole methodology for the labelling of cellular glycans with engineered GalNAc transferases that accept bumped GalNAc donors.^{168, 169} Following on from this work, Debets *et al.* were able to develop a new metabolic labelling probe (GalNAzMe) that selectively labels mucin type *O*-linked glycans when combined with an appropriate GalNAc transferase, but is not converted into GlcNAc and therefore leads to high specificity in *O*-glycan labelling.¹⁷⁰ Though promising results have been obtained by 'bump-and-hole', some challenges to this method remain including the stable expression of mutant enzymes in cells and the delivery of modified sugar nucleotides across the cell membrane.¹⁶⁹ With 'bump-and-hole' techniques for glycosyltransferases in their infancy, there is certainly potential for this method to expand the scope of chemical reporter strategies for glycan labelling.^{171, 172}

2.6 References

77. A. Varki, *Glycobiology*, 2017, **27**, 3-49.
78. K. T. Schjoldager, Y. Narimatsu, H. J. Joshi and H. Clausen, *Nat. Rev. Mol. Cell Biol.*, 2020, **21**, 729-749.
79. B. Lin, X. Qing, J. Liao and K. Zhuo, *Cells*, 2020, **9**, 1022.
80. H. Haukedal and K. K. Freude, *Front. Neurosci.*, 2021, **14**, 1432.
81. S. Mereiter, M. Balmaña, D. Campos, J. Gomes and C. A. Reis, *Cancer Cell*, 2019, **36**, 6-16.
82. H. C. Hang and C. R. Bertozzi, *Bioorg. Med. Chem.*, 2005, **13**, 5021-5034.
83. X. Yang and K. Qian, *Nat. Rev. Mol. Cell Biol.*, 2017, **18**, 452-465.
84. M. L. W. J. Smeenk, L. W. Mike, J. Agramunt and K. M. Bongers, *Curr. Opin. Chem. Bio.*, 2021, **60**, 79-88.
85. D. M. Patterson, L. A. Nazarova and J. A. Prescher, *ACS Chem. Biol.*, 2014, **9**, 592-605.
86. Q. Wang, T. R. Chan, R. Hilgraf, V. V. Fokin, K. B. Sharpless and M. G. Finn, *J. Am. Chem. Soc.*, 2003, **125**, 3192-3193.
87. A. E. Speers, G. C. Adam and B. F. Cravatt, *J. Am. Chem. Soc.*, 2003, **125**, 4686-4687.
88. C. G. Gahmberg and L. C. Andersson, *J. Biol. Chem.*, 1977, **252**, 5888-5894.
89. C. G. Gahmberg and S. Hakomori, *J. Biol. Chem.*, 1973, **248**, 4311-4317.
90. M. Critcher, T. O'Leary and M. L. Huang, *Biochem. J.*, 2021, **478**, 703-719.
91. N. Nischan and J. J. Kohler, *Glycobiology*, 2016, **26**, 1-8.
92. P.-A. Gilormini, A. R. Batt, M. R. Pratt and C. Biot, *Chem. Sci.*, 2018, **9**, 7585-7595.
93. T. J. Sminia, H. Zuilhof and T. Wennekes, *Carbohydr. Res.*, 2016, **435**, 121-141.
94. A. Lopez Aguilar, J. G. Briard, L. Yang, B. Ovrzyn, M. S. Macauley and P. Wu, *ACS Chem. Biol.*, 2017, **12**, 611-621.
95. N. J. Pedowitz and M. R. Pratt, *RSC Chem. Bio.*, 2021, **2**, 306-321.
96. N. K. Devaraj, *ACS Cent. Sci.*, 2018, **4**, 952-959.
97. Y. Zeng, T. N. C. Ramya, A. Dirksen, P. E. Dawson and J. C. Paulson, *Nat. Methods*, 2009, **6**, 207-209.
98. J. Nilsson, U. Rüetschi, A. Halim, C. Hesse, E. Carlsohn, G. Brinkmalm and G. Larson, *Nat. Methods*, 2009, **6**, 809-811.
99. E. Klement, Z. Lipinszki, Z. Kupihár, A. Udvardy and K. F. Medzihradszky, *J. Proteome Res.*, 2010, **9**, 2200-2206.
100. T. N. C. Ramya, E. Weerapana, B. F. Cravatt and J. C. Paulson, *Glycobiology*, 2013, **23**, 211-221.
101. A. P. Matthey, W. R. Birmingham, P. Both, N. Kress, K. Huang, J. M. Van Munster, G. S. Bulmer, F. Parmeggiani, J. Voglmeir, J. E. R. Martinez, N. J. Turner and S. L. Flitsch, *ACS Catal.*, 2019, **9**, 8208-8212.
102. J. Huang, H. Qin, Z. Sun, G. Huang, J. Mao, K. Cheng, Z. Zhang, H. Wan, Y. Yao, J. Dong, J. Zhu, F. Wang, M. Ye and H. Zou, *Sci. Rep.*, 2015, **5**, 10164.
103. F. Sun, S. Suttapitugsakul and R. Wu, *Anal. Chem.*, 2019, **91**, 4195-4203.
104. J. E. McCombs and J. J. Kohler, *Bioconjug. Chem.*, 2016, **27**, 1013-1022.
105. H. Kayser, R. Zeitler, C. Kannicht, D. Grunow, R. Nuck and W. Reutter, *J. Biol. Chem.*, 1992, **267**, 16934-16938.
106. L. K. Mahal, K. J. Yarema and C. R. Bertozzi, *Science*, 1997, **276**, 1125-1128.
107. E. Saxon and C. R. Bertozzi, *Science*, 2000, **287**, 2007-2010.
108. M. Sawa, T. L. Hsu, T. Itoh, M. Sugiyama, S. R. Hanson, P. K. Vogt and C. H. Wong, *Proc. Natl. Acad. Sci. U. S. A.*, 2006, **103**, 12371-12376.
109. S. T. Laughlin, J. M. Baskin, S. L. Amacher and C. R. Bertozzi, *Science*, 2008, **320**, 664-667.
110. D. J. Vocadlo, H. C. Hang, E. J. Kim, J. A. Hanover and C. R. Bertozzi, *Proc. Natl. Acad. Sci. U. S. A.*, 2003, **100**, 9116-9121.

111. B. W. Zaro, Y. Y. Yang, H. C. Hang and M. R. Pratt, *Proc. Natl. Acad. Sci. U. S. A.*, 2011, **108**, 8146-8151.
112. A. R. Batt, B. W. Zaro, M. X. Navarro and M. R. Pratt, *Chembiochem*, 2017, **18**, 1177-1182.
113. M. Boyce, I. S. Carrico, A. S. Ganguli, S. H. Yu, M. J. Hangauer, S. C. Hubbard, J. J. Kohler and C. R. Bertozzi, *Proc. Natl. Acad. Sci. U. S. A.*, 2011, **108**, 3141-3146.
114. C. M. Whitman, F. Yang and J. J. Kohler, *Bioorg. Med. Chem. Lett.*, 2011, **21**, 5006-5010.
115. C. Büll, T. Heise, D. M. H. Beurskens, M. Riemersma, A. Ashikov, F. P. J. T. Rutjes, T. H. Van Kuppevelt, D. J. Lefeber, M. H. Den Brok, G. J. Adema and T. J. Boltje, *ACS Chem. Biol.*, 2015, **10**, 2353-2363.
116. K. N. Chuh, B. W. Zaro, F. Piller, V. Piller and M. R. Pratt, *J. Am. Chem. Soc.*, 2014, **136**, 12283-12295.
117. R. Xie, L. Dong, Y. Du, Y. Zhu, R. Hua, C. Zhang and X. Chen, *Proc. Natl. Acad. Sci. U. S. A.*, 2016, **113**, 5173-5178.
118. Z. S. Chinoy, C. Bodineau, C. Favre, K. W. Moremen, R. V. Durán and F. Friscourt, *Angew. Chem. Int. Ed. Engl.*, 2019, **58**, 4281-4285.
119. A. Kitowski and G. J. L. Bernardes, *Chembiochem*, 2020, **21**, 2696-2700.
120. J. L. Daughtry, W. Cao, J. Ye and J. M. Baskin, *ACS Chem. Biol.*, 2020, **15**, 318-324.
121. B. W. Zaro, A. R. Batt, K. N. Chuh, M. X. Navarro and M. R. Pratt, *ACS Chem. Biol.*, 2017, **12**, 787-794.
122. J. E. G. A. Dold, J. Pfozter, A. K. Späte and V. Wittmann, *Chembiochem*, 2017, **18**, 1242-1250.
123. J. E. G. A. Dold and V. Wittmann, *Chembiochem*, 2021, **22**, 1243-1251.
124. A. K. Späte, J. E. G. A. Dold, E. Batroff, V. F. Schart, D. E. Wieland, O. R. Baudendistel and V. Wittmann, *Chembiochem*, 2016, **17**, 1374-1383.
125. A. K. Späte, V. F. Schart, S. Schöllkopf, A. Niederwieser and V. Wittmann, *Eur. J. Chem.*, 2014, **20**, 16502-16508.
126. N. D. Pham, C. S. Fermaintt, A. C. Rodriguez, J. E. McCombs, N. Nischan and J. J. Kohler, *Glycoconj. J.*, 2015, **32**, 515-529.
127. C. Ma, H. Takeuchi, H. Hao, C. Yonekawa, K. Nakajima, M. Nagae, T. Okajima, R. S. Haltiwanger and Y. Kizuka, *Int. J. Mol. Sci.*, 2020, **21**, 1-18.
128. W. Qin, K. Qin, X. Fan, L. Peng, W. Hong, Y. Zhu, P. Lv, Y. Du, R. Huang, M. Han, B. Cheng, Y. Liu, W. Zhou, C. Wang and X. Chen, *Angew. Chem. Int. Ed. Engl.*, 2018, **57**, 1817-1820.
129. N. Darabedian, B. Yang, R. Ding, G. Cutolo, B. W. Zaro, C. M. Woo and M. R. Pratt, *Front. Chem.*, 2020, **8**, 1-14.
130. Y. Hao, X. Fan, Y. Shi, C. Zhang, D. e. Sun, K. Qin, W. Qin, W. Zhou and X. Chen, *Nat. Commun.*, 2019, **10**, 4065.
131. R. T. Almaraz, U. Aich, H. S. Khanna, E. Tan, R. Bhattacharya, S. Shah and K. J. Yarema, *Biotechnol. Bioeng.*, 2012, **109**, 992-1006.
132. A. K. Späte, H. Bußkamp, A. Niederwieser, V. F. Schart, A. Marx and V. Wittmann, *Bioconjug. Chem.*, 2014, **25**, 147-154.
133. P. A. Gilormini, C. Lion, D. Vicogne, T. Levade, S. Potelle, C. Mariller, Y. Guérardel, C. Biot and F. Foulquier, *Chem. Commun.*, 2016, **52**, 2318-2321.
134. A. Niederwieser, A. K. Späte, L. D. Nguyen, C. Jüngst, W. Reutter and V. Wittmann, *Angew. Chem. Int. Ed. Engl.*, 2013, **52**, 4265-4268.
135. V. F. Schart, J. Hassenrück, A. K. Späte, J. E. G. A. Dold, R. Fahrner and V. Wittmann, *Chembiochem*, 2019, **20**, 166-171.
136. Y. Zhu, L. I. Willems, D. Salas, S. Cecioni, W. B. Wu, L. J. Foster and D. J. Voadlo, *J. Am. Chem. Soc.*, 2020, **142**, 15729-15739.
137. F. Doll, A. Buntz, A. K. Späte, V. F. Schart, A. Timper, W. Schrimpf, C. R. Hauck, A. Zumbusch and V. Wittmann, *Angew. Chem. Int. Ed. Engl.*, 2016, **55**, 2262-2266.
138. H. Y. Tan, R. Eskandari, D. Shen, Y. Zhu, T. W. Liu, L. I. Willems, M. G. Alteen, Z. Madden and D. J. Voadlo, *J. Am. Chem. Soc.*, 2018, **140**, 15300-15308.

139. K. K. Palaniappan and C. R. Bertozzi, *Chem. Rev.*, 2016, **116**, 14277-14306.
140. M. E. Griffin and L. C. Hsieh-Wilson, *Cell Chem. Biol.*, 2016, **23**, 108-121.
141. L. A. Walter, A. R. Batt, N. Darabedian, B. W. Zaro and M. R. Pratt, *Chembiochem*, 2018, **19**, 1918-1921.
142. D. Soares da Costa, J. C. Sousa, S. D. Mesquita, N. I. Petkova-Yankova, F. Marques, R. L. Reis, N. Sousa and I. Pashkuleva, *Molecules*, 2020, **25**, 795.
143. R. Xie, S. Hong, L. Feng, J. Rong and X. Chen, *J. Am. Chem. Soc.*, 2012, **134**, 9914-9917.
144. H. Wang, R. Wang, K. Cai, H. He, Y. Liu, J. Yen, Z. Wang, M. Xu, Y. Sun, X. Zhou, Q. Yin, L. Tang, I. T. Dobrucki, L. W. Dobrucki, E. J. Chaney, S. A. Boppart, T. M. Fan, S. Lezmi, X. Chen, L. Yin and J. Cheng, *Nat. Chem. Biol.*, 2017, **13**, 415-424.
145. A. Lamoot, A. Uvyn, S. Kasmi and B. G. De Geest, *Angew. Chem. Int. Ed. Engl.*, 2021, **60**, 6320-6325.
146. S. Lim, W. Kim, S. Song, M. K. Shim, H. Y. Yoon, B. S. Kim, I. C. Kwon and K. Kim, *Bioconjug. Chem.*, 2021, **32**, 199-214.
147. J. C. Paulson, J. E. Sadler and R. L. Hill, *J. Biol. Chem.*, 1979, **254**, 2120-2124.
148. Q. Chao, Y. Ding, Z. H. Chen, M. H. Xiang, N. Wang and X. D. Gao, *Front. Chem.*, 2020, **8**, 513.
149. E. Kim, *Molecules*, 2018, **23**.
150. F. Tang, M. Zhou, K. Qin, W. Shi, A. Yashinov, Y. Yang, L. Yang, D. Guan, L. Zhao, Y. Tang, Y. Chang, L. Zhao, H. Yang, H. Zhou, R. Huang and W. Huang, *Nat. Chem. Biol.*, 2020, **16**, 766-775.
151. M. Noel, P.-A. Gilormini, V. Coge, N. Yamakawa, D. Vicogne, C. Lion, C. Biot, Y. Guérardel and A. Harduin-Lepers, *Chembiochem*, 2017, **18**, 1251-1259.
152. S. H. Yu, P. Zhao, T. Sun, Z. Gao, K. W. Moremen, G. J. Boons, L. Wells and R. Steet, *J. Biol. Chem.*, 2016, **291**, 3982-3989.
153. A. Lopez Aguilar, L. Meng, X. Hou, W. Li, K. W. Moremen and P. Wu, *Bioconjug. Chem.*, 2018, **29**, 1231-1239.
154. N. E. Mbua, X. Li, H. R. Flanagan-Steet, L. Meng, K. Aoki, K. W. Moremen, M. A. Wolfert, R. Steet and G. J. Boons, *Angew. Chem. Int. Ed. Engl.*, 2013, **52**, 13012-13015.
155. T. Zheng, H. Jiang, M. Gros, D. S. del Amo, S. Sundaram, G. Lauvau, F. Marlow, Y. Liu, P. Stanley and P. Wu, *Angew. Chem. Int. Ed. Engl.*, 2011, **50**, 4113-4118.
156. Q. Li, Z. Li, X. Duan and W. Yi, *J. Am. Chem. Soc.*, 2014, **136**, 12536-12539.
157. J.-L. Chabard, C. Krishnamurthy, W. Yi, D. F. Smith and L. C. Hsieh-Wilson, *J. Am. Chem. Soc.*, 2012, **134**, 4489-4492.
158. L. Wen, Y. Zheng, K. Jiang, M. Zhang, S. M. Kondengaden, S. Li, K. Huang, J. Li, J. Song and P. G. Wang, *J. Am. Chem. Soc.*, 2016, **138**, 11473-11476.
159. H. Zhu, S. Wang, D. Liu, L. Ding, C. Chen, Y. Liu, Z. Wu, R. Bollag, K. Liu, W. M. Alexander, J. Yin, C. Ma, L. Li and P. G. Wang, *Anal. Chem.*, 2020, **92**, 6297-6303.
160. T. Sun, S.-H. Yu, P. Zhao, L. Meng, K. W. Moremen, L. Wells, R. Steet and G.-J. Boons, *J. Am. Chem. Soc.*, 2016, **138**, 11575-11582.
161. Z. L. Wu, M. Whittaker, J. M. Ertelt, A. D. Person and V. Kalabokis, *Glycobiology*, 2020, **30**, 970-980.
162. Z. L. Wu, A. Luo, A. Grill, T. Lao, Y. Zou and Y. Chen, *Bioconjug. Chem.*, 2020, **31**, 2098-2102.
163. T. Abukar, S. Rahmani, N. K. Thompson, C. N. Antonescu and W. W. Wakarchuk, *Carbohydr. Res.*, 2021, **500**, 108249.
164. L. Wen, M. R. Gadi, Y. Zheng, C. Gibbons, S. M. Kondengaden, J. Zhang and P. G. Wang, *ACS Catal.*, 2018, **8**, 7659-7666.
165. S. Hong, Y. Shi, N. C. Wu, G. Grande, L. Douthit, H. Wang, W. Zhou, K. B. Sharpless, I. A. Wilson, J. Xie and P. Wu, *Nat. Commun.*, 2019, **10**, 1799.
166. S. H. Yu, M. Boyce, A. M. Wands, M. R. Bond, C. R. Bertozzi and J. J. Kohler, *Proc. Natl. Acad. Sci. U. S. A.*, 2012, **109**, 4834-4839.
167. B. Ramakrishnan and P. K. Qasba, *J. Biol. Chem.*, 2002, **277**, 20833-20839.

168. J. Choi, L. J. S. Wagner, S. B. P. E. Timmermans, S. A. Malaker, B. Schumann, M. A. Gray, M. F. Debets, M. Takashima, J. Gehring and C. R. Bertozzi, *J. Am. Chem. Soc.*, 2019, **141**, 13442-13453.
169. B. Schumann, S. A. Malaker, S. P. Wisnovsky, M. F. Debets, A. J. Agbay, D. Fernandez, L. J. S. Wagner, L. Lin, Z. Li, J. Choi, D. M. Fox, J. Peh, M. A. Gray, K. Pedram, J. J. Kohler, M. Mrksich and C. R. Bertozzi, *Mol. Cell*, 2020, **78**, 824–834.e815.
170. M. F. Debets, O. Y. Tastan, S. P. Wisnovsky, S. A. Malaker, N. Angelis, L. K. R. Moeckl, J. Choi, H. Flynn, L. J. S. Wagner, G. Bineva-Todd, A. Antonopoulos, A. Cioce, W. M. Browne, Z. Li, D. C. Briggs, H. L. Douglas, G. T. Hess, A. J. Agbay, C. Roustan, S. Kjaer, S. M. Haslam, A. P. Snijders, M. C. Bassik, W. E. Moerner, V. S. W. Li, C. R. Bertozzi and B. Schumann, *Proc. Natl. Acad. Sci. U S A*, 2020, **117**, 25293-25301.
171. K. Islam, *Cell Chem. Biol.*, 2018, **25**, 1171-1184.
172. A. Cioce, S. A. Malaker and B. Schumann, *Curr. Opin. Chem. Bio.*, 2021, **60**, 66-78.

Chapter 3: Synthesis of 1-Azido-D-Ribitol-5-Phosphate Probes

3.1 Abstract

Glycans play an essential role in a wide range of cellular processes, and this is reflected in the great diversity in their structure and function. In recent years, the cell surface protein α -dystroglycan has been shown to possess a unique tandem D-ribitol-5-phosphate linker. This linear pentitol was not previously known to exist within mammalian cells, though it is commonly found within teichoic acids produced by Gram-positive bacteria. The possibility remains for this unique monosaccharide to be present elsewhere within mammalian cell glycans. Described in this Chapter is the synthesis of a panel of 1-azido analogues of ribitol-5-phosphate, suitable for *in vitro* and *in vivo* metabolic labelling studies. Utilising newly developed chemistry for the addition of the S-Acetyl-ThioEthyl (SATE) protected phosphate moiety, a 12-step synthetic route has been developed from D-ribose to a fully protected, cell-permeable D-ribitol-5-phosphate analogue. Adjustments to this route allowed for the synthesis of an array of 1-azido ribitol based probes with varied protecting group strategies, both with and without phosphate, for *in vivo* labelling. Additionally, a fully deprotected phosphate-containing probe was formed for *in vitro* studies. Treatment of live cells with these probes possesses the potential to metabolically label D-ribitol-5-phosphate containing glycans *in vivo*, revealing new insight into the presence of this unique monosaccharide within mammalian cells. The successful synthesis of these 1-azido analogues, combined with the phosphotriester method development on the path to their synthesis, will also pave the way for the production of future generations of D-ribitol-5-phosphate based metabolic labelling probes.

3.2 Introduction

D-Ribitol-5-phosphate is typically associated with teichoic acids; the major component of bacterial cell walls.⁵⁶ It was not until 2016 that this unique sugar moiety was identified as a tandem linker in a cell surface glycan within mammalian cells.^{39, 44, 45} Contained within the Core M3 'functional' glycan of α -dystroglycan (α -DG), this linking unit is responsible for connecting matriglycan (the unit responsible directly for the interactions between α -DG and extracellular matrix components) to the core M3 trisaccharide (which is directly bound to α -DG). Incorrect formation of the tandem D-ribitol-5-phosphate linker, through mutation of the enzymes responsible for its formation, ISPD, FKTN and FKRP, has been shown to cause a subset of muscular dystrophies, termed dystroglycanopathies.^{2, 10, 73}

To date D-ribitol-5-phosphate within mammalian cells is only known to exist within α -DG, so this provides a unique target for the labelling of functional α -DG, for example through the use of ribitol-phosphate-derived probes for metabolic labelling (see Chapter 2, pg. 40). In addition to the selective targeting of α -DG, metabolic labelling with D-ribitol-5-phosphate provides us with the possibility of unveiling other sites where this unique sugar moiety is present in mammalian cells. In the design of metabolic labelling probes there are three main considerations; 1) the structure of the probes, 2) the bioorthogonal handle for labelling, and 3) the protecting group strategy.

Structure

The biosynthetic pathway of D-ribitol-5-phosphate within cells is currently unknown. Therefore, the structure of our probes will be based on this phospho-pentitol structure, specifically the D-isomer of ribitol-5-phosphate. Phosphate-containing probes can increase the efficiency by which nucleoside analogues are metabolically converted within cells, as they bypass the initial rate-limiting phosphorylation step,^{173, 174} and studies have indeed shown the increased efficiency of protected phosphate prodrugs vs non-phosphorylated nucleotides.¹⁷⁵ There is, however, also evidence that at high cellular concentrations of D-ribitol, the enzyme FGGY can directly convert D-ribitol into D-ribitol-5-phosphate,^{45, 57} and the uptake and conversion of ¹³C labelled D-ribitol into ¹³C labelled CDP-ribitol has been shown within cells.¹⁷⁶ This opens up the possibility of testing non-phosphorylated ribitol derivatives as metabolic labelling tools. As well as shining further light on the biosynthetic pathway of D-ribitol-5-phosphate in cells, if successful, D-ribitol based probes will also provide an easier to synthesise structure to utilise in future metabolic labelling studies.

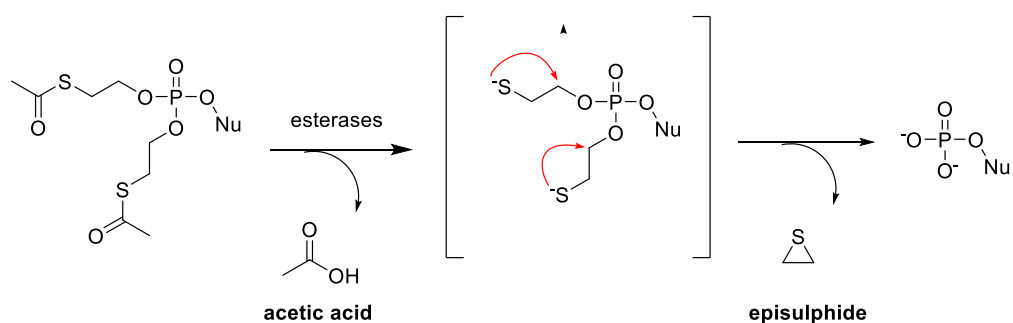
Bioorthogonal Handle

Metabolic incorporation of labelled sugars is a commonplace technique to gain insight into biological systems and relies on the use of bioorthogonal reactions to allow specific labelling of the incorporated metabolic handle (see Chapter 2, pg. 40). The term 'bioorthogonal' was first coined by Bertozzi in 2003,¹⁷⁷ and is used to describe a reaction that "neither interacts nor interferes with a biological system".¹⁷⁸ The most frequently utilised bioorthogonal reaction at present, is the Copper (I) catalysed Azide-Alkyne Cycloaddition (CuAAC) reaction, more commonly referred to as the Cu-catalysed 'Click reaction'. The Click reaction relies on the metabolic incorporation of either an azide or alkyne moiety. The development of the ring-Strain Promoted Azide-Alkyne Cycloaddition (SPAAC), which utilises highly reactive strained alkynes, avoids the use of the cytotoxic copper catalyst and allows *in vivo* labelling. To be able to utilise this copper-free method, an azide will be utilised as the metabolic tag in the D-ribitol-5-phosphate derived probes.

Protecting Group Strategy

When considering a protecting group strategy for metabolic labelling probes there are two potential hurdles: 1) being able to cross the cell membrane, and 2) being utilised in the required biosynthetic pathway for incorporation into the biological target. For sugars, the high proportion of highly polar hydroxyl groups makes crossing the cell membrane to the site of action a difficult task, and this is only increased further with the addition of a negatively charged phosphate. Therefore the use of cell-permeable, cell-cleavable protecting groups of both sugar and phosphate hydroxyl groups is required.

Acetate groups are commonplace in the protection of cell-permeable sugar-based metabolic labelling probes. These small ester groups have been shown to increase the cell permeability of chemical probes,¹⁷⁹ and they are readily cleaved within the cell by non-specific esterase and/or lipase activity. Recent studies have raised concerns about the non-enzymatic labelling of cysteine residues caused by acetate protection,^{128, 130} though these effects depend heavily on the structure of the acetylated chemical reporter.^{18, 19} As phosphotriester cleaving enzymes have not been discovered within mammalian cells, the cleavage of phosphate protecting groups relies on other known enzymatic and biochemical processes. *S*-Acetyl-2-ThioEthyl (SATE) phosphate protecting groups display high stability, and their degradation products have been shown to not exhibit cytotoxicity.¹⁸⁰ The cellular cleavage of SATE groups is initiated by the cleavage of the terminal thioacetate groups. Once cleaved, the newly-uncovered thiols can undergo self-cyclisation, releasing episulfide alongside the free phosphate mono-ester within the cell as shown in Scheme 3.¹⁸⁰



Scheme 3: Enzymatic cleavage of SATE protected phosphates

3.3 Aims

This chapter aims to describe the synthesis of a panel of ribitol-5-phosphate and ribitol based metabolic labelling probes. Of the various sites of azide incorporation proposed (see 1.7 *Project Aims*, Figure 7, pg. 335), the probes with an azide substituting the primary hydroxyl group at C-1 (Figure 12) were expected to have the most straightforward synthesis so were focused on

initially. The ribitol-5-phosphate probes **1-Az-OAc-SATE** and **1-Az-OH-SATE**, and ribitol based probes **1-Az-OH** and **1-Az-OAc** will be utilised for *in vivo* labelling experiments (where protection is required for cell permeability), and synthesis of the fully deprotected probe **1-Az-OH-Phos** will allow for *in vitro* testing (where unprotected probes serve as enzyme substrates).

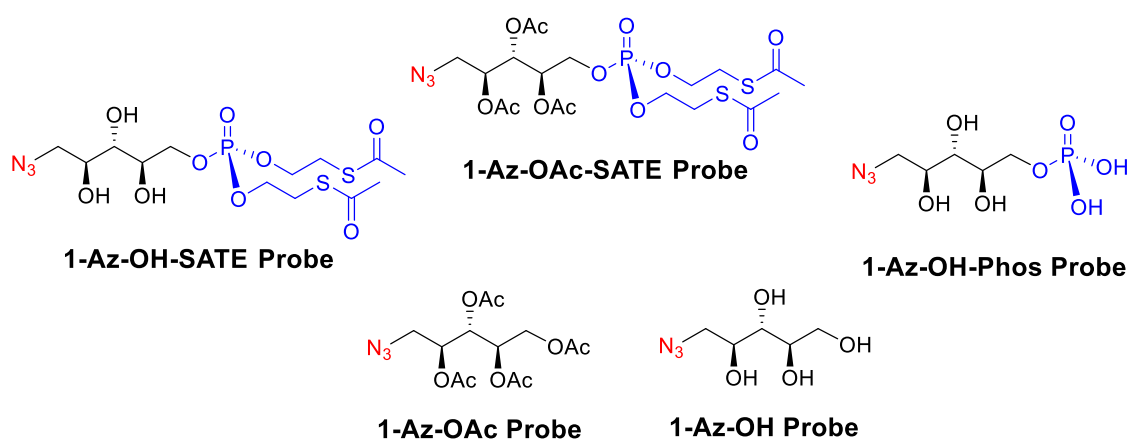


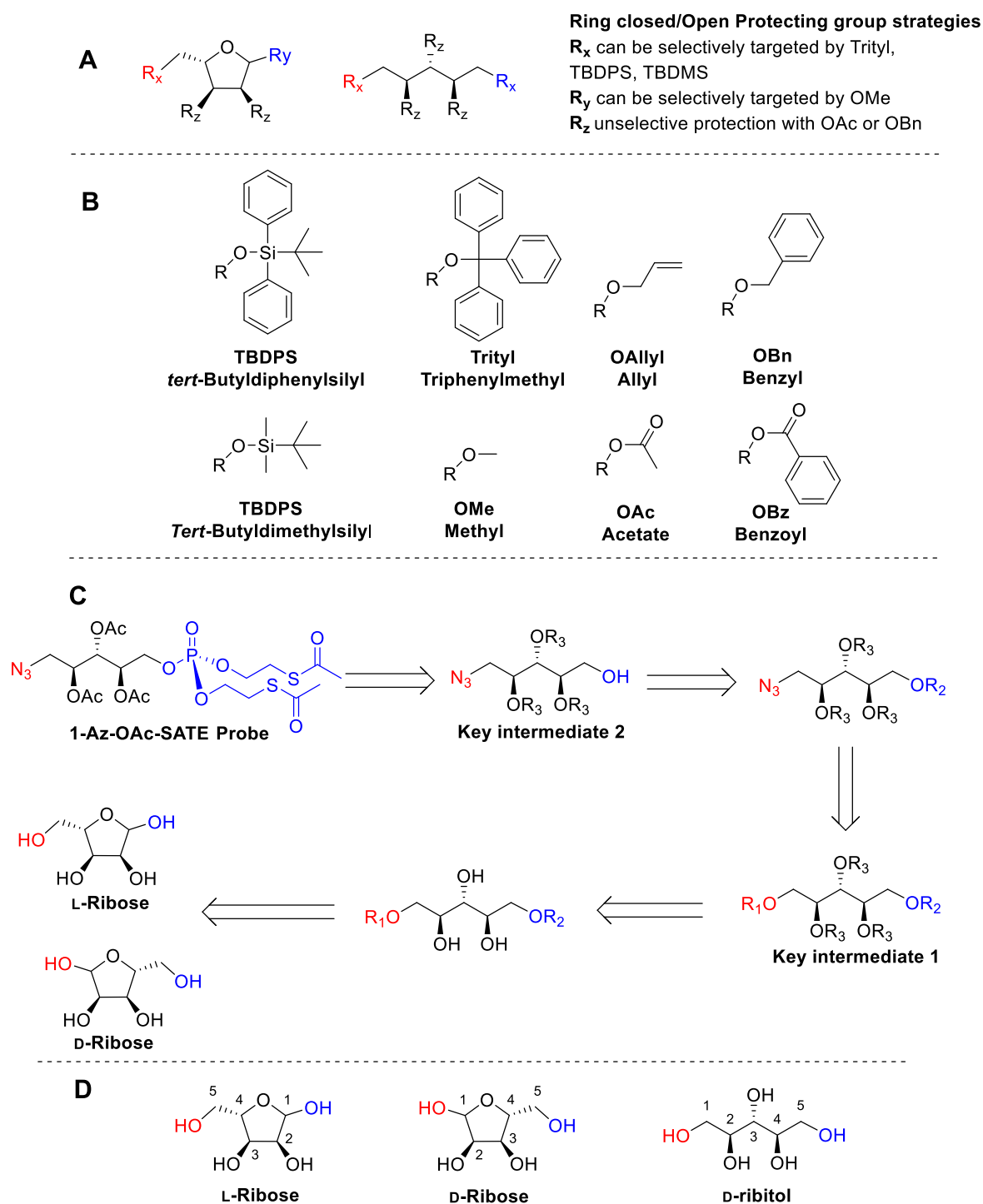
Figure 12: Structure of 1-azido-2,3,4-tri-O-acetyl-D-ribitol-5-bis(S-acetyl-thioethyl)phosphate (1-Az-OAc-SATE) and related probes

3.4 Results and Discussion

Retrosynthesis Design

An array of azide-tagged ribitol-based probes were designed for use within metabolic labelling studies targeting ribitol-containing glycoconjugates (Figure 12). Having the site of azide incorporation at the 1-position of D-ribitol meant that this site could be effectively targeted with the use of primary selective protecting groups (Scheme 4A). Equally, due to the site of azide incorporation being achiral, the inversion of stereochemistry when performing S_N2 substitution of a hydroxyl group to an azide would not be an issue. The ribitol pentitol structure is symmetrical, and this, combined with the achiral site of azide addition, meant synthesis could proceed from either L- or D-ribose (Scheme 4C).

For ease of clarity within all schemes, the site of phosphate incorporation is shown in blue, and the site of azide addition is shown in red. When referring to numbered carbons, ring-closed ribose numbering follows the standard for sugars, where C-1 is the anomeric carbon, and C-5 is the CH_2 . Once either D- or L-ribose is ring-opened to give ribitol, the pentitol is numbered as for D-ribitol, where the site of phosphate incorporation is numbered C-5 and the site of azide incorporation C-1 (Scheme 4D).



Scheme 4: Protecting group strategies for the synthesis of 1-Az probes: A) protecting group strategies for pentose (ring closed) and pentitol (ring-opened) sugars; B) structures of protecting groups discussed within this thesis; C) proposed retrosynthetic pathway from the fully protected 1-Az-OAc-SATE probe to ribose starting materials. R = protecting group. D) Compound numbering for D- and L-ribose and D-ribitol

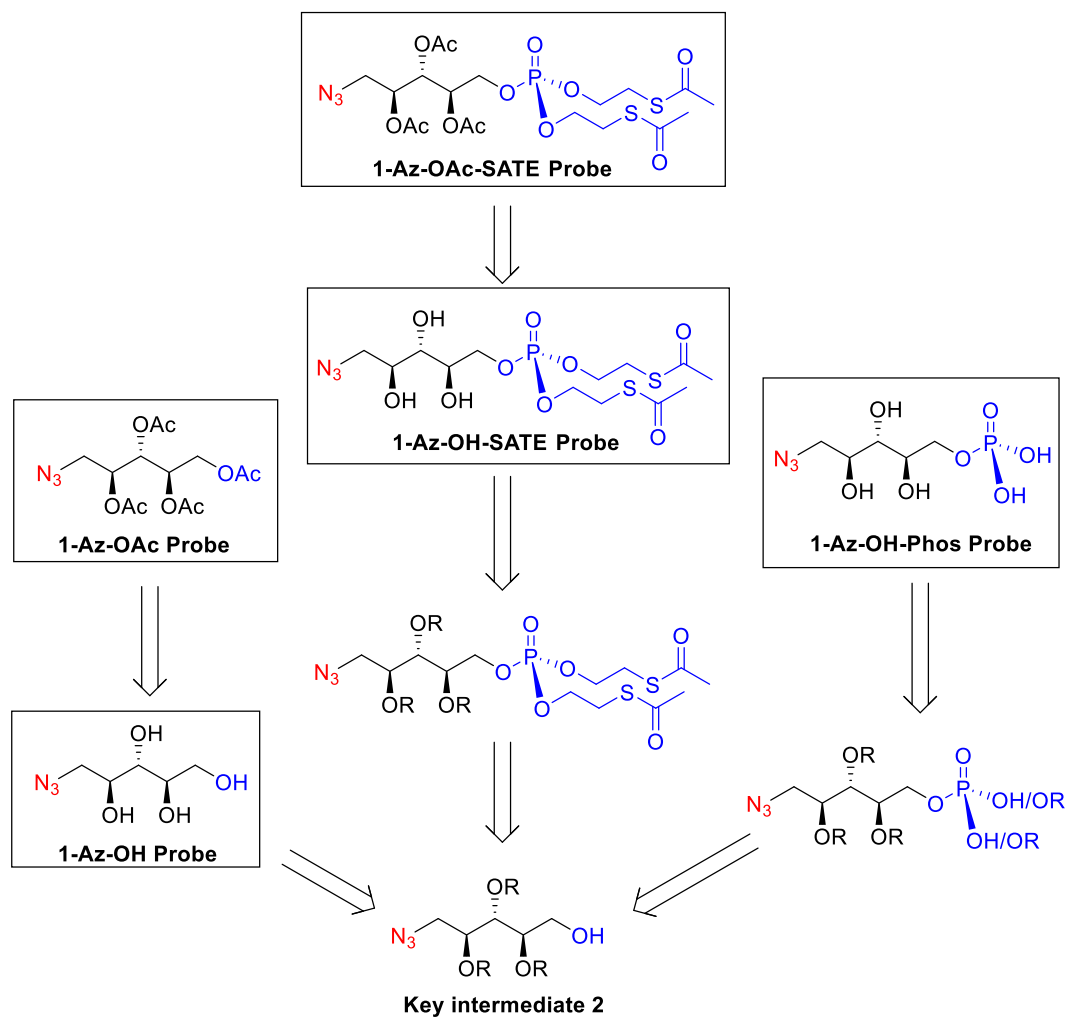
The synthesis of the 1-Azido probes can proceed with either the site of azide or phosphate incorporation initially uncovered depending on whether D- or L- ribose is utilised. This primary hydroxyl group can be selectively protected with various protecting groups (Scheme 4A,B). Ring-opening exposes the second primary alcohol site for alternative functionality with an azide or phosphate, which can be protected by the use of a second, orthogonal, primary selective protecting

group. This requires the use of two orthogonal primary selective protecting groups (R_1 and R_2). The triphenylmethyl (trityl) and the *tert*-butyldiphenyl/methyl silyl (TBDPS/TBDMS) groups are the most readily utilised primary protecting groups within carbohydrate chemistry. While the trityl group is readily cleaved under acidic conditions,¹⁸¹⁻¹⁸³ silyl ethers are cleaved under more selective conditions, utilising fluoride sources such as TBAF^{184, 185} or HF.^{186, 187} Additionally, the ability to protect the anomeric hydroxyl group by Fisher glycosylation provides a third alternative method for the site-selective protection of the 1-position of D- or L-ribose (Scheme 4A). Typically protected by methyl groups, these groups are cleaved under much harsher conditions than trityl or silyl ethers, requiring low pH and a high temperature.^{188, 189}

Protecting the remaining secondary hydroxyl groups with non-selective protecting groups (R_3) provides a pentitol with a general structure referred to as **Key Intermediate 1** (Scheme 4C), where both azide and phosphate sites can be selectively unmasked by the removal of R_1 or R_2 respectively. For non-selective protection, acetate and benzyl groups are commonplace. Acetate groups are beneficial to the synthesis of the target probes as they are required in the final product, however, the ester structure has been shown to undergo migration in the presence of free hydroxyl groups.^{190, 191} This makes benzyl groups a favourable alternative. Their structure prevents migration from occurring, however the need to convert them to acetate groups in the final product does increase the number of synthetic steps required to reach the final products. Another ether-based protecting group is the allyl group, though their use within carbohydrate chemistry is less common, and more typically limited to selective anomeric protection.^{192, 193} Therefore, strategies utilising both benzyl and acetyl groups will be investigated to reach the final 1-Az probes.

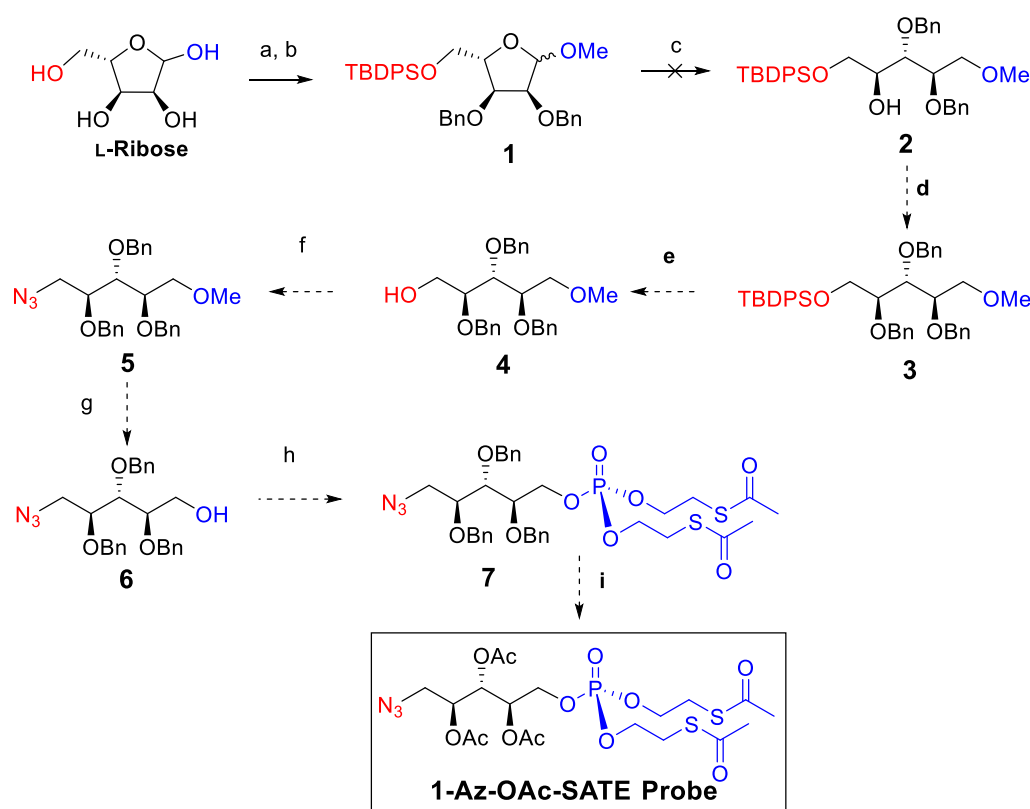
Removal of the primary protecting group (R_1) at C-1 of **Key Intermediate 1** allows for the selective incorporation of an azide moiety. Following azide incorporation, removal of the protecting group at C-5 (R_2) produces **Key Intermediate 2**. This intermediate is of high significance as not only does this allow for the site-specific addition of phosphate to take place at C-5, but the route at this point can also diversify, allowing for the formation of an array of differentially protected 1-azido-ribitol phosphate derivatives (Scheme 5). From **Key Intermediate 2** the ribitol based probes can be obtained from an acetylated intermediate by acetylation of the free OH and global de-acetylation to form the **1-Az-OAc** and **1-Az-OH** probes, respectively, or from a benzylated intermediate by the removal of the benzyl groups and global acetylation. The **1-Az-OAc-SATE** and **1-Az-OH-SATE** probes are formed after the *bis*-SATE-phosphate addition in a similar manner. The fully deprotected **1-Az-OH-Phos** probe is the largest digression from the overall route, with the incorporation of a phosphate monoester requiring different chemistry than the addition of the fully protected SATE

phosphate. The synthetic route to this probe depends on either the direct incorporation of a free phosphate moiety or the addition of a protected phosphate which can be subsequently deprotected.



Scheme 5: Retrosynthetic pathway of 1-Az Probes from Key Intermediate 2

Route 1



Scheme 6: Route 1 from L-Ribose to the 1-Az-OAc-SATE probe. **Reagents and Conditions:** a) i) HCl, MeOH, r.t., 2 hr, ii) TBDPS-Cl, pyridine, r.t., 24 hrs, (55%), b) BnBr, NaH, TBAI, DMF, r.t. 2 hrs, (67%) c) DIBAL-H, toluene, 10 min, 60°C (0%) **Proposed Conditions:** d) BnBr, TBAI, DMF, e) TBAF, THF, f) i) TsCl, pyridine, ii) NaN₃, DMF, g) AcOH, 80°C, h) i) PO(OEt-2Br)₃, Tf₂O, pyridine, DCM, ii) KSAc, acetone, i) BCl₃, DCM, ii) Ac₂O, pyridine

The initially proposed synthetic route to the **1-Az-OAc-SATE** probe (Scheme 6) proceeds by the selective protection of the anomeric position with a methoxy group and the primary alcohol at C-5 with TBDPS. This provides selective protection of the sites of addition for phosphate and azide respectively. Benzylation of the remaining hydroxyl groups leads to the formation of the fully protected compound **1**. After the ring-opening step, benzylation of the newly uncovered alcohol group in compound **2** would give compound **3** which follows the general structure previously referred to as **Key Intermediate 1**. This fully protected intermediate can then undergo selective deprotection of the C-1 or C-5 positions, enabling the site-selective addition of the azide and phosphate groups. The azide moiety was chosen to be installed first, as the phosphate triester was expected to be unstable towards the conditions needed for deprotection of the TBDPS group at C-1, as well as the elevated temperature required for azide introduction. Therefore, from compound **3**, TBDPS would be removed to give compound **4** which would allow site-specific azide incorporation to afford compound **5**. With the azide introduced to the ribitol compound, removal of the methoxy group would provide the **Key Intermediate 2** structure **6**, which can undergo SATE phosphate incorporation to yield the bis-SATE-phosphate compound **7**. The benzyl protecting groups can then

be substituted for acetate to provide the final fully protected probe **1-Az-OAc-SATE**. This final protecting group conversion from OBn to OAc would utilise BCl_3 for the benzyl group removal, as using the typical debenzoylation conditions of hydrogenation with Pd/C would cause reduction of the azide to an amine group.¹⁹⁴⁻¹⁹⁶

The initially proposed route to obtain **1-Az-OAc-SATE** (Scheme 6) was attempted as discussed from the starting sugar L-ribose. Fischer glycosylation to yield the 1-methoxy intermediate, followed by protection of the primary alcohol at C-5 with TBDPS-Cl was successful and provided selective protection of the sites of phosphate and azide addition. Benzoylation of the remaining free alcohol groups yielded the desired fully protected product **1**. Ring-opening of compound **1** was attempted by the procedure reported by Sollogoub and co-workers with the reducing agent DIBAL-H.¹⁹⁷ Their method was shown to be both successful on five-membered sugars with an anomeric methoxy group, and tolerant of benzyl protecting groups.

This reaction was attempted on compound **1**, however, none of the desired compound **2** was obtained. Instead, the isolation of the side products **8** and **9** (Figure 13) suggested that the TBDPS group was cleaved before the ring-opening reaction had occurred. Analysis of these side products with MS, IR and ^1H NMR showed the loss of signals relating to the presence of TBDPS, as well as the lack of an anomeric peak for compound **8** proving that the ring-opening had occurred.

Unsurprisingly, the lack of a free alcohol at the anomeric position of **1** meant that ring-opening with NaBH_4 , a procedure typically used for reductive carbohydrate ring-opening, was unsuccessful even after leaving the reaction for several days.¹⁹⁸ An alternative procedure, using TFA to cleave the methyl group, which would allow for ring-opening with NaBH_4 ,¹⁹⁹ would also cause possible cleavage of TBDPS,^{200, 201} so was not attempted. The ring-opened product that was formed (compound **8**) could, theoretically, be converted into compound **2**, however, this would require multiple additional protection and deprotection steps to allow for selective azide addition. Therefore, an alternative route for the synthesis of the **1-Az-SATE** probe was designed, utilising trityl ether protection as shown in Scheme 7.

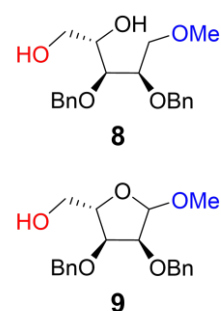
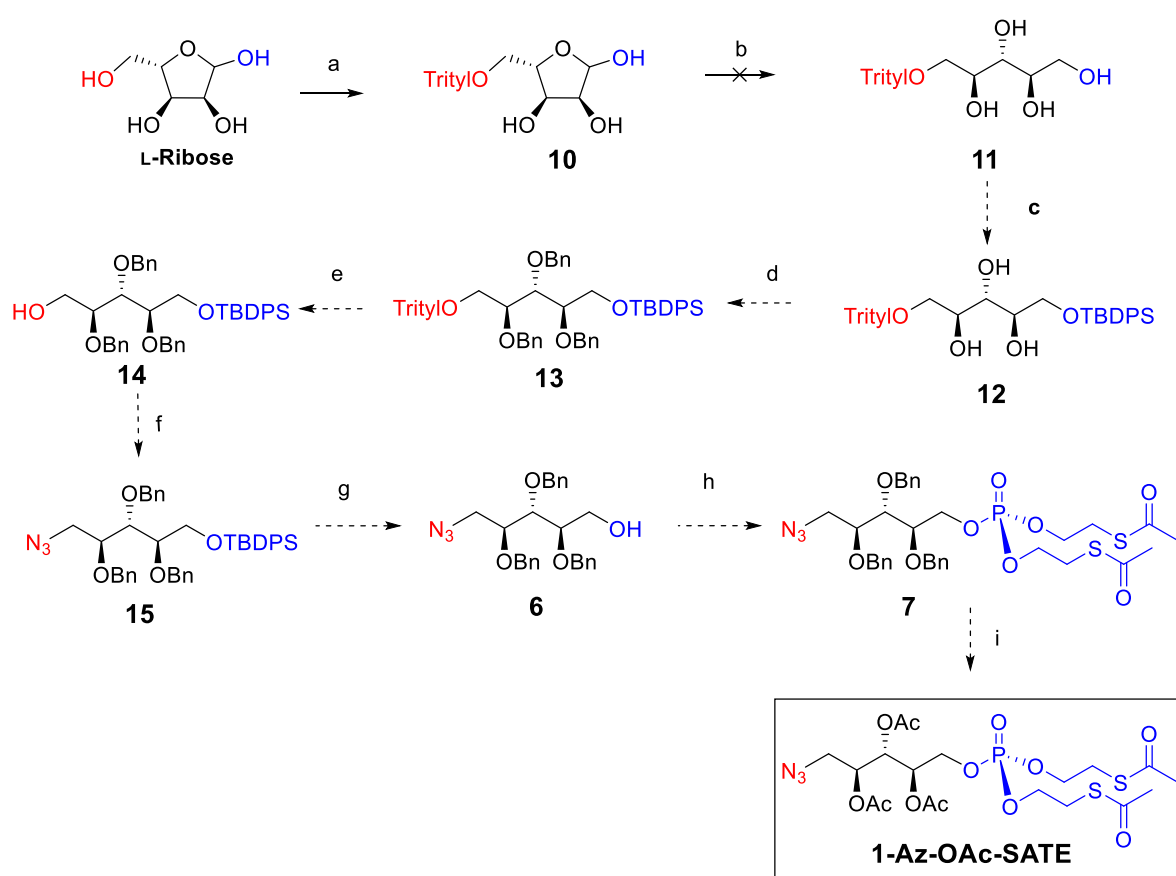


Figure 13: Ring opening side products **8** and **9** formed by the reaction of compound **1** with DIBAL-H, in respective yields of 45% and 55%.

Route 2

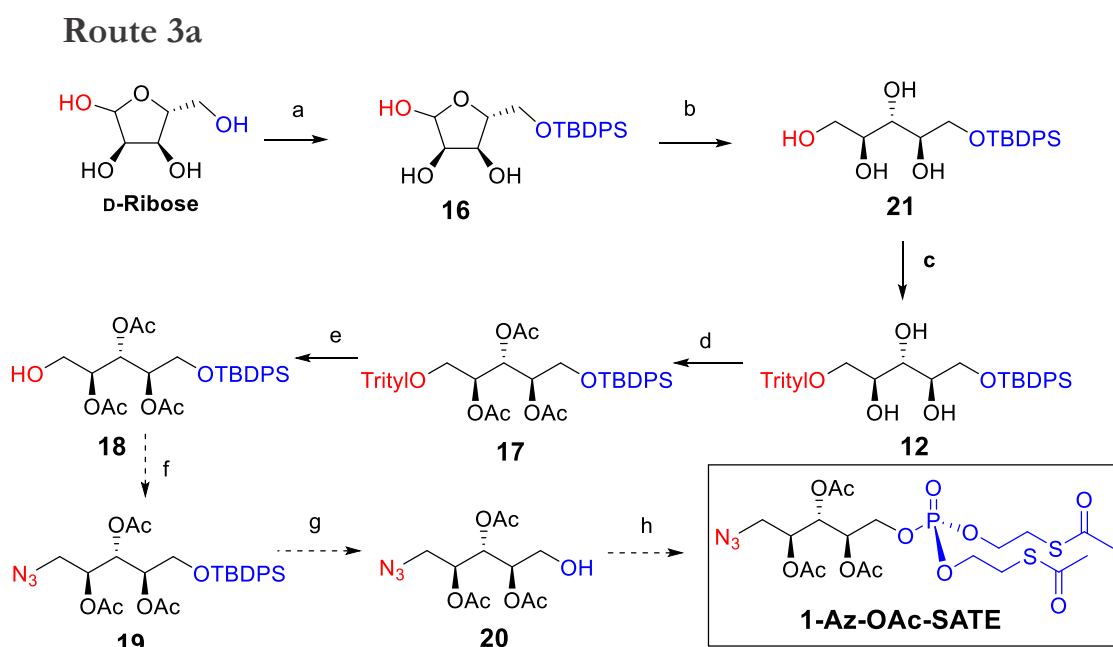


Scheme 7: Route 2 for the synthesis of the **1-Az-OAc-SATE** Probe. **Reagents and Conditions** a) TrCl, pyridine, r.t., 24 h, (48%) b) NaBH₄, EtOH, r.t., 2 h, (0%) **Proposed Conditions** c) TBDPS-Cl, pyridine, d) BnBr, TBAI, DMF, e) *p*-TsOH, MeOH, f) i) TsCl, pyridine, ii) NaN₃, DMF, 60°C, g) TBAF, DMF, h) PO(OEt-2Br)₃, Tf₂O, pyridine, DCM, ii) KSAC, acetone, i) Ac₂O, H₂SO₄,

The newly proposed route (Scheme 7) proceeded with the protection of the primary alcohol at the site of azide substitution, directly followed by ring-opening. By avoiding the use of Fischer glycosylation to install an anomeric methoxide, this ring-opening step could proceed with NaBH₄. The site of phosphate addition would then be selectively protected, with the use of a second, orthogonal, primary selective protecting group. The protecting group at the site of phosphate addition would need to withstand harsh conditions, such as the elevated temperatures required for azide substitution, so TBDPS was selected for the protection of this site rather than a trityl group. Additionally, trityl ethers had been shown within the literature to withstand ring-opening with both DIBAL-H^{202, 203} and NaBH₄,^{204, 205} so the trityl group was chosen to be installed on the ring-closed sugar. Route 2 was initiated with primary protection with trityl to give compound **10**. After the subsequent ring-opening to form compound **11**, TBDPS protection of the newly uncovered primary alcohol would provide compound **12**, in which the positions for azide and phosphate are selectively protected. Subsequent benzyl protection would give compound **13** which fits the general structure of **Key Intermediate 1**. Removal of the trityl group under acidic conditions would provide **14** and allow for azide addition at the desired position to form compound **15**. Selective removal of the

TBDPS group would lead to compound **6** in the structure of **Key Intermediate 2**, which would allow for the continuation of the route to the **1-Az-OAc-SATE** probe as described within Route 1 (Scheme 6).

Attempts at following this newly proposed route were unsuccessful. Though the tritylation of L-ribose appeared to proceed by TLC of the crude reaction, following purification and isolation the resulting tritylated sugar **10** was found to be highly unstable and decomposed within both the ring-opening reaction and samples of pure compound dissolved for use as a TLC standard. Despite the successful synthesis of the similar 5-trityl-D-ribose sugar in literature,²⁰⁶ a repeat of this synthesis following the same procedure was again found to be unsuccessful. More recent literature for the synthesis of this sugar proceeds *via* the corresponding trityl lactone intermediate, however, the reported conditions and yields for this synthesis matched those without the additional oxidation step.²⁰⁷ To test the compatibility of the trityl group with NaBH₄, the ring-opening reaction was repeated on a sample of 5-trityl-D-arabinose available within the lab.²⁰⁸ This starting material was found to not only be much more stable but also able to undergo the ring-opening reaction with moderate yields (68%). These findings indicate a stability issue of the trityl group specific to the ring closed L-ribose sugar, with the trityl group stable on both the D-arabinose substrate, and able to withstand ring-opening. This demonstrates the great effects of differing ring-closed structures on trityl group stability. These findings led to the adapted route presented within Scheme 8.



Scheme 8: Route 3 for the synthesis of 1-Az-OAc-SATE **Reagents and Conditions** a) TBDPS-Cl, pyridine, r.t. 48 h, (60%) b) NaBH₄, EtOH, r.t., 2 h (43%), c) TrCl, pyridine, 60°C, 48 h, (60%) d) Ac₂O, pyridine, r.t., 48 h, (78%), e) HCl, AcOH, DCM, r.t., 1 h, (22%) **Proposed Conditions** f) i) TsCl, pyridine, ii) NaN₃, DMF, 60°C, g) TBAF, DMF, h) PO(OEt-2Br)₃, Tf₂O, pyridine, DCM, ii) KSAc, acetone

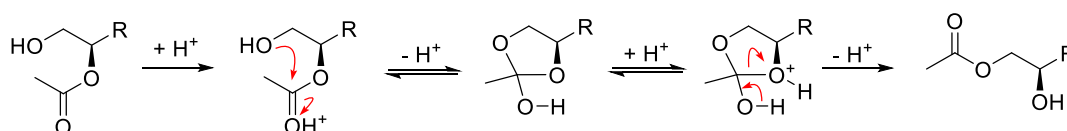
In a third proposed route, the starting sugar was changed from L- to D-ribose, meaning that the sites for the addition of the azide and phosphotriester groups were reversed. Therefore the primary alcohol initially available for protection is the position of phosphorylation, and the later uncovered primary alcohol is the site of azidation. Having the position of phosphorylation initially available meant this could be protected with TBDPS, which was previously shown to be much more stable on the ring-closed sugar than trityl, and trityl would be utilised second, meaning it was only required to be stable for one protection step before its removal. Initial protection of D-ribose with a TBDPS group would yield compound **16**, which could then be ring-opened to allow for selective trityl protection to form compound **12**. To avoid the need for additional substitution steps at the end of the route, this route then investigated the protection of the secondary alcohols with acetate, instead of benzyl groups. From the now acetylated **Key Intermediate 1 (17)** the **1-Az-SATE-Probe** was synthesised as seen previously with the removal of trityl (**18**), azidation (**19**), and the removal of TBDPS to provide the **Key Intermediate 2** compound **20**. The incorporation of the SATE phosphate group would then yield the final **1-Az-OAc-SATE** probe without the need for conversion to OAc from OBn groups.

Utilising acetate groups would not only be more efficient for the synthesis of **1-Az-OAc-SATE** but also for the non-phosphorylated ribitol-based probes. Acetylation of the free alcohol in compound **20** would now lead directly to the **1-Az-OAc** probe and the unprotected derivative **1-Az-OH** could then be obtained through subsequent de-acetylation. The synthesis of **1-Az-OH-Phos** could proceed as previously presented, with the removal of acetates rather than benzyl groups after phosphate incorporation. However, the synthesis of the **1-Az-OH-SATE** probe would not be possible as the removal of the acetate groups also causes deacetylation of the SATE thioesters.²⁰⁹⁻²¹¹

Following this route initially proved successful. Primary protection with TBDPS gave a good yield of 59%, with the major side product formed being the double addition product. This double addition TBDPS product was observed even when TBDPS-Cl was utilised in 0.8 equivalents, indicating a preference for the formation of the double addition product. Once purified, compound **16** was effectively ring-opened with the use of NaBH₄ in EtOH. The high overall polarity of compound **21** caused a low recovery of sugar from the aqueous workup of the reaction mixture (75%), which led to a lower than expected yield after purification (40%). To increase yields, attempts were made to purify the product from the crude reaction mixture following quenching of the reaction with AcOH and removal by rotary evaporation without a work-up, however, the presence of acid in the crude reaction mixture caused issues when purifying by column chromatography and gave only a small increase in yield (43%). The addition of trityl to the newly uncovered primary position was found to be much slower than the initial TBDPS protection and required extended reaction times (72 h) at

elevated temperature (60°C). The obtained yield of mono-substituted product **12** was also affected by the formation of double-addition side products, though the reaction gave a reasonable yield of 60%. Subsequent acetylation of this product lead to the desired fully protected ribitol intermediate **17** which mimicked the **Key Intermediate 1** structure.

The next step in this route was the selective removal of the trityl protecting group to allow for site-selective azidation. The selective removal of the trityl group was found to be challenging due to ensuing acid catalysed acetate migration forming side products **22** and **23** presented within Table 1. This migration is believed to progress in acidic conditions by the mechanism shown in Scheme 9.²¹² The mixture of products formed led to low yields, and the similarity in the polarity of the side products caused challenging purification. Various reaction times, solvents, and acid catalysts were trialled for this deprotection as detailed within Table 1.



Scheme 9: Acid catalysed acetate migration mechanism

Table 1: Reagents and conditions for acid catalysed trityl deprotection

Entry	Acid (Quantity)	Solvent	Time	Trityl Deprotection Combined Yield (19, 22 + 23)	Ratio of products (19:22:23)	Desired Product Yield (10)
1	p-TsOH (0.3 equiv)	MeOH	5 h	29%	- ^a	- ^a
2	p-TsOH (0.2 equiv)	MeOH	4 days	22%	- ^a	- ^a
3	CSA (0.2 equiv)	4:1 DCM:MeOH ^b	24 h	54%	1:1.5:1	14%
4	CSA (0.1 equiv)	4:1 DCM: MeOH ^b	3 days	33%	1:1:1	11%
5	HCl (cat.)	1:1 DCM:AcOH	1 h	45%	1:0.5:0.5	22%
6	Pyr p-TsOH (0.5 equiv)	DCM	4 days	50%	1:1:1	17%
7	Pyr p-TsOH (0.5 equiv) with TIPS as ion scavenger	DCM	4 days	Results are the same as without TIPS addition. (Entry 6)		

^aSide products **22** and **23** not known at this point, only yield of combined products known
^bCSA only partially soluble in DCM

Initial trityl deprotection strategies followed literature conditions with p-TsOH in methanol, and CSA in DCM: MeOH (Entries 1-4).²¹³⁻²¹⁵ These procedures gave varied reaction times from hours

to days, however, even after days with TsOH as a catalyst (entry 2), the trityl starting material **18** remained mostly intact with only a small amount of conversion to the deprotected product. Upon following the alternate reaction with CSA (entries 3 and 4), the presence of the undesired side products from acetate migration were identified. Despite the much higher rate for loss of the trityl group (i.e. faster conversion of starting material), the presence of the undesired acetate migration products lead to low overall product yields. Following this, an alternative procedure utilising catalytic HCl in DCM: AcOH was investigated as detailed in literature on a trityl and acetate protected disaccharide.²¹⁶ This procedure (entry 5) had a much higher rate of trityl deprotection with the majority of the starting material **18** consumed within 1 hour. The overall yield of trityl deprotected product from the HCl catalysed deprotection was 45% with small amounts of side product from the loss of the TBDPS group also observed. Despite the fast reaction rates seen, acetate migration products were still formed in large quantities reducing the yield of the desired product to 22%.

Estimates of pKa values for the conjugate acids of the trityl ether in comparison to the acetyl carbonyl show the acetate to have a pKa value that is 2 units lower (Table 2), meaning it is 100 times more acidic than the trityl oxygen. This means that the trityl oxygen should be preferentially protonated, and therefore deprotected in preference to the migration of acetate. An alternative procedure, which utilised the pyridinium salt of p-TsOH was investigated, which had been shown in literature as a catalyst for trityl deprotection.²¹⁷⁻²¹⁹ As its pKa was much higher than the previously utilised catalysts, and the reaction mixture much less acidic, it was hoped this would even more greatly favour trityl deprotection over acetate migration. As expected the rate for trityl deprotection was much lower than seen before (entry 6), however, acetate migration was still observed. As a way of aiming to accelerate the trityl removal, the addition of 2 equivalents of TIPS to the p-TsOH pyridinium salt deprotection was investigated. This compound is commonly utilised as an ion scavenger for trityl-derived cations during peptide synthesis,²²⁰ and it was hoped that scavenging the trityl ion as it was formed would drive the equilibrium to cause further trityl deprotection. However, this did not occur and reaction rates and yields were found to match those without the addition of TIPS (entry 7).

Table 2: Approximate pKa values for the acetate-carbonyl and trityl-ether conjugate acids and acid catalysts²²¹⁻²²³

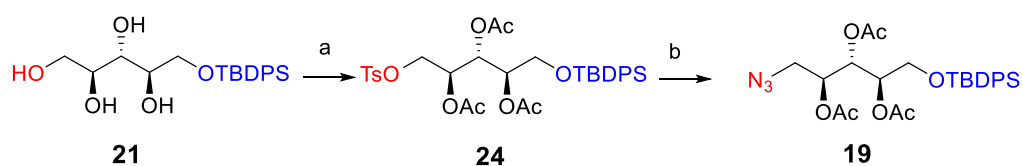
Compound	pKa
Protonated trityl ether oxygen	-3 (approx.)
Protonated ester carbonyl oxygen	-7 (approx.)
p-Toluene sulphonic acid	-2.8
Camphor sulphonic acid	1.2
HCl	-6.3
Pyridinium p-Toluene sulphonate	5.2

The much higher rates for acetate migration on the ribitol substrate vs the rates reported for the previously mentioned disaccharide in literature²¹⁶ can be rationalised by the ring-opened structure of ribitol. This structure offers a much higher amount of flexibility which allows the deprotected alcohol to more easily adapt to the conformation required for an attack on the neighbouring acetate group. Conversely, it is much harder for a primary alcohol on a ring closed pyranose sugar to reach the desired orientation. As well as the loss of flexibility, the fixed orientation of neighbouring groups on opposite faces of the ring, as seen within the abovementioned disaccharide, further increases the relative distances between the free alcohol and acetyl groups preventing migration. This same effect is also seen later within Chapter 5: *Synthesis of Glucose Substrates*, (pg. 144), where a C-6-deprotected acetylated glucose derivative is efficiently synthesised through trityl deprotection in moderate yields. In that case acetate migration was observed to a much lesser degree than for the ribitol compound.

Following the results from acidic cleavage, the removal of the trityl group in the presence of hydrogen with activated Pd/C was attempted as reported by Wróblewski and Bąk-Sypień in 2007.²²⁴ After leaving the reaction in a hydrogen atmosphere under balloon pressure for 24 h, no change was seen by either TLC or MS (ESI) of the crude reaction mixture. After filtering through celite, the filtrate was dried *in vacuo* to give only pure starting material, as evidenced by ¹H NMR. Other literature procedures for hydrogenation of trityl ethers utilise high-pressure hydrogenation to achieve results, but with no sign of reaction seen under atmospheric pressure and the lack of easily accessible high-pressure hydrogenation equipment available this methodology was not further investigated

Route 3b

Moving forward, an alternative pathway to synthesis of the desired azido ribitol compound **19** was investigated, this time utilising a toluene sulphonate group (tosylate) as a primary hydroxyl selective group. As well as being selective for the primary hydroxyl group, this group also serves as an efficient leaving group for the conversion of alcohols to azides.^{225, 226} The alternative proposed route from compound **21** to **19** is presented in Scheme 10.



Scheme 10: Alternative route to the synthesis of compound **19**, **Reagents and Conditions** a) TsCl, pyridine, 0°C, 3 h, then Ac₂O, 0°C, 4 h (27%) b) NaN₃, DMF, 60°C, 24 h (25%)

Initial attempts at this synthesis found that leaving the tosylation step overnight, followed by acetylation overnight at room temperature, led to very low formation of the desired tosyl intermediate **24**. Instead, the major product isolated was the fully acetylated side-product **25**, alongside a small amount of non-fully acetylated tosylated product. A mixture of mono- and *di*-acetylated tosyl-containing side products were obtained, and leaving these to acetylate overnight at 4 °C produced mainly the fully acetylated side product **25** (70%). These results suggested that the tosyl group was unstable to the acetylation conditions. In an attempt to monitor both reactions more closely and prevent the loss of the tosyl group, each of the steps was run for 3 hours at 0°C. This led to the formation of the desired intermediate **24** and fully acetylated product **25** in addition to a new undesired side product. This side product is believed to be compound **26** (Scheme 11A), formed by the ring-closing elimination of tosylic acid through S_N2 substitution by the attack of the alcohol at the 4-position. Evidence for the identification of this product came from the presence of an ESI-MS peak correlating to the elimination of tosylic acid. Furthermore, no double bond or carbonyl peaks were seen within the ¹H NMR or ¹³C NMR spectra which would have been present had elimination occurred to form the corresponding elimination product **27** or its tautomer **28** (Scheme 11B). Additional proof of the formation of compound **26** came from the lack of reaction with the reducing agent NaBH₄. This would be expected to reduce a ketone or double bond-containing species **27** and **28**.²²⁷⁻²²⁹ Although this reagent is also used for ring-opening reduction, the absence of an anomeric alcohol in **26** prevents this from occurring.

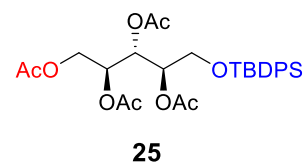
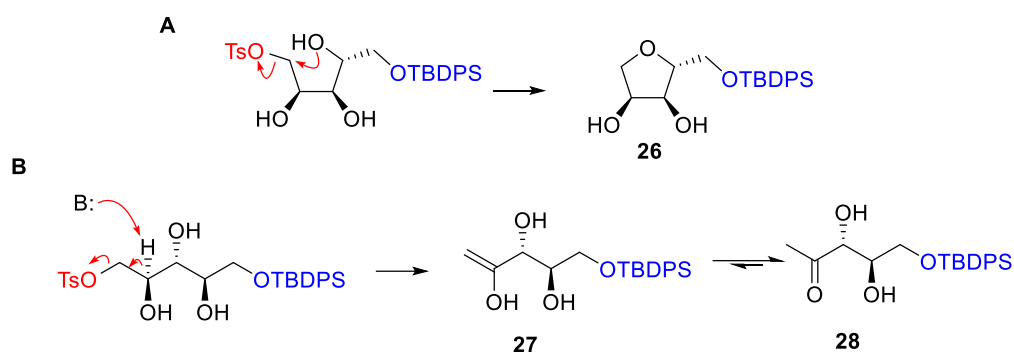
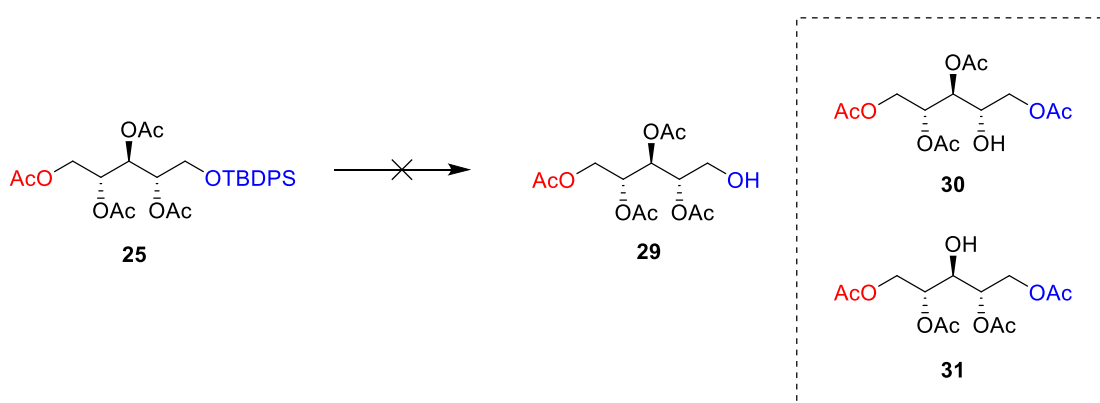


Figure 14: Fully acetylated major side product **25** formed in the synthesis of compound **19** from **21**



Scheme 11: A) Formation of elimination product compound **26**, B) Mechanism for the formation of alternative possible elimination products **27** or **28**

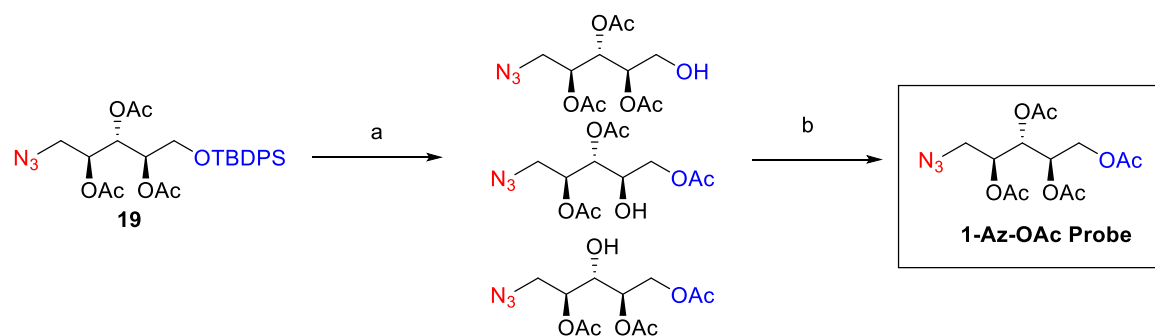
From compound **21** the tosylated, acetylated intermediate **24** was obtained by an optimised method running each step for 3 hours at 0°C, giving a yield of 27% over two steps with the product obtained in quantities of around 100 mg. Azide substitution of the tosylate in **24** at 60°C overnight gave a yield of 25%. Overall, this produced compound **19** in a yield of 7.1% from compound **21** (Scheme 10). Though the overall yield for these steps was low (4% from D-ribose), this synthesis required fewer synthetic and purification steps and took less time than the previously proposed method (route 3A utilising acidic removal of trityl, yielding 7% up to the point of azide substitution). Additionally, the starting material for this reaction (**21**) was easy to synthesise in the large quantities required for the scale-up of this route.



Scheme 12: Attempted synthesis of 1,2,3,4-tetra-O-acetyl ribitol **29** and side products formed **30** and **31** Reagents and Conditions: TBAF, THF, 0°C-r.t. 18 h (44% 2:3 mixture of **30** and **31**)

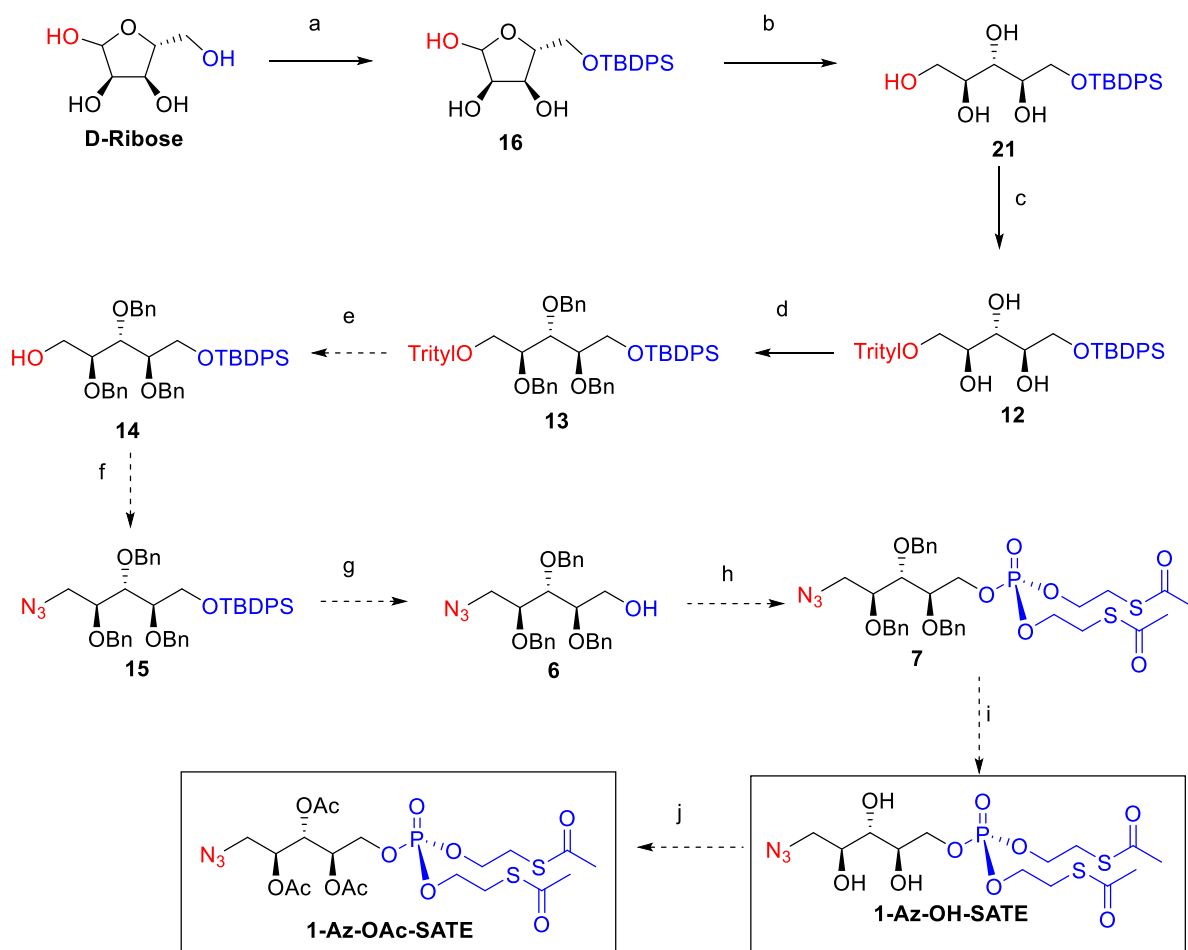
It was realised that side-product **25** provided a useful intermediate towards a *tetra*-acetylated ribitol derivative on which the SATE phosphate addition could be explored (**29**). TBDPS deprotection was attempted, however, similarly to the trityl deprotection seen previously, removal of the TBDPS group also caused acetate migration. Rather than the desired 5-position being deprotected, migration caused formation of the side products 1,2,3,5-*tetra*-O-acetyl-ribitol **30** and 1,2,4,5-*tetra*-O-acetyl-ribitol **31** (Scheme 12). As this prevented the addition of a phosphate selectively at C-5, the synthesis of **1-Az-OAc-SATE** *via* the use of acetate protecting groups (Scheme

10) was abandoned. All of the previously synthesised azido-containing ribitol compound (**19**) was pooled to synthesise the fully acetylated, non-phosphorylated probe **1-Az-OAc**. Synthesis of this acetylated probe was conducted as presented in Scheme 13 *via* a one-pot deprotection-acetylation procedure. This method gave an overall yield of 85% over 2 steps affording 5.5 mg of the pure **1-Az-OAc** probe. This probe can be utilised for metabolic labelling of cells, with successful labelling of functional α -DG providing insight into the biosynthetic pathway of D-ribitol-5-phosphate.



Scheme 13: Synthesis of the **1-Az-OAc** probe **Reagents and Conditions:** a) TBAF, THF, 3 h, 0°C-r.t. b) Ac_2O , pyridine, DMAP cat., r.t., 20 h, (91% over 2 steps)

Route 4a



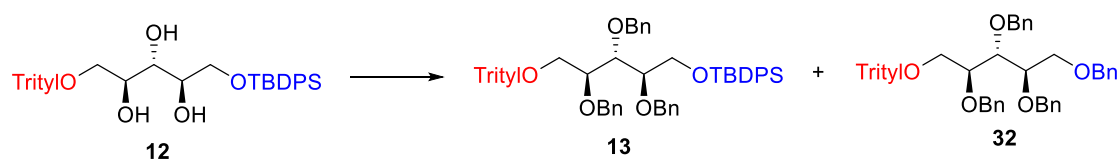
Scheme 14: Route 4a for the synthesis of the 1-Az-OAc-SATE probe **Reagents and Conditions:** a) TBDPS-Cl, DMAP cat., pyridine, r.t., 72 h, (60%) b) NaBH₄, EtOH, r.t., 5 h, (43%) c) TrCl, NEt₃, DCM, r.t., 72 h, (60%) d) BnBr, NaH, TBAI, DMF, 0°C-r.t., 2 h, (25%) **Proposed Conditions:** e) *p*-TsOH, MeOH, r.t., 4.5 h, f) MsCl, NEt₃, DCM, r.t., 24 h, then, NaN₃, DMF, 60°C, 24 h, g) TBAF, THF, 0°C-r.t., 2 h, h) PO(OEt-2Br)₃, Tf₂O, pyridine, DCM, ii) KSAC, acetone, i) BCl₃, DCM, -78°C, 2 h, j) Ac₂O, pyridine, DMAP, r.t., 24 h.

To avoid the issues arising from the use of acetate groups, a new route was designed that reverts back to the use of benzyl groups. The benzyl ether structure (as previously discussed and presented within Scheme 4) prevents migration from occurring as the ester carbonyl structure required for acetate migration (Scheme 9) is not present. It should be noted that the migration of the bulkier benzoyl and pivaloyl ester groups would also be expected to be much slower, and unspecific cleavage less likely to occur than for acetate groups.¹⁹⁰ Though commonly utilised protecting groups within carbohydrate chemistry, these alternative ester groups were unsuitable for the synthesis of our SATE containing probes as the conditions for their cleavage (NaOMe in MeOH) would also cleave thioacetate groups on the SATE phosphate.^{210, 211, 230}

Route 4A (Scheme 14), which utilises benzyl groups, proceeds by the initial formation of **12** as seen in previous routes 2 (Scheme 7) and 3A (Scheme 8). Continuing on, the protection of the secondary alcohols with benzyl groups instead of acetates would yield the fully protected compound

13, in the structure of **Key Intermediate 1**. Selective removal of the trityl group would then allow for site-selective azide substitution at C-1 yielding **15**. Removal of the TBDPS group would then provide the **Key Intermediate 2** compound **6** which allows for the formation of all 5 **1-Az** probes as previously discussed (Scheme 5).

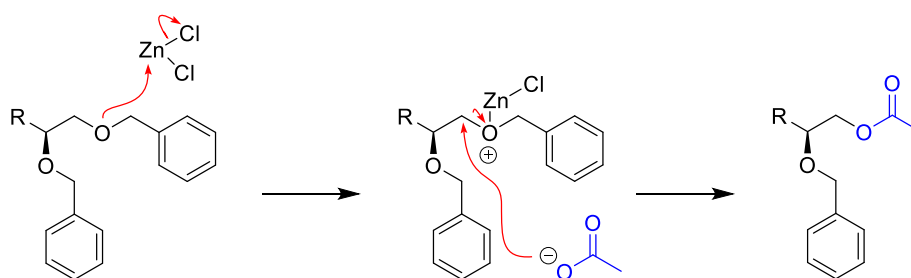
Unfortunately, the benzylation of compound **12** to form the fully protected compound **13** was found to cause the loss of the TBDPS group. This led to the formation of the undesired side product **32** alongside the desired **13** (Scheme 15).



Scheme 15: Benzylation of compound **12** Reagents and Conditions: NaH, BnBr, TBAI, DMF, 0°C – r.t., 4 h (**13** = 25%, **32** = 20%)

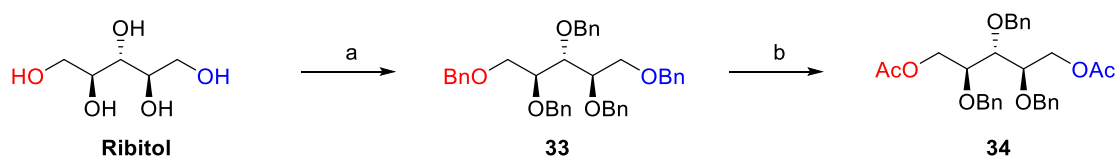
This side reaction is referenced within literature,^{231, 232} though it is reported to occur to a much lesser degree. Even when following these literature conditions, the desired compound was obtained in a ratio of 1.3:1 to the undesired side-product, as well as in low overall benzylation yield (44%). The close polarity of these two products led to difficulties in isolating them from one another by flash column chromatography. Different conditions to optimise the benzylation of compound **12** were attempted. These included varying reaction times, increasing the equivalents of reagents, and adding reagents portion-wise over longer periods. These reactions all gave evidence of the loss of TBDPS, in addition to the incomplete benzylation of the rest of the free hydroxyl groups. Large amounts of incompletely protected product were obtained, even when following the same conditions as for the high yielding formation of 1,2,3,4,5-*O*-penta-benzyl-ribose **33** (Scheme 17). Upon closer monitoring of the reaction by TLC, the loss of TBDPS was shown to occur on the addition of NaH before adding BnBr. To avoid this issue, an alternative benzylation procedure utilising BaO and Ba(OH)₂ was investigated but this was still shown to cause loss of TBDPS and resulted in no formation of desired compound **13**.

It was hypothesised that compound **6** could be synthesised from the 1-azido-2,3,4,5-*tetra-O*-benzylated-ribose sugar **36**, by utilising primary selective debenylation of the benzyl group at the 5-position. In literature, the selective acetolysis of primary benzyl groups has been successful on a wide range of sugars of varied structures both ring-closed,^{233, 234} ring-opened,²³⁵ and in the presence of azides.²³⁶ This methodology utilises ZnCl₂ in the presence of acetic anhydride in acetic acid. The selectivity of this site-specific acetolysis is believed to be promoted by the higher accessibility of the primary site to be activated by ZnCl₂ as shown in Scheme 16. Once the benzyl group is converted to an acetate group, this can be selectively cleaved with the use of sodium methoxide in methanol.



Scheme 16: General mechanism of the ZnCl_2 -mediated site-selective acetolysis of benzylated sugars

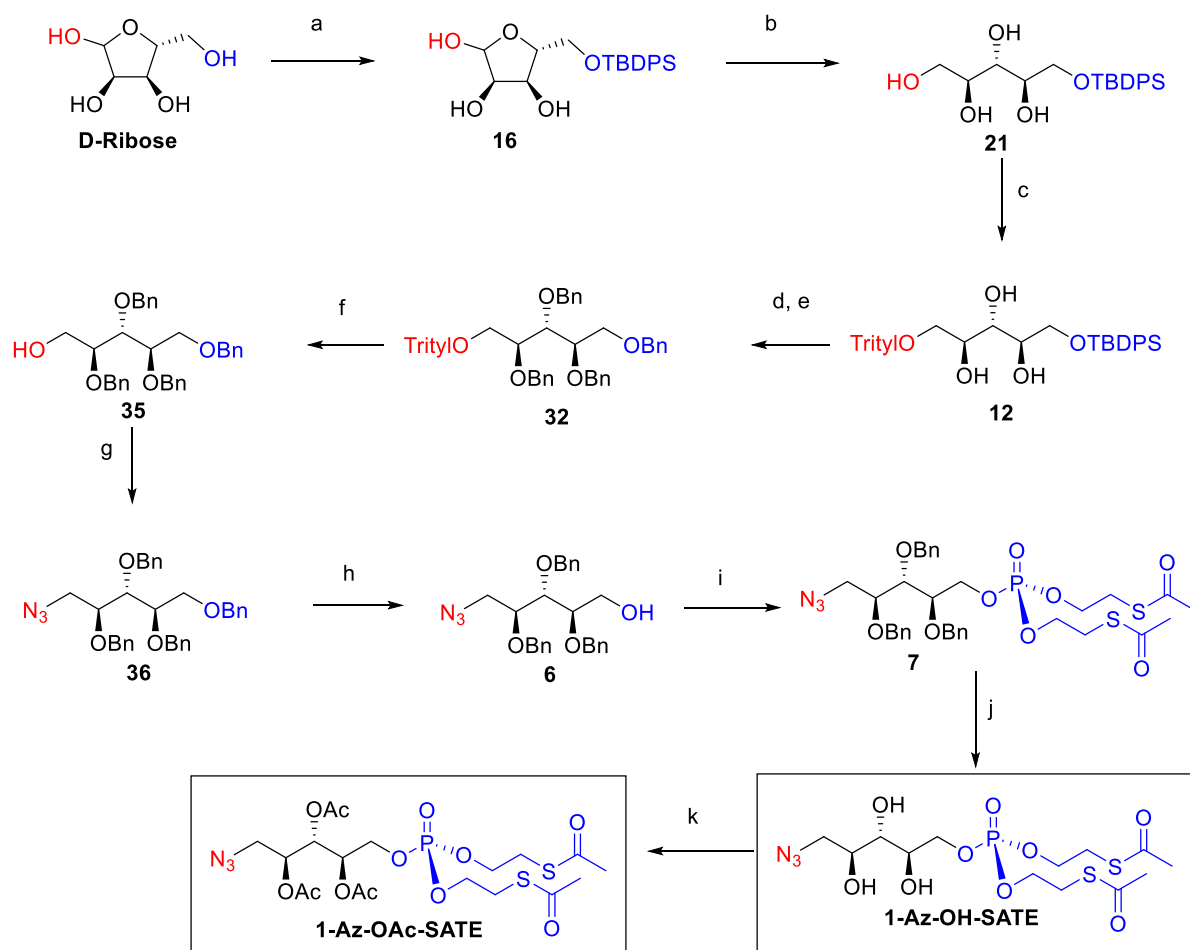
To test the primary-selective acetolysis reaction on a ribitol substrate, the reaction was initially run on the fully benzylated ribitol substrate, 1,2,3,4,5-*penta-O*-benzyl-ribitol **33** (Scheme 17).



Scheme 17: Selective debenzylation test with fully benzylated ribitol **33** **Reagents and Conditions:** a) BnBr , NaH , TBAI, DMF, 0°C -r.t., 24 h, (67%) b) ZnCl_2 , Ac_2O , AcOH , r.t., 3 h, (92%)

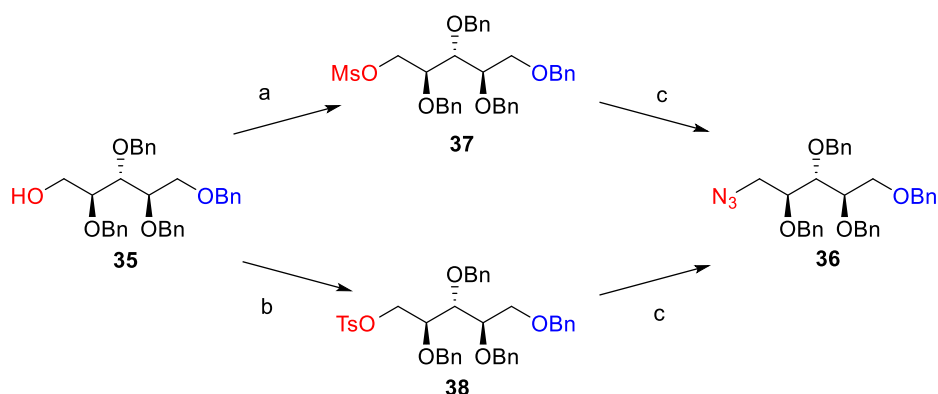
This reaction was found to be successful, providing the expected acetylated intermediate **34** in very high yields (92%). Following on from the success of this reaction, the final route to **1-Az-OAc-SATE** was designed (Scheme 18), utilising the selective deprotection of the primary benzyl group in an optimised strategy to compound **6**.

Route 4b



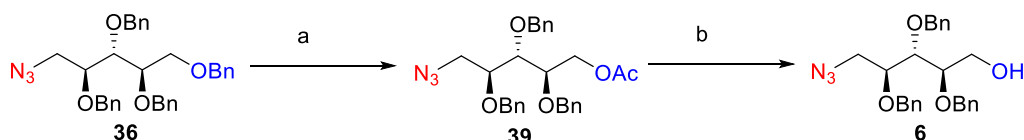
Scheme 18: Route 4b for the synthesis of **1-Az-OAc-SATE** Reagents and Conditions: a) TBDPS-Cl, DMAP cat., pyridine, r.t., 72 h, (60%) b) NaBH₄, EtOH, r.t., 5 h, (43%) c) TrCl, NEt₃, DCM, r.t., 72 h, (60%) d) TBAF, THF, 0°C-r.t., 2 h, (75%) e) BnBr, NaH, TBAI cat., DMF, 0°C-r.t., 2 h, (82%) f) *p*-TsOH, MeOH, r.t., 4.5 h, (75%) g) MsCl, NEt₃, DCM, r.t., 24 h, then, NaN₃, DMF, 60°C, 24 h, (46%) h) i) ZnCl, Ac₂O, AcOH, r.t., 2 h, ii) NaOMe, MeOH, r.t., 2 h, (69% over 2 steps) i) PO(OEt-2Br)₃, Tf₂O, pyridine, DCM, (42%) ii) KSAC, acetone, (quant.) j) BCl₃, DCM, -78°C, 2 h, (quant.) k) Ac₂O, pyridine, DMAP, r.t., 24 h (quant).

The synthesis was adapted as presented within Scheme 18, with de-silylation of the ring opened compound **12** and subsequent benzylation providing compound **32** which was then selectively de-tritylated under acidic conditions to afford compound **35**. With a new method for the synthesis of compound **6** from **35** designed, an investigation into the best method for azidation of **35** to form **36** took place. As azidation *via* a tosyl intermediate had previously been investigated and utilised within Route 3B, this was chosen as a starting point in the synthesis of **36**. Previously the primary selectivity arising from the larger steric bulk of the tosyl group was required, so the use of a mesyl group was not considered. However, with only the site of azide addition uncovered in **35**, the use of this smaller group was considered. To investigate the effect on reaction time and yields between the two intermediates, the azidation of compound **35** to reach **36** was attempted utilising both tosylation and mesylation (Scheme 19).



Scheme 19: Synthesis of **36** via OMs and OTs intermediates **Reagents and Conditions:** a) MsCl, pyridine, DCM, 0°C-r.t., 3 h, b) TsCl, pyridine, DCM, 0°C-r.t., 24 h c) NaN₃, DMF, 80°C, 24 h, (46% via OMs, 28% via OTs)

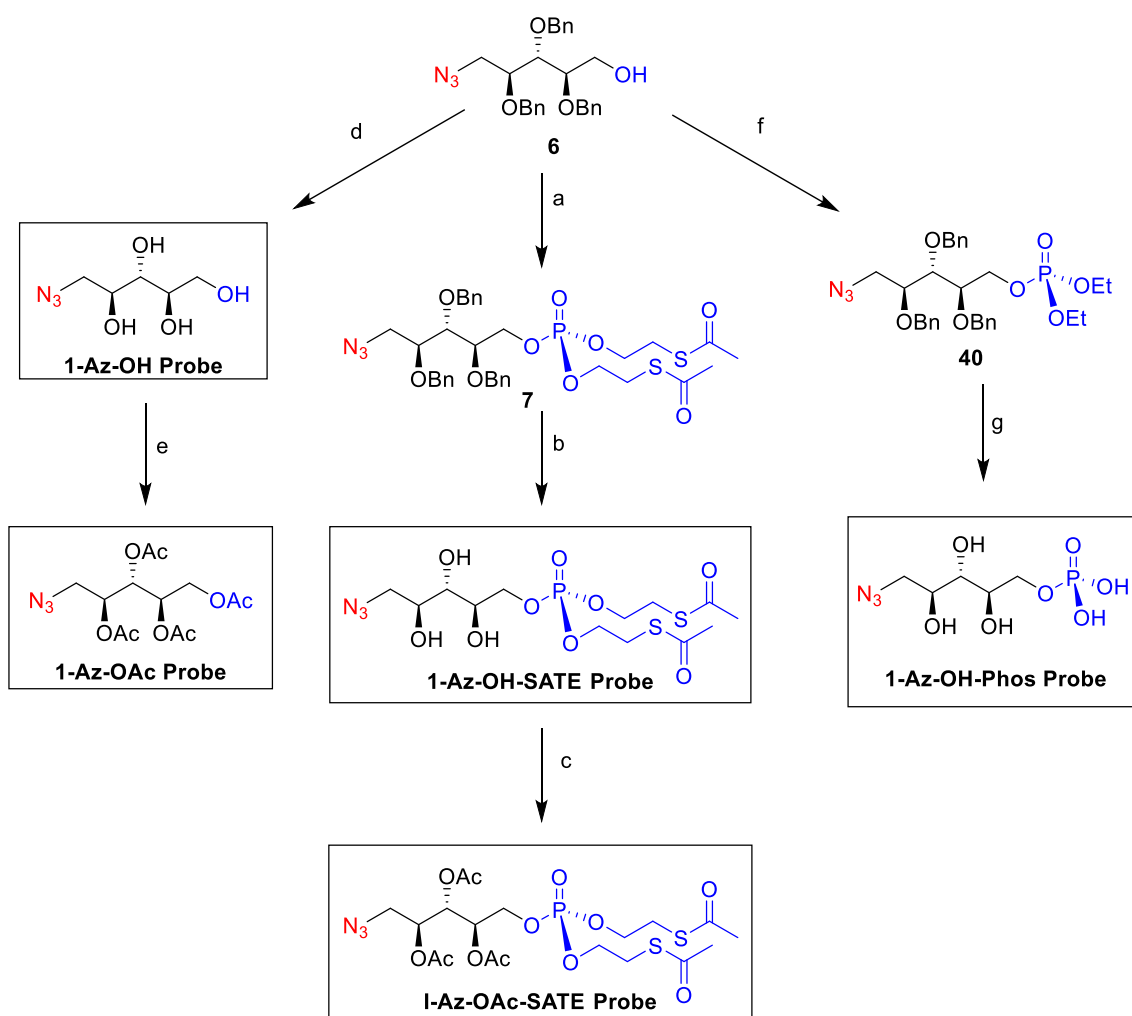
As anticipated from their respective sizes, the mesyl intermediate **37** formed much faster than the tosyl compound, requiring 3 h for full conversion compared to the 24 h of the tosyl intermediate **38**. In addition, azidation *via* the mesylate intermediate was found to provide higher yields of product **36** (46% vs 28%). In both cases, the unreacted starting material was recovered, and no intermediate mesyl or tosyl product was recovered from the reaction. Additionally, no side products from elimination reactions were seen, despite this being reported elsewhere.²²⁵ With compound **36** successfully synthesised, the selective debenzylation of intermediate **36** was run following the same procedure as before (Scheme 20), providing **39** in a yield of 93%. NMR showed the product to be pure after work-up, so this product was directly used without further purification for the de-acetylation step to form **6** in 75% yield (69% over two steps from **36**).



Scheme 20: Two-step selective debenzylation of the primary benzyl group of **36** to form **6** a) ZnCl₂, Ac₂O, AcOH, r.t., 2 h (93%) b) NaOMe, MeOH, r.t., 3.5 h, (73%)

With the synthesis of compound **6** now successful, all 5 **1-Az probes** could be produced as previously discussed (Scheme 5). Incorporation of the SATE phosphate moiety proceeded *via* a newly developed methodology for SATE phosphate synthesis based on 2018 literature for the synthesis of *di*-ethyl phosphates (See Chapter 4, pg. 107).^{237, 238} This two-step procedure involves the initial incorporation of a *bis*(2-bromoethyl) protected phosphate and subsequent substitution of bromine with thioacetate to yield the desired *bis*(SATE) protected phosphotriester probe. SATE phosphate incorporation at the 5- position of compound **6** by this method was successful, yielding the desired SATE containing benzylated intermediate **7** in an initial yield of 13%, which after the optimisation conducted within Chapter 5 (see Table 8, pg. 141) rose to 42% (Scheme 21). To synthesise the desired **1-Az-OH-SATE** and **1-Az-OAc-SATE** probes, in which the ribitol hydroxyl groups are unprotected or acetylated, respectively, compound **7** was treated with an excess of BCl₃ in

anhydrous DCM to cleave the benzyl groups and subjected to column chromatography to yield the **1-Az-OH-SATE** probe. This was then acetylated in a 1:2 ratio of acetic anhydride: pyridine to yield the fully protected **1-Az-OAc-SATE** probe. Both the debenzoylation and acetylation *via* these methods were found to give quantitative yields. This led to overall yields of 42% from the key intermediate **6** to both the **1-Az-OH-SATE** and **1-Az-OAc-SATE** probes, and an overall yield of 0.93% over 12 steps from D-ribose.

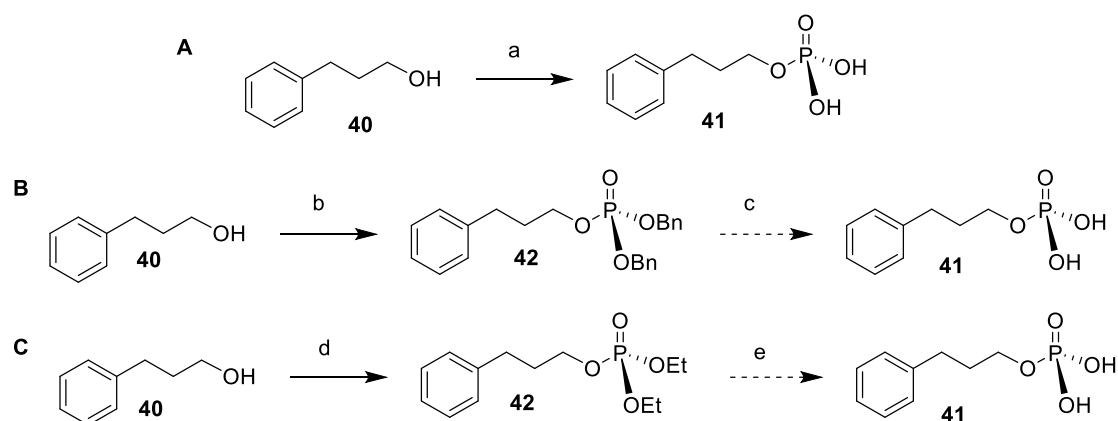


Scheme 21: Synthesis of final ribitol and ribitol-5-phosphate probes from Key Intermediate compound 6: Reagents and Conditions a) i) PO(OEt-2Br)₃, Tf₂O, pyridine, DCM ii) KSAC, acetone, (42%) b) BCl₃, DCM, -78°C, 4h, (quant.) c) Ac₂O, pyridine, DMAP r.t., 24h, (quant.) d) BCl₃, DCM, -78°C, 4h, (quant.) e) Ac₂O, pyridine, DMAP, r.t., 24h, (quant.) f) EtO₃PO, Tf₂O, pyridine, r.t., 1.5 h, (55%) g) i) TMSBr, DCM, r.t., 16 h, ii) BCl₃, DCM, -78°C, 4 h, (56% over two steps)

To obtain ribitol-based non-phosphorylated probes compound **6** was subjected to the same conditions for debenzoylation providing the **1-Az-OH** probe. Acetylation then afforded the **1-Az-OAc** probe in quantitative yield, and an overall yield from D-ribose of 2.3% over 10 steps. In future, the synthesis of the non-phosphorylated probes can be further simplified by obtaining them from the fully benzylated azido-ribitol substrate **36** because they do not require selective deprotection of the 5-position.

Incorporation of a Deprotected Phosphate Monoester for the Synthesis of 1-Az-OH-Phos

The formation of the fully deprotected **1-Az-OH-Phos** probe was the largest divergence from the route to the alternative probes. Initial tests for the formation of this probe considered the addition of a phosphate group by reaction with POCl_3 , followed by hydrolysis (Scheme 22A). This procedure was investigated utilising the model alcohol 3-phenyl-propanol (**40**). Despite a peak for the desired phosphate product (**41**) being seen by ESI-MS, ion-exchange chromatography was found to be unsuccessful in isolating the desired product, and no product was recovered. Additional concerns about this methodology were raised over the use of POCl_3 in the presence of benzyl groups, as benzyl groups are deprotected by the use of Cl^- ions.²³⁹⁻²⁴¹



Scheme 22: Investigated methodologies for the synthesis of the free-phosphate containing probe utilising the simple alcohol 3-phenyl-propanol as a model substrate **Reagent and Conditions** a) POCl_3 , pyridine, THF, H_2O (0%), b: via Mitsunobu) DIAD, PPh_3 , NEt_3 , THF, r.t., 16 h (0%), via DCC coupling) DCC, NEt_3 , DCM, r.t., 18 h (16%) via dibenzyl-chlorophosphate) oxalyl chloride, NaH , DCM, r.t., 3 h, (32%) d) triethyl phosphate, Tf_2O , pyridine, DCM, (39%) **Proposed Reagents and Conditions** c) BCl_3 , DCM, e) TMSBr

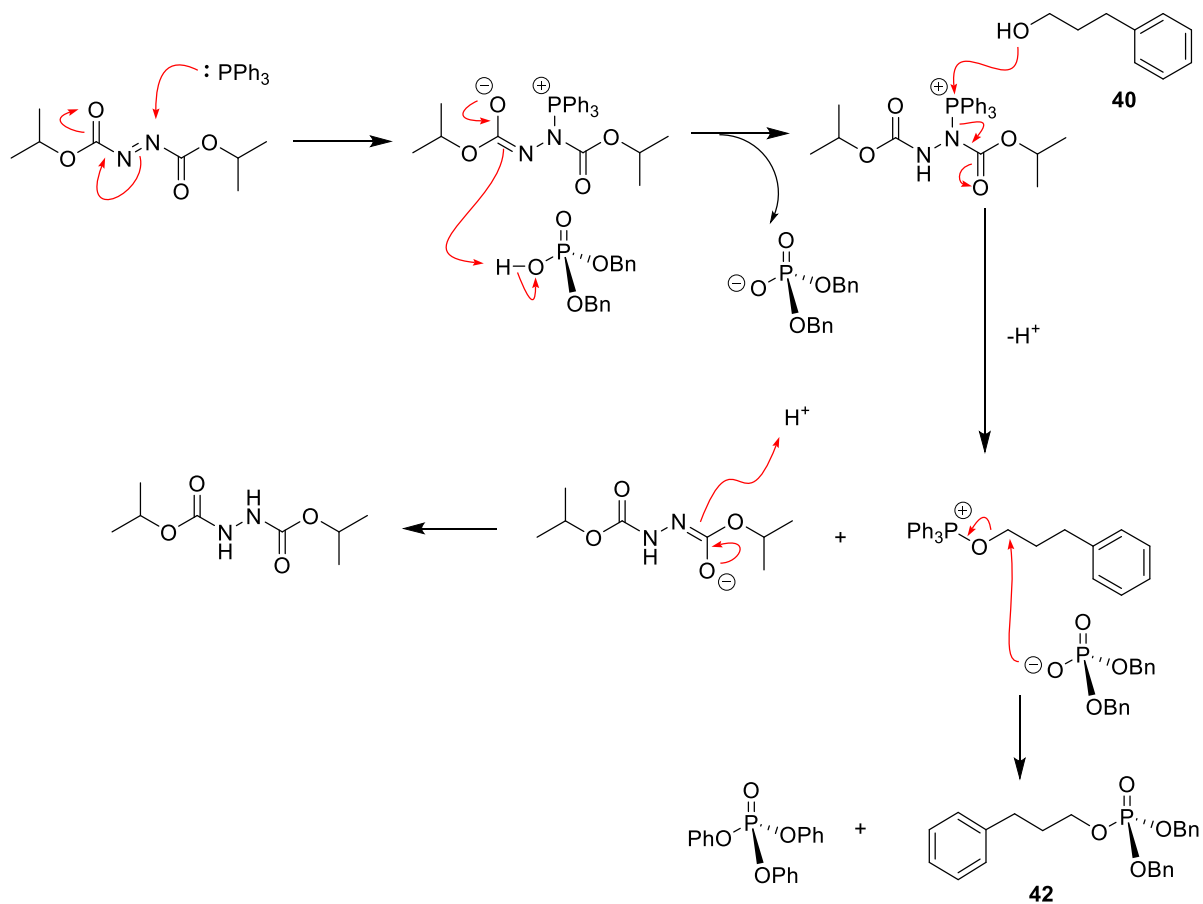
Alternative methods for the synthesis of the **1-Az-OH-Phos** probe were based on the incorporation of a protected phosphate moiety which could subsequently be cleaved to produce the deprotected probe. Incorporation of a protected phosphate would enable column chromatography for purification, which is not possible after the incorporation of a free phosphate. The initially investigated phosphate for this addition was dibenzyl phosphate. Not only was the diphosphate starting material required for this synthesis commercially available, but the removal of benzyl groups to form the free phosphate would utilise BCl_3 , which simultaneously would cause desirable deprotection of the benzyl groups on the sugar.^{240, 241}

Literature shows numerous methods for the coupling of diester phosphates to alcohols. These include Mitsunobu reaction,^{242, 243} the use of coupling reagents such as DCC,²⁴⁴ and by activation with oxalyl chloride to form an acid chloride *in situ* which can undergo substitution to

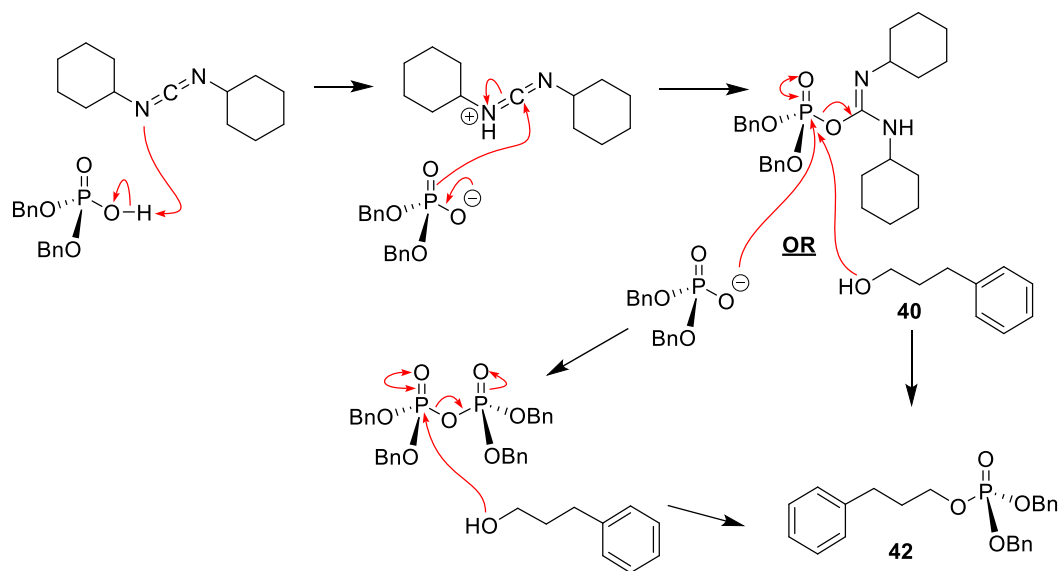
form the benzylated phosphate product.^{245, 246} Each of these methodologies was attempted on the model alcohol 3-phenyl-propanol.

The Mitsunobu methodology, utilising PPh₃ and DIAD, was found to be unsuccessful on the simple 3-phenyl-propanol substrate with no product obtained following column chromatography (Scheme 22B). Contrastingly the DCC coupling method was found to be successful, though in low yield (16%, Scheme 22B). A higher yield was obtained through the chlorophosphate methodology, by activation of the *di*-benzyl phosphate with oxalyl chloride. On substitution of this activated phosphate with 3-phenyl-propanol, a yield of 32% for compound **42** was obtained (Scheme 22B).

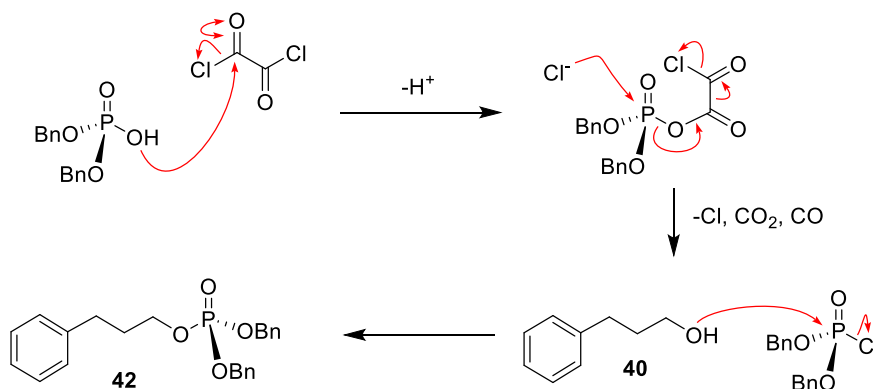
The reduced reactivity seen for the phosphate addition with both Mitsunobu and DCC coupling conditions can be rationalised by the mechanisms for these reactions (Scheme 23 and Scheme 24 respectively). In the case of both the mechanisms for the DCC coupling and Mitsunobu methodology the nucleophilic attack of the reacting alcohol (3-phenyl-propanol) occurs at a large sterically hindered intermediate formed by the reaction with DCC or DIAD respectively. As well as steric hindrance for the attack of the alcohol, the higher bulk of the dibenzyl phosphate will also negatively affect interaction between the phosphate and either DCC or DIAD. Contrastingly, in the case of the chlorophosphate reaction, the attack of the alcohol occurs at a less sterically hindered, more highly reactive activated phosphate intermediate (Scheme 25).



Scheme 23: Mechanism for the Mitsunobu reaction between dibenzyl phosphate and 3-phenyl-propanol **40**



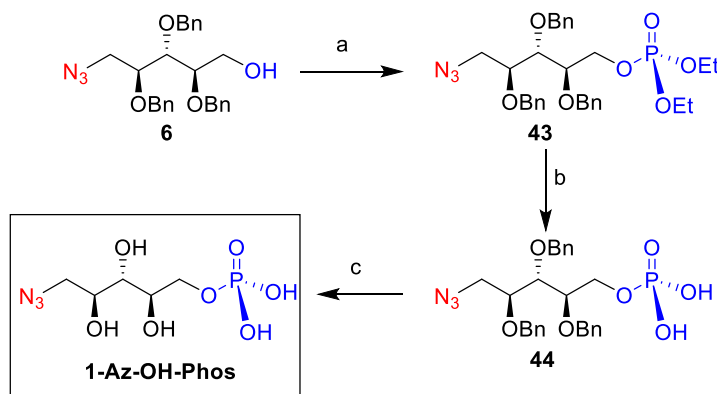
Scheme 24: Mechanism for the DCC coupling reaction between dibenzyl phosphate and 3-phenyl-propanol **40**



Scheme 25: Mechanism for the oxalyl chloride activated reaction between dibenzyl phosphate and 3-phenyl-propanol **40**

With the pre-activation with oxalyl chloride providing the highest yield in the 3-phenyl-propanol screens, this reaction was attempted on the *tetra*-benzyl-ribitol compound **35** (Scheme 26). Initial tests utilising the same reaction conditions for the reaction with 3-phenyl-propanol provided the desired fully benzylated product in yields of 20%. To increase the yield for this reaction, attempts were made to increase the activation of the diphosphate starting material by using a higher number of equivalents of oxalyl chloride. Rather than increase yields, however, this led to the formation of no desired product and instead degradation and loss of starting material was seen (only 50% of the starting material sugar was recovered by column chromatography). Alongside this, the presence of a major diphosphate side product was noticed and this was identified as the product forming through the addition of dibenzyl phosphate to itself. The inability to increase the final yield of this reaction above the initial 20%, and the difficulties in isolating this compound from the starting sugar, led to an alternative methodology being investigated.

One promising possibility was the triflic anhydride/pyridine activation of phosphotriesters, which was explored in great depth for the synthesis of SATE protected phosphates (See Chapter 4, pg. 104). The literature procedure on which the SATE methodology was based,²³⁷ utilised incorporation of a *bis*-ethyl phosphate by reaction with *tri*-ethyl-phosphate and this reaction was shown to be successful on a benzylated substrate during the development of the SATE methodology. Indeed, the formation of the ethyl phosphate derivative of **6** was successful with yields of 55% and the purification of this product was much simpler than for the benzyl phosphate product (Scheme 26)



Scheme 26: Formation of the **1-Az-OH-Phos** probe from compound **6** **Reagents and Conditions** a) tri-ethyl phosphate, Tf_2O , pyridine, DCM, r.t., 1h, (55%) b) TMSBr, c) BCl_3 , DCM, $-78^\circ C$, 3 h, (56% over 2 steps)

With compound **43** successfully synthesised, work moved towards deprotection of this compound to yield the **1-Az-OH** probe. This was attempted *via* a two-step deprotection. Initially, the phosphate protecting groups were cleaved by the use of TMSBr. This reaction was found to be successful, yielding compound **44** with no loss of benzyl groups observed. There was no evidence of incompletely deprotected phosphate, though a sugar side product was present which is believed to be an alkyl bromide formed by substitution of the phosphate moiety by bromine as indicated within the crude 1H NMR spectrum. No evidence was seen for any ethyl- or silyl-containing side products indicating these were all removed by co-evaporation of the crude reaction mixture with toluene. The crude product of this reaction was carried through to the next step without purification.

Debenzylation of compound **44** with BCl_3 was found to be successful as evidenced by a peak in ESI-MS for the desired product and NMR analysis. There was no longer evidence for the brominated side-product within the ESI-MS or by NMR, and instead, the only other product seen within the NMR was the side product **45**. This is believed to have formed similarly to the tosylation side products described previously (Scheme 11, pg. 71). 1H and ^{13}C NMR data obtained for the crude product confirmed the desired **1-Az-OH-Phos** probe, and all other peaks correlated with literature data for the side product **45**.

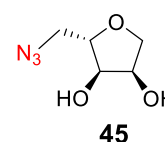


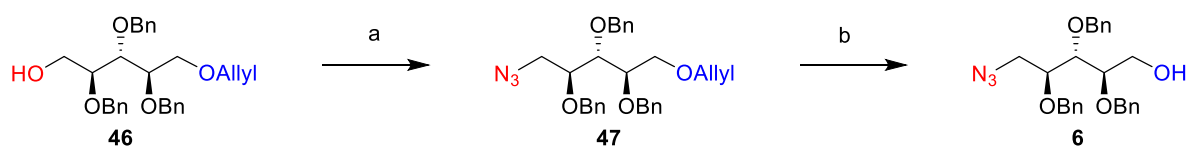
Figure 15: Side product **45** formed by the deprotection of **44**

With the crude deprotected phosphate probe now in hand, ion-exchange chromatography was explored for purification of this probe using a model system consisting of glucose and glucose-1-phosphate. However, this was unsuccessful and showed decomposition of the sugar-phosphate. Literature for the synthesis of similar phospho-sugars typically utilises purification by HPLC, however, the lack of access to preparative HPLC meant this was not possible. Since the only identified side

product **45** does not carry a phosphate, it will likely not interfere with any planned biological tests and *in vitro* studies of the **1-Az-OH-Phos** probe in the presence of compound **45** can still be run.^a

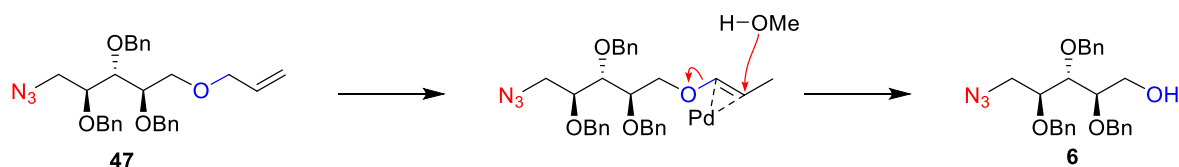
In summary, through the development and optimisation of a synthetic route to compound **6**, all 5 of the **1-Az** probes were successfully synthesised, while only the **1-Az-OH-Phos** probe has been synthesised but not yet fully purified.

Synthesis of Probes from Commercially Available Starting Sugar 5-Allyl-2,3,4-*tri-O*-Benzyl-D-Ribitol



Scheme 27: Synthesis of compound **6** from commercially available 5-allyl-2,3,4-*tri-O*-benzyl-ribose **Reagents and Conditions** a) i) MsCl, pyridine, r.t., 3 h ii) NaN₃, DMF, 100°C, 72 h, (57%) b) PdCl₂, MeOH, r.t., 18 h (63%)

Having developed a successful route to all five of the **1-Az** probes from D-ribose, an alternative procedure to synthesise compound **6** starting from commercially available 5-allyl-2,3,4-*tri-O*-benzyl-D-ribose (**46**) was explored. Efficient synthesis of the key intermediate **6** was achieved in 2 steps (Scheme 27). Initial azidation of the free alcohol utilising a mesylate intermediate yielded the allyl containing ribitol substrate **47**, after which the selective cleavage of the allyl group was achieved by the use of catalytic quantities of palladium(II)dichloride (PdCl₂) in dry methanol. This gave selective cleavage of the allyl group leaving the benzyl groups fully untouched, with the only other recovered sugar being identified as the unreacted starting material.



Scheme 28: Proposed mechanism for the selective allyl deprotection with PdCl₂ based on literature observations reported by Barbier et al²⁴⁷

The proposed mechanism for the selective allyl deprotection is presented within Scheme 28. Evidence for this mechanism is based on observations within literature.²⁴⁷ The majority of allyl deprotection reactions reported with Pd catalysts run in the presence of KCO₃ or a copper-containing regeneration catalyst.²⁴⁸ In our case these are not present, though the reaction was still found to be moderately high yielding with only catalytic quantities of PdCl₂ (63%, 0.2 equivalents). A

^a Preliminary tests run by Willems group PhD student Tom Ward using recombinant ISPD with ribose-phosphate as a substrate and a CMP-Glo kinetic assay for the readout of enzymatic activity showed no turnover, indicating that pentose sugars are unlikely to cause issues and suggesting the side-product **45** will indeed not interfere with *in vitro* testing.

publication by Barbier and co-workers reports a variety of different allyl deprotection conditions.²⁴⁷ They note that the selective removal of allyl groups with PdCl₂ is successful in methanol, but not dichloromethane, tert-butanol, or butylamine. This indicates that methanol itself is essential for the deprotection to proceed. Within the same publication, they propose a mechanism for a similar mercury catalysed allyl deprotection. This mechanism relies on the rearrangement of the allyl double bond, and coordination of mercury to the allyl ether group. This coordination then allows the removal of the allyl group through the attack of water at this coordinated site. As well as explaining why in the absence of alcohol the palladium catalysed deprotection is unable to proceed, and the lack of regeneration catalyst, this also explains why only the allyl groups are cleaved and the benzyl ethers remain untouched, as benzyl groups do not include a site for this metal coordination.

The new synthesis of the **Key Intermediate 2** compound **6** from commercially available 5-allyl-2,3,4-*tri-O*-benzyl-ribose gave an overall yield of 37% over two steps. This provides a much more efficient and shorter method for the synthesis of the **1-Az** probes. Overall this route is 7 steps shorter and gives an overall yield 32% higher than the route to **6** starting from D-ribose.

3.5 Conclusion

The synthesis of a panel of 1-azido-ribose-5-phosphate metabolic labelling probes has been successful, with five probes of varied protecting group strategy obtained for biological testing. As well as accessing final compounds, these routes have utilized the newly developed method of SATE phosphate synthesis which is described in Chapter 4. In addition to the 12-step route from the starting sugar D-ribose, a shorter, higher-yielding, route from the commercially available 5-allyl-2,3,4-*tri-O*-benzyl-ribose sugar has been proven to be successful. While this starting material is more expensive, the costs are compensated by the faster, more efficient method that is 7 steps shorter and improves the yield of key intermediate **6** by over 30%, which will be particularly useful for larger-scale synthesis. Furthermore, the method development and protecting group manipulations discovered will provide a foundation on which routes to alternative ribitol-5-phosphate based probes can be built.

By obtaining probes for use in both *in vivo* and *in vitro* studies we can monitor these probes both in live-cell systems and on the relevant recombinant enzymes ISPD, FKTN and FKRP *in vitro* to confirm whether the 1-azido modifications are tolerated by the enzymes which incorporate ribitol-5-phosphate onto α -DG. Additionally, the non-phosphate-containing ribitol-based probes will allow us to not only gain further information about the biosynthesis of ribitol-5-phosphate within cells, but, if successful, will provide an easier-to-synthesise structure for future generations of probes.

3.6 Experimental

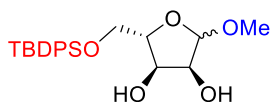
General Experimental

All reactions were conducted in oven dried glass wear under nitrogen, and where specified dry solvents used were either freshly distilled (DCM, DMF, toluene, THF) or from a SureSeal bottle, (DCE, pyridine). Flash column chromatography was run either manually with high purity 220-400 μm particle size silica (Sigma) or on an automated system (Teledyne, CombiFlash NextGen 300+) with 20 to 40 μm particle size silica (RediSep Rf Gold Normal-Phase Silica columns) here specified. Reactions and column fractions were monitored by TLC and visualised by UV and staining. For sugars, the staining consisted of charring with 10% H_2SO_4 in MeOH; for phosphate reactions a KMnO_4 stain was used; and for azido compounds the procedure involved initial reaction with 10% PPh_3 in DCM, followed by staining with ninhydrin.

For phosphate addition reactions all starting materials were dried prior to use by co-evaporation with toluene three times and drying on a high vacuum manifold overnight. Triflic anhydride was distilled over P_2O_5 prior to use and pyridine was used from a SureSeal stored over molecular sieves.

^1H and ^{13}C NMR spectra were obtained either on a JEOL ECS400A spectrometer (400 and 101 MHz respectively) or a Bruker AVIIIHD600 spectrometer (600 and 150 MHz respectively) where specified. Structural assignments were corroborated by homo- and heteronuclear 2D NMR methods (COSY, HMQC and DEPT) where necessary. Chemical shifts are reported in parts per million (ppm, δ) relative to the solvent (CDCl_3 , δ 7.26; CD_3OD , δ 3.31; D_2O , δ 4.79). ^1H NMR splitting patterns are designated as singlet (s), doublet (d), triplet (t), quartet (q), doublet of doublets (dd), doublet of doublets of doublets (ddd), doublet of triplets (dt), apparent triplet (apt t), and so forth. Splitting patterns that could not be visualized or easily interpreted were designated as multiplet (m). Coupling constants are reported in Hertz (Hz). Where sugar NMR data is reported in a ratio of anomers, the NMR data is assigned with integrals as whole integers corresponding to the number of protons within the peak. Where one anomer is greatly preferred, ^{13}C NMR may not be visible for the minor anomer and in those cases the ^{13}C NMR data is reported for only the major anomer. This is denoted by ' ^{13}C NMR (α) δ '

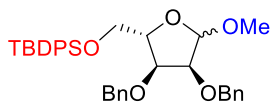
IR spectra were obtained by thin film ATR on a Perkin Elmer Spectrum 2 and $[\alpha]_D$ measurements obtained on a Bellingham Stanley ADP400 polarimeter at the in the given solvent at specified concentration where $C = 1 = 10 \text{ mg/mL}$.



Methyl-5-*O*-*tert*-butyldiphenylsilyl- α,β -L-ribofuranoside

To a stirring solution of L-Ribose (495 mg, 3.30 mmol, 1.00 equiv.) in dry MeOH (20 mL), was added HCl (2 M solution in Et₂O, 0.60 mL, 1.2 mmol, 0.36 equiv.). The resulting solution was allowed to stir at RT for 1 h after which pyridine (10 mL) was added and the solvents removed *in vacuo*. The residue was co-evaporated with pyridine (2 x 7 mL) and left under high vacuum for 30 mins. Pyridine (5 mL) and TBDPS-Cl (1.1 mL, 4.2 mmol, 1.3 equiv.) were added and the resulting solution was stirred for 24 hrs. The reaction mixture was concentrated under reduced pressure and the resulting residue was dissolved in EtOAc (20 mL) and washed with H₂O (20 mL). The aqueous layer was further extracted with EtOAc (3 x 10 mL) before the combined organic layers were dried over MgSO₄, filtered and concentrated *in vacuo*. The crude product was purified by flash column chromatography on an automated system (gradient 0% to 60% EtOAc in hexane) to afford the title compound as a pale yellow oil (706 mg, 1.82 mmol, 55%) in a ratio of 1:8 α : β .

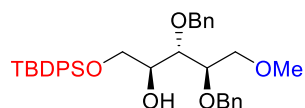
HRMS-ESI: Calculated for: [C₂₂H₃₀O₅Si + Na⁺]: 425.1863, found: 425.1858 **¹H NMR** (400 MHz, CHLOROFORM-*D*) δ 1.05 (s, 9H, α C(CH₃)₃ TBDPS), 1.07 (s, 9H, β C(CH₃)₃ TBDPS), 2.33 (d, *J* = 5.6 Hz, 1H, β OH), 2.55 (d, *J* = 8.2 Hz, 1H, α OH), 2.66 (d, *J* = 3.4 Hz, 1H, β OH), 2.89 (d, *J* = 9.6 Hz, 1H, α OH), 3.31 (s, 3H, β OCH₃), 3.49 (s, 3H, α OCH₃), 3.77 (dd, *J* = 10.5, 5.5 Hz, 2H, α CH-5, β CH-5), 3.83 (dd, *J* = 10.6, 4.9 Hz, 2H, α CH-5', β CH-5'), 4.00 – 4.07 (m, 4H, α CH-3, CH-4, β CH-3, CH-4), 4.19 – 4.26 (m, 1H, α CH-2), 4.30 – 4.39 (m, 1H, β CH-2), 4.85 (d, *J* = 1.3 Hz, 1H, β CH-1), 4.94 (d, *J* = 4.1 Hz, 1H, α CH-1), 7.35 – 7.47 (m, 12H, CH arom.), 7.63 – 7.72 (m, 8H, CH arom.) **¹³C NMR** (101 MHz, CHLOROFORM-*D*) (β) δ ppm: 19.34 (C(CH₃)₃ TBDPS), 26.92 (C(CH₃)₃ TBDPS), 55.31 (OCH₃), 65.17 (CH-5), 72.73 (CH-2), 75.41 (CH-3), 83.06 (CH-4), 108.19 (CH-1), 127.84 129.88, 133.29, 135.66 ((CH arom.)) **IR** (ν_{\max} , film) 3392, 3074, 2930, 2857, 1593, 1471, 1427, 1105, 1050, 974, 893, 699, 502 cm⁻¹



Methyl-2,3-*di-O*-benzyl-5-*O*-*tert*-butyldiphenylsilyl- α,β -L-ribofuranoside (1)

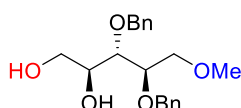
To a stirring solution of Methyl-5-*O*-*tert*-butyldiphenylsilyl- α,β -L-ribofuranoside (187 mg, 0.465 mmol, 1.00 equiv.) in dry DMF (6.5 mL) at 0°C was added BnBr (0.25 mL, 1.9 mmol, 4.1 equiv.), TBAI (5.0 mg, 14 μ mol, 0.029 equiv.) and NaH (60% dispersion in mineral oil, 78 mg, 2.0 mmol, 4.2 equiv.) under N₂. The reaction was allowed to stir at RT for 2 hrs before the reaction was quenched by the addition of MeOH (7 mL) and the reaction mixture was concentrated under reduced pressure. The crude residue was purified by automated flash column chromatography (gradient 0% to 50% EtOAc in hexane) to afford the title compound as a colourless oil (181 mg, 0.310 mmol, 67%) in a ratio of 1:8 α : β .

HRMS-ESI: Calculated for: [C₃₆H₄₂O₅Si + Na⁺]: 605.2699, found: 605.2698. **¹H NMR** (400 MHz, CHLOROFORM-*D*) δ 1.04 (s, 9H, β C(CH₃)₃ TBDPS), 1.08 (s, 9H, α C(CH₃)₃ TBDPS), 3.32 (s, 6H, α OCH₃, β OCH₃), 3.72 (dd, *J* = 11.1, 4.2 Hz, 2H, α CH-5, β CH-5), 3.79 – 3.92 (m, 4H, α CH-4, CH-5', β CH-4, CH-5'), 4.18 (dd, *J* = 6.8, 4.3 Hz, 2H, α CH-3, β CH-3), 4.27 (dt, *J* = 6.8, 4.0 Hz, 2H, α CH-2, β CH-2), 4.46 (d, *J* = 11.9 Hz, 2H, α/β CH₂ OBn), 4.53 (d, *J* = 11.8 Hz, 2H, α/β CH₂ OBn), 4.60 (d, *J* = 12.1 Hz, 2H, α/β CH₂ OBn), 4.68 (d, *J* = 12.0 Hz, 2H, α/β CH₂ OBn), 4.95 (s, 1H, β CH-1), 5.11 (s, 1H, α CH-1), 7.27 – 7.46 (m, 32H, CH arom.), 7.64 – 7.71 (m, 8H, CH arom.) **¹³C NMR** (101 MHz, CHLOROFORM-*D*) (β) δ ppm: 19.56 (C(CH₃)₃ TBDPS), 27.08 (C(CH₃)₃ TBDPS), 55.54 (OCH₃), 64.38 (CH-5), 72.57, 72.68 (CH OBn), 77.88 (CH-4), 80.20, 82.25 (CH-2, CH-3), 106.50 (CH-1), 127.98, 128.08, 128.30, 128.64, 128.70, 129.91, 129.96, 133.72, 135.92 (CH arom.) **IR** (ν_{\max} , film) 3023, 2928, 2856, 1452, 1427, 1105, 608, 503 cm⁻¹



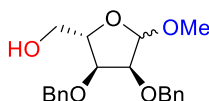
Attempted Synthesis of methyl-2,3-di-O-benzyl-5-O-tert-butylidiphenylsilyl- α,β -L-ribofuranoside (1)

To a stirring solution of methyl-2,3-di-O-benzyl-5-O-tert-butylidiphenylsilyl- α,β -L-ribofuranoside (**1**) (45 mg, 77 μ mol, 1.0 equiv.) in dry toluene (0.75 mL) was added a solution of DIBAL-H (in toluene, 2 M, 0.45 mL, 6.0 equiv) at RT. The reaction was heated to 60°C for 10 mins, after which the reaction was cooled to 0°C and quenched by the addition of 10% NaOH sol. (5 mL). The organic products were extracted with DCM (3 \times 10 mL), and the organic layers were combined, dried over MgSO₄, filtered and concentrated *in vacuo*. The resulting crude residue was purified by flash column chromatography (20%-33% EtOAc in hexane) but gave no desired product, instead partially deprotected side products including both ring opened methyl-2,3-di-O-benzyl-ribofuranoside (**8**) (12 mg, 34 μ mol, 45%) and ring closed methyl-2,3-di-O-benzyl- α,β -L-ribofuranoside (**9**) (15 mg, 43 μ mol, 55%) were obtained as clear oils.



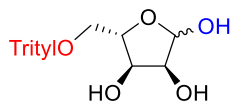
Ring Opened methyl-2,3-di-O-benzyl-D-ribofuranoside (**8**)

HRMS-ESI: Calculated for: [C₂₀H₂₆O₅ + Na⁺]: 369.1678, found: 369.1675 **¹H NMR** (400 MHz, CHLOROFORM-D) δ 2.03 (s, 1H, OH), 2.73 (br s, 1H, OH) 3.37 (s, 3H, OCH₃) 3.58 (ddd, *J* = 10.4, 4.1, 1.6 Hz, 1H, CH-5), 3.65 – 3.77 (m, 4H, CH-1, CH-2, CH-1', CH-5'), 3.77 – 3.88 (m, 2H, CH-2, CH-3), 4.61 (d, *J* = 11.7 Hz, 2H), 4.67 (d, *J* = 11.4 Hz, 2H), 4.75 (d, *J* = 11.7 Hz, 1H), 7.27 - 7.42 (m, 10H, CH arom.) **¹³C NMR** (101 MHz, CHLOROFORM-D) δ 59.36 (OCH₃), 63.70 (CH-1), 71.30 (CH-5), 72.23 (CH OBn), 74.09 (CH-2), 79.01, 79.18 (CH-3, CH-4), 128.08, 128.10, 128.20, 128.66, 137.85 (CH arom.). **IR** (ν_{\max} , film) 3400, 2876, 1496, 1530, 1206, 1097, 1027, 735, 696, 604 cm⁻¹ $[\alpha]_D^{20}$ = +2.53 (*c* = 1.0, DCM)



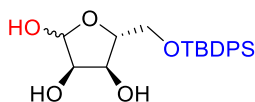
Ring Closed methyl-2,3-di-O-benzyl- α,β -L-ribofuranoside (**9**)

HRMS-ESI: Calculated for: [C₂₀H₂₄O₅ + Na⁺]: 367.1521, found: 367.1515 **¹H NMR** (400 MHz, CHLOROFORM-D) δ 3.37 (s, 3H, CH₃), 3.52 - 3.60 (m, 1H, CH-5), 3.74 - 3.81 (m, 1H, CH-5'), 3.87 (d, *J* = 4.7 Hz, 1H, CH-4), 4.06 – 4.17 (m, 1H, CH-2/3), 4.24 – 4.33 (m, 1H, CH-2/3), 4.50 (d, *J* = 11.4 Hz, 1H, CH OBn), 4.57 (d, *J* = 11.5 Hz, 1H, CH OBn), 4.63 (d, *J* = 11.6 Hz, 1H, CH OBn), 4.67 (d, *J* = 11.8 Hz, 1H, CH OBn), 4.89 (s, 1H, CH-1), 7.28 – 7.43 (m, 10H, CH arom.). **¹³C NMR** (101 MHz, CHLOROFORM-D) δ 55.15 (OCH₃), 62.79 (CH-5), 72.64 (CH-4), 72.82 (CH₂ OBn), 82.45 (CH-2, CH-3), 106.98 (CH-1), 128.03, 128.07, 128.15, 128.60 (CH arom.) **IR** (ν_{\max} , film) 3455, 3035, 2920, 1496, 1453, 1320, 1094, 1027, 934, 735, 696, 567 cm⁻¹



5-O-trityl- α,β -L-ribofuranose (**11**)

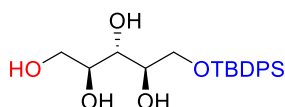
To a stirring solution of L-Ribose (493 mg, 3.28 mmol, 1.00 equiv.) in dry pyridine (7 mL) was added TrCl (1.05 g, 3.75 mmol, 1.14 equiv.) and the resulting solution was allowed to stir for 27 hours at RT after which DMAP (40 mg, 0.32 mmol 0.1 equiv.) was added and the reaction was continued at RT for a further 24 hours. The reaction was quenched by the addition of MeOH (1 mL) and the reaction mixture was concentrated under reduced pressure and co-evaporated with toluene (2 \times 5 mL). The resulting residue was dissolved in DCM (10 mL), washed with sat. NaHCO₃ solution (10 mL), dried over MgSO₄, filtered and concentrated *in vacuo* to afford the crude product. The crude product was purified by flash column chromatography (gradient 20-33% ethyl acetate in hexane) to afford the title product as a white foam (621 mg, 1.58 mmol, 48%) that was found to degrade to ribose and the free trityl group. NMR Data unable to be obtained.



5-*O*-*tert*-butyl-diphenyl-silyl- α,β -D-ribofuranose (**21**)

To two stirring solutions of D-ribose (6.50 g, 43.3 mmol, 1.00 equiv.) and DMAP (50 mg, 0.41 mmol, 0.010 equiv.) in dry pyridine (150 mL) at 0°C was added TBDPS-Cl (11.2 mL, 43.3 mmol, 1.00 equiv.) dropwise. The reactions were allowed to stir at RT for 72 hrs after which each reaction was quenched by the addition of MeOH (20 mL) and the reaction mixture was concentrated under reduced pressure and co-evaporated with toluene (3 x 50 mL). The resulting residues were combined and dissolved in DCM (500 mL), washed with 0.5 M HCl (150 mL), water (150 mL) and brine (150 mL). Each aqueous layer was re-extracted with EtOAc (200 mL) and the combined organic layers were dried over MgSO₄, filtered and concentrated *in vacuo* to afford the crude product. The crude product was purified by automated flash column chromatography (gradient 20 to 70% EtOAc in hexane) to afford the title product as a pale yellow oil (20.1 g, 51.8 mmol, 60%) in a 3:1 ratio of $\alpha:\beta$.

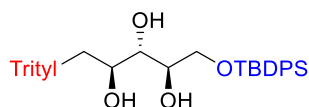
HRMS-ESI Calculated for [C₂₁H₂₈O₅Si + Na⁺]: 411.1498 found: 411.1500 **¹H NMR** (400 MHz, CHLOROFORM-*D*) δ 1.03 (s, 9H, β C(CH₃)₃ TBDPS), 1.06 (s, 9H, α C(CH₃)₃ TBDPS), 3.64 – 3.77 (m, 2H, α CH-5, CH-5'), 3.78 – 3.85 (m, 1H, CH-5), 3.85 – 3.92 (m, 1H, β CH-5'), 3.97 – 4.07 (m, 1H, β CH-4), 4.14 – 4.24 (m, 3H, α CH-2, CH-3, CH-4), 4.47 (t, *J* = 5.3 Hz, 1H, β CH-3), 4.66 – 4.76 (m, 1H, β CH-2), 5.24 (s, 1H, β CH-1), 5.35 (s, 1H, α CH-1), 7.30 – 7.53 (m, 12H, CH arom.), 7.53 – 7.84 (m, 8H, CH arom.) **¹³C NMR** (101 MHz, CHLOROFORM-*D*) (α) δ ppm: 18.44 (C(CH₃)₃ TBDPS), 26.94 (C(CH₃)₃ TBDPS), 64.23 (CH-5), 71.97, 73.70 (CH-2, CH-3), 85.86 (CH-4), 95.87 (CH-1), 127.43, 128.57, 129.99, 130.59, 131.73, 133.33, 135.67, 136.49 (CH arom.) **IR** (ν_{\max} , film) 3380, 3079, 2931, 2858, 1427, 1111, 737, 701 cm⁻¹



5-*O*-*tert*-butyl-diphenyl-silyl-D-ribitol (**21**)

To a stirring solution of 5-*O*-*tert*-butyl-diphenyl silyl- α,β -D-ribofuranose (**16**) (10.0 g, 25.7 mmol, 1.00 equiv.) in EtOH (250 mL) at 0°C was added NaBH₄ (1.96 g, 51.5 mmol, 2.00 equiv.). The reaction was allowed to warm to RT and allowed to stir for 6 hours. The reaction was quenched by the dropwise addition of AcOH (35 mL) and the solvents were removed *in vacuo*. The resulting residue was dissolved in EtOAc (200 mL). After stirring for 10 mins the resulting salt was removed by filtration and the reaction mixture concentrated under reduced pressure. The crude product was purified by automated flash column chromatography (gradient 10 to 100% EtOAc in hexane) to afford the title compound as a pale yellow foam (4.31 g, 11.1 mmol, 43%).

HRMS-ESI Calculated for [C₂₁H₃₀O₅Si + Na⁺]: 413.1755, found: 413.1750 **¹H NMR** (400 MHz, CHLOROFORM-*D*) δ ppm 1.04 (s, 9H, C(CH₃)₃ TBDPS) 3.50-3.80 (m, 7H, CH-1, CH-2, CH-3, CH-4, CH-5), 7.34-7.40 (m, 6H, CH arom.), 7.62-7.68 (m, 4H, CH arom.) **¹³C NMR** (101 MHz, CHLOROFORM-*D*) δ ppm 19.28 (C(CH₃)₃ TBDPS), 26.95 (C(CH₃)₃ TBDPS), 63.31 (CH-1), 65.62 (CH-5), 72.24, 72.91, 73.10, (CH-2, CH-3, CH-4), 127.99, 130.26, 133.22, 135.63, 138.57 (CH arom.) **IR** (ν_{\max} , film) 3369, 3071, 2930, 2888, 2857, 1427, 1105, 1046, 699, 486 cm⁻¹
[α]_D²⁰ = +4.40 (*c* = 1.0, DCM)

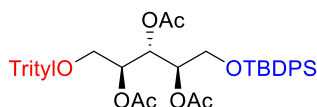


5-*O*-*tert*-butyl-diphenylsilyl-1-*O*-trityl-ribitol (**12**)

To a stirring solution of 5-*O*-*tert*-butyl-diphenyl-silyl-D-ribitol (**21**) (4.40 g, 11.1 mmol, 1.00 equiv.) in dry DCM (180 mL) was added NEt₃ (3.3 mL, 24 mmol, 2.1 equiv.) and TrCl (3.75 g, 13.5 mmol, 1.22 equiv.), and the resulting solution was heated to 60°C for 48 hours. The reaction was quenched with MeOH (10 mL) and the solvent removed *in vacuo*. The crude mixture was then dissolved in EtOAc (500 mL) and washed consecutively with 1M HCl (200 mL), sat. aqueous NaHCO₃ solution (200 mL) and brine (200 mL), and the combined organic layers were dried over MgSO₄, filtered and concentrated *in vacuo*. The crude product was purified by

automated flash column chromatography (gradient from 0 to 60% EtOAc in hexane) to afford the title compound as a pale yellow oil (4.18 g, 6.61 mmol, 60%)

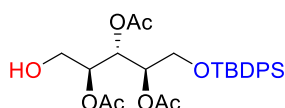
HRMS-ESI Calculated for $[C_{40}H_{45}O_5Si + Na^+]$: 655.2850, found: 655.2863 **1H NMR** (400 MHz, CHLOROFORM-*D*) δ ppm 1.05 (s, 9H, $C(CH_3)_3$ TBDPS), 2.91 – 3.14 (m, 2H, *CH*-1, *CH*-1'), 3.35 (dd, 1H, $J=9.9, 4.7$ Hz, *CH*-5) 3.48 (dd, $J = 9.9, 4.0$ Hz, 1H, *CH*-5), 3.68 (m, 1H, *CH*-2), 3.63 – 3.70 (m, 1H, *CH*-2), 3.70 – 3.79 (m, 1H, *CH*-4), 3.83 (dd, $J = 4.7, 1.8$ Hz, 1H, *CH*-3), 7.22 - 7.52 (m, 21H, *CH* arom.), 7.49 - 7.73 (m, 4H, *CH* arom.) **^{13}C NMR** (101 MHz, CHLOROFORM-*D*) δ ppm 19.19($C(CH_3)_3$ TBDPS), 21.01 26.84 ($C(CH_3)_3$ TBDPS), 65.13 (*CH*-1), 65.35 (*CH*-5), 71.84 (*CH*-3), 72.53 (*CH*-2), 73.26 (*CH*-3), 87.35 ($C(Ph)_3$ Trityl), 127.22, 127.83, 127.91, 127.99, 128.51, 129.95, 132.62, 135.49, 143.48 (*CH* arom.) **IR** (ν_{max} , film) 3466, 3056, 2930, 2857, 1471, 1111, 1053, 700, 504 cm^{-1} $[\alpha]_D^{20} = -3.61$ ($c = 1.00$, DCM)



2,3,4-tri-O-acetyl-5-O-tert-butyl-diphenylsilyl-1-O-trityl-ribose (17)

To a stirring solution of 5-*O*-tert-butyl-diphenylsilyl-1-*O*-trityl-ribose (**12**) (910 mg, 1.44 mmol, 1.00 equiv.) in dry pyridine (10 mL), was added Ac_2O (1.4 mL, 5.4 mmol, 3.8 equiv.) and DMAP (40 mg, 0.33 mmol, 0.24 equiv.). The reaction was allowed to stir for 72 hours at RT before the solvents were removed *in vacuo* and co-evaporated with toluene (3 x 10 mL). The resulting residue was dissolved in DCM (30 mL) and washed with H_2O (30 mL), the aqueous layer was further extracted with DCM (3 x 30 mL) and the combined organic layers washed with sat. aqueous $NaHCO_3$ solution, dried over $MgSO_4$, filtered and concentrated *in vacuo* to afford the crude product. The crude product was purified by automated column chromatography (gradient 0-50% EtOAc in hexane) to afford the title compound as a clear oil (850 mg, 1.12 mmol, 78%)

HRMS-ESI Calculated for $[C_{46}H_{54}O_8Si + Na^+]$: 781.3167, found: 781.3184 **1H NMR** (400 MHz, CHLOROFORM-*D*) δ ppm 1.08 (s, 9H, $C(CH_3)_3$ TBDPS), 1.83 (s, 3H, CH_3 OAc), 1.85 (s, 3H, CH_3 OAc), 1.96 (s, 3H, CH_3 OAc) 3.18 (dd, $J = 10.3, 6.1$ Hz, 1H, *CH*-1) 3.32 (dd, $J=10.3, 3.2$ Hz, 1H, *CH*-1') 3.73 (dd, $J=11.2, 6.1$ Hz, 1H, *CH*-5) 3.83 (dd, $J=11.2, 3.7$ Hz, 1H, *CH*-5'), 5.25 - 5.28 (m, 1H, *CH*-4), 5.36 - 5.42 (td, $J = 6.1, 3.2, 1H, CH$ -2), 5.48 (dd, $J = 6.1, 4.8$ Hz, 1H, *CH*-3), 7.17 – 7.31 (m, 10H, *CH* arom.), 7.32 – 7.45 (m, 12H, *CH* arom.), 7.57 – 7.66 (m, 3H, *CH* arom.) **^{13}C NMR** (101 MHz, CHLOROFORM-*D*) δ ppm 18.60 ($C(CH_3)_3$ TBDPS), 23.54 ($C(Ph)_3$ Trityl), 25.06 ($C(CH_3)_3$ TBDPS), 25.16, 25.22, 25.29 (CH_3 OAc), 66.45 (*CH*-1), 66.58 (*CH*-5), 73.88 (*CH*-3), 75.51 (*CH*-2), 77.00 (*CH*-4), 86.66 ($C(Ph)_3$ Trityl), 131.45, 132.12, 133.01, 134.16, 137.44, 137.47, 139.99, 147.97, (*CH* arom.) 173.63, 173.66, 174.21 ($C=O$) **IR** (ν_{max} , film) 2940, 2853, 1750, 1431, 1360, 1219, 1114, 1049, 702, 510 cm^{-1} $[\alpha]_D^{20} = +1.28$ ($c = 1.0$, DCM)

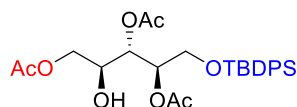


2,3,4-tri-O-acetyl-5-O-tert-butyl-diphenylsilyl-ribose (18)

To a stirring solution of 2,3,4-tri-O-acetyl-5-O-tert-butyl-diphenylsilyl-1-O-trityl-ribose (**17**) (101 mg, 0.133 mmol, 1.00 equiv.) in 1:1 DCM:MeOH (2.5 mL) was added HCl (cat.). After 5 hours at RT the reaction was quenched with addition of sat. aqueous $NaHCO_3$ solution (10 mL) and the aqueous layer was further extracted with EtOAc (3 x 15 mL). The combined organic layers were washed with brine (10 mL), dried over $MgSO_4$, filtered and concentrated *in vacuo* to afford the crude product which was purified by automated column chromatography (gradient 0-30%) to afford the title product as a clear oil (20 mg, 38 μ mol, 22%) alongside 1,3,4-tri-O-acetyl-5-O-tert-butyl-diphenylsilyl-ribose (10 mg, 19 μ mol, 11%) and 1,2,4-tri-O-acetyl-5-O-tert-butyl-diphenylsilyl-ribose (10 mg, 19 μ mol, 11%)

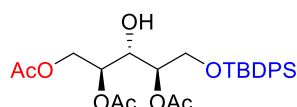
HRMS-ESI Calculated for $[C_{27}H_{36}O_8Si + Na^+]$: 539.2072, found: 539.2067 **1H NMR** (400 MHz, CHLOROFORM-*D*) δ 1.06 (s, 9H, $C(CH_3)_3$ TBDPS), 2.02 (s, 3H, CH_3 OAc), 2.05 (s, 3H, CH_3 OAc), 2.08 (s, 3H, CH_3 OAc), 3.57 (dd, $J = 10.5, 5.5$ Hz, 1H, *CH*-5), 3.70 (dd, $J = 10.5, 3.2$ Hz, 1H, *CH*-5'), 4.12 (dd, $J = 8.0, 4.4$ Hz, 1H, *CH*-3), 4.27 (dd, $J = 11.7, 7.4$ Hz, 1H, *CH*-1), 4.38 (dd, $J = 11.7, 3.2$ Hz, 1H, *CH*-1'), 5.19 (dd, $J = 8.0, 3.2$ Hz, 1H, *CH*-2), 5.47 (ddd, $J = 8.0, 5.5, 3.2$ Hz, 1H, *CH*-4), 7.35 – 7.52 (m, 7H, *CH* arom.), 7.64 (dddd, $J = 8.7, 6.4, 4.6, 2.2$ Hz, 4H, *CH* arom.) **^{13}C NMR** (101 MHz, CHLOROFORM-*D*) δ 19.26 ($C(CH_3)_3$ TBDPS), 20.95, 21.03 (CH_3 OAc), 26.77 ($C(CH_3)_3$ TBDPS),

62.14 (CH-1), 65.23 (CH-5), 68.64 (CH-2), 72.12 (CH-3), 72.37 (CH-4), 127.59, 130.04, 132.70, 135.72 (CH arom.), 170.08, 170.59, 171.35 C=O). IR (ν_{\max} , film) 3474, 2931, 2857, 1741, 1427, 1369, 1215, 1111, 1045, 504 cm^{-1} $[\alpha]_{\text{D}}^{20} = -4.21$ ($c = 1.0$, DCM)



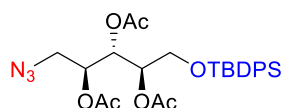
1,3,4-tri-O-acetyl-5-O-tert-butylidiphenylsilyl-ribose (22)

$^1\text{H NMR}$ (400 MHz, CHLOROFORM-*D*) δ 1.05 (s, 9H, C(CH₃)₃ TBDPS), 2.02 (s, 3H, CH₃ OAc), 2.06 (s, 3H, CH₃ OAc), 2.08 (s, 3H, CH₃ OAc), 3.85 (dd, $J = 12.3, 3.2$ Hz, 1H, CH-5), 3.98 (dd, $J = 11.4, 4.6$ Hz, 1H, CH-5'), 4.05 – 4.19 (m, 1H, CH-2), 4.26 (dd, $J = 12.4, 6.0$ Hz, 1H, CH-1), 4.48 (dd, $J = 12.4, 3.2$ Hz, 1H, CH-1'), 4.90 – 4.95 (m, 1H, CH-3), 5.13 (td, $J = 6.2, 3.0$ Hz, 1H, CH-4), 7.35 – 7.50 (m, 6H, CH arom.), 7.60 – 7.71 (m, 4H, CH arom.)



1,3,4-tri-O-acetyl-5-O-tert-butylidiphenylsilyl-ribose (23)

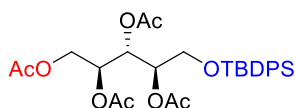
$^1\text{H NMR}$ (400 MHz, CHLOROFORM-*D*) δ 1.05 (s, 9H, C(CH₃)₃ TBDPS), 2.02 (s, 3H, CH₃ OAc), 2.02 (s, 3H, CH₃ OAc), 2.08 (s, 3H, CH₃ OAc), 3.81 (dd, $J = 11.0, 5.0$ Hz, 1H, CH-5), 3.89 (dd, $J = 11.0, 4.8$ Hz, 1H, CH-5'), 4.08 – 4.23 (m, 3H, CH-1, CH-1', CH-3), 5.23 (dd, $J = 6.6, 3.9$ Hz, 1H, CH-2), 5.32 (dd, $J = 5.0, 4.8$ Hz, 1H, CH-4), 7.42 (ddd, $J = 14.2, 7.6, 5.7$ Hz, 6H), 7.66 (td, $J = 7.8, 1.8$ Hz, 4H).



1-Azido-2,3,4-tri-O-acetyl-5-O-tert-butylidiphenylsilyl-ribose (19)

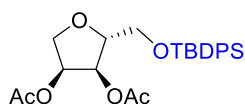
To a stirring solution of 5-*O*-tert-butyl-diphenylsilyl-D-ribose (**21**) (156 mg, 0.400 mmol, 1.00 equiv.) in dry pyridine (2 mL) at 0°C was added TsCl (110 mg 0.575 mmol, 1.43 equiv.). The reaction was maintained at 0°C for 3 hrs before the addition of Ac₂O (0.60 mL, 2.3 mmol, 6.1 equiv.). The reaction was maintained at 0°C for a further 3 hrs before quenching by the addition of MeOH (1 mL) and the reaction mixture was concentrated under reduced pressure. The crude product was purified by automated flash column chromatography (gradient 0 to 50% EtOAc in hexane) to afford the desired tosyl intermediate (67 mg, 0.11 mmol, 27%) which was dissolved in dry DMF (1 mL) and NaN₃ (28 mg, 0.42 mmol, 4.2 equiv.) added. The resulting solution was heated to 60°C for 24 hours before the reaction was quenched by the addition of sat. aqueous NaHCO₃ solution (10 mL) and the product was extracted with EtOAc (3 x 10 mL). The combined organic layers were washed consecutively with sat. aqueous NaHCO₃ solution (20 mL) and brine (20 mL), dried over MgSO₄, filtered and concentrated *in vacuo*. The crude product was purified by automated flash column chromatography (gradient 0 to 100% EtOAc on hexane) to afford the title product as a yellow oil (15 mg, 27 μmol , 25% from the tosylated intermediate, 7.1% overall)

HRMS-ESI Calculated for [C₂₇H₃₅O₇N₃Si + Na⁺]: 564.2136, found: 564.2150 $^1\text{H NMR}$ (400 MHz, CHLOROFORM-*D*) δ ppm 1.09 (s, 9H, C(CH₃)₃ TBDPS), 1.86 (m, 3H, CH₃ OAc), 2.03 (s, 3H, CH₃ OAc), 2.08 (s, 3H, CH₃ OAc), 3.34 (dd, $J = 13.4, 7.0$ Hz, 1H, CH-1), 3.41 (dd, $J = 13.4, 3.3$ Hz, 1H, CH-1'), 3.96-4.06 (m, 3H, CH-2, CH-5, CH-5'), 5.20 (dd, $J = 5.5, 3.9$ Hz, 1H, CH-3), 5.36 - 5.43 (m, 1H, CH-4), 7.22 - 7.48 (m, 6H, CH arom.), 7.55 – 7.61 (m, 2H, CH arom.), 7.68 – 7.73 (m, 2H, CH arom.) $^{13}\text{C NMR}$ (101 MHz, CHLOROFORM-*D*) δ ppm 19.26, 20.35, 20.68 (CH₃ OAc), 25.55 (C(CH₃)₃ TBDPS), 26.27 (C(CH₃)₃ TBDPS), 50.11 (CH-1), 64.78 (CH-5), 67.92 (CH-3), 70.45 (CH-2), 72.06 (CH-4), 127.58, 130.24, 135.61, 136.06, (CH arom.), 169.30, 169.69, 170.51 (C=O OAc) IR (ν_{\max} , film) 2931, 2858, 2103, 1743, 1427, 1368, 1222, 1104, 701, 504 cm^{-1}



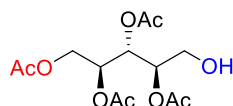
1,2,3,4,5-tetra-O-acetyl-5-O-tert-butylidiphenylsilyl-ribose (25)

HRMS-ESI Calculated for $[C_{29}H_{38}O_9 + Na^+]$: 581.2177, found: 581.2173 **1H NMR** (400 MHz, CHLOROFORM-*D*) δ 1.05 (s, 9H, $C(CH_3)_3$ TBDPS), 1.97 (s, 3H, CH_3 OAc), 2.01 – 2.07 (m, 9H, CH_3 OAc), 3.73 (dd, $J = 11.4, 5.5$ Hz, 1H, $CH-5$), 3.79 (dd, $J = 11.4, 3.7$ Hz, 1H, $CH-5'$), 4.06 – 4.19 (m, 1H, $CH-1$), 4.32 (td, $J = 11.4, 3.0$ Hz, 1H, $CH-1'$), 5.14 – 5.28 (m, 1H, $CH-4$), 5.28 – 5.38 (m, 1H, $CH-2$), 5.43 (app t, $J = 4.9$ Hz, 1H, $CH-3$), 7.34 – 7.42 (m, 6H, CH arom.), 7.61 – 7.74 (m, 4H, CH arom.) **^{13}C NMR** (101 MHz, CHLOROFORM-*D*) δ 19.59 ($C(CH_3)_3$ TBDPS), 21.16, 21.24, 21.37, 27.03, 27.22, (CH_3 OAc, $C(CH_3)_3$ TBDPS) 62.45, 62.49 ($CH-1, CH-5$), 69.84 ($CH-2$), 70.25 ($CH-4$), 72.58 ($CH-3$), 128.22, 130.29, 130.32, 133.33, 133.38, 136.00, 136.06, 136.60 (CH arom.), 169.85, 170.31, 170.41, 171.09 ($C=O$ OAc).



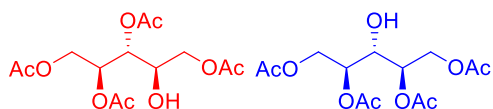
1,4-anhydro-2,3-di-O-acetyl-5-O-tert-butylidiphenylsilyl-deoxy-D,L-ribose (26)

1H NMR (400 MHz, CHLOROFORM-*D*) δ 1.06 (s, 9H, $C(CH_3)_3$ TBDPS), 1.95 (s, 3H, CH_3 OAc), 2.08 (s, 3H, CH_3 OAc), 3.67 (dd, $J = 10.5, 6.0$ Hz, 1H, $CH-5$), 3.74 (dd, $J = 10.5, 3.7$ Hz, 1H, $CH-5'$), 3.96 (ddd, $J = 6.9, 5.5, 3.7$ Hz, 1H, $CH-4$), 4.15 – 4.23 (m, 2H, $CH-2, CH-3$), 4.97 (dd, $J = 6.9, 5.0$ Hz, 1H, $CH-1$), 5.17 – 5.26 (m, 1H, $CH-1'$), 7.36 – 7.47 (m, 6H, CH arom.), 7.56 – 7.76 (m, 4H, CH arom.).

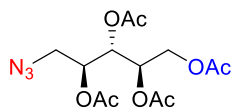


1,2,3,4-tetra-O-acetyl-D-ribose (29)

To a stirring solution of 1,2,3,4-tetra-O-acetyl-5-O-tert-butylidiphenylsilyl-ribose (120 mg, 0.215 mmol, 1.00 equiv) in THF (3.5 mL) was added TBAF (1 M in THF, 0.40 mL, 0.40 mmol, 1.9 equiv). After 18 hours at RT, the reaction was quenched by the addition of sat. aqueous NH_4Cl solution (20 mL) and EtOAc (20 mL). The layers separated, and the organic layer was washed with water (20 mL), dried over $MgSO_4$, filtered and concentrated *in vacuo* to afford the crude product which was purified by flash column chromatography (20% EtOAc in hexane) to afford a clear oil (31 mg, 90 μ mol, 44%). NMR analysis shows a 2:3 ratio of 1,2,3,5-tetra-O-acetyl-D-ribose **30** and 1,2,4,5-tetra-O-acetyl-D-ribose **31**



HRMS-ESI Calculated for $[C_{13}H_{20}O_9 + Na^+]$: 343.1000, found: 343.0998 **1H NMR** (400 MHz, CHLOROFORM-*D*) δ 2.06 (s, 2H, CH_3 OAc), 2.06 (s, 7H, CH_3 OAc), 2.08 (s, 3H, CH_3 OAc), 2.08 (s, 3H, CH_3 OAc), 2.09 (d, $J = 1.4$ Hz, 4H, CH_3 OAc), 2.12 (s, 8H, CH_3 OAc), 3.96 (t, $J = 6.0$ Hz, 1H, $CH-3$), 4.05 (td, $J = 7.1, 3.4$ Hz, 1H, $CH-4$), 4.12 (dd, $J = 12.5, 7.3$ Hz, 1H, $CH-5$), 4.19 (dd, $J = 12.5, 3.4$ Hz, 1H, $CH-5'$), 4.23 – 4.26 (m, 1H), 4.26 – 4.30 (m, 2H), 4.36 – 4.45 (m, 3H) ($CH-1, CH-1', CH-1, CH-1', CH-5, CH-5'$) 5.09 (td, $J = 5.7, 3.4$ Hz, 2H, $CH-2, CH-4$), 5.15 (dd, $J = 7.1, 4.1$ Hz, 1H, $CH-3$), 5.42 (ddd, $J = 7.3, 4.1, 3.0$ Hz, 1H, $CH-2$). **^{13}C NMR** (101 MHz, CHLOROFORM-*D*) δ 20.91 (CH_3 OAc), 21.05 (CH_3 OAc), 21.09 (CH_3 OAc), 62.22, 62.29 ($CH-1, CH-1, CH-5$), 65.27 ($CH-5$), 69.02 ($CH-4$), 69.33 ($CH-3$), 70.43 ($CH-2$), 71.45 ($CH-3$), 71.79 ($CH-2, CH-4$), 169.97, 170.24, 170.48, 171.02, 171.16 ($C=O$ OAc)

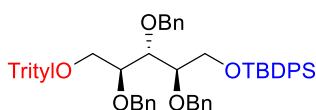


2,3,4,5-tetra-O-acetyl-1-azido-D-ribose (1-Az-OAc Probe)

To a stirring solution of 1-Azido-2,3,4-tri-O-acetyl-5-O-tert-butyl-diphenylsilyl-ribose (4.0 mg, 0.0074 mmol, 1.0 equiv.) in 200 μ L THF was added 16 μ L TBAF (1 M in THF, 16 μ mol, 2.2 equiv.) at 0°C. After 3.3 hours at RT the reaction was quenched by the addition of MeOH (2 mL) and the reaction mixture was concentrated under reduced pressure. The resulting residue was dissolved in EtOAc (0.5 mL) and washed with sat. NH_4Cl solution (0.5 mL). The aqueous layer was further extracted with EtOAc (5 x 0.5 mL) before the combined organic layers were dried over MgSO_4 , filtered and concentrated *in vacuo* to afford the crude de-silylated intermediate.* The crude residue was dissolved in pyridine (200 μ L) and treated with Ac_2O (15 μ L, 80 μ mol, 11 equiv.). The reaction mixture was allowed to stir at RT for 18 h before the reaction mixture was concentrated under reduced pressure and co-evaporated with toluene (3 x 2 mL). The crude product was purified by manual flash column chromatography (gradient 25% EtOAc in hexane) to afford the pure compound as a clear oil (2.1 mg, 0.0068 mmol, 91%)

HRMS-ESI Calculated for $[\text{C}_{13}\text{H}_{19}\text{N}_3\text{O}_8 + \text{Na}^+]$: 368.1064, found: 368.1063 **$^1\text{H NMR}$** (400 MHz, CHCl_3 -*D*) δ ppm 2.04 (s, 3H, CH_3 OAc), 2.09 (s, 6H, CH_3 OAc), 2.12 (s, 3H, CH_3 OAc), 3.41 (dd, $J = 13.4, 6.9$ Hz, 1H, *CH-1*), 3.50 (dd, $J = 13.4, 3.6$ Hz, 1H, *CH-1*), 4.13 (dd, $J = 12.2, 6.0$ Hz, 1H, *CH-5*), 4.31 (dd, $J = 12.2, 3.2$ Hz, 1H, *CH-5*), 5.15 – 5.23 (m, 1H, *CH-2*), 5.24 (ddd, $J = 5.9, 6.0, 3.2$ Hz, 1H, *CH-4*), 5.32 (dd, $J = 5.8, 5.3$ Hz, 1H, *CH-3*), **$^{13}\text{C NMR}$** (101 MHz, CHCl_3 -*D*) δ ppm 20.57, 20.71, 20.74 (CH_3 OAc), 50.14 (*CH-1*), 61.65 (*CH-5*), 69.41, 69.65 (*CH-2, CH-4*), 70.38 (*CH-3*), 169.26, 169.71, 169.76, 170.43 (C=O OAc) $[\alpha]_D^{20} = +12.59$ ($c = 0.67$, DCM)

*Crude $^1\text{H NMR}$ showed a messy profile with a side product formed from the loss of an additional acetate and acetate migration products, the reaction was continued without further purification.



2,3,4-tri-O-benzyl-5-O-tert-butyl-diphenylsilyl-1-O-trityl-D-ribose (13)

With BnBr and NaH

To a stirring solution of 5-O-tert-butyl-diphenylsilyl-1-O-trityl-D-ribose (**12**) (178 mg, 0.282 mmol, 1.00 equiv.) in DMF (5 mL) was added NaH (60% in mineral oil, 60 mg, 1.5 mmol, 5.4 equiv.) and BnBr (0.18 mL, 1.5 mmol, 5.4 equiv.) at 0°C. After 2 h at RT the reaction was quenched by the addition of MeOH (1 mL), and dissolved in EtOAc (20 mL). The solution was washed with 1M HCl (10 mL), sat. aqueous NaHCO_3 solution (10 mL) and brine (10 mL), dried over MgSO_4 , filtered and concentrated *in vacuo*. The crude product was purified by automated flash column chromatography (gradient 0-20% EtOAc in hexane) to afford title compound as a yellow oil (65 mg, 70 μ mol, 25%) and the side product 2,3,4,5-tetra-O-benzyl-1-trityl-D-ribose (**32**) as a clear oil (50 mg, 60 μ mol, 20%)

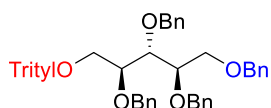
With BnBr, BaO and Ba(OH)₂

To a stirring solution of 5-O-tert-butyl-diphenylsilyl-1-O-trityl-D-ribose (**12**) (100 mg, 0.158 mmol, 1.00 equiv.) in DMF (1 mL) was added BaO (212 mg, 0.840 mmol, 5.30 equiv.) and Ba(OH)₂ (27 mg, 0.10 mmol, 0.66 equiv.) followed by dropwise addition of BnBr (85 μ L, 0.71 mmol, 4.5 equiv.) at 0°C. After 24 h at RT the reaction was diluted with DCM (10 mL) and quenched by the addition of 1M HCl till the pH remained acidic (5 mL), and allowed to stir for 30 mins. Crude ESI-MS showed no presence of desired compound **17**, and instead showed evidence for formation of side product **30** and incompletely benzylated product.

2,3,4-tri-O-benzyl-5-O-tert-butyl-diphenylsilyl-1-O-trityl-D-ribose (13)

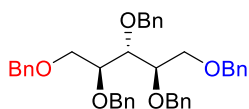
HRMS-ESI Calculated for $[\text{C}_{61}\text{H}_{62}\text{O}_5\text{Si} + \text{Na}^+]$: 925.4258, found: 925.4271 **$^1\text{H NMR}$** (400 MHz, CHCl_3 -*D*) δ ppm 1.09 (s, 9 H, $\text{C}(\text{CH}_3)_3$ TBDPS), 3.19 – 3.60 (m, 2H, *CH-1*), 3.62 – 3.80 (m, 1H, *CH-4*), 3.81 – 3.98 (m, 2H, *CH-5*), 4.03 – 4.14 (m, 1H, *CH-2*), 4.20 – 4.33 (m, 1H, *CH-3*), 4.38 – 4.77 (m, 6H, *CH* OBn), 6.89 – 7.75 (m, 40H, *CH*

arom.) $^{13}\text{C NMR}$ (101 MHz, CHLOROFORM-*D*) δ ppm 14.25 ($\text{C}(\text{CH}_3)_3$ TBDPS), 27.01 ($\text{C}(\text{Ph})_3$ Trityl), 27.21 ($\text{C}(\text{CH}_3)_3$ TBDPS), 64.17 (CH-1), 65.36 (CH-5), 72.61, 73.22, 73.56 (CH OBn), 78.84 (CH-2), 79.78 (CH-3), 80.40 (CH-4), 126.93, 127.28, 127.40, 127.51, 127.56, 127.65, 127.71, 127.73, 127.76, 127.81, 127.97, 128.12, 128.16, 128.22, 128.28, 128.35, 128.53, 128.83, 128.94, 129.64, 133.54, 135.77, 135.83, 136.03, 136.38, 138.58, 138.91 (CH arom.) IR (ν_{max} , film) 3030, 2930, 2856, 1493, 1450, 1108, 1027, 737, 699 cm^{-1}
 $[\alpha]_{\text{D}}^{20} = +7.71$ ($c = 1.0$, DCM)



2,3,4,5-tetra-O-benzyl-1-O-trityl-D-ribose (32)

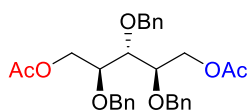
HRMS-ESI Calculated for $[\text{C}_{52}\text{H}_{50}\text{O}_5 + \text{Na}^+]$: 777.3550, found: 777.3572 $^1\text{H NMR}$ (400 MHz, CHLOROFORM-*D*) δ 3.42 (dd, $J = 10.2, 5.6$ Hz, 1H, CH-5), 3.49 (dd, $J = 10.3, 2.6$ Hz, 1H, CH-5'), 3.72 (dd, $J = 10.4, 5.4$ Hz, 1H, CH-1), 3.77 (dd, $J = 10.5, 3.1$ Hz, 1H, CH-1), 3.90 – 4.06 (m, 3H, CH-2, CH-3, CH-4), 4.52 (d, $J = 2.8$ Hz, 2H, CH OBn), 4.57 (d, $J = 10.9$ Hz, 1H, CH OBn), 4.60 (d, $J = 11.6$ Hz, 1H, CH OBn), 4.65 (d, $J = 11.0$ Hz, 2H, CH OBn), 4.73 (d, $J = 11.6$ Hz, 1H, CH OBn), 4.83 (d, $J = 11.5$ Hz, 1H, CH OBn), 7.01 – 7.65 (m, 35H, CH arom.) $^{13}\text{C NMR}$ (101 MHz, CHLOROFORM-*D*) δ ppm 64.08 (CH-1), 70.52 (CH-5), 72.60, 72.77, 73.38, 73.76, (CH OBn), 78.88 (CH-2), 78.99 (CH-3), 79.06 (CH-4), 127.02, 127.49, 127.53, 127.60, 127.78, 127.89, 127.93, 128.08, 128.30, 128.38, 128.42, 128.45, 128.98, 138.59, 138.64, 138.85, 138.88 (CH arom.) IR (ν_{max} , film) 3030, 2859, 1740, 1450, 1099, 1028, 740, 697 cm^{-1} $[\alpha]_{\text{D}}^{20} = +7.87$ ($c = 0.5$, DCM)



1,2,3,4,5-penta-O-benzyl-D-ribose (33)

To a stirring solution of D-ribose (purchased from Sigma, 27 mg, 0.18 mmol, 1.0 equiv.) in DMF (1 mL) was added NaH (60% in mineral oil, 40 mg, 0.55 mmol, 3.1 equiv.). After 30 mins at RT the reaction was cooled in an ice bath to 0°C and BnBr (7.0 μL , 0.59 mmol, 3.3 equiv.) was added. After 2.5 hrs NaH (60% in mineral oil, 40 mg, 0.55 mmol, 3.1 equiv.) added at RT and after 30 mins the reaction was cooled in an ice bath to 0°C and BnBr (7.0 μL , 0.59 mmol, 3.3 equiv.) was added. After a further 2.5 hrs NaH (60% in mineral oil, 40 mg, 0.55 mmol, 3.1 equiv.) was added at RT and after 30 mins the reaction was cooled in an ice bath to 0°C and BnBr (7.0 μL , 0.59 mmol, 3.3 equiv.) added. The resulting suspension was allowed to stir at RT for 16 hrs. The reaction was quenched by the addition of MeOH (2 mL) and the reaction mixture was concentrated under reduced pressure. The resulting residue was dissolved in DCM (10 mL) and washed with H₂O (3 x 10 mL). The aqueous layer was further extracted with DCM (20 mL) and the organic layers combined, washed with brine (2 x 20 mL), dried over MgSO₄, filtered and concentrated *in vacuo* to afford the crude product. The crude product was purified by automated flash column chromatography (gradient from 0 to 15% EtOAc in hexane) to afford the title compound as a clear oil (73 mg, 0.12 mmol, 67%)

HRMS-ESI Calculated for $[\text{C}_{42}\text{O}_5 + \text{Na}^+]$: 625.6924, found: 625.2936 $^1\text{H NMR}$ (400 MHz, CHLOROFORM-*D*) δ ppm 3.60 – 3.71 (m, 4H, CH-1, CH-1', CH-5, CH-5'), 3.82 – 3.90 (m, 3H, CH-2, CH-3, CH-4), 4.38 – 4.70 (m, 10H, CH OBn), 7.24-7.29 (m, 25H, CH arom.) $^{13}\text{C NMR}$ (101 MHz, CHLOROFORM-*D*) δ ppm 69.8 (CH-5, CH-1), 72.04, 72.55, 73.49, 74.14 (CH OBn), 77.1 (CH-3), 78.4, 78.9 (CH-2, CH-4), 127.7, 127.8, 127.9, 128.0, 128.0, 128.2, 128.5, 128.5, 128.5, 138.2, 138.3, 138.4 (CH arom.) IR (ν_{max} , film) 3063, 3029, 2861, 1495, 1453, 1095, 1027, 734, 696 cm^{-1} $[\alpha]_{\text{D}}^{20} = +2.27$ ($c = 1.0$, DCM)



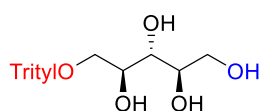
1,5-di-O-acetyl-2,3,4-tetra-O-benzyl-D-ribose (34)

To a stirring solution of 1,2,3,4,5-penta-O-benzyl-ribose (33) (22 mg, 35 μmol , 1.0 equiv.) in 1:5 AcOH:Ac₂O (320 μL) at 0°C was added ZnCl₂ (28 mg, 0.21 mmol, 5.7 equiv.). The resulting solution was stirred for 3 h at RT before addition of H₂O (5 mL) and Et₂O (5 mL). The layers were separated and the resulting organic layer was

further washed with H₂O (2 x 5 mL) and brine (5 mL), and dried over MgSO₄, filtered and concentrated *in vacuo*. The solution was concentrated *in vacuo* and co-evaporated with toluene (5mL) to afford the title compound as a clear oil (14 mg, 33 μmol, 92%)

HRMS-ESI Calculated for [C₃₀H₃₄O₇ + Na⁺]: 529.2197, found: 529.2199 **¹H NMR** (400 MHz, CHLOROFORM-*D*) 1.97 (2 x s, 6H, CH₃), 3.76 – 3.90 (m, 3H, CH-2, CH-3, CH-4), 4.16 (dd, *J* = 12.0, 5.4 Hz, 2H, CH-1, CH-5), 4.40 (tt, *J* = 12.0, 3.1 Hz, 2H, CH-1', CH-5') **¹³C NMR** (101 MHz, CHLOROFORM-*D*) δ ppm δ 21.06 (CH₃ OAc), 63.57, (CH-1, CH-5), 72.40, 73.77 (CH OBn) 76.94, (CH-3), 77.81 (CH-2, CH-4), 127.84, 127.91, 128.13, 128.30, 128.47, 129.01, 137.89, 137.99, (CH arom.), 170.98. (C=O OAc) **IR** (ν_{max}, film) 2920, 1739, 1495, 1453, 1231, 1100, 740, 698 cm [α]_D²⁰ = +2.56 (*c* = 0.5, DCM)

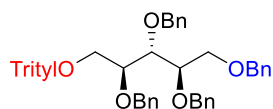
Data in accordance with literature values²⁴⁹



1-O-trityl-D-ribitol (11)

To a stirring solution of 5-*O*-*tert*-butyldiphenylsilyl-1-*O*-trityl-D-ribitol (**12**) (2.48 g, 3.96 mmol, 1.00 equiv.) in dry THF (50 mL) was added TBAF (1M in THF, 4.8 mL, 4.8 mmol, 1.2 equiv.) at 0°C. The resulting solution was allowed to warm to RT and stirred for 2.5 h. The reaction was diluted with EtOAc (100 mL), washed with sat. aqueous NH₄Cl solution (100 mL) and extracted with EtOAc (2 x 100 mL). The combined organic layers were dried over MgSO₄, filtered and concentrated *in vacuo*. The crude product was purified by automated flash column chromatography (gradient 0 to 100% EtOAc in hexane) to afford the title compound as a white foam. (1.16 g, 2.97 mmol, 75%)

HRMS-ESI Calculated for [C₂₄H₂₆O₅ + Na⁺]: 417.1672, found: 417.1681 **¹H NMR** (400 MHz, CHLOROFORM-*D*) δ ppm 3.12 – 4.04 (m, 7H, CH-1, CH-2, CH-3, CH-4, CH-5), 7.26 (m, 9H, CH arom), 7.43 (d, *J* = 7.6 Hz, 5H, CH arom.) **¹³C NMR** (101 MHz, CHLOROFORM-*D*) δ ppm 19.80 (C(Ph)₃), 63.43 (CH-5), 65.35 (CH-1), 71.78, 72.98, 73.29 (CH-2, CH-3, CH-4), 127.37, 128.12, 128.70, 143.65 (CH arom.) **IR** (ν_{max}, film) 3368, 3058, 2932, 1596.54, 1490, 1448, 1265, 1220, 1155, 1054, 901, 766, 746, 704, 633 cm⁻¹ [α]_D²⁰ = +0.31 (*c* = 0.5, DCM)

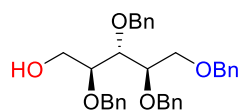


2,3,4,5-tetra-O-benzyl-1-O-trityl-D-ribitol (32)

To a stirring solution of 1-*O*-trityl-D-ribitol (**11**) (1.61 g, 4.09 mmol, 1.00 equiv.) in DMF (33 mL) at 0°C, was added NaH (60% in mineral oil, 380 mg, 9.50 mmol, 2.32 equiv.). The resulting suspension was maintained at 0°C for 30 mins before the dropwise addition of BnBr (1.2 mL, 10 mmol, 2.4 equiv.). The resulting solution was allowed to warm to RT and left stirring for 2 h before the reaction was cooled to 0°C and NaH (60% in mineral oil, 380 mg, 9.5 mmol, 2.3 equiv.) was added. After 30 mins at 0°C, additional BnBr (1.2 mL, 10 mmol, 2.4 equiv.) was added and the reaction warmed to RT. After a further 2h at RT the reaction was cooled to 0°C and NaH (60% in mineral oil, 380 mg, 9.5 mmol, 2.3 equiv.) was added again. After 30 mins at 0°C, BnBr (1.2 mL, 10 mmol, 2.4 equiv.) was again added dropwise and the resulting reaction mixture was left to react overnight at RT. After 17 h the reaction was quenched by the addition of MeOH (10 mL) and the reaction mixture was concentrated under reduced pressure. The resulting residue was dissolved in DCM (100 mL) and washed with H₂O (100 mL). The aqueous layer was further extracted with DCM (2 x 50 mL) and the combined organic layers washed with brine (100 mL), dried over MgSO₄, filtered and concentrated *in vacuo* to afford the crude product which was purified by automated flash column chromatography (gradient from 0 to 60% EtOAc in hexane) to afford the title compound as a colourless oil (2.45 g, 3.35 mmol, 82%)

HRMS-ESI Calculated for [C₅₂H₅₀O₅ + Na⁺]: 777.3550, found: 777.3572 **¹H NMR** (400 MHz, CHLOROFORM-*D*) δ 3.42 (dd, *J* = 10.2, 5.6 Hz, 1H, CH-1), 3.49 (dd, *J* = 10.2, 2.6 Hz, 1H, CH-1'), 3.72 (dd, *J* = 10.4, 5.4 Hz, 1H, CH-5), 3.77 (dd, *J* = 10.4, 3.1 Hz, 1H, CH-5'), 3.90 – 4.06 (m, 3H, CH-2, CH-3, CH-4), 4.52 (d, *J* = 2.8 Hz, 2H, CH OBn), 4.57 (d, *J* = 10.9 Hz, 1H, CH OBn), 4.60 (d, *J* = 11.6 Hz, 1H, CH OBn), 4.65 (d, *J* = 11.0 Hz, 2H, CH OBn), 4.73 (d, *J* =

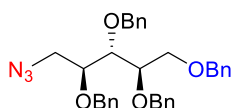
11.6 Hz, 1H, CH OBn), 4.83 (d, $J = 11.5$ Hz, 1H, CH OBn), 7.12 (dd, $J = 6.7, 3.0$ Hz, 2H, CH arom.), 7.18 – 7.41 (m, 27H, CH arom.), 7.51 (dd, $J = 7.7, 1.8$ Hz, CH arom.). $^{13}\text{C NMR}$ (101 MHz, CHLOROFORM- D) δ 64.03 (CH-1), 70.48 (CH-5), 72.56, 72.73, 73.34, 73.73 (CH OBn), 78.84, 78.94, 79.01 (CH-2, CH-3, CH-4), 86.75 (C(Ph) $_3$), 126.98, 127.37, 127.46, 127.49, 127.56, 127.74, 127.85, 127.89, 128.04, 128.26, 128.34, 128.38, 128.41, 128.93, 138.54, 138.60, 138.80, 138.84, (CH arom.) IR (ν_{max} , film) 3030, 2859, 1740, 1450, 1099, 1028, 740, 697 cm^{-1} $[\alpha]_{\text{D}}^{20} = +7.87$ ($c = 0.5$, DCM)



2,3,4,5-tetra-O-benzyl-D-ribose (35)

To a stirring solution of 2,3,4,5-tetra-O-benzyl-1-O-trityl-D-ribose (**32**) (283 mg, 0.375 mmol, 1.00 equiv.) in 2:1 MeOH:DCM (15 mL) was added TsOH (38 mg, 0.22 mmol, 0.59 equiv.). The pH was checked to be pH 3 and the reaction was allowed to stir at RT for 2.5 h. The reaction mixture was concentrated under reduced pressure, and the resulting residue was dissolved in EtOAc (20 mL) and washed with sat. NaHCO_3 (20 mL). The aqueous layer was further extracted with EtOAc (3 x 20 mL) and the combined organic were dried over MgSO_4 , filtered and concentrated *in vacuo*. The crude product was purified by automated flash column chromatography (gradient 0-30% EtOAc in hexane) to afford the title compound as a clear oil (144 mg, 0.281 mmol, 75%)

HRMS-ESI Calculated for $[\text{C}_{33}\text{H}_{36}\text{O}_5 + \text{Na}^+]$: 535.2455, found: 535.2453 $^1\text{H NMR}$ (400 MHz, CHLOROFORM- D) δ ppm 3.59 – 3.71 (m, 5H, CH-1, CH-1', CH-2, CH-5, CH-5'), 3.79 – 3.86 (m, 1H, CH-3), 3.95 (t, 1H, $J = 4.8$ Hz, CH-4), 4.49 (d, $J = 12.3$ Hz, 1H, CH OBn), 4.53 (d, $J = 11.9$ Hz, 1H, CH OBn), 4.58 (s, 2H, CH OBn), 4.64 (d, $J = 11.9$ Hz, 1H, CH OBn), 4.68 (d, $J = 11.0$ Hz, 1H, CH OBn), 4.71 (d, $J = 11.9$ Hz, 1H, CH OBn), 4.74 (d, $J = 11.9$ Hz, 1H, CH OBn), 7.25 (m, 20H, CH arom.) $^{13}\text{C NMR}$ (101 MHz, CHLOROFORM- D) δ ppm 61.2 (CH-1), 69.8 (CH-5), 72.04, 72.55, 73.49, 74.14 (CH OBn), 77.1 (CH-2), 78.4 (CH-3), 78.9 (CH-4), 127.7, 127.8, 127.9, 128.0, 128.0, 128.2, 128.5, 128.5, 128.5, 138.2, 138.3, 138.4 (CH arom.) IR (ν_{max} , film) 3029, 2863, 1496, 1453, 1096, 1027, 735, 696 cm^{-1} $[\alpha]_{\text{D}}^{20} = +5.67$ ($c = 1.0$, DCM)



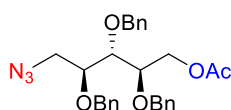
1-azido-2,3,4,5-tetra-O-benzyl-D-ribose (36)

via OMs To a stirring solution of 2,3,4,5-tetra-O-benzyl-D-ribose (**33**) (24 mg, 47 μmol , 1.0 equiv.) and pyridine (82 μL , 0.47 mmol, 10 equiv.) in dry DCM (0.3 mL) at 0°C was added MsCl (18 μL , 0.23 mmol, 4.9 equiv.) dropwise. The resulting solution was left to warm to RT over 2 h. The reaction was quenched by the addition of MeOH (1 mL) and diluted with DCM (10 mL). This reaction mixture was washed with 1M HCl (10 mL), sat. NaHCO_3 (10 mL) and brine (10 mL). The resulting organic layer was dried over MgSO_4 , filtered and concentrated *in vacuo*, followed by a high vacuum line for 30 min to afford the crude mesylate intermediate **1.35** which was used in the next step without further purification. This intermediate was dissolved in dry DMF (0.25 mL) and treated with NaN_3 (14 mg, 0.21 mmol, 4.5 equiv.). The reaction was heated to 80°C. After 22 h the reaction was diluted with EtOAc (10 mL), washed with sat. NaHCO_3 (10 mL) brine (10 mL), dried over MgSO_4 , filtered and concentrated *in vacuo*. The crude product was purified by flash column chromatography (gradient 10% EtOAc in hexane) to afford the title compound as a clear oil (12 mg, 21 μmol , 46%)

via OTs To a stirring solution of 2,3,4,5-tetra-O-benzyl-D-ribose (20 mg, 39 μmol , 1.0 equiv.) and pyridine (69 μL , 0.39 mmol, 10 equiv.) in dry DCM (0.3 mL) at 0°C was added TsCl (37 mg, 0.2 mmol, 5.1 equiv.). The resulting solution was allowed to warm to RT and after 24 h the reaction was quenched by the addition of MeOH (1 mL). The resulting solution was diluted with DCM (10 mL) and washed with 1M HCl (10 mL), sat. NaHCO_3 (10 mL) and brine (10 mL). The resulting organic layer was dried over MgSO_4 , filtered and concentrated *in vacuo*, followed by high vacuum line for 30 min to afford the crude tosyl intermediate (**3.36**) which was used in the next step without further purification. This intermediate was dissolved in dry DMF (0.25

mL) and treated with NaN₃ (8.0 mg, 0.12 mmol, 3 equiv.). The reaction was heated to 80°C and after 22 h the reaction was diluted with EtOAc (10 mL), washed with sat. NaHCO₃ (10 mL) and brine (10 mL). The resulting organic layer was then dried over MgSO₄, filtered and concentrated *in vacuo*. The crude product was purified by flash column chromatography (gradient 10% EtOAc in hexane) to afford the title compound as a clear oil (6.0 mg, 11 μmol, 28%)

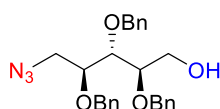
HRMS-ESI Calculated for [C₃₃H₃₅N₃O₅ + Na⁺]: 560.2525, found: 560.2527 **¹H NMR** (400 MHz, CHLOROFORM-*D*) δ ppm 3.34 (dd, *J* = 13.1, 2.7 Hz, 1H, CH-1), 3.45 (dd, *J* = 13.1, 6.0 Hz, 1H, CH-1'), 3.66 (dd, *J* = 10.5, 5.0 Hz, 1H, CH-5), 3.72 (dd, *J* = 10.5, 3.7 Hz, 1H, CH-5'), 3.78 – 3.84 (m, 1H, CH-3), 3.83 – 3.91 (m, 2H, CH-2, CH-4), 4.47 (d, *J* = 11.8 Hz, 1H, CH₂ Bn), 4.50 (d, *J* = 12.5 Hz, 1H, CH₂ Bn), 4.56 – 4.63 (m, 3H, CH₂ Bn), 4.63 – 4.69 (m, 2H, CH₂ Bn), 4.72 (d, *J* = 11.4 Hz, 1H, CH₂ Bn), 7.13 – 7.43 (m, 20H, CH arom.) **¹³C NMR** (101 MHz, CHLOROFORM-*D*) δ ppm 51.43 (CH-1), 69.65 (CH-5), 72.42, 72.52, 73.46, 73.97, (CH₂ Bn), 77.93, (CH-3), 78.30, 78.61 (CH-2, CH-4), 127.76, 127.81, 127.83, 128.04, 128.12, 128.47, 137.92, 138.30 (CH arom.) **IR** (ν_{max}, film) 3068, 3069, 3031, 2965, 2918, 2095, 1496, 1454, 1291, 1207, 1096, 1027, 912, 736, 697 cm⁻¹ [α]_D²⁰ = -6.09 (*c* = 0.75, DCM)



5-O-acetyl-1-azido-2,3,4-tri-O-benzyl-D-ribose (39)

To a stirring solution of 1-azido-2,3,4,5-tetra-O-benzyl-D-ribose (**36**) (471 mg, 0.877 mmol, 1.00 equiv.) in 1:5 AcOH:Ac₂O (3.5 mL) at 0°C was added ZnCl (300 mg, 2.21 mmol, 2.52 equiv.). The resulting solution was stirred for 3 h before the addition of H₂O (25 mL) and EtOAc (25 mL). The layers were separated and the aqueous layer further extracted with EtOAc (2 x 25 mL). The organic layers were combined and washed with brine (25 mL), dried over MgSO₄, filtered and concentrated *in vacuo*, and co-evaporated toluene (5mL x 2) to afford the title compound as a clear oil (398 mg, 0.815 mmol, 93%)

HRMS-ESI Calculated for [C₂₈H₃₁N₃O₅ + Na⁺]: 512.2156, found: 512.2159 **¹H NMR** (400 MHz, CHLOROFORM-*D*) 1.97 (s, 3H, CH₃), 3.37 (dd, *J* = 13.1, 2.4 Hz, 1H, CH-1), 3.43 (dd, *J* = 13.1, 5.4 Hz, 1H, CH-1'), 3.73 – 3.86 (m, 3H, CH-2, CH-3, CH-4), 4.15 (dd, *J* = 12.0, 5.3 Hz, 1H, CH-5), 4.41 (dd, *J* = 12.0, 2.7 Hz, 1H, CH-5'), 4.51 – 4.73 (m, 6H, CH OBn), 7.02 – 7.44 (m, 15H, CH arom.) **¹³C NMR** (101 MHz, CHLOROFORM-*D*) δ ppm 21.05 (CH₃), 51.17 (CH-1), 63.45 (CH-5), 72.26, 72.69, 73.99 (CH OBn), 76.72, 77.92, 78.24 (CH-2, CH-3, CH-4), 127.97, 128.19, 128.21, 128.25, 128.37, 128.51, 128.54, 128.67, 137.69, 137.80, 137.86, (CH arom.), 170.94 (C=O) **IR** (ν_{max}, film) 3031, 2920, 2853, 2099, 1738, 1496, 1454, 1231, 1094, 789, 687 cm⁻¹ [α]_D²⁰ = +8.78 (*c* = 1.0, DCM)



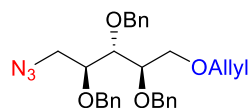
1-azido-2,3,4-tri-O-benzyl-D-ribose (6)

To a stirring solution of 5-O-acetyl-1-azido-2,3,4-tri-O-benzyl-D-ribose (**39**) (398 mg, 0.815 mmol, 1.00 equiv.) in MeOH (7.7 mL) was added NaOMe (0.5 M in MeOH, 0.40 mL, 0.19 mmol, 0.23 equiv.). After 3.5 h the reaction was quenched to pH 7 by the addition of DOWEX H⁺ resin and the resulting suspension filtered and concentrated under reduced pressure. The desired product was isolated by automated flash column chromatography (gradient of 0 to 30% EtOAc in hexane) to afford the title compound as a clear oil (265 mg, 0.593 mmol, 73%)

Alternative procedure from 5-O-allyl-1-azido-2,3,4-tri-O-benzyl-D-ribose (47)

To a stirring solution of 5-O-allyl-1-azido-2,3,4-tri-O-benzyl-D-ribose (**47**) (900 mg, 1.85 mmol, 1.00 equiv.) in dry MeOH (27 mL) was added PdCl₂ (65 mg, 0.37 mmol, 0.19 equiv.). The resulting suspension was kept at RT for 16 h, after which the palladium was removed by filtering through celite, and a short pass silica column. The crude product was purified by automated flash column chromatography (gradient 0-20% EtOAc in hexane) to afford the title compound as a pale yellow oil (444 mg, 0.993 mmol, 54%)

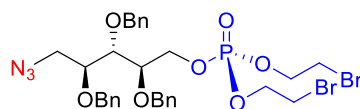
HRMS-ESI Calculated for $[C_{26}H_{29}O_4 + Na^+]$: 470.2050, found: 470.2061 **1H NMR** (400 MHz, CHLOROFORM-*D*) δ ppm 3.36 (dd, $J = 13.2, 3.5$ Hz, 1H, CH-1), 3.49 (dd, $J = 13.2, 6.4$ Hz, 1H, CH-1), 3.61 – 3.67 (m, 1H, CH-4), 3.74 (d, $J = 4.2$ Hz, 2H, CH-5, CH-5'), 3.79 – 3.84 (m, 1H, CH-2), 3.85 – 3.93 (m, 1H, CH-3), 4.57 (d, $J = 11.9$ Hz, 1H, CH OBn), 4.60 (d, $J = 11.1$ Hz, 1H, CH OBn), 4.63 (t, $J = 11.4$ Hz, 1H), CH OBn, 4.66 (d, $J = 11.3$ Hz, 1H, CH OBn), 4.70 (t, $J = 7.3$ Hz, 2H, CH OBn), 7.27 – 7.44 (m, 15H, CH arom.) **^{13}C NMR** (101 MHz, CHLOROFORM-*D*) δ ppm 51.21 (CH-1), 61.23 (CH-5), 72.14, 72.62, 74.33 (CH-OBn), 78.45, 78.48 (CH-2, CH-4), 78.57 (CH-3), 128.13, 128.17, 128.27, 128.31, 128.63, 128.68, 137.65, 137.83, 137.88. (CH arom.) **IR** (ν_{max} , film), 3068, 3069, 3031, 2964, 2016, 2098, 1496, 1453, 1291, 1207, 1096, 1027, 912, 736, 697, 460 cm^{-1} $[\alpha]_D^{20} = -0.12$ ($c = 0.6$, DCM)



5-O-allyl-1-azido-2,3,4-tri-O-benzyl-D-ribose (47)

To a stirring solution of 5-O-Allyl-2,3,4-tri-O-benzyl-D-ribose (**46**) (1.90 g, 4.12 mmol, 1.00 equiv, purchased from CarboSynth) in dry DCM (60 mL) at 0°C was added dry pyridine (7.6 mL, 43 mmol, 10 equiv.) and MsCl (1.7 mL, 22 mmol, 5.3 equiv.) dropwise. The resulting solution was allowed to warm to RT and stirred for 2 h after which the reaction was quenched by the addition of MeOH (10 mL). The resulting reaction mixture was diluted with DCM (100 mL) and washed with 1M HCl (100 mL), sat. aqueous NaHCO₃ solution (100 mL) and brine (100 mL). The resulting organic layer was dried over MgSO₄, filtered and concentrated *in vacuo* to afford the crude mesylate intermediate. This crude was suspended in DMF (35 mL) and NaN₃ (2.8 g, 43 mmol, 10 equiv.) added. The resulting suspension was heated to 80°C for 72 h, before cooling to RT and diluting with EtOAc (150 mL). The solution was washed with sat. aqueous NaHCO₃ solution (2 x 100 mL) and brine (100 mL). The resulting organic layer dried over MgSO₄, filtered and concentrated *in vacuo* to afford the crude product. The purified product was obtained by automated flash column chromatography (gradient 0 to 30% EtOAc in hexane) to afford the title product as a pale yellow oil (1.15 g, 2.36 mmol, 57%)

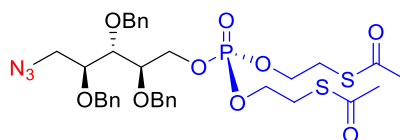
HRMS-ESI Calculated for $[C_{29}H_{33}N_3O_4 + Na^+]$: 510.2364, found: 510.2361 **1H NMR** (400 MHz, CHLOROFORM-*D*) δ 3.37 (dd, $J = 12.7, 2.4$ Hz, 1H, CH-1), 3.49 (dd, $J = 12.7, 5.4$ Hz, 1H, CH-1), 3.62 (dd, $J = 10.4, 5.1$ Hz, 1H, CH-5), 3.70 (dd, $J = 10.4, 3.8$ Hz, 1H, CH-5), 3.80 (dt, $J = 8.4, 5.1$ Hz, 1H, CH-4), 3.85 – 3.95 (m, 2H, CH-2, CH-3), 3.97 (dt, $J = 5.4, 1.5$ Hz, 2H, CH₂ OAllyl), 4.59 – 4.78 (m, 6H, CH₂ OBn), 5.24 (ddd, $J = 16.9, 5.0, 1.5$ Hz, 2H, CH=CH₂ OAllyl), 5.80 – 5.98 (m, 1H, CH=CH₂ OAllyl), 7.29 – 7.45 (m, 15H, CH arom.). **^{13}C NMR** (101 MHz, CHLOROFORM-*D*) δ 51.44 (CH-1), 69.63 (CH-5), 72.38, 72.45, 72.51 (CH₂ OBn x 2, CH₂ OAllyl), 73.99 (CH₂ OBn), 77.88 (CH-4), 78.33, 78.61 (CH-2, CH-3), 117.11 (CH₂=CH OAllyl), 127.78, 127.83, 127.87, 128.07, 128.14, 128.48, 128.51 (CH arom.), 134.84 (CH=CH₂ OAllyl), 137.94, 138.28, 138.32 (CH arom.) **IR** (ν_{max} , film) 3065, 3038, 2926, 2867, 2100, 1699, 1652, 1497, 1454, 1288, 1094, 1028, 920, 736, 628 cm^{-1} $[\alpha]_D^{20} = -1.54$ ($c = 0.18$, DCM)



1-azido-2,3,4-tri-O-benzyl-D-ribose-5-(bis(2-bromoethyl)phosphate) (7)

To a stirring solution of *tri*-2-bromoethyl-phosphate **65** (30 mg, 72 μ mol, 1.0 equiv.) in dry DCM (700 μ L) was added Tf₂O (18 μ L, 0.11 mmol, 1.5 equiv.). After 10 mins at RT dry pyridine (12 μ L, 0.14 mmol, 2.0 equiv.) was added and the resulting suspension was allowed to stir at RT for 10 mins before the addition of 1-azido-2,3,4-tri-O-benzyl-D-ribose (**1.06**) (64 mg in 300 μ L of DCM, 0.14 mmol, 2.0 equiv.). The sugar flask was rinsed with an additional dry DCM (150 μ L) which was added to the reaction and the resulting solution was allowed to stir at RT for 1.5 h. The reaction was diluted with DCM (1 mL), and concentrated under reduced pressure *in vacuo* to afford the crude product which was purified by flash column chromatography (gradient 30% EtOAc in hexane) to afford the pure product as a clear oil (23 mg, 31 μ mol, 44%)

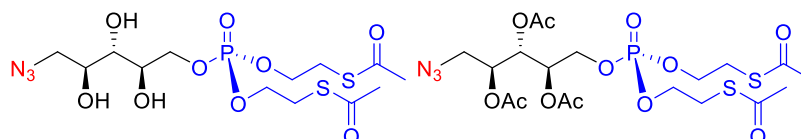
HRMS-ESI Calculated for [C₃₀H₃₆Br₂N₃O₇P⁺ + Na⁺]: 762.0550, found: 762.0560. **¹H NMR** (600 MHz, CHLOROFORM-*D*) δ ppm 3.27 – 3.55 (m, 6H, *CH*-1, *CH*-1', *CH*₂Br) 3.70 – 3.90 (m, 3H, *CH*-2, *CH*-3, *CH*-4), 4.14 – 4.33 (m, 5H, *OCH*₂CH₂Br, *CH*-5), 4.33 – 4.44 (m, 1H, *CH*-5'), 4.52 – 4.78 (m, 6H, *CHO*Bn), 7.28 – 7.43 (m, 15H, *CH* arom.) **¹³C NMR** (101 MHz, CHLOROFORM-*D*) δ ppm 29.50 (d, *J* = 7.5 Hz, *CH*₂Br), 29.60 (d, *J* = 7.3 Hz, *CH*₂Br), 51.07 (*CH*-1), 67.02 (dd, *J* = 5.2, 2.4 Hz, *CH*-5), 67.20 (d, *J* = 6.0 Hz, *CH*₂CH₂Br), 72.55, 72.65, 74.02, (*CH*₂ *OB*n), 77.39, 77.64, (*CH*-2, *CH*-4), 78.17 (*CH*-3), 128.00, 128.03, 128.10, 128.12, 128.19, 128.54, 128.57, 128.61, 137.58, 137.61, 137.77 (*CH* arom.) **IR** (*v*_{max}, film) 3289, 2898, 2101, 2049, 1977, 1709, 1454, 1395, 1352, 1221, 1175, 1164, 1102, 1050, 1020, 977, 918, 832, 745, 709, 699, 586 cm⁻¹ [α]_D²⁰ = +11.36 (*c* = 0.1, DCM)



1-azido-2,3,4-*tri-O*-benzyl-D-ribose-5-(*bis-S*-acetyl-2-thioethyl-phosphate)

To a stirring solution of 1-azido-2,3,4-*tri-O*-benzyl-D-ribose-5-(*di*-2-bromoethyl-phosphate) (**7**) (62 mg, 77 μmol, 1.0 equiv.) in acetone (2.5 mL) was added KSAC (51 mg, 0.43 mmol, 5.7 equiv.) The resulting suspension was allowed to stir at RT for 18 h before the reaction mixture was concentrated under reduced pressure. The crude product was purified by flash column chromatography (gradient 40% EtOAc in hexane) to afford the title compound as a clear oil (50 mg, 68 μmol, 88%)

HRMS-ESI Calculated for [C₃₄H₄₂N₃O₉PS₂ + Na⁺]: 754.1992, found: 754.2012, **¹H NMR** (600 MHz, CHLOROFORM-*D*) δ 2.29 (s, 6H, *CH*₃), 3.09 (td, *J* = 12.3, 6.1 Hz, 4H, *CH*₂SAC), 3.35 (dd, *J* = 12.9, 2.5 Hz, 1H, *CH*-1), 3.45 (dd, *J* = 12.9, 2.2 Hz, 1H, *CH*-1'), 3.74 – 3.89 (m, 3H, *CH*-2, *CH*-3, *CH*-4), 4.00 – 4.13 (m, 4H, *OCH*₂-*CH*₂SAC), 4.21 (ddd, *J* = 11.3, 7.3, 3.9 Hz, 1H, *CH*-5), 4.35 (ddd, *J* = 11.3, 6.2, 2.1 Hz, 1H, *CH*-5'), 4.51 – 4.78 (m, 6H, *CH*₂ *OB*n), 7.26 – 7.44 (m, 15H, *CH* arom.) **¹³C NMR** (101 MHz, CHLOROFORM-*D*) δ ppm 29.26 (d, *J* = 2.8 Hz), 29.31 (d, *J* = 3.0 Hz), (*CO-CH*₃), 30.66, 32.07, (*CH*₂SAC), 51.22 (*CH*-1), 66.11, 66.15, (*OCH*₂CH₂SAC), 67.04 (d, *J* = 6.0 Hz, *CH*-5), 72.59, 72.73, 74.08 (*CH*₂ *OB*n), 77.4642, 77.79, (*CH*-2, *CH*-4), 78.31 (*CH*-3), 128.04, 128.19, 128.24, 128.59, 128.61, 137.73, 137.74, 137.91, (*CH* arom.), 194.82 (*C=O*). **³¹P NMR** (162 MHz, C CHLOROFORM-*D*) δ -0.90. **IR** (*v*_{max}, film) 3031, 2917, 2100, 1694, 1497, 1454, 1355, 1278, 1098, 1060, 1017, 957, 738, 699, 624 cm⁻¹ [α]_D²⁰ = -2.66 (*c* = 0.125, DCM)



1-azido-D-ribose-5-(*bis-S*-acetyl-2-thioethyl-phosphate) (1-Az-OH-SATE Probe) and 2,3,4-*tri-O*-acetyl-1-azido-D-ribose-5-(*bis-S*-acetyl-2-thioethyl-phosphate) (1-Az-OAc-SATE Probe)

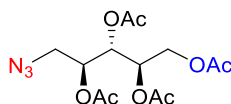
To a stirring solution of 1-azido-2,3,4-*tri-O*-benzyl-5-ribose-5-(*di-S*-Acetyl-2-ThioEthyl-phosphate) (47 mg, 65 μmol, 1.0 equiv.) in dry DCM (1.3 mL) at -78°C was added BCl₃ (1M in DCM, 0.65 mL, 0.65 mmol, 10 equiv.). The reaction was allowed to stir at -78°C for 3 hours before the reaction was quenched by the addition of 1:1 DCM: MeOH (1 mL) which was cooled to -78°C. The resulting reaction was left to warm to RT over 30 mins before the reaction mixture was concentrated under reduced pressure. The resulting crude intermediate was split in half, with half being purified by flash column chromatography (gradient 2 to 4% MeOH in DCM) to afford 1-azido-5-ribose-5-(*di-S*-Acetyl-2-ThioEthyl-phosphate) (1-Az-OH-SATE Probe) (17 mg, 37 μmol, quant.) as a clear oil. The other half was dissolved in 1:2 Ac₂O: pyridine (1.2 mL) and allowed to stir at RT for 18 h. The reaction was quenched by the addition of MeOH (1 mL) at 0°C and the reaction mixture was concentrated under reduced pressure. The crude product was purified by flash column chromatography (gradient 50% EtOAc in hexane) to afford 2,3,4-*tri-O*-acetyl-1-azido-5-ribose-5-(*di-S*-Acetyl-2-ThioEthyl-phosphate) as a pale yellow oil (18 mg, 31 μmol, quant.)

1-Az-OH-SATE Probe

HRMS-ESI Calculated for $[C_{13}H_{24}N_3O_9PS_2 + Na^+]$: 484.0584, found: 484.0597 **1H NMR** (600 MHz, CHLOROFORM-*D*) δ 2.40 (s, 6H, CH_3 SAc), 3.22 (dt, $J = 6.2, 6.6$ Hz, 4H, CH_2 SAc), 3.59 (dd, $J = 12.6, 6.2$ Hz, 1H, *CH-1*), 3.67 (dd, $J = 12.6, 2.9$ Hz, 1H, *CH-1'*), 3.74 (t, $J = 7.7$ Hz, 1H, *CH-3*), 3.92 (dd, $J = 8.1, 4.2$ Hz, 1H, *CH-4*), 3.98 (dd, $J = 6.9, 2.9$ Hz, 1H, *CH-2*), 4.11 – 4.25 (m, 4H, OCH_2CH_2 SAc), 4.31 (td, $J = 11.5, 2.3$ Hz, 1H, *CH-5*), 4.45 (dd, $J = 11.5, 4.2$ Hz, 1H, *CH-5'*). **^{13}C NMR** (151 MHz, CHLOROFORM-*D*) δ 29.14 (CH_3 SAc), 30.77 (CH_2 SAc), 53.90 (*CH-1*), 66.60 (d, $J = 6.2$ Hz, OCH_2CH_2 SAc), 69.41 (d, $J = 5.2$ Hz, *CH-5*), 70.10 (*CH-2*), 73.06 (*CH-3*), 73.41 (d, $J = 3.7$ Hz, *CH-4*), 195.48 (C=O SAc). **^{31}P NMR** (162 MHz, CHLOROFORM-*D*) δ 0.63. **IR** (ν_{max} , film) 3382, 2910, 2853, 2088, 1588, 1058, 1015, 955 cm^{-1} $[\alpha]_D^{20} = -21.85$ ($c = 0.045$, DCM)

1-Az-OAc-SATE Probe

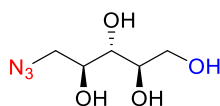
HRMS-ESI Calculated for $[C_{19}H_{30}N_3O_{12}PS_2 + Na^+]$: 610.0901, found: 610.0917 **1H NMR** (400 MHz, CHLOROFORM-*D*) δ 2.14 (s, 3H, OAc CH_3), 2.16 (s, 6H, OAc CH_3), 2.38 (s, 3H, SAc CH_3), 2.39 (s, 3H, SAc CH_3), 3.16 (dt, $J = 6.4, 5.7$ Hz, 4H, OCH_2CH_2 SAc), 3.43 (dd, $J = 13.3, 7.0$ Hz, 1H, *CH-1*), 3.50 (dd, $J = 13.3, 4.1$ Hz, 1H, *CH-1'*), 4.06 – 4.17 (m, 5H, *CH-5*, OCH_2CH_2), 4.27 (ddd, $J = 11.6, 6.3, 2.9$ Hz, 1H, *CH-5'*), 5.18 – 5.24 (m, 1H, *CH-2*), 5.23 (dd, $J = 5.9, 2.9$ Hz, 1H, *CH-4*), 5.30 (dd, $J = 5.9, 4.4$ Hz, 1H, *CH-3*). **^{13}C NMR** (151 MHz, CHLOROFORM-*D*) δ 20.64, 20.76, 20.82 (OAc CH_3), 29.00, 29.05 (SAc CH_3), 29.64, 30.50 (CH_2 SAc), 50.09 (*CH-1*), 65.27 (d, $J = 5.2$ Hz, *CH-5*), 66.19 (2 x d, $J = 2.6$ Hz, OCH_2CH_2 SAc), 69.32 (*CH-2*), 69.93 (d, $J = 7.8$ Hz, *CH-4*), 70.55 (*CH-3*), 169.27, 169.75 (C=O OAc), 194.66 (C=O SAc). **^{31}P NMR** (162 MHz, CHLOROFORM-*D*) δ -1.15. **IR** (ν_{max} , film) 2911, 2852, 2088, 1750, 1705, 1205, 1058, 1000 cm^{-1} $[\alpha]_D^{20} = +6.34$ ($c = 0.025$, DCM)



2,3,4,5-tetra-O-acetyl-1-azido-D-ribose (1-Az-OAc Probe)

To a stirring solution of 1-azido-2,3,4-*tri-O*-benzyl-D-ribose (**6**) (30 mg, 56 μ mol, 1.0 equiv.) in dry DCM (1 mL) at $-78^\circ C$ was added BCl_3 (1 M in DCM, 0.56 mL, 0.56 mmol, 10 equiv.) dropwise. The reaction was maintained at $-78^\circ C$ for 3 h before the reaction was quenched by the dropwise addition of 1:1 DCM: MeOH (1 mL) which had been cooled to $-78^\circ C$. The reaction was allowed to stir at $-78^\circ C$ for 15 mins, $0^\circ C$ for 15 mins and RT for 15 mins before the reaction mixture was concentrated under reduced pressure. The resulting crude was dissolved in 1:2 Ac₂O: pyridine (1 mL) and allowed to stir at RT for 18 h. The reaction was quenched by the addition of MeOH (1 mL) at $0^\circ C$ and the reaction mixture was concentrated under reduced pressure. The crude product was purified by flash column chromatography (gradient 20-33% EtOAc in hexane) to afford the title compound as a clear oil (18 mg, 53 μ mol, 95%)

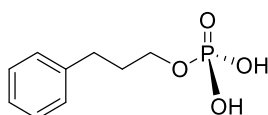
HRMS-ESI Calculated for $[C_{13}H_{19}N_3O_8 + Na^+]$: 368.1064, found: 368.1065 **1H NMR** (400 MHz, CHLOROFORM-*D*) δ 2.05 (s, 3H, CH_3 OAc), 2.10 (s, 6H, CH_3 OAc x 2), 2.13 (s, 3H, CH_3 OAc), 3.42 (dd, $J = 13.4, 6.9$ Hz, 1H, *CH-1*), 3.51 (dd, $J = 13.4, 3.4$ Hz, 1H, *CH-1'*), 4.14 (dd, $J = 12.2, 6.2$ Hz, 1H, *CH-5*), 4.32 (dd, $J = 12.2, 3.3$ Hz, 1H, *CH-5'*), 5.19 (ddd, $J = 6.9, 5.3, 3.4$ Hz, 1H, *CH-2*), 5.25 (td, $J = 5.9, 3.3$ Hz, 1H, *CH-4*), 5.33 (app. t, $J = 5.3$ Hz, 1H, *CH-3*). **^{13}C NMR** (101 MHz, CHLOROFORM-*D*) δ 20.81, 20.95, 20.98, (CH_3 OAc), 50.30 (*CH-1*), 61.85 (*CH-5*), 69.57 (*CH-2*), 69.78 (*CH-4*), 70.57 (*CH-3*), 169.51, 169.97, 170.01, 170.70 (C=O OAc) **IR** (ν_{max} , film) 2105, 1747, 1371, 1216, 1050 cm^{-1} $[\alpha]_D^{20} = +12.59$ ($c = 0.67$, DCM)



1-azido-ribitol (1-Az-OH Probe)

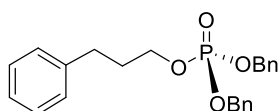
To a stirring solution of 2,3,4,5-*tetra-O*-acetyl-1-azido-D-ribitol (**1-Az-OAc Probe**) (4.7 mg, 14 μ mol, 1.0 equiv.) in MeOH (0.3 mL) was added NaOMe (0.5 M in MeOH) till the pH reached pH 10 (approx. 7 drops). The resulting solution was allowed to stir at RT for 24 h. The reaction was neutralised with DOWEX H⁺ resin and filtered to afford the crude product which was purified by flash column chromatography (gradient 10% MeOH in DCM) to afford the title compound as a white solid (1.6 mg, 9.0 μ mol, 64%)

HRMS-ESI Calculated for [C₅H₁₀N₃O₄]⁻: 176.0677, found: 176.0668. **¹H NMR** (600 MHz, D₂O) δ 3.45 (dd, J = 13.1, 7.5 Hz, 1H, CH-1), 3.54 (dd, J = 13.1, 3.0 Hz, 1H, CH-1'), 3.58 – 3.66 (m, 1H, CH-5), 3.68 (t, J = 6.2 Hz, 1H, CH-5'), 3.75 – 3.82 (m, 2H, CH-3, CH-4), 3.92 (ddd, J = 7.5, 6.4, 3.0 Hz, 1H, CH-2). **¹³C NMR** (151 MHz, D₂O) δ 52.83 (CH-1), 62.30 (CH-5), 70.76 (CH-2), 72.08 (CH-4), 72.29 (CH-3). **IR** (ν_{\max} , film) 3396, 3084, 3003, 29256, 2837, 2109, 1601, 1514, 1302, 1181, 1148, 1050, 1088, 564 cm⁻¹ [α]_D²⁰ = +3.33 (c = 0.05, MeOH)



3-phenylpropyl-1-phosphate (41)

To a stirring solution of MeCN (1.6 mL) and H₂O (180 μ L) at 0°C was added POCl₃ (0.20 mL, 2.2 mmol, 6.1 equiv.). Pyridine (0.15 mL, 2.2 mmol, 6.1 equiv.) was added dropwise and the solution kept at 0°C for 10 mins before the addition of 3-phenyl-1-propanol (50 μ L, 0.36 mmol, 1.0 equiv.). After 6 h the reaction was quenched by the addition of H₂O (12 mL) and the solution stirred for 1 h before concentrating under reduced pressure to afford the crude product. ESI-MS confirmed presence of the desired phosphorylated product and ion exchange chromatography (Dowex 1X8 Resin Cl⁻ form, eluting with increasing strength of formic acid: 0 to 1M in 0.2M increments) was attempted. No title product observed following purification.



3-phenylpropyl-1-(bis-benzyl-phosphate) (42)

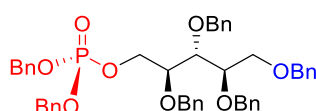
via Mitsunobu To a stirring solution of dibenzyl phosphate (204 mg, 0.733 mmol, 4.89 equiv.), PPh₃ (193 mg, 0.736 mmol, 4.91 equiv.) and 3-phenyl-1-propanol (20 mg, 0.15 mmol, 1.0 equiv.) in dry THF (5 mL) was added NEt₃ (0.20 mL, 1.5 mmol, 10 equiv.) and DIAD (0.13 mL, 0.74 mmol, 5.0 equiv.). The reaction mixture was allowed to stir at RT for 18 h, and the reaction mixture was concentrated under reduced pressure onto silica. The crude product was purified by flash column chromatography (gradient 30% EtOAc in hexane). No desired product was obtained.

via DCC Coupling A solution of dibenzyl phosphate (120 mg, 0.431 mmol, 1.95 equiv.) and DCC (90 mg, 0.436 mmol, 1.98 equiv.) in dry DCM (5.5 mL) was stirred at RT for 4 h before the reaction mixture was filtered through a cotton wool plug. To the resulting clear pale yellow solution was added 3-phenyl-1-propanol (30 μ L, 0.22 mmol, 1.0 equiv.). After 16 h the reaction mixture was concentrated under reduced pressure and the crude product was purified by manual flash column chromatography (gradient of 30% EtOAc in hexane) to afford the title compound as a clear oil (14 mg, 40 μ mol, 16%)

via Oxalyl Chloride Chloro-phosphate formation To a stirring solution of dibenzyl phosphate (30 mg, 0.18 mmol, 3.2 equiv.) in dry DCM (0.5 mL) with 3 drops of dry DMF (cat.) at 0°C was added oxalyl chloride (13 μ L, 0.12 mmol, 3.0 equiv.). After 1 h DCM (0.2 mL) was added to a dry flask containing 3-phenyl-1-propanol (5.0

μL , 34 μmol , 1.0 equiv.) and NaH (60% in mineral oil, 2.0 mg, 70 μmol , 1.7 equiv.). To this solution at 0°C was added half by volume of the activated phosphate solution diluted with DMF (0.4 mL). After 3 h the reaction was quenched by the addition of H₂O (5 drops) and the reaction mixture was concentrated under reduced pressure. The desired title product was obtained by flash column chromatography (gradient 20-40% EtOAc in hexane) to afford the pure product as a clear oil (3.8 mg, 0.0098 mmol, 32%).

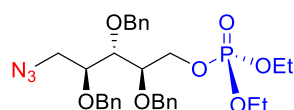
HRMS-ESI Calculated for [C₂₃H₂₅O₄P + Na⁺]: 419.1383, found: 419.1378 **¹H NMR** (400 MHz, CHLOROFORM-*D*) δ 1.87 – 1.97 (m, 2H, Ph-CH₂-CH₂), 2.64 (t, J = 7.4 Hz, 2H, Ph-CH₂), 4.00 (dd, J = 6.6, 6.2 Hz, 2H, Ph-CH₂), 4.99 – 5.09 (m, 4H, CH₂ OBn), 7.09 – 7.24 (m, 5H, CH arom.), 7.30-7.38 (s, 10H, CH arom.). **¹³C NMR** 400 MHz, CHLOROFORM-*D*), 31.55 (OCH₂CH₂CH₂Ph), 31.94 (OCH₂CH₂CH₂Ph), 67.09 (J = 6.07 Hz, OCH₂), 69.18 (CH₂ OBn), 69.24 CH₂ OBn), 127.93, 128.42, 128.51, 128.57 (CH arom.) **³¹P NMR** (162 MHz, CHLOROFORM-*D*) δ -0.17. **IR** (ν_{max} , film) 2925, 2852, 1694, 1596, 1455, 1266, 1011, 880, 790, 697, 456 cm⁻¹



2,3,4,5-tetra-O-benzyl-ribitol-1-(bis-benzylphosphate)

To a stirring solution of dibenzyl phosphate (30 mg, 0.18 mmol, 3.2 equiv.) in dry DCM (0.5 mL) with 3 drops of dry DMF (cat.) at 0°C was added oxalyl chloride (13 μL , 0.12 mmol, 3.0 equiv.). After 1 h DCM (0.2 mL) was added to a dry flask containing 2,3,4,5-tetra-O-benzyl-ribitol (**33**) (18 mg, 34 μmol , 1.0 equiv.) and NaH (60% in mineral oil, 2.0 mg, 70 μmol , 1.7 equiv.). To this solution at 0°C was added half by volume of the activated phosphate solution diluted with DMF (0.4 mL). After 3 h the reaction was quenched by the addition of H₂O (5 drops) and the reaction mixture was concentrated under reduced pressure. The crude product was purified by flash column chromatography (gradient 20-40% EtOAc in hexane) to afford the title compound as a clear oil (5.0 mg, 7.0 μmol , 20%).

HRMS-ESI Calculated for [C₄₇H₄₉O₈P + Na⁺]: 795.3057 found: 795.3092 **¹H NMR** (400 MHz, CHLOROFORM-*D*) δ 3.60 – 3.70 (m, 2H, CH-5, CH-5'), 3.81 – 3.91 (m, 3H, CH-2, CH-3, CH-4), 4.21 (ddd, J = 11.1, 7.2, 5.3 Hz, 1H, CH-1), 4.34 (ddd, J = 11.1, 6.1, 2.7 Hz, 1H, CH-1'), 4.46 (d, J = 1.3 Hz, 2H, CH₂ OBn), 4.51 (d, J = 11. Hz, 1H, CH₂ OBn), 4.57 (d, J = 11.8 Hz, 1H, CH₂ OBn), 4.59 – 4.70 (m, 4H, CH₂ OBn), 4.90 – 5.04 (m, 4H, POCH₂Ph), 7.18 – 7.24 (m, 4H, CH arom.), 7.25 – 7.33 (m, 26H, CH arom.). **¹³C NMR** (101 MHz, CHLOROFORM-*D*) δ 67.34 (d, J = 6.1 Hz, CH-1), 69.23 (d, J = 2.1 Hz, POCH₂Ph), 69.29 (d, J = 2.2 Hz, POCH₂Ph), 69.90, CH-5), 72.51, 72.53, 73.42, 73.86 (CH₂ OBn), 78.07 (d, J = 7.5 Hz, CH-2), 78.21 (CH-3), 78.26 (CH-4), 127.63, 127.69, 127.74, 127.79, 127.91, 127.94, 127.96, 128.03, 128.09, 128.42, 128.47, 128.51, 128.55, 128.66, 135.98 (d, J = 2.9 Hz), 136.08 (d, J = 2.9 Hz), 138.21, 138.33, 138.58 (CH arom.). **³¹P NMR** (162 MHz, CHLOROFORM-*D*) δ -0.08. **IR** (ν_{max} , film) 2960, 2918, 2852, 2105, 1733, 1458, 1261, 1094, 1027, 699 cm⁻¹ [α]_D²⁰ = + 28.52 (c = 0.85, DCM)

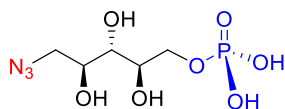


1-azido-2,3,4-tri-O-benzyl-D-ribitol-5-(diethyl-phosphate) (43)

To a stirring solution of triethyl phosphate (18 mg, 0.10 mmol, 1.0 equiv.) in DCM (0.5 mL) was added freshly distilled Tf₂O (25 μL , 0.15 mmol, 1.5 equiv.) at RT. The reaction was allowed to stir for 10 mins before the addition of pyridine (16 μL , 0.20 mmol, 2.0 equiv.). After a further 10 mins a solution of 1-azido-2,3,4-tri-O-benzyl-D-ribitol (**33**) (80 mg, 0.18 mmol, 1.8 equiv.) in DCM (400 μL) was added dropwise. The resulting solution was allowed to stir at RT for 1.5 hours before the reaction mixture was concentrated under reduced pressure onto silica. The pure product was obtained by column chromatography on an automated system (gradient 0-70% EtOAc in hexane) to afford the title compound as a golden oil (32 mg, 54 μmol , 55%)

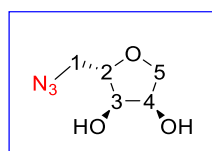
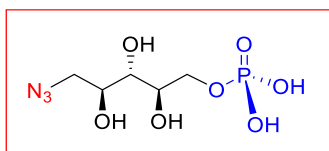
HRMS-ESI Calculated for [C₂₆H₂₉N₃O₇P]: 526.1749, found: 526.1768. **¹H NMR** (400 MHz, CHLOROFORM-*D*) δ 1.24 – 1.32 (m, 6H, CH₃), 3.35 (dd, J = 13.1, 2.4 Hz, 1H, CH-1), 3.46 (dd, J = 13.1, 5.6 Hz, 1H, CH-1'), 3.81 – 3.88 (m, 3H, CH-2, CH-3, CH-4), 4.00 – 4.13 (m, 4H, OCH₂-H₃), 4.19 (ddd, J = 11.6, 6.9, 4.1 Hz, 1H, CH-5), 4.33 (ddd, J

= 11.6, 6.1, 2.4 Hz, 1H, CH-5'), 4.57 – 4.76 (m, 6H, CH₂ OBn), 7.26 – 7.40 (m, 15H, CH arom.). ¹³C NMR (101 MHz, CHLOROFORM-D) δ 16.25 (d, J = 6.0 Hz, CH₃), 51.23 (CH-1), 63.95 (d, J = 5.8 Hz, OCH₂CH₃), 66.57 (d, J = 6.0 Hz, CH-5), 72.55, 72.70, 74.04 (CH₂ OBn), 77.63 (d, J = 7.1 Hz, CH-2), 77.89 (CH-4), 78.35 (CH-3), 127.96, 128.16, 128.54, 128.57, 137.76, 137.84, 137.95 (CH arom.) IR (ν_{max}, film) 3065, 3034, 2984, 2908, 2872, 2100, 1499, 1455, 1394, 1267, 1099, 1029, 745, 698 cm⁻¹ ³¹P NMR (162 MHz, CHLOROFORM-D) δ -0.15. [α]_D²⁰ = -7.95 (c = 0.475, DCM)



1-azido-D-ribose-5-phosphate (1-Az OH Phos Probe)

To a stirring solution of 1-azido-2,3,4-tri-O-benzyl-D-ribose-(diethyl-phosphate) (**43**) (38 mg, 60 μmol, 1.0 equiv.) in dry DCM (1.3 mL) at 0°C was added TMSBr (0.10 mL, 0.60 mmol, 10 equiv.) the resulting solution was allowed to warm to RT and left for 21 h after which the solvents were removed *in vacuo* and the excess TMSBr was removed by co-evaporation with MeOH and toluene. Crude ESI-MS and ¹H NMR showed evidence of the free phosphate intermediate, and the crude was used in the following step without purification. The crude was dissolved in DCM (0.8 mL) and cooled to -78°C. BCl₃ (1M in DCM, 0.60 mL, 0.60 mmol, 12 equiv.) was added dropwise. After 4 h the reaction was quenched by the addition of 1:1 MeOH:DCM (1 mL) and the reaction slowly warmed to RT. The solvents were removed *in vacuo* to yield a 3:1 ratio of product:side product 1,4-anhydro-5-azido-5-deoxy-D,L-ribose as a clear oil (11 mg, 36 μmol, 60%).



HRMS-ESI Calculated for [C₅H₁₁N₃O₇P + Na⁺]: 256.0340, found: 256.0330. Calculated for [C₅H₈N₃O₃ + Na⁺]: 158.0571, found: 158.0569 ¹H NMR (600 MHz, D₂O) δ 3.41 (dd, J = 13.5, 5.6 Hz, 1H, CH-1), 3.48 (dd, J = 13.1, 7.5 Hz, 1H, CH-1), 3.55 (dd, J = 13.1, 3.0 Hz, 1H, CH-1), 3.68 (dd, J = 13.5, 3.2 Hz, 1H, CH-1), 3.76 (t, J = 6.4 Hz, 1H, CH-3), 3.82 (dd, J = 10.2, 2.4 Hz, 1H, CH-5), 3.93 (td, J = 6.4, 2.9 Hz, 1H, CH-2), 3.95 – 4.00 (m, 2H, CH-2, CH-4), 4.02 (dt, J = 12.1, 6.2 Hz, 1H, CH-5), 4.07 – 4.15 (m, 3H, CH-3, CH-5, CH-5), 4.30 (td, J = 4.5, 2.4 Hz, 1H, CH-4). ¹³C NMR (151 MHz, D₂O) δ 51.83 (CH-1), 52.78 (CH-1), 66.59 (d, J = 4.4 Hz, CH-5), 70.74 (CH-2), 70.82 (d, J = 7.9 Hz, CH-4), 70.96 (CH-4), 71.74 (CH-3), 72.45 (CH-5), 72.58 (CH-3), 79.85 (CH-2). ³¹P NMR (162 MHz, D₂O) δ 1.30.

3.7 References

2. L. Wells, *J. Biol. Chem.*, 2013, **288**, 6930-6935.
10. M. Riemersma, D. S. Froese, W. van Tol, U. F. Engelke, J. Kopec, M. van Scherpenzeel, A. Ashikov, T. Krojer, F. von Delft, M. Tessari, A. Buczkowska, E. Swiezewska, L. T. Jae, T. R. Brummelkamp, H. Manya, T. Endo, H. van Bokhoven, W. W. Yue and D. J. Lefeber, *Chem. Biol.*, 2015, **22**, 1643-1652.
39. J. L. Praissman, T. Willer, M. O. Sheikh, A. Toi, D. Chitayat, Y.-Y. Lin, H. Lee, S. H. Stalnaker, S. Wang, P. K. Prabhakar, S. F. Nelson, D. L. Stemple, S. A. Moore, K. W. Moremen, K. P. Campbell and L. Wells, *Elife*, 2016, **5**, 1-18.
44. M. Kanagawa, K. Kobayashi, M. Tajiri, H. Manya, A. Kuga, Y. Yamaguchi, K. Akasaka-Manya, J.-I. Furukawa, M. Mizuno, H. Kawakami, Y. Shinohara, Y. Wada, T. Endo and T. Toda, *Cell Rep.*, 2016, **14**, 2209-2223.
45. I. Gerin, B. Ury, I. Breloy, C. Bouchet-Seraphin, J. Bolsée, M. Halbout, J. Graff, D. Vertommen, G. G. Muccioli, N. Seta, J.-M. Cuisset, I. Dabaj, S. Quijano-Roy, A. Grahn, E. Van Schaftingen and G. T. Bommer, *Nat. Commun.*, 2016, **7**, 11534.
56. S. Baur, J. Maries-Wright, S. Buckenmaier, R. J. Lewis and W. Vollmer, *J. Bacteriol.*, 2009, **191**, 1200-1210.
57. C. Singh, E. Glaab and C. L. Linster, *J. Biol. Chem.*, 2017, **292**, 1005-1028.
73. J. Sasaki, K. Ishikawa, K. Kobayashi, E. Kondo-Iida, M. Fukayama, H. Mizusawa, S. Takashima, Y. Sakakihara, Y. Nakamura and T. Toda, *Hum. Mol. Genet.*, 2000, **9**, 3083-3090.
128. W. Qin, K. Qin, X. Fan, L. Peng, W. Hong, Y. Zhu, P. Lv, Y. Du, R. Huang, M. Han, B. Cheng, Y. Liu, W. Zhou, C. Wang and X. Chen, *Angew. Chem. Int. Ed. Engl.*, 2018, **57**, 1817-1820.
130. Y. Hao, X. Fan, Y. Shi, C. Zhang, D. e. Sun, K. Qin, W. Qin, W. Zhou and X. Chen, *Nat. Commun.*, 2019, **10**, 4065.
173. U. Pradere, E. C. Garnier-Amblard, S. J. Coats, F. Amblard and R. F. Schinazi, *Chem. Rev.*, 2014, **114**, 9154-9218.
174. A. R. Van Rompay, M. Johansson and A. Karlsson, *Pharmacol. Ther.*, 2000, **87**, 189-198.
175. Y. Ding, J.-L. Girardet, Z. Hong, V. C. H. Lai, H. An, Y.-H. Koh, S. Z. Shaw and W. Zhong, *Bioorg. Med. Chem. Lett.*, 2005, **15**, 709-713.
176. M. P. Cataldi, P. Lu, A. Blaeser and Q. L. Lu, *Nat. Commun.*, 2018, **9**, 3448.
177. H. C. Hang, C. Yu, D. L. Kato and C. R. Bertozzi, *Proc. Natl. Acad. Sci. U. S. A.*, 2003, **100**, 14846-14851.
178. E. M. Sletten and C. R. Bertozzi, *Acc. Chem. Res.*, 2011, **44**, 666-676.
179. A. K. Sarkar, T. A. Fritz, W. H. Taylor and J. D. Esko, *Proc. Natl. Acad. Sci. U. S. A.*, 1995, **92**, 3323-3327.
180. A. J. Wiemer and D. F. Wiemer, *Top. Curr. Chem.*, 2015, **360**, 115-160.
181. M. Komabayashi, T. Stiller and S. Jopp, *J. Mol. Liq.*, 2021, **325**, 115167.
182. T. Kamkhachorn, A. R. Parameswar and A. V. Demchenko, *Org. Lett.*, 2010, **12**, 3078-3081.
183. S. Ohkawabata, M. Kanemaru, S.-y. Kuawahara, K. Yamamoto and J.-i. Kadokawa, *J. Carbohydr. Chem.*, 2012, **31**, 659-672.
184. K. Takashima, M. Sakano, E. Kinouchi, S. Nakamura, S. Marumoto, F. Ishikawa, K. Ninomiya, I. Nakanishi, T. Morikawa and G. Tanabe, *Bioorg. Med. Chem. Lett.*, 2021, **33**, 127751.
185. T. Lasek, J. Dobias, M. Budesinsky, J. Kozak, B. Lapunikova, I. Rosenberg, G. Birkus and O. Pav, *Tetrahedron*, 2021, **89**, 132159.
186. G. Zhao, W. Yao, J. N. Mauro and M. Y. Ngai, *J. Am. Chem. Soc.*, 2021, **143**, 1728-1734.
187. S. Valverde, M. García, A. M. Gómez and J. C. López, *Chem. Commun.*, 2000, DOI: 10.1039/b000771o, 813-814.
188. A. Shaw, P. Das and S. Ajay, *Synthesis*, 2016, **48**, 3753-3762.
189. A. Chronowska, E. Gallienne, C. Nicolas, A. Kato, I. Adachi and O. R. Martin, *Tetrahedron Lett.*, 2011, **52**, 6399-6402.

190. M. U. Roslund, O. Aitio, J. Wärnå, H. Maaheimo, D. Y. Murzin and R. Leino, *J. Am. Chem. Soc.*, 2008, **130**, 8769-8772.
191. O. P. Chevallier and M. E. Migaud, *Beilstein J. Org. Chem.*, 2006, **2**, 14.
192. G. Zhang, M. Fu and J. Ning, *Carbohydr. Res.*, 2005, **340**, 155-159.
193. M. Islam, G. P. Shinde and S. Hotha, *Chem. Sci.*, 2017, **8**, 2033-2038.
194. M. Fusari, S. Fallarini, G. Lombardi and L. Lay, *Bioorg Med Chem*, 2015, **23**, 7439-7447.
195. L. Cattiaux, A. Mee, M. Pourcelot, G. Sfihi-Loualia, T. Hurtaux, E. Maes, C. Fradin, B. Sendid, D. Poulain, E. Fabre, F. Delplace, Y. Guerardel and J. M. Mallet, *Bioorg. Med. Chem.*, 2016, **24**, 1362-1368.
196. E. Zhang, S. Wang, L. L. Li, Y. G. Hua, J. F. Yue, J. F. Li and C. Y. Jin, *Bioorg. Med. Chem. Lett.*, 2018, **28**, 497-502.
197. C. Jia, Y. Zhang, L.-H. Zhang, P. Sinaÿ and M. Sollogoub, *Carbohydr. Res.*, 2006, **341**, 2135-2144.
198. C. Chbib, A. J. Sobczak, M. Mudgal, C. Gonzalez, D. Lumpuy, J. Nagaj, K. Stokowa-Soltys and S. F. Wnuk, *J. Sulphur Chem.*, 2016, **37**, 307-327.
199. P. Das, S. Ajay and A. K. Shaw, *Synthesis*, 2016, **48**, 3753-3762.
200. G. W. J. Fleet and P. W. Smith, *Tetrahedron*, 1986, **42**, 5685-5692.
201. Y. S. Shin, D. B. Jarhad, M. H. Jang, K. Kovacicova, G. Kim, J.-S. Yoon, H.-R. Kim, Y. E. Hyun, A. S. Tipnis, T.-S. Chang, M. J. van Hemert and L. S. Jeong, *Eur. J. Med. Chem.*, 2020, **187**, 111956.
202. M. Fouché, L. Rooney and A. G. M. Barrett, *J. Org. Chem.*, 2012, **77**, 3060-3070.
203. A. Venkanna, E. Sreedhar, B. Siva, K. S. Babu, K. R. Prasad and J. M. Rao, *Tetrahedron Asymmetry*, 2013, **24**, 1010-1022.
204. S. Šesták, M. Bella, T. Klunda, S. Gurská, P. Džubák, F. Wöls, I. B. H. Wilson, V. Sladek, M. Hajdúch, M. Poláková and J. Kóňa, *ChemMedChem*, 2018, **13**, 373-383.
205. G. Chandra, Y. W. Moon, Y. Lee, J. Y. Jang, J. Song, A. Nayak, K. Oh, V. A. Mulamoottil, P. K. Sahu, G. Kim, T.-S. Chang, M. Noh, S. K. Lee, S. Choi and L. S. Jeong, *J. Med. Chem.*, 2015, **58**, 5108-5120.
206. P. J. Garegg, R. Johansson, I. Lindh and B. Samuelsson, *Carbohydr. Res.*, 1986, **150**, 285-289.
207. K. Napora, T. M. Wrodnigg, P. Kosmus, M. Thonhofer, K. Robins and M. Winkler, *Bioorg. Med. Chem. Lett.*, 2013, **23**, 3393-3395.
208. M. Miyazawa, T. Takahashi, I. Horibe and R. Ishikawa, *Tetrahedron*, 2012, **68**, 2007-2010.
209. B. Ren, M. Wang, J. Liu, J. Ge, X. Zhang and H. Dong, *Green Chem.*, 2015, **17**, 1390-1394.
210. J.-F. Longevial, K. El Cheikh, D. Aggad, A. Lebrun, A. van der Lee, F. Tielens, S. Clément, A. Morère, M. Garcia, M. Gary-Bobo and S. Richeter, *Eur. J. Chem.*, 2017, **23**, 14017-14026.
211. S. A. Svarovsky, Z. Szekely and J. J. Barchi, *Tetrahedron Asymmetry*, 2005, **16**, 587-598.
212. C. G. Casinovi, M. Framondino, G. Randazzo and F. Siani, *Carbohydr. Res.*, 1974, **36**, 67-73.
213. A. E. Christina, D. v. d. Es, J. Dinkelaar, H. S. Overkleeft, G. A. v. d. Marel and J. D. C. Codée, *Chem. Commun.*, 2012, **48**, 2686.
214. M. Tortosa, N. A. Yakelis and W. R. Roush, *J. Am. Chem. Soc.*, 2008, **130**, 2722-2723.
215. F. Kleinbeck and E. M. Carreira, *Angew. Chem. Int. Ed.*, 2009, **48**, 578-581.
216. A. S. Sofian and C. Kuan Lee, *J. Carbohydr. Chem.*, 2003, **22**, 185-206.
217. K. R. Prasad and P. Gutala, *Tetrahedron*, 2011, **67**, 4514-4520.
218. S. Mouné, G. Niel, M. Busquet, I. Eggleston and P. Jouin, *J. Org. Chem.*, 1997, **62**, 3332-3339.
219. J. Hao, X. Zhang, P. Zhang, J. Liu, L. Zhang and H. Sun, *Tetrahedron*, 2009, **65**, 7975-7984.
220. I. Raji, F. Yadudu, E. Janeira, S. Fathi, L. Szymczak, J. R. Kornacki, K. Komatsu, J.-D. Li, M. Mrksich and A. K. Oyelere, *Bioorg. Med. Chem.*, 2017, **25**, 1202-1218.
221. pKa Values for Organic and Inorganic Bronsted Acids at 25°C,
<https://owl.oit.umass.edu/departments/OrganicChemistry/appendix/pKaTable.html>,
 (accessed 12/4/2020).

222. pKa Table, https://edisciplinas.usp.br/pluginfile.php/1885601/mod_resource/content/1/pKa%20table_organic.pdf, (accessed 12/4/2020).
223. Approximate pKa chart of the functional groups: values to know, <https://www.chem.indiana.edu/wp-content/uploads/2018/03/pka-chart.pdf>, (accessed 12/4/2020).
224. A. E. Wróblewski and I. I. B ak-Sypień, *Tetrahedron Asymmetry*, 2007, **18**, 2218-2226.
225. A. Nagy, B. Csordás, V. Zsoldos-Mády, I. Pintér, V. Farkas and A. Perczel, *Amino Acids*, 2017, **49**, 223-240.
226. A. S. Figueredo, L. O. B. Zamoner, M. Rejzek, R. A. Field and I. Carvalho, *Tetrahedron Lett.*, 2018, **59**, 4405-4409.
227. C. Pasti, E. Rinaldi, C. Cervellati, F. Dallochio, R. Hardré, L. Salmon and S. Hanau, *Bioorg. Med. Chem.*, 2003, **11**, 1207-1214.
228. C. Wiles, P. Watts and S. J. Haswell, *Tetrahedron Lett.*, 2006, **47**, 5261-5264.
229. Y. Koga, S. Sakamaki, M. Hongu, E. Kawanishi, T. Sakamoto, Y. Yamamoto, H. Kimata, K. Nakayama, C. Kuriyama, Y. Matsushita, K. Ueta, M. Tsuda-Tsukimoto and S. Nomura, *Bioorg. Med. Chem.*, 2013, **21**, 5561-5572.
230. W. Ndugire, B. Wu and M. Yan, *Molecules*, 2019, **24**.
231. C. M. Liu, C. D. Warren and R. W. Jeanloz, *Carbohydr. Res.*, 1985, **136**, 273-284.
232. R. C. Pinto, M. M. Andrade and M. T. Barros, *Tetrahedron Lett.*, 2012, **53**, 6633-6636.
233. D. Alvarez-Dorta, E. I. Leon, A. R. Kennedy, A. Martin, I. Perez-Martin, C. Riesco-Fagundo and E. Suarez, *Chemistry*, 2013, **19**, 10312-10333.
234. W. Lu, L. Navidpour and S. D. Taylor, *Carbohydr. Res.*, 2005, **340**, 1213-1217.
235. H. Che, Y. Fang, S. K. Gurung, J. Luo, D. H. Yoon, G.-H. Sung, T. W. Kim and H. Park, *Bull. Korean. Chem. Soc.*, 2014, **35**, 2038-2042.
236. T. S. Rasmussen, H. Koldso, S. Nakagawa, A. Kato, B. Schiott and H. H. Jensen, *Org. Biomol. Chem.*, 2011, **9**, 7807-7813.
237. H. Huang, J. Ash and J. Y. Kang, *Org. Lett.*, 2018, **20**, 4938-4941.
238. H. Huang, J. Denne, C.-H. Yang, H. Wang and J. Y. Kang, *Angew. Chem. Int. Ed. Engl.*, 2018, **57**, 6624-6628.
239. C. D. Spicer, M. Pujari-Palmer, H. Autefage, G. Insley, P. Procter, H. Engqvist and M. M. Stevens, *ACS Cent. Sci.*, 2020, **6**, 226-231.
240. L. Liang, T. Y. Wade Wei, P. Y. Wu, W. Herrebout, M. D. Tsai and S. P. Vincent, *ChemBioChem*, 2020, **21**, 2982-2990.
241. K. M. Sureshan, M. Trusselle, S. C. Tovey, C. W. Taylor and B. V. L. Potter, *J. Org. Chem.*, 2008, **73**, 1682-1692.
242. R. G. Bhat, N. S. Kumar and B. M. Pinto, *Carbohydr. Res.*, 2007, **342**, 1934-1942.
243. A. Borio, A. Hofinger, P. Kosma and A. Zamyatina, *Tetrahedron Lett.*, 2017, **58**, 2826-2829.
244. B. Xiong, G. Wang, C. Zhou, Y. Liu, J. Li, P. Zhang and K. Tang, *Phosphorus Sulfur Silicon Relat. Elem.*, 2018, **193**, 239-244.
245. S. P. Vincent and L. N. Gastinel, *Carbohydr. Res.*, 2002, **337**, 1039-1042.
246. H. Miyazawa, H. Yokokura, Y. Ohkubo, Y. Kondo and N. Yoshino, *J. Fluor. Chem.*, 2004, **125**, 1485-1490.
247. M. Barbier, E. Grand and J. Kovensky, *Carbohydr. Res.*, 2007, **342**, 2635-2640.
248. M. Nagaraju, A. Krishnaiah and H. B. Mereyala, *Synth. Commun.*, 2007, **37**, 2467-2472.
249. K. Burgess, D. A. Chaplin, I. Henderson, Y. T. Pan and A. D. Elbein, *J. Org. Chem.*, 1992, **57**, 1103-1109.

Chapter 4: Development of Novel Methodology for Synthesis of *S*-Acetyl-2-Thioethyl-Protected Phosphates

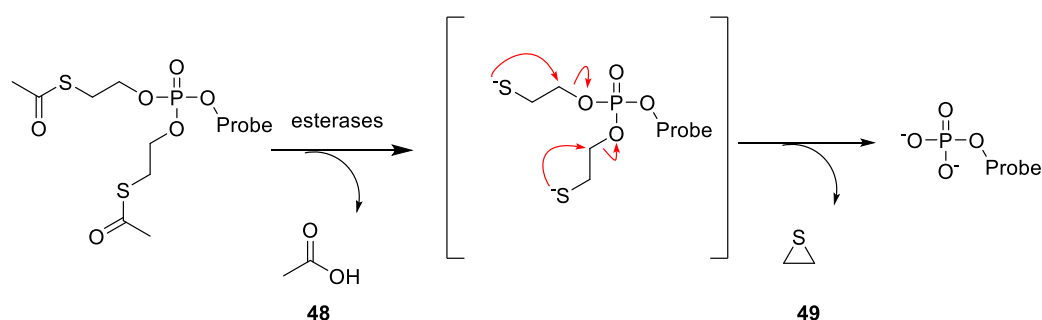
4.1 Abstract

S-acetyl-2-thioethyl (SATE) groups are commonly utilised in chemical biology within metabolic labelling studies which utilise carbohydrate phosphate derivatives as cell permeable labelling probes. These protecting groups are used to mask negatively charged phosphate groups, which increases the cell-permeability of phosphorylated small-molecule probes. Once taken up in cells, the acetyl groups are cleaved, initiating further decomposition of the remaining thioethyl groups to reveal the deprotected phosphate monoester. Though SATE protection is commonplace, the majority of recent literature on the synthesis of SATE-protected phosphates relies on the use of highly hazardous dichlorophosphine intermediates for the formation of an activated phosphoramidite intermediate. This chapter describes the research undertaken to uncover a new methodology for the synthesis of SATE-protected phosphates by a two-step process that utilises an easy-to-synthesise *tris*(2-bromoethyl)phosphate starting material. This methodology avoids the use of dichlorophosphine intermediates, not only improving the safety of the SATE-protected phosphate formation, but also increasing the ease of purification and isolation of the required phosphorylation reagent. By utilising readily available, affordable starting materials, this methodology is much more accessible than the phosphoramidite approach that is commonly reported and therefore has the potential to make the use of SATE protecting groups more prevalent, not only within metabolic labelling studies but also for their wider applications in phosphate-containing prodrugs.

4.2 Introduction

S-Acetyl-2-ThioEthyl (SATE) groups are commonly utilised phosphate protecting groups for small molecule phosphate-containing probes and pro-drugs which need to cross the cell membrane. Despite the inherently low cell permeability of phosphate-containing molecules, phosphate groups are often used to increase the efficiency of carbohydrate- or nucleoside-based molecules. Nucleotide analogues, for instance, are generally more efficient than their non-phosphorylated derivatives as they bypass the initial rate-limiting biosynthetic phosphorylation step.^{173, 174} One study published in 2005 demonstrated this point by comparing the inhibitory effects of C-6 substituted purine nucleosides to that of SATE-protected prodrugs of the corresponding 5'-monophosphate

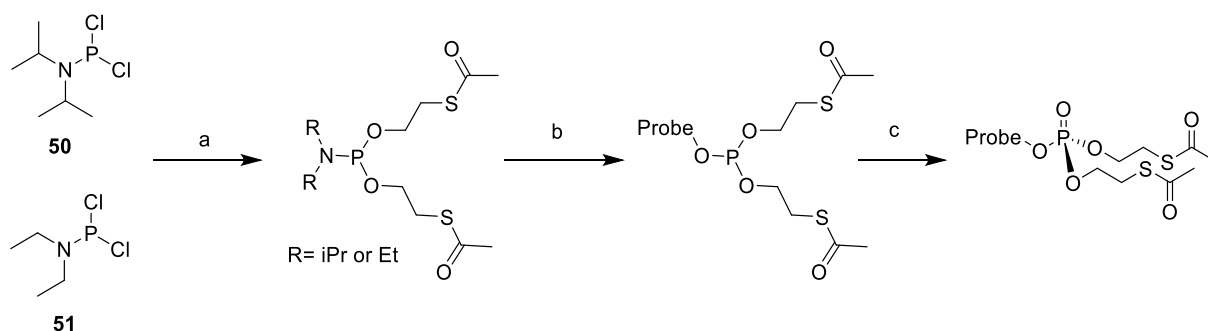
nucleotide derivatives, with the latter displaying a much greater potency than their non-phosphorylated counterparts.¹⁷⁵ SATE groups mask the high polarity and charged nature of phosphate monoesters, enhancing cell permeability. Once the protected probe is taken up in the cell, non-specific esterase and lipase activity cleaves the terminal acetate of the SATE group, unveiling a thioethyl moiety that can self-cyclise releasing the deprotected phosphate (Scheme 29).¹⁸⁰ SATE groups give high stability in solution, and the by-products formed by their cleavage mechanism, acetic acid (**48**) and episulfide (**49**), have been shown not to induce additional cytotoxicity.²⁵⁰⁻²⁵³



Scheme 29: Enzymatic cleavage of SATE protected phosphates

The synthesis of SATE groups was first published by Lefebvre and co-workers in 1995,²⁵⁴ and their phosphoramidite approach remains the most commonly utilised method for the synthesis of SATE-protected phosphates in recent literature.^{120, 255} This method proceeds from the highly reactive dichlorophosphine intermediate **50** (Scheme 30).^{138, 175, 254} Initially, the two chlorines in **50** are substituted with S-acetyl-2-thioethanol to yield a SATE-protected phosphoramidite intermediate. Once protected, this phosphoramidite is then coupled to the required probe by the use of 1*H*-tetrazole to yield a phosphite intermediate. This phosphite is then oxidised with *m*-CPBA to yield the final *bis*(SATE)-protected phosphate product (Scheme 30). The compound diisopropylamido-(dichlorophosphine) **50** is pyrophoric and highly reactive in air and moisture making its isolation challenging. Due to safety concerns, the dichlorophosphine **50** is not commercially available in the UK and therefore the synthesis of this highly hazardous species is required in-house. More recently, safer alternatives for this intermediate have been investigated, the most notable being diethylamido(dichlorophosphine) **51**, which has been utilised to incorporate SATE phosphates onto sugars and peptides.^{256, 257} Not only does the ethyl derivative have fewer safety concerns than its diisopropyl counterpart, but it is also commercially available in the UK. No direct comparisons for the yield of diisopropyl vs diethyl phosphoramidite intermediates are available, however, comparison of the yields on similar sugar substrates shows that yields are lower for the diethylamido(dichlorophosphine) **51** (6-42%)^{257, 258} compared to diisopropylamido-(dichlorophosphine) **50** (25-61%).^{120, 138} Another issue with both of these reagents is that the yields

vary greatly between substrates^{138, 257} and the syntheses are not always reproducible.²⁵⁹ Though diethylamido(dichlorophosphine) **51** provides a safer approach to SATE phosphoramidite synthesis, the reagent's highly reactive nature, and greatly varying yields fuel a desire to find a safer, more efficient methodology for the synthesis of SATE protected phosphates.



Scheme 30: Traditional synthesis route towards bis(SATE) protected phosphorprobes, first presented by Lefebvre and co-workers in 1995. **Reagents and Conditions:** a) *S*-Acetyl-2-thioethanol, NEt_3 , THF, -78°C -r.t, b) Probe-OH, 1H-tetrazole, THF, c) *m*CPBA, DCM, -40°C -r.t

While the work described in this chapter was ongoing a modified approach to SATE-protected hexosamine-1-phosphates, utilising bis(diisopropylethylamino)chlorophosphine **52** (Figure 16), has been developed.²⁵⁹ This method incorporates a phosphoramidite intermediate onto the target sugar first by substitution of the chlorine atom of **52**, after which the amines are substituted for SATE groups by the use of *S*-acetyl-2-thioethanol. This yields a *bis*(SATE)phosphite which, as for the phosphoramidite procedure described previously (Scheme 30), is then oxidised with *m*-CPBA to form the desired SATE phosphate. This methodology gave an overall yield of 45% over 3 steps using 3,4,6-tri-*O*-acetylated *N*-acetylglucosamine as a substrate. This yield is comparable to that obtained by the conventional phosphoramidite methodology on a similar azido glucosamine substrate (40% over 2 steps),¹³⁸ and 2,3,4,6-*tetra-O*-acetylated glucose (42% over 2 steps).²⁵⁸

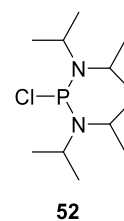
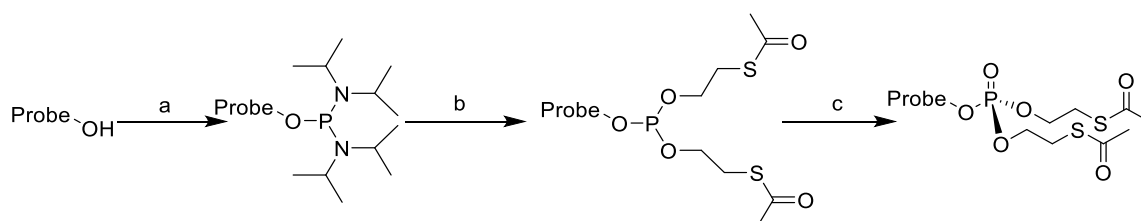


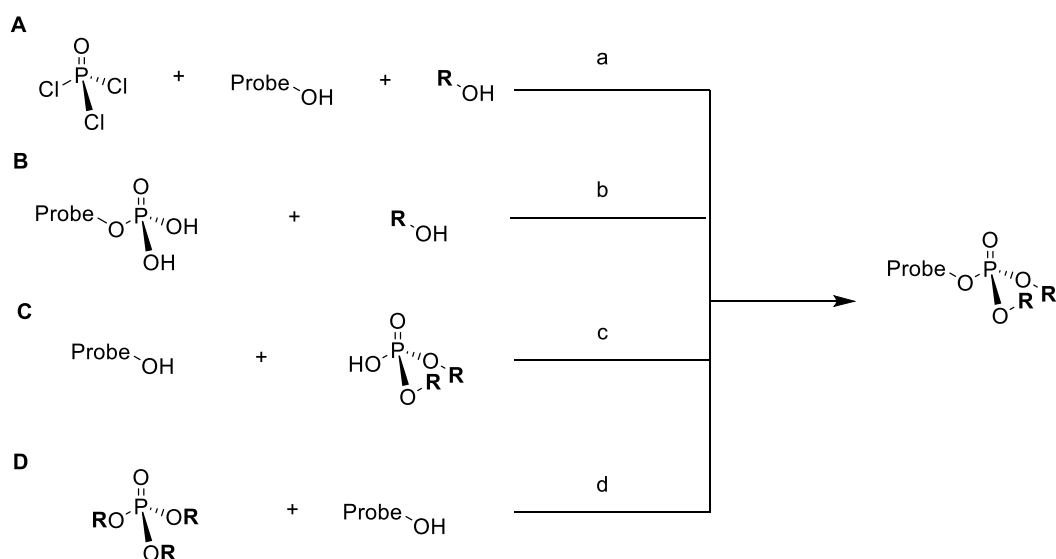
Figure 16: Structure of bis(diisopropylamino)chlorophosphine **52**



Scheme 31: Modified phosphoramidite approach to SATE-protected phosphates published by Kohler and colleagues in 2021²⁵⁹ **Reagents and Conditions** a) bis(diisopropylamino)chlorophosphine **52**, DBU, DCM, r.t., 1 h, b) *S*-acetyl-2-thioethanol, 1H-tetrazole, DCM, r.t., 12 h, c) *m*-CPBA, DCM, -40°C to r.t., 3 h

Though alternative methodologies for the synthesis of SATE protected phosphates are not commonplace, there are numerous strategies for the synthesis of protected or mixed phosphate

triesters.¹⁷³ These can be classed into three major categories (Scheme 32A-C); A) chloride substitution methods, highlighted in Scheme 32A is a newly published one-pot procedure that utilises the sequential substitution of the chlorides in POCl₃ with hydroxyl groups of both probe and protecting groups;²³⁹ B) the coupling of protecting groups onto a free phosphate monoester already attached to the probe, and C) the addition of a partially protected phosphate (phosphodiester) to the free hydroxyl group of a probe. Additional to these core synthetic methodologies, more recent literature has utilised the activation of phosphotriesters with triflic anhydride as a method to generate mixed phosphates (Scheme 32D), though this methodology has not yet been applied more widely.²⁶⁰



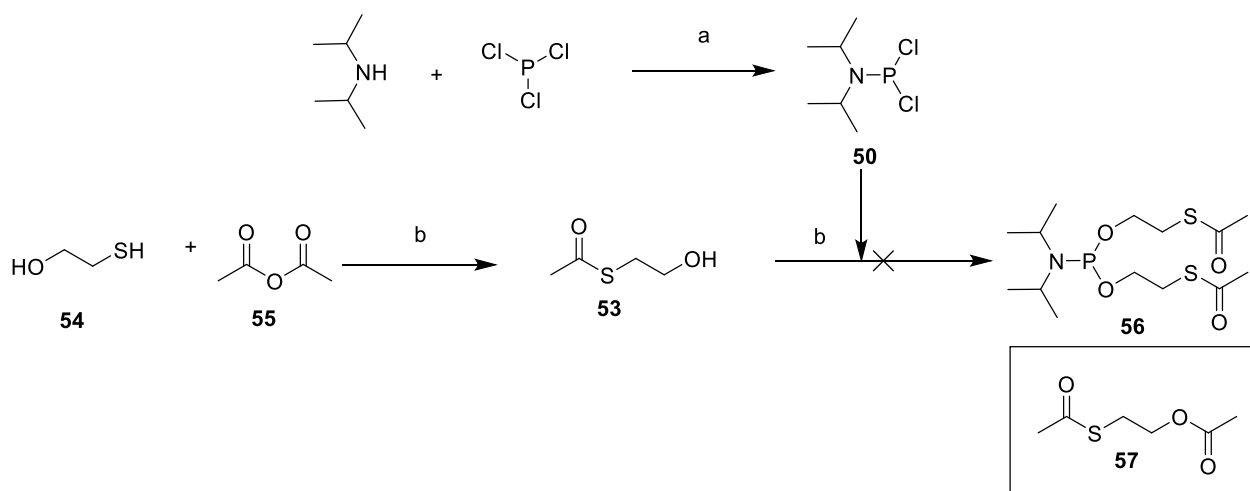
*Scheme 32: Reported methodologies for the synthesis of protected phosphates A) Chlorine substitution methods, here illustrated by tri-substitution of POCl₃, B) Protection of a phosphate monoester, C) Coupling of a probe to a protected phosphate, D) Synthesis of mixed phosphates by activation of phosphotriesters with triflic anhydride and pyridine **Reagents and Conditions:** a) NEt₃, DCM b) MSNT, pyridine, or accessed via varied coupling conditions including via DCC coupling) DCC, NEt₃, DCM, c) varied coupling conditions including via Mistunobu) DIAD, PPh₃, NEt₃, THF, via DCC coupling) DCC, NEt₃, DCM, via dichlorophosphate formation) oxalyl chloride, NaH, DCM d) Tf₂O, pyridine, DCM*

4.3 Aims

This chapter aims to explore the development of a new methodology for the synthesis of SATE-protected phosphates which avoids the use of highly hazardous dichlorophosphine intermediates. This method will be based on the more general methodologies used for mixed phosphotriester synthesis within the field (Scheme 35). The main purpose of this new methodology is for the synthesis of protected ribitol-5-phosphate derivatives, which are relevant as metabolic labelling probes for O-mannosyl glycans (Chapter 3, pg. 55). For this method to be applicable to the synthesis of these probes, it needs to be tolerant towards both azide and benzyl groups as well as an open-chain sugar structure. Once successful, broader application of the methodology to different classes of molecules will also be explored (Chapter 5, pg. 128).

4.4 Results and Discussion

Initially the synthesis of SATE-protected phosphates was attempted *via* the already established phosphoramidite approach utilising diisopropylamido(dichlorophosphine) (**50**). With this intermediate being non-commercially available,²⁶¹ the synthesis of the SATE-protected phosphoramidite was attempted through an adapted method published by Bhat and colleagues in a 2017 patent (Scheme 33).²⁶² Their method relies on the formation of *S*-acetyl-2-thioethanol (**53**) *in situ* by the reaction of β -mercaptoethanol (**54**) with acetic anhydride (**55**), rather than the much more toxic 2-iodoethanol and thioacetic acid utilised in the Lefebvre procedure. This reaction mixture is then treated with a crude mixture of the separately prepared dichlorophosphine intermediate **50**, therefore avoiding isolation of this highly hazardous intermediate. Once protected with SATE groups, compound **56** can then be purified by column chromatography.



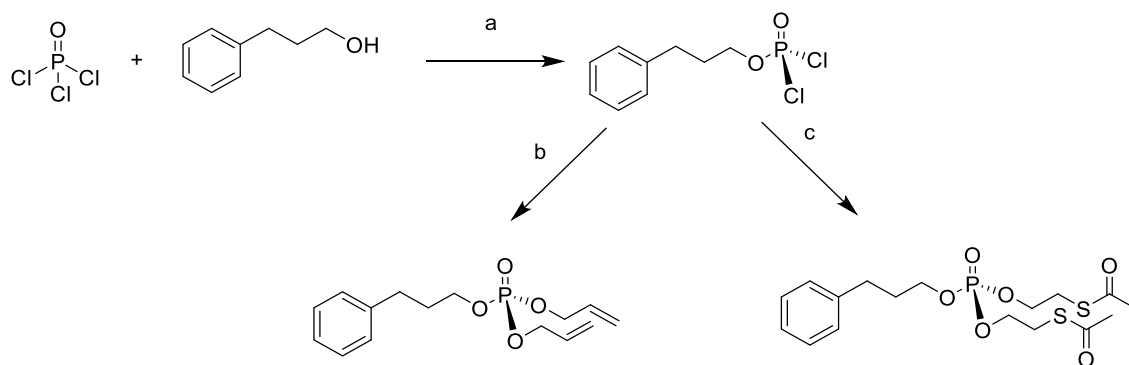
Scheme 33: Attempted synthesis of phosphoramidite **56** through an adapted phosphoramidite methodology published by Bhat and colleagues²⁶² **Reagents and Conditions** a) DBU, toluene, 0°C-r.t., b) NEt₃, THF, 0°C-r.t. (0%)

Unfortunately, on attempting this reaction no evidence of the desired SATE-protected phosphoramidite **56** was seen by ESI-MS analysis of the crude reaction mixture, and ¹H NMR showed that the only product obtained after column chromatography was doubly acetylated β -mercaptoethanol (**57**). The fact that this attempt at producing the required SATE-phosphate (**56**) was unsuccessful provided further evidence for the requirement of a methodology which utilises more accessible intermediates.

Methods A and B: Discussion

A methodology for the synthesis of allyl protected phosphates was recently described by the sequential reaction of two different alcohols with phosphorous oxychloride (POCl₃).²³⁹ This two-step one-pot procedure (described by the general procedure in Scheme 34) utilises an excess of POCl₃ (1.5 equiv.), which allows for the selective addition of one alcohol group to the phosphine oxide

(step a). After a reaction time of 3 hours, an excess of the second alcohol (in the paper's case allyl alcohol) is then added to substitute the remaining chloride groups on the phosphate, forming the desired allyl-protected phosphate (step b). It was hypothesised that by using the SATE alcohol **53** in the second step instead (step c), this methodology would be able to yield SATE-protected phosphates.



*Scheme 34: Synthesis of protected phosphates through the reaction of alcohols selectively with POCl₃ Reagents and Conditions a) NEt₃, DCM, r.t., 3 h, b) allyl alcohol, NEt₃, DCM, r.t., 16 h, (70%) c) S-acetyl-2-thioethanol **53**, NEt₃, DCM, r.t., 16 h, (46%)*

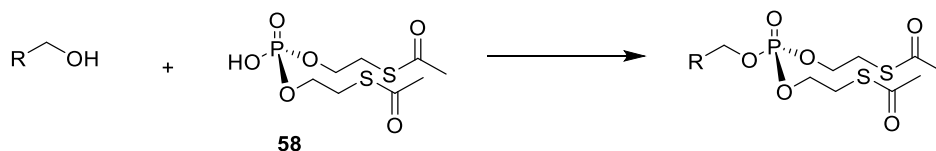
Despite this methodology proving successful for the synthesis of SATE-protected phosphates on the model alcohol 3-phenyl propanol (Scheme 34), ongoing work on the ribitol-based metabolic labelling probes (Chapter 3) lead to the conclusion that this methodology would be incompatible with the optimised protecting group strategy. With acetate migration issues being encountered in the synthesis of the 1-Azido probes, the routes to ribitol probes were adapted to utilising benzyl groups (see the explanation for protecting group choice in Chapter 3 –Route 4a, pg. 73). Therefore a phosphate synthesis strategy that was compatible with benzyl groups was required. In their publication, Spicer *et al* note that on running their reaction with a benzyl alcohol substrate, ‘chloride substitution of the alcohol[s is] instead isolated as the major product’.²³⁹ The same issues with deprotection of benzyl groups were believed to occur on a benzylated sugar substrate.^b

An alternative methodology for the formation of protected phosphates utilises the initial incorporation of a deprotected phosphate monoester onto a probe, which is later protected (approach B in Scheme 32), and this methodology had been previously utilised for the synthesis of S-pivaloyl-2-thioethyl (tBu-SATE) phosphates.^{263, 264} The direct addition of a free phosphate onto a ribitol probe had indeed been attempted previously (See Chapter 3: Incorporation of a Deprotected Phosphate Monoester for the Synthesis of 1-Az-OH-Phos pg. 79), but issues with the isolation and

^b This was also later corroborated by work within the Willems group conducted by PhD student Lloyd Murphy (*unpublished findings*).

purification of the deprotected phosphate species had caused this method to be unsuccessful. Therefore, this methodology (approach B in Scheme 32) was not investigated for SATE-phosphate synthesis. The next set of experiments instead focused on the coupling of phosphodiester onto a free hydroxyl group of the probe (approach C in Scheme 32).

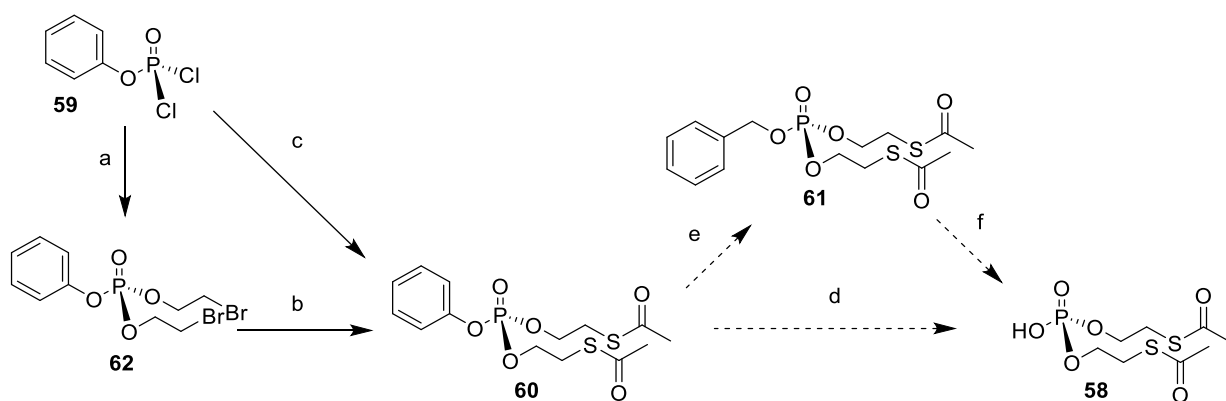
Method C: Addition of a Phosphodiester



Scheme 35: General synthesis strategy to SATE protected Phosphates utilising a bis(SATE)phosphate starting material
Proposed reagents and Conditions: varied coupling conditions including via Mitsunobu) DIAD, PPh₃, NEt₃, THF, via DCC coupling) DCC, NEt₃, DCM, via dichlorophosphate formation) oxalyl chloride, NaH, DCM d) Tf₂O, pyridine, DCM

In literature, the coupling of phosphodiester to alcohols is a commonly used strategy for the formation of protected phosphates, as earlier discussed (approach C in Scheme 32). Benefits from this methodology are its compatibility with benzyl protecting groups, and the great variety of conditions possible for the coupling reaction; for example, coupling with DCC, *via* Mitsunobu reaction, and *via* a chloro-phosphate intermediate have all been utilised in previous work with the commercially available *di*-benzyl-phosphate (see Chapter 3: Incorporation of a Deprotected Phosphate Monoester for the Synthesis of 1-Az-OH-Phos, pg. 79). To utilise this chemistry for the synthesis of SATE-protected phosphoprobe, first, a method to synthesise a *bis*-SATE phosphate reagent **58** (Scheme 35) was required.

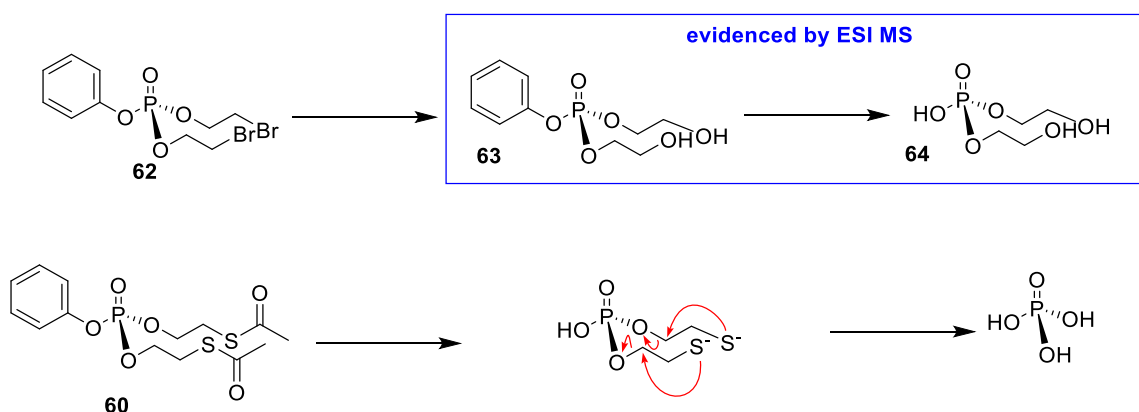
It was hypothesised that the desired *bis*-SATE phosphate **58** could be synthesised by the formation of a mixed phosphotriester bearing one protecting group that could be selectively cleaved in the presence of SATE groups. A method was proposed that utilised the commercially available starting material phenyl-dichlorophosphate **59**. This would allow for the formation of a phenyl-*bis*(SATE)phosphate **60**, either directly or through a *bis*-(2-bromoethyl) intermediate (see Chapter 3), after which the phenyl group could either be directly removed, or substituted for a benzyl group (**61**) which could then be selectively removed to afford **58** (Scheme 36).



Scheme 36: Proposed synthesis and deprotection strategies for the synthesis of bis(SATE)phosphate from phenyl-dichlorophosphate **Reagents and Conditions** a) 2-bromoethanol, NEt_3 , DCM, r.t., 16 h, (64%) b) KSAc, acetone, r.t., 16 h, (74%) c) S-acetyl-2-thioethanol, NEt_3 , DCM, r.t., 16 h, (9%), **Proposed Reagents and Conditions** d) NaOH, e) BnOH , NaH, THF, f) BCl_3 , DCM

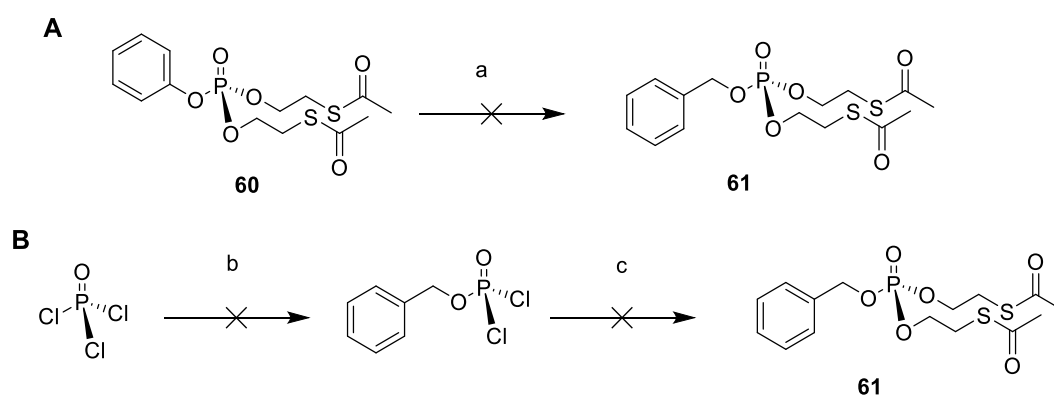
The synthesis of both *bis*(SATE) (**60**) and *bis*(2-bromoethyl) (**62**) phenyl phosphates was successful with the introduction of the 2-bromoethyl group providing much higher yields than the addition of the SATE alcohol (56% vs 7%). Substitution of bromine with potassium thioacetate, as shown previously, gave **60** in a yield of 64% from intermediate **62** and an overall yield of 40% from the phenyl dichlorophosphate starting material **59**. Then direct, selective deprotection of the phenyl group was attempted on each of these substrates as presented by Yoshino and co-workers using sodium hydroxide under aqueous conditions.²⁴⁶

The products identified after deprotection of **62** by mass spectrometry analysis showed evidence of substitution of bromine with hydroxide. The presence of masses corresponding to both compounds **63** and **64**, shown in Scheme 37, suggests that this substitution occurred before the removal of the phenyl group. In the negative and positive ion mode mass spectra of the products identified after deprotection of **60**, no peaks for the SATE-protected product **58** could be identified, and no starting material was seen either, showing that decomposition of the SATE groups had likely occurred. This is believed to be due to hydrolysis of the terminal acetate causing the cyclisation of the thiol to occur and total deprotection of the phosphate.



Scheme 37: Decomposition pathway of the 2-bromoethyl compound **62** following ESI-MS evidence of both compounds **63** and **64** and the proposed decomposition of the SATE compound **60**

Alternative methodologies for the removal of the phenyl group from phosphate relied on either high-pressure hydrogenation or hydrogenation with a platinum catalyst.²⁶⁵ To avoid these more harsh conditions, transesterification of the phenyl phosphate with benzyl alcohol and sodium hydride to give compound **61** was attempted as reported in literature.²⁶⁶⁻²⁶⁸ The removal of the benzyl group could then proceed under much milder conditions with either atmospheric pressure hydrogenation,²⁶³ or by reaction with BCl_3 .^{241, 269} This substitution was attempted as displayed in Scheme 38A, however, no reaction was observed over varied reaction times and reagent equivalencies. Direct formation of compound **61** was also attempted utilising the POCl_3 methodology utilised for the synthesis of 3-phenyl-propyl substrates (Scheme 38B) however this was unsuccessful and afforded none of the desired benzyl phosphate.

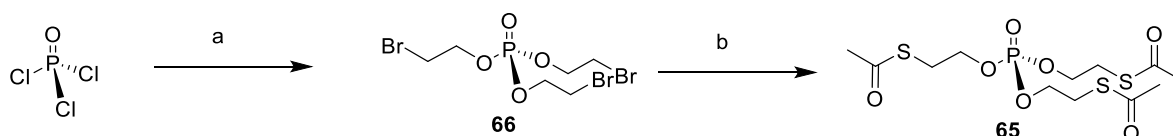


Scheme 38: Attempted synthesis of benzyl-bis(SATE)phosphate through A) transesterification of phenyl-bis(SATE)phosphate B) the POCl_3 methodology **Reagents and Conditions** a) BnOH , NaH , THF , 0°C -r.t. (0%) b) BnOH , NEt_3 , DCM , r.t., 3 h, c) *S*-acetyl-2-thioethanol **53**, NEt_3 , DCM , r.t., 18 h (0%)

Method D: Triflic Anhydride Activation of a Phosphotriester

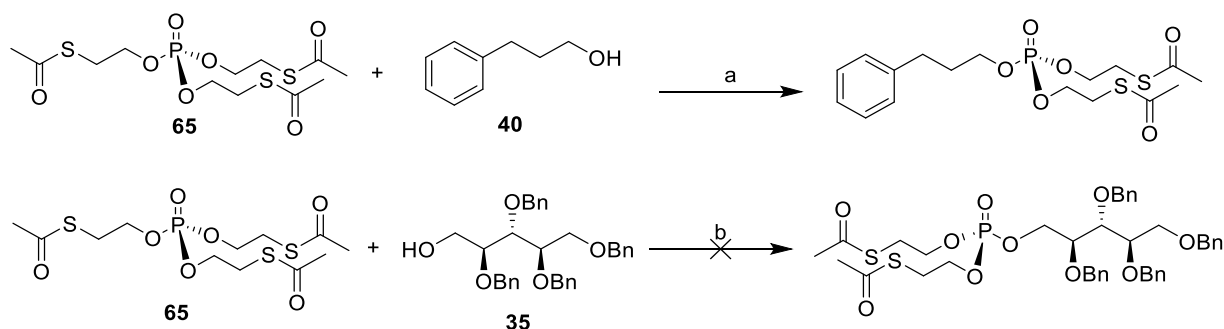
In a final strategy, the synthesis of SATE-protected phosphates was investigated based on a 2018 paper by Huang and co-workers²³⁷ which presents a method for synthesising *bis*-ethyl-protected phosphates from triethyl phosphate. Their method proceeds by the initial activation of

triethyl phosphate with triflic anhydride, and then reaction with pyridine. Following the formation of a reactive pyridinium species, substitution with a range of substrates provided an array of diethyl-protected phosphates. It was hypothesised that this method could not only be useful in synthesising the desired benzyl-*bis*(SATE) phosphate **61** but may also provide a potential method for the direct formation of the SATE-protected phosphoprobosc, by-passing the need for synthesis of the *bis*(SATE) phosphate intermediate **58**. To test this hypothesis, the *tris*(SATE) phosphate **65** was synthesised from POCl₃ *via* the 2-bromoethyl derivative **66** (Scheme 39).



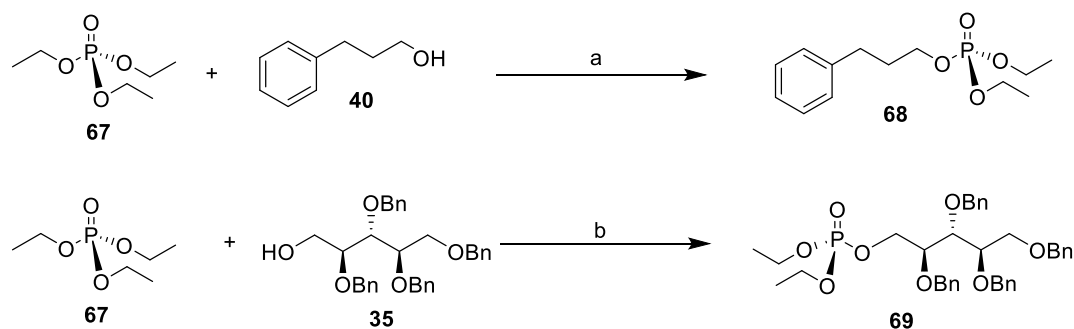
Scheme 39: Synthesis of *tris*(SATE)phosphate **Reagents and Conditions** a) i) 2-bromo-ethanol, NEt₃, DCM, r.t., 16 h, (50%) b) KSAC, acetone, r.t., 18 h, (60%, 30% over two steps)

The triflic anhydride/pyridine reaction was then attempted with *tris*(SATE) phosphate **65** and the substrates 3-phenyl-propanol **40** and previously synthesised sugar derivative 2,3,4,5-*tetra-O*-benzyl ribitol **35** (Scheme 40), which was an intermediate in the route to the 1-azido-probes described in Chapter 3.



Scheme 40: Test Reactions for the synthesis of SATE-protected phosphates with triflic anhydride and pyridine utilising *tris*(SATE)phosphate **Reagents and Conditions** a) i) Tf₂O, pyridine, DCM, r.t., 10 min, ii) 3-phenyl-propanol, DCM, r.t., 30 min, (33%) d) i) Tf₂O, pyridine, DCM, r.t., 10 min, then 2,3,4,6-*tetra-O*-benzyl-ribitol, r.t., 30 min (0%)

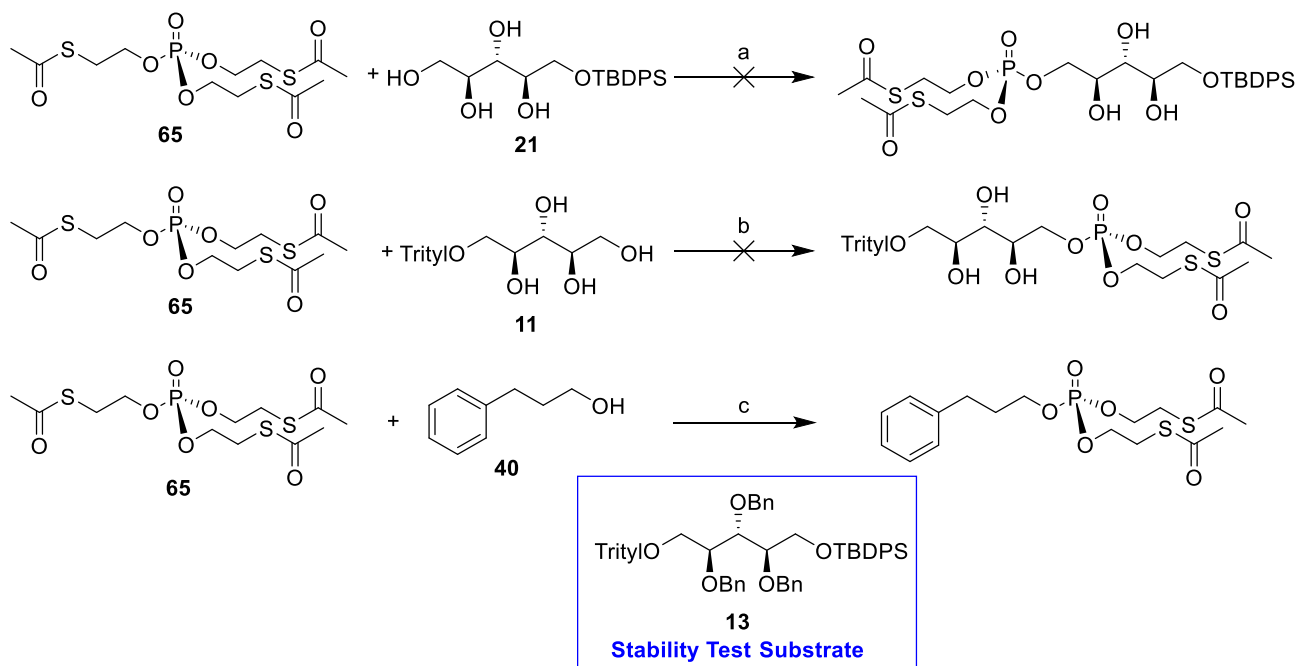
Despite this new SATE methodology proving successful on the model alcohol 3-phenyl-propanol (33%), no product was seen from the reaction with the ribitol substrate **35**. To compare these yields with the values obtained by Huang and co-workers, the reaction of both compounds **40** and **35** with commercially available triethyl phosphate **67** was attempted (Scheme 41).



Scheme 41: Test Reactions for the synthesis of ethyl phosphates with triflic anhydride and pyridine utilising triethyl phosphate **Reagents and Conditions** a) i) Tf_2O , pyridine, DCM, r.t., 10 min, ii) 3-phenyl-propanol, DCM, r.t. 30 min, (45%) b) i) Tf_2O , pyridine, DCM, r.t. 10 min, then 2,3,4,6-tetra-O-benzyl-ribose, r.t., 30 min, (14%)

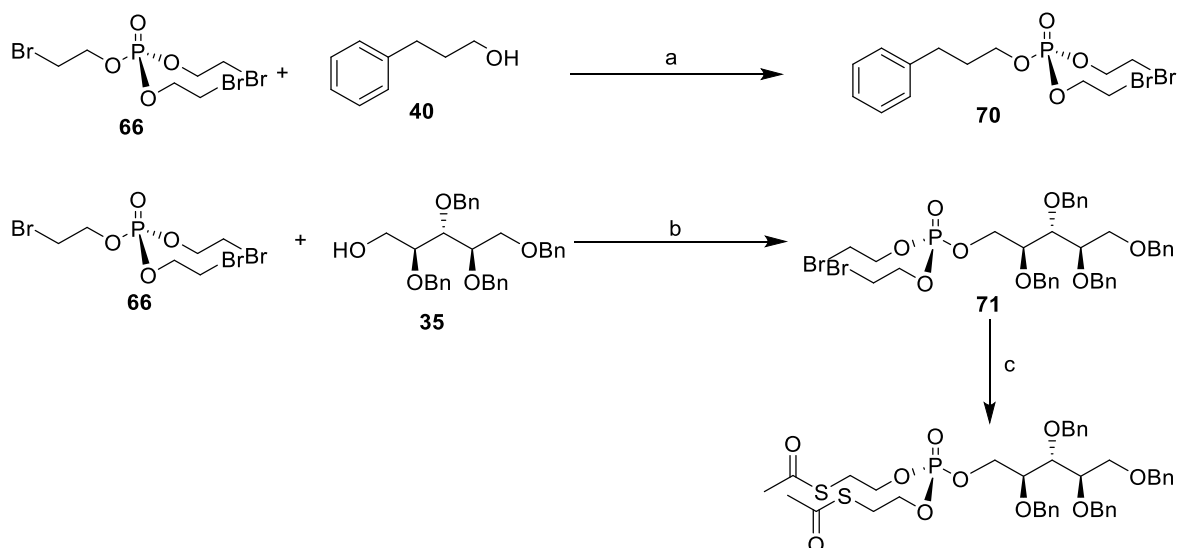
The reaction with 3-phenyl-propanol **40** and triethyl-phosphate **67** was found to give yields of product **68** which were comparable to those seen for the *tris*(SATE)phosphate, though lower than yields for the same reaction reported by Huang and co-workers. Significantly, the reaction with triethyl phosphate **67** and the *tetra*-benzylated ribitol substrate **35** was also successful yielding the desired ribitol-5-*bis*-ethyl phosphate **69** in a yield of 14%. In their publication, based on test reactions and DFT calculations, Huang *et al* propose an $\text{S}_{\text{N}}1$ type reaction. Ethanol has a pKa of 16, while *S*-acetyl-2-thioethanol has a lower calculated pKa (13.6) due to the electron-withdrawing thioacetate groups. This means that the *S*-acetyl-2-thioethyl group should be a preferential leaving group over ethyl and give a higher reactivity. Given, however, that the triethyl phosphate reagent was able to react with the benzylated sugar while the *tris*(SATE) phosphate was not, it was hypothesised that the large size of the *tris*(SATE) phosphate, and not electronic effects, was dominating the reaction efficiency and that steric hindrance may explain the lack of reactivity between *tris*(SATE) phosphate **65** and the benzylated ribitol substrate **35**.

With the SATE phosphate **65** being bulkier than Huang's original phosphate reagent, it was hypothesised that the addition of SATE-protected phosphates using this method could be performed selectively on the primary site of a partially protected (and therefore less sterically hindered) ribitol substrate. Therefore, the reaction was attempted on the 1-trityl (**11**), and 5-TBDPS (**21**) ribitol substrates previously synthesised in the routes towards 1-Az probes (Scheme 42, for synthesis, see Chapter 3). Unfortunately, both reactions with 1-trityl and 5-TBDPS substrates **11** and **21** were unsuccessful, with none of the desired products formed and no evidence of phosphate addition occurring. In addition to this, TLC analysis of the reaction showed degradation of the starting sugars and loss of TBDPS and Trityl groups, respectively.



Scheme 42: Attempted synthesis of bis(SATE) phosphate products **Reagents and Conditions**: a) i) Tf_2O , pyridine, DCM, r.t. 10 min then ii) **21**, DCM, r.t., 1 h. (0%) b) i) TfO_2 , pyridine, DCM, r.t. 10 min then ii) **11**, DCM, r.t., 1 h. (0%) c) i) TfO_2 , pyridine, CDCl_3 , r.t. 10 min then ii) **40**, 2,3,4-tri-*O*-benzyl-5-TBDPS-1-trityl ribitol, CDCl_3 , r.t., 1 h. (sugar shown to have degraded by crude NMR)

To further corroborate these findings, the test reaction of **65** with 3-phenyl-propanol **40** was repeated in the presence of the fully protected ribitol compound **13** (Scheme 42). While the benzyl groups were seen to be stable to the reaction conditions, crude ^1H NMR showed degradation of the ribitol material, with loss of TBDPS and Trityl groups. Since the primary protecting groups utilised in the synthesis of the 1-Az probes were shown to not be stable to the reaction conditions, successful use of this phosphate methodology would require the addition of the phosphate moiety to the benzylated ribitol compound **35**. However, as steric hindrance was believed to cause issues in adding the SATE phosphate directly to **35**, it was hypothesised that the intermediate from the *tris*(SATE) phosphate synthesis, *tris*(2-bromoethyl)phosphate **66** may be more suitable for the triflic anhydride/pyridine catalysed reaction. The bromine provides a similar electron-withdrawing effect to the thioacetate, boosting the leaving group potential of the halogenated alkyl group over the ethyl leaving group, and bromine with its much smaller size should better mimic the size of the ethyl phosphate originally utilised in the literature procedure. The use of the alternative phosphate reagent **66** was thus explored on both the 3-phenyl-propanol and the *tetra*-benzylated ribitol substrates (Scheme 43).



Scheme 43: Test Reactions for the synthesis of SATE Phosphates with triflic anhydride and pyridine utilising tris(SATE) phosphate **Reagents and Conditions** a) i) Tf_2O , pyridine DCM, r.t. 10 min, ii) 3-phenyl-propanol, DCM, r.t. 30 min (17%) b) i) Tf_2O , pyridine, DCM, r.t. 10 min then 2,3,4,6-tetra-O-benzyl-ribose, r.t., 30 min (11%), c) KSAC, acetone, r.t., 24 h, (72%)

The reaction of tris(2-bromoethyl)phosphate **66** with 3-phenyl-propanol **40** was successful, yielding compound **70** in a yield of 17%. More significantly, the reaction of the 2-bromo-ethyl-phosphate **66** was also found to be successful on the benzylated ribitol compound **35**, providing the bis(2-bromoethyl) ribitol compound **71** in a yield of 11%. This benzylated ribitol-phosphate product **71** was subsequently able to be converted to the corresponding SATE-protected phosphate by substitution with potassium thioacetate in acetone (72%) providing the corresponding SATE containing ribitol-phosphate compound in a yield of 8% over two steps. With a successful methodology now in hand, this procedure was applied to the synthesis of 1-azido-ribose-5-phosphate probes (Chapter 3) while concurrently work was continued to further optimise this methodology to increase yields and explore the scope of the reaction on a range of different substrates (Chapter 5).

4.5 Conclusion

This chapter has explored the development of a new methodology for the synthesis of SATE-protected phosphates. Adapted from Huang and co-workers' methodology, the successful procedure utilises an easy-to-access phosphotriester starting material, tris(2-bromoethyl)phosphate, followed by a reaction with potassium thioacetate to incorporate SATE-protected phosphates onto a substrate hydroxyl group through a two-step synthesis. This methodology avoids the use of highly hazardous, and difficult to handle dichlorophosphine intermediates, and the improved stability of the 2-bromoethyl-phosphate intermediates allows for easier isolation and storage. With this methodology now in hand, future work will not only apply this approach to the synthesis of cell-permeable ribitol-5-phosphate probes but also look into the application of this methodology to a

wider scope of substrates. Alongside this investigation, further work will be undertaken to optimise the yields of this reaction on the ribitol substrate above the initially reported 11%.

4.6 Experimental

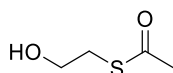
General Experimental

All reactions were conducted in oven dried glass wear under nitrogen, and where specified dry solvents used were either freshly distilled (DCM, DMF, toluene, THF) or from a SureSeal bottle, (DCE, pyridine). Flash column chromatography was run either manually with high purity 220-400 μm particle size silica (Sigma) or on an automated system (Teledyne, CombiFlash NextGen 300+) with 20 to 40 μm particle size silica (RediSep Rf Gold Normal-Phase Silica columns) here specified. Reactions and column fractions were monitored by TLC and visualised by UV and staining. For sugars: charring with 10% H_2SO_4 in MeOH; for phosphate reactions: KMnO_4 stain.

^1H and ^{13}C NMR spectra were obtained either on a JEOL ECS400A spectrometer (400 and 101 MHz respectively) or a Bruker AVIIIHD600 spectrometer (600 and 150 MHz respectively) where specified. Structural assignments were corroborated by homo- and heteronuclear 2D NMR methods (COSY, HMQC and DEPT) where necessary. Chemical shifts are reported in parts per million (ppm, δ) relative to the solvent (CDCl_3 , δ 7.26; CD_3OD , δ 3.31; D_2O , δ 4.79). ^1H NMR splitting patterns are designated as singlet (s), doublet (d), triplet (t), quartet (q), doublet of doublets (dd), doublet of doublets of doublets (ddd), doublet of triplets (dt), apparent triplet (apt t), and so forth. Splitting patterns that could not be visualized or easily interpreted were designated as multiplet (m). Coupling constants are reported in Hertz (Hz).

IR spectra were obtained by thin film ATR on a Perkin Elmer Spectrum 2 and $[\alpha]_D$ measurements obtained on a Bellingham Stanley ADP400 polarimeter at the in the given solvent at specified concentration where $C = 1 = 10 \text{ mg/mL}$.

Synthesis of compounds **11**, **13**, **21**, and **35** is described in Chapter 3.

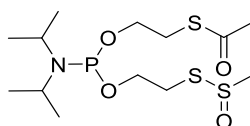


S-acetyl-2-thioethanol (53)

To a stirring solution of 2-bromo-ethanol (1.0 mL, 14 mmol, 1.0 equiv) in acetone (40 mL) was added KSAC (1.7 g, 16 mmol, 1.1 equiv) The resultant reaction mixture was allowed to stir at RT for 18 hours before the precipitated KBr was removed by filtration. The filtrate was evaporated *in vacuo* and subjected to automated flash column chromatography (gradient 0 to 100% EtOAc in hexane) to afford the title compound as a pale yellow oil (890 mg, 7.4 mmol, 53%).

HRMS-ESI Calculated for $[C_4H_8O_2S + Na^+]$: 143.0137, found: 143.0141 **1H NMR** (400 MHz, CHLOROFORM-*D*) δ ppm 1.93 (t, 1H, $J = 5.95$ Hz, OH) 2.35 (s, 3H, CH_3) 3.07 (t, 2H, $J = 5.95$ Hz, CH_2S) 3.75 (q, 2 H, $J = 5.95$ Hz, CH_2OH) **^{13}C NMR** (101 MHz, CHLOROFORM-*D*) δ ppm 30.78 (CH_3) 32.23 (CH_2S), 61.94 (CH_2OH), 196.50 (C=O) **IR** (V_{max} , film) 3363, 2964, 2879, 1686, 1354, 1133, 623 cm^{-1}

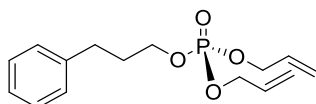
Data in accordance with literature values²⁷⁰



Attempted Synthesis of bis-S-Acetyl-2-thioethyl-N,N-diisopropyl phosphoramidate (50)

To a stirring solution of PCl_3 (50 μ L, 0.57 mmol, 1.0 equiv.) in dry hexane (1 mL) at 0°C was added diisopropylamine (0.16 mL, 0.92 mmol, 1.6 equiv.) over 15 mins. The solution was allowed to warm to RT and the formed inorganic salts were removed by filtration and rinsed with hexane (3 x 2 mL). The resulting solution was diluted with dry THF (10 mL) and the volume was reduced to approximately 3 mL *in vacuo*. This process was repeated three times to yield the crude phosphoramidate in a 3 mL solution of dry THF.

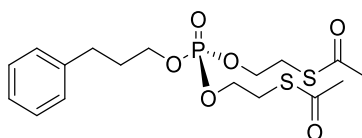
To a stirring solution of 2-mercaptoethanol (70 μ L, 1.0 mmol, 2.3 equiv) in dry DCM (1 mL) at 0°C was added NEt_3 (60 μ L, 0.43 mmol, 1.0 equiv.) and Ac_2O (70 μ L, 0.74 mmol, 1.7 equiv.). The reaction was left for 1 h at 0°C followed by 2 h at RT, before the reaction was diluted with DCM (5 mL) and washed sequentially with H_2O (5 mL), sat. aqueous $NaHCO_3$ solution (5 mL) and brine (5 mL). The organic layer was concentrated *in vacuo* to yield the crude intermediate as a clear oil. This residue was dissolved in dry THF (1 mL) and to this solution was added NEt_3 (60 μ L, 0.43 mmol, 1.0 equiv.) and activated 4A molecular sieves. The reaction mixture was cooled to 0°C and the crude phosphoramidate in 3 mL of dry THF was added dropwise. After 2 hours at 0°C dry hexane (5 mL) was added and the resulting precipitate was removed by filtration. The resultant solution was dried *in vacuo* and purified by flash column chromatography (gradient 0 to 50% EtOAc in hexane). No desired title product was obtained.



3-Phenyl-propyl-1-bis-allyl-phosphate

To a stirring solution of $POCl_3$ (0.10 mL, 1.1 mmol, 1.5 equiv.) and NEt_3 (0.18 mL, 1.1 mmol, 1.5 equiv.) in dry DCM (10 mL) was added 3-phenyl-propanol (0.10 mL, 0.74 mmol, 1.5 equiv.). The resulting solution was stirred at RT for 3 h before the addition of allyl alcohol (0.25 mL, 3.8 mmol, 5.0 equiv.) and NEt_3 (0.52 mL, 3.8 mmol, 5.0 equiv.). The solution was left to stir at RT for 16 hours before the addition of THF (20 mL). The resulting suspension was left at RT for 15 mins before the precipitated $NEt_3.HCl$ was removed by filtration, and the solvents were removed *in vacuo*. The resulting crude product was purified by automated flash column chromatography (gradient of 0 to 100% ethyl acetate in hexane) yielding the pure product as a pale yellow oil (150 mg, 0.51 mmol, 70%)

HRMS-ESI Calculated for $[C_{15}H_{21}O_4P + Na^+]$: 319.1070, found: 319.1056 **1H NMR** (400 MHz, CHLOROFORM-*D*) δ ppm 1.96-2.03 (m, 2H, $CH_2CH_2CH_2OP$) 2.66-2.72 (m, 2H, CH_2CH_2OP) 4.03-4.17 (m, 2H, CH_2OP) 4.51-4.70 (m, 4H, CH_2 OAllyl) 5.21-5.39 (m, 4H, m, $CH=CH_2$ OAllyl) 5.87-5.95 (m, 2H, $CH=CH_2$ OAllyl) 7.15-7.19 (m, 2H, CH arom.) 7.23- 7.28 (m, 2H, CH arom.) 7.37-7.39 (m, 1H, CH arom.) **^{13}C NMR** (101 MHz, CHLOROFORM-*D*) δ ppm 31.75 ($CH_2CH_2CH_2OP$) 31.96 (d, $J = 6.7$ Hz, CH_2CH_2OP) 67.21 (d, $J = 5.8$ Hz, CH_2OP) 68.25 (d, $J = 5.3$ Hz, CH_2 OAllyl) 118.41 (d, $J = 3.8$ Hz, $CH=CH_2$ OAllyl), 122.67, 126.20, 128.60 (CH arom.) 132.63 (d, $J = 6.7$ Hz, $CH=CH_2$) **IR** (V_{max} , film) 3026, 2951, 1496, 1278, 1013 cm^{-1} **^{31}P NMR** (162 MHz, CHLOROFORM-*D*) δ -0.11



3-Phenyl-propyl-1-bis(SATE)phosphate

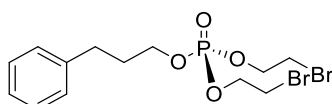
Synthesis from $POCl_3$

To a stirring solution of $POCl_3$ (0.10 mL, 1.1 mmol, 1.5 equiv.) and NEt_3 (0.18 mL, 1.1 mmol, 1.5 equiv.) in dry DCM (10 mL) was added 3-phenyl-propanol (0.10 mL, 0.74 mmol, 1.0 equiv.). The resulting solution was stirred at RT for 3 h before the addition of S-acetyl-2-thioethanol (430 mg in 1 ml dry DCM, 3.7 mmol, 5.0 equiv.) and NEt_3 (0.52 mL, 3.8 mmol, 5.1 equiv.). The solution was left to stir at RT for 16 hours before the addition of THF (20 mL). The resulting suspension was left at RT for 15 mins before the precipitated $NEt_3.HCl$ was removed by filtration, and the solvents were removed *in vacuo*. The resulting crude product was purified by automated flash column chromatography (gradient of 0 to 100% EtOAc in hexane) to afford the title compound as a pale yellow oil (140 mg, 0.33 mmol, 46%)

Synthesis by *tris*(SATE)phosphate activation with Tf_2O and Pyridine

To a stirring solution of *tris*(SATE)phosphate **64** (23 mg, 56 μ mol, 1.0 equiv.) in dry DCM (0.13 mL), was added Tf_2O (12 μ L, 71 μ mol, 1.3 equiv) and pyridine (9 μ L, 0.11 mmol, 2.0 equiv.). The resulting solution was left to stir at RT for 10 mins before the addition of 3-phenyl-propanol (25 μ L, 0.18 mmol, 3.2 equiv.). The resulting solution was left to stir for a further 30 mins. The reaction mixture was concentrated *in vacuo* onto silica and purified by automated flash column chromatography (gradient 0 to 100% EtOAc in hexane) to afford the title compound as a pink oil (7.3 mg, 18 μ mol, 33%)

HRMS-ESI Calculated for $[C_{17}H_{25}O_6PS_2 + Na^+]$: 420.0810, found: 420.0830 **1H NMR** (400 MHz, CHLOROFORM-*D*) δ ppm 2.05-2.13 (m, 2H, $CH_2CH_2CH_2OP$) 2.32 (s, 6H, CH_3 SAC) 2.79 (tt, 2H, $J = 2.7, 6.6$ Hz, CH_2CH_2OP) 3.12-3.21 (m, 4H, CH_2SAC) 4.03-4.13 (m, 4H, CH_2CH_2SAC) 4.20-4.45 (m, 2H, CH_2OP) 7.15-7.18 (m, 3H, CH arom.) 7.25-7.28 (m, 2H, CH arom.) **^{13}C NMR** (101 MHz, CHLOROFORM-*D*) δ ppm 28.69, 28.82 (CH_2SAC) 30.19, 30.11 (CH_3 SAC) 31.13 ($CH_2CH_2CH_2OP$) 31.58 (CH_2CH_2OP) 66.02 (d, $J = 5.3$ Hz, CH_2CH_2SAC) 66.07 (d, $J = 5.7$ Hz, CH_2CH_2SAC) 68.97 (d, $J = 6.3$ Hz, CH_2OP) 125.66, 128.02, 128.04, 140.37 (CH arom.), 194.17, 194.33 ($C=O$ SAC) **^{31}P NMR** (162 MHz, CHLOROFORM-*D*) δ 1.17. **IR** (V_{max} , film) 2956, 1690, 1452, 1232, 1011 cm^{-1}

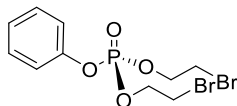


3-Phenyl-propyl-1-bis(2-bromo-ethyl)phosphate (70)

To a stirring solution of *tris*(2-bromoethyl)phosphate **66** (38 mg, 92 μ mol, 1.0 equiv.) in dry DCM (0.5 mL) was added Tf_2O (23 μ L, 0.14 mmol, 1.5 equiv.) and pyridine (15 μ L, 0.19 mmol, 2.1 equiv.). After 10 mins 3-phenyl-propanol (25 μ L, 0.18 mmol, 2.0 equiv.) was added and the resultant solution was allowed to stir for 1.5 h before the reaction mixture was concentrated *in vacuo* onto silica. The crude product was purified by automated flash column chromatography (gradient 0 to 60% EtOAc in hexane) to afford the title compound as a clear oil (6.7 mg, 16 μ mol, 17%)

HRMS-ESI Calculated for $[C_{13}H_{19}Br_2O_4P + Na^+]$: 452.9260, found: 452.9249 **1H NMR** (400 MHz, CHLOROFORM-*D*) δ 1.94-2.08 (m, 2H, $CH_2CH_2CH_2OP$), 2.66-2.79 (m, 2H, CH_2CH_2OP), 3.56 (dt, $J = 9.7, 6.0$ Hz, 4H, CH_2Br), 4.13

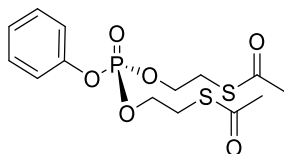
(q, $J = 6.7$ Hz, 2H, CH_2OP), 4.37 (ddt, $J = 19.7, 8.1, 6.1$ Hz, 4H, $\text{CH}_2\text{CH}_2\text{Br}$), 7.16–7.24 (m, 2H, CH arom.), 7.29–7.33 (m, 3H, CH arom.). ^{13}C NMR (101 MHz, $\text{CHLOROFORM-}D$) δ 29.59, 29.66 (CH_2Br), 31.61 (CH_2Ph), 31.80 (d, $J = 6.9$, $\text{CH}_2\text{CH}_2\text{Ph}$), 67.00 (d, $J = 5.6$ Hz, $\text{CH}_2\text{CH}_2\text{Br}$), 67.79 (d, $J = 6.5$ Hz, $\text{CH}_2\text{CH}_2\text{CH}_2\text{Ph}$), 126.26, 128.59, 140.83 (CH arom.), ^{31}P NMR (162 MHz, $\text{CHLOROFORM-}D$) δ -1.51. IR (Vmax, film) 2972, 2269, 1672, 1496, 1454, 1203, 1071, 1007, 745, 699, 483 cm^{-1}



Phenyl-*bis*(2-bromoethyl)phosphate (**62**)

To a stirring solution of phenyl dichlorophosphate (1.0 mL, 6.9 mmol, 1.0 equiv) in dry DCM (45 mL) at 0°C, was added NEt_3 (5.0 mL, 34 mmol, 5.0 equiv.) and 2-bromoethanol (2.0 mL, 28 mmol, 4.0 equiv.). The resulting solution was left to stir at RT for 24 h. THF (60 mL) was added and the precipitated $\text{NEt}_3\cdot\text{HCl}$ was removed by filtration, and the filtrate concentrated *in vacuo*. The crude product was purified by automated flash column chromatography (gradient 0 to 100% EtOAc in hexane) to afford the title compound as a clear oil (1.7 g, 4.4 mmol, 64%)

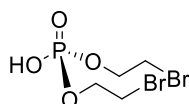
HRMS-ESI Calculated for [$\text{C}_{10}\text{H}_{14}\text{Br}_2\text{O}_4\text{P} + \text{Na}^+$]: 408.8810, found: 408.8805 ^1H NMR (400 MHz, $\text{CHLOROFORM-}D$) δ 3.53 (td, $J = 6.2, 2.1$ Hz, 4H, CH_2Br), 4.34 – 4.51 (m, 4H, $\text{CH}_2\text{CH}_2\text{Br}$), 7.17 – 7.26 (m, 3H, CH arom.), 7.32 – 7.39 (m, 2H, CH arom.) ^{13}C NMR (101 MHz, $\text{CHLOROFORM-}D$) δ 29.22 (d, $J = 7.6$ Hz, CH_3Br), 67.64 (d, $J = 5.7$ Hz, $\text{CH}_2\text{CH}_2\text{Br}$), 120.14 (d, $J = 4.78$ Hz), 125.65, 130.00 (CH arom.), 150.32 (d, $J = 7.6$ Hz, POCH arom.) ^{31}P NMR (162 MHz, $\text{CHLOROFORM-}D$) δ -6.60. IR (Vmax, film) 3061, 2968, 1771, 1673, 1591, 1489, 1276, 1207, 1067, 1013, 945, 760, 735, 689, 538 cm^{-1}



Phenyl-*bis*(SATE)phosphate (**60**)

To a stirring solution of Phenyl-*bis*(2-bromoethyl)phosphate (**62**) (261 mg, 0.678 mmol, 1.00 equiv) in acetone (17 mL) at RT, was added KSAC (170 mg, 1.49 mmol, 2.20 equiv). The resultant solution was allowed to stir at RT for 24 h after which the reaction was dissolved in DCM (100 mL) and washed with H_2O (50 mL). The resultant organic layer was dried over MgSO_4 , filtered, and the solvents concentrated *in vacuo*. The resulting crude product was purified by automated flash column chromatography (gradient 0 to 100% EtOAc in hexane) to yield the pure product as a pale yellow oil (190 mg, 0.506 mmol, 74%)

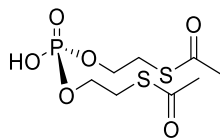
HRMS-ESI Calculated for [$\text{C}_{14}\text{H}_{19}\text{O}_6\text{PS}_2 + \text{Na}^+$]: 401.0253, found: 401.0253 ^1H NMR (400 MHz, $\text{CHLOROFORM-}D$) δ 3.17 (t, $J = 6.5$ Hz, 4H, CH_2SAC), 4.22 (dtd, $J = 8.5, 6.5, 2.1$ Hz, 4H, $\text{CH}_2\text{CH}_2\text{SAC}$), 7.12 – 7.24 (m, 3H, CH arom.), 7.30 – 7.39 (m, 2H, CH arom.). ^{13}C NMR (101 MHz, $\text{CHLOROFORM-}D$) δ 29.24 (d, $J = 7.6$ Hz, CH_2SAC), 30.67 (SAC), 66.74 (d, $J = 5.8$ Hz, $\text{CH}_2\text{CH}_2\text{SAC}$), 120.15, 125.45, 129.94 (CH arom), 150.53 (d, $J = 7.0$ Hz, POCH arom.), 194.90 ($\text{C}=\text{O}$) ^{31}P NMR (162 MHz, $\text{CHLOROFORM-}D$) δ -6.47. IR (Vmax, film) 3043, 2948, 2905, 1690, 1591, 1490, 1355, 1278, 1206, 1136, 1063, 1007, 940, 760, 660, 622, 541 cm^{-1}



Attempted synthesis of *bis*(2-bromoethyl)phosphate

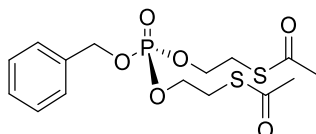
Phenyl-*bis*(2-bromoethyl)phosphate (**62**) (32 mg, 76 μmol , 1.0 equiv.) in 1,4-dioxane (0.4 mL) and 4M NaOH (0.15 mL) and heated to 50°C for 2 hours. The reaction was then cooled to RT and 1M HCl was added until the solution reached pH 4 and the resulting solution was allowed to stir for 20 mins. Sat. aqueous NaHCO_3 solution was then added until the solution reached pH 7. The solvents were removed under reduced pressure. No

starting material or desired product were observed by ESI-MS, instead, the substitution of the Br for OH was observed both before and after Ph deprotection.



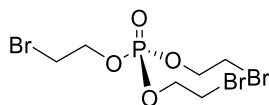
Attempted synthesis of bis(SATE)phosphate (58)

Phenyl-bis(SATE)phosphate (**60**) (18 mg, 58 μmol , 1.0 equiv.) was dissolved in 1,4-dioxane (0.2 mL) and 4M NaOH (0.1 mL) and heated to 50°C for 2 hours. The reaction was then cooled to RT and 1M HCl was added until the solution reached pH 4. The resulting solution was allowed to stir for 20 mins. The resulting precipitate was removed by filtration and suspended in sat NaHCO₃ (1.5 mL) with stirring for 20 mins. The solvents were removed under reduced pressure. No starting material or desired product was observed by ESI-MS.



Attempted synthesis of Benzyl-bis(SATE)phosphate (61)

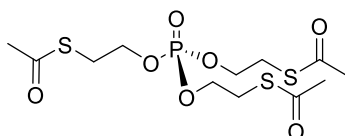
To a stirring solution of Phenyl-bis(SATE)phosphate (**60**) (60 mg, 0.16 mmol, 1.0 equiv.) in dry THF (5.5 mL) was added NaH (60% in mineral oil, 19 mg, 0.48 mmol, 3.0 equiv.) and BnOH (40 μL , 0.48 mmol, 3.0 equiv.). After 3.5 h the reaction was quenched with sat. aqueous citric acid solution (4 mL) and the solvents were removed *in vacuo*. The resulting residue was suspended in brine (25 mL), and the products extracted with Et₂O (3 x 25 mL). The combined organic layers were dried over MgSO₄, filtered and the solvents removed *in vacuo*. No desired product was identified by crude ESI-MS or NMR analysis.



tris(2-bromoethyl)phosphate (66)

To a stirring solution of POCl₃ (0.25 mL, 2.2 mmol, 1.0 equiv.) in dry DCM (15 mL) at 0°C was added 2-BrEtOH (0.77 mL, 11 mmol, 5.0 equiv) and NEt₃ (1.5 mL, 11 mmol, 5.0 equiv.) The resulting allowed to warm to RT and left stirring for 18 h. The reaction was diluted with THF (20 mL) and the precipitated NEt₃.HCl was removed by filtration. The resulting crude was concentrated *in vacuo*, and the crude residue purified by automated flash column chromatography (gradient 0 to 100% EtOAc in hexane) to afford the title compound as a clear oil (450 mg, 1.08 mmol, 50%).

HRMS-ESI Calculated for [C₆H₁₂Br₃O₄P + Na⁺]: 440.7895, found: 440.7892 ¹H NMR (400 MHz, CHLOROFORM-*D*) δ ppm 3.56 (t, 6 H, J = 6.2 Hz, BrCH₂) 4.38 (dt, 6H, J = 6.2, 8.2 Hz, CH₂CH₂Br) ¹³C NMR (101 MHz, CHLOROFORM-*D*) δ ppm 29.53 (d, J = 7.6 Hz, CH₂Br) 67.34 (d, J = 5.0 Hz, CH₂CH₂Br) ³¹P NMR (162 MHz, CHLOROFORM-*D*) δ - 1.94. IR (Vmax, film) 2967, 2885, 1455, 1422, 1270, 1235, 1064, 1004, 960, 944, 781, 572 cm⁻¹

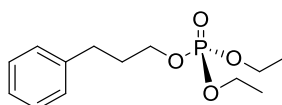


tris(SATE)phosphate (65)

To a stirring solution of tris(2-bromoethyl)phosphate (**66**) (400 mg, 0.959 mmol, 1.00 equiv) in acetone (10 mL) was added KSAc (450 mg, 3.95 mmol, 4.12 equiv.) and the resulting solution was allowed to stir for 24 hours at RT. The solvent was removed *in vacuo*, and the resulting residue was dissolved in DCM (25 mL) and washed with water (20 mL). The aqueous layer was re-extracted with DCM (2 x 25 mL), and the organic layers were

combined, dried over MgSO₄, filtered and concentrated *in vacuo* to afford the crude product. The crude product was purified by automated flash column chromatography (gradient of 0 to 100% ethyl acetate in hexane) to afford the title compound as a pink oil (234 mg, 0.579 mmol, 60%).

HRMS-ESI Calculated for [C₁₂H₂₁O₇PS₃ + Na⁺]: 427.0079, found: 427.0088 **¹H NMR** (400 MHz, CHLOROFORM-*D*) δ ppm 2.32 (s, 9H, CH₃), 3.14 (t, 6H, CH₂SAC), 4.09 (dt, *J* = 7.4, 6.5 Hz, 6H, CH₂CH₂SAC) **¹³C NMR** (101 MHz, CHLOROFORM-*D*) δ ppm 29.21 (d, *J* = 7.2 Hz, CH₂SAC), 30.60 (CH₃ SAC), 66.14 (d, *J* = 5.8 Hz, CH₂CH₂SAC) 194.76 (C=O) **³¹P NMR** (162 MHz, CHLOROFORM-*D*) δ -1.59. **IR** (Vmax, film) 2919, 2850, 1734, 1695, 1460, 1376, 1264, 1133, 1062, 1015, 956, 623 cm⁻¹

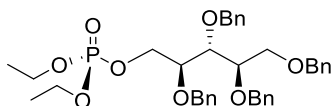


3-phenyl-propyl-bis-ethyl-phosphate (70)

To a stirring solution of PO(OEt)₃ (16 mg, 87 μmol, 1.0 equiv) in DCM (0.4 mL), was added Tf₂O (21 μL, 0.12 mmol, 1.4 equiv) and pyridine (13 μL, 0.17 mmol, 2.1 equiv). The solution was allowed to stir at RT for 10 mins before the addition of 3-phenyl-propanol (100 μL, 1.6 M solution in DCM, 0.17 mmol, 2.1 equiv.) and the resultant solution was left to stir for a further 30 mins. The reaction mixture was concentrated *in vacuo* onto silica and purified by automated flash column (gradient 0 to 100% ethyl acetate in hexane) to afford the title compound as a clear oil (11 mg, 39 μmol, 43%)

HRMS-ESI Calculated for [C₁₃H₂₁O₄P + Na⁺]: 295.1071, found: 295.1070 **¹H NMR** (400 MHz, CHLOROFORM-*D*) δ ppm 1.38 (dt, 6H *J* = 1.0, 7.1 Hz, CH₂CH₃) 1.98-2.01 (m, 2H, PhCH₂CH₂) 2.74 (dd, 2H, *J* = 6.7, 8.6 z, PhCH₂) 4.04-4.17 (m, 6H, POCH₂CH₃ + POCH₂CH₂) 7.18-7.46 (5 H, m, CH arom.) **¹³C NMR** (101 MHz, CHLOROFORM-*D*) δ 16.26 (d, *J* = 6.7 Hz, CH₃), 31.76 (OCH₂CH₂CH₂Ph), 31.99 (d, *J* = 6.8 Hz, OCH₂CH₂CH₂Ph), 63.84 (d, *J* = 5.8 Hz, OCH₂CH₃), 66.87 (d, *J* = 5.6 Hz, OCH₂CH₂), 126.16, 128.57, 141.11. (CH arom.) **³¹P NMR** (162 MHz, CHLOROFORM-*D*) δ -0.15.

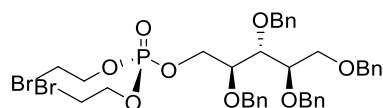
Data in accordance with literature values.²³⁷



2,3,4,5-tetra-O-benzyl-ribose-5-(bis-ethyl-phosphate) (69)

To a stirring solution of PO(OEt)₃ (6.0 μL, 32 μmol, 1.0 equiv.) in dry DCM (0.24 mL), was added Tf₂O (9 μL, 54 μmol, 1.6 equiv) and pyridine (8 μL, 0.1 mmol, 2.3 equiv). The resulting solution was left to stir at RT for 10 mins before 120 μL of the reaction mixture was transferred to a dry flask containing 2,3,4,5-tetra-O-benzyl-D-ribose (35) (27 mg, 52 μmol, 2.0 equiv.). The resulting solution was allowed to stir for a further hour at RT before the solvents were removed *in vacuo* and co-evaporated with toluene (2 mL). The crude product was purified by manual flash column (gradient 0 to 33% EtOAc in hexane) to afford the title compound as a pale orange oil (2.8 mg, 4.3 μmol, 14%)

HRMS-ESI Calculated for [C₃₇H₄₅O₈P + Na⁺]: 671.2744, found: 671.2745 **¹H NMR** (400 MHz, CHLOROFORM-*D*) δ ppm 1.28 (dt, 6H, CH₃) 3.57 – 3.78 (m, 3H, CH-2, CH-3, CH-4) 3.82 – 3.95 (m, 2H, CH-5) 4.02 (dddt, *J* = 14.3, 6.9, 4.6, 2.6 Hz, 4H, CH₂CH₃) 4.19 (ddd, *J* = 11.0, 6.9, 5.5 Hz, 1H, CH-1) 4.33 (ddd, *J* = 11.0, 5.9, 2.7 Hz, 1H, CH-1) 4.58 (d, *J* = 11.4 Hz, 1H, CH₂ OBn), 4.63 (d, *J* = 11.7 Hz, 1H, CH₂ OBn), 4.66 (s, 2H, CH₂ OBn), 4.69 (d, *J* = 11.4 Hz, 1H, CH₂ OBn), 4.72 (d, *J* = 11.7 Hz, 1H, CH₂ OBn), 7.20 – 7.36 (m, 20H, CH arom.) **¹³C NMR** (151 MHz, CHLOROFORM-*D*) δ 16.22 (d, *J* = 3.5 Hz, CH₃), 16.27 (d, *J* = 3.1 Hz, CH₃), 63.84 (d, *J* = 5.9 Hz, CH₂CH₃), 63.86 (d, *J* = 5.9 Hz, CH₂CH₃) 67.18 (d, *J* = 6.3 Hz, CH-1), 69.98 (CH-5), 72.59, 72.61, 73.47, 73.91 (CH OBn) 78.22 (d, *J* = 7.7 Hz, CH-2), 78.38 (CH-3), 78.42 (CH-4), 127.64, 127.70, 127.76, 127.81, 127.93, 128.01, 128.08, 128.48, 138.33, 138.41, 138.47, 138.65 (CH arom.) **³¹P NMR** (162 MHz, CHLOROFORM-*D*) δ -0.15. **IR** (Vmax, film) 2961, 2918, 1852, 2105, 1733, 1459, 1262, 1095, 1028, 700 cm⁻¹ [α]_D²⁰ = + 11.80 (c = 0.045, DCM)

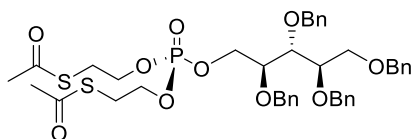


2,3,4,5-tetra-O-benzyl-ribose-5-bis(2-bromoethyl)phosphate (71)

To a stirring solution of tris(2-bromoethyl)phosphate (**66**) (30 mg, 72 μmol , 3.0 equiv) in DCM (0.36 mL), was added TiF_2O (18 μL , 0.11 mmol, 4.5 equiv) and pyridine (12 μL , 0.15 mmol, 6.3 equiv). The solution was allowed to stir at RT for 10 mins before 120 μL of the reaction mixture was transferred to a dry flask containing 2,3,4,5-tetra-O-benzyl-D-ribose (**35**) (20 mg, 40 μmol , 1.6 equiv). The resultant solution was allowed to stir for a further hour at RT before the solvents were removed *in vacuo* and co-evaporated with toluene (2 mL). The crude product was purified by manual flash column (gradient 0 to 33% ethyl acetate in hexane) to afford the title compound as a pale orange oil (2.0 mg, 2.5 μmol , 11%)

HRMS-ESI Calculated for $[\text{C}_{37}\text{H}_{43}\text{Br}_2\text{O}_8\text{P} + \text{Na}^+]$: 827.0955, found: 827.0951 **$^1\text{H NMR}$** (600 MHz, CHLOROFORM-*D*) δ 3.37 (t, $J = 6.2$ Hz, 2H, CH_2Br), 3.41 (q, $J = 6.7$ Hz, 2H, CH_2Br), 3.67 (dd, $J = 10.4, 5.1$ Hz, 1H, CH-5), 3.71 (dd, $J = 10.4, 3.5$ Hz, 1H, $\text{CH-5}'$), 3.87 – 3.95 (m, 3H, CH-2, CH-3, CH-4), 4.14 – 4.29 (m, 5H, $\text{CH}_2\text{CH}_2\text{Br, CH-1}$), 4.40 (ddd, $J = 11.2, 6.3, 2.8$ Hz, 1H, $\text{CH-1}'$), 4.49 (d, $J = 2.6$ Hz, 2H, CH_2 OBn), 4.58 (d, $J = 11.5$ Hz, 1H, CH_2 OBn), 4.63 (d, $J = 11.4$ Hz, 2H, CH_2 OBn), 4.66 (t, $J = 2.0$ Hz, 2H, CH_2 OBn), 4.73 (d, $J = 11.8$ Hz, 1H, CH_2 OBn), 7.27 – 7.36 (m, 20H, CH arom.).

$^{13}\text{C NMR}$ (151 MHz, CHLOROFORM-*D*) δ 29.51 (d, $J = 7.6$ Hz, CH_2Br), 29.57 (d, $J = 7.5$ Hz, CH_2Br), 66.93 (d, $J = 5.4$ Hz, $\text{CH}_2\text{CH}_2\text{Br}$), 66.96 (d, $J = 5.2$ Hz, $\text{CH}_2\text{CH}_2\text{Br}$), 67.81 (d, $J = 6.0$ Hz, CH-1), 69.82 (CH-5), 72.59, 72.61, 73.51, 73.91 (CH_2 OBn), 78.04 (d, $J = 7.2$ Hz, CH-2), 78.20 (CH-4), 78.24 (CH-3), 127.73, 127.77, 127.84, 127.85, 127.95, 128.10, 128.51, 128.52, 138.12, 138.31, 138.40, 138.56 (CH arom.). **IR** (Vmax, film) 2923, 2853, 1723, 1454, 1376, 1264, 1071, 1017, 800, 737, 701 cm^{-1} **$[\alpha]_D^{20}$** = - 2.20 ($c = 0.105$, DCM)



2,3,4,5-tetra-O-benzyl-ribose-5-bis(SATE)phosphate

To a stirring solution of 2,3,4,5-tetra-O-benzyl-ribose-5-bis(2-bromoethyl)phosphate (**71**) (2.0 mg, 2.5 μmol , 1.0 equiv.) in acetone (200 μL) was added KSAc (5.0 mg, 30 μmol , 12 equiv). The resulting suspension was stirred at RT for 24 hours before the acetone was removed *in vacuo*. The resulting residue was dissolved in DCM (0.5 mL) and the salts were removed by filtration to afford the title compound as a pink oil (1.4 mg 1.8 μmol , 72%)

HRMS-ESI Calculated for $[\text{C}_{41}\text{H}_{49}\text{O}_{10}\text{PS}_2 + \text{Na}^+]$: 819.2397, found: 819.2406 **$^1\text{H NMR}$** (400 MHz, CHLOROFORM-*D*) δ ppm 2.28 (s, 6H, CH_3) 3.05 (dt, 4H, $J = 10.7, 6.5$ Hz, CH_2S) 3.56 – 3.79 (m, 3H, CH-2, CH-3, CH-4) 3.79 – 3.96 (m, 2H, CH-5) 3.96 – 4.09 (m, 4H, $\text{CH}_2\text{CH}_2\text{S}$) 4.17 – 4.42 (2H, m, CH-1) 4.50 – 4.76 (8H, m, CH_2 OBn) 7.20-7.47 (m, 20H, CH arom.) **$^{13}\text{C NMR}$** (151 MHz, CHLOROFORM-*D*) δ 29.33, 29.51 (CH_2SAC), 30.64 (CH_3 SAC), 66.06 (d, $J = 6.1$ Hz, $\text{CH}_2\text{CH}_2\text{SAC}$), 66.31 (d, $J = 6.3$ Hz, CH-1) 69.92 (CH-5), 72.59, 72.61, 73.49, 73.92 (CH_2 OBn), 78.05 (d, $J = 7.14$, CH-2) 78.28 (CH-3), 78.30 (CH-4), 127.69, 127.73, 127.82, 127.95, 128.07, 128.10, 128.48, 128.50 (CH arom.), 194.82 (C=O SAC). **$^{31}\text{P NMR}$** (162 MHz, CHLOROFORM-*D*) δ -0.90 **IR** (Vmax, film) 3034, 2921, 2851, 1696, 1496, 1454, 1261, 1097, 1064, 1017, 955, 801, 736, 698 cm^{-1} **$[\alpha]_D^{20}$** = + 0.31 ($c = 0.085$, DCM)

4.7 References

120. J. L. Daughtry, W. Cao, J. Ye and J. M. Baskin, *ACS Chem. Biol.*, 2020, **15**, 318-324.
138. H. Y. Tan, R. Eskandari, D. Shen, Y. Zhu, T. W. Liu, L. I. Willems, M. G. Alteen, Z. Madden and D. J. Voadlo, *J. Am. Chem. Soc.*, 2018, **140**, 15300-15308.
173. U. Pradere, E. C. Garnier-Amblard, S. J. Coats, F. Amblard and R. F. Schinazi, *Chem. Rev.*, 2014, **114**, 9154-9218.
174. A. R. Van Rompay, M. Johansson and A. Karlsson, *Pharmacol. Ther.*, 2000, **87**, 189-198.
175. Y. Ding, J.-L. Girardet, Z. Hong, V. C. H. Lai, H. An, Y.-H. Koh, S. Z. Shaw and W. Zhong, *Bioorg. Med. Chem. Lett.*, 2005, **15**, 709-713.
180. A. J. Wiemer and D. F. Wiemer, *Top. Curr. Chem.*, 2015, **360**, 115-160.
237. H. Huang, J. Ash and J. Y. Kang, *Org. Lett.*, 2018, **20**, 4938-4941.
239. C. D. Spicer, M. Pujari-Palmer, H. Autefage, G. Insley, P. Procter, H. Engqvist and M. M. Stevens, *ACS Cent. Sci.*, 2020, **6**, 226-231.
241. K. M. Sureshan, M. Trusselle, S. C. Tovey, C. W. Taylor and B. V. L. Potter, *J. Org. Chem.*, 2008, **73**, 1682-1692.
246. H. Miyazawa, H. Yokokura, Y. Ohkubo, Y. Kondo and N. Yoshino, *J. Fluor. Chem.*, 2004, **125**, 1485-1490.
250. S. Benzaria, H. Pelicano, R. Johnson, G. Maury, J. L. Imbach, A. M. Aubertin, G. Obert and G. Gosselin, *J. Med. Chem.*, 1996, **39**, 4958-4965.
251. C. Périgaud, J. L. Girardet, I. Lefebvre, M. Y. Xie, A. M. Aubertin, A. Kirn, G. Gosselin, J. L. Imbach and J. P. Sommadossi, *Antivir. Chem. Chemother.*, 1996, **7**, 338-345.
252. S. Peyrottes, D. Egron, I. Lefebvre, G. Gosselin, J. L. Imbach and C. Périgaud, *Mini Rev. Med. Chem.*, 2004, **4**, 395-408.
253. C. Schultz, *Bioorg. Med. Chem.*, 2003, **11**, 885-898.
254. I. Lefebvre, C. Périgaud, A. Pompon, A. M. Aubertin, J. L. Girardet, A. Kirn, G. Gosselin and J. L. Imbach, *J. Med. Chem.*, 1995, **38**, 3941-3950.
255. H. Y. Tan, R. Eskandari, D. Shen, Y. Zhu, T.-W. Liu, L. I. Willems, M. G. Alteen, Z. Madden and D. J. Voadlo, *J. Am. Chem. Soc.*, 2018, **140**, 15300-15308.
256. W.-Q. Liu, M. Vidal, C. Olszowy, E. Million, C. Lenoir, H. Dhôtel and C. Garbay, *J. Med. Chem.*, 2004, **47**, 1223-1233.
257. J. F. A. Pijnenborg, E. A. Visser, M. Noga, E. Rossing, R. Veizaj, D. J. Lefeber, C. Büll and T. J. Boltje, *Chemistry*, 2021, **27**, 4022-4027.
258. J. F. A. Pijnenborg, E. Rossing, J. Merx, M. J. Noga, W. H. C. Titulaer, N. Eerden, R. Veizaj, P. B. White, D. J. Lefeber and T. J. Boltje, *Nat. Commun.*, 2021, **12**, 7024.
259. B. N. Kakde, E. Capota, J. J. Kohler and U. K. Tambar, *J. Org. Chem.*, 2021, **86**, 18257-18264.
260. H. Huang and J. Y. Kang, *Synlett*, 2019, **30**, 635-641.
261. Diisopropylphosphoramidous dichloride,
<https://www.sigmaaldrich.com/GB/en/sds/aldrich/307254>, (accessed 13/2/22).
262. *US Pat. Pat.*, 183373 A1, 2017.
263. Y.-H. Koh, J. H. Shim, J. Z. Wu, W. Zhong, Z. Hong and J.-L. Girardet, *J. Med. Chem.*, 2005, **48**, 2867-2875.
264. H. Li, J.-C. Yoo, Y.-C. Baik, W.-J. Lee and J.-H. Hong, *Bull. Korean. Chem. Soc.*, 2010, **31**, 2514-2518.
265. M. K. Patel and B. G. Davis, *Org. Biomol. Chem.*, 2010, **8**, 4232-4235.
266. M. T. Liu, N. N. Nagre and K. Ryan, *Bioorg. Med. Chem.*, 2014, **22**, 834-841.
267. B. R. Sculimbrene, Y. Xu and S. J. Miller, *J. Am. Chem. Soc.*, 2004, **126**, 13182-13183.
268. J. Schulz, M. W. Beaton and D. Gani, *J. Chem. Soc., Perkin Trans. 1*, 2000, , 943-954.
269. L. Linderoth, P. Fristrup, M. Hansen, F. Melander, R. Madsen, T. L. Andresen and G. H. Peters, *J. Am. Chem. Soc.*, 2009, **131**, 12193-12200.

270. M. T. Cook, S. A. Schmidt, E. Lee, W. Samprasit, P. Opanasopit and V. V. Khutoryanskiy, *J. Mater. Chem. B.*, 2015, **3**, 6599-6604.

Chapter 5: Optimisation and Substrate Scope of the New *S*-Acetyl-2-Thioethyl-Protected Phosphate Synthesis

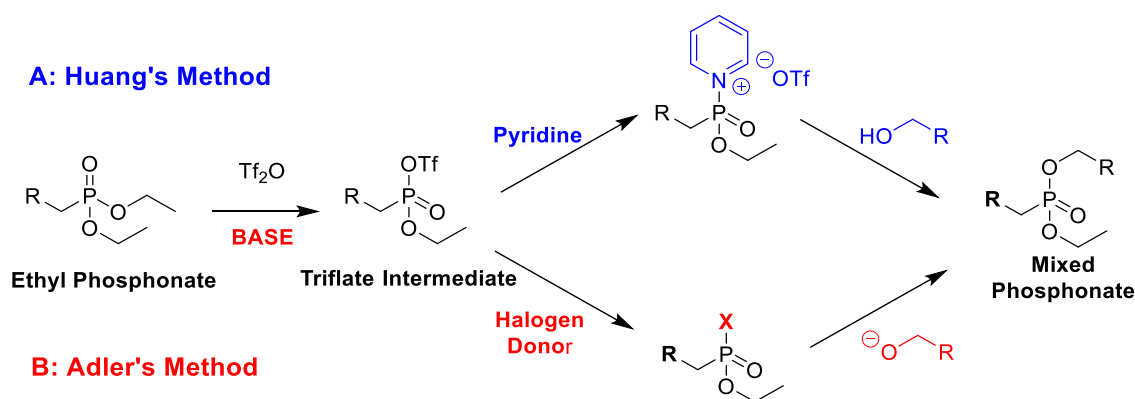
Methodology

5.1 Abstract

S-Acetyl-2-Thioethyl (SATE) groups are commonly used phosphate protecting groups in phosphate-containing small-molecule probes. These cell-permeable, cleavable groups are typically synthesised utilising highly hazardous phosphoramidite intermediates. In 2018, two research groups published methodologies for the synthesis of mixed phosphonates with the use of triflic anhydride for the activation of diethyl phosphonates.^{238, 271} This methodology was later applied to the synthesis of diethyl phosphotriesters,²³⁷ and the adaption of this method to the synthesis of *bis*(SATE) phosphates has been previously described (Chapter 4, pg. 107). With this new method in hand, work to optimise yields and explore the substrate scope of this reaction was undertaken. This chapter describes the optimisation of the SATE methodology, improving yields on a standard glucose substrate from 25% up to 64%. This method is compatible with common hydroxyl protecting groups including acetate, allyl, benzyl, and benzoyl, as well as the amine protecting groups Fmoc and CBz. In addition to these findings, the synthesis of an azide-containing metabolic glycan labelling probe previously described in literature further demonstrates the potential impact of this method to the wider field. By avoiding the use of highly hazardous dichlorophosphine intermediates and making use of readily available starting materials, this method will make the synthesis of SATE-protected phosphoprobables more practical and accessible.

5.2 Introduction

In 2018 multiple papers were published by two separate groups detailing the synthesis of mixed phosphonates by new methodologies which employ the initial electrophilic activation of a diethyl phosphonate with triflic anhydride.^{237, 238, 260, 271} Following activation with triflic anhydride, both methods then convert the intermediate species to a more reactive intermediate by addition of either a halogen donor or pyridine (Scheme 44).



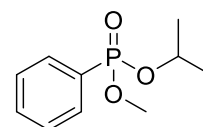
Scheme 44: Comparison of the Adler *et al* and Huang *et al* methodologies for the synthesis of mixed phosphonates. Unique elements of the Huang *et al* method are shown in blue, and of the Adler *et al* method in red.

Huang's Method

The Huang *et al* methodology was initially published for the synthesis of mixed phosphonates²³⁸ but later adapted by the same group to the synthesis of mixed phosphates.²³⁷ Their method proceeds by initial electrophilic activation of the phosphonate with triflic anhydride, yielding a phospho-triflate species which then can undergo substitution with pyridine to form a highly reactive pyridinium species. This species undergoes substitution with the target alcohol to afford the mixed phosphonate product (Scheme 44A). Significantly, these studies showed that the reaction did not proceed without the addition of pyridine, revealing the importance of the reactive intermediate for the alcohol substitution step.

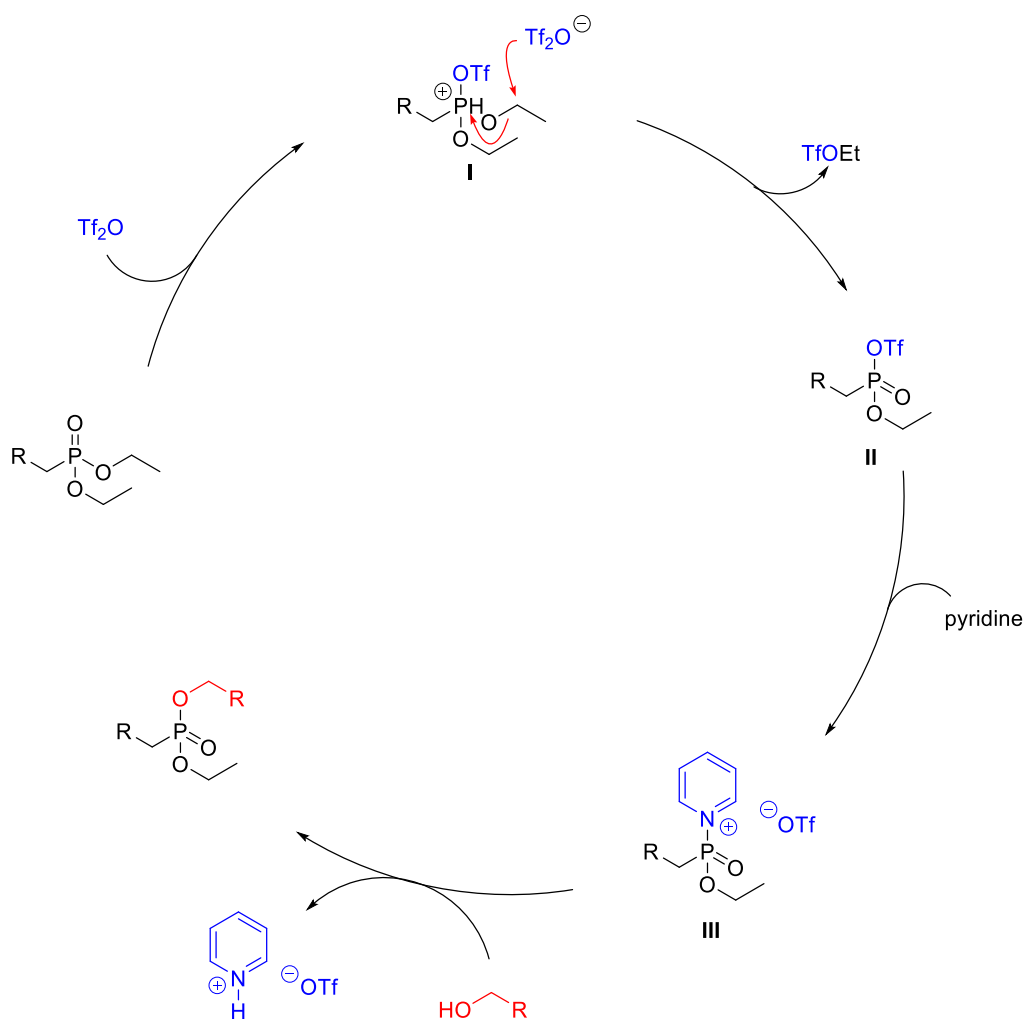
Evidence for mechanism

The group were able to prove the formation of all reactive intermediates presented within their mechanism (Scheme 45) by ¹H and ³¹P NMR studies alongside additional test reactions which were conducted to determine whether the substitution step between intermediates I and II was S_N1 or S_N2-like. They were able to prove an S_N1-type substitution by the alcohol substrate through a reaction with the mixed methyl and isopropyl starting phosphonate **72**. Substitution of only the more stable isopropyl leaving group suggests an S_N1-type reaction mechanism for this activation. In a second test reaction, the reactivity of the double bonded oxygen atom of the phosphonate with triflate was investigated by a one-pot reaction in the presence of both a phenyl and nitro-phenyl phosphonate. Lack of reaction with the electron-withdrawing nitro-phenol substrate helped provide evidence that the terminal oxygen performs a nucleophilic attack on triflic anhydride. A final control experiment with ¹⁸O-labelled phosphonate starting material gave an unlabelled product, further demonstrating that the terminal oxygen acts as a nucleophile to generate a triflate intermediate that is subsequently lost from the product, supporting their proposed mechanism.



72

Figure 17: Test substrate to prove the mechanism of substitution for the Huang *et al* method



Scheme 45: Mechanism proposed by Huang and co-workers for their method of synthesising mixed phosphonates

Reported Optimisation

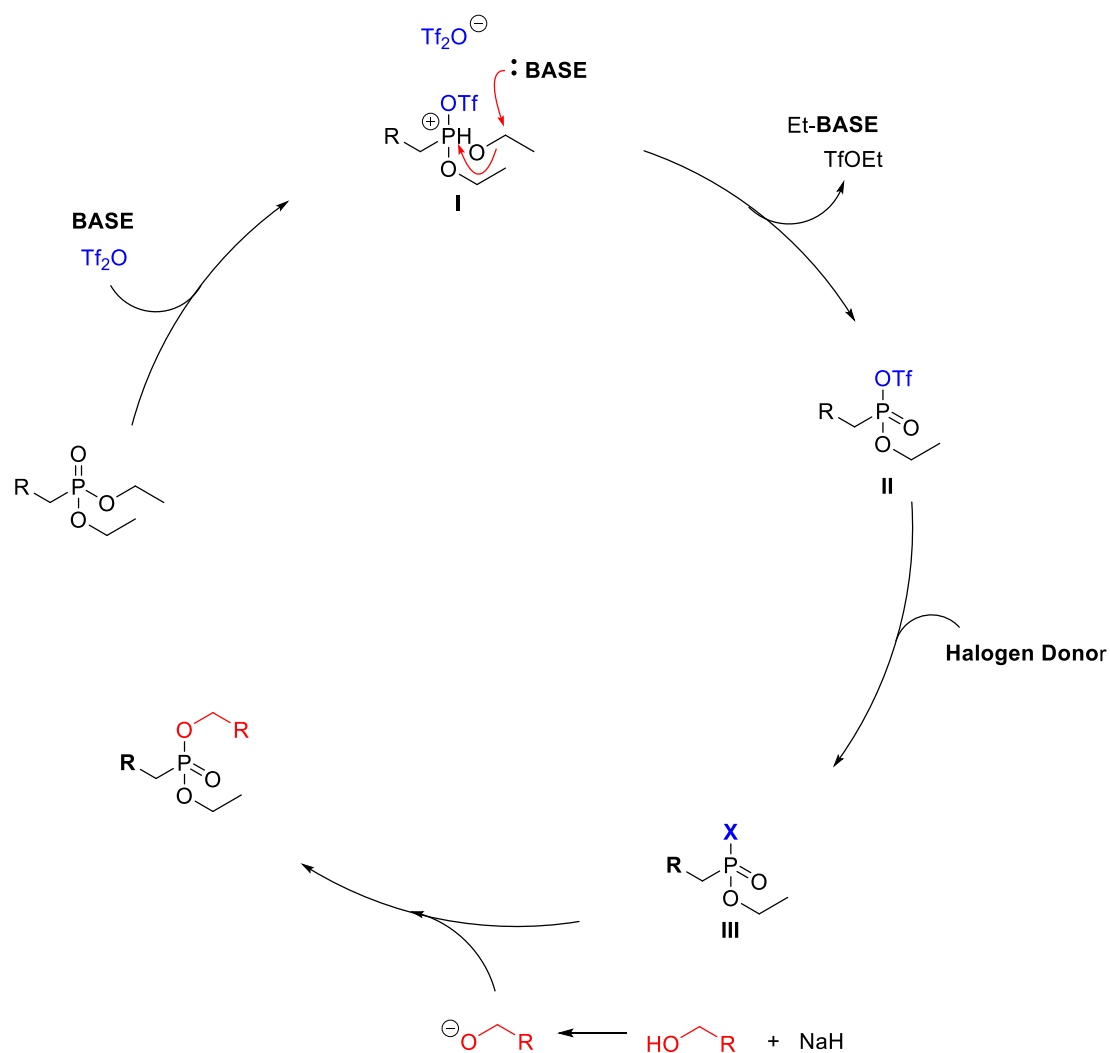
When conducting optimisation of their method, Huang *et al* investigated a wide range of reaction conditions. The initial scope of nucleophiles found that phenols were tolerated, but sterically bulky substrates resulted in the isolation of triflated side-products. Amines and thiols were also shown to be incompatible. When screening different activating agents, the group investigated triflic, acetic and trifluoroacetic anhydrides as well as bromotrimethylsilane, however only triflic anhydride was successful. Further screens tested a range of bases for the initial substitution step, including pyridine, 2,6-lutidine, DMAP, Et₃N, DBU and K₂CO₃. Interestingly, the only base to give a positive result was pyridine, with all other bases yielding a triflated alcohol side-product as the major product. Additionally, no reaction was seen without the addition of a base, further reinforcing the need for formation of the activated pyridinium species to allow for substitution with the alcohol substrate. Solvents were also screened, with DCM being highest yielding.

Adler's Method

As seen for the Huang *et al* methodology, the method published by Adler *et al* proceeds with phosphonate activation by triflic anhydride. Adler *et al* then propose that this initiates an Arbuzov reaction to the phospho-triflate species, in contrast to the Huang *et al* methodology, in the presence of base. After activation, a halogen donor is added, forming a halo-phosphonate which upon addition of the deprotonated alcohol substrate undergoes substitution to the final product (Scheme 44B). In contrast to the Huang paper, the Adler method was found to be successful with a wide range of substrates including both alcohols and thiols with primary, secondary and tertiary configurations, though their reaction requires higher equivalents of nucleophile than the Huang method (4 vs 2 equiv.). Additionally, sugar and aryl species were screened alongside a vast range of functional groups including, but not limited to, alkynes, CF₃, and halo alkane moieties.

Evidence for mechanism

The proposed mechanism for the synthesis of mixed phosphonates *via* this method is presented in Scheme 46. Evidence for this mechanism and the formed intermediates came from ¹H and ³¹P NMR studies, with a proposed Arbuzov reaction converting intermediate I to II. Significantly, the group notes that when using 2-iodopyridine as the base, they do not see evidence for the formation of the pyridinium species observed by Huang *et al* in their proposed mechanism (Scheme 45). This may be explained by the order of addition of the pyridine to the reaction, with the pyridine added before triflic anhydride by Adler *et al*, but only after the addition of triflic anhydride in the Huang *et al* methodology. It should also be noted that the Alder *et al* publication makes no reference to the requirement for prior deprotonation of their nucleophiles with NaH, and no attempts of the reaction without this deprotonation step are reported.



Scheme 46: Mechanism proposed by Alder and co-workers for their method of synthesising mixed phosphonates.

Reported Optimisation

The Adler publication lists optimisation through the screening of a variety of bases including pyridine and substituted pyridines, as well as DBU, 1,8-bis(dimethylamino)naphthalene (a.k.a. proton sponge) and Et₃N. Ultimately, they determined 2-iodopyridine as the highest yielding base, in 1.5 equivalents relative to the phosphonate starting material. With the phospho-triflate formed, substitution to a reactive chloro-intermediate was optimised through the screening of various halogen sources, including tetrabutyl- and tetraethylammonium salts with the tetraethyl-ammonium chloride salt providing the highest yields. Interestingly, yields from the use of the tetrabutylammonium chloride and bromide salts were outperformed by the yield obtained without a halogen source. This indicates an alternate mechanism to the desired product in the absence of halogen source, either stemming from a direct reaction with the triflate intermediate, or another potential intermediate formed through interaction with 2-iodopyridine.

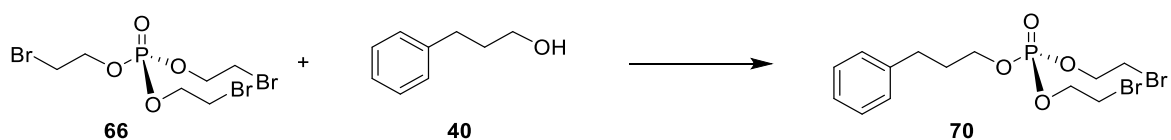
Though both publications explore a wide scope of substituted alcohol substrates, both in terms of structure and functionality, no alternative phosphonate or phosphate protecting groups were described, with only ethyl-protected substrates being tested.^{271, 272} Therefore, questions remain regarding the applicability of this methodology to alternative phosphate substrates. In addition, while a wide range of optimisation steps has already been conducted by both groups, further optimisation of the reaction conditions, such as reaction timings, and substrate scope can be investigated.

5.3 Aims

Previously the synthesis of SATE protected phosphates on a model substrates 3-phenyl-propanol and the linear sugar 2,3,4,5-*tetra-O*-benzyl-D-ribitol has proven successful utilising the Huang *et al* methodology to install an intermediate *di*-2-bromo-ethyl phosphate (see Chapter 4, pg. 104). This chapter explores optimisation of this newly developed methodology for *bis*(SATE) protected phosphates (to increase yields above the initially reported 13% for the reaction between *tris*(2-bromoethyl)phosphate and 1-azido-*tri*-2,3,4-benzyl-D-ribitol, the key intermediate for the synthesis of 1-azido-ribitol-5-phosphate probes (Chapter 3, pg. 55). In addition to this, the synthesis of SATE-protected phosphate derivatives from alternative substrates containing a range of different protecting groups and at various sites of addition are explored to demonstrate the scope of this reaction, and verify its application to the wider field.

5.4 Results and Discussion

Leading on from the successful addition of a *bis*(SATE) phosphate on a benzylated ribitol compound utilising new methodology based on the Huang *et al* procedure (Chapter 4, pg. 104), optimisation was carried out to improve the yield of this reaction above the preliminary 13% for the synthesis of the protected 1-azido-5-phosphate ribitol probes (Chapter 3, pg. 55). Initially, only the Huang *et al* method had been attempted for the synthesis of SATE phosphates as this methodology had been applied in literature to the synthesis of protected phosphates. To test whether the Adler *et al* methodology would also be successful for SATE phosphate synthesis, and encouraged by the reported use of the reaction on a much wider range of nucleophiles, the reaction of *tris*(2-bromoethyl)phosphate **66** with the model alcohol 3-phenyl-propanol **40** was attempted under the reaction conditions described by Adler *et al*. Upon attempting this reaction (Scheme 47), however, none of the desired product **70** was obtained, and the majority (85%) of the phosphate starting material was recovered. Because of this poor result, subsequent optimisation continued with the previously utilised Huang *et al* methodology.



Scheme 47: Attempted synthesis of **70** via the Adler method for mixed phosphonate synthesis **Reagents and Conditions** i) Tf_2O , pyridine, DCM, ii) TBAI ii) 3-phenyl-propanol **40**, NaH, THF (0%)

Initially, efforts were focused on improving the yields for the literature reaction with triethyl phosphate **67** and 3-phenyl-propanol **40** as the yields were lower (45%) than recorded within the literature (89%), and yields were even lower with the 2-bromoethyl-phosphate **66** (17%). A combination of distilling Tf_2O prior to use and introducing the 3-phenyl-propanol to the reaction as a solution in DCM instead of neat were shown to positively affect yields in line with the values reported within the literature (82%) (Table 3).

Table 3: Optimisation of the synthesis of 3-phenyl-propyl-diethyl-phosphate through the distillation of triflic anhydride and adding 3-phenyl-propanol as a solution in DCM

	Phosphate (tri-ethyl- phosphate) equiv.	Tf_2O equiv.	Pyridine equiv.	Pre- activation Time	Alcohol (3- phenyl- propanol) equiv.	Alcohol addition method	Reaction time	Yield
Run 1	1.0	1.5 (not distilled)	2.0	10 mins	2.0	Added neat	1 h	45%
Run 2	1.5	1.5 (not distilled)	2.0	10 mins.	2.0	Added in 1.6 M sol.	1 h	53%
Run 3	1.0	1.5 (distilled)	2.0	10 mins	2.0	Added in 1.6 M sol.	1 h	82%
Run 4	1.0	1.5 (distilled)	2.0	10 mins	2.0	Added in 0.8 M sol.	1 h	76%
Run 5	1.0	1.5 (distilled)	2.0	10 mins	2.0	Added in 0.55 M sol.	1 h	42%

The initial increase in yield from 45% up to 53% (Run 1 vs Run 2) can be attributed to the accuracy with which the 3-phenyl-propanol could be added to the reaction in solution vs the neat highly viscous oil. Further boosts to yields were observed upon the distillation of triflic anhydride, which increased yields up to 82% (Run 3). Therefore, in all following reactions distillation of triflic anhydride was conducted before the reaction. To further investigate the effect of reaction concentration, lower concentrations of starting alcohol were investigated (Runs 4 and 5). The

decrease in yields upon these lower alcohol concentrations shows the clear requirement for high reaction concentrations to achieve high yields. With the yields now in line with literature (Run 3), the same conditions were applied to the reaction of 3-phenyl-propanol with *tris*(2-bromoethyl)-phosphate **66**, however, the yield for this reaction remained low at 17%. Attempts at improving this yield by adding double the equivalents of phosphate and activating agents led to exclusive recovery of the triflated side-product (see section Phosphate Addition Side Product, pg. 141), while none of the desired product **70** was formed.

Since the reaction with the 2-bromoethyl phosphate derivative was much lower yielding than for the triethyl phosphate, and an excess of activated phosphate had further reduced yields, the conditions for phosphate pre-activation were changed. The effects of these changes were initially screened on the model reaction with triethyl phosphate **67** to identify any potential negative effects of changing reaction conditions (Table 4). Within the Adler *et al* procedure, the base was added to the reaction mixture before the addition of triflic anhydride so this was attempted in the Huang procedure (Run 6). In addition, the reaction was conducted with increasing equivalents of pyridine to investigate whether the conversion of the triflate to the pyridinium species was the cause of lower yields (Runs 7 and 8).

Table 4: Optimisation of the synthesis of 3-phenyl-propyl-diethyl phosphate through changing the order of reagent addition and the number of equivalents of pyridine

	Phosphate (ethyl-phosphate) equiv.	Tf ₂ O equiv.	Pyridine equiv.	Pre-activation time	Alcohol (3-phenyl-propanol) (added in 1.6M sol.)	Reaction time	Yield
Prev.	1.0	1.5	2	10 mins	2.0	1 h	82%
Run 6	1.0	1.5	2 (added before Tf ₂ O)	10 mins	2.0	1 h	27%
Run 7	1.0	1.5	4	10 mins	2.0	1 h	42%
Run 8	1.0	1.5	8	10 mins	2.0	1 h	27%

Adding in pyridine before triflic anhydride (Run 6) was shown to have a largely negative effect on yield. Additionally, the yields seen on increasing the equivalents of pyridine (Runs 7 and 8) were also greatly reduced. For this reason, this alteration to the method was not attempted with the 2-bromoethyl phosphate **66**. Significantly, these observations suggested that pyridine was

deactivating the unreacted triflic anhydride, thereby preventing the reaction from proceeding. Furthermore, the fact that higher equivalents of pyridine reduced yields indicated that the triflic anhydride had not fully activated the phosphate by the time pyridine was added (approx. 1 min after triflic anhydride addition). The effect of increasing the pre-activation time before pyridine was added to the reaction was then investigated for the reaction of *tris*(2-bromoethyl)phosphate **66** with 3-phenyl-propanol **40** as presented in Table 5. Notably, the Huang *et al* procedure does not report a waiting time between triflic anhydride and pyridine addition.

Table 5: Optimisation of the synthesis of 3-phenyl-propyl-bis(2-bromoethyl) phosphate by inserting a pre-activation time after the addition of triflic anhydride, and before the addition of pyridine

	Phosphate (2-bromoethyl-phosphate) equiv.	Tf ₂ O equiv.	Waiting time before adding pyridine	Pyridine equiv.	Pre-activation time	Alcohol (3-phenyl-propanol) (added in 1.6M sol.)	Reaction time	Yield
Prev.	1.0	1.5	None (approx. 1 min)	2.0	10 mins	2.0	1 h	17%
Run 9	1.0	1.5	5 min	2.0	10 mins	2.0	1 h	37%
Run 10	1.0	1.5	10 min	2.0	10 mins	2.0	1 h	50% 52% (51%)
Run 11	1.0	1.5	20 min	2.0	10 mins	2.0	1 h	45%
Run 12	1.0	1.5	30 min	2.0	10 mins	2.0	1 h	43%

a) where two separate yields are reported, the reaction was performed in duplicate with averages given in brackets

As previously hypothesised, a clear increase in yields was seen on the introduction of a pre-activation time before pyridine addition (Run 9). With as little as 5 minutes of triflic anhydride pre-activation, the yield of the reaction more than doubled, and further increases were seen after increasing the waiting time to 10 mins (Run 10). On increasing the waiting time further, up to 30 mins (Run 11 and 12), a drop-off in yield was seen indicating instability of the formed phospho-triflate species in solution (in line with observations made by Huang *et al*). Since the introduction of a 10 min gap between the addition of triflic anhydride and pyridine had a significant positive effect on yields, the effect of changing the pre-activation time (after addition of pyridine and before

addition of the alcohol) was also investigated (Table 6). In contrast to the increase in yields observed above, increasing the waiting time after the addition of pyridine reduced yields (Runs 13 and 14).

Table 6: Optimisation of the synthesis of 3-phenyl-propyl- bis(2-bromoethyl) phosphate by investigating the effect of increasing the pre-activation time after pyridine addition to the reaction

	Phosphate (2-bromo- ethyl- phosphate) equiv.	Tf ₂ O	Waiting time before adding pyridine	Pyridine	Pre- activation time	Alcohol (3- phenyl- propanol) (added in 1.6M sol.)	Reaction time	Yield
Prev.	1.0	1.5	10 mins	2.0	10 mins	2.0	1 h	51%
Run 13	1.0	1.5	10 mins	2.0	20 mins	2.0	1 h	42%
Run 14	1.0	1.5	10 mins	2.0	30 mins	2.0	1 h	36%

At this point, optimisation of the pre-activation of the phosphate reagent was considered complete. By distillation of triflic anhydride before the reaction, addition of the alcohol to the reaction as a solution in DCM, and the introduction of a pre-activation time before the addition of pyridine to the reaction, yields for the model reaction with *tris*(2-bromoethyl)phosphate were improved from 17% to 51%. As previously discussed, the solvent (DCM), activating agent (Tf₂O) and base (pyridine) for the reaction had been screened in the original Huang paper, so these were not considered for further optimisation.²³⁸

Next, these conditions were applied to a carbohydrate substrate 1,2,3,4-*tetra-O*-benzyl-glucose **73** (for synthesis see Synthesis of Glucose Substrates, pg. 144). This benzylated sugar provided a substrate that was more similar to the benzylated ribitol substrate utilised in the synthesis of the ribitol-based probes than the model alcohol used previously, yet easier to synthesise in high quantities. Due to the higher steric hindrance around the free hydroxyl group in this substrate, reaction of the phosphate at this site was expected to be slower. Therefore final optimisation of the reaction conditions investigated the effects on yield of increasing the reaction length (Table 7). Increased yields were observed up to a reaction time of 1.5 hours, with longer times after this point causing a reduction in yield indicating an instability of the formed phosphate under the reaction conditions.

Table 7: Optimisation of the synthesis of 1,2,3,4-tetra-*O*-benzyl-glucose-6-bis(2-bromoethyl)phosphate by the investigation of the effect of reaction length on yields

	Phosphate (2-bromo-ethyl-phosphate) equiv.	Tf ₂ O	Wait before adding Pyridine	Pyridine	Pre- activation time	Alcohol (1,2,3,4- tetra- <i>O</i> - benzyl glucose, added in 1.6M sol.)	Reaction time	Yield ^a
Prev.	1.0	1.5	10 mins	2.0	10 mins	2.0	1 h	51%
Run 15	1.0	1.5	10 mins	2.0	10 mins	2.0	30 mins	36%, 25% (31%)
Run 16	1.0	1.5	10 mins	2.0	10 mins	2.0	1 h 30 mins	56%, 62% (59%)
Run 17	1.0	1.5	10 mins	2.0	10 mins	2.0	2 h	41%, 42% (42%)
Run 18	1.0	1.5	10 mins	2.0	10 mins	2.0	3 h	38%, 42% (40%)
Run 19	1.0	1.5	10 mins	2.0	10 mins	2.0	4 h	39%, 43% (41%)

a) in cases where two separate yields are reported, the reaction was performed in duplicate with averages given in brackets

Optimisation Summary

Overall optimisation of the *bis*(2-bromoethyl)phosphate forming reaction was achieved through the introduction of an additional phosphate pre-activation waiting time prior pyridine addition, the use of distilled triflic anhydride, optimisation of the method of alcohol addition, and an increase in reaction time for more sterically hindered substrates up to 1.5 hours. These optimisations are presented alongside the pre-optimised methodology in Table 8. With the optimisation of the *bis*(bromoethyl)phosphate synthesis methodology now complete, the reaction was reattempted for the synthesis of the 1-azido SATE-protected-ribose phosphate probe (Chapter 3, pg. 55). While previous yields had averaged 13%, the optimised procedure described above increased yields to 48% (Table 8).

Table 8: Comparison of the original, and optimised procedure for the formation of 2-bromo-ethyl phosphates by the Huang *et al* methodology

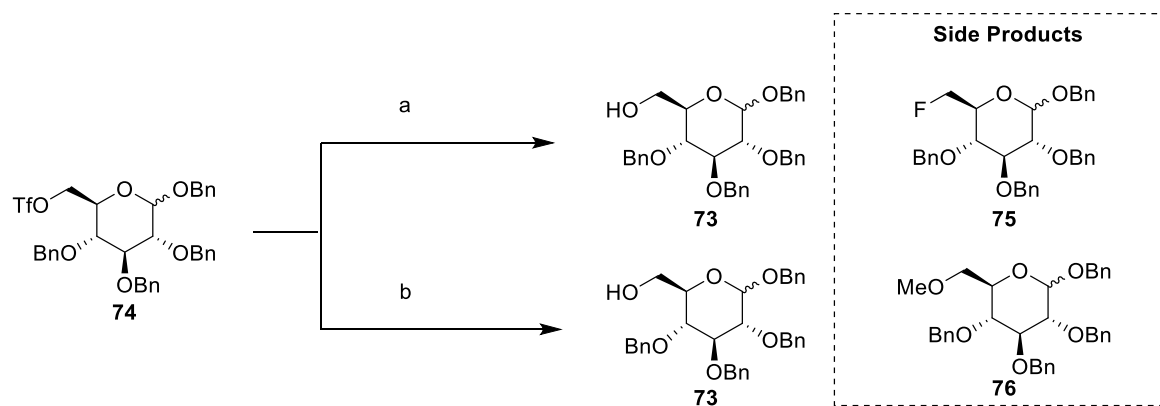
	Phosphate (2-bromo-ethyl-phosphate) equiv.	Tf ₂ O equiv.	Waiting time before adding pyridine	Pyridine equiv.	Pre-activation time	Alcohol equiv. (1-Azido-2,3,4-tri-O-benzyl-D-ribitol, added in 1.6M sol.)	Reaction time	Yield
Original	1.0	1.5	No wait (approx. 1 min)	2.0	10 mins	2.0	30 mins	13%
Optimised		1.5*	10 mins	2.0**			1 h 30 mins	48%

*freshly distilled over P₂O₅
 **it should be noted that the best yields are obtained with recently opened, sure seal-protected bottles of pyridine which are stored over molecular sieves (data not shown)

Phosphate Addition Side Product

With an optimised procedure that was applied to the synthesis of the protected ribitol-5-phosphate-probes, the focus now moved on to the identification of the main side product of the reaction. The only additional sugar product obtained from the phosphate addition reaction on the glucose substrate **73** ran higher on TLC than the starting material, indicating a decrease in polarity, and was found to decompose to a brown solid when left under a vacuum to dry after purification by flash column chromatography. ¹H NMR of this side product shows a shift of the carbohydrate CH protons and no loss or addition of peaks. Huang *et al* describe the formation of triflated side products when using bulky nucleophiles.²³⁸ To confirm that the identity of the formed side-product was indeed a triflated species, samples were analysed by ¹⁹F NMR. Freshly purified side-product showed one clear peak in the ¹⁹F NMR spectrum, with older discoloured samples showing the reduction of this peak and a large new peak at -79.0 ppm which is consistent with values reported in literature for the free triflate ion.^{273, 274} With the only fluorine within the reaction mixture coming from triflic anhydride, this provided clear evidence for the formation of the triflated side product **74**.

With evidence supporting the formation of a triflated glucose derivative, this isolated species was subjected to two literature procedures for the conversion of triflates to alcohols in an attempt to recover the starting material (Scheme 48).



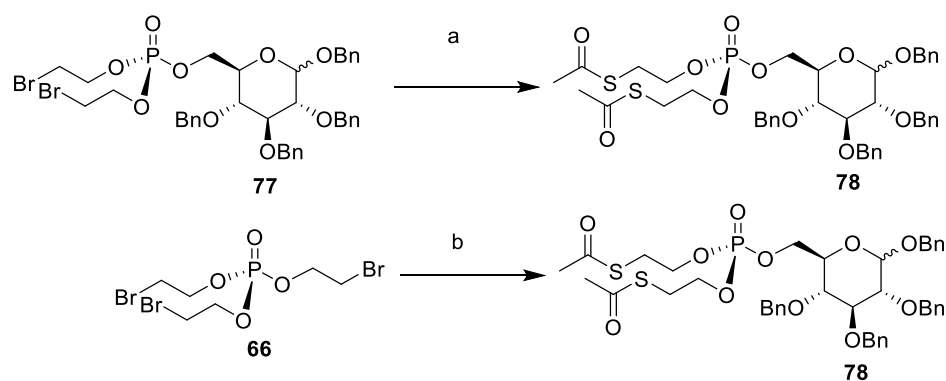
Scheme 48: Reactions attempted to recover the free alcohols from the triflated side product. **Reagents and Conditions:** a) TBAF, THF, r.t., 16 h, (**73**: 51%) b) NaOH, MeOH, THF, r.t., 16 h, (**73**: 59%)

The first method investigated for recovery of the starting sugar was treatment with TBAF (Scheme 48b).²⁷⁶ While this did provide a moderate amount of starting sugar **73** (51%), evidence of a side-product formed by the substitution of the triflate with fluorine to afford **75** was observed, as well as decomposition side products. This was evidenced by both ¹³C NMR and ESI-MS. New peaks within the ¹³C NMR spectrum at 81 and 74 ppm correlate well with C-6 and C-5 peaks for 6-fluoro glucose compounds within the literature.²⁷⁷ Furthermore, the peaks at 64 ppm relating to C-6 in the non-substituted glucose substrate were much less intense, further suggesting that substitution had taken place.

A second method for the substitution of the triflate group back to the starting alcohol was by reaction with aqueous NaOH in a solution of THF and MeOH (Scheme 48c).²⁷⁸ Crude TLC showed an approximate 1:1 ratio of the desired alcohol **72** product to a new side product, which was confirmed by ¹H and ¹³C NMR to be the result of substitution by a methoxy group producing compound **76**. Comparison to literature data for the similar 6-methoxy-1,2,3,4-*tetra-O*-benzylmannosyl compound gave a strong correlation with the new CH₃ and C-6 peaks.²⁷⁹

Of the two methods tested, treatment with aq. NaOH in THF and MeOH gave the highest yield for recovery of the starting material. With the major product being the OMe substituted product **76**, it is hypothesised that using a different solvent, for instance, just THF on its own, may prevent the undesired side reaction from occurring, and could thereby allow more of the desired starting material to be recovered in future.

SATE Phosphate Formation



Scheme 49: SATE phosphate formation of 1,2,3,4-tetra-O-benzyl-D-glucose-6-bis(2-bromoethyl)phosphate **Reagents and Conditions a**) KSAc, acetone, r.t., 24 h, (quant.) **b**) i) Tf₂O, DCM, r.t., 10 mins., then pyridine, 10 min, then 1,2,3,4-tetra-O-benzyl-D-glucose, r.t., 1.5 h, ii) KSAc, acetone, r.t., 24 h, (51% over 2 steps)

With the addition of 2-bromoethyl phosphates now fully optimised, the next step of the process towards the formation of SATE phosphates, involving substitution of the bromines by thioacetate, was investigated (Scheme 49). Substitution of the 2-bromoethyl phosphate derivative of benzylated glucose **77** was run in triplicate. The yields of each of these reactions were found to be quantitative, with the only other product being a KBr salt which precipitated out of the reaction mixture. Next, tests were run to see whether the SATE formation reaction, including both the synthesis of the *bis*(2-bromoethyl)phosphotriester **77** and the subsequent conversion into SATE phosphate **78**, could be run as a one-pot procedure from the starting phosphate **66** (Scheme 49). Following the *bis*(2-bromoethyl)phosphate formation the solvents were removed by rotary evaporation, the crude residue was dissolved in acetone, KSAc was added, and the reaction allowed to stir overnight. Following purification, a yield of 51% was obtained for the corresponding SATE product 1,2,3,4-tetra-O-benzyl-6-bis(SATE)-phosphate **78**. Though slightly lower yielding than the two-step reaction, which led to an overall yield of approximately 60% over two steps (see Table 7, run 16 and Scheme 49), the higher polarity of the SATE-protected phosphate as compared to the 2-bromoethyl phosphate made purification of the product after phosphotriester formation much easier. Though the one pot reaction was more straightforward and the desired product easier to purify, the unreacted starting material **73** was recovered in very low yields (4% of the 2 equiv. added compared to 30% from the 2-bromoethyl phosphate addition step alone). Regardless, this methodology could prove beneficial in cases where significant issues are seen in the separation of the phosphorylated product from the *tris*(2-bromoethyl)phosphate **66** after the first step of the reaction.

Substrate Synthesis and Testing

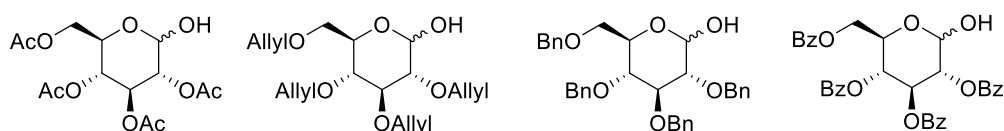
Having developed and optimised a new methodology for the synthesis of *bis*(SATE) phosphates, a panel of substrates were synthesised to investigate the scope of this SATE forming reaction and demonstrate the versatility of this reaction outside of its use in the synthesis of the 1-azido-ribitol-5-phosphate probes. In addition to sugar nucleotides and the use of phosphosugars as metabolic labelling probes, phosphate derivatives are also common in amino acids such as tyrosine and serine. With these structures in mind, the following classes of substrates were tested: 1) glucose derivatives, 2) tyrosine derivatives, and 3) azide containing GlcNAc derivatives as an example of commonly used metabolic glycan labelling probes. Through the synthesis and testing of these classes of compounds, the compatibility of various O-(OAc, OAllyl, OBn, OBz) and N-(Boc, CBz, Fmoc) protecting groups could be explored, as well as the reaction efficiency on both sugar-based structures (with incorporation of a protected phosphate at either the 1- or 6-position) and aromatic alcohols.

Glucose Sugar Derivatives

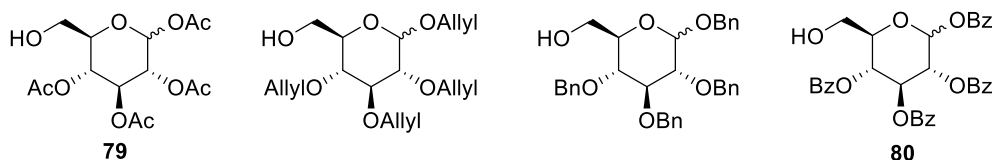
Synthesis of Glucose Substrates

Glucose and GlcNAc derivatives are commonly used in the context of metabolic glycan labelling. In recent literature, several probes have been described in which a SATE-protected phosphate is installed at the anomeric position.^{257-259, 280} Furthermore, C6-phosphate derivatives occur naturally within the metabolic pathways towards the biosynthesis of glycosylation donors.^{281, 282} Therefore, the newly developed methodology was applied to the synthesis of a number of protected C1- and C6-phosphate derivatives of glucose (Scheme 50). Within carbohydrate chemistry, some of the most commonly utilised protecting groups are acetate esters (OAc), allyl ethers (OAllyl), benzyl ethers (OBn) and benzoyl esters (OBz) and these were chosen to investigate the scope of the SATE phosphate formation. Glucose substrates with either the 1- or 6- position selectively deprotected were synthesised through one of three different methods, as presented within Scheme 50.

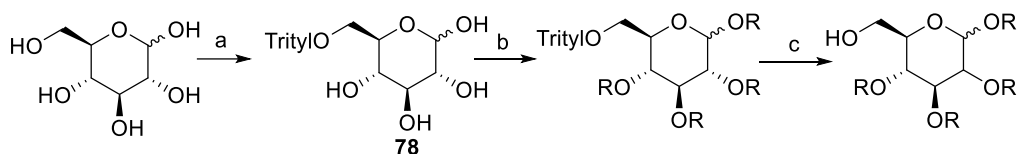
Glucose 1-Phosphate Precursor



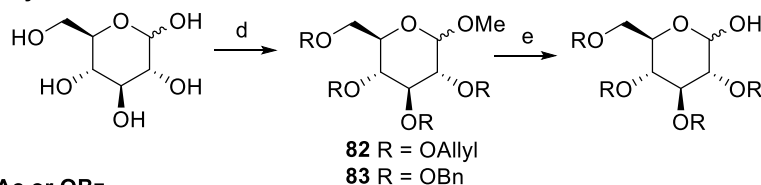
Glucose 6-Phosphate Precursor



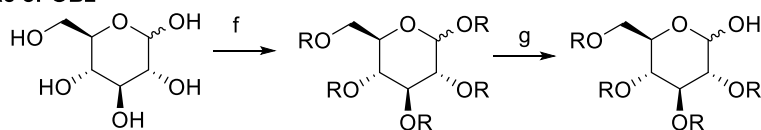
A R = OAc, OAllyl, OBn or OBz



B R = OAllyl or OBn



C R = OAc or OBz



Scheme 50: Glucose substrate structures and general methods of synthesis. **Reagents and Conditions:** a) TrCl, pyridine, r.t., 72 h (50%) b) OAc) Ac₂O, pyridine, DMAP cat., r.t., 56 h, (70%) OAllyl) AllylBr, NaH, DMF, 0°C-r.t., 18 h (70%) OBn) BnBr, NaH, DMF, 0°C-r.t., 18 h, (71%) OBz) BzCl, pyridine, DMAP cat., r.t., 56 h, (80%) c) HBr, AcOH, DCM, 10°C, 5 min, (55-70%) d) OBn) i) AcCl, MeOH, 60°C, ii) BnBr, NaH, DMF, (94%) OAllyl) i) AcCl, MeOH, 60°C, ii) AllylBr, NaH, DMF, (45%) e) H₂SO₄, AcOH, 100°C, 2.5 h, (50-57%) f) OBz) BzCl, pyridine, DMAP cat., 18 h, (72%) g) BnNH₂, THF, r.t., 18 h, (72-90%)

Synthesis of the C6-unprotected substrates was the most streamlined, with the synthesis of all four differentially protected substrates proceeding *via* the trityl protected intermediate **78** and subsequent global protection with the protecting group of choice. The removal of the trityl group was then conducted with hydrogen bromide in acetic acid. Initial trityl deprotection tests had utilised p-TsOH, however, the slower rate of deprotection using this acid caused migration of the ester protecting groups in compounds **79** and **80**. The reaction with hydrogen bromide was found to reach completion in very fast reaction times (approx. one minute) and gave no evidence of migration for the benzoylated substrate. Between 10% and 33% of the migrated side product 1,2,3,6-*tetra-O*-acetyl-D-glucose (**81**) was observed for the acetylated substrate. To mitigate against the presence of the C4-unprotected side product, the phosphate reaction with the acetylated substrate was run with 3 equivalents of

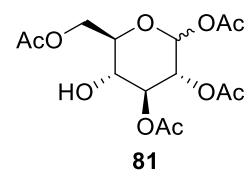


Figure 18: Migration side product 1,2,3,6-*tetra-O*-acetyl glucose **81**

glucose substrate instead of the typical 2 equivalents used in the standard reaction.

The synthesis of the anomeric deprotected glucose derivatives was performed through two different routes. For the benzyl and allyl ether protected derivatives, initial Fischer glycosylation to form the 1-OMe compound was followed by global allylation or benzylation, providing the fully protected compounds **82** and **83** respectively. The anomeric methoxy group was then cleaved by reaction with acetic acid in sulfuric acid at 100°C. On running the Fischer glycosylation and benzylation steps initially, short reaction times (3 h) for the addition of the OMe group gave only the formation of the furanoside product **84**. This was the kinetically favoured product, and the desired thermodynamically favoured pyranoside product was obtained by leaving the Fischer glycosylation step overnight. The removal of the anomeric methyl group was successful for both the OAllyl and OBn substrates in moderate yields of 50-57%, with some side products formed due to decomposition under harsh reaction conditions.

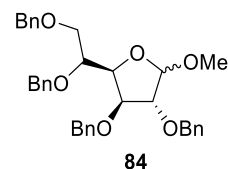


Figure 19: Furanoside side product formed from Fischer glycosylation and benzylation

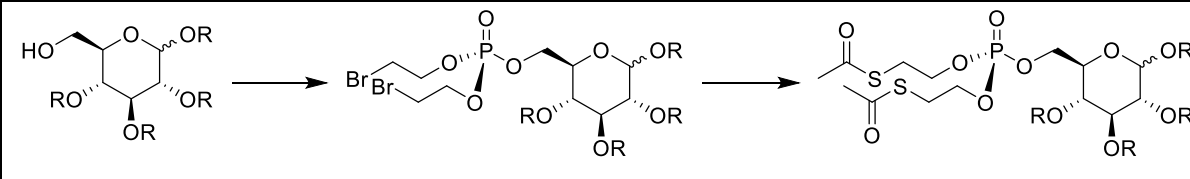
Because of potential ester migration under acidic conditions, synthesis *via* Fischer glycosylation was not possible for the acetylated and benzoylated substrates due to the acidic conditions and extended reaction times required for the OMe cleavage. Therefore, the synthesis of these anomericly unprotected substrates proceeded through the initial global protection of the sugar with OAc or OBz. Once fully protected, selective removal of the anomeric ester groups was conducted with benzylamine yielding the desired anomeric deprotected substrates. This reaction was found to be successful with both fully acetylated and fully benzoylated glucose. The cleavage of the anomeric benzoyl group was found to be much slower than for acetate (72 h vs. 18 h) and gave slightly lower yields (72% vs 90%) but for both sugars no migration was observed.

Overall, all eight of the 1-OH and 6-OH substrates were efficiently synthesised *via* two- or three-step procedures from D-glucose. With these in hand, they could be tested with the new methodology for SATE-protected phosphotriester synthesis.

Testing C6 Glucose Substrate Compatibility in the Developed SATE Phosphate Methodology

With the optimisation of the SATE reaction proceeding on the 6-position, the C6- unprotected glucose derivatives were investigated first. The results of this initial screening are presented in Table 9.

Table 9: Yields for the phosphorylation of C6 unprotected glucose derivatives



Substrate	2-BrOEt phosphate formation ^a	SATE Substitution ^a	Overall Yield
R = OBn	62%	Quant.	62%
R = OAc ^c	56%, 55%	57%, 53%	30%
R = OAllyl	33%, 31% ^b	Quant.	31%
R = OBz	39%, 35% ^b	Quant.	35%

a) in cases where two separate yields are reported, the reaction was performed in duplicate

b) product unable to be fully isolated from the *tri*-2-bromo-ethyl phosphate reagent, yields calculated from ¹H NMR peak integrals of starting phosphate and product

c) 3 equiv. of starting sugar was utilised in the 2-bromoethyl phosphate forming steps to mitigate against the presence of acetate migration product – no migrated phosphate product observed

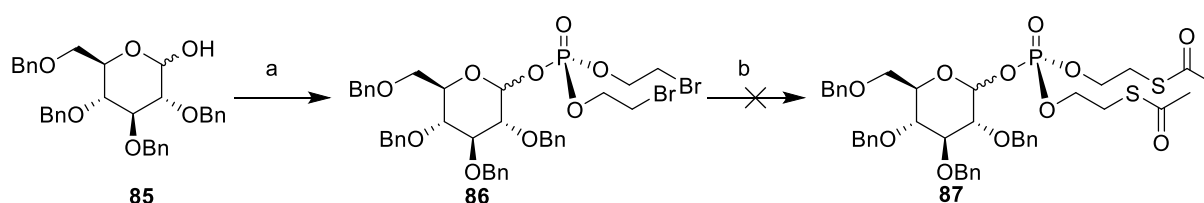
d) **Reagents and Conditions** a) i) (2BrEtO)₃PO, Tf₂O (1.5 equiv.), DCM, r.t., 10 mins ii) pyridine (2 equiv.), DCM, r.t., 10 mins. iii) sugar (2 equiv. in DCM), r.t., 1.5 h. b) KSAC, pyridine, r.t., 18 h

The *bis*(2-bromoethyl)phosphate addition was successful for all protecting groups. The benzylated product gave the highest yield of 62% with the acetylated derivative also showing high yields of 56%. These results were encouraging as OBn and OAc groups are very commonly utilised within carbohydrate chemistry. The allyl and benzoyl protected sugars had lower yields of 32% and 37% respectively. In addition to this, their purification was more challenging due to the proximity of the phosphorylated products and the 2-bromoethyl phosphate starting material on TLC. For these products, yields were calculated from a combination of fully purified product and estimated yields from ¹H NMR data on a mixture of the product and the phosphate reagent.

The subsequent SATE substitution reactions proceeded in quantitative yields for this reaction with the OAllyl, OBn and OBz substrates. Contrastingly, the SATE substitution of the OAc derivative only produced yields of 57%. No other sugar products were obtained by column chromatography or seen by TLC of the crude reaction, indicating that the side-product formed was removed by filtration. The obtained product showed no sign of degradation which would cause a loss in mass. It remains therefore unclear why the yield of the reaction on the acetylated substrate is significantly lower than the other protected derivatives.

Testing C1 Glucose Substrate Compatibility in the Developed SATE Phosphate Methodology

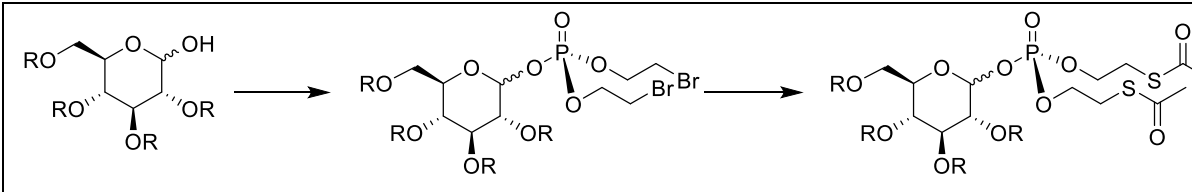
With all four protecting groups found to be able to withstand the reaction conditions for the addition of phosphate at the 6-position of glucose, testing continued for the synthesis of the phosphates at C1. Tests were initially conducted on the benzyl-protected anomerically free glucose derivative **85** (Scheme 51). The initial formation of the 2-bromoethyl phosphate **86** was successful, however, on the conversion to the corresponding SATE phosphate **87**, no phosphorylated product was detected and instead only non-phosphorylated starting sugar **85** was obtained. Testing the pH of the reaction mixture showed it had become acidic. Within the reaction, potassium thioacetate substitutes the bromine atom forming a KBr salt side product. Due to the reaction being performed with non-dry acetone under atmospheric conditions there were concerns that moisture within the reaction may be causing dissociation of KBr releasing bromide ions. HBr is utilised as a reagent for the cleavage of anomeric ester groups,²⁸³⁻²⁸⁵ and it is possible that bromide ions were acting similarly to cleave the anomeric phosphate.



Scheme 51: Initial attempted synthesis of compound **87** Reagents and Conditions a) $(2\text{BrEtO})_3\text{PO}$, Tf_2O (1.5 equiv.), DCM, r.t., 10 mins ii) pyridine (2 equiv.), DCM, r.t., 10 mins. iii) 2,3,4,6-tetra-O-benzyl-D-glucose (2 equiv. in DCM), DCM, r.t., 1.5 h. (26%) b) KSAc, acetone, r.t., 18 h, (0%)

To mitigate against any effects from acidity in the reaction mixture, resulting from either the potential formation of HBr or from potassium thioacetate in the presence of moisture forming thioacetic acid, the reaction conditions were changed as follows. Four trials of the SATE substitution reaction were run 1) utilising freshly distilled acetone, 2) utilising freshly distilled acetone with the addition of 10 equiv. dry NEt_3 3) utilising freshly distilled acetone with the addition of 10 equiv. dry pyridine and 4) running the reaction in dry pyridine as the solvent. These conditions were initially tested on the more readily available benzylated 6-bis(2-bromoethyl)phosphate glucose substrate **73**. All four reactions were found to be successful and provided quantitative yields for the SATE substitution reaction and the reaction was carried forward using dry pyridine as the solvent (see Table 9, R = OBn). These conditions were then tested for the formation of the C1-SATE-protected phosphate derivative of benzylated glucose, **87**. This reaction was found to be successful, with conversion to the SATE phosphate proceeding in a purified yield of 90%. None of the de-phosphorylated side-product was obtained, proving the stability of the 1-position phosphate under basic anhydrous conditions. Following these results, all SATE forming reactions were conducted in pyridine, and the SATE phosphate formation was tested on the other 1-OH substrates (Table 10).

Table 10: Yields for the Phosphorylation of C1 unprotected glucose derivatives



Substrate	2-BrOEt phosphate formation	Ratio $\alpha:\beta$ (SM ratio) ^a	SATE Substitution	Overall Yield
R = OBn	26%	9:1 (2:1)	90%	23%
R = OAc	35%	1:5 (4:1)	69%	24%
R = OAllyl	20%	1:0 (4:1)	72%	14%
R = OBz	41%	5:1 (4:1)	74%	30%

a) anomeric ratios determined from ¹H NMR spectra (SM = starting material)

b) **Reagents and Conditions** a) i) (2BrEtO)₃PO, Tf₂O (1.5 equiv.), DCM, RT, 10 mins ii) pyridine (2 equiv.), DCM, r.t., 10 mins. iii) sugar (2 equiv. in DCM), DCM, r.t., 1.5 h. b) KSAC, pyridine, r.t., 18 h

Overall, the yields for the ether protecting groups OBn and OAllyl were lower than for the esters OAc and OBz. Within glycosylation reactions, ester groups are considered ‘disarming’ as they disrupt the stability of the oxocarbenium ion formed upon loss of the C-1 leaving group, while ether groups, which do not destabilise this intermediate, are thought of as ‘arming’.²⁸⁶ In contrast to glycosylation reactions, however, the phosphorylation reaction occurs through nucleophilic attack of the C-1 hydroxyl group at the activated phosphate, instead of through formation of an oxocarbenium ion, and therefore the effects of ‘arming’ and ‘disarming’ groups are expected to be different. The electron withdrawing esters at C-2 may, through induction, increase the reactivity of the anomeric hydroxyl group, while the ethers do not, and this could be the cause of the increased reactivity and yield of the ester-protected derivatives. In addition, for the ‘armed’ substrates, it is possible that yields are further negatively affected by competing oxocarbenium ion formation through elimination of the phosphate group or the triflated side-product in the presence of an acid. Furthermore, the ‘armed’ ether groups may encourage triflated side-product formation which will further negatively impact on yields for these groups.

Also significant for the 1-position phosphates is the ratio of $\alpha:\beta$ anomers formed. Typically the phosphoramidite methodology yields the α product due to the anomeric effect leading to an increased stability of the alpha anomer of the intermediate phosphite (Chatoer 4: 4.2 Introduction pg. 107). The same is true for the newly developed methodology, with the α anomer preferred over the β anomer. It should be kept in mind that it is possible for the anomericly unprotected starting materials to undergo mutarotation under the reaction conditions, with reaction of the α -anomer expected to exhibit faster reactivity due to the anomeric effect. This leads to the anomeric ratio of

products differing from the ratio of starting material. As predicted, for the OAllyl, OBn and OBz substrates the more stabilized α -anomer was preferentially formed, as expected by the anomeric effect. Contrastingly, for the OAc group the β -anomer was formed preferentially. Further investigation into the anomeric ratio of products when using anomerically pure starting materials, and elucidation of the reaction mechanism, is required to further explore these findings.

Though the yields for the anomeric phosphates were lower than the phosphorylation at the 6-position, these yields are still comparable to reported yields for anomeric SATE-protected phosphate addition *via* the phosphoramidite approach.²⁵⁸ It is also important to note that the reaction times for the reaction at the anomeric position have not yet been optimised. With this alcohol group possessing different reactivity than the primary alcohol at C-6, and the larger steric bulk at this site, a longer reaction time could increase yields for these substrates further.

Tyrosine Derivatives

In 2020, the development of a new route to the synthesis of phospho-serine and -tyrosine derivatives was published.²³⁹ This report scoped a range of substrates containing a number of different nitrogen protecting groups, including the tyrosine mimics shown in Figure 20.

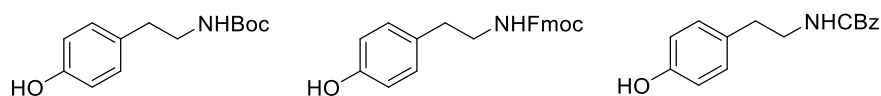
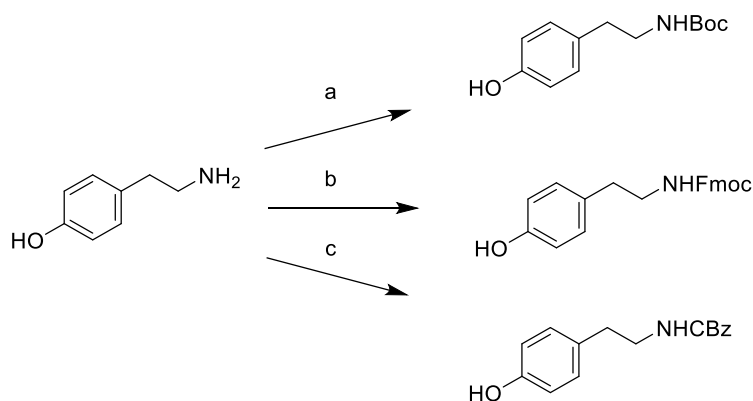


Figure 20: Tyrosine mimics for testing the SATE phosphate reaction

Using these substrates within the SATE-phosphate synthesis reaction would allow testing of the compatibility with additional protecting groups, including Boc, Fmoc and CBz groups (groups previously inaccessible through the use of glucose substrates), in addition to testing the efficiency of the reaction on phenol derivatives. These substrates were easily accessible from commercially available tyramine, allowing efficient synthesis following routes previously described by Spicer *et al*²³⁹ (Scheme 52).



Scheme 52: Synthesis of serine and threonine analogues for SATE phosphate testing **Reagents and Conditions** a) Boc anhydride, NaHCO₃, THF, H₂O, r.t., 4 h, (50%) b) Fmoc chloride, NaHCO₃, THF, H₂O, r.t., 4 h, (30%) c) benzyl chloroformate, NaHCO₃, THF, H₂O, r.t., 4 h, (64%)

Testing Thr Substrate Compatibility in the Developed SATE Phosphate Methodology

Initial tests were run with the Fmoc, Boc and CBz protected tyramine derivatives under the conditions optimised for the glucose derivatives.

Table 11: Yields for the phosphorylation of Thr derivatives

Substrate	2-BrOEt phosphate formation ^a	SATE Substitution	Overall Yield
Fmoc Tyramine	60%, 50%	83%	42%
CBz Tyramine	32%, 26%	Quant.	25%
Boc Tyramine	<1% ^b	-	-

a) in cases where two separate yields are reported, the reaction was performed in duplicate

b) product unable to be fully isolated from the *tris*(2-bromoethyl)phosphate reagent, yields calculated from NMR of starting phosphate and product

c) **Reagents and Conditions** a) i) (2BrEtO)₃PO, Tf₂O (1.5 equiv.), DCM, r.t., 10 mins ii) pyridine (2 equiv.), DCM, r.t., 10 mins. iii) sugar (2 equiv. in DCM), DCM, r.t., 1.5 h. b) KSAC, pyridine, r.t., 18 h

Upon testing the phosphate reaction on the tyramine derivatives, the Fmoc substrate gave the highest yields (50-60%), followed by CBz with lower yields (around 30%) while for the Boc substrate only trace amounts of product were detected by ¹H NMR (<1%). Despite the varied yields for the reaction, moderate amounts of starting material (Fmoc = 36%, CBz = 61%, Boc = 54%) were recovered, alongside the corresponding triflated side products. This indicated that the low yield for the Boc substrate was not due to the starting material decomposing under the reaction conditions, but instead due to low reactivity and potentially low solubility of the substrate.

Both the CBz and Fmoc substrates were able to undergo substitution to form the corresponding SATE phosphates in high yields, and the overall SATE formation yields were in line with those observed for the glucose substrates.

GlcNAc Derivatives

GlcNAc is a commonly utilised sugar for metabolic labelling purposes, and SATE-protected phosphates have been used to allow GlcNAc-1-phosphate derivatives to enter into the cell.^{138, 166, 259} A panel of GlcNAc substrates^c (Figure 21) was therefore subjected to the new phosphotriester synthesis methodology (Table 12).

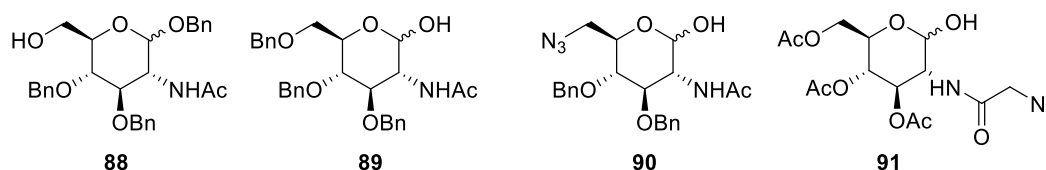


Figure 21: GlcNAc substrates for the testing of the SATE phosphate methodology

Table 12: Yields for the phosphorylation of GlcNAc derivatives

Substrate	2-BrOEt phosphate formation ^a	SATE Substitution	Overall Yield
88	0%	-	-
89	0%	-	-
90	0%	-	-
91	8.3%	Quant.	8.3%

a) **Reagents and Conditions** a) i) (2BrEtO)₃PO, Tf₂O (1.5 equiv.), DCM, r.t., 10 mins ii) pyridine (2 equiv.), DCM, r.t., 10 mins. iii) sugar (2 equiv. in DCM), DCM, r.t., 1.5 h. b) KSAC, pyridine, r.t., 18 h

Testing initially investigated the reaction of benzylated substrates **88**, **89** and **90** within the 2-bromoethyl phosphate forming reaction. With benzyl groups yielding the highest results for the SATE methodology on glucose substrates, it was believed the corresponding GlcNAc substrates would be most likely to be successful. On attempting the reaction with these substrates, however, no desired product was obtained. There were concerns about the *N*-acyl moiety being unstable to the reaction conditions, however, the majority of the starting material could be recovered from the

^c GlcNAc substrates **88**, **89**, **90** and **91** were synthesised following literature procedures by Willems group member Quentin Foucart.

reaction in each case, and their identity was proven by NMR analysis to be unchanged. Additionally, the only carbohydrate side-products from the reaction were triflated side products similar to those seen for the glucose substrates. Even with much longer reaction times (3 h) there was still no desired product obtained, and again starting material was recovered from the reaction. The one-pot SATE synthesis was also attempted on these substrates, to check whether or not GlcNAc was stable to the SATE substitution conditions. Again the majority of the starting sugar was reobtained unchanged, however, still none of the desired product was observed.

With the reaction being unsuccessful on the benzylated GlcNAc substrates, the acetylated substrate **91** was tested as the synthesis of the corresponding SATE product had been reported previously in the literature.¹³⁸ The reaction to form the 2-bromoethyl phosphate was successful on this substrate, indicating that the deactivation of the *N*-acyl ester by the azido group may have aided the reaction to be successful.^d While the SATE formation was also successful, with crude ¹H NMR showing peaks that match those reported in the literature for the corresponding SATE-protected GlcNAc probe,¹³⁸ yields obtained for the SATE formation were low (8.3% over 2 steps) compared to the reported phosphoramidate approach (40%).

Further optimisation of the method is required to make it applicable to a wider range of GlcNAc substrates. A major reason for the lack of reactivity seen for the benzylated derivatives within the phosphate reaction may arise from their low solubility in DCM. Within the original Huang paper, DCM is by far the best solvent for the reaction²³⁸ however with the optimisation conducted it may be possible that a more polar solvent could be applicable. Despite the general lack of reactivity of GlcNAc substrates, the fact that they can be recovered and are thus stable to the reaction conditions for both the phosphate addition and SATE substitution is encouraging for the further optimisation and possible application of this methodology to additional hexosamine substrates in the future.

5.5 Conclusion

In conclusion, the optimisation of the new SATE-protected phosphate synthesis has been described. Thorough optimisation of this methodology continuing from the previously reported method development by Huang *et al* has increased the yield of the reaction to form the 1-azido ribitol probes from 13% to 48%. In addition to this optimisation, it was shown that the major sugar side product of the reaction, identified as a triflated species, can be converted back to the starting alcohol substrate to recover precious starting materials. Furthermore, the reaction was shown to be

^d Test of this reaction with the non-azido acetylated GlcNAc substrate has since been found to be unsuccessful. Reaction conducted by Willems group PhD student Lloyd Murphy (*unpublished findings*).

successful on various glucose substrates, with both addition of phosphate at the 6- and 1-positions successful, and on phenol derivatives, showing compatibility with a wide range of both hydroxyl and amine protecting groups. Finally, the use of this method has been successful in the synthesis of an azide containing GlcNAc metabolic labelling probe described in literature. These results demonstrate the significance of the newly developed methodology to the wider chemical biology community, with this methodology utilising less hazardous intermediates than the previously utilised phosphoramidite chemistry, while producing comparable yields on optimised substrates. Further work on *N*-acetylhexosamine substrates is needed to make the reaction more widely applicable to this class of compounds.

5.6 Experimental

General Experimental

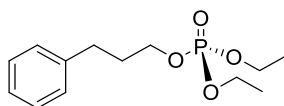
All reactions were conducted in oven dried glass wear under nitrogen, and where specified dry solvents used were either freshly distilled (DCM, DMF, toluene, THF) or from a SureSeal bottle, (DCE, pyridine). Flash column chromatography was run either manually with high purity 220-400 μm particle size silica (Sigma) or on an automated system (Teledyne, CombiFlash NextGen 300+) with 20 to 40 μm particle size silica (RediSep Rf Gold Normal-Phase Silica columns) here specified. Reactions and column fractions were monitored by TLC and visualised by UV and staining. For sugars: charring with 10% H_2SO_4 in MeOH; for phosphate reactions: KMnO_4 stain; and for azido compounds: initial reaction with 10% PPh_3 in DCM, followed by staining with ninhydrin.

For phosphate addition reactions all starting materials were dried prior to use by co-evaporation with toluene three times and drying on a high vacuum manifold overnight. Triflic anhydride was distilled over P_2O_5 prior to use and pyridine used from a SureSeal bottle stored over molecular sieves.

^1H and ^{13}C NMR spectra were obtained either on a JEOL ECS400A spectrometer (400 and 101 MHz respectively) or a Bruker AVIIIHD600 spectrometer (600 and 150 MHz respectively) where specified. Structural assignments were corroborated by homo- and heteronuclear 2D NMR methods (COSY, HMQC and DEPT) where necessary. Chemical shifts are reported in parts per million (ppm, δ) relative to the solvent (CDCl_3 , δ 7.26; CD_3OD , δ 3.31; D_2O , δ 4.79). ^1H NMR splitting patterns are designated as singlet (s), doublet (d), triplet (t), quartet (q), doublet of doublets (dd), doublet of doublets of doublets (ddd), doublet of triplets (dt), apparent triplet (apt t), and so forth. Splitting patterns that could not be visualized or easily interpreted were designated as multiplet (m). Coupling constants are reported in Hertz (Hz). Where sugar NMR data is reported in a ratio of anomers, the NMR data is assigned with integrals as whole integers corresponding to the number of protons within the peak (normalised for each anomer separately). Where one anomer is greatly preferred, ^{13}C NMR may not be visible for the minor anomer and in those cases the ^{13}C NMR data is reported for only the major anomer. This is denoted by $^{13}\text{C NMR } (\alpha) \delta'$.

IR spectra were obtained by thin film ATR on a Perkin Elmer Spectrum 2 and $[\alpha]_D$ measurements obtained on a Bellingham Stanley ADP400 polarimeter at the in the given solvent at specified concentration where $C = 1 = 10 \text{ mg/mL}$.

Synthesis of compound **66** is described previously in Chapter 4. Compounds **88**, **89**, **90**, and **91** were synthesised by Quentin Foucart.



3-phenyl-propyl-bis-ethyl-phosphate (68)

Optimisation Conditions

To a stirring solution of PO(OEt)₃ (A mg, 1.0 equiv) in DCM (0.2 M), was added Tf₂O (B. equiv) and pyridine (C. equiv). The solution was left to stir at RT for 10 mins before the addition of 3-phenyl-propanol (D equiv. by E method) and the resulting solution was left to stir for a further 30 mins. The reaction mixture was evaporated *in vacuo* onto silica and dry loaded onto an automated flash column (gradient 0 to 100% ethyl acetate in hexane) to afford the title compound as a clear oil (F%).

	Tri-ethyl-phosphate Mass (A mg)	Tf ₂ O (B equiv.)	Pyridine (C equiv.)	3-phenyl- propanol (D equiv.)	Alcohol addition method (E)	Yield (F)
Run 1	15 mg	1.5 (not distilled)	2.0	2.0	Added neat	45%
Run 2	15 mg	1.5 (not distilled)	2.0	2.0	Added in 1.6 M sol.	53%
Run 3	15 mg	1.5 (distilled)	2.0	2.0	Added in 1.6 M sol.	82%
Run 4	15 mg	1.5 (distilled)	2.0	2.0	Added in 0.8 M sol.	76%
Run 5	15 mg	1.5 (distilled)	2.0	2.0	Added in 0.55 M sol.	42%
Run 6	15 mg	1.5 (distilled)	2 (added before Tf ₂ O)	2.0	Added in 1.6 M sol.	27%
Run 7	15 mg	1.5 (distilled)	4	2.0	Added in 1.6 M sol.	42%
Run 8	15 mg	1.5 (distilled)	8	2.0	Added in 1.6 M sol.	27%

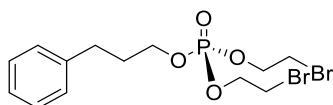
Optimised Conditions

To a stirring solution of PO(OEt)₃ (16 mg, 87 μmol, 1.0 equiv) in DCM (0.4 mL), was added Tf₂O (21 μL, 0.12 mmol, 1.4 equiv) and pyridine (13 μL, 0.17 mmol, 2.1 equiv). The solution was left to stir at RT for 10 mins before the addition of 3-phenyl-propanol (100 μL of a 1.6 M solution in DCM, 0.17 mmol, 2.1 equiv.) and the resulting solution was left to stir for a further 30 mins. The reaction mixture was evaporated *in vacuo* onto silica and dry loaded onto an automated flash column (gradient 0 to 100% ethyl acetate in hexane) to afford the title compound as a clear oil (20 mg, 74 μmol, 85%)

HRMS-ESI Calculated for [C₁₃H₂₁O₄P + Na⁺]: 295.1071, found: 295.1070 **¹H NMR** (400 MHz, CHLOROFORM-*D*) δ ppm 1.38 (dt, 6H *J* = 1.0, 7.1 Hz, CH₂-CH₃) 1.98-2.01 (m, 2H, Ph-CH₂-CH₂) 2.74 (dd, 2H, *J* = 6.7, 8.6 z, Ph-CH₂) 4.04-4.17 (m, 6H, P-O-CH₂-CH₃ + P-O-CH₂-CH₂) 7.18-7.46 (5 H, m, CH arom.) **¹³C NMR** (101 MHz, CHLOROFORM-*D*) δ 16.26 (d, *J* = 6.7 Hz, CH₃), 31.76 (OCH₂CH₂CH₂Ph), 31.99 (d, *J* = 6.8 Hz, OCH₂CH₂CH₂Ph), 63.84 (d, *J* = 5.8 Hz,

OCH₂CH₃), 66.87 (d, *J* = 5.6 Hz, OCH₂CH₂), 126.16, 128.57, 141.11. (CH arom.) ³¹P NMR (162 MHz, CHLOROFORM-*D*) δ -0.15.

Data in accordance with literature values.²³⁷



3-phenyl-propyl-1-bis(2-bromoethyl)phosphate (70)

Optimisation conditions

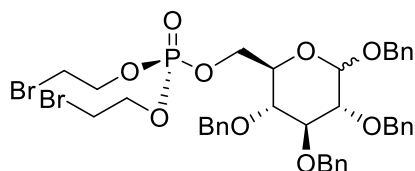
To a stirring solution of **65** (A mg, 1.0 equiv) in DCM (0.2 M), was added Tf₂O (1.5 equiv) and after B mins pyridine (2 equiv) was added. The solution was left to stir at RT for C mins before the addition of 3-phenyl-propanol (2 equiv. as a 1.6M solution in DCM) and the resulting solution was left to stir for [D time]. The reaction mixture was evaporated *in vacuo* onto silica and dry loaded onto an automated flash column (gradient 0 to 100% ethyl acetate in hexane) to afford the title compound as a clear oil (E%)

	Tri-2-bromoethyl-phosphate Mass (A mg)	Waiting time before adding pyridine (B mins)	Preactivation time (C mins)	Reaction length (D)	Yield (E%)
Unoptimised	22 mg	None (approx. 1 min)	10 mins	1 h	17%
Run 9	40 mg	5 min	10 mins	1 h	37%
Run 10	40 mg	10 min	10 mins	1 h	50% 52% (51%)
Run 11	40 mg	20 min	10 mins	1 h	45%
Run 12	40 mg	30 min	10 mins	1 h	43%
Run 13	42 mg	10 mins	20 mins	1 h	42%
Run 14	42 mg	10 mins	30 mins	1 h	36%

Optimised Conditions

To a stirring solution of *tri*-2-bromoethyl phosphate (**66**) (38 mg, 92 μmol, 1.0 equiv.) in dry DCM (0.5 mL) was added Tf₂O (23 μL, 0.14 mmol, 1.5 equiv.). After 10 mins at RT, pyridine (15 μL, 0.19 mmol, 2.1 equiv.) was added, and after a further 10 mins at RT, 3-phenyl-propanol (120 μL of a 1.6 M solution in DCM, 0.18 mmol, 2.0 equiv.) was added. The resultant solution was allowed to stir for 1 h before the reaction mixture was dried onto silica, and the crude product was purified by automated flash column chromatography (gradient 0 to 60% EtOAc in hexane) to afford the title compound as a clear oil (19 mg, 45 μmol, 49%)

HRMS-ESI Calculated for [C₁₃H₁₉Br₂O₄P + Na⁺]: 452.9260, found: 452.9249 **¹H NMR** (400 MHz, CHLOROFORM-*D*) δ 1.94 – 2.08 (m, 2H, CH₂CH₂CH₂OP), 2.66 – 2.79 (m, 2H, CH₂CH₂OP), 3.56 (dt, *J* = 9.7, 6.0 Hz, 4H, CH₂Br), 4.13 (q, *J* = 6.7 Hz, 2H, CH₂OP), 4.37 (ddt, *J* = 19.7, 8.1, 6.1 Hz, 4H, CH₂CH₂Br), 7.16 – 7.24 (m, 2H, CH arom.), 7.29 – 7.33 (m, 3H, CH arom.). **¹³C NMR** (101 MHz, CHLOROFORM-*D*) δ 29.59, 29.66 (CH₂Br), 31.61 (CH₂Ph), 31.80 (d, *J* = 6.9, CH₂CH₂Ph), 67.00 (d, *J* = 5.6 Hz, CH₂CH₂Br), 67.79 (d, *J* = 6.5 Hz, CH₂CH₂CH₂Ph), 126.26, 128.59, 140.83 (CH arom.), **³¹P NMR** (162 MHz, CHLOROFORM-*D*) δ -1.51. **IR** (Vmax, film) 2972, 2269, 1672, 1496, 1454, 1203, 1071, 1007, 745, 699, 483 cm⁻¹



1,2,3,4,-tetra-O-Benzyl-6-bis(2-bromoethyl)phosphate- α,β -D-glucose

Optimisation conditions

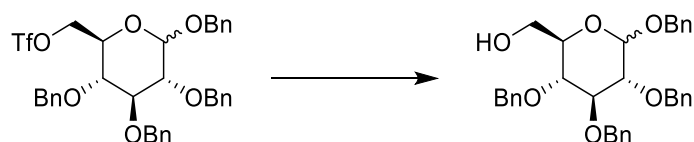
To a stirring solution of *tri*-2-bromoethyl phosphate (**66**) (**A** mg, 1.0 equiv) in DCM (0.2 M), was added Tf_2O (1.5 equiv) and after 10 mins pyridine (2 equiv) was added. The solution was left to stir at RT for 10 mins before the addition of 1,2,3,4,-tetra-*O*-benzyl- α,β -D-glucose (2 equiv. as a 1.6M solution in DCM) and the resulting solution was left to stir for [**B** time]. The reaction mixture was evaporated *in vacuo* onto silica and dry loaded onto an automated flash column (gradient 0 to 100% ethyl acetate in hexane) to afford the title compound as a clear oil (**C**%)

Tri-2-bromoethyl-phosphate Mass (A mg)	Reaction time	Yield^a
23 mg	30 mins	25%
23 mg	1 h	51%
23 mg	1 h 30 mins	62%
24 mg	2 h	41%, 42%, 42%
24 mg	3 h	38%, 42%, 40%
24 mg	4 h	39%

Optimised Conditions

To a stirring solution of *tri*-2-bromoethyl-phosphate **66** (30 mg, 72 μmol , 1.0 equiv.) in DCM (0.36 mL) was added freshly distilled Tf_2O (18 μL , 0.11 mmol, 1.5 equiv.). After stirring at RT for 10 mins dry pyridine (12 μL , 0.14 mmol, 2.0 equiv.) was added. After a further 10 mins at RT, a solution of **73** (78 mg, 0.14 mmol, 2.0 equiv.) in DCM (0.18 mL) was added. The reaction was allowed to continue at RT for a further 1.5 h before the solvents were removed *in vacuo* and the residue dried onto silica. The crude product was purified by automated flash column chromatography (gradient 0 to 60% EtOAc in hexane) to afford the title compound as a white solid (45 mg, 54 μmol , 62%) in a mixture of anomers (2:3 $\alpha:\beta$).

HRMS-ESI Calculated for $[\text{C}_{38}\text{H}_{43}\text{Br}_2\text{O}_9\text{P} + \text{Na}^+]$: 855.0904, found: 855.0945 **¹H NMR** (400 MHz, CHLOROFORM-*D*) δ 3.42 – 3.63 (m, 9H, CH_2Br , α CH-2, CH-4, β CH-2, CH-4, CH-5), 3.68 (t, J = 8.9 Hz, 1H, β CH-3), 3.84 (ddt, J = 10.0, 4.0, 2.4 Hz, 1H, α CH-5), 4.08 (t, J = 9.2 Hz, 1H, α CH-3), 4.19 – 4.48 (m, 8H, $\text{CH}_2\text{CH}_2\text{SAC}$, α/β CH-6 x 2), 4.55 (d, J = 7.8 Hz, 1H, β CH-1), 4.81 (d, J = 3.8 Hz, 1H, α CH-1), 4.53 – 5.08 (m, 16H, CH_2 OBn), 7.27 – 7.51 (m, 40H CH arom.). **¹³C NMR** (101 MHz, CHLOROFORM-*D*) δ 29.38, 29.48, 29.58, 29.67 (CH_2Br), 66.93 (d, J = 5.9 Hz, α CH-6), 67.03 (d, J = 5.9 Hz, β CH-6), 67.03 (d, J = 5.9 Hz, $\text{CH}_2\text{CH}_2\text{Br}$) 67.08 (d, J = 6.0 Hz, $\text{CH}_2\text{CH}_2\text{Br}$), 69.50 (α CH-5), 71.36, 73.21, 73.53, 73.60 (d, J = 7.8 Hz, α CH-5), 75.08, 75.23 (CH_2 OBn), 75.23 (d, J = 7.8 Hz, β CH-5), 75.86 (CH_2 OBn), 77.24 (α CH-4), 77.46 (β CH-4), 79.98 (α CH-2), 81.97 (α CH-3), 82.29 (β CH-2), 84.56 (β CH-3), 95.67 (α CH-1), 102.55 (β CH-1), 127.81, 127.85, 127.88, 128.00, 128.06, 128.09, 128.29, 128.52, 128.57, 128.62, 128.66, 137.28, 137.92, 138.07, 138.14, 138.34, 138.48 (CH arom.) **³¹P NMR** (162 MHz, CHLOROFORM-*D*) δ -1.31, -1.19. **IR** (V_{max} , film) 3031, 2885, 1421, 1453, 1360, 1273, 1012, 1067, 736, 698 cm^{-1}



Recovery of Starting Sugar from Triflated Side-product

Method A: Reaction with TBAF

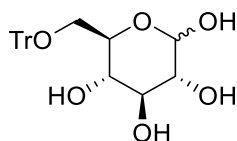
To a stirring solution of **74** (30 mg, 44 μmol , 1.0 equiv.) in THF (1 mL) was added TBAF (1 M in THF, 0.10 mL, 0.10 mmol, 2.3 equiv.). The resulting solution was left stirring at RT for 18 h and the reaction mixture was diluted with EtOAc (5 ml) and washed with NH_4Cl (5 mL), dried with MgSO_4 and the solvents removed *in vacuo*. The crude product as analysed by ^1H , ^{13}C NMR and MS to show a yield of 51% for the reobtained SM **73**.

Method B: Reaction with Sodium Hydroxide

To a stirring solution of **74** (30 mg, 44 μmol , 1.0 equiv.) in THF (2 mL) and MeOH (2 mL) was added 1M NaOH (0.15 mL). After 18 h the reaction was quenched by the addition of DOWEX H^+ resin, washed with MeOH and filtered with the resulting solution concentrated *in vacuo*. The crude product as analysed by ^1H , ^{13}C NMR and MS to show a yield of 59% for the reobtained SM **73**.

Substrates

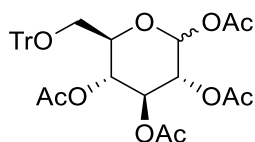
Glucose



6-O-trityl- α,β -D-glucose

To a stirring solution of D-glucose (2.6 g, 14 mmol, 1.0 equiv.) in pyridine (50 mL) at 0°C , was added a solution of trityl chloride (4.3 g, 15 mmol, 1.1 equiv.) in pyridine (13 mL) dropwise. The resulting solution was allowed to warm to RT and left stirring for 72 h before the reaction was quenched by the addition of MeOH (5 mL). The solvents were removed *in vacuo* and the resulting residue was co-evaporated with toluene (3 x 10 mL). The resulting residue was dissolved in DCM (250 mL) and washed consecutively with 1M HCl (100 mL), saturated aqueous NaHCO_3 solution (100 mL), and brine (100 mL). The organic layer was dried over MgSO_4 , filtered, and dried *in vacuo* to afford the crude product. The crude product was purified by flash column chromatography on an automated system (gradient 0 to 10% MeOH in DCM) to afford the title compound, as a mixture of anomers, as a white foam (3.0 g, 7.3 mmol, 50%)

HRMS-ESI Calculated for $[\text{C}_{25}\text{H}_{26}\text{O}_6 + \text{Na}^+]$: 445.1622, found: 445.1625, **^1H NMR** (600 MHz, CHLOROFORM-*D*) δ 3.11 – 3.60 (m, 6H), 3.60 – 4.02 (m, 2H), 4.38 – 5.15 (m, 4H), 5.15 – 5.68 (m, 2H, CH-1), 7.01 – 7.53 (m, 15H, CH arom.). **^{13}C NMR** (151 MHz, CHLOROFORM-*D*) δ 21.50 (OC(Ph) $_3$), 63.46 (CH-6 α), 64.07 (CH-6 β), 70.32, 71.15, 71.95, 73.47, 74.47, 82.06, 86.76, 87.15, 92.31 (CH-1 α), 96.36 (CH-1 β), 125.33, 127.08, 127.16, 127.30, 127.75, 127.90, 127.95, 127.97, 128.26, 128.71, 129.07, 129.71, 137.91, 143.56, 143.75, 146.86, (CH arom.) **IR** (ν_{max} , film) 3358, 3058, 3030, 2928, 2883, 1490, 1448, 1035, 1002, 900, 764, 732, 697, 645 cm^{-1}

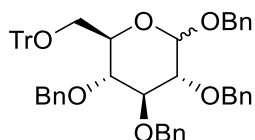


1,2,3,4-tetra-O-acetyl-6-O-trityl- α,β -D-glucose

To a stirring solution of 6-O-trityl- α,β -D-glucose (500 mg, 1.18 mmol, 1.00 equiv.) in dry pyridine (10 mL) at 0°C, was added Ac₂O (0.85 mL, 9.1 mmol, 8.3 equiv.) and DMAP (cat.). The resulting solution was allowed to warm to RT and left stirring for 56 h before the reaction was quenched by the addition of MeOH (2.5 mL). The solvents were removed *in vacuo* followed by co-evaporation with toluene (3 x 5 mL). The resulting residue was dissolved in DCM (50 mL) and washed consecutively with 1M HCl (25 mL), saturated aqueous NaHCO₃ solution (25 mL), and brine (25 mL), dried over MgSO₄, filtered, and dried *in vacuo*. The resulting crude product was purified by flash column chromatography on an automated system (gradient 0 to 50% EtOAc in hexane) to afford the title compound in a mixture of anomers (4:6 $\alpha:\beta$), as a colourless foam (470 mg, 0.79 mmol, 70%),

HRMS-ESI Calculated for [C₃₃H₃₄O₁₀ + Na⁺]: 613.2044, found: 613.2035, **¹H NMR** (400 MHz, CHLOROFORM-D) δ 1.92 – 2.03 (m, 24H, CH₃), 2.99 (dd, *J* = 10.7, 4.1 Hz, 1H, α CH-6), 3.03 (dd, *J* = 10.6, 4.2 Hz, 1H, β CH-6), 3.30 (dd, *J* = 10.7, 2.3 Hz, 1H, α CH-6'), 3.32 (dd, *J* = 10.7, 2.4 Hz, 1H, β CH-6') 3.67 (ddd, *J* = 9.8, 4.1, 2.4 Hz, 1H, β CH-5) 4.00 (ddd, *J* = 8.4, 4.1, 2.3 Hz, 1H, α CH-5), 5.11 – 5.19 (m, 3H, α CH-2, β CH-2, CH-4), 5.22 – 5.28 (m, 1H, α CH-4) 5.32 (t, *J* = 10.0 Hz, 1H, β CH-3), 5.39 (t, *J* = 9.8 Hz, 1H, α CH-3), 5.71 (d, *J* = 8.4 Hz, 1H, β CH-1), 6.42 (d, *J* = 3.7 Hz, 1H, α CH-1), 7.15 – 7.22 (m, 8H, CH arom.), 7.22 – 7.29 (m, 10H, CH arom.), 7.37 – 7.43 (m, 16H, CH arom.). **¹³C NMR** (101 MHz, CHLOROFORM-D) δ 20.48, 20.54, 20.65, 20.68, 20.79, 20.91, 20.97, 21.09, (CH₃), 61.19 (α CH-6), 61.64 (β CH-6), 68.26 (α CH-4), 68.31 (β CH-4), 69.52 (α CH-2), 70.38 (α CH-3), 70.56 (β CH-2), 71.28 (α CH-5), 73.21 (β CH-3), 74.08 (β CH-5), 86.54 (α (C(Ph)₃), 86.65 (β (C(Ph)₃), 89.38, (α CH-1) 91.97, (β CH-1) 127.08, 127.85, 127.88, 128.74, 128.77, 143.50, 143.53, (CH arom.) 168.94, 168.97, 169.03, 169.40, 169.84, 170.31, 170.49, 171.17. (C=O) IR (Vmax, film) 3059, 3026, 2938, 2882, 1753, 1491, 1449, 1368, 1247, 1213, 1014, 985, 930, 900, 783, 767, 736, 702, 645 cm⁻¹

Data in accordance with literature values^{287, 288}



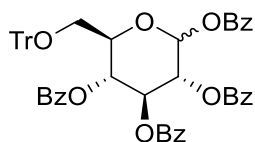
1,2,3,4-tetra-O-benzyl-6-O-trityl- α,β -D-glucose

To a stirring solution of 6-O-trityl- α,β -D-glucose (500 mg, 1.18 mmol, 1.00 equiv.) in dry DMF at 0°C was added NaH (60% in mineral oil, 300 mg, 7.40 mmol, 6.27 equiv.). The resulting reaction mixture was left at 0°C for 30 mins before the addition of BnBr (0.85 mL, 6.8 mL, 6.2 equiv.) and TBAI (cat.). Additional DMF (2 mL) was added to solubilise the reaction before allowing the resulting suspension to warm to RT. After 18 h the reaction was quenched by the addition of MeOH (5 mL) and the solvents were removed *in vacuo*. The resulting residue was dissolved in DCM (50 mL) and washed consecutively with sat. aqueous NH₄Cl (25 mL) solution, water (25 mL) and brine (25 mL). The resulting organic layer was dried over MgSO₄, filtered and solvents removed *in vacuo*. The crude product was purified by automated flash column chromatography (0 to 15% EtOAc in hexane) to afford the title compound in a mixture of anomers ($\alpha:\beta$ 2:3), as a clear foam (630 mg, 0.80 mmol, 71%).

HRMS-ESI Calculated for [C₅₃H₅₀O₆ + Na⁺]: 805.3500, found: 805.3518 **¹H NMR** (400 MHz, CHLOROFORM-D) δ 3.19 (dd, *J* = 10.2, 4.4 Hz, 1H, α CH-6), 3.27 (dd, *J* = 10.1, 4.0 Hz, 1H, β CH-6), 3.36 – 3.53 (m, 1H, β CH-5, α CH-6'), 3.57 – 3.73 (m, 5H, α CH-2, CH-4, β CH-2, CH-4, CH-6'), 3.79 – 3.90 (m, 2H, α CH-5, β CH-3), 4.02 (t, *J* = 9.3 Hz, 1H, α CH-3), 4.30 (d, *J* = 10.5 Hz, 1H, α CH₂ OBn), 4.37 (d, *J* = 10.4 Hz, 1H, β CH₂ OBn), 4.56 (d, *J* = 6.7 Hz, 1H, β CH-1), 4.59 – 4.92 (m, 12H, CH₂ OBn), 4.94 (d, *J* = 3.9 Hz, 1H, α CH-1), 4.96 – 5.12 (m, 4H, CH₂ OBn), 7.14 – 7.65 (m, 40H, CH arom.) **¹³C NMR** (101 MHz, CHLOROFORM-D) δ 62.49 ($\alpha+\beta$ CH-6), 68.68 (CH₂ OBn), 70.64 (α CH-5), 70.79, 73.05 (CH₂ OBn), 74.72 (β CH-5), 75.08, 75.14, 75.19, 76.07, 76.12 (CH₂ OBn), 77.98 (β CH-4),

78.22 (α CH-2), 80.30 (α CH-4), 82.46 (α CH-3), 82.67 (β CH-2), 84.83 (β CH-3), 86.38 (α C(Ph)₃), 86.47 (β C(Ph)₃), 94.69 (α CH-1), 102.34 (β CH-1), 127.06, 127.08, 127.71, 127.77, 127.84, 127.89, 127.92, 127.98, 128.01, 128.15, 128.23, 128.27, 128.32, 128.48, 128.50, 128.53, 128.62, 128.82, 128.91, 128.94, 137.10, 137.46, 137.94, 138.38, 138.62, 144.03, 144.07 (CH arom.) IR (Vmax, film) 3031, 2923, 2876, 1494, 1450, 1359, 1211, 1153, 1071, 1028, 739, 697 cm⁻¹

Data in accordance with literature values²⁸⁹

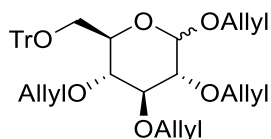


1,2,3,4-tetra-O-benzoyl-6-O-trityl- α,β -D-glucose

To a stirring solution of 6-O-trityl- α,β -D-glucose (500 mg, 1.18 mmol, 1.00 equiv.) in dry pyridine (10 mL) at 0°C, was added BzCl (0.80 mL, 6.9 mmol, 6.3 equiv.) and DMAP (cat.). The resulting solution was allowed to warm to RT and left stirring for 56 h before the reaction was quenched by the addition of MeOH (2.5 mL). The solvents were removed *in vacuo* and co-evaporated with toluene (3 x 5 mL). The resulting residue was dissolved in DCM (50 mL) and washed consecutively with 1M HCl (25 mL), sat. aqueous NaHCO₃ solution (25 mL), and brine (25 mL), dried over MgSO₄, filtered, and the solvents removed *in vacuo*. The resulting crude product was purified by flash column chromatography on an automated system (gradient 0 to 30% EtOAc in hexane) to afford the title compound in a mixture of anomers (2:1 $\alpha:\beta$) as a colourless foam (760 mg, 0.90 mmol, 80%)

HRMS-ESI Calculated for [C₅₃H₄₂O₁₀ + Na⁺]: 861.2670, found: 861.2702, **¹H NMR** (400 MHz, CHLOROFORM-D) δ 3.28 (ddt, J = 14.9, 10.8, 4.3 Hz, 2H, α CH-6, β CH-6), 3.51 (dtd, J = 16.7, 6.7, 3.3 Hz, 2H, α CH-6', β CH-6'), 4.13 – 4.33 (m, 1H, β CH-5), 4.21 – 4.65 (m, 1H, α CH-5), 5.74 – 5.83 (m, 1H, α CH-2), 5.87 – 6.04 (m, 4H, α CH-4, β CH-2, CH-3, CH-4), 6.17 – 6.29 (m, 1H, α CH-3), 6.32 (d, J = 7.3 Hz, 1H, β CH-1), 6.94 – 7.06 (m, 1H, α CH-1), 7.04 – 7.23 (m, 20H, CH arom.), 7.28 – 7.71 (m, 42H, CH arom.), 7.80 (dd, J = 7.6, 3.7 Hz, 4H, CH arom.), 7.94 (dtd, J = 9.6, 7.1, 6.7, 3.8 Hz, 8H, CH arom.), 8.11 – 8.25 (m, 4H, CH arom.). **¹³C NMR** (101 MHz, CHLOROFORM-D) δ 61.83 (α CH-6), 62.19 (β CH-6), 68.74 (α CH-4), 69.04 (β CH-4), 70.86 (α CH-2), 71.00 (α CH-3), 71.26 (β CH-2), 72.11 (α CH-5), 73.37 (β CH-3), 74.67 (β CH-5), 86.74 (α C(Ph)₃), 86.82 (β C(Ph)₃), 90.35 (α CH-1), 92.92 (β CH-1), 126.97, 127.79, 127.82, 128.30, 128.33, 128.41, 128.43, 128.48, 128.65, 128.68, 128.76, 128.81, 128.93, 128.97, 129.09, 129.19, 129.28, 129.80, 129.83, 129.87, 129.90, 129.93, 130.07, 130.26, 133.23, 133.33, 133.51, 133.88, 143.54, 143.57 (CH arom.), 164.58, 164.77, 164.81, 165.25, 165.54, 165.86, 166.08 (C=O) .IR (Vmax, film) 3061, 2942, 1732, 1601, 1450, 1256, 1104, 1091, 1021, 736, 705, 644 cm⁻¹

Data in accordance with literature values²⁹⁰



1,2,3,4-tetra-O-allyl-6-O-trityl- α,β -D-glucose

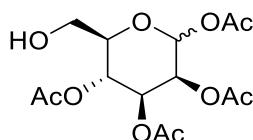
To a stirring solution of 6-O-trityl- α,β -D-glucose (500 mg, 1.18 mmol, 1.00 equiv) in dry DMF at °C was added NaH (60% in mineral oil, 300 mg, 7.40 mmol, 6.27 equiv.). The reaction was left at 0°C for 30 mins before the addition of AllylBr (0.70 mL, 6.8 mL, 6.2 equiv.) and TBAI (cat.). Additional DMF (2 mL) was added to solubilise the reaction before warming to RT. After 18 h the reaction was quenched by the addition of MeOH (5 mL), and the solvents were removed *in vacuo*. The resulting residue was dissolved in DCM (50 mL) and washed consecutively with sat. aqueous NH₄Cl solution (25 mL), water (25 mL) and brine (25 mL) dried over MgSO₄, filtered, and concentrated *in vacuo*. The crude product was purified by automated flash column chromatography (0 to 15% EtOAc in hexane) to afford the separated pure anomers α (160 mg, 0.27 mmol, 23%) and β (320 mg, 0.54 mmol, 46%) as clear oils.

α-anomer (major)

HRMS-ESI Calculated for [C₃₇H₄₂O₆ Na⁺]: 605.2874, found: 605.2883, **¹H NMR** (400 MHz, CHLOROFORM-*D*) δ 3.07 (dd, *J* = 10.1, 3.8 Hz, 1H, *CH*-6), 3.26 (ddd, *J* = 9.5, 3.8, 2.0 Hz, 1H, *CH*-5), 3.32 (d, *J* = 2.3 Hz, 1H, *CH*-2), 3.33 – 3.34 (m, 1H, *CH*-3), 3.43 (dd, *J* = 10.1, 2.0 Hz, 1H, *CH*-6'), 3.55 (ddd, *J* = 9.5, 6.1, 2.9 Hz, 1H, *CH*-4), 3.79 – 3.88 (m, 1H, OCH₂ OAllyl), 4.05 – 4.14 (m, 1H, OCH₂ OAllyl), 4.14 – 4.29 (m, 2H, OCH₂ OAllyl), 4.29 – 4.50 (m, 4H, OCH₂ OAllyl), 4.95 (d, *J* = 1.6 Hz, 1H, *CH*-1), 4.96 – 5.04 (m, 2H, CH=CH₂ OAllyl), 5.09 – 5.43 (m, 6H, CH=CH₂ OAllyl), 5.56 (ddt, *J* = 17.3, 9.6, 6.0 Hz, 1H, CH=CH₂ OAllyl), 5.88 – 6.07 (m, 3H, CH=CH₂ OAllyl), 7.15 – 7.36 (m, 9H, *CH* arom.), 7.38 – 7.55 (m, 6H, *CH* arom.). **¹³C NMR** (101 MHz, CHLOROFORM-*D*) δ 62.53 (*CH*-6), 67.97 (CH₂ OAllyl), 70.44 (*CH*-5), 72.48 (CH₂ OAllyl), 73.97 (CH₂ OAllyl), 74.69 (CH₂ OAllyl), 78.09, 79.80 (*CH*-2, *CH*-3), 81.90 (*CH*-4), 86.34 (C(Ph)₃), 95.49 (*CH*-1), 117.52, 118.38 (CH=CH₂ OAllyl), 127.07, 127.88, 128.92, 134.00, 134.83, 135.13, 135.45, (CH arom.), 144.14 (CH=CH₂ OAllyl), **IR** (Vmax, film) 3057, 2984, 2924, 2875, 1737, 1449, 1265, 1071, 1048, 926, 735, 703, 644 cm⁻¹ [α]_D²⁰ = +71.7 (*c* = 0.19, DCM)

β-anomer (minor)

HRMS-ESI Calculated for [C₃₇H₄₂O₆ + Na⁺]: 605.2874, found: 605.2883, **¹H NMR** (400 MHz, CHLOROFORM-*D*) δ 3.14 (dd, *J* = 10.0, 4.2 Hz, 1H, *CH*-6), 3.45 (dd, *J* = 10.0, 1.9 Hz, 1H, *CH*-6'), 3.48 – 3.54 (m, 2H, *CH*-2, *CH*-3), 3.75 (t, *J* = 10 Hz, 1H, *CH*-5), 3.78 – 3.85 (m, 1H, *CH*-4), 4.14-4.26 (m, 5H, OCH₂ OAllyl), 4.36 – 4.45 (m, 1H, OCH₂ OAllyl), 4.96 – 5.05 (m, 2H, CH=CH₂ OAllyl), 5.07 (d, *J* = 3.6 Hz, 1H, *CH*-1), 5.14 – 5.40 (m, 6H, CH=CH₂ OAllyl), 5.59 (ddt, *J* = 16.4, 10.1, 6.0 Hz, 1H, CH=CH₂ OAllyl), 5.90 – 6.12 (m, 3H, CH=CH₂ OAllyl), 7.19 – 7.38 (m, 12H, *CH* arom.), 7.52 (dd, *J* = 7.2, 2.0 Hz, 6H, *CH* arom.). **¹³C NMR** (101 MHz, CHLOROFORM-*D*) δ 62.45 (*CH*-6), 70.09 (*CH*-5), 73.83, 73.89, 74.60, 74.82 (CH₂ OAllyl), 77.63, 81.96 (*CH*-2, *CH*-3), 84.38 (*CH*-4), 86.36 (C(Ph)₃), 102.65 (*CH*-1), 117.01, 117.15, 117.25, 117.31 (CH=CH₂ OAllyl), 127.06, 127.87, 128.92, 134.32, 134.77, 135.31, 135.36 (CH arom.), 144.08 (CH=CH₂ OAllyl), **IR** (Vmax, film) 3057, 2984, 2924, 2875, 1737, 1449, 1265, 1071, 1048, 926, 735, 703, 644 cm⁻¹ [α]_D²⁰ = +8.25 (*c* = 0.8, DCM)



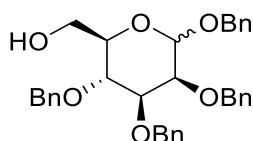
1,2,3,4-tetra-*O*-acetyl- α,β -D-glucose

To a stirring solution of 1,2,3,4-*tetra-O*-acetyl-6-*O*-trityl- α,β -D-glucose (240 mg, 0.407 mmol, 1.00 equiv.) in AcOH (0.95 mL) at 10°C, was added HBr (33% in acetic acid, 0.80 mL, 0.47 mmol, 1.2 equiv.). The resulting solution was stirred for 30 seconds before the reaction mixture was filtered, and rinsed with AcOH into a separating funnel containing DCM (10 mL) and H₂O (10 mL). The aqueous layer was further extracted with DCM (3 x 10 mL) and the combined organic layers were washed with sat. aqueous NaHCO₃, dried over MgSO₄, filtered, and concentrated *in vacuo*. The resulting crude product was purified by automated flash column chromatography (0 to 100% EtOAc in hexane) to afford the title compound as a clear foam (100 mg, 0.29 mmol, 72%), in a mixture of anomers (1:1 $\alpha:\beta$), alongside side migration product 1,2,3,6-*tetra-O*-acetyl glucose (30%)

HRMS-ESI Calculated for [C₃₃H₃₄O₁₀ + Na⁺]: 613.2044, found: 613.2035 **¹H NMR** (400 MHz, CHLOROFORM-*D*) δ 2.00 (s, 6H, CH₃ OAc), 2.02 (s, 6H, CH₃ OAc), 2.05 (s, 6H, CH₃ OAc), 2.09 (s, 3H, CH₃ OAc), 2.15 (s, 3H, CH₃ OAc), 3.50 – 3.66 (m, 3H, α *CH*-6, β *CH*-6, *CH*-5), 3.67 – 3.83 (m, 2H, α *CH*-6', β *CH*-6'), 3.90 (ddd, *J* = 10.3, 4.1, 2.2 Hz, 1H, α *CH*-5), 4.98 – 5.09 (m, 2H, α *CH*-2, β *CH*-4), 5.06 – 5.13 (m, 2H, α *CH*-4, β *CH*-2), 5.29 (t, *J* = 10.1 Hz, 1H, β *CH*-3), 5.47 – 5.54 (m, 1H, α *CH*-3), 5.70 (d, *J* = 8.2 Hz, 1H, β *CH*-1), 6.32 (d, *J* = 3.7 Hz, 1H α *CH*-1). **¹³C NMR** (101 MHz, CHLOROFORM-*D*) δ 20.45, 20.79, 20.96, 21.28 (CH₃ OAc), 60.72 (α *CH*-6), 61.08 (β *CH*-6), 68.16 (β *CH*-4), 68.50 (α *CH*-4), 69.25 (α *CH*-2), 69.66 (α *CH*-3), 70.44 (β *CH*-2), 72.13 (α *CH*-5), 74.97 (β *CH*-5), 89.31 (α *CH*-1),

91.79 (β CH-1), 169.16, 169.41, 169.83, 170.29 (C=O OAc). IR (Vmax, film) 3521, 3018, 2921, 2859, 1753, 1370, 1223, 1036, 944 cm^{-1}

Data in accordance with literature values²⁸⁸

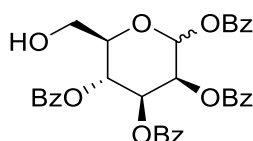


1,2,3,4-tetra-O-benzyl- α,β -D-glucose

To a stirring solution of 1,2,3,4-tetra-O-benzyl-6-O-trityl- α,β -D-glucose (450 mg, 0.579 mmol, 1.00 equiv.) in AcOH (5 mL) and DCM (5 mL) at 10°C, was added HBr (33% in acetic acid, 0.12 mL, 0.88 mmol, 1.2 equiv.) dropwise. The resulting solution was stirred for 5 mins before the reaction mixture was filtered and rinsed with AcOH into a separating funnel containing DCM (10 mL) and H₂O (10 mL). The aqueous layer was further extracted with DCM (3 x 10 mL) and the combined organic layers were washed with sat. aqueous NaHCO₃ solution, dried over MgSO₄, filtered and concentrated *in vacuo*. The resulting crude product was purified by automated flash column chromatography (0 to 30% EtOAc in hexane) to afford the title compound in a mixture of anomers (1:1 $\alpha:\beta$) as a clear foam (170 mg, 0.314 mmol, 55%).

HRMS-ESI Calculated for [C₃₄H₃₆O₆ + Na⁺]: 563.2404, found: 563.2412, **¹H NMR** (400 MHz, CHLOROFORM-D) δ 3.37 (ddd, J = 9.6, 4.6, 2.7 Hz, 1H, β CH-5), 3.46 – 3.57 (m, 2H, β CH-2, α CH-2), 3.58 (t, J = 9.2 Hz, 1H, α CH-4), 3.60 (t, J = 9.3 Hz, 1H, β CH-4), 3.65 – 3.79 (m, 5H, α CH-5, CH-6 x 2, β CH-3, CH-6), 3.84 – 3.91 (m, 1H, β CH-6'), 4.09 (t, J = 9.4 Hz, 1H, α CH-3), 4.53 (d, J = 4.5 Hz, 1H, CH₂ OBn), 4.55 – 4.60 (m, 2H, β CH-1, CH₂ OBn), 4.62 – 4.69 (m, 4H, CH₂ OBn), 4.70 (d, J = 4.6 Hz, 2H, CH₂ OBn), 4.74 (d, J = 10.9 Hz, 1H, CH₂ OBn), 4.81 (d, J = 3.8 Hz, 1H, CH-1), 4.83 (d, J = 5.8 Hz, 2H, CH₂ OBn), 4.85 (d, J = 4.7 Hz, 2H, CH₂ OBn), 4.88 (d, J = 5.0 Hz, 2H, CH₂ OBn), 4.91 (d, J = 1.9 Hz, 1H, CH₂ OBn), 4.94 (d, J = 6.0 Hz, 2H, CH₂ OBn), 4.97 (d, J = 6.0 Hz, 1H, CH₂ OBn), 5.02 (d, J = 10.9 Hz, 2H, CH₂ OBn), 7.21 – 7.42 (m, 40H, CH arom.). **¹³C NMR** (101 MHz, CHLOROFORM-D) δ 61.69 (β CH-6), 61.96 (α CH-6), 69.21 (CH₂ OBn), 71.08 (α CH-5), 71.63 (β CH-5), 73.06, 75.00, 75.07, 75.11, 75.15, 75.73 (CH₂ OBn), 77.43 (α CH-4), 77.54 (β CH-4), 80.05 (α CH-2), 81.96 (α CH-3), 82.35 (β CH-2), 84.54 (β CH-3), 95.55 (α CH-1), 102.83 (β CH-1), 137.10, 137.29, 138.01, 138.17, 138.32, 138.54, 138.84 (CH arom.). IR (Vmax, film) 3454, 3088, 3063, 3030, 2918, 2873, 1734, 1601, 1585, 1496, 1453, 1361, 1210, 1068, 1027, 735, 697 cm^{-1}

Data in accordance with literature values²⁹¹



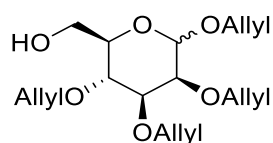
1,2,3,4-tetra-O-benzoyl- α,β -D-glucose

To a stirring solution of 1,2,3,4-tetra-O-benzoyl-6-O-trityl- α,β -D-glucose (500 mg, 0.583 mmol, 1.00 equiv.) in AcOH (1.4 mL) with 10 drops of DCM at 10°C, was added HBr (33% in acetic acid, 0.12 mL, 0.69 mmol, 1.2 equiv.) dropwise. The resulting solution was stirred for 30 seconds before the reaction mixture was filtered and rinsed with AcOH into a separating funnel containing DCM (10 mL) and H₂O (10 mL). The aqueous layer was further extracted with DCM (3 x 10 mL) and the combined organic layers were washed with sat. saturated NaHCO₃, dried over MgSO₄, filtered, and concentrated *in vacuo*. The resulting crude product was purified by automated flash column chromatography (0 to 35% EtOAc in hexane) to afford the title compound in a mixture of anomers, (2:1 $\alpha:\beta$) as a clear foam (212 mg, 0.357 mmol, 62%).

HRMS-ESI Calculated for [C₃₄H₂₈O₁₀ + Na⁺]: 619.1575, found: 619.1586, **¹H NMR** (400 MHz, CHLOROFORM-D) δ 3.74 (ddd, J = 13.0, 5.8, 3.9 Hz, 2H, $\alpha+\beta$ CH-6), 3.89 (ddd, J = 27.8, 13.0, 2.2 Hz, 2H, $\alpha+\beta$ CH-6'), 4.02 (ddd, J =

9.9, 3.9, 2.2 Hz, 1H, β CH-5), 4.26 (ddd, $J = 10.3, 3.7, 2.2$ Hz, 1H, α CH-5), 5.57 – 5.78 (m, 4H, α CH-2, CH-3, β CH-3), 5.85 (dd, $J = 10.0, 8.2$ Hz, 1H, β CH-2), 6.09 (t, $J = 9.6$ Hz, 1H, β CH-4), 6.25 (d, $J = 8.2$ Hz, 1H, β CH-1), 6.36 (t, $J = 10.1$ Hz, 1H, α CH-4), 6.85 (d, $J = 3.7$ Hz, 1H, α CH-1), 7.32 (ddt, $J = 12.2, 6.0, 1.9$ Hz, 8H, CH arom.), 7.37 – 7.51 (m, 10H, CH arom.), 7.51 – 7.61 (m, 6H, CH arom.), 7.61 – 7.72 (m, 4H, CH arom.), 7.80-9.1 (m, 4H, CH arom.), 7.95 – 8.08 (m, 6H, CH arom.), 8.11 – 8.21 (m, 2H, CH arom) $^{13}\text{C NMR}$ (101 MHz, CHLOROFORM-*D*) δ 60.50 (CH-6 α), 60.93 (CH-6 β), 68.93 (α CH-2), 69.18 (β CH-3), 70.24 (α CH-4), 70.53 (α CH-3), 70.91 (β CH-2), 72.71 (β CH-4), 72.86 (α CH-5), 75.67 (β CH-5), 90.19 (CH-1 α), 92.85 (CH-1 β), 128.47, 128.51, 128.65, 128.81, 128.88, 128.92, 129.04, 129.81, 129.86, 129.91, 130.10, 130.13, 130.29, 133.50, 133.53, 133.59, 133.92, 133.97, 134.03 (CH arom.), 164.60, 164.88, 165.19, 165.42, 165.81, 166.03, 166.24 (C=O) IR (Vmax, film) 3509, 3066, 2958, 1728, 1601, 1451, 1257, 1090, 1068, 1023, 707, 686, 641 cm^{-1}

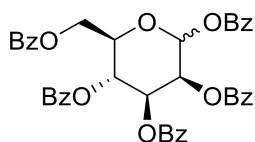
Data in accordance with literature values²⁹²



1,2,3,4-tetra-O-allyl- α,β -D-glucose

To a stirring solution of 1,2,3,4-tetra-O-allyl-6-O-trityl- α,β -D-glucose (163 mg, 0.281 mmol, 1.00 equiv.) in AcOH (0.65 mL) at 10°C, was added HBr (33% in acetic acid, 60 μL , 0.31 mmol, 1.2 equiv.) dropwise. The resulting solution was stirred for 30 seconds before the reaction mixture was filtered and rinsed with AcOH into a separating funnel containing DCM (10 mL) and H₂O (10 mL). The aqueous layer was further extracted with DCM (3 x 10 mL) and the combined organic layers were washed with sat. aqueous NaHCO₃ solution, dried over MgSO₄, filtered and concentrated *in vacuo*. The resulting crude product was purified by automated flash column chromatography (0 to 100% EtOAc in hexane) to afford the title compound in a mixture of anomers (1:1 $\alpha:\beta$) as a clear foam (54 mg, 0.16 mmol, 60%)

HRMS-ESI Calculated for [C₁₈H₂₈O₆ + Na⁺]: 363.1778, found: 363.1781, $^1\text{H NMR}$ (400 MHz, CHLOROFORM-*D*) δ 3.19 (t, $J = 8.3$ Hz, 1H, β CH-3), 3.25 (ddd, $J = 9.4, 4.5, 2.8$ Hz, 1H, β CH-5), 3.29 – 3.45 (m, 4H, α CH-5, CH-3, β CH-4, CH-2), 3.63 (dt, $J = 10.0, 3.6$ Hz, 1H, α CH-2), 3.69 (dd, $J = 11.8, 4.6$ Hz, 1H, β CH-6), 3.69 (dd, $J = 12.8, 4.6$ Hz, 1H, α CH-6), 3.79 (dd, $J = 12.8, 3.1$ Hz, 1H, α CH-6'), 3.84 (dd, $J = 11.8, 2.7$ Hz, 1H, β CH-6'), 3.97 – 4.45 (m, 16H, OCH₂ OAllyl), 4.89 (d, $J = 3.6$ Hz, 1H, α CH-1), 5.07 – 5.30 (m, 16H, CH=CH₂ OAllyl), 5.31 – 5.34 (m, 2H, β CH-1), 5.82 – 6.03 (m, 8H, CH=CH₂ OAllyl) $^{13}\text{C NMR}$ (101 MHz, CHLOROFORM-*D*) δ 61.90 (α CH-6), 62.09 (β CH-6), 68.22 (α CH-5), 70.60 (β CH-5), 70.90, 72.43, 73.81, 73.92, 74.00, 74.37, 74.53 (O-CH₂), 75.02 (β CH-4), 77.33 (α CH-4), 79.54 (α CH-2), 81.44 (α CH-3), 81.69 (β CH-2), 84.06 (CH-3), 95.78 (α CH-1), 102.70 (β CH-1), 116.59, 116.87, 117.06, 117.29, 117.35, 117.40, 118.25 (CH=CH₂ OAllyl), 133.80, 133.99, 134.74, 134.88, 134.94, 135.09, 135.25, 135.39 (CH=CH₂). IR (Vmax, film) 3408, 3084, 2821, 2867, 1462, 1347, 1268, 1074, 1044, 990, 923, 735 cm^{-1}

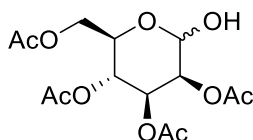


1,2,3,4,6-penta-O-benzoyl- α -D-glucose

To a stirring solution of D-glucose (250 mg, 1.39 mmol, 1.00 equiv.) in dry pyridine (5 mL) at 0°C was added BzCl (1.3 mL, 11 mmol, 7.9 equiv.) and DMAP (cat.). The reaction was allowed to warm to RT and left stirring for 18 h before the reaction was quenched by the addition of MeOH (2 mL). The solvents were removed *in vacuo* followed by co-evaporation with toluene (3 x 2 mL). The resulting residue was dissolved in DCM (60 mL) and washed consecutively with 1M HCl (30 mL), sat. aqueous NaHCO₃ solution (30 mL) and brine (30 mL). The organic layer was dried over MgSO₄ filtered and concentrated *in vacuo*. The resulting crude product was purified by automated flash column chromatography (gradient 0 to 30%) to afford the title compound as a waxy white solid (630 mg, 0.90 mmol, 65%).

HRMS-ESI Calculated for $[C_{41}H_{32}O_{11} + Na^+]$: 723.1837, found: 723.1852, 1H NMR (400 MHz, CHLOROFORM-*D*) δ 4.50 (ddd, $J = 13.1, 5.3, 2.3$ Hz, 1H, *CH*-6), 4.57 – 4.74 (m, 2H, *CH*-5, *CH*-6'), 5.70 (dd, $J = 10.1, 3.6$ Hz, 1H, *CH*-2), 5.89 (td, $J = 9.8, 2.8$ Hz, 1H, *CH*-4), 6.34 (td, $J = 10.1, 2.8$ Hz, 1H, *CH*-3), 6.87 (d, $J = 3.6$ Hz, 1H, *CH*-1), 7.20 – 7.60 (m, 16H, *CH* arom.), 7.60 – 7.74 (m, 1H, *CH* arom.), 7.81 – 8.01 (m, 6H, *CH* arom.), 8.04 (dq, $J = 8.4, 1.6$ Hz, 2H), 8.08 – 8.26 (m, 2H, *CH* arom.) ^{13}C NMR (101 MHz, CHLOROFORM-*D*) δ 62.21 (*CH*-6), 68.56 (*CH*-4), 70.18 (*CH*-5), 70.24 (*CH*-2), 89.79 (*CH*-1), 128.18, 128.22, 128.24, 128.30, 128.44, 128.57, 128.60, 128.72, 129.28, 129.53, 129.57, 129.63, 129.67, 129.82, 132.95, 133.17, 133.31, 133.35, 133.74, (*CH* arom.) 164.20, 164.91, 165.15, 165.69, 165.88 (C=O). IR (Vmax, film) 3069, 3030, 2961, 1724, 1601, 1451, 1315, 1254, 1176, 1020, 1067, 1091 cm^{-1}

Data in accordance with literature values²⁹³

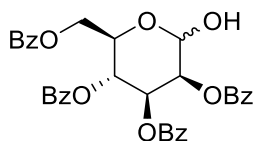


2,3,4,6-tetra-*O*-acetyl- α,β -D-glucose

To a stirring solution of 1,2,3,4,5-tetra-*O*-acetyl- α -D-glucose (Purchased from Sigma, 410 mg, 1.11 mmol, 1.00 equiv.) in THF (4 mL) was added $BnNH_2$ (0.22 mL, 2.1 mmol, 2.0 equiv.) at RT. After 18 h the reaction was quenched by the addition of 1 M HCl (25 mL). The resulting solution was extracted with DCM (50 mL), and the organic layer was further washed sequentially with sat. aqueous $NaHCO_3$ solution (25 mL) and brine (25 mL). The resulting organic layer was dried with $MgSO_4$, filtered, and the solvents were removed *in vacuo*. The resulting crude product was purified by automated flash column chromatography (gradient 0 to 100% EtOAc in hexane) to afford the title compound in a mixture of anomers (5:2 $\alpha:\beta$) as a clear oil (320 mg, 0.92 mmol 90%)

HRMS-ESI Calculated for $[C_{14}H_{20}O_{10} + Na^+]$: 371.0949, found: 371.0953 1H NMR (400 MHz, CHLOROFORM-*D*) δ 2.01 (s, 3H, OAc), 2.03 (s, 3H), 2.04 (s, 3H, OAc), 2.08 (s, 3H, OAc), 2.09 (s, 12H, OAc), 3.75 (ddd, $J = 10.1, 4.7, 2.3$ Hz, 1H, β *CH*-5), 4.05 – 4.19 (m, 2H, α *CH*-6, β *CH*-6), 4.19 – 4.33 (m, 3H, α *CH*-5, *CH*-6', β *CH*-6'), 4.73 (d, $J = 8.2$ Hz, 1H, β *CH*-1), 4.84 – 4.92 (m, 2H, α *CH*-2, β *CH*-2), 5.08 (td, $J = 9.8, 1.7$ Hz, 2H, α *CH*-4, β *CH*-4), 5.25 (t, $J = 9.6$ Hz, 1H, β *CH*-3), 5.46 (d, $J = 3.6$ Hz, 1H, α *CH*-1), 5.53 (t, $J = 9.8$ Hz, 1H, α *CH*-3) ^{13}C NMR (101 MHz, CHLOROFORM-*D*) δ 20.60, 20.64, 20.70, 20.73 20.76, (CH_3), 60.58 (β *CH*-6), 62.02 (α *CH*-6), 66.99 (α *CH*-5), 68.41 (β *CH*-4), 68.53 (α *CH*-4), 69.94 (α *CH*-2) 71.18 (α *CH*-3) 71.93 (β *CH*-5), 72.45 (β *CH*-3), 72.99 (β *CH*-2), 90.00 (α *CH*-1), 95.36 (β *CH*-1), 169.66, 169.82, 170.35, 170.38, 170.61, 170.99, 171.09. (C=O) IR (Vmax, film) 3468, 2961, 1747, 1443, 1369, 1227, 1153, 1038 cm^{-1}

Data is in accordance with literature values²⁹⁴

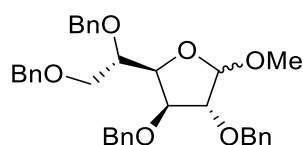


2,3,4,6-tetra-*O*-benzoyl- α,β -D-glucose

To a stirring solution of 2,3,4,6-tetra-*O*-benzoyl- α,β -D-glucose (470 mg, 0.671 mmol, 1.00 equiv.) in THF (4 mL) was added $BnNH_2$ (0.24 mL, 2.1 mmol, 2.7 equiv.) at RT. After 72 h the reaction was quenched by the addition of 1 M HCl (25 mL). The resulting solution was extracted with DCM (50 mL), and the organic layer was further washed with sat. aqueous $NaHCO_3$ solution (25 mL) and brine (25 mL). The resulting organic layer was dried with $MgSO_4$, filtered and the solvents were removed *in vacuo*. The resulting crude product was purified by automated flash column chromatography (gradient 0 to 40% EtOAc in hexane) to afford the title compound in a mixture of anomers (4:1 $\alpha:\beta$) as a white foam (310 mg, 0.52 mmol, 77%)

HRMS-ESI Calculated for $[C_{34}H_{28}O_{10} + Na^+]$: 619.1575, found: 619.1583, **1H NMR** (400 MHz, CHLOROFORM-*D*) δ 4.22 (ddd, $J = 10.0, 4.2, 3.0$ Hz, 1H, β CH-5), 4.47 (dd, $J = 12.3, 4.2$ Hz, 1H, β CH-6), 4.49 (ddd, $J = 19.7, 12.3, 4.5$ Hz, 1H, α CH-6), 4.52 (dd, $J = 12.3, 4.9$ Hz, 1H, β CH-6'), 4.59 – 4.83 (m, 2H, α CH-5, CH-6'), 5.16 (d, $J = 7.7$ Hz, 1H, β CH-1), 5.37 (dd, $J = 10.0, 3.5$ Hz, 1H, α CH-2), 5.49 (ddd, $J = 10.0, 7.7, 2.3$ Hz, 1H, β CH-2), 5.69 – 5.87 (m, 3H, α CH-1, α CH-4, β CH-4), 6.00 (t, $J = 10.0$ Hz, 1H, β CH-3), 6.34 (t, $J = 10.1$ Hz, 1H, α CH-3), 7.24 – 7.66 (m, 24H, CH arom.), 7.77 – 8.19 (m, 16H, CH arom.). **^{13}C NMR** (101 MHz, CHLOROFORM-*D*) δ 63.00 (α CH-6), 63.13 (β CH-6), 67.52 (α CH-5), 67.97 (β CH-5), 69.59 (α CH-4), 70.36 (α CH-3), 72.33 (β CH-3), 72.43 (α CH-2), 72.62 (β CH-4), 73.92 (β CH-2), 90.40 (α CH-1), 95.98 (β CH-1), 127.04, 127.61, 127.91, 128.32, 128.40, 128.45, 128.61, 128.77, 128.94, 129.06, 129.20, 129.50, 129.66, 129.70, 129.74, 129.81, 129.87, 129.93, 131.67, 133.16, 133.20, 133.36, 133.43, 133.54, 134.16 (CH-arom.), 165.36, 165.91, 165.94, 166.33, 166.40 (C=O) **IR** (Vmax, film) 3437, 3081, 2961, 1726, 1456, 1269, 1095 cm^{-1}

Data in accordance with literature values²⁹⁵



Methyl-2,3,4,6-tetra-O-benzyl- α,β -D-glucofuranose

To a stirring solution of D-glucose (500 mg, 2.78 mmol, 1.00 equiv.) in MeOH (13 mL) was added AcCl (0.45 mL, 6.3 mmol, 2.3 equiv.) dropwise. After 6 h at RT, the reaction was quenched by the addition of NEt_3 (1.2 mL) and the solvents were removed *in vacuo*. The residue was dissolved in DMF (13 mL) and NaH (60% in mineral oil, 900 mg, 22.6 mmol, 8.13 equiv.) was added at 0°C. After 10 mins at 0°C, BnBr (2.6 mL, 22 mmol, 7.9 equiv.) was added dropwise followed by the addition of TBAI (cat.). The resulting suspension was allowed to warm to RT and left stirring for 16 h before the reaction was quenched by the addition of MeOH (5 mL). The solvents were removed *in vacuo* and the resulting residue dissolved in DCM (100 mL) and washed consecutively with sat. aqueous NH_4Cl solution (50 mL), H_2O (50 mL), and brine (50 mL). The resulting organic layer was dried over $MgSO_4$, filtered, and concentrated *in vacuo*. The resulting crude product was purified by automated flash column chromatography (gradient 0 to 25% EtOAc in hexane) to afford the title compound in a mixture of anomers (2:3 $\alpha:\beta$) as a clear oil (841 mg, 1.52 mmol 54%)

β -anomer

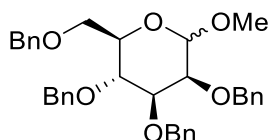
HRMS-ESI Calculated for $[C_{34}H_{36}O_6 + Na^+]$: 577.2561, found: 577.2576. **1H NMR** (400 MHz, CHLOROFORM-*D*) δ 3.37 (s, 3H, OMe), 3.72 (dd, $J = 10.8, 5.5$ Hz, 1H, CH-6), 3.90 (dd, $J = 10.8, 1.9$ Hz, 1H, CH-6'), 3.92 – 3.94 (m, 1H, CH-4), 4.08 (dd, $J = 4.7, 1.1$ Hz, 2H, CH-2), 4.10 (dd, $J = 5.5, 1.9$ Hz, 1H, CH-5), 4.35 (dd, $J = 9.2, 4.7$ Hz, 1H, CH-3), 4.43 (s, 2H, CH OBn), 4.52 (d, $J = 11.4$ Hz, 1H, CH OBn), 4.52 (s, 2H, CH OBn), 4.60 (s, 2H, CH OBn), 4.78 (d, $J = 11.4$ Hz, 1H, CH OBn), 4.90 (d, $J = 1.1$ Hz, 1H, CH-1), 7.12 – 7.50 (m, 20H, CH arom.). **^{13}C NMR** (101 MHz, CHLOROFORM-*D*) δ 56.07 (CH₃), 70.85 (CH-6), 71.86, 72.25, 72.49, 73.46 (CH OBn), 76.66 (CH-5), 80.25 (CH-4), 80.61 (CH-2), 85.81 (CH-3), 108.75 (CH-1), 127.46, 127.50, 127.70, 127.74, 127.83, 127.90, 127.96, 128.00, 128.10, 128.23, 128.34, 128.38, 128.46, 128.56, 137.63, 137.96, 138.77, 139.01 (CH arom.) **IR** (Vmax, film) 3092, 3065, 3029, 2909, 2867, 1496, 1453, 1099, 1056, 1027, 995, 735, 697 cm^{-1} $[\alpha]_D^{20} = -28.4$ c = 1.25, DCM)

α -anomer

1H NMR (400 MHz, CHLOROFORM-*D*) δ 3.73 (dd, $J = 10.6, 6.2$ Hz, 1H, CH-6), 3.89 (dd, $J = 10.6, 2.4$ Hz, 1H, CH-6'), 4.00 (app. t, $J = 4.1$ Hz, 1H, CH-4), 4.04 (ddd, $J = 6.2, 2.4, 1.3$ Hz, 1H, CH-5), 4.28 (dd, $J = 5.9, 3.9$ Hz, 1H, CH-2), 4.39 (dd, $J = 7.3, 5.9$ Hz, 1H, CH-3), 4.48 – 4.61 (m, 6H, CH OBn), 4.68 (d, $J = 12.0$ Hz, 1H, CH OBn), 4.82 (d, $J = 11.7$ Hz, 1H, CH OBn) 4.91 (d, $J = 3.9$ Hz, 1H, CH-1), 7.16 – 7.47 (m, 20H, CH arom.) **^{13}C NMR** (101 MHz, CHLOROFORM-*D*) δ 55.61 (CH₃), 71.45 (CH-6), 72.31, 72.63, 72.72, 73.45 (CH OBn), 76.78, 76.92 (CH-5 and CH-

4), 82.16 (CH-2), 83.72 (CH-3), 101.62 (CH-1), 127.44, 127.50, 127.62, 127.68, 127.73, 128.04, 128.22, 128.33, 128.40, 128.44, 128.55, 137.81, 138.16, 138.78, 139.08 (CH arom.). $[\alpha]_D^{20} = 57.5$ ($c = 0.765$, DCM))

Data in accordance with literature values²⁹⁶



Methyl-2,3,4,6-tetra-O-benzyl- α,β -D-glucose

To a stirring solution of D-glucose (500 mg, 2.78 mmol, 1.00 equiv.) in MeOH (13 mL) was added AcCl (0.45 mL, 6.3 mmol, 2.3 equiv.) dropwise. The resulting solution was heated to 60°C for 18 h before the reaction was quenched with the addition of NEt₃ (1.2 mL) and the solvents were removed *in vacuo*. The residue was dissolved in DMF (13 mL) and NaH (60% in mineral oil, 900 mg, 22.6 mmol, 8.13 equiv.) was added at 0°C. After 10 mins at 0°C, BnBr (2.6 mL, 22 mmol, 7.9 equiv.) was added dropwise followed by TBAI (cat.). The resulting suspension was allowed to warm to RT and react for 16 h before the reaction was quenched by the addition of MeOH (5 mL). The solvents were removed *in vacuo* and the resulting residue dissolved in DCM (100 mL) and washed successively with sat. NH₄Cl (50 mL), H₂O (50 mL), and brine (50 mL). The resulting organic layer was dried with MgSO₄, filtered and concentrated *in vacuo*. The resulting crude product was purified by automated flash column chromatography (gradient 0 to 25% EtOAc in hexane) to afford the title compound in a mixture of anomers (2:1 $\alpha:\beta$) as a white foam (1.4 g, 2.6 mmol 94%).

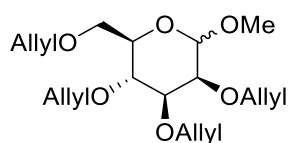
α -anomer

HRMS-ESI Calculated for [C₃₅H₃₈O₆ + Na⁺]: 577.2561, found: 577.2570. **¹H NMR** (400 MHz, CHLOROFORM-D) δ 3.43 (s, 3H, CH₃), 3.57 – 3.86 (m, 3H, CH-4, CH-5, CH-6), 3.99 – 4.10 (m, 1H, CH-6), 4.48 – 4.57 (m, 2H, CH-2, CH-3), 4.62 – 4.77 (m, 3H, CH₂ OBn), 4.80 – 4.97 (m, 3H, CH-1, CH₂ OBn), 5.02 (d, $J = 10.8$ Hz, 1H, CH₂ OBn), 5.06 (d, $J = 10.8$ Hz, 1H, CH₂ OBn), 7.19 – 7.24 (m, 2H), 7.28–7.45 (m, 18H, CH arom.). **¹³C NMR** (101 MHz, CHLOROFORM-D) δ 55.21 (CH₃), 68.48 (CH-6), 70.08 (CH-5), 73.43, 73.51, 75.08, 75.81 (CH OBn), 77.68 (CH-4), 79.86 (CH-2), 82.17 (CH-3), 98.25 (CH-1), 126.96, 127.58, 127.65, 127.73, 127.91, 127.97, 128.03, 128.20, 128.41, 128.45, 128.50, 137.95, 138.21, 138.30, 138.84 (CH arom.) **IR** (Vmax, film) 3090, 3064, 3030, 2906, 1496, 1453, 1360, 1070, 1046, 1028, cm⁻¹ $[\alpha]_D^{20} = 64.3$ ($c = 2.10$, DCM)

β -anomer

¹H NMR (400 MHz, CHLOROFORM-D) δ 3.47 – 3.56 (m, 2H, CH-4, CH-5), 3.64 (s, 3H, CH₃ OMe), 3.65 – 3.75 (m, 3H, CH-2, CH-3, CH-6), 3.81 (dd, $J = 10.8, 1.8$ Hz, 1H, CH-6'), 4.38 (d, $J = 7.7$ Hz, 1H, CH-1), 4.59 (d, $J = 11.3$ Hz, 1H, CH₂ OBn), 4.62 (d, $J = 11.4$ Hz, 1H, CH₂ OBn), 4.68 (d, $J = 11.9$ Hz, 1H, CH₂ OBn), 4.77 (d, $J = 11.0$ Hz, 1H, CH₂ OBn), 4.85 (d, $J = 11.0$ Hz, 1H, CH₂ OBn), 4.88 (d, $J = 11.0$ Hz, 1H, CH₂ OBn), 4.99 (d, $J = 11.0$ Hz, 2H, CH₂ OBn), 7.19 – 7.24 (m, 2H, CH arom.), 7.27 – 7.44 (m, 18H, CH arom.). **¹³C NMR** (101 MHz, CHLOROFORM-D) δ 57.22 (CH₃), 68.98 (CH-6), 73.57 (CH-5), 74.85, 74.92, 75.12, 75.78, (CH₂ OBn), 77.95 (CH-4), 82.41 (CH-2), 84.73 (CH-3), 104.79 (CH-1), 127.70, 127.74, 127.87, 127.98, 128.07, 128.21, 128.46, 128.49, 138.18, 138.26, 138.61, 138.69. (CH arom.). $[\alpha]_D^{20} = -1.74$ ($c = 1.18$, DCM)

Data in accordance with literature values^{297, 298}



Methyl-2,3,4,6-tetra-O-allyl- α,β -D-glucose

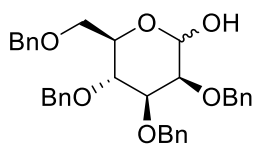
To a stirring solution of D-glucose (500 mg, 2.78 mmol, 1.00 equiv.) in MeOH (13 mL) was added AcCl (0.45 mL, 6.3 mmol, 2.7 equiv.) dropwise. The resulting solution was heated to 60°C for 18 h before the reaction was quenched by the addition of NEt₃ (1.2 mL) and the solvents were removed *in vacuo*. The residue was dissolved in DMF (13 mL) and NaH (60% in mineral oil, 900 mg, 22.6 mmol, 8.13 equiv.) was added at 0°C. After 10 mins at 0°C, AllylBr (1.9 mL, 22 mmol, 8.1 equiv.) was added dropwise followed by TBAI (cat.). The resulting suspension was allowed to warm to RT and after 16 h quenched by the addition of MeOH (5 mL). The solvents were removed *in vacuo* and the resulting residue dissolved in DCM (100 mL) and washed successively with sat. aqueous NH₄Cl solution (50 mL), H₂O (50 mL), and brine (50 mL). The resulting organic layer was dried over MgSO₄, filtered and concentrated *in vacuo*. The resulting crude product was obtained by automated flash column chromatography (gradient 0 to 25% EtOAc in hexane) to afford the title compound as a mixture of anomers (2:1 $\alpha:\beta$) as a clear oil (440 mg, 1.24 mmol 45%)

α -anomer

HRMS-ESI Calculated for [C₁₉H₃₀O₆ + Na⁺]: 377.1935, found: 377.1935. **¹H NMR** (400 MHz, CHLOROFORM-*D*) δ 3.28 – 3.41 (m, 5H, OCH₃, CH-2, CH-4), 3.53 – 3.76 (m, 4H, CH-3, CH-5, CH-6 x 2), 3.84 – 4.45 (m, 8H, OCH₂ OAllyl), 4.71 (d, *J* = 3.6 Hz, 1H, CH-1), 5.04 – 5.28 (m, 8H, CH₂=CH OAllyl), 5.78 – 5.98 (m, 4H, CH=CH₂ OAllyl). **¹³C NMR** (101 MHz, CHLOROFORM-*D*) δ 55.08 (CH₃), 68.49 (CH-6), 69.98 (CH-5), 72.48, 72.61, 73.88, 74.29 (OCH₂ OAllyl), 77.35 (CH-4), 79.39 (CH-2), 81.49 (CH-3), 98.29 (CH-1), 116.51, 116.53, 116.77, 116.80, 117.30, 117.68 (CH=CH₂ OAllyl), 134.59, 134.88, 134.98, 135.39 (CH=CH₂ OAllyl). **IR** (Vmax, film) 3075, 3016, 2994, 2917, 2864, 1648, 1460, 1156, 1047, 1000, 922 cm⁻¹ [α]_D²⁰ = 76.1 (*c* = 1.38, DCM)

β -anomer

¹H NMR (400 MHz, CHLOROFORM-*D*) δ 3.10 – 3.18 (m, 1H, CH-5), 3.25 – 3.41 (m, 3H, CH-2, CH-3, CH-4), 3.48 (s, 3H, OCH₃), 3.58 (dd, *J* = 10.8, 4.3 Hz, 1H, CH-6), 3.67 (dd, *J* = 10.8, 1.3 Hz, 1H, CH-6'), 3.94 – 4.16 (m, 4H, OCH₂ OAllyl), 4.14 (d, *J* = 7.8 Hz, 1H, CH-1), 4.18 – 4.40 (m, 4H, OCH₂ OAllyl), 5.06 – 5.29 (m, 8H, CH=CH₂ OAllyl), 5.78 – 6.02 (m, 4H, CH=CH₂ OAllyl) **¹³C NMR** (101 MHz, CHLOROFORM-*D*) δ 57.03 (CH₃), 68.91 (CH-6), 72.49 (CH-5), 73.56, 73.82, 74.42, 74.80 (OCH₂ OAllyl), 77.51 (CH-4), 81.63 (CH-2), 84.18 (CH-3), 104.47 (CH-1), 116.66, 116.81, 116.95, 116.98, (CH=CH₂ OAllyl) 134.76, 134.87, 135.18, 135.28 (CH=CH₂ OAllyl) [α]_D²⁰ = +8.79 (*c* = 1.79, DCM)

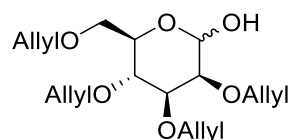


2,3,4,6-tetra-O-benzyl- α,β -D-glucose

To a stirring solution of methyl-2,3,4,6-tetra-O-benzyl- α,β -D-glucose (640 mg, 1.2 mmol, 1.0 equiv.) in AcOH (13 mL) was added 1M H₂SO₄ (1.6 mL). The resulting solution was heated to 100°C for 2.5 h before the reaction was cooled to RT and the pH was adjusted to pH 4 with the addition of 1 M NaOH. The quenched reaction mixture was then diluted with DCM (50 mL) and washed with sat. aqueous NaHCO₃ solution (50 ml). The aqueous layer was further extracted with DCM (3 x 25 mL) and the combined organic layers dried over MgSO₄, filtered and concentrated *in vacuo*. The resulting crude product was purified by automated flash column chromatography (gradient 0 to 35% EtOAc in hexane) to afford the title compound in a mixture of anomers (2:1 $\alpha:\beta$) as a white solid (310 mg, 0.574 mmol, 50%)

HRMS-ESI Calculated for $[C_{34}H_{36}O_6 + Na^+]$: 563.2404, found: 563.2408 **1H NMR** (400 MHz, CHLOROFORM-*D*) δ 3.40 (dd, $J = 9.0, 7.6$ Hz, 1H, β CH-2), 3.49 – 3.67 (m, 8H, α CH-2 CH-3, CH-6, β CH-6 CH-3, CH-4, CH-5, CH-6), 3.71 (dd, $J = 10.9, 3.5$ Hz, 1H, α CH-6), 3.96 (t, $J = 9.3$ Hz, 1H, α CH-4), 4.03 (ddd, $J = 10.1, 3.8, 2.1$ Hz, 1H, α CH-5), 4.44 – 5.01 (m, 17H, β CH-1, CH₂ OBn), 5.23 (d, $J = 3.6$ Hz, 1H, α CH-1), 7.08 – 7.18 (m, 6H, CH arom.), 7.27 – 7.41 (m, 34H, CH arom.). **^{13}C NMR** (101 MHz, CHLOROFORM-*D*) δ 68.64 (α CH-6), 68.99 (β CH-6) 70.45 (α CH-4), 73.40, 73.61, 73.66, 74.86, 74.92 (β CH-4), 75.11, 75.82 (CH₂ OBn), 77.73 (α CH-3), 77.88 (β CH-3), 80.09 (α CH-2), 81.84 (α CH-5), 83.22 (β CH-2), 84.66 (β CH-5) 91.45 (α CH-1), 97.60 (β CH-1) 127.74, 127.80, 127.90, 127.97, 128.03, 128.06, 128.11, 128.16, 128.27, 128.47, 128.51, 128.62, 137.92, 137.96, 138.29, 138.60, 138.76 (CH arom.). **IR** (Vmax, film) 3365, 2928, 2861, 1456, 1145, 1089 cm^{-1}

Data in accordance with literature values^{299, 300}

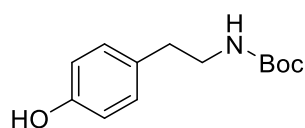


2,3,4,6-tetra-O-allyl- α,β -D-glucose

To a stirring solution of methyl-2,3,4,6-tetra-O-allyl- α,β -D-glucose (440 mg, 1.24 mmol, 1.00 equiv.) in AcOH (13 mL) was added 1M H₂SO₄ (1.5 mL). The resulting solution was heated to 100°C for 2.5 h before the reaction was cooled to RT and the pH was adjusted to pH 4 with the addition of 1M NaOH. The quenched reaction mixture was then diluted with DCM (50 mL) and washed with sat. aqueous NaHCO₃ solution (50 ml). The aqueous layer was further extracted with DCM (3 x 25 mL) and the combined organic layers were dried over MgSO₄, filtered and concentrated *in vacuo*. The resulting crude product was purified by automated flash column chromatography (gradient 0 to 35% EtOAc in hexane) to afford the title compound in a mixture of anomers. (4:1 $\alpha:\beta$) as a white solid (219 mg, 0.644 mmol, 57%)

HRMS-ESI Calculated for $[C_{18}H_{28}O_6 + Na^+]$: 363.1778 found: 363.1771, **1H NMR** (400 MHz, CHLOROFORM-*D*) δ 3.16 (dd, $J = 8.9, 7.7$ Hz, 1H, β CH-2), 3.30 – 3.46 (m, 5H, α CH-2, CH-4, β CH-4, CH-6 x 2), 3.56 – 3.62 (m, 1H, β CH-5), 3.62 – 3.65 (m, 2H, α CH-5, CH-6'), 3.65 – 3.67 (m, 1H, β CH-3), 3.70 (t, $J = 9.4$ Hz, 1H, α CH-3), 3.93 – 4.44 (m, 16H, OCH₂ OAllyl), 4.62 (d, $J = 7.7$ Hz, 1H, β CH-1), 5.11 – 5.34 (m, 17H, CH-CH₂, OAllyl, α CH-1), 5.81 – 6.07 (m, 8H, CH=CH₂ OAllyl). **^{13}C NMR** (101 MHz, CHLOROFORM-*D*) δ (α) 68.65 (CH-6), 70.34 (CH-4) 72.48, 72.58, 73.93, 74.40 (OCH₂ OAllyl), 79.64 (CH-2), 81.22 (CH-5), 91.54 (CH-1), 116.69, 117.59 (CH=CH₂ OAllyl), 134.58, 134.63, 134.98, 135.36 (CH=CH₂ OAllyl). **IR** (Vmax, film) 3432, 3054, 2931, 2873, 2244, 1736, 1651, 1462, 1422, 1351, 1265, 1071, 996, 907, 730, 704, 649 cm^{-1}

Phospho-Tyrosine



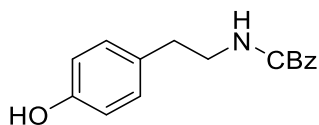
N-tert-butoxy carbonyl tyramine

To a stirring solution of tyramine (250 mg, 1.82 mmol, 1.00 equiv.) and NaHCO₃ (180 mg, 2.13 mmol, 1.17 equiv) in THF (7.5 mL) and H₂O (5 mL) was added a solution of *di-tert-butyl* dicarbonate (404 mg, 1.85 mmol, 1.02 equiv.) in THF (5 mL) dropwise. The resulting reaction mixture was left to stir at RT for 4 hours before diluting with EtOAc (75 mL). The resulting organic layer was washed consecutively with H₂O (50 mL) and brine (50 mL), dried over MgSO₄, filtered and concentrated *in vacuo*. The resulting crude product was purified by automated flash column chromatography (gradient 20% to 40% EtOAc in hexane) to afford the title compound as a clear oil (217 mg, 0.916 mmol, 50%)

HRMS-ESI Calculated for $[C_{13}H_{19}NO_3 + Na^+]$: 260.1257, found: 260.1261 **1H NMR** (400 MHz, CHLOROFORM-*D*) δ 1.44 (s, 9H, (CH₃)₃) 2.70 (t, $J = 7.1$ Hz, 2H, CH₂CH₂NH) 3.33 (dt, $J = 6.8$ Hz, 2H, CH₂NH) 4.62 (br s, 1H, NH) 6.17 (br s, 1H, OH) 6.78 (dt, $J = 8.4, 2.8, 2.2$ Hz, 2H, CH arom.) 7.01 (d, $J = 8.4$ Hz, 2H, CH arom.) **^{13}C NMR** (101 MHz,

CHLOROFORM-*D*) δ 28.54 ((CH₃)₃), 35.39 (CH₂CH₂NH), 42.18 (CH₂NH), 79.69 (C(CH₃)₃), 115.60, 129.96, 130.60, 154.78 (CH arom.), 156.32 (NHC=O).

Data in accordance with literature values³⁰¹

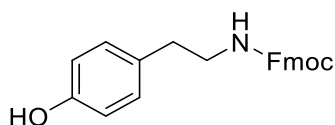


N-tert-butoxy carbonyl tyramine

To a stirring solution of tyramine (250 mg, 1.82 mmol, 1.00 equiv.) and NaHCO₃ (180 mg, 2.13 mmol, 1.17 equiv.) in THF (5 mL) and H₂O (10 mL) was added a solution of benzyl chloroformate (0.30 mL, 2.0 mmol, 1.1 equiv.) in THF (5 mL) dropwise. The resulting reaction mixture was left to stir at RT for 4 hours before dilution with EtOAc (75 mL). The resulting organic later was washed with consecutively H₂O (50 mL) and brine (50 mL), dried over MgSO₄, filtered and concentrated *in vacuo*. The resulting crude product was purified by automated flash column chromatography (gradient 20% to 40% EtOAc in hexane) to afford the title compound as a white sticky solid (280 mg, 1.20 mmol, 66%)

HRMS-ESI Calculated for [C₁₆H₁₇NO₃ + Na⁺]: 294.11001, found: 294.1100 **¹H NMR** (400 MHz, CHLOROFORM-*D*) δ 2.73 (t, *J* = 7.0 Hz, 2H, CH₂CH₂NH), 3.42 (dt, *J* = 6.7 Hz, 2H, CH₂NH), 4.81 (s, 1H, NH), 5.09 (s, 2H, CH₂ CBz), 5.84 (br s, 1H, OH) 6.70 – 6.80 (m, 2H, CH arom.), 7.02 (d, *J* = 8.1 Hz, 2H, CH arom.), 7.27 – 7.40 (m, 5H, CBz arom.). **¹³C NMR** (101 MHz, CHLOROFORM-*D*) δ 35.27 (CH₂CH₂NH), 42.55 (CH₂NH), 66.92 (COCH₂), 115.64, 128.17, 128.29, 128.68, 130.00, 136.54, 154.66 (CH arom.), 156.64 (C=O).

Data in accordance with literature values³⁰¹



N-Fmoc tyramine

To a stirring solution of tyramine (250 mg, 1.82 mmol, 1.00 equiv.) and NaHCO₃ (150 mg, 1.78 mmol, 0.981 equiv.) in THF (5 mL) and H₂O (10 mL) was added a solution of Fmoc chloride (980 mL, 1.8 mmol, 1.0 equiv.) in THF (5 mL) dropwise. The resulting reaction mixture was left to stir at RT for 4 hours before dilution with EtOAc (75 mL). The resulting organic later was washed consecutively with H₂O (50 mL) and brine (50 mL), dried over MgSO₄, filtered and concentrated *in vacuo*. The resulting crude product was purified by automated flash column chromatography (gradient 30% EtOAc in hexane) to afford the title compound as a white solid (200 mg, 0.55 mmol, 31%)

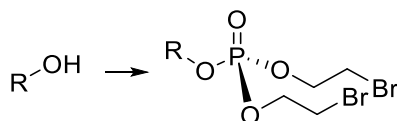
¹H NMR (400 MHz, Methanol-*d*₄) δ 2.64 (t, *J* = 7.3 Hz, 2H, CH₂CH₂NH), 3.24 (t, *J* = 7.3 Hz, 2H, CH₂CH₂NH), 4.15 (t, *J* = 6.8 Hz, 1H, CH Fmoc), 4.29 (d, *J* = 6.9 Hz, 2H, CH₂ Fmoc) 6.67 (d, *J* = 8.6 Hz, 1H, CH arom.), 6.98 (d, *J* = 8.6 Hz, 2H, CH arom), 7.29 (d, *J* = 7.5 Hz, 2H, CH arom. Fmoc), 7.36 (t, *J* = 7.5 Hz, 2H, CH arom. Fmoc), 7.77 (d, *J* = 7.5 Hz, 2H, CH arom. Fmoc). **¹³C NMR** (101 MHz, Methanol-*d*₄) δ 34.88 (CH₂CH₂NH), 43.68 (CH₂NH), 66.25 (CH₂ Fmoc), 114.86, 119.57, 124.86, 126.80, 127.42, 129.47, 144.01 (CH arom), 155.89 (C=O).

Data in accordance with literature values³⁰¹

SATE Compounds

General Procedures

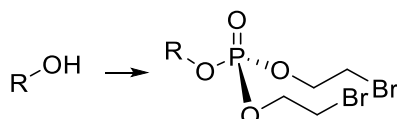
General Procedure 1 for 2-bromoethyl phosphate addition



To a stirring solution of *tri*-2-bromoethyl-phosphate **66** (1.0 equiv.) in DCM (5 mL/mmol) was added freshly distilled TiF_2O (1.5 equiv.). After stirring at RT for 10 mins dry pyridine (2.0 equiv.) was added. After a further 10 mins at RT, a solution of the starting alcohol (2.0 equiv.) in DCM (2.0 mL/mmol) was added*. The reaction was allowed to continue at RT for a further 1.5 h before the solvents were removed *in vacuo* and the residue dried onto silica and the crude product was purified by column chromatography with an appropriate solvent.

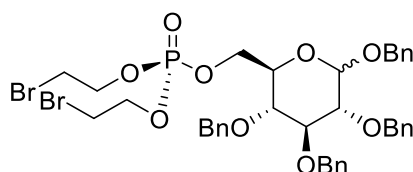
*note: where the starting alcohol was not soluble in DCM, the solution of activated phosphate was added to a flask of dried alcohol

General Procedure 2 for SATE phosphate substitution



To a stirring solution of the appropriate *di*-2-bromo-ethyl phosphate (1.0 equiv.) in dry pyridine (25 mL/mmol) was added KSAc (5.0 equiv.). The resultant solution was left stirring for 18 h at RT before the precipitated KBr salt was removed through filtration. The resulting crude solution was dried onto silica, and the crude product was purified by column chromatography with an appropriate solvent.

Glucose

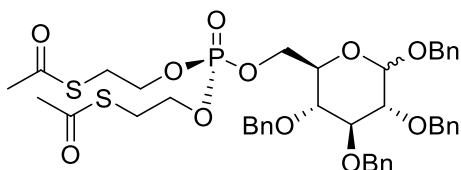


1,2,3,4-tetra-O-benzyl-6-bis(2-bromoethyl)phosphate- α,β -D-glucose

Following general procedure 1, the reaction was run with *tris*(2-bromoethyl)phosphate **65** on a 30 mg (72 μmol) scale on 1,2,3,4-tetra-O-benzyl- α,β -D-glucose. The crude product was purified by automated flash column chromatography (gradient 0 to 60% EtOAc in hexane) to afford the title compound in a mixture of anomers (2:3 $\alpha:\beta$) as a white solid (45 mg, 54 μmol , 62%).

HRMS-ESI Calculated for $[\text{C}_{38}\text{H}_{43}\text{Br}_2\text{O}_9\text{P} + \text{Na}^+]$: 855.0904, found: 855.0945 **$^1\text{H NMR}$** (400 MHz, CHLOROFORM-*D*) δ 3.42 – 3.63 (m, 9H, CH_2Br , α CH-2, CH-4, β CH-2, CH-4, CH-5), 3.68 (t, J = 8.9 Hz, 1H, β CH-3), 3.84 (ddt, J = 10.0, 4.0, 2.4 Hz, 1H, α CH-5), 4.08 (t, J = 9.2 Hz, 1H, α CH-3), 4.19 – 4.48 (m, 8H, $\text{CH}_2\text{CH}_2\text{SAC}$, α/β CH-6 x 2), 4.55 (d, J = 7.8 Hz, 1H, β CH-1), 4.81 (d, J = 3.8 Hz, 1H, α CH-1), 4.53 – 5.08 (m, 16H, CH_2 OBn), 7.27 – 7.51 (m, 40H CH arom.). **$^{13}\text{C NMR}$** (101 MHz, CHLOROFORM-*D*) δ 29.38, 29.48, 29.58, 29.67 (CH_2Br), 66.93 (d, J = 5.9 Hz, α CH-6), 67.03 (d, J = 5.9 Hz, β CH-6), 67.03 (d, J = 5.9 Hz, $\text{CH}_2\text{CH}_2\text{Br}$), 67.08 (d, J = 6.0 Hz, $\text{CH}_2\text{CH}_2\text{Br}$), 69.50 (α CH-5), 71.36, 73.21, 73.53, 73.60 (d, J = 7.8 Hz, α CH-5), 75.08, 75.23 (CH_2 OBn), 75.23 (d, J = 7.8 Hz, β CH-5), 75.86 (CH_2 OBn), 77.24 (α CH-4), 77.46 (β CH-4), 79.98 (α CH-2), 81.97 (α CH-3), 82.29 (β CH-2), 84.56 (β CH-3), 95.67 (α CH-1), 102.55 (β CH-1), 127.81, 127.85, 127.88, 128.00, 128.06, 128.09, 128.29, 128.52, 128.57, 128.62,

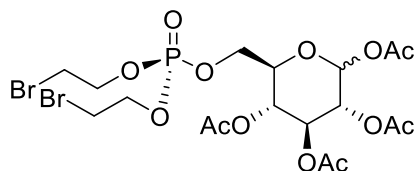
128.66, 137.28, 137.92, 138.07, 138.14, 138.34, 138.48 (CH arom.) ³¹P NMR (162 MHz, CHLOROFORM-D) δ -1.31, -1.19. IR (Vmax, film) 3031, 2885, 1421, 1453, 1360, 1273, 1012, 1067, 736, 698 cm⁻¹



1,2,3,4,-tetra-O-benzyl-6-bis(SATE)phosphate-α,β-D-glucose

Following general procedure 2, the reaction was run with 1,2,3,4-tetra-O-Benzyl-6-bis(2-bromoethyl)-phosphate-α,β-D-glucose on a 30 mg (40 μmol) scale. The crude product was purified by automated flash column chromatography (gradient 0 to 70% EtOAc in hexane) to afford the title compound in a mixture of anomers (3:2 α:β) as a yellow oil (30 mg, 40 μmol, quant.)

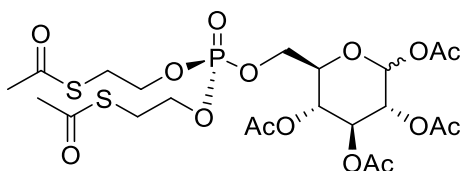
HRMS-ESI Calculated for [C₄₂H₄₉O₁₁PS₂ + Na⁺]: 847.2346, found: 847.2380 ¹H NMR (400 MHz, CHLOROFORM-D) δ 2.30 (s, 5H, CH₃ SAC), 2.31 (s, 5H, CH₃ SAC), 2.31 (s, 2H, CH₃ SAC), 3.15 (qd, J = 6.6, 3.3 Hz, 8H, CH₂SAC), 3.45 – 3.63 (m, 5H, α CH-2, CH-4, β CH-2, CH-4, CH-5), 3.67 (t, J = 8.9 Hz, 1H, β CH-3), 3.78 – 3.88 (m, 1H, α CH-5), 4.06 (d, J = 9.4 Hz, 1H, α CH-3), 4.09 – 4.20 (m, 8H, OCH₂CH₂SAC), 4.24 (tdd, J = 11.1, 7.9, 3.3 Hz, 2H, α/β CH-6), 4.38 (ddd, J = 11.1, 6.3, 1.8 Hz, 2H, α/β CH-6'), 4.54 (d, J = 5.5 Hz, 1H, β CH-1), 4.51 – 5.05 (m, 16H, CH₂OBn), 4.81 (d, J = 3.6 Hz, 1H, α CH-1), 7.27 – 7.44 (m, 40H, CH arom.). ¹³C NMR (101 MHz, CHLOROFORM-D) δ 29.26, 29.33 (CH₃), 30.64, (CH₂SAC) 66.14 (d, J = 1.9 Hz), 66.18 (d, J = 1.3 Hz) (CH₂CH₂SAC), 66.25 (d, J = 6.0 Hz, α CH-6), 66.66 (d, J = 4.4 Hz, β CH-6), 69.41 (CH OBn), 69.73 (α CH-5), 71.29, 73.15, 73.59 (CH₂ OBn), 73.66 (β CH-5), 75.06, 75.22, 75.31, 75.85 (CH₂ OBn), 77.26 (α CH-4), 77.37 (β CH-4), 80.04 (α CH-2), 81.97 (α CH-3), 82.30 (β CH-2), 84.58 (β CH-3), 95.57 (α CH-1), 102.50 (β CH-1), 127.70, 127.82, 127.85, 127.95, 127.99, 128.05, 128.08, 128.12, 128.29, 128.50, 128.54, 128.59, 128.65, 137.32, 137.93, 138.17, 138.37, 138.51 (CH arom.), 194.82 (C=O SAC). ³¹P NMR (162 MHz, CHLOROFORM-D) δ -1.08, -0.94. IR (Vmax, film) 3063, 3031, 2904, 1692, 1496, 1454, 1356, 1272, 1065, 1009, 735, 698, 622 cm⁻¹



1,2,3,4,-tetra-O-acetyl-6-bis-(2-bromoethyl)phosphate-α,β-D-glucose

Following general procedure 1, the reaction was run with tris(2-bromoethyl)phosphate 65 on a 30 mg (72 μmol) scale on 1,2,3,4-tetra-O-acetyl-α,β-D-glucose (3 equiv. instead of 2). The crude product was purified by automated flash column chromatography (gradient 0 to 60% EtOAc in hexane) to afford the title compound in a mixture of anomers (2:3 α:β) as a clear oil (25 mg, 35 μmol, 55%).

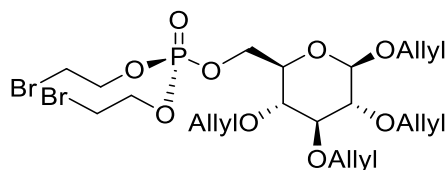
HRMS-ESI Calculated for [C₁₈H₂₇Br₂O₁₃P + Na⁺]: 662.9448, found: 662.9445 ¹H NMR (400 MHz, CHLOROFORM-D) δ 1.99 – 2.22 (m, 24H, CH₃ OAc), 3.56 (dt, J = 10.9, 6.8 Hz, 8H, CH₂Br), 3.73 (dt, J = 11.5, 5.8 Hz, 1H, α CH-5), 3.87 (ddd, J = 8.0, 4.6, 2.0 Hz, 1H, β CH-5), 4.10 – 4.20 (m, 3H, α CH-6, β CH-6 x 2) 4.22 (ddd, J = 11.5, 5.4, 2.3 Hz, 1H, α CH-6'), 4.27 – 4.41 (m, 8H, CH₂O), 4.47 – 4.56 (m, 1H, α CH-4), 5.05 – 5.18 (m, 3H, α CH-2, β α CH-2, CH-4), 5.27 (t, J = 10.6 Hz, 1H, β CH-3), 5.48 (t, J = 9.9 Hz, 1H, α CH-3), 5.72 (d, J = 8.3 Hz, 1H, β CH-1), 6.33 (d, J = 3.7 Hz, 1H, α CH-1). ¹³C NMR (101 MHz, CHLOROFORM-D) δ 20.43, 20.53, 20.55, 20.64, 20.88 (CH₃) 29.24, 29.34, 29.39, 29.47, 29.52, 29.59, 29.68 (CH₂Br) 65.34 (d J = 5.05, α CH-6) 65.47 (d, J = 5.75, β CH-6) 67.18 (d, J = 5.75, CH₂CH₂Br) 67.59 (α CH-4) 67.70 (β CH-4) 69.09 (α CH-2) 69.72 (α CH-3) 70.10 (β CH-2) 70.24 (α CH-5) 72.69 (β CH-3) 72.95 (d, J = 7.67, β CH-5) 88.90 (α CH-1) 91.61 (β CH-1) ³¹P NMR (162 MHz, CHLOROFORM-D) δ -1.75, -1.64. IR (Vmax, film) 2944, 2852, 1754, 1428, 1369, 1216, 1069, 1038, 1015, 942 cm⁻¹



1,2,3,4,-tetra-O-acetyl-6-bis(SATE)phosphate- α,β -D-glucose

Following general procedure 2, the reaction was run with 1,2,3,4-tetra-O-acetyl-6-bis(2-bromoethyl)-phosphate- α,β -D-glucose on a 9.6 mg (15 μ mol) scale. The crude product was purified by automated flash column chromatography (gradient 0 to 70% EtOAc in hexane) to afford the title compound in a mixture of anomers (1:1 $\alpha:\beta$) as a yellow oil (5.1 mg, 8.1 μ mol, 54%).

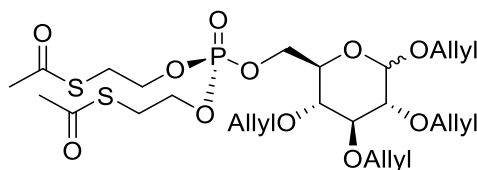
HRMS-ESI Calculated for [C₂₂H₃₃O₁₅PS₂ + Na⁺]: 655.0891, found: 655.0900 **¹H NMR** (400 MHz, CHLOROFORM-D) δ 1.97 – 2.23 (m, 24H, CH₃ OAc), 2.36 (s, 12H, CH₃ SAc), 3.18 (td, J = 6.5, 3.5 Hz, 8H, CH₂SAc), 3.71 (q, J = 4.9 Hz, 1H, α CH-5), 3.81 – 3.91 (m, 1H, β CH-5), 4.06 – 4.22 (m, 11H, CH₂CH₂SAc, α CH-6, β CH-6 x 2), 4.23 – 4.32 (m, 1H, α CH-6'), 5.05 – 5.19 (m, 3H, α CH-2, β α CH-2, CH-4), 5.26 (t, J = 9.5 Hz, 1H, β CH-3), 5.47 (t, J = 9.9 Hz, 1H, α CH-3), 5.72 (d, J = 8.4 Hz, 1H, β CH-1), 6.33 (d, J = 3.8 Hz, 1H, α CH-1). **¹³C NMR** (151 MHz, CHLOROFORM-D) δ 20.59, 20.70, 20.72, 20.76, 20.92, 21.02 (CH₃ OAc), 29.26, 29.85, 30.69 (CH₂OAc), 65.37 – 65.46 (m, CH-6 x 2), 66.46 – 66.35 (m, CH₂O x 2), 67.86 (α CH-4), 67.93 (β CH-4), 69.28 (α CH-2), 70.00 (α CH-3), 70.32 (β CH-2), 70.51 (α CH-5), 72.92 (β CH-3), 73.29 (β CH-5), 89.11 (α CH-1), 91.78 (β CH-1), 169.04, 169.35, 169.52, (C=O OAc) 170.25, 170.42 (C=O SAc). **³¹P NMR** (162 MHz, CHLOROFORM-D) δ -1.42, -1.35. **IR** (Vmax, film) 2964, 2923, 2848, 1754, 1693, 1429, 1368, 1247, 1213, 1016, 1133, 1017, 735, 713, 623, 546, 481 cm⁻¹



1,2,3,4,-tetra-O-allyl-6-bis(2-bromoethyl)phosphate- α,β -D-glucose

Following general procedure 1, the reaction was run with *tris*(2-bromoethyl)phosphate 65 on a 30 mg (72 μ mol) scale on 1,2,3,4-tetra-O-acetyl- α,β -D-glucose. The crude product was purified by automated flash column chromatography (gradient 0 to 60% EtOAc in hexane) to afford the title compound in a mixture of anomers (1:6 $\alpha:\beta$) as a white solid (14 mg, 22 μ mol, 31%).

HRMS-ESI Calculated for [C₂₂H₃₅Br₂O₉P + Na⁺]: 655.0278, found: 655.0301 **¹H NMR** (400 MHz, CHLOROFORM-D) δ 3.21 (dd, J = 9.1, 7.8 Hz, 1H, β CH-2), 3.27 – 3.45 (m, 4H, α CH-2, CH-4, β CH-3, CH-4), 3.46 – 3.60 (m, 8H, CH₂Br), 3.70 – 3.78 (m, 2H, α CH-3, CH-5), 4.04 – 4.28 (m, 8H, CH₂ OAllyl, α CH-6, β CH-6), 4.28 – 4.44 (m, 22H, α CH-6, β CH-1, CH-5, CH-6', OCH₂ OAllyl, CH₂CH₂Br), 5.13 – 5.22 (m, 4H, CH=CH₂ OAllyl), 5.22 – 5.36 (m, 4H, CH=CH₂ OAllyl), 5.78 – 6.03 (m, 8H, CH=CH₂ OAllyl). **¹³C NMR** (101 MHz, CHLOROFORM-D) (β) δ 29.43, 29.51 (CH₂Br), 66.97 (d, J = 5.9 Hz, CH₂CH₂Br), 67.03 (d, J = 5.9 Hz, CH₂CH₂Br) 67.12 (d, J = 5.9 Hz CH-6), 70.33 (CH-5), 73.47, 73.79, 73.94, 74.56 (OCH₂ OAllyl), 76.69 (CH-4), 81.57 (CH-2), 84.03 (CH-3), 102.47 (CH-1), 116.97, 117.12, 117.25, 117.53 (CH=CH₂ OAllyl), 133.90, 134.56, 135.04, 135.12 (CH=CH₂). **³¹P NMR** (162 MHz, CHLOROFORM-D) δ -2.47. **IR** (Vmax, film) 3088, 2894, 1736, 1647, 1456, 1426, 1348, 1270, 1067, 1009, 942 cm⁻¹

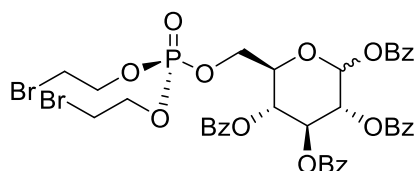


1,2,3,4,-tetra-O-allyl-6-bis(SATE)phosphate- α,β -D-glucose

Following general procedure 2, the reaction was run with 1,2,3,4-tetra-O-allyl-6-bis(2-bromoethyl)-phosphate- α,β -D-glucose on an 8.0 mg (16 μ mol) scale. The crude product was purified by automated flash column

chromatography (gradient 0 to 70% EtOAc in hexane) to afford the title compound in a mixture of anomers (3:7 α : β) as a yellow oil (8.0 mg, 16 μ mol, quant.).

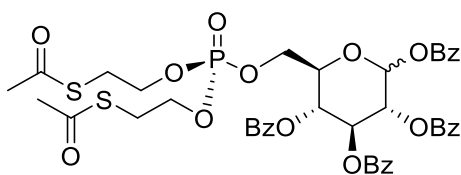
HRMS-ESI Calculated for $[C_{26}H_{41}O_{11}P + Na^+]$: 647.1720, found: 647.1741. **1H NMR** (600 MHz, CHLOROFORM-*D*) δ 2.35 (t, J = 1.3 Hz, 12H, CH_3 SAc), 3.12 – 3.23 (m, 9H, CH_2 SAc, β CH -2), 3.24 – 3.33 (m, 2H, α CH -2, β CH -4), 3.33 – 3.44 (m, 3H, α CH -4, β CH -3, β CH -5), 3.70 – 3.80 (m, 2H, α CH -3, α CH -5), 4.01 – 4.21 (m, 18H, CH_2 OAllyl, OCH_2CH_2 SAc, α CH -6, β CH -6), 4.24 (dddd, J = 10.8, 8.5, 7.1, 5.4 Hz, 4H, CH_2 OAllyl), 4.29 – 4.41 (m, 7H, α CH -6', β CH -1, β CH -6', CH_2 OAllyl), 4.90 (d, J = 3.6 Hz, 1H, α CH -1), 5.11 – 5.23 (m, 4H, $CH=CH_2$ OAllyl), 5.23 – 5.33 (m, 4H, $CH=CH_2$ OAllyl), 5.83 – 6.00 (m, 4H, $CH=CH_2$ OAllyl). **^{13}C NMR** (151 MHz, CHLOROFORM-*D*) δ 29.32, 29.37 (CH_3 SAc), 66.17 (d, J = 6.8 Hz, CH_2CH_2 SAc), 66.27 (d, J = 5.8 Hz, CH_2CH_2 SAc), 66.68 – 66.84 (m, α CH -6, β CH -6), 68.35 (O- CH_2 OAllyl), 69.63 (d, J = 8.3 Hz, α CH -5), 70.31 (β CH -5), 72.46 (O- CH_2 OAllyl), 73.57 (α CH -4), 73.61, 73.81, 73.97, 74.06, 74.44, 74.58 (O- CH_2 OAllyl), 76.88 (β CH -4), 79.52 (α CH -2), 81.50 (α CH -3), 81.67 (β CH -2), 84.15 (β CH -3), 95.81 (α CH -1), 102.50 (β CH -1), 116.68, 116.93, 117.08, 117.26, 117.35, 117.50, 117.62, 118.32 (O- CH_2 -CH- CH_2 OAllyl), 133.79, 134.03, 134.68, 134.81, 134.95, 135.15, 135.23, 135.36 (O- CH_2 -CH OAllyl), 194.80, 194.84 (C=O SAc). **^{31}P NMR** (162 MHz, CHLOROFORM-*D*) δ -1.17, -0.98. **IR** (V_{max} , film) 2922, 2868, 1693, 1459, 1422, 1394, 1270, 1129, 1065, 1006, 957, 923, 776, 684, 622, 490 cm^{-1}



11,2,3,4-*tetra-O*-benzoyl-6-*bis*(2-bromoethyl)phosphate- α,β -D-glucose

Following general procedure 1, the reaction was run with *tris*(2-bromoethyl)phosphate 65 on a 15 mg (36 μ mol) scale on 1,2,3,4-*tetra-O*-benzoyl- α,β -D-glucose. The crude product was purified by automated flash column chromatography (gradient 0 to 60% EtOAc in hexane) to afford the title compound in a mixture of anomers (1:1 α : β) as a clear oil (6.1 mg, 14 μ mol, 39%).

HRMS-ESI Calculated for $[C_{38}H_{35}Br_2O_{13}P + Na^+]$: 911.0074, found: 911.0111 **1H NMR** (400 MHz, CHLOROFORM-*D*) δ 3.41 – 3.54 (m, 8H, CH_2 Br), 4.22 – 4.43 (m, 12H, CH_2CH_2 Br, α CH -6, β CH -5, CH -6 x 2), 4.46 – 4.55 (m, 1H, α CH -5), 5.60 – 5.68 (m, 2H, α CH -2 β CH -4), 5.72 (t, J = 10.2 Hz, 1H, α CH -4), 5.83 (dd, J = 9.7, 8.0 Hz, 1H, β CH -2), 6.01 (t, J = 9.6 Hz, 1H, β CH -3), 6.25 (d, J = 8.2 Hz, 1H, β CH -1), 6.28 (d, J = 10.0 Hz, 1H, α CH -2), 6.83 (d, J = 3.7 Hz, 1H, α CH -1), 7.26 – 7.37 (m, 8H, CH arom.), 7.33 – 7.62 (m, 16H, CH arom.), 7.81 – 8.01 (m, 12H, CH arom.), 8.01 – 8.08 (m, 2H, CH arom.), 8.13 – 8.20 (m, 2H, CH arom.). **^{13}C NMR** (101 MHz, CHLOROFORM-*D*) δ 29.39, 29.47, 29.62 (CH_2 Br), 65.97 (d, J = 4.8 Hz, α CH -6, β CH -6), 67.16 – 67.39 (m, CH_2CH_2 Br), 68.42 (α CH -4), 68.65 (α CH -2), 70.37 (β CH -4), 70.45 (α CH -3), 70.78 (β CH -2), 71.07 (d, J = 7.9 Hz, α CH -5), 72.76 (β CH -3), 73.84 (d, J = 6.9 Hz, β CH -5), 89.97 (α CH -1), 92.72 (β CH -1), 128.44, 128.52, 128.56, 128.67, 128.71, 128.77, 128.95, 128.99, 129.88, 129.94, 129.97, 130.06, 130.20, 130.34, 133.55, 133.68, 133.88, 134.15 (CH arom.), 164.72, 165.27, 165.45, 165.76, 166.00 (C=O OBz). **^{31}P NMR** (162 MHz, CHLOROFORM-*D*) δ -1.89, -1.75. **IR** (V_{max} , film) 2961, 1731, 1582, 1452, 1257, 1067, 1012, 962, 709 cm^{-1}

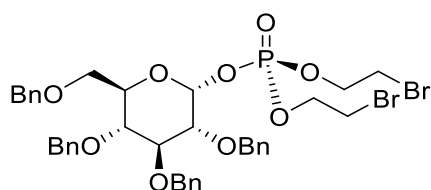


1,2,3,4-*tetra-O*-benzoyl-6-*bis*(SATE)phosphate- α,β -D-glucose

Following general procedure 2, the reaction was run with 1,2,3,4-*tetra-O*-benzoyl-6-*bis*(2-bromoethyl)-phosphate- α,β -D-glucose on a 12 mg (13 μ mol) scale. The crude product was purified by automated flash

column chromatography (gradient 0 to 70% EtOAc in hexane) to afford the title compound in a mixture of anomers (1:1 α : β) as a yellow oil (12 mg, 13 μ mol, quant.).

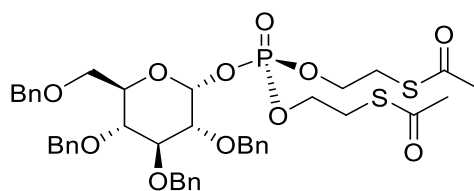
HRMS-ESI Calculated for $[C_{42}H_{41}O_{15}PS_2 + Na^+]$: 903.1517, found: 903.1561 **1H NMR** (400 MHz, CHLOROFORM-*D*) δ 2.23 – 2.39 (m, 12H, CH_3 SAc), 3.03 – 3.23 (m, 8H, CH_2 SAc), 4.04 – 4.20 (m, 8H, CH_2CH_2 SAc), 4.20 – 4.37 (m, 5H, α CH -6 x 2, β CH -5, CH -6 x 2), 4.45 – 4.54 (m, 1H, α CH -5), 5.61 – 5.70 (m, 2H, α CH -2 β CH -4), 5.74 (t, J = 9.9 Hz, 1H, α CH -4), 5.79 – 5.86 (m, 1H, β CH -2), 6.01 (d, J = 9.7 Hz, 1H, β CH -3), 6.21 – 6.32 (m, 2H, α CH -3 β CH -1), 6.83 (d, J = 3.8 Hz, 1H, α CH -1), 7.28 – 8.19 (m, 40H, CH arom.) **^{13}C NMR** (151 MHz, CHLOROFORM-*D*) δ 29.23, 29.25, 29.28, 29.30, 29.32 (CH_2 SAc), 30.60, 30.63, 30.65 (CH_3), 65.55 (d, J = 5.53 Hz α CH -6), 65.62 (d, J = 5.53 Hz, β CH -6), 66.23 (d, J = 4.42 Hz), 66.26 (d, J = 5.53 Hz) (CH_2 -OP), 68.44 (α CH -4), 68.73 (α CH -2), 70.49 (α CH -3, β CH -4), 70.85 (β CH -2), 71.15 (α CH -5), 72.87 (β CH -3), 73.82 (β CH -5), 90.04 (α CH -1), 92.74 (β CH -1), 128.50, 128.53, 128.56, 128.67, 128.68, 128.74, 128.97, 129.89, 129.94, 129.96, 129.98, 130.06, 130.07, 130.20, 130.36, 133.51, 133.59, 133.63, 133.78, 133.80, 134.06, 134.10 (CH arom. OBz) 164.47, 165.23, 165.43, 166.02, 166.12 ($C=O$ OBz) **^{31}P NMR** (162 MHz, CHLOROFORM-*D*) δ -1.62, -1.50. **IR** (V_{max} , film) 3073, 2964, 2922, 2852, 1731, 1652, 1253, 1066, 1015, 707 cm^{-1}



2,3,4,6-tetra-O-benzyl-1-bis(2-bromoethyl)phosphate- α,β -D-glucose

Following general procedure 1, the reaction was run with *tris*(2-bromoethyl)phosphate 65 on a 30 mg (72 μ mol) scale on 2,3,4,6-tetra-O-benzyl- α,β -D-glucose. The crude product was purified by automated flash column chromatography (gradient 0 to 60% EtOAc in hexane) to afford the title product in a mixture of anomers (α : β 9:1) as a white solid (14 mg, 18 μ mol, 26%).

HRMS-ESI Calculated for $[C_{38}H_{43}Br_2O_9P + Na^+]$: 855.0904, found: 855.0940 **1H NMR** (400 MHz, CHLOROFORM-*D*) δ 3.29 – 3.48 (m, 4H, CH_2 Br), 3.62 – 3.77 (m, 4H, CH -2, CH -5, CH -6 x 2), 3.87 – 4.06 (m, 2H, CH -3, CH -4), 4.18 – 4.39 (m, 4H, CH_2CH_2 Br), 4.44 – 5.04 (m, 8H, CH_2 OBn), 5.17 – 5.26 (m, 1H, β CH -1), 5.90 (dd, J = 6.8, 3.2 Hz, 1H, α CH -1), 7.07 – 7.47 (m, 20H, CH arom.) **^{13}C NMR** (101 MHz, CHLOROFORM-*D*) (α) δ 29.32, 29.39 (CH_2 Br), 66.95 (d, J = 4.8 Hz, CH_2CH_2 Br), 67.11 (d, J = 5.6 Hz, CH_2CH_2 Br), 68.31 (CH -6), 72.85 (CH -5), 73.44, 73.66, 75.35, 75.83 (CH_2 OBn), 77.01 (CH -4), 79.21 (d, J = 8.1 Hz, CH -2), 81.15 (CH -3), 96.22 (d, J = 6.3 Hz, CH -1), 127.89, 127.97, 128.01, 128.10, 128.12, 128.19, 128.33, 128.52, 128.57, 128.64, 137.53, 137.82, 138.02, 138.49 (CH arom.). **IR** (V_{max} , film) 3363, 3030, 2880, 2916, 1735, 1496, 1452, 1416, 1212, 1071, 1017, 741, 695 cm^{-1} $[\alpha]_D^{20} = +32.41$ ($c=0.2$, DCM)

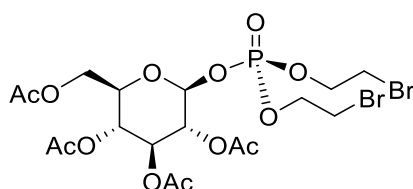


2,3,4,6-tetra-O-benzyl-1-bis(SATE)phosphate- α,β -D-glucose

Following general procedure 2, the reaction was run with 2,3,4,6-tetra-O-benzyl-1-bis(2-bromoethyl)phosphate- α,β -D-glucose on a 7.0 mg (8.4 μ mol) scale. The crude product was purified by manual flash column chromatography (gradient 20 to 50% EtOAc in hexane) to afford the title compound as the α -anomer as a yellow oil (5.4 mg, 6.5 μ mol, 78%).

HRMS-ESI Calculated for $[C_{42}H_{49}O_{11}PS_2 + Na^+]$: 847.2346, found: 847.2338. **1H NMR** (400 MHz, CHLOROFORM-*D*) δ 2.30 (d, J = 4.0 Hz, 6H, CH_3 SAc), 2.98 – 3.15 (m, 4H, CH_2 SAc), 3.50 – 3.79 (m, 4H, CH -2, CH -5, CH -6 x 2), 3.86 – 4.03 (m, 2H, CH -3, CH -4), 4.11 (dddd, J = 12.8, 10.9, 7.6, 5.0 Hz, 4H, CH_2CH_2 SAc), 4.48 (t, J = 11.8 Hz, 2H, CH_2 OBn), 4.59 (d, J = 12.0 Hz, 1H, CH_2 OBn), 4.68 (d, J = 11.3 Hz, 1H, CH_2 OBn), 4.76 (d, J = 11.4 Hz, 1H, CH_2

OBn), 4.83 (dd, $J = 10.8, 6.8$ Hz, 2H, CH_2 OBn), 4.95 (d, $J = 10.9$ Hz, 1H, CH_2 OBn), 5.87 (dd, $J = 6.8, 3.2$ Hz, 1H, $CH-1$), 7.15 (dd, $J = 7.0, 2.5$ Hz, 2H, CH arom.), 7.27 – 7.41 (m, 18H CH arom.). ^{13}C NMR (151 MHz, CHLOROFORM- D) δ 29.25 (d, $J = 7.5$ Hz), 29.28 (d, $J = 7.5$ Hz), 30.65, 66.10 (d, $J = 6.1$ Hz, CH_2CH_2S Ac), 66.30 (d, $J = 6.1$ Hz, CH_2CH_2S Ac), 68.23 ($CH-6$), 72.78 ($CH-5$), 73.27, 73.66, 75.33, 75.82 (CH_2 OBn), 79.27 (d, $J = 7.4$ Hz, $CH-2$) 81.25 ($CH-3$), 95.97 (d, $J = 5.8$ Hz, $CH-1$), 127.84, 127.92, 128.00, 128.07, 128.10 (d, $J = 2.8$ Hz), 128.30, 128.55, 128.62, 137.67, 137.94, 138.20, 138.65 (CH arom.), 194.85 ($C=O$ SAc). ^{31}P NMR (162 MHz, CHLOROFORM- D) δ -2.35. IR (Vmax, film) 3031, 2923, 2852, 1743, 1693, 1497, 1454, 1268, 1068, 1015, 993, 737, 698, 623, 530 cm^{-1} $[\alpha]_D^{20} + 9.89$ ($c = 0.455$, DCM)

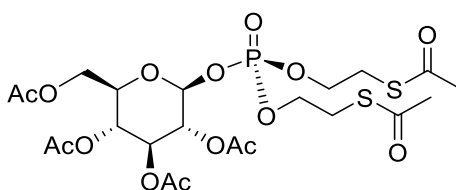


2,3,4,6-tetra-O-acetyl-1-bis(2-bromoethyl)phosphate- α,β -D-glucose

Following general procedure 1, the reaction was run with *tris*(2-bromoethyl)phosphate 65 on a 30 mg (72 μ mol) scale on 2,3,4,6-tetra-O-acetyl- α,β -D-glucose*. The crude product was purified by automated flash column chromatography (gradient 0 to 60% EtOAc in hexane) to afford the title compound in a mixture of anomers ($\alpha:\beta$ 1:5) as a white solid (15 mg, 25 μ mol, 35%)

HRMS-ESI Calculated for $[C_{18}H_{27}Br_2O_{13}P + Na^+]$: 662.945, found: 662.945. 1H NMR (400 MHz, CHLOROFORM- D) δ 2.02 (s, 6H, CH_3 OAc), 2.04 (s, 6H, CH_3 OAc), 2.09 (s, 6H, CH_3 OAc), 2.10 (s, 6H, CH_3 OAc), 3.54 (dd, $J = 12.1, 6.0$ Hz, 8H, CH_2Br), 3.65 – 3.78 (m, 3H, α $CH-5$, $CH-6 \times 2$) 3.84 (dt, $J = 9.9, 3.5$ Hz, 1H, β $CH-5$), 4.20 – 4.24 (m, 2H, β $CH-6 \times 2$), 4.30-4.46 (m, 8H, CH_2CH_2Br), 5.00 – 5.07 (m, 1H, α $CH-4$), 5.06 – 5.17 (m, 2H, β $CH-2$, $CH-4$), 5.23 (dd, $J = 9.8, 9.0$ Hz, 1H, β $CH-3$), 5.32 (dd, $J = 7.8, 6.9$ Hz, 1H, β $CH-1$) 5.44 – 5.54 (m, 2H, α $CH-2$, $CH-3$), 5.90 (dd, $J = 6.4, 3.2$ Hz, 1H, α $CH-1$). ^{13}C NMR (101 MHz, CHLOROFORM- D) (β) δ 20.54, 20.65, 20.74 (CH_3) 28.62, 28.70, 28.81, 28.90 (CH_2Br) 61.31 ($CH-6$) 67.13 (d, $J = 5.75$, CH_2CH_2Br) 67.31 (d, $J = 4.79$, CH_2CH_2Br) 67.63 ($CH-4$) 71.03 ($CH-2$) 72.19 ($CH-5$) 72.79 ($CH-3$) 96.41 (d, $J = 4.79$, $CH-1$) 169.27, 169.35, 169.98, 170.46 ($C=O$) ^{31}P NMR (162 MHz, CHLOROFORM- D) δ -1.86. IR (Vmax, film) 2968, 2919, 2849, 1593, 1490, 1278, 1215, 1071, 1019, 963 cm^{-1}

*3 equiv. of starting sugar utilised to mitigate the presence of migrated 1,3,4,6-tetra-O-acetyl sugar, no migrated phosphate product detected.

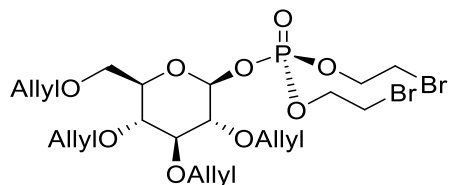


2,3,4,6-tetra-O-acetyl-1-bis(SATE)phosphate- α,β -D-glucose

Following general procedure 2, the reaction was run with 2,3,4,6-tetra-O-acetyl-1-bis(2-bromoethyl)-phosphate- α,β -D-glucose on a 5.0 mg (7.8 μ mol) scale. The crude product was purified by manual flash column chromatography (gradient 20 to 50% EtOAc in hexane) to afford the title compound in a mixture of anomers ($\alpha:\beta$ 3:7) as a yellow oil (3.4 mg, 5.4 μ mol, 69%).

HRMS-ESI Calculated for $[C_{22}H_{33}O_{15}PS_2 + Na^+]$: 655.0891; Found; 655.0902 1H NMR (400 MHz, CHLOROFORM- D) δ 1.96 – 2.11 (m, 24H, CH_3 OAc), 2.31 – 2.39 (m, 12H, CH_3 SAc), 3.10 – 3.25 (m, 8H, CH_2S Ac), 3.62 – 3.75 (m, 1H, α $CH-5$), 3.82 (ddd, $J = 10.1, 4.6, 2.4$ Hz, 1H, β $CH-5$), 4.01 – 4.33 (m, 12H, α/β $CH-6$, CH_2CH_2Br), 5.00 (ddd, $J = 10.4, 3.4, 2.7$ Hz, 1H, α $CH-2$), 5.05 – 5.15 (m, 3H, α $CH-4$, β $CH-2$, $CH-4$), 5.21 (t, $J = 9.4$ Hz, 1H, β $CH-3$), 5.29 (dd, $J = 8.0, 7.7$ Hz, 1H, β $CH-1$), 5.39 – 5.59 (m, 1H, α $CH-3$), 5.84 (dd, $J = 6.7, 3.4$ Hz, 1H, α $CH-1$) ^{13}C NMR (101 MHz, CHLOROFORM- D) δ 20.70, 20.73, 20.78, 20.85 (CH_3 OAc), 29.03, 29.12, 29.15, 29.25 (CH_3 SAc), 61.32 (β

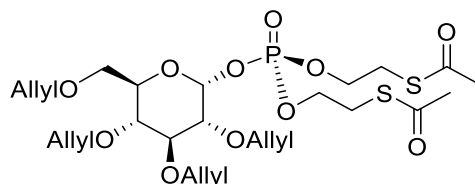
CH-6), 61.44 (α CH-6), 66.46 (d, $J = 6.08$, CH₂CH₂SAC), 66.50 (d, $J = 5.48$, CH₂CH₂SAC), 66.54 (d, $J = 5.6$ Hz, CH₂CH₂SAC), 66.69 (d, $J = 6.2$ Hz, CH₂CH₂SAC), 67.57 (β CH-4), 67.69 (α CH-4), 69.28 (α CH-5), 69.47 (β CH-5), 69.70 (d, $J = 7.71$, α CH-2), 71.09 (d, $J = 9.63$, β CH-2), 72.28 (d, $J = 2.2$ Hz, α CH-3), 72.66 (β CH-3), 94.22 (d, $J = 5.0$ Hz, α CH-1), 96.4 (d, $J = 5.0$ Hz, β CH-1), 169.40, 169.52, 169.89, 170.16, 170.65 (C=O). ³¹P NMR (162 MHz, CHLOROFORM-D) δ -2.89 IR (Vmax, film) 2960, 1747, 1694, 1429, 1367, 1216, 1032, 955, 735, 623 cm⁻¹



2,3,4,6-tetra-O-allyl-1-bis(2-bromoethyl)phosphate- α,β -D-glucose

Following general procedure 1, the reaction was run with *tris*(2-bromoethyl)phosphate 65 on a 60 mg, (0.14 mmol) scale on 2,3,4,6-tetra-O-allyl- α,β -D-glucose. The crude product was purified by automated flash column chromatography (gradient 0 to 60% EtOAc in hexane) to afford the α -anomer of the title compound as a clear oil (18 mg, 28 μ mol, 20%).

HRMS-ESI Calculated for [C₂₂H₃₅Br₂O₉P + Na⁺]: 655.0278; Measures: 655.0291 ¹H NMR (600 MHz, CHLOROFORM-D) δ 3.43 (dt, $J = 9.7, 3.2$ Hz, 1H, CH-2), 3.47 (app. t, $J = 9.9$ Hz, 1H, CH-4), 3.54 (dt, $J = 15.8, 6.4$ Hz, 4H, CH₂Br), 3.65 (d, $J = 3.0$ Hz, 2H, CH-6 x 2), 3.67 (t, $J = 9.7$ Hz, 1H, CH-3), 3.88 (dt, $J = 9.9, 3.0$ Hz, 1H, CH-5), 3.96 – 4.02 (m, 1H, CH₂ Allyl), 4.05 (ddt, $J = 12.8, 5.7, 1.4$ Hz, 1H, CH₂ Allyl), 4.09 – 4.18 (m, 2H, CH₂ Allyl), 4.18 – 4.23 (m, 1H, CH₂ Allyl), 4.23 – 4.30 (m, 1H, CH₂ Allyl), 4.30 – 4.42 (m, 5H, CH₂ Allyl, OCH₂CH₂Br), 5.11 – 5.23 (m, 4H, CH=CH₂), 5.23 – 5.36 (m, 4H, CH=CH₂), 5.81 (dd, $J = 6.8, 3.3$ Hz, 1H, CH-1), 5.85 – 6.01 (m, 4H, CH=CH₂). ¹³C NMR (151 MHz, CHLOROFORM-D) δ 29.23, 29.28, 29.32, 29.37 (CH₂Br), 66.91 (d, $J = 4.8$ Hz, CH₂CH₂Br), 67.05 (d, $J = 5.5$ Hz, CH₂CH₂Br), 68.31 (CH-6), 72.51, 72.63 (CH₂ Allyl), 72.82 (CH-5), 74.13, 74.48 (CH₂ Allyl), 76.63 (CH-4), 78.87 (d, $J = 7.3$ Hz, CH-2), 80.64 (CH-3), 96.51 (d, $J = 6.3$ Hz, CH-1), 116.93, 117.17, 117.65, 117.98 (CH=CH₂), 134.45, 134.52, 134.82, 135.29 (CH=CH₂). ³¹P NMR (162 MHz, CHLOROFORM-D) δ -6.58. IR (Vmax, film) 2920, 2853, 1737, 1538, 1455, 1376, 1260, 1096, 1820, 800 cm⁻¹ [α]_D²⁰ = + 6.32 (c=0.2, DCM)

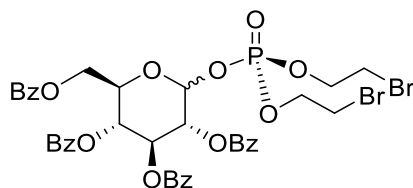


2,3,4,6-tetra-O-allyl-1-bis(SATE)phosphate- α,β -D-glucose

Following general procedure 2, the reaction was run with 2,3,4,6-tetra-O-benzoyl-1-bis(2-bromoethyl)-phosphate- α,β -D-glucose on a 1.8 mg (2.8 μ mol) scale. The crude product was purified by manual flash column chromatography (gradient 20 to 50% EtOAc in hexane) to afford the title compound in a mixture of anomers ($\alpha:\beta$ 3:1) as a yellow oil (1.3 mg, 2.0 μ mol, 72%).

HRMS-ESI Calculated for [C₂₆H₄₁Br₂O₁₁PS₂ + Na⁺]: 647.1720; Measures: 647.1741 ¹H NMR (400 MHz, CHLOROFORM-D) δ 2.33 (d, $J = 1.9$ Hz, 12H, CH₃ SAc), 3.11 – 3.21 (m, 8H, CH₂ SAc), 3.26 (t, $J = 7.5$ Hz, 1H, β CH-4), 3.36 – 3.43 (m, 2H, α CH-2, CH-4), 3.47 (dd, $J = 10.0, 9.3$ Hz, 1H, α CH-3), 3.56 – 3.72 (m, 5H, α/β CH-6 x 2, β CH-2, CH-3, CH-5), 3.83 (ddd, $J = 10.1, 3.4, 2.1$ Hz, 1H, α CH-5), 3.92 – 4.06 (m, 4H, CH₂ Allyl), 4.06 – 4.20 (m, 12H, CH₂ Allyl, CH₂CH₂SAC), 4.20 – 4.38 (m, 4H, CH₂ Allyl), 5.00 (dd, $J = 7.8, 6.9$ Hz, 1H, β CH-1), 5.12-5.18 (m, 8H, CH=CH₂), 5.20 – 5.32 (m, 4H, CH=CH₂), 5.76 (dd, $J = 6.9, 3.3$ Hz, 1H, α CH-1), 5.78 – 6.00 (m, 8H, CH=CH₂). ¹³C NMR (101 MHz, CHLOROFORM-D) δ 29.20, 29.24, 29.26, 29.31, 29.34, 30.68 (CH₃ SAc), 66.02 (d, $J = 5.2$ Hz), CH₂CH₂SAC, 66.24 (d, $J = 5.7$ Hz, CH₂CH₂SAC), 68.14 (α CH-6), 68.42 (β CH-6), 72.30, 72.45, 72.59 (α CH-5), 72.63, 73.83, 73.96, 74.08, 74.44, 74.53, 75.45 (CH₂ OAllyl), 76.51 (α CH-4), 78.81 (d, $J = 7.1$ Hz, α CH-2), 80.66 (α CH-3), 81.22 (d, $J = 8.5$ Hz, β CH-2) 83.90 (β CH-3) 96.12 (d, $J = 6.2$ Hz, α CH-1), 98.98 (d, $J = 6.7$ Hz, β CH-1), 116.82, 117.06, 117.17, 117.36, 117.57, 117.83 (CH=CH₂), 134.49, 134.54, 134.76, 134.87, 135.07, 135.32

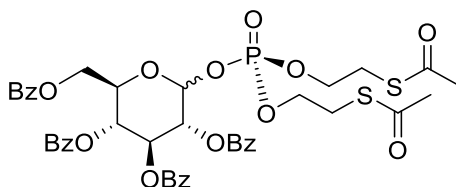
(CH=CH₂) ³¹P NMR (162 MHz, CHLOROFORM-D) δ -2.41. IR (Vmax, film) 3079, 2922, 2867, 1693, 1461, 1421, 1355, 1270, 1065, 1009, 949, 622, 515 cm⁻¹



2,3,4,6-tetra-O-benzoyl-1-bis(2-bromoethyl)phosphate- α,β -D-glucose

Following general procedure 1, the reaction was run with *tris*(2-bromoethyl)phosphate 65 on a 30 mg (72 μ mol) scale on 2,3,4,6-tetra-O-benzoyl- α,β -D-glucose. The crude product was purified by automated flash column chromatography (gradient 0 to 60% EtOAc in hexane) to afford the title product in a mixture of anomers ($\alpha:\beta$ 5:1) as a clear oil (26 mg, 2.9 μ mol, 41%).

HRMS-ESI Calculated for [C₃₈H₃₅Br₂O₁₃P + Na⁺]: 911.0074; Found; 911.0109 ¹H NMR (400 MHz, CHLOROFORM-D) δ 3.35 (qdd, *J* = 17.0, 8.6, 5.0 Hz, 8H, CH₂Br), 4.15 – 4.36 (m, 8H, CH₂CH₂Br), 4.35 – 4.47 (m, 2H, β CH-6 x 2), 4.51 (dd, *J* = 12.2, 4.6 Hz, 1H, α CH-6), 4.66 (dd, *J* = 12.2, 3.3 Hz, 1H, α CH-6), 4.68 – 4.76 (m, 1H, α/β CH-5), 5.43 (dt, *J* = 10.1, 3.1 Hz, 1H, α CH-2), 5.59 – 5.74 (m, 2H, β CH-2, CH-4), 5.78 (t, *J* = 10.1 Hz, 1H, α CH-4), 5.93 (t, *J* = 9.4 Hz, 1H, β CH-3), 6.16 – 6.24 (m, 2H, α CH-1, CH-3, β CH-1), 7.27 – 7.62 (m, 24H, CH arom.), 7.80 – 8.12 (m, 16H, CH arom.) ¹³C NMR (101 MHz, CHLOROFORM-D) δ (α) 28.92, 28.99, 29.05 (CH₂Br), 62.58 (CH-6), 67.35 (d, *J* = 5.6 Hz, CH₂CH₂Br), 67.40 (d, *J* = 4.4 Hz, CH₂CH₂Br), 68.67 (CH-4), 69.60 (CH-3), 70.30 (CH-5), 71.19 (d, *J* = 8.0 Hz, CH-2), 94.69 (d, *J* = 6.7 Hz, CH-1), 128.51, 128.65, 128.78, 128.91, 129.62, 129.87, 129.91, 130.06, 133.44, 133.51, 133.77, 133.94 (CH arom.) 165.27, 165.55, 165.83, 166.15 (C=O) ³¹P NMR (162 MHz, CHLOROFORM-D) δ -3.44, -2.98. IR (Vmax, film) 3073, 2961, 2926, 2852, 1725, 1601, 1451, 1260, 1068, 1003, 959, 708 cm⁻¹

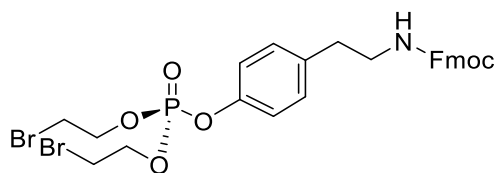


2,3,4,6-tetra-O-benzoyl-1-bis(SATE)phosphate- α,β -D-glucose

Following general procedure 2, the reaction was run with 2,3,4,6-tetra-O-benzoyl-1-bis(2-bromoethyl)-phosphate- α,β -D-glucose on a 24 mg (2.7 μ mol) scale. The crude product was purified by manual flash column chromatography (gradient 20 to 50% EtOAc in hexane) to afford the title compound in a mixture of anomers ($\alpha:\beta$ 5:1) as a yellow oil (18 mg, 2.0 μ mol, 74%).

HRMS-ESI Calculated for [C₄₂H₄₁O₁₅PS₂ + Na⁺]: 903.1561; Found; 903.1517 ¹H NMR (400 MHz, CHLOROFORM-D) δ 2.31 (s, 3H, CH₃ SAc), 2.32 (s, 3H, CH₃ SAc), 3.02 (dt, *J* = 19.9, 6.4 Hz, 8H, CH₂SAC), 3.96 – 4.16 (m, 8H, CH₂CH₂SAC), 4.43 – 4.55 (m, 2H, β CH-6 x 2), 4.51 (dd, *J* = 12.2, 4.5 Hz, 1H, α CH-6), 4.64 (dd, *J* = 12.2, 2.8 Hz, 1H, α CH-6), 4.69 (ddd, *J* = 10.1, 4.5, 2.8 Hz, 1H, α/β CH-5), 5.43 (dt, *J* = 10.1, 3.2 Hz, 1H, α CH-2), 5.59 – 5.75 (m, 2H, β CH-2, CH-4), 5.79 (t, *J* = 10.1 Hz, 1H, α CH-4), 5.91 (t, *J* = 9.6 Hz, 1H, β CH-3), 6.10 – 6.24 (m, 3H, α CH-1, CH-3, β CH-1), 7.25 – 7.61 (m, 24H, CH arom.), 7.79 – 8.09 (m, 16H, CH arom.) ¹³C NMR (101 MHz, CHLOROFORM-D) δ (α) 29.01, 29.09, 29.16 (CH₂SAC), 30.64, (CH₃ SAC), 62.56 (CH-6), 66.60 (d, *J* = 5.1 Hz, CH₂CH₂SAC), 66.65 (d, *J* = 5.8 Hz, CH₂CH₂SAC), 68.67 (CH-4), 69.73 (CH-3), 70.14 (CH-5), 71.11 (d, *J* = 8.0 Hz, CH-2), 94.51 (d, *J* = 5.8 Hz, CH-1), 128.49, 128.61, 128.70, 128.73, 128.77, 128.99, 129.87, 129.92, 130.07, 133.37, 133.45, 133.71, 133.83 (CH arom.) 165.25, 165.56, 165.79, 166.18 (C=O) ³¹P NMR (162 MHz, CHLOROFORM-D) δ -3.19, -2.87. IR (Vmax, film) 3064, 2959, 2972, 1727, 1694, 1452, 1264, 1092, 1069, 1025, 952, 707, 623, 484 cm⁻¹

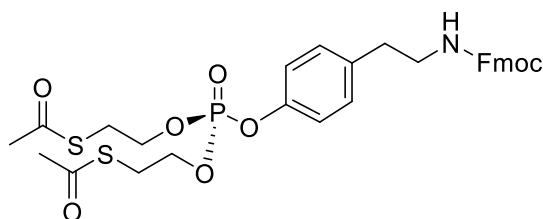
Phospho-Tyrosine



***N*-Fmoc-3-(bis(2-bromoethyl)phosphate)-tyramine**

Following general method 1, the reaction was run with *tris*(2-bromoethyl)phosphate 65 on a 30 mg (72 μ mol) scale on *N*-Fmoc-tyramine. The crude product was purified by manual flash column chromatography (gradient 50% EtOAc in hexane) to afford the title compound as a clear oil (25 mg, 39 μ mol, 55%)

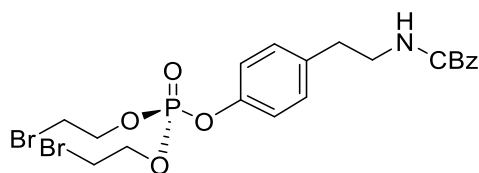
HRMS-ESI Calculated for $[C_{27}H_{28}Br_2NO_6P + Na^+]$: 673.9913, found: 673.9932 **1H NMR** (400 MHz, CHLOROFORM-*D*) δ 2.79 (t, J = 6.9 Hz, 2H, CH_2CH_2NH), 3.43 (t, J = 7.8 Hz, 2H, CH_2CH_2NH), 3.51 – 3.56 (m, 4H, CH_2Br), 4.21 (t, J = 6.9 Hz, 1H, CH Fmoc), 4.41 – 4.47 (m, 6H, OCH_2CH_2Br , CH_2 Fmoc), 7.09 – 7.23 (m, 4H, CH arom.), 7.31 (t, J = 7.4 Hz, 2H, CH arom. Fmoc), 7.40 (t, J = 7.5 Hz, 2H, CH arom. Fmoc), 7.57 (d, J = 7.4 Hz, 2H, CH arom. Fmoc), 7.77 (d, J = 7.3 Hz, 2H, CH arom. Fmoc). **^{13}C NMR** (101 MHz, CHLOROFORM-*D*) δ 29.22, 29.30 (CH_2Br), 35.56 (CH_2CH_2NH), 42.31 (CH_2NH), 47.39 (CH Fmoc), 66.63 (CH_2 Fmoc), 67.65, 67.70 (OCH_2CH_2Br), 120.11, 120.29 (d, J = 4.6 Hz, *C*-3 arom.), 125.13, 127.17, 127.83, 130.32, 136.28, 141.45, 144.03, 149.02 (CH arom.), 156.42 ($C=O$). **IR** (V_{max} , film) 3319, 3038, 2943, 1707, 1505, 1449, 1267, 1214, 1068, 1019, 957, 781, 759, 741, 668 cm^{-1}



***N*-Fmoc-3-(bis(SATE)phosphate)-tyramine**

Following general procedure 2, the reaction was run with *N*-Fmoc-3-(bis(2-bromoethyl)phosphate)-tyramine on a 24 mg (39 μ mol) scale. The crude product was purified by manual flash column chromatography (gradient 50% EtOAc in hexane) to afford the title compound as a yellow oil (20 mg, 32 μ mol, 83%).

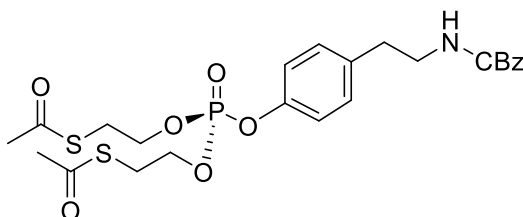
HRMS-ESI Calculated for $[C_{31}H_{34}NO_8PS_2 + Na^+]$: 666.1356, found: 666.1370 **1H NMR** (400 MHz, CHLOROFORM-*D*) δ 2.34 (s, 6H, CH_3 SAc), 2.79 (t, J = 6.9 Hz, 2H, CH_2CH_2NH), 3.17 (dt, J = 6.8, 1.7 Hz, 4H, CH_2SAc), 3.43 (q, J = 6.1 Hz, 2H, CH_2CH_2NH), 4.16 – 4.32 (m, 4H, CH_2CH_2SAc), 4.42 (d, J = 6.8 Hz, 2H, CH Fmoc), 7.15 (s, 4H, CH_2 arom.), 7.32 (t, J = 7.3 Hz, 2H, CH_2 arom. Fmoc), 7.35 – 7.49 (m, 2H, CH_2 arom. Fmoc), 7.57 (d, J = 7.5 Hz, 2H, CH_2 arom. Fmoc), 7.77 (d, J = 7.4 Hz, 2H, CH_2 arom. Fmoc). **^{13}C NMR** (151 MHz, CHLOROFORM-*D*) δ 29.28 (d, J = 7.3 Hz, CH_2SAc), 30.67 (CH_3 SAc), 35.60 (CH_2CH_2NH), 42.37 (CH_2NH), 47.45 (CH Fmoc), 66.67 (CH_2 Fmoc), 66.77 (dd, J = 5.7 Hz, OCH_2CH_2SAc), 120.13, 120.34 (d, J = 5.1 Hz, COP arom.), 125.16, 127.18, 127.84, 130.29, 141.48, 144.08 (CH arom.), 194.86 ($C=O$ SAc). **^{31}P NMR** (162 MHz, CHLOROFORM-*D*) δ -6.30. **IR** (V_{max} , film) 3322, 3069, 2927, 2848, 1693, 1506, 1450, 1355, 1272, 1244, 1215, 1133, 1061, 1012, 952, 880, 759, 731, 741, 621, 529 cm^{-1}



***N*-CBz-3-(bis(2-bromoethyl)phosphate)-tyramine**

Following general procedure 1, the reaction was run with *tris*(2-bromoethyl)phosphate **65** on a 30 mg (72 μ mol) scale on *N*-CBz-tyramine. The crude product was purified by manual flash column chromatography (gradient 50% EtOAc in hexane) to afford the title compound as a clear oil (12 mg, 22 μ mol, 32%)

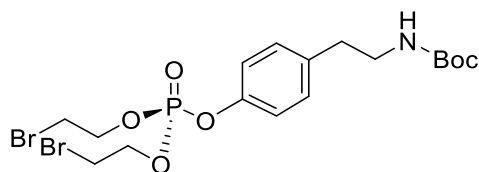
HRMS-ESI Calculated for [C₂₂H₂₃Br₂NO₆P + Na⁺]: 585.9624, found: 585.9612 **¹H NMR** (400 MHz, CHLOROFORM-*D*) δ 2.79 (t, *J* = 6.9 Hz, 2H, CH₂CH₂NH), 3.42 (app. q, *J* = 6.7 Hz, 2H, CH₂NH), 3.46 – 3.58 (m, 4H, CH₂Br), 4.31 – 4.48 (m, 4H, CH₂CH₂Br), 4.78 (s, 1H, NH), 5.09 (s, 2H, CH₂ CBz), 7.15 (s, 4H, CH arom.), 7.34 (d, *J* = 5.7 Hz, 5H, CBz arom.). **¹³C NMR** (101 MHz, CHLOROFORM-*D*) δ 29.21, 29.28 (CH₂Br), 35.76 (CH₂CH₂NH), 43.16 (CH₂NH), 65.83 (COCH₂), 67.65, 67.71 (O-CH₂-CH₂), 120.32 (d, *J* = 4.8 Hz, COP arom.), 128.32, 128.69, 130.31 (CH arom.), 156.41 (C=O). **IR** (Vmax, film) 3319, 2932, 1707, 1505, 1449, 1268, 1213, 1070, 1018, 959, 778, 746, 698 cm⁻¹



***N*-CBz-3-(bis(SATE)phosphate)-tyramine**

Following general procedure 2, the reaction was run with *N*-CBz-3-(bis(2-bromoethyl)phosphate)-tyramine on a 10 mg (18 μ mol) scale. The crude product was purified by manual flash column chromatography (gradient 50% EtOAc in hexane) to afford the title compound as a yellow oil (10 mg, 18 μ mol, quant.).

HRMS-ESI Calculated for [C₂₄H₃₀NO₈PS₂ + Na⁺]: 578.1043, found: 578.1038 **¹H NMR** (400 MHz, CHLOROFORM-*D*) δ 2.33 (s, 6H, CH₃), 2.78 (t, *J* = 7.0 Hz, 2H, CH₂CH₂NH), 3.08 – 3.23 (m, 4H, CH₂SAC), 3.42 (q, *J* = 6.7 Hz, 2H, CH₂NH), 4.14 – 4.25 (m, 4H, CH₂CH₂SAC), 4.80 (s, 1H, NH), 5.08 (s, 2H, CH₂ CBz), 7.13 (s, 4H, CH arom.), 7.33 (d, *J* = 5.5 Hz, 5H, CBz arom.). **¹³C NMR** (101 MHz, CHLOROFORM-*D*) δ 29.20, 29.27 (CH₃), 29.83, 30.67 (CH₂SAC), 35.52 (CH₂CH₂NH), 42.33 (CH₂NH), 66.71, 66.77 (COCH₂), 77.36, 120.33 (d, *J* = 4.8 Hz, COP arom.), 128.28 (d, *J* = 2.4 Hz), 128.68, 130.25 (CH arom.), 194.90 (C=O). **³¹P NMR** (162 MHz, CHLOROFORM-*D*) δ -6.34. **IR** (Vmax, film) 3321, 2932, 1692, 1506, 1455, 1355, 1246, 1214, 1132, 1059, 1013, 953, 835, 776, 738, 698, 622, 527 cm⁻¹



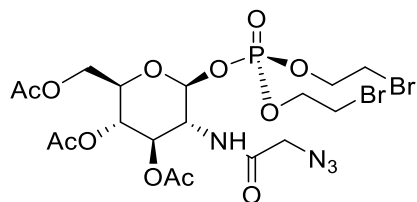
***N*-Boc-3-(bis(2-bromoethyl)phosphate)-tyramine**

Following general procedure 1, the reaction was run with *tris*(2-bromoethyl)phosphate **65** on a 30 mg (72 μ mol) scale on *N*-Boc-tyramine. The crude product was purified by manual flash column chromatography (gradient 50% EtOAc in hexane) to afford the title compound as a clear oil (0.2 mg, 0.4 μ mol, 0.57%)*

*yield calculated by ¹H NMR of product obtained as a mixture with starting *tris*(2-bromoethyl)phosphate **65**

HRMS-ESI Calculated for $[C_{17}H_{26}Br_2NO_6P + Na^+]$: 551.9757, found: 551.9774 **1H NMR** (400 MHz, CHLOROFORM-*D*) δ 1.43 (s, 9H, $(CH_3)_3$ Boc), 2.77 (t, $J = 7.2$ Hz, 2H, CH_2CH_2NH), 3.34 (t, $J = 6.9$ Hz, 2H, CH_2NH), 3.74 (dq, $J = 11.4$, 5.7 Hz, 4H, CH_2Br), 4.43 – 4.51 (m, 4H, CH_2CH_2Br), 7.17 (d, $J = 4.4$ Hz, 4H, CH arom.).

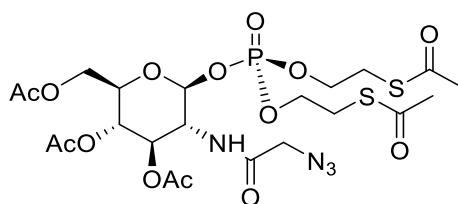
Glucosamine



3,4,6-tri-O-acetyl-2-N-azido-acetimido-1-bis(2-bromoethyl)phosphate- α -D-glucosamine

Following general procedure 1, the reaction was run with *tris*(2-bromoethyl)phosphate **65** on a 30 mg (72 μ mol) scale on 3,4,6-tri-O-acetyl-2-N-azido-acetimido- α,β -D-glucosamine. The crude product was purified by manual flash column chromatography (gradient 8% MeOH in DCM) to afford the title compound as a clear oil (4.0 mg, 6.0 μ mol, 8.3%)

HRMS-ESI Calculated for $[C_{18}H_{27}Br_2N_4O_{12}P + Na^+]$: 702.9622, found: 702.9629 **1H NMR** (600 MHz, CHLOROFORM-*D*) δ 2.03 (s, 3H, CH_3 OAc), 2.05 (s, 3H, CH_3 OAc), 2.06 (s, 3H, CH_3 OAc), 2.11 (s, 3H, CH_3 OAc), 3.58 (dtd, $J = 12.9$, 6.1, 0.9 Hz, 4H, CH_2Br), 3.98 (d, $J = 4.1$ Hz, 2H, CH_2N_3), 4.12 – 4.16 (m, 1H, CH-6), 4.20 – 4.25 (m, 1H, CH-6'), 4.28 (dd, $J = 12.4$, 4.1 Hz, 1H, CH), 4.37 – 4.46 (m, 5H, CH_2CH_2Br , CH), 5.22 (t, $J = 9.9$ Hz, 1H, CH), 5.31 (dd, $J = 10.6$, 9.6 Hz, 1H, CH), 5.80 (dd, $J = 5.9$, 3.3 Hz, 1H, CH-1), 6.65 (d, $J = 8.8$ Hz, 1H, NH).



3,4,6-tri-O-acetyl-2-N-azido-acetimido-1-bis(SATE)phosphate- α -D-glucosamine

Following general procedure 2, the reaction was run with 3,4,6-tri-O-acetyl-2-N-azido-acetimido-1-bis(2-bromoethyl)phosphate- α -D-glucosamine on a 4.0 mg (6.0 μ mol) scale. The crude product was analysed by 1H NMR, and full conversion to the title compound was observed.

HRMS-ESI Calculated for $[C_{22}H_{33}N_4O_{14}PS_2 + Na^+]$: 695.1065, found: 695.1048 **1H NMR** (600 MHz, CHLOROFORM-*D*) δ 2.01 (s, 3H), 2.03 (s, 3H), 2.05 (s, 3H), 2.09 (s, 3H), 3.15 – 3.21 (m, 4H), 3.97 (d, $J = 1.5$ Hz, 2H), 4.10 – 4.31 (m, 7H), 5.21 (t, $J = 9.9$ Hz, 1H), 5.29 (dd, $J = 10.9$, 9.8 Hz, 1H), 5.75 (dd, $J = 6.1$, 3.1 Hz, 1H), 6.75 (d, $J = 8.9$ Hz, 1H).

Data in accordance with literature values¹³⁸

5.7 References

138. H. Y. Tan, R. Eskandari, D. Shen, Y. Zhu, T. W. Liu, L. I. Willems, M. G. Alteen, Z. Madden and D. J. Vocadlo, *J. Am. Chem. Soc.*, 2018, **140**, 15300-15308.
166. S. H. Yu, M. Boyce, A. M. Wands, M. R. Bond, C. R. Bertozzi and J. J. Kohler, *Proc. Natl. Acad. Sci. U. S. A.*, 2012, **109**, 4834-4839.
237. H. Huang, J. Ash and J. Y. Kang, *Org. Lett.*, 2018, **20**, 4938-4941.
238. H. Huang, J. Denne, C.-H. Yang, H. Wang and J. Y. Kang, *Angew. Chem. Int. Ed. Engl.*, 2018, **57**, 6624-6628.
239. C. D. Spicer, M. Pujari-Palmer, H. Autefage, G. Insley, P. Procter, H. Engqvist and M. M. Stevens, *ACS Cent. Sci.*, 2020, **6**, 226-231.
257. J. F. A. Pijnenborg, E. A. Visser, M. Noga, E. Rossing, R. Veizaj, D. J. Lefeber, C. Büll and T. J. Boltje, *Chemistry*, 2021, **27**, 4022-4027.
258. J. F. A. Pijnenborg, E. Rossing, J. Merx, M. J. Noga, W. H. C. Titulaer, N. Eerden, R. Veizaj, P. B. White, D. J. Lefeber and T. J. Boltje, *Nat. Commun.*, 2021, **12**, 7024.
259. B. N. Kakde, E. Capota, J. J. Kohler and U. K. Tambar, *J. Org. Chem.*, 2021, **86**, 18257-18264.
260. H. Huang and J. Y. Kang, *Synlett*, 2019, **30**, 635-641.
271. P. Adler, A. Pons, J. Li, J. Heider, B. R. Brutiu and N. Maulide, *Angew. Chem. Int. Ed. Engl.*, 2018, **57**, 13330-13334.
272. B. J. Foust, J. Li, C.-H. C. Hsiao, D. F. Wiemer and A. J. Wiemer, *ChemMedChem*, 2019, **14**, 1597-1603.
273. D. J. Anderson, R. McDonald and M. Cowie, *Angew. Chem. Int. Ed. Engl.*, 2007, **46**, 3741-3744.
274. D. Gasperini, S. E. Neale, M. F. Mahon, S. A. Macgregor and R. L. Webster, *ACS Catal.*, 2021, **11**, 5452-5462.
275. S. Singh, Z. Su, M. Grossutti and F. I. Auzanneau, *Carbohydr Res*, 2014, **390**, 50-58.
276. G. T. Giuffredi, L. E. Jennings, B. Bernet and V. Gouverneur, *J. Fluor. Chem.*, 2011, **132**, 772-778.
277. N. Santschi, N. Aiguabella, V. Lewe and R. Gilmour, *J. Fluor. Chem.*, 2015, **179**, 96-101.
278. T. Hamada, A. Chieffi, J. Ahman and S. L. Buchwald, *J. Am. Chem. Soc.*, 2002, **124**, 1261-1268.
279. Z. Khedri, M. M. Muthana, Y. Li, S. M. Muthana, H. Yu, H. Cao and X. Chen, *Chem. Commun. (Camb)*, 2012, **48**, 3357-3359.
280. N. Darabedian, J. Gao, K. N. Chuh, C. M. Woo and M. R. Pratt, *J. Am. Chem. Soc.*, 2018, **140**, 7092-7100.
281. F. Rajas, A. Gautier-Stein and G. Mithieux, *Metabolites*, 2019, **9**.
282. J. Fettke, T. Albrecht, M. Hejazi, S. Mahlow, Y. Nakamura and M. Steup, *New Phytol*, 2010, **185**, 663-675.
283. S. N. Jager, E. O. J. Porta and G. R. Labadie, *Steroids*, 2019, **141**, 41-45.
284. J. C. Lee, S. W. Chang, C. C. Liao, F. C. Chi, C. S. Chen, Y. S. Wen, C. C. Wang, S. S. Kulkarni, R. Puranik, Y. H. Liu and S. C. Hung, *Chemistry*, 2004, **10**, 399-415.
285. S. Mohamed, Q. Q. He, R. J. Lepage, E. H. Krenske and V. Ferro, *Eur. J. Org. Chem.*, 2018, **2018**, 2214-2227.
286. B. Fraser-Reid, Z. Wu, U. E. Udodong and H. Ottosson, *J. Org. Chem.*, 1990, **55**, 6068-6070.
287. T. Utamura, K. Kuromatsu, K. Suwa, K. Koizumi and T. Shingu, *Chem. Pharm. Bull.*, 1986, **34**, 2341-2353.
288. K. Hiruma-Shimizu, A. P. Kalverda, P. J. Henderson, S. W. Homans and S. G. Patching, *J. Labelled Comp. Radiopharm.*, 2014, **57**, 737-743.
289. E. Kaji, T. Komori, M. Yokoyama, T. Kato, T. Nishino and T. Shirahata, *Tetrahedron*, 2010, **66**, 4089-4100.
290. Y. Konda, T. Toida, E. Kaji, K. Takeda and Y. Harigaya, *Carbohydr. Res.*, 1997, **301**, 123-143.
291. S. Hackbusch, A. Watson and A. H. Franz, *Carbohydr. Res.*, 2018, **458-459**, 1-12.

292. V. Kumar, N. Yadav and K. P. R. Kartha, *Carbohydr. Res.*, 2014, **397**, 18-26.
293. L. M. Doyle, S. O'Sullivan, C. Di Salvo, M. McKinney, P. McArdle and P. V. Murphy, *Org. Lett.*, 2017, **19**, 5802-5805.
294. J. Dinkelaar, M. D. Witte, L. J. van den Bos, H. S. Overkleeft and G. A. van der Marel, *Carbohydr. Res.*, 2006, **341**, 1723-1729.
295. L. Kerins, S. Byrne, A. Gabba and P. V. Murphy, *J. Org. Chem.*, 2018, **83**, 7714-7729.
296. S. Ghorai, R. Mukhopadhyay, A. P. Kundu and A. Bhattacharjya, *Tetrahedron*, 2005, **61**, 2999-3012.
297. M. A. Fernández-Herrera, S. Mohan, H. López-Muñoz, J. M. V. Hernández-Vázquez, E. Pérez-Cervantes, M. L. Escobar-Sánchez, L. Sánchez-Sánchez, I. Regla, B. M. Pinto and J. Sandoval-Ramírez, *Eur. J. Med. Chem.*, 2010, **45**, 4827-4837.
298. T. Nokami, A. Shibuya, H. Tsuyama, S. Suga, A. A. Bowers, D. Crich and J. Yoshida, *J. Am. Chem. Soc.*, 2007, **129**, 10922-10928.
299. K. Gulbe, J. Luginina, E. Jansons, A. Kinens and M. Turks, *Beilstein J. Org. Chem.*, 2021, **17**, 964-976.
300. W. Ouyang, H. Huang, R. Yang, H. Ding and Q. Xiao, *Mar. Drugs*, 2020, **18**.
301. C. Cassani, G. Bergonzini and C. J. Wallentin, *Org. Lett.*, 2014, **16**, 4228-4231.

Chapter 6: Towards the Synthesis of 2-Azido- and 3-Azido-D-Ribitol-5-Phosphate Probes

6.1 Abstract

Metabolic Oligosaccharide Engineering (MOE) relies on the incorporation of modified monosaccharides into target glycans by exploiting the flexibility of the cell's metabolic machinery. With multiple enzymes typically involved in the metabolic pathway of a metabolic labelling probe, the tolerance towards the modification made to the probe relative to the cell's native substrate is difficult to predict. Therefore the determination of optimal labelling type and position often relies on a 'trial-and-error' approach, exploring different sites of label incorporation and varied labelling strategies. To explore the tolerance of human enzymes that act on ribitol-5-phosphate (FKTN, FKRP and ISPD) towards modification of the pentitol with an azide tag, routes to 2- and 3-azido-ribitol-5-phosphate probes suitable for the synthesis of both protected and unprotected probes for use *in vivo* and *in vitro*, respectively, is described. These routes build on the development of the 1-azido-ribitol-5-phosphate probes described in Chapter 3, while also exploring new protecting group strategies and manipulations. A key ring-opened benzylated lyxitol intermediate has been synthesised on route to the 2-azido probes, from which the fully-protected SATE probe can be synthesised in 7-steps, following protecting group manipulations previously achieved in the 1-azido probe routes. Initial investigation into synthesis of the 3-azido probe from D-xylose has also taken place, and a fully protected xylose intermediate, in which the sites of azide and phosphate incorporation have been orthogonally protected, has been synthesised. An additional route, based on literature reported by Gao *et al* in their synthesis of an azido adenosine reporter,³⁰² is also proposed, again building upon previous protecting group compatibilities identified during the synthesis of the 1-azido-ribitol probe. These routes pave the way to the synthesis of these alternative azido-containing probes, with which we hypothesise being able to better understand the enzyme tolerance of FKTN, FKRP and ISPD to substrate modification.

6.2 Introduction

When designing metabolic labelling probes, the site of label incorporation often relies on prior knowledge of the biosynthetic transformations the probe will need to undergo as well as the tolerance of the various enzymes to different sites of modification. The issue of enzyme tolerance is typically established through previous metabolic labelling studies, on which new generations of chemical probes are based. In the case of hexopyranose and hexosamine sugars such as glucose and *N*-acetylglucosamine, modification typically occurs at the 2- and 6- positions,¹¹¹⁻¹¹³ while for sialic acids it is typically the 9-position or the *N*-acyl group.^{117,303} In the case of the linear pentitol structure of ribitol, there is no literature precedent for metabolic labelling of ring-opened sugars, though the metabolic labelling of choline, a small linear molecule, has been reported utilising both azide and alkyne modification.³⁰⁴⁻³⁰⁶ Therefore, to fully investigate the tolerance of the human enzymes that act on ribitol-5-phosphate (FKTN, FKR and ISPD) to modification of the ribitol structure, several sites of azide incorporation were investigated.

Previously the synthesis of a series of 1-azido probes has been discussed in great detail (Chapter 3, pg. 55). Alongside the development of the 1-azido-probes, investigations into the synthesis of 2- and 3-azido ribitol-5-phosphate probes (Figure 22) were carried out. This chapter describes the initial findings towards the synthesis of these probes. Complete synthetic routes to these final probes are proposed, based on the protecting group compatibilities revealed during the synthesis of the 1-azido probes, alongside alternative, shorter approaches that make use of different protecting groups, such as benzoyl groups and acetonides for the protection of 1,2-diols, and a variety of different pentose starting sugars. The installation of an azide at the 4-position was not pursued, as the incorporation of this probe into the core M3 *O*-mannosyl glycan by FKR would prevent further extension with matriglycan (see Chapter 1, pg. 20).



Figure 22: Structures of the fully protected 2-azido and 3-azido-D-ribitol-5-phosphate probes carrying acetate and SATE protection for the purpose of *in vivo* metabolic labelling.

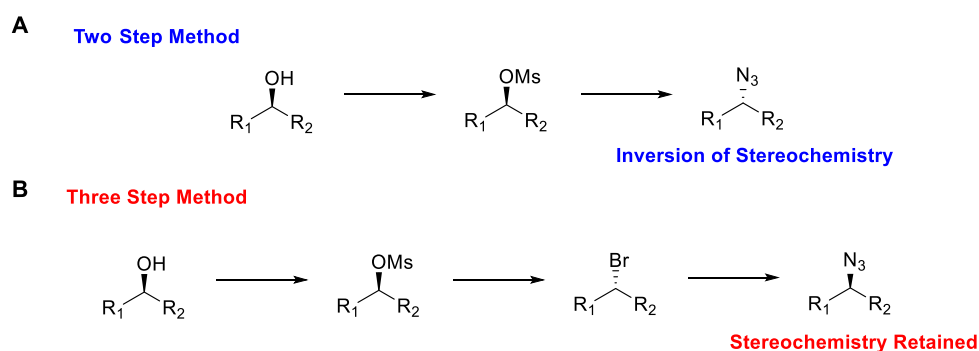
6.3 Aims

This chapter aims to explain the rationale behind the newly proposed synthetic routes to 2- and 3-azido-D-ribitol-5-phosphate probes. Building upon the routes to the 1-azido probes (Chapter 3, pg. 55), it will explore methods for the regioselective installation of an azide at the 2- or 3-position and appropriate protection to generate probes for both *in vivo* and *in vitro* application. The synthesis

of these probes will, combined with the 1-azido probes synthesised previously, enable better interrogation of the tolerance of the biosynthetic machinery in mammalian cells towards tagged ribitol-5-phosphate derivatives.

6.4 Results and Discussion

Typically, the conversion of hydroxyl groups to azides proceeds via a two-step procedure. Initially, the hydroxyl group is activated with a group such as a methanesulfonate (mesylate, OMs) or p-toluene sulfonate (tosylate, OTs), to make it into a more efficient leaving group. This then allows for substitution with an azide source, such as sodium azide, *via* an S_N2 reaction to afford the desired azide-containing product with inversion of stereochemistry at the reaction centre (Scheme 53A). Alternative methods proceed *via* a double inversion approach, initially substituting the hydroxyl group for a halide, typically bromine, which can then be substituted to form the azide. This double inversion approach retains the overall stereochemistry at the reaction centre (Scheme 53B).



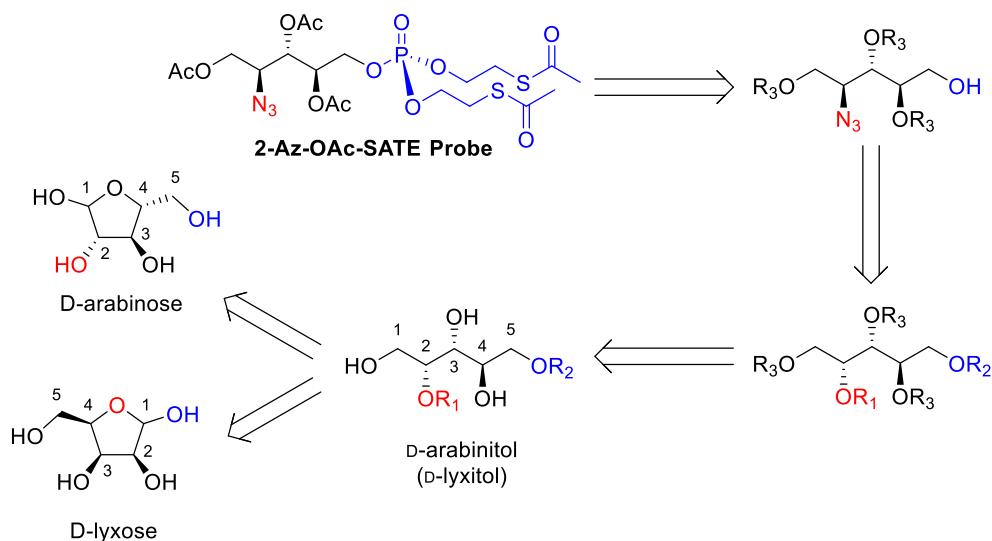
Scheme 53: Difference in stereochemical outcome of azide substitution reactions using A) two- and B) three-step conversion of alcohols to azides through mesylated intermediates.

When designing routes to the 2- and 3-azido-ribitol compounds, it was clear that the synthetic routes would diverge greatly from the previous 1-azido routes because of different protecting group requirements needed for the correct positioning of the azide substitution. Due to this, there was little benefit to utilising a double inversion approach to proceed from D-ribose as was the case for the 1-azido probe. Therefore, the routes to the 2- and 3-azido probes instead utilise different starting sugars and make use of inversion of stereochemistry in the conversion of an appropriate hydroxyl group to an azide.

2-Azido Ribitol-5-Phosphate Probe

Due to the azide incorporation at the 2-position occurring at a chiral position, inversion of stereochemistry meant that synthesis could proceed from either of two different pentose sugars; D-arabinose and D-lyxose, with phosphate addition occurring at the 5- or the 1-position of the pentose ring, respectively (Scheme 54). It should be noted that, for consistency throughout this Chapter, the

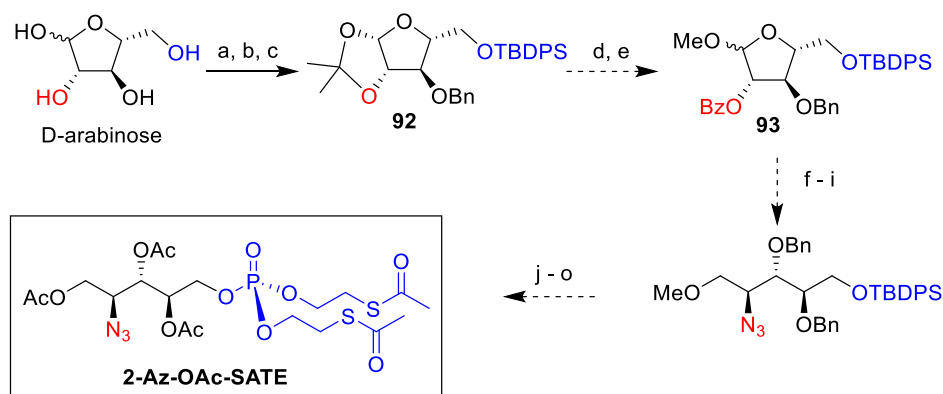
numbering of ring opened sugars is such that the site of phosphate addition is always numbered as C-5 (even if it originated from C-1 of a furanose sugar).



Scheme 54: Proposed retrosynthetic pathway from the fully protected 2-azido-ribitol probe to pentose starting materials *D*-arabinose and *D*-lyxose, *R* = protecting group. Compound numbering for ring closed and ring-open structures shown, with the sites of azide incorporation shown in red, and the sites for phosphate incorporation in blue.

The ring-open structure *D*-arabinitol (also termed *D*-lyxitol) can be formed from either *D*-lyxose or *D*-arabinose as shown (Scheme 54). Investigations into the use of *D*-arabinose were carried out together with an MChem student within the Willems group, Henrietta Amy McIntosh (referred to from now on as Amy), as detailed in Scheme 55 and Scheme 56.

Amy McIntosh^e: 2-Azido-ribitol probe route from D-arabinose



Scheme 55: Proposed synthesis of 2-azido-1,3,4-tri-O-acetyl-ribitol-5-(bis(SATE)phosphate) **Reagents and Conditions** a) TBDPSCI, dry pyridine, DMAP, r.t., 18 h, (72%) b) DMP, CSA, DCM, r.t., 16 h, (72%) c) BnBr, NaH, TBAI, THF, r.t., 16 h (90%) d) 1% HCl in MeOH, r.t., 45 min (16%) **Proposed Reagents and Conditions:** e) BzCl, pyridine, r.t. f) DIBAL-H, THF, g) BnBr, NaH, DMF, TBAI cat., h) NaOMe, MeOH, i) i) MsCl, pyridine, ii) NaN₃, DMF, j) TBAF, THF, k) PO(OEt-2Br)₃, Tf₂O, pyridine, DCM, l) KSAC, acetone, m) 1M HCl, n) BCl₃, MeOH, o) Ac₂O, pyridine, DMAP cat.

^e The synthesis detailed in Schemes 55 and 56 was conducted by Willems group MChem student Amy McIntosh

The initially proposed route, from starting sugar D-arabinose, is shown above (Scheme 55).

After protection of the primary position, the addition of an isopropylidene group across the 1- and 2-positions allowed for the protection of the remaining C-3 hydroxyl group with benzyl to give the fully protected compound **92** in an overall yield of 47% over three steps.

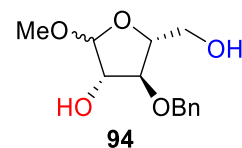
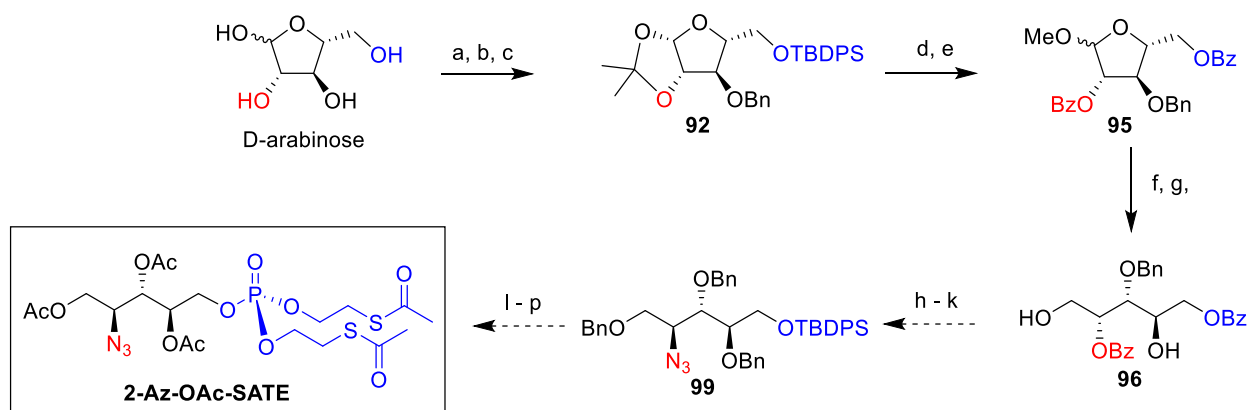


Figure 23: 1-methoxy-3-benzyl-D-arabinose side product

Once fully protected, a one-step procedure in methanol under acidic conditions was hypothesised to both cleave the isopropylidene group and allow the addition of a methoxy group at the anomeric centre by Fisher glycosylation, which would allow for the selective protection of the site of azide addition (C-2) with a benzoyl group to afford compound **93**. Unfortunately, the use of HCl in methanol for the Fisher glycosylation step in the formation of **93** was low yielding, with the desired compound formed in a yield of 19% and the major product obtained occurring from the loss of TBDPS (**94**, Figure 23). To use the formation of this product to our advantage, a new route was devised as shown below in Scheme 56.

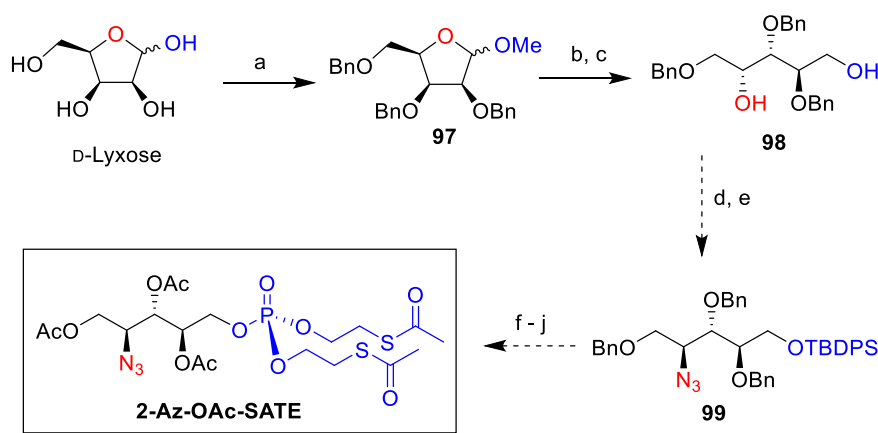


Scheme 56: Revised synthesis of 2-azido-1,3,4-tri-O-acetyl-ribitol-5-(bis(SATE)phosphate) **Reagents and Conditions** a) TBDPS-Cl, pyridine, DMAP, r.t., 18 h (72%) b) DMP, CSA, DCM, r.t., 16 h (72%) c) BnBr, NaH, TBAI, THF, r.t., 16 h (90%) d) 1% HCl in MeOH, r.t., 45 min e) BzCl, DMAP, pyridine, r.t., 72hr, f) 50% TFA, 50°C, 3hr; g) NaBH₄, EtOH, 0°C, 30min (2.5% over four steps) **Proposed Reagents and Conditions** h) BnBr, NaH, DMF, TBAI cat. i) NaOMe, MeOH, j) TBDPS-Cl, pyridine, r.t., 24 h, k) i) MsCl, pyridine, ii) NaN₃, DMF, 100°C, l) TBAF, THF, m) PO(OEt-2Br)₃, Tf₂O, pyridine, DCM, n) KSAC, acetone, o) BCl₃ MeOH, p) Ac₂O, pyridine, DMAP cat.

This alternative route utilised the doubly deprotected side-product **94** and successfully protected it with benzoyl groups at both positions to yield **95**, providing an orthogonal protecting strategy for both sites of modification. Upon removal of the methoxy group to allow for ring-opening, however, yields were very poor (2.5% over four steps (**96**)).

New Route to 2-Azido-ribitol probe route from D-Lyxose

Since Amy's route utilising D-arabinose involved more than 15 transformations and several steps in the early stages proved to be low yielding, the use of an alternative starting material was explored in order to reduce the number of steps. As stated previously (Scheme 54), the ring-opened form of D-lyxose is D-lyxitol, which has the same structure as D-arabinitol. Utilising D-lyxose, the site of azide incorporation is the ring oxygen, and the site of phosphate addition is the anomeric alcohol. New routes starting from D-lyxose could therefore harness the unique reactivity of the anomeric hydroxyl group, as well as the uncovered site of azide incorporation in the ring-closed pentose sugar, to achieve orthogonal protection (Scheme 57).

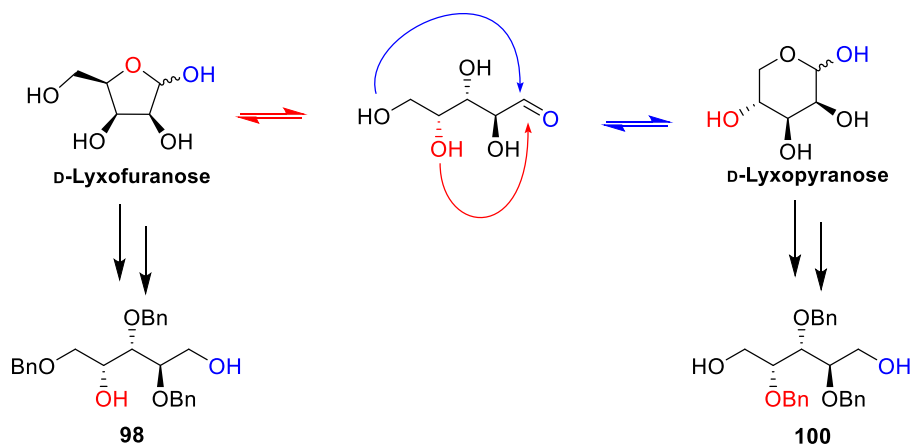


Scheme 57: New route to 2-azido-1,3,4-tri-O-acetyl-ribitol-5-(bis(SATE)phosphate) from D-lyxose **Reagents and Conditions** a) i) AcCl, MeOH, 18 h, 0°C-r.t., ii) BnBr, NaH, DMF, 0°C-r.t., 2 h (50%) b) H₂SO₄, AcOH, 100°C, 1 h, c) NaBH₄, EtOH, r.t., 5 h (8.3% over 2 steps) **Proposed Reagents and Conditions** d) TBDPS-Cl, pyridine, e) i) MsCl, pyridine, ii) NaN₃, DMF, 100°C, f) TBAF, THF g) PO(OEt-2Br)₃, Tf₂O, pyridine, DCM h) KSAc, acetone

A new approach towards formation of a ring opened intermediate was proposed following a procedure reported by van Rijssel *et al*, who utilise the intermediate **97** for the synthesis of compound **98** (Scheme 57).³⁰⁷ This can then undergo primary protection with TBDPS to allow for site-selective azidation at C-2 to yield key intermediate **99** as presented previously (Scheme 56).

Following the published procedure for the formation of **97**, a mixture of α and β forms of both pyranose and furanose conformations was seen (Scheme 58) with the major product being the β furanoside (50%). Upon ring-opening, moderate yields of ring-opened products were seen (41%), with no starting material present upon completion of the reaction. The corresponding ring-open products from the furanose and pyranose sugars could be separated by column chromatography, giving a ratio of 1:4 of desired product **98** to side product **100**, providing a yield of 8.3% for **98**. The only other sugar products detected within the ring opening reaction were decomposition products. Alternative procedures for the removal of the anomeric OMe groups proceed under less harsh conditions, using HCl in 1,4-dioxane and water at 60°C.^{308, 309} It is expected that using milder conditions in future attempts at this synthesis may prevent decomposition and lead to an increase in

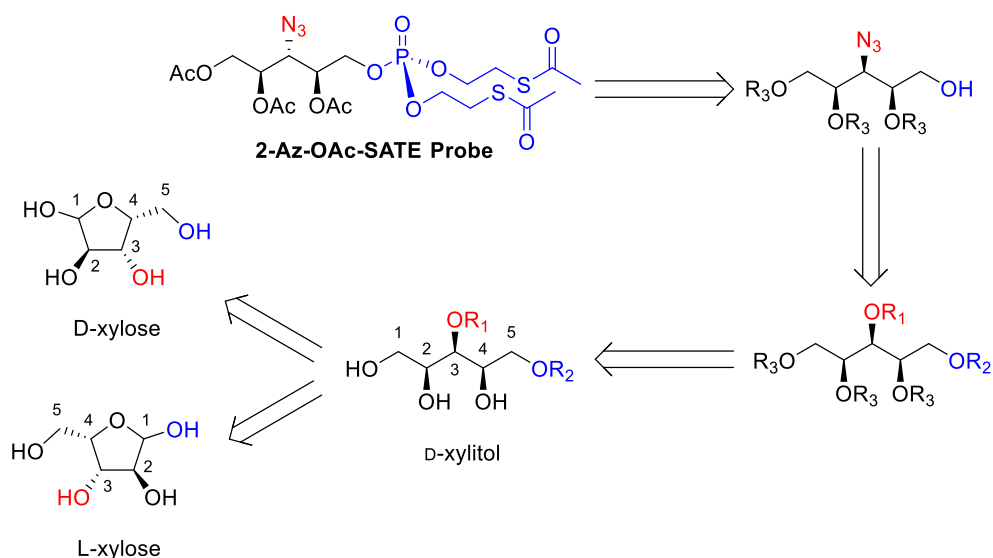
yield. Additionally, as seen in the Fischer glycosylation of glucose during the synthesis of substrates for the SATE phosphate reaction (Chapter 5, pg. 130) there is a great effect of reaction time for the Fischer glycosylation on the ratio of furanose to pyranose products, with the pyranose form greatly favoured over longer reaction times. Therefore, shorter reaction times for the initial OMe protection might help to favour the kinetic furanose product and further increase yields of the desired product.



Scheme 58: Schematic representation of the formation of both furanose and pyranose forms of D-lyxose and the corresponding ring-opened products after the reaction sequence shown in Scheme 57 (steps a-c).

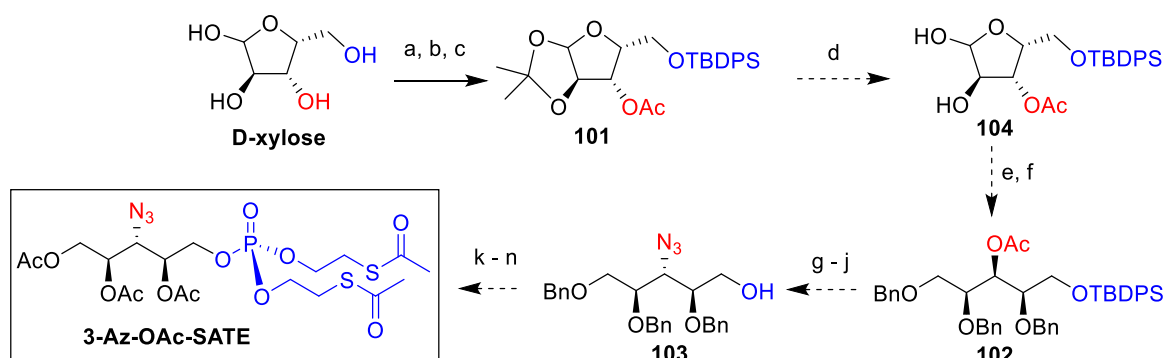
3-Azido Ribitol-5-Phosphate Probe

In a similar manner to the 2-azido probes being obtained from either D-arabinose or D-lyxose, the 3-azido probes can be obtained from D- and L-xylose. Due to its plane of symmetry, the product resulting from ring opening of both enantiomers of xylose is the same (D-xylitol, Scheme 59). Within the ring-closed starting sugars, the site of phosphate addition is either at the primary or the anomeric hydroxyl group of D- and L-xylose, respectively, while regioselective azidation of xylitol requires selective protection at either C-2 or C-3.



Scheme 59: Proposed Retrosynthetic pathway from the fully protected 3-azido-ribitol probe to pentose starting materials *D*- and *L*-xylose, *R* = protecting group. Compound numbering for ring closed and ring-open structures shown, with the sites of azide incorporation shown in red, and the sites for phosphate in blue.

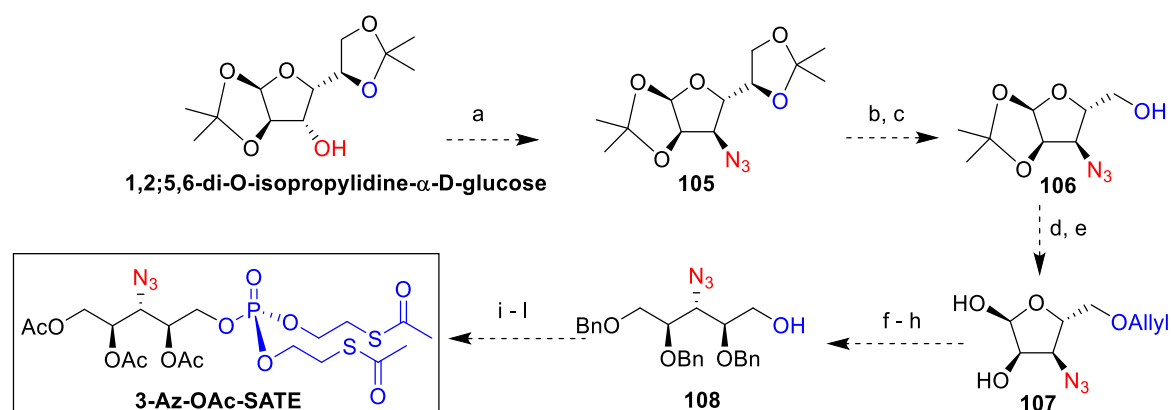
The sites of azide and phosphate addition within *L*-xylose were more difficult to selectively target with protecting groups than those in *D*-xylose, so the latter was chosen as the starting point for the synthesis of the 3-Azido probes.



Scheme 60: Synthesis of the 3-azido probes from *D*-xylose Reagents and Conditions a) TBDPSCl, pyridine, r.t., 72 h (36%) b) 2,2-DMP, *p*-TSA, acetone, r.t. 72 h (45%) c) Ac_2O , pyridine, r.t. 24 h (86%) **Proposed Reagents and Conditions** d) HCl, DCM, e) NaBH_4 , EtOH, f) BnBr , NaH, DMF, g) NaOMe, MeOH, h) i) MsCl , pyridine ii) NaN_3 , DMF, 100°C, j) TBAF, THF, 0°C-r.t., k) $\text{PO}(\text{OEt}-2\text{Br})_3$, Tf₂O, pyridine, DCM l) KSAc , acetone, m) BCl_3 , DCM, n) Ac_2O pyridine

The route from *D*-xylose proceeded with the initial protection of the primary hydroxyl group with TBDPS, protection of the 1- and 2- positions with an isopropylidene group and finally protection of the site of azide incorporation as an acetyl ester. This yielded the fully protected compound **101** with moderate to high yields for each of the 3 steps. Subsequent steps have not yet been attempted but include removal of the isopropylidene group and ring-opening, which allows all other sites to be protected with benzyl groups (**102**). Selective removal of the OAc group would then enable site-specific incorporation of azide at C-3 (**103**), and removal of the TBDPS group provides the free hydroxyl group to which a *bis*(SATE)-protected phosphate can be added to form the final probe.

Alongside the development of this route, issues with acetate migration under acidic conditions were observed (Chapter 3: Route 3b, pg. 69), which may cause issues with removal of the isopropylidene group within compound **104**. To mitigate against these effects, both the use of a benzoyl group instead of acetate, and the development of a new route that avoids the use of ester protecting groups are proposed (Scheme 61).

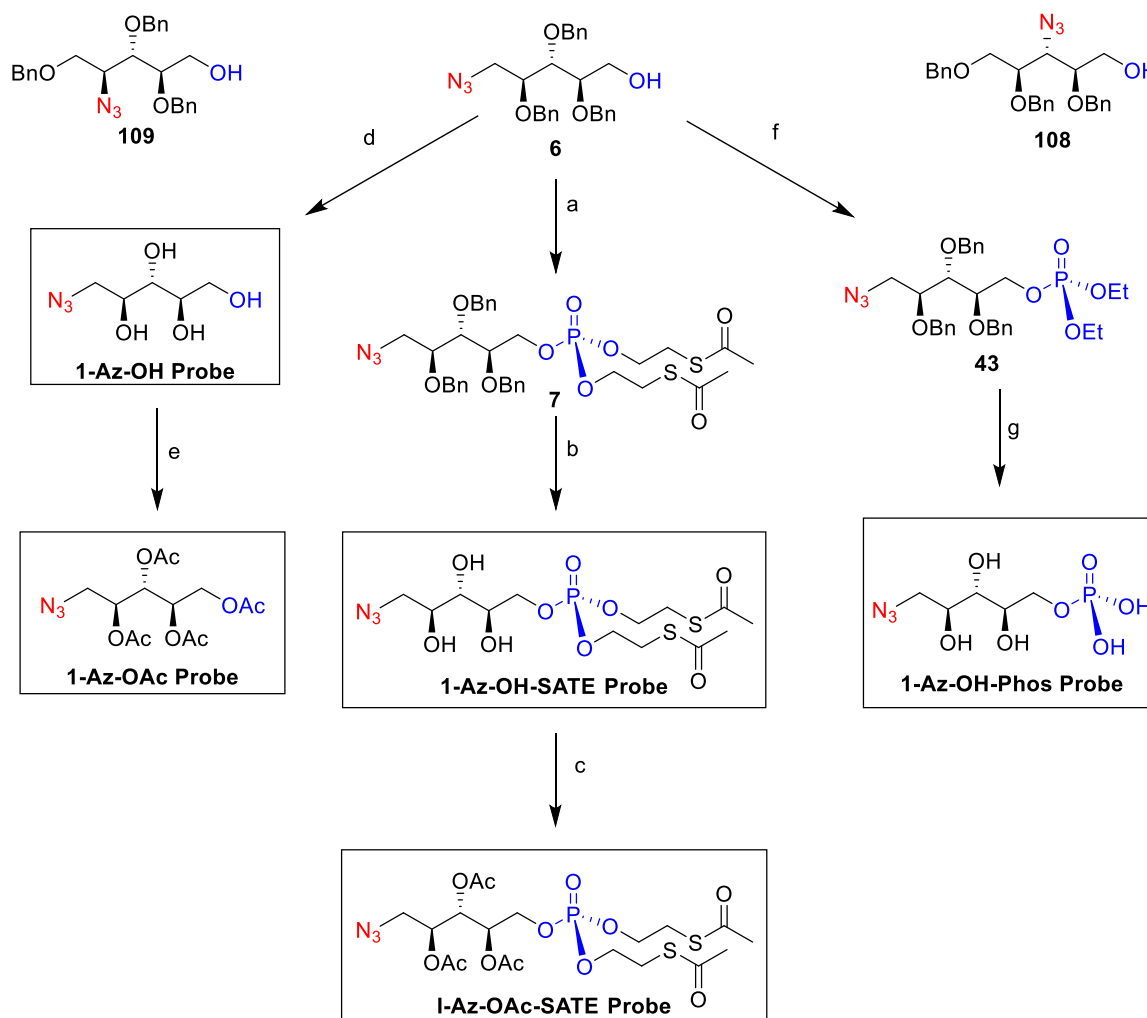


Scheme 61: **Proposed reagents and conditions** a) i) Tf₂O, pyridine, 0 °C, ii) NaN₃, DMF, r.t., b) 75% AcOH, 55 °C, 1.5 h, c) NaIO₄/H₂O, EtOH, 0 °C, 20 min then NaBH₄, d) AllylBr, NaH, DMF, e) p-TsOH, DCM, f) NaBH₄, EtOH, g) BnBr, NaH, DMF, h) PdCl₂ MeOH, i) PO(OEt-2Br)₃, Tf₂O, pyridine, DCM, j) KSAC, acetone, k) BCl₃, DCM, l) Ac₂O, pyridine

Gao *et al* in 2006 detailed the synthesis of a 3-azido-ribose derivative as an intermediate in the synthesis of modified adenosine.³⁰² Rather than proceeding from ribose or xylose, their methodology utilised the starting sugar 1,2:5,6-di-O-isopropylidene-α-D-glucose. This sugar is commercially available, and Gao *et al* were able to show the substitution of the free hydroxyl group with an azide directly onto this ring-closed sugar (**105**). Once the azide was incorporated, they were able to selectively remove the isopropylidene group across the 5- and 6-sites with acetic acid and utilise oxidative cleavage of the resulting 1,2-diol and subsequent reduction to form the ribose derivative **106**. By diverging from their route here, allyl protection of the alcohol at C-5 will give selective protection of the site of phosphate addition. Removal of the second isopropylidene group (**107**) allows for ring-opening with NaBH₄ and protection of the rest of the hydroxyl groups with benzyl groups. Selective removal of the allyl group to form **108** is then possible by the use of PdCl₂, which has been utilised previously for the successful removal of the allyl group on the regioisomeric product 5-O-Allyl-1-Azido-2,3,4-tri-O-benzyl-ribitol (Chapter 3: Synthesis of Probes from Commercially Available Starting Sugar 5-Allyl-2,3,4-tri-O-Benzyl-D-Ribitol pg. 84). From this intermediate, the route can proceed as presented previously (Scheme 60). Though this route has not been attempted yet, it is likely to be successful as the formation of compound **105** has been readily reported in literature via this method,³¹⁰⁻³¹² and past that point, all protecting group manipulations have been conducted in previous synthetic routes described in this Thesis.

Alternatively protected probes

While the strategies above have focused on the synthesis of the fully protected probes with both SATE and acetate protection, it is important to note that an array of different protecting group arrangements for *in vivo* and *in vitro* probes can be accessed by the same methodology utilised for the synthesis of the 1-azido probes (Chapter 3, pg. 55). As shown below using 1-azido compound **6** as an example, but also true for the 2- and 3-azido probe intermediates **109** and **108** respectively, the synthetic routes can diverge to give the alternatively protected probes. Debenzylation and acetylation can yield the differentially protected and non-phosphorylated azido-ribitol probes Az-OH and Az-OAc. Debenzylation after SATE addition, on the other hand, yields the partially protected Az-OH-SATE probes. Finally, the addition of an ethyl phosphate instead of SATE allows for the synthesis of the fully deprotected phosphate probes, which can be utilised for *in vitro* analysis of enzyme activity.



Scheme 62: Synthesis of final ribitol and ribitol-5-phosphate probes from key intermediate compound **6**: **Reagents and Conditions** a) i) PO(OEt-2Br)₃, Tf₂O, pyridine, DCM, ii) KSAC, acetone, (42%) b) BCl₃, DCM, -78°C, 4h, (quant.) c) Ac₂O, Pyridine, DMAP, r.t., 24h, (quant.) d) BCl₃, DCM, -78°C, 4h, (quant.) e) Ac₂O, pyridine, DMAP, r.t., 24h (quant.) f) EtO₃PO, Tf₂O, pyridine, r.t., 1.5 h, (55%) g) i) TMSBr, DCM, r.t., 16 h ii) BCl₃, DCM, -78°C, 4 h, (56% over two steps)

6.5 Conclusions

This chapter has explored the development of synthetic routes to ribitol-5-phosphate based probes that incorporate an azide at the 2- and 3- positions. A route to the 2-azido probes has been developed from the starting sugar *D*-lyxose, where the sites of azide and phosphate functionalisation are the ring-oxygen and anomeric position, respectively, in the ring-closed sugar. A key pentitol intermediate in this route, in which the sites of azide and phosphate addition are selectively deprotected, has been successfully synthesised, and the proceeding steps have been previously shown successful within previous routes. A fully protected ring-closed intermediate, in which the sites of azide and phosphate have been selectively protected with orthogonal protecting groups, has been synthesised from *D*-xylose on the route to the 3-azido probes. This route has potential for regioselectivity issues in subsequent steps due to the acetate migration, and therefore an alternative route which mitigates these issues has also been designed, based on literature precedent for the synthesis of 3-azido-ribose compounds from the starting sugar 1,2:5,6-di-*O*-isopropylidene- α -*D*-glucose.³¹⁰⁻³¹² These findings pave the way for expansion of the currently available set of azide-tagged ribitol-phosphate derivatives, which can be utilised to better understand the enzyme tolerance of FKTN, FKRP and ISPD to substrate modification and enhance the likelihood of successful incorporation of azide-tagged ribitol-phosphate into glycans.

6.6 Experimental

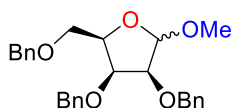
General Experimental

All reactions were conducted in oven dried glass wear under nitrogen, and where specified dry solvents used were either freshly distilled (DCM, DMF, toluene, THF) or from a SureSeal bottle, (DCE, pyridine). Flash column chromatography was run either manually with high purity 220-400 μm particle size silica (Sigma) or on an automated system (Teledyne, CombiFlash NextGen 300+) with 20 to 40 μm particle size silica (RediSep Rf Gold Normal-Phase Silica columns) here specified. Reactions and column fractions were monitored by TLC and visualised by UV and staining. For sugars, the staining consisted of charring with 10% H_2SO_4 in MeOH; and for azido compounds the procedure involved initial reaction with 10% PPh_3 in DCM, followed by staining with ninhydrin.

^1H and ^{13}C NMR spectra were obtained either on a JEOL ECS400A spectrometer (400 and 101 MHz respectively) or a Bruker AVIIIHD600 spectrometer (600 and 150 MHz respectively) where specified. Structural assignments were corroborated by homo- and heteronuclear 2D NMR methods (COSY, HMQC and DEPT) where necessary. Chemical shifts are reported in parts per million (ppm, δ) relative to the solvent (CDCl_3 , δ 7.26; CD_3OD , δ 3.31; D_2O , δ 4.79). ^1H NMR splitting patterns are designated as singlet (s), doublet (d), triplet (t), quartet (q), doublet of doublets (dd), doublet of doublets of doublets (ddd), doublet of triplets (dt), apparent triplet (apt t), and so forth. Splitting patterns that could not be visualized or easily interpreted were designated as multiplet (m). Coupling constants are reported in Hertz (Hz). Where sugar NMR data is reported in a ratio of anomers, the NMR data is assigned with integrals as whole integers corresponding to the number of protons within the peak.

IR spectra were obtained by thin film ATR on a Perkin Elmer Spectrum 2 and $[\alpha]_D$ measurements obtained on a Bellingham Stanley ADP400 polarimeter at the in the given solvent at specified concentration where $C = 1 = 10 \text{ mg/mL}$.

Compounds **92**, **93**, **94**, **95**, and **96** were synthesised by Amy McIntosh, see her MChem Thesis for experimental data and characterisation

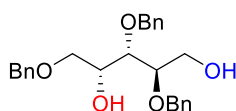


Methyl-2,3,5-tri-O-benzyl-D-lyxofuranoside (96)

To a stirring solution of D-lyxose (500 mg, 3.33 mmol, 1.00 equiv.) in MeOH (12 mL) was added AcCl (50 μ L in 2.5 mL MeOH, 0.67 mmol, 0.20 equiv.) dropwise. The resulting solution was allowed to stir overnight at RT before the reaction was neutralised with 3 M NaOH to pH 7 (approx. 0.7 mL). The resulting mixture was concentrated *in vacuo* and co-evaporated with toluene (3 x 5 mL) to afford the crude product. This crude was dissolved in dry DMF (12 mL) and cooled to 0°C. NaH (850 mg, 60% in mineral oil, 21.3 mmol, 6.4 equiv.) was added portion-wise followed by BnBr (1.6 mL, 11 mmol, 3.3 equiv.) and TBAI (cat.). After 30 mins the resulting reaction mixture was allowed to warm to RT and kept stirring for 2 hours before the reaction was quenched by the addition of MeOH (5 mL) and the solvents removed *in vacuo*. The resulting residue was dissolved in EtOAc (100 mL) and washed sequentially with 1 M HCl (100 mL), sat. aqueous NaHCO₃ solution (100 mL) and brine (100 mL). The resulting organic layer was dried over MgSO₄, filtered, and concentrated *in vacuo*. The resulting crude was purified by automated flash column chromatography (gradient 0 to 100% EtOAc in hexane) to afford the title compound as a clear oil (1.3 g, 2.9 mmol, 87%). The obtained product was a mixture of the α and β forms of Methyl-2,3,4-tri-O-benzyl-lyxopyranoside and α and β forms of Methyl-2,3,4-tri-O-benzyl-lyxofuranoside, with the major product methyl-2,3,4-tri-O-benzyl- β -D-lyxofuranoside (50%).

HRMS-ESI Calculated for [C₂₇H₃₀O₅ + Na⁺]: 457.1985, found: 457.1981 **¹H NMR** (400 MHz, CHLOROFORM-D) δ 3.38 (s, 0.7H, OCH₃), 3.42 (s, 1.5H, OCH₃), 3.48 (s, 0.3H, OCH₃), 3.52 (s, 0.4H, OCH₃), 3.57 (dd, J = 9.1, 2.5 Hz, 0.2H), 3.66 (dd, J = 6.5, 3.3 Hz, 0.15H), 3.72 – 3.91 (m, 2.2H), 3.94 (dd, J = 4.6, 2.4 Hz, 0.5H, β_{fur}), 4.00 (dt, J = 8.8, 4.2 Hz, 0.2H), 4.07 – 4.14 (m, 0.2H), 4.24 (t, J = 5.0 Hz, 0.6H, β_{fur}), 4.41 (dt, J = 7.0, 5.3 Hz, 0.5H, β_{fur}), 4.49 – 4.88 (m, 6.5H, CH₂), 5.07 (d, J = 2.5 Hz, 0.5H, β_{fur} CH-1), 7.27 – 7.48 (m, 15H, CH arom.). **¹³C NMR** (101 MHz, CHLOROFORM-D) δ 55.12 (α_{py} OCH₃), 55.65 (β_{py} OCH₃), 55.71, 56.66 (β_{fur} OCH₃), 61.02 (β_{pyr} CH-5), 61.49 (α_{py} CH-5), 69.74 (α_{fur} CH-5), 70.34 (β_{fur} CH-5), 72.15, 72.36, 72.41, 72.56, 72.74, 72.86, 73.14, 73.25, 73.29, 73.47, 73.50, 73.66 (CH₂ OBn), 73.95 (β_{pyr} CH-2), 74.76 (β_{pyr} CH-4), 74.85 (α_{py} CH-4), 75.48 (α_{py} CH-2), 77.94 (β_{fur} CH-3), 78.96 (β_{fur} CH-4), 79.28 (α_{py} CH-3), 79.31 (α_{fur} CH-2), 82.53 (β_{fur} CH-2), 99.96 (α_{py} CH-1), 100.98 (β_{pyr} CH-1), 101.40 (α_{fur} CH-1), 106.44 (β_{fur} CH-1), 127.57, 127.62, 127.65, 127.67, 127.69, 127.74, 127.79, 127.80, 127.83, 127.88, 127.90, 127.96, 127.98, 128.15, 128.18, 128.27, 128.30, 128.40, 128.43, 128.47, 137.83, 137.93, 138.15, 138.25, 138.31, 138.45, 138.49, 138.57, 138.65, 138.75 (CH arom.).

Data in accordance with literature values^{307, 313, 314}

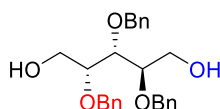


2,3,5-tri-O-benzyl-lyxofuranose (98)

To a stirring solution of methyl-2,3,5-tri-O-benzyl-lyxofuranoside and pyranoside (350 mg, 0.806 mmol, 1.00 equiv.) in acetic acid (6 mL) at RT, was added H₂SO₄ (3M in H₂O, 1.6 mL, 4.8 mmol, 5.9 equiv.). The resulting solution was heated to 100°C. After 1 h the reaction was cooled back to RT and the reaction was quenched by the addition of sat. NaHCO₃ (25 mL) and extracted with DCM (3 x 50 mL). The organic layers were combined, dried with MgSO₄, filtered and concentrated *in vacuo* to yield the crude product. The crude residue was purified by automated flash column chromatography (0 to 50% EtOAc in hexane) to yield the desired product as a clear oil (67 mg, 0.18 mmol, 22%). This intermediate product was dissolved in EtOH (1.6 mL) and cooled to 0°C. NaBH₄ (20 mg, 0.54 mmol, 3.0 equiv.) was added and the resulting reaction mixture was warmed to RT. After 5 hours the reaction was quenched by the addition of acetic acid (0.1 mL) and the solvents were removed *in vacuo*. The resulting residue was dissolved in EtOAc (25 mL) and washed with 1 M HCl (20 mL), sat. NaHCO₃ (20 mL) and brine (20 mL). The resulting organic layer was dried with MgSO₄ and the solvents were removed *in vacuo* to yield the crude product. The crude product was purified by automated flash column chromatography (0 to 60% EtOAc in hexane) to afford the title compound as a clear oil (6.7 mg, 15 μ mol, 8.3%) alongside the major product 2,3,4-tri-O-benzyl-D-lyxitol (26 mg, 60 μ mol, 33%)

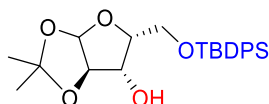
HRMS-ESI Calculated for $[C_{26}H_{30}O_5 + Na^+]$: 445.1985, found: 445.1990. **1H NMR** (400 MHz, CHLOROFORM-*D*) δ 2.11 (s, 1H, OH), 3.47 (dd, $J = 9.6, 6.0$ Hz, 1H, CH-5), 3.55 (dd, $J = 9.4, 6.2$ Hz, 1H, CH-5'), 3.67 – 3.93 (m, 4H, CH-1, CH-1', CH-2, CH-3), 3.98 – 4.05 (m, 1H, CH-4), 4.44 – 4.57 (m, 3H, CH₂ OBn), 4.63 (s, 2H, CH₂ OBn), 4.74 (d, $J = 11.0$ Hz, 1H, CH₂ OBn), 7.24 – 7.40 (m, 16H, CH arom.). **^{13}C NMR** (101 MHz, CHLOROFORM-*D*) δ 60.65 (CH-1), 69.87 (CH-4), 71.40 (CH-5), 72.56, 73.59, 74.56 (CH₂ OBn), 77.36 (CH-3), 79.67 (CH-2), 127.98, 128.06, 128.11, 128.41, 128.61, 128.70, 129.91, 137.97. (CH arom.)

Data in accordance with literature values³⁰⁷



2,3,4-tri-O-benzyl-D-lyxitol (100)

1H NMR (400 MHz, CHLOROFORM-*D*) δ 3.68 – 3.81 (m, 5H), 3.82 – 3.87 (m, 1H), 3.89 (dd, $J = 12.1, 4.4$ Hz, 1H), 7.27 – 7.40 (m, 15H, CH arom.). **^{13}C NMR** (101 MHz, CHLOROFORM-*D*) δ 60.73, 61.36 (CH-1, CH-5), 72.10, 72.75, 74.34 (CH₂ OBn), 78.89 (CH-3), 79.16, 79.36 (CH-2, CH-4), 127.94, 128.02, 128.12, 128.39, 128.45, 128.62, 128.66, 137.92, 137.98, 138.13 (CH arom.).

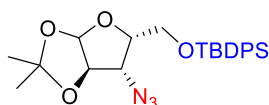


5-O-tert-butylidiphenylsilyl-1,2-O-isopropylidene- α -D-xylofuranose

To a stirring solution of D-xylose (3.3 g, 20 mmol, 1.0 equiv.) in dry pyridine (60 mL) at 0°C was added TBDPS-Cl (5.2 mL, 27 mmol, 1.4 equiv.). The resulting solution was allowed to warm to RT and stirred for 72 h before the reaction was quenched by the addition of MeOH (5 mL). The solvents were removed *in vacuo*, and the resulting residue co-evaporated with toluene (3 x 10 mL). The crude product was dissolved in DCM (100 mL) and washed with 1 M HCl (100 mL), sat. aqueous NaHCO₃ solution (100 mL) and brine (100 mL), dried over MgSO₄, filtered, and the solvents removed *in vacuo*. The crude product was purified by automated flash column chromatography (0 to 60% EtOAc in hexane) to afford the TBDPS protected intermediate as a yellow oil (3.1 g, 7.4 mmol, 36%). To half of this intermediate product (1.6 g, 4.1 mmol, 1.0 equiv.) in acetone (30 mL) at 0°C was added TsOH (76 mg, 0.41 mmol, 0.10 equiv.) and 2,2-DMP (1 mL, 8.3 mmol, 2.0 equiv.). The resulting solution was warmed to RT and left stirring for 3.5 h before the reaction was quenched by the addition of NEt₃ (1 mL). The solvents were removed *in vacuo*, and the crude product was subjected to automated flash column chromatography (gradient 0-60% EtOAc in hexane) to yield the pure product as a clear solid (780 mg, 1.8 mmol, 44%, 15% over two steps)

HRMS-ESI Calculated for $[C_{24}H_{32}O_5 + Na^+]$: 451.1911, found: 451.1909. **1H NMR** (400 MHz, CHLOROFORM-*D*) δ 1.05 (s, 9H, C(CH₃)₃ TBDPS), 1.33 (s, 3H, CH₃ *i*Pr), 1.47 (s, 3H, CH₃ *i*Pr), 4.05 – 4.17 (m, 3H, CH-5, CH-3), 4.37 (d, $J = 3.2$ Hz, 1H, CH-4), 4.55 (d, $J = 3.7$ Hz, 1H, CH-2), 6.01 (d, $J = 3.7$ Hz, 1H, CH-1), 7.33 – 7.49 (m, 6H, CH arom.), 7.63 – 7.74 (m, 4H, CH arom.). **^{13}C NMR** (101 MHz, CHLOROFORM-*D*) δ 19.18 (C(CH₃)₃ TBDPS), 26.30, 26.80 (CH₃ *i*Pr), 26.91 (C(CH₃ TBDPS), 62.91 (CH-5), 76.97 (CH-4), 78.50 (CH-3), 85.56 (CH-2), 105.11 (CH-1), 111.63 (C(CH₃)₂), 127.85, 127.90, 128.02, 128.05, 130.18, 132.02, 132.56, 135.62, 135.75, 135.82 (CH arom.)

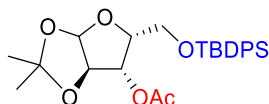
Data in accordance with literature values³¹⁵



Attempted synthesis of 3-azido-5-O-tert-butylidiphenylsilyl-1,2-O-isopropylidene- α -D-xylofuranose

To a stirring solution of 5-O-tert-Butyl (diphenyl)silyl-1,2-O-isopropylidene-D-xylofuranose (172 mg, 0.402 mmol, 1.00 equiv.) in dry pyridine (1 mL) at 0°C, was added TsCl (86 mg, 0.45 mmol, 1.1 equiv.). After 2 h at 0°C, the reaction was warmed to RT and allowed to react for 18 h. The solvents were removed *in vacuo* and

the crude was co-evaporated with toluene (3 x 2 mL). The resulting residue was suspended in 1M HCl (50 mL), extracted with EtOAc (3 x 50 mL), dried over MgSO₄, filtered and concentrated *in vacuo*. The resulting tosylate intermediate was dissolved in dry DMF (2 mL) and NaN₃ (33 mg, 0.5 mmol, 1.3 equiv.) was added. The resulting solution was warmed to 80°C for 24 h before cooling back down to RT. No evidence of azide containing sugar seen by crude ESI-MS analysis or ¹H NMR.



3-acetyl-5-*O*-*tert*-butyldiphenylsilyl-1,2-*O*-isopropylidene- α -D-xylose (101)

To a stirring solution of 5-*O*-*tert*-Butyl(diphenyl)silyl-1,2-*O*-isopropylidene-D-xylofuranose (1.4 g, 3.3 mmol, 1.0 equiv.) in dry pyridine (11 mL) at 0°C was added acetic anhydride (1.7 mL, 6.5 mmol, 2.0 equiv.). The resulting solution was allowed to warm to RT and left for 18 h before the solvents were removed *in vacuo* and the residue was co-evaporated with toluene (3 x 20 mL). The resulting residue was dissolved in EtOAc (100 mL) and sequentially washed with 1M HCl (30 mL), sat. aqueous NaHCO₃ solution (30 mL) and brine (30 mL), dried over MgSO₄, filtered and concentrated *in vacuo*. The resulting crude product was purified by manual flash column chromatography (gradient 0 to 60% EtOAc in hexane) to yield the product as a clear oil (1.3 g, 2.8 mmol, 86%)

HRMS-ESI Calculated for C₂₆H₃₄O₆ + Na: 493.2017, found: 493.2009. **¹H NMR** (400 MHz, CHLOROFORM-*D*) δ 1.04 (s, 9H, C(CH₃)₃ TBDPS), 1.32 (s, 3H, CH₃ *i*Pr), 1.53 (s, 3H, CH₃ *i*Pr), 1.97 (s, 3H, CH₃ OAc), 3.81 (dd, *J* = 10.1, 8.0 Hz, 1H, CH-5), 3.89 (dd, *J* = 10.1, 5.5 Hz, 1H, CH-5'), 4.44 (ddd, *J* = 8.0, 5.5, 3.2 Hz, 1H, CH-4), 4.51 (d, *J* = 4.1 Hz, 1H, CH-2), 5.33 (d, *J* = 3.2 Hz, 1H CH-3), 5.88 (d, *J* = 3.7 Hz, 1H, CH-1), 7.34 – 7.47 (m, 6H, CH arom.), 7.64 (dt, *J* = 7.8, 1.4 Hz, 4H, CH arom.). **¹³C NMR** (101 MHz, CHLOROFORM-*D*) δ 19.24 (C(CH₃)₃ TBDPS), 20.81 (CH₃ OAc), 22.77, 26.36, 26.83 (C(CH₃)₂ *i*Pr), 60.51 (CH-5), 75.97 (CH-4), 79.12 (CH-3), 83.44 (CH-2), 104.93 (CH-1), 112.25 (C(CH₃)₂), 127.86, 129.92, 133.20, 133.27, 135.65, 135.67, 135.88 (CH arom.), 169.83 (C=O OAc).

6.7 References

111. B. W. Zaro, Y. Y. Yang, H. C. Hang and M. R. Pratt, *Proc. Natl. Acad. Sci. U. S. A.*, 2011, **108**, 8146-8151.
112. A. R. Batt, B. W. Zaro, M. X. Navarro and M. R. Pratt, *Chembiochem*, 2017, **18**, 1177-1182.
113. M. Boyce, I. S. Carrico, A. S. Ganguli, S. H. Yu, M. J. Hangauer, S. C. Hubbard, J. J. Kohler and C. R. Bertozzi, *Proc. Natl. Acad. Sci. U. S. A.*, 2011, **108**, 3141-3146.
117. R. Xie, L. Dong, Y. Du, Y. Zhu, R. Hua, C. Zhang and X. Chen, *Proc. Natl. Acad. Sci. U. S. A.*, 2016, **113**, 5173-5178.
302. Z.-G. Gao, H. T. Duong, T. Sonina, S.-K. Kim, P. Van Rompaey, S. Van Calenbergh, L. Mamedova, H. O. Kim, M. J. Kim, A. Y. Kim, B. T. Liang, L. S. Jeong and K. A. Jacobson, *J. Med. Chem.*, 2006, **49**, 2689-2702.
303. B. Cheng, L. Dong, Y. Zhu, R. Huang, Y. Sun, Q. You, Q. Song, J. C. Paton, A. W. Paton and X. Chen, *ACS Chem. Biol.*, 2019, **14**, 2141-2147.
304. C. Y. Jao, M. Roth, R. Welti and A. Salic, *Proc. Natl. Acad. Sci. U S A*, 2009, **106**, 15332-15337.
305. A. Dixit, G. P. Jose, C. Shanbhag, N. Tagad and J. Kalia, 2022, DOI: bioRxiv doi:10.1101/2022.03.31.486572.
306. Y. Li, S. Kinting, S. Hoppner, M. E. Forstner, O. Uhl, B. Koletzko and M. Griese, *Biochim. Biophys. Acta. Mol. Cell. Biol. Lipids*, 2019, **1864**, 158516.
307. E. R. van Rijssel, T. P. M. Goumans, G. Lodder, H. S. Overkleeft, G. A. van der Marel and J. D. C. Codée, *Org. Lett.*, 2013, **15**, 3026-3029.
308. A. H. Viuff and H. H. Jensen, *Org. Biomol. Chem.*, 2016, **14**, 8545-8556.
309. T. Wennekes, K. M. Bongers, K. Vogel, R. J. B. H. N. van den Berg, A. Strijland, W. E. Donker-Koopman, J. M. F. G. Aerts, G. A. van der Marel and H. S. Overkleeft, *Eur. J. Org. Chem.*, 2012, **2012**, 6420-6454.
310. S. K. Maurya and R. Rana, *Beilstein J. Org. Chem.*, 2017, **13**, 1106-1118.
311. E. Raluy, O. Pàmies and M. Diéguez, *Adv. Synth. Catal.*, 2009, **351**, 1648-1670.
312. F. John and V. Wittmann, *J. Org. Chem.*, 2015, **80**, 7477-7485.
313. S. Li, J. Jaszczyk, X. Pannecoucke, T. Poisson, O. R. Martin and C. Nicolas, *Adv. Synth. Catal.*, 2020, **363**, 470-483.
314. S. N. Dhawan, T. L. Chick and W. J. Goux, *Carbohydr. Res.*, 1988, **172**, 297-307.
315. O. Baszczyński, J. M. Watt, M. D. Rozewitz, A. H. Guse, R. Fliegert and B. V. L. Potter, *J. Org. Chem.*, 2019, **84**, 6143-6157.

Chapter 7: Summary and Future Work

7.1 Summary

α -dystroglycan is a cell-surface protein which provides essential links between the extracellular matrix and the cytoskeleton through interactions between *O*-linked glycans on α -dystroglycan, and extracellular proteins involved in regulating tissue architecture and signalling pathways. Some of these binding interactions are essential for maintaining muscle integrity and, as a result, loss of these binding interactions causes a subset of muscular dystrophies named dystroglycanopathies.¹⁻³ The unit responsible for binding to the extracellular matrix proteins is a linear polysaccharide – named matriglycan – which is linked to the core glycan by two ribitol-5-phosphate units.^{39, 44, 45} Loss of activity of any of the enzymes responsible for forming the tandem ribitol-5-phosphate linker is known to cause α -dystroglycanopathies, so better understanding how cells utilise and process ribitol-5-phosphate will aid in further understanding these disorders.

Currently the only known occurrence of ribitol-5-phosphate within mammalian cells is in the matriglycan-carrying glycan of α -DG. This presents ribitol-5-phosphate as a unique target for cellular studies of this glycan. By metabolic incorporation of modified ribitol-5-phosphate analogues, we hypothesise being able to effectively identify the localisation and levels of functionally glycosylated α -dystroglycan, and at the same time identify potential other ribitol-5-phosphate containing cell-surface glycans.

This Thesis has explored the synthesis of a panel of azido-D-ribitol-5-phosphate derived metabolic labelling probes, with various degrees of protection to enable biological testing both *in vivo* and *in vitro*. In Chapter 3, a 12-step synthetic route to the fully-protected 1-azido probe has been developed from the starting sugar D-ribose. This synthesis involves a key tetrabenzylated, 1-deoxy-1-azido intermediate from which the primary benzyl group can be selectively removed to enable subsequent phosphate installation. In addition, it was shown that a shorter, higher-yielding, route from commercially available 5-allyl-2,3,4-tri-O-benzyl-ribitol allows a faster, more efficient method for large-scale synthesis of the final probes. The method development and protecting group manipulations discovered within these synthetic routes also aided in the development of synthetic routes to 2- and 3-azido-D-ribitol-5-phosphate probes from the starting sugars D-lyxose and D-xylose respectively (Chapter 6). Because of the differences in reactivity and regioselectivity required for azide substitution at the secondary hydroxyl groups of the 2- and 3- azido probes, compared to the primary site leading to the 1-azido-probes, the synthetic routes utilised different protecting group strategies and manipulations such as the use of isopropylidene and allyl groups, in addition to anomeric selective Fischer glycosylation. An alternative strategy to the 3-azido-probes has also been

designed based on literature precedent for the synthesis of 3-azido-ribose compounds from the starting sugar 1,2:5,6-di-*O*-isopropylidene- α -D-glucose.³¹⁰⁻³¹²

The key challenge in the synthesis of D-ribitol-5-phosphate probes was the incorporation of the *bis*(SATE)phosphate group, which was overcome by the development of a new methodology for the synthesis of protected carbohydrate phosphates (Chapter 4). Adapted from Huang and co-workers' methodology, the newly developed 2-step approach utilises an easy-to-access phosphotriester starting material, *tris*(2-bromoethyl)phosphate. Mono-substitution of one of the bromoethyl groups by the free hydroxyl group of a partially protected carbohydrate substrate, followed by efficient substitution of the remaining bromines with potassium thioacetate, yields the SATE-protected phosphorylated product. This methodology avoids the use of highly hazardous, difficult to isolate dichlorophosphine intermediates, while the improved stability of the 2-bromoethylphosphates allows for straightforward isolation and storage of intermediates.

Thorough optimisation of this methodology was performed to increase the yield of the reaction on the 1-azido-ribitol substrate from 11% to 48% (Chapter 5). The major sugar by-product of the reaction has been identified as the corresponding triflated ribitol species, which can be converted back to the free alcohol by treatment with sodium hydroxide to recover precious starting materials. The novel SATE methodology was shown to be compatible with a wide range of substrates, including glucose substrates to which a SATE-protected phosphate was added at the 6- and 1-positions, tyramine derivatives, and a GlcNAc-based metabolic labelling probe previously described in literature.¹³⁸ Furthermore, compatibility with a wide range of both hydroxyl and amine protecting groups has been shown, showcasing the significance of this new methodology in a wider chemical biology and medicinal chemistry context, where SATE-protected phosphotriesters are commonly used for metabolic labelling and as prodrugs, respectively.

7.2 Future Work

Biological Testing: *in vivo* Analysis

Having completed the synthesis of a panel of 1-azido-ribitol-5-phosphate probes, future work will initially focus on the biological testing of the probes both *in vivo* and *in vitro*. *In vivo* testing will utilise the fully and semi-protected ribitol and ribitol-5-phosphate analogues, which to aid cell permeability possess a combination of acetate protection of hydroxyl groups and S-acetyl-2-thioethyl (SATE) groups for phosphate protection. Once taken up into the cell, these groups are cleaved unveiling the deprotected ribitol-5-phosphate probes for uptake into the biosynthetic pathway for *O*-mannosylation of α -DG.

Initial analysis of azide-tagged biomolecules can take place following the treatment of cultured, immortalised human cell lines with the probes and cell lysis (Figure 24). Once the cell is lysed, copper-catalysed click chemistry can be utilised (as the cytotoxicity of copper(I) is no longer an issue) for labelling with an alkyne reagent carrying either a fluorescent tag or a biotin affinity tag. Labelling with a fluorescent tag such as Cy3 or AlexaFluor allows for the direct fluorescent imaging of the labelled biomolecules by Sodium Dodecyl Sulphate–PolyAcrylamide Gel Electrophoresis (SDS-PAGE). Conversely, biotin-containing alkynes allow for the enrichment of labelled materials by the use of streptavidin beads which allows the capture and subsequent release of biotinylated molecules. Once separated, the enriched glycoproteins can undergo MS/MS analysis to confirm their identity. Additionally, upon glycan release and fragmentation, glycan composition can be characterised.

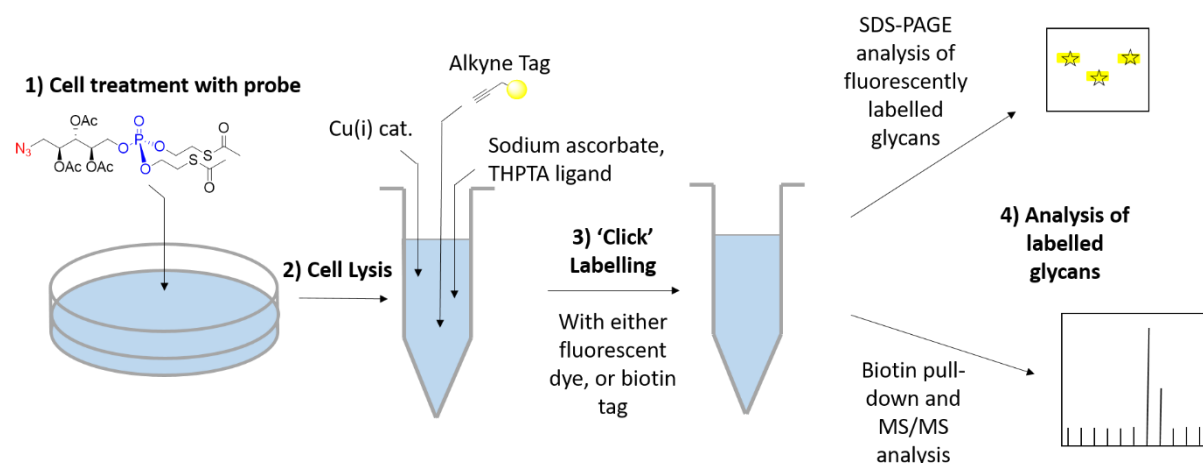


Figure 24: Overview of *in vivo* metabolic incorporation of 1-azido-ribitol-5-phosphate: 1) upon uptake of the probe into cells, the protecting groups are cleaved by non-specific esterase and lipase activity releasing the free probe for incorporation into enzymatic pathways, 2) cell lysis is conducted breaking down the cell membrane, 3) copper(I) catalysed azide-alkyne cycloaddition (CuAAC) labelling allows the conjugation of a fluorescent or biotin tag, 4) labelled biomolecules can be characterised by either SDS-PAGE or MS/MS analysis following the conjugation of a fluorescent or biotin tag respectively. Cat. = catalyst, THPTA = tris(benzyltriazolylmethyl)amine

By incorporation of an azide moiety into the metabolic labelling probe the ring-strain promoted copper-free click reaction, in which the reaction is catalysed by the relief of ring strain from a cyclo-octyne group, can also be utilised. The lack of copper catalyst means this reaction can be run on the surface of living cells, allowing for the direct visualisation of labelled D-ribose-5-phosphate within cell-surface glycans through conjugation with a fluorescent tag.

Successful incorporation of azide labelled ribitol-5-phosphate onto α -DG in wild-type cultured cells will confirm the presence of this unique sugar within the glycoprotein's glycans, which up until now has only been demonstrated after overexpression of α -DG.^{39, 44, 45} If labelling is specific to the core M3 O-mannosyl glycan, the use of ribitol-derived metabolic labelling probes will provide us with an efficient method for selective and covalent labelling of this glycan, providing an advantage over current methods that rely on the use of low affinity and less specific anti- α -DG antibodies. The specific labelling of functional α -DG will also provide a tool for the study of healthy vs diseased cells, where the effects of mutations in genes of the core M3 O-mannosyl biosynthesis pathway on the level of functional α -DG glycosylation can be studied. Alternatively, there is a possibility that these metabolic labelling probes will label additional glycans in which ribitol-5-phosphate may be present, allowing for potential identification of as yet unknown glycoconjugate structures and providing further insight into the role of this sugar in mammalian glycans. Ribitol-based non-phosphorylated probes will also be tested to provide insight into the as-of-yet-unknown biosynthesis of ribitol-5-phosphate within mammalian cells. If successful, these probes provide an easier-to-synthesise target for future generations of ribitol-based metabolic labelling probes.

Biological Testing: *in vitro* Analysis

As well as *in vivo* analysis, the fully deprotected ribitol-phosphate probe allows for the analysis of the tolerance of ISPD, FKTN and FKRP to the 1-azido modification *in vitro*. These tests can be run by incubation of the recombinant enzyme of interest, produced by overexpression and purification of a HIS-tagged protein construct in mammalian cells,^{44, 66} with their respective modified substrates. ISPD reactions will further require the co-factor CTP, while the product of the ISPD reaction provides the CDP-activated substrate for FKTN and FKRP and acceptor substrates for FKTN and FKRP can be accessed either commercially or through chemical synthesis (Figure 25).^{44, 66} The corresponding tagged products can then be analysed by MALDI-MS or LCMS analysis. In addition to *in vitro* testing allowing troubleshooting of the tolerance of the enzymes to the 1-azido modification, this also allows the enzyme kinetics of this modified substrate to be compared to the natural ribitol-5-phosphate substrate. It is important to note that azido modification at the 1-position of ribitol-5-

phosphate will prevent further extension by FKRP after its incorporation onto the Core M3 glycan by FKTN. Alternative probes, where incorporation of azide occurs at the 2- or 3- position, and for which determination of suitable synthetic routes has begun (see Chapter 6), will circumvent this issue, and potentially lead to higher labelling efficiency.

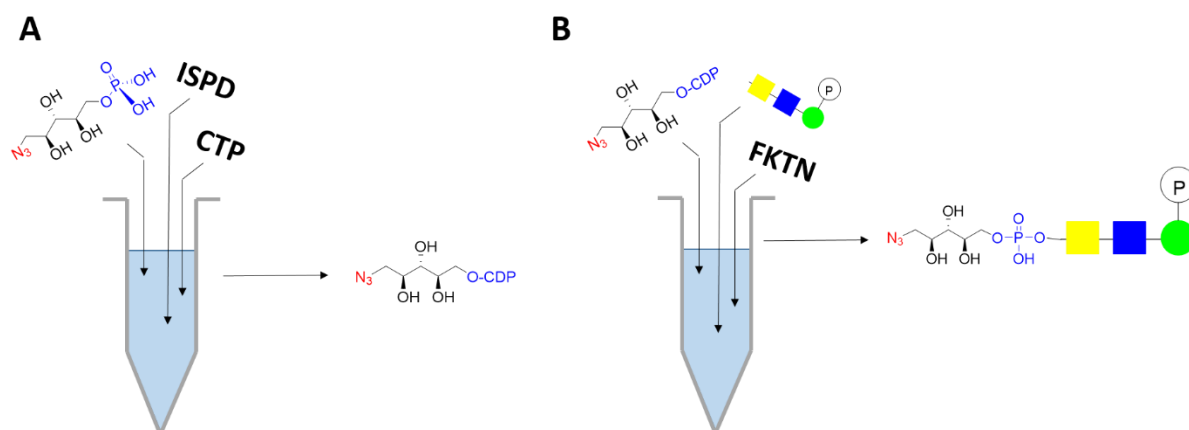


Figure 25: Schematic representation of the *in vitro* studies of modified ribitol-5-phosphate, showing the conversion of ribitol-5-phosphate into CDP-ribitol by ISPD and B) the modification of a core M3 trisaccharide with ribitol-5-phosphate by FKTN, using the ISPD reaction product CDP-ribitol as a donor.

Future Probe Generations

Further insight into the tolerance of the relevant enzymes, *ISPD*, *FKTN*, and *FKRP* towards modification can be obtained by the synthesis and biological testing of the 2- and 3-azido-D-ribitol-5-phosphate probes following the previously designed synthetic routes (Chapter 6). In addition to the panel of azido probes, a similarly-structured panel of metabolic labelling probes which utilise alkyne tags may also be beneficial (Figure 26A). Alkyne tags are smaller than the azide, and are uncharged so may be better tolerated by the enzyme active site than azido modification, though the non-strained alkynes prevent the use of copper-free azide-alkyne cycloaddition for live cell-surface labelling. Propargyl ethers also offer an alternative strategy to incorporate alkyne tags for metabolic labelling as they keep the hydroxyl group oxygen intact and are synthetically more easily accessible than probes requiring the substitution of hydroxyl groups with an azide (Figure 26B). Furthermore propargyl ethers have also been utilised within literature for click labelling when incorporated on phosphate.³¹⁶ This offers a further alternative site of label incorporation should the 1-, 2-, and 3-, sites be intolerant of modification.

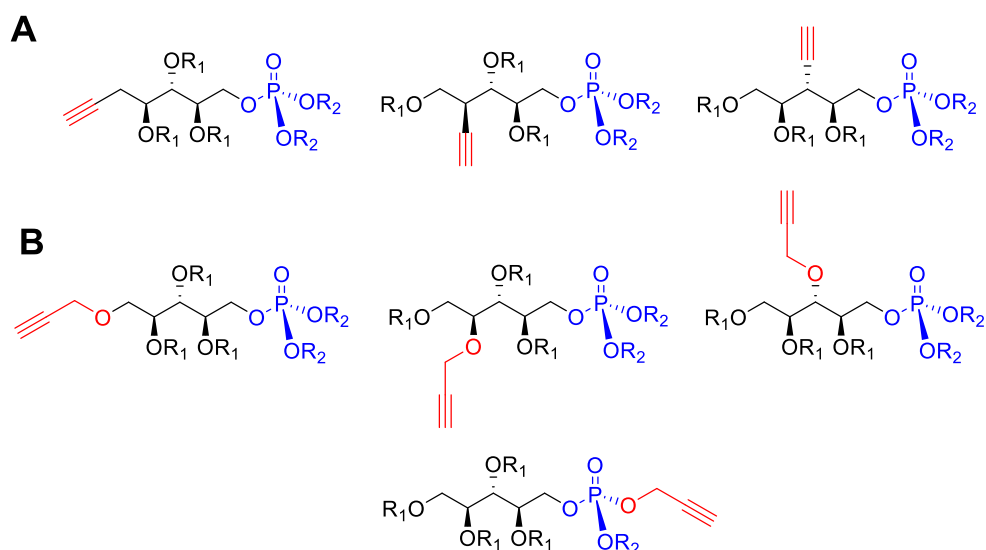


Figure 26: Proposed structures for additional panels of ribitol-5-phosphate metabolic labelling probes: A) alkyne labelled probes B) propargyl ether labelled probes, including alternative site of label incorporation on the phosphate. For *in vivo* probes $R_1 = \text{OAc}$ and $R_2 = \text{SATE}$, for *in vitro* probes $R_1 = R_2 = \text{OH}$

As well as expanding the metabolic labelling work undertaken within this Thesis, future ribitol-based compounds can be developed which aim to act as activity-based probes. Activity based probes (ABPs) are highly selective, mechanism-based enzyme probes that are able to reveal further insight into enzyme-substrate interactions and aid in elucidating enzyme mechanisms, as well as providing tools for the direct covalent labelling of catalytically active enzymes.³¹⁷ The data obtained from metabolic labelling studies regarding the tolerance of the enzymes acting on ribitol-phosphate can help to guide the design of ribitol-based activity-based probes and enzyme inhibitors.

The active site of FKTN is yet to be elucidated, and the catalytic mechanism of both FKTN and FKRP remains unknown. Therefore the design of activity-based probes that target the active site of FKTN and FKRP is both challenging and potentially of great value to the research community. With FKTN and FKRP responsible for the transfer of ribitol-5-phosphate from a CDP-ribitol donor, inhibitors that intervene with donor binding can be designed (Figure 27). Phosphonates and phosphorothioates,³¹⁸ in which phosphate group oxygen atoms are replaced by carbon or sulfur respectively, mimic the phosphate group structure but cannot function as enzyme substrates, thereby acting as inhibitors. Similarly, fully substituting the phosphate for a phosphate mimick such as a vinyl sulphone/sulphonate has been shown to yield successful inhibitors for different enzymes.^{319, 320} Acrylamides are commonly utilised as inhibitors in ABPs,³¹⁷ so incorporation of a structurally similar acrylate group may act similarly within a ribitol-based probe.

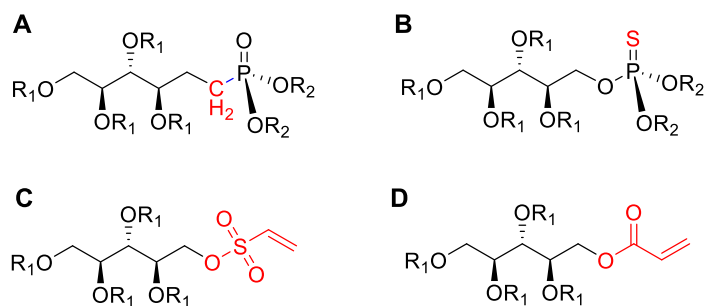


Figure 27: Proposed activity-based probes and inhibitors of FKTN and FKRP utilising A) phosphonate, B) phosphothionate C) vinyl sulphone and D) acrylate groups. For *in vivo* probes $R_1 = \text{OAc}$ $R_2 = \text{SATE}$, for *in vitro* $R_1 = R_2 = \text{OH}$

The phenotypic and symptomatic diversity of muscular dystrophy and associated dystroglycanopathies means that the ability to utilise a combination of both metabolic labelling probes and activity-based probes for the efficient detection of problems with *ISPD*, *FKTN* or *FKRP* activity will speed up the diagnosis of disorders caused by mutations in the corresponding genes. The development of more targeted future generations of probes will aid in achieving a better understanding of the action of these enzymes, and will increase our knowledge base for the development of therapies for the associated dystroglycanopathies. Furthermore, dosing with ribitol and CDP-ribitol has been proposed for the treatment of patients exhibiting *ISPD* deficiency.^{45, 52} Utilising metabolic labelling probes to better understand the fates of ribitol and its CDP-derivative in cells, by detecting any additional sites of ribitol or ribitol-5-phosphate modification within the cell, as well as potential side-effects from elevated dosing, will better inform the suitability of this therapy for the treatment of muscular dystrophies.

Phosphate Future Work

In addition to the design, synthesis and use of metabolic labelling probes, further work can also be undertaken to further develop the new SATE synthesis methodology. In this Thesis, the incorporation of SATE phosphates via this methodology onto the anomeric site of protected glucose derivatives has been described, though further investigation into the optimised reaction length for this reaction is yet to be conducted. Furthermore, the anomeric ratios obtained by this method for the varying protecting groups deserves further investigation to be able to fully rationalise the anomeric preference of this reaction. In addition to further work on anomeric glucose derivatives, further work should also investigate the optimisation of the methodology on the glucosamine substrates. All three of the unsuccessful derivatives possessed an *N*-acyl group, so a test of the reaction on a simpler substrate such as *N*-Acetylated-tyramine (Figure 28) will confirm whether this group itself is incompatible with the reaction conditions or whether the observed

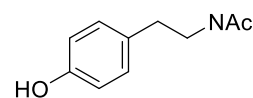


Figure 28: NAc-tyramine on which the compatibility of NAc groups within the SATE methodology can be tested

issues are specific to the hexosamine substrates. Though a large scope of different protecting groups and structures have been investigated, the applicability of the new methodology to SATE protected nucleotides, which have been synthesised by other methods within literature,¹⁷³ would be of interest to investigate. As well as alternative structures, this substrate class also provides the ability to demonstrate the compatibility of isopropylidene groups in the reaction, while unprotected nucleotides allow for the comparison of primary vs secondary alcohol selectivity (Figure 29).

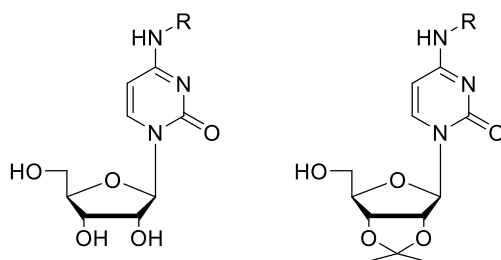


Figure 29: Examples of cytidine structures of interest for the testing of the SATE phosphate synthesis on nucleotides. R = Fmoc or CBz

Another avenue for investigation into the SATE methodology includes the investigation of the applicability of this method to the use of tris(2-chloroethyl)phosphate. Use of this commercially available low-cost phosphate intermediate negates the need to synthesise the bromo intermediate in-house, further increasing safety by negating the use of phosphorous oxychloride, and increasing the accessibility and appeal of this methodology to a wider audience.

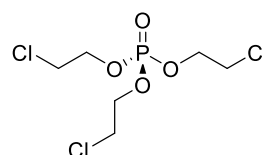
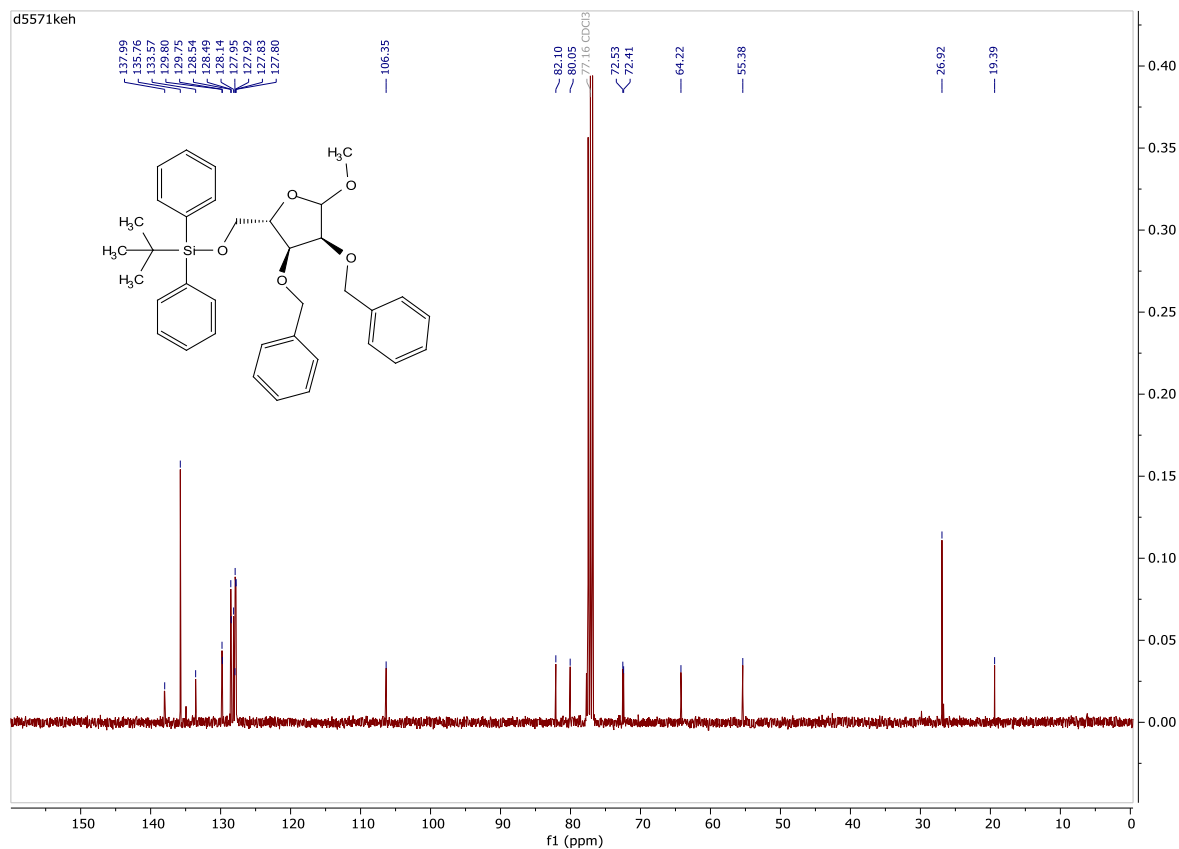
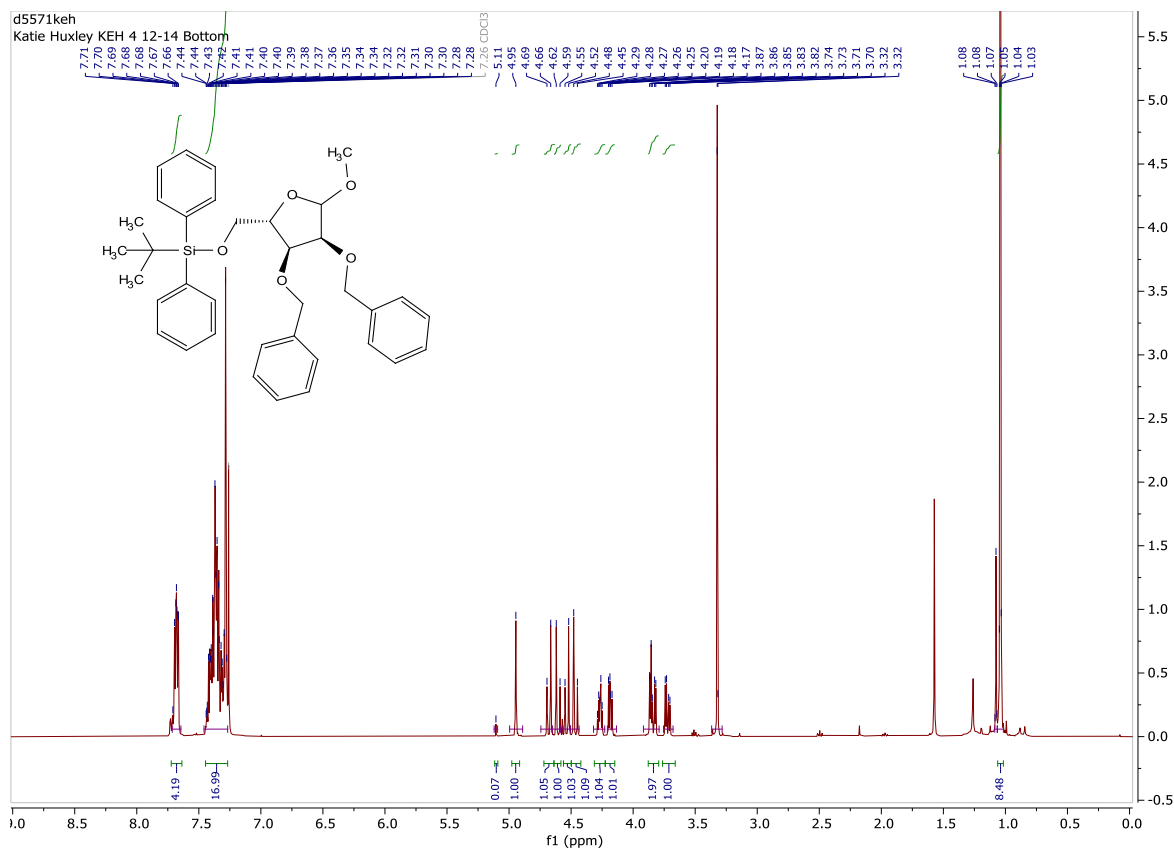


Figure 30: Commercially available tris(2-chloroethyl)phosphate on which the SATE methodology can be tested

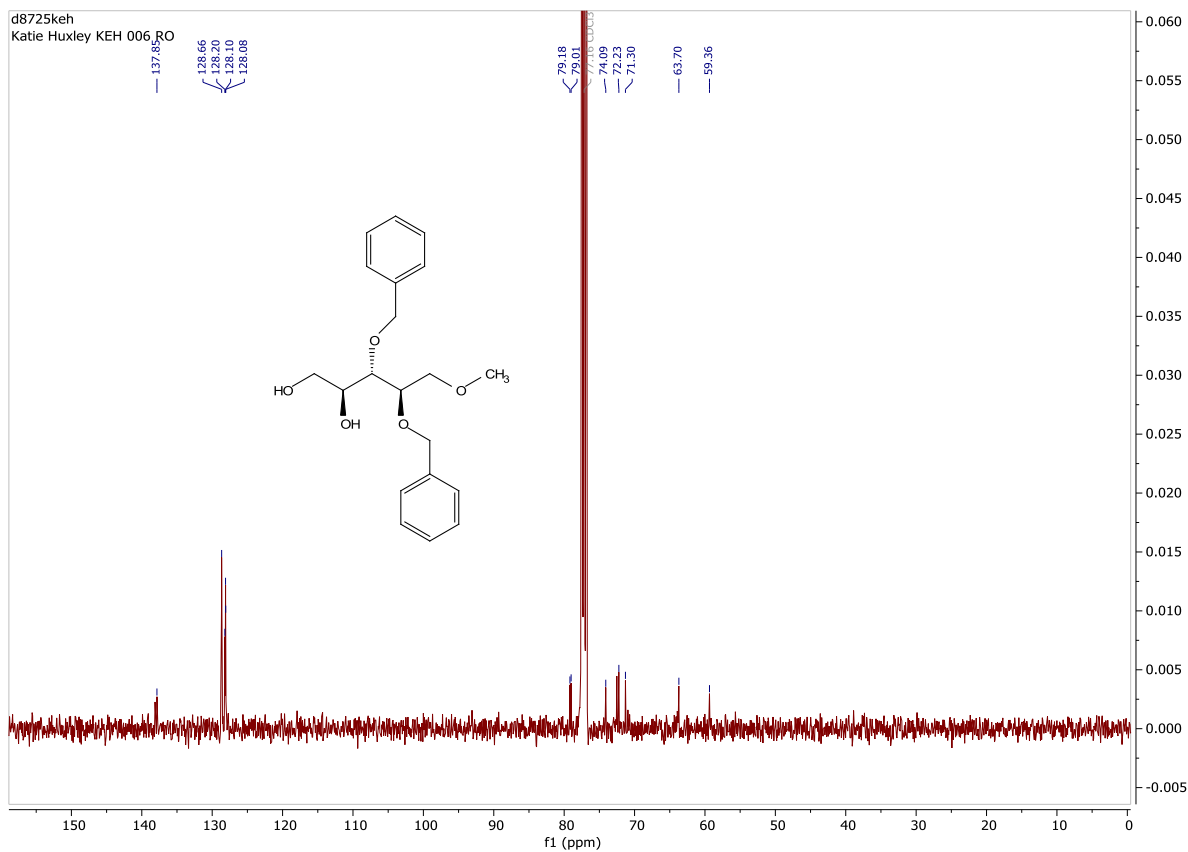
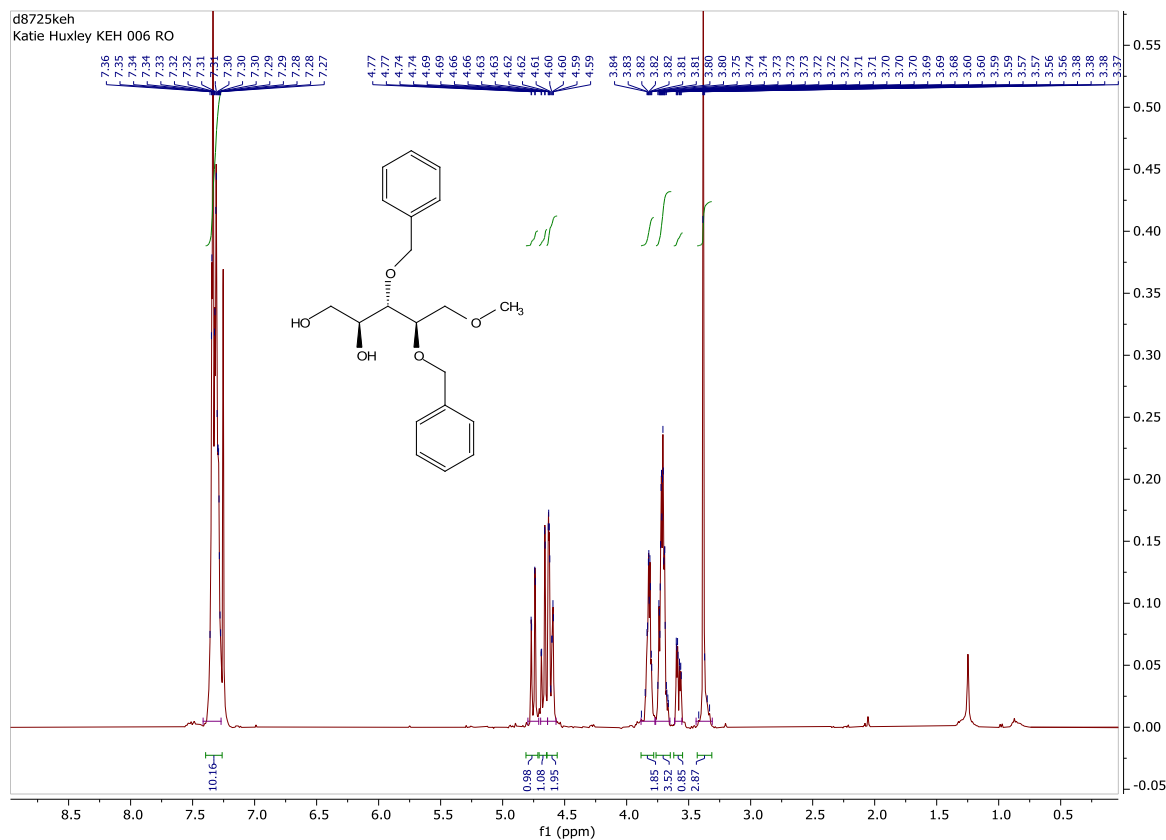
7.3 References

1. M. Kanagawa and T. Toda, *J. Neuromuscul. Dis.*, 2017, **4**, 259-267.
2. L. Wells, *J. Biol. Chem.*, 2013, **288**, 6930-6935.
3. H. Manya and T. Endo, *Biochim. Biophys. Acta Gen. Subj.*, 2017, **1861**, 2462-2472.
39. J. L. Praissman, T. Willer, M. O. Sheikh, A. Toi, D. Chitayat, Y.-Y. Lin, H. Lee, S. H. Stalnaker, S. Wang, P. K. Prabhakar, S. F. Nelson, D. L. Stemple, S. A. Moore, K. W. Moremen, K. P. Campbell and L. Wells, *Elife*, 2016, **5**, 1-18.
44. M. Kanagawa, K. Kobayashi, M. Tajiri, H. Manya, A. Kuga, Y. Yamaguchi, K. Akasaka-Manya, J.-I. Furukawa, M. Mizuno, H. Kawakami, Y. Shinohara, Y. Wada, T. Endo and T. Toda, *Cell Rep.*, 2016, **14**, 2209-2223.
45. I. Gerin, B. Ury, I. Breloy, C. Bouchet-Seraphin, J. Bolsée, M. Halbout, J. Graff, D. Vertommen, G. G. Muccioli, N. Seta, J.-M. Cuisset, I. Dabaj, S. Quijano-Roy, A. Grahn, E. Van Schaftingen and G. T. Bommer, *Nat. Commun.*, 2016, **7**, 11534.
52. H. Tokuoka, R. Imae, H. Nakashima, H. Manya, C. Masuda, S. Hoshino, K. Kobayashi, D. J. Lefeber, R. Matsumoto, T. Okada, T. Endo, M. Kanagawa and T. Toda, *Nat. Commun.*, 2022, **13**, 1847.
66. J. I. Tamura, T. Tamura, S. Hoshino, R. Imae, R. Kato, M. Yokono, M. Nagase, S. Ohno, N. Manabe, Y. Yamaguchi, H. Manya and T. Endo, *ACS Chem. Biol.*, 2022, **17**, 1513-1523.
138. H. Y. Tan, R. Eskandari, D. Shen, Y. Zhu, T. W. Liu, L. I. Willems, M. G. Alteen, Z. Madden and D. J. Vocadlo, *J. Am. Chem. Soc.*, 2018, **140**, 15300-15308.
173. U. Pradere, E. C. Garnier-Amblard, S. J. Coats, F. Amblard and R. F. Schinazi, *Chem. Rev.*, 2014, **114**, 9154-9218.
310. S. K. Maurya and R. Rana, *Beilstein J. Org. Chem.*, 2017, **13**, 1106-1118.
311. E. Raluy, O. Pàmies and M. Diéguez, *Adv. Synth. Catal.*, 2009, **351**, 1648-1670.
312. F. John and V. Wittmann, *J. Org. Chem.*, 2015, **80**, 7477-7485.
316. C. M. Dojahn, M. Hesse and C. Arenz, *Chem. Commun.*, 2013, **49**, 3128-3130.
317. H. Fang, B. Peng, S. Y. Ong, Q. Wu, L. Li and S. Q. Yao, *Chem. Sci.*, 2021, **12**, 8288-8310.
318. D. Kubacka, M. Kozarski, M. R. Baranowski, R. Wojcik, J. Panecka-Hofman, D. Strzelecka, J. Basquin, J. Jemielity and J. Kowalska, *Pharmaceuticals (Basel)*, 2022, **15**.
319. S. Liu, B. Zhou, H. Yang, Y. He, Z. X. Jiang, S. Kumar, L. Wu and Z. Y. Zhang, *J. Am. Chem. Soc.*, 2008, **130**, 8251-8260.
320. S. Pan, S. Y. Jang, S. S. Liew, J. Fu, D. Wang, J. S. Lee and S. Q. Yao, *Angew. Chem. Int. Ed. Engl.*, 2018, **57**, 579-583.

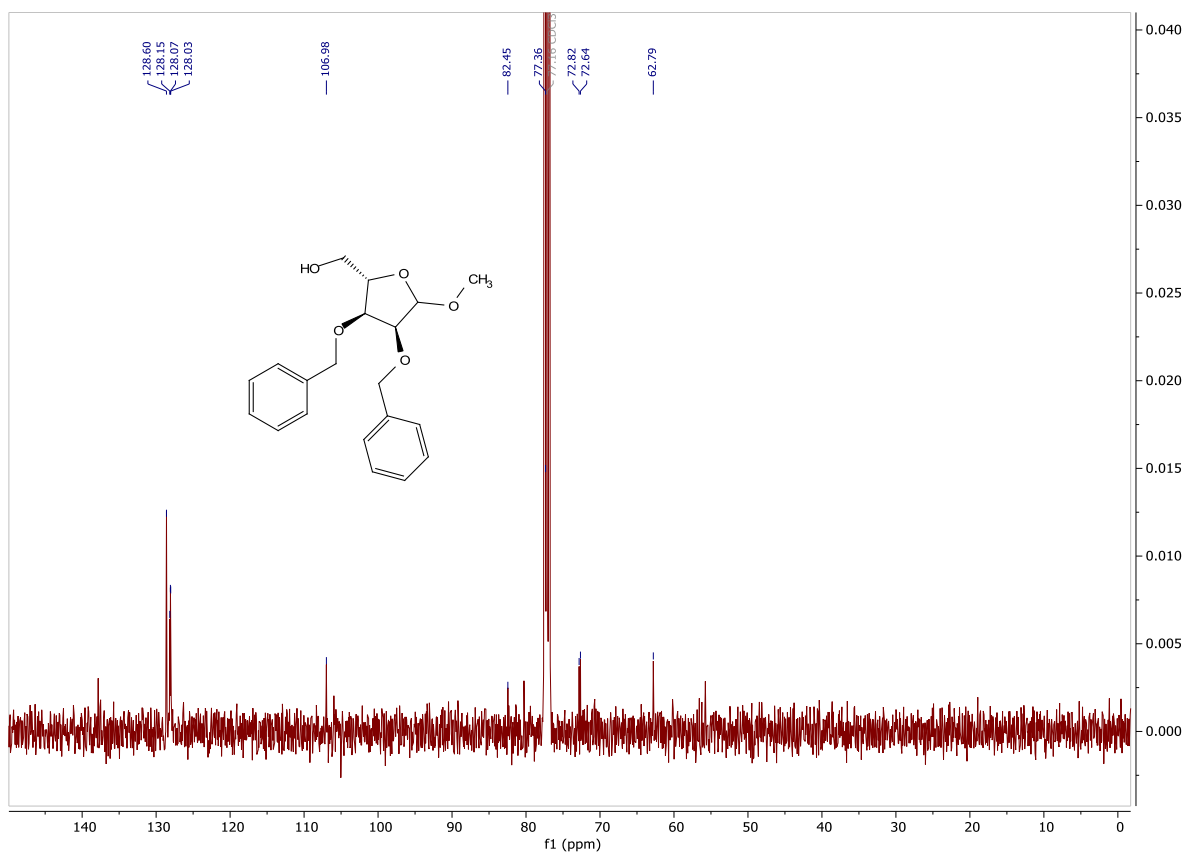
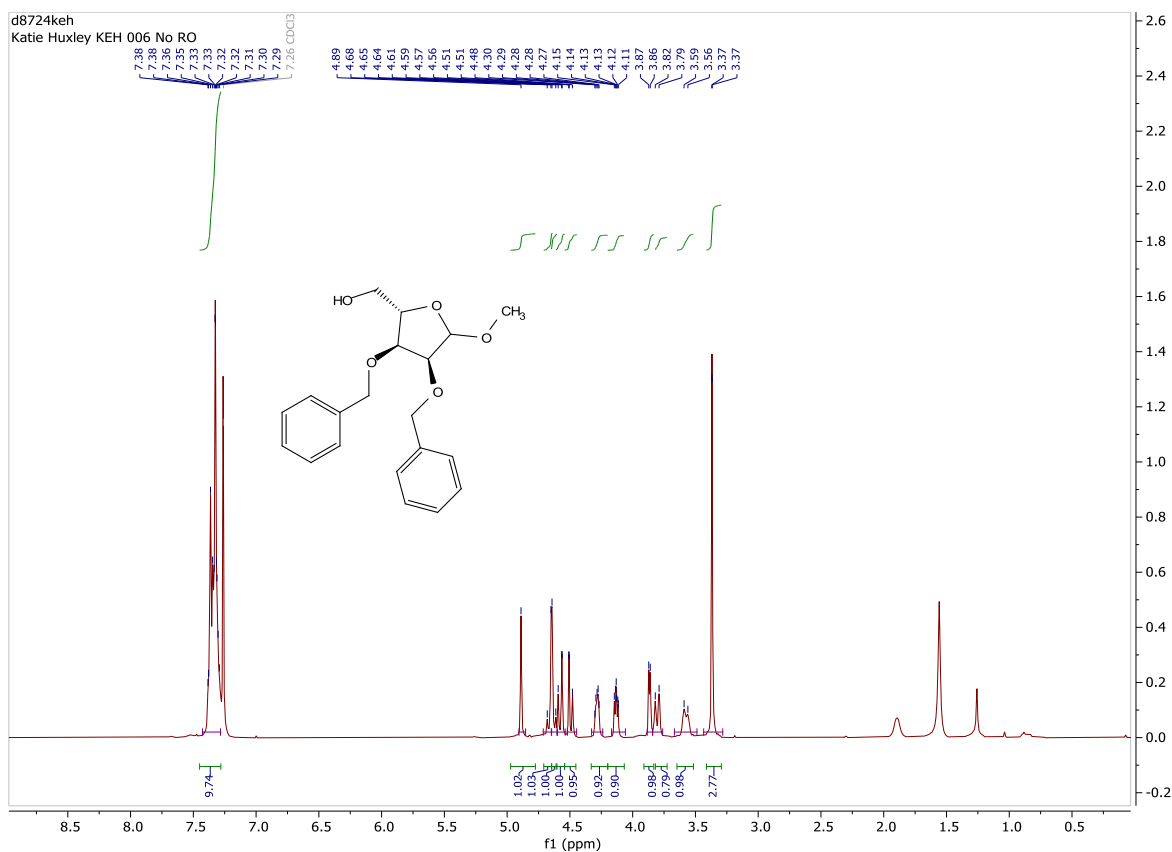
Methyl-2,3-di-O-benzyl-5-O-tert-butylidiphenylsilyl- α,β -L-ribofuranoside (1)



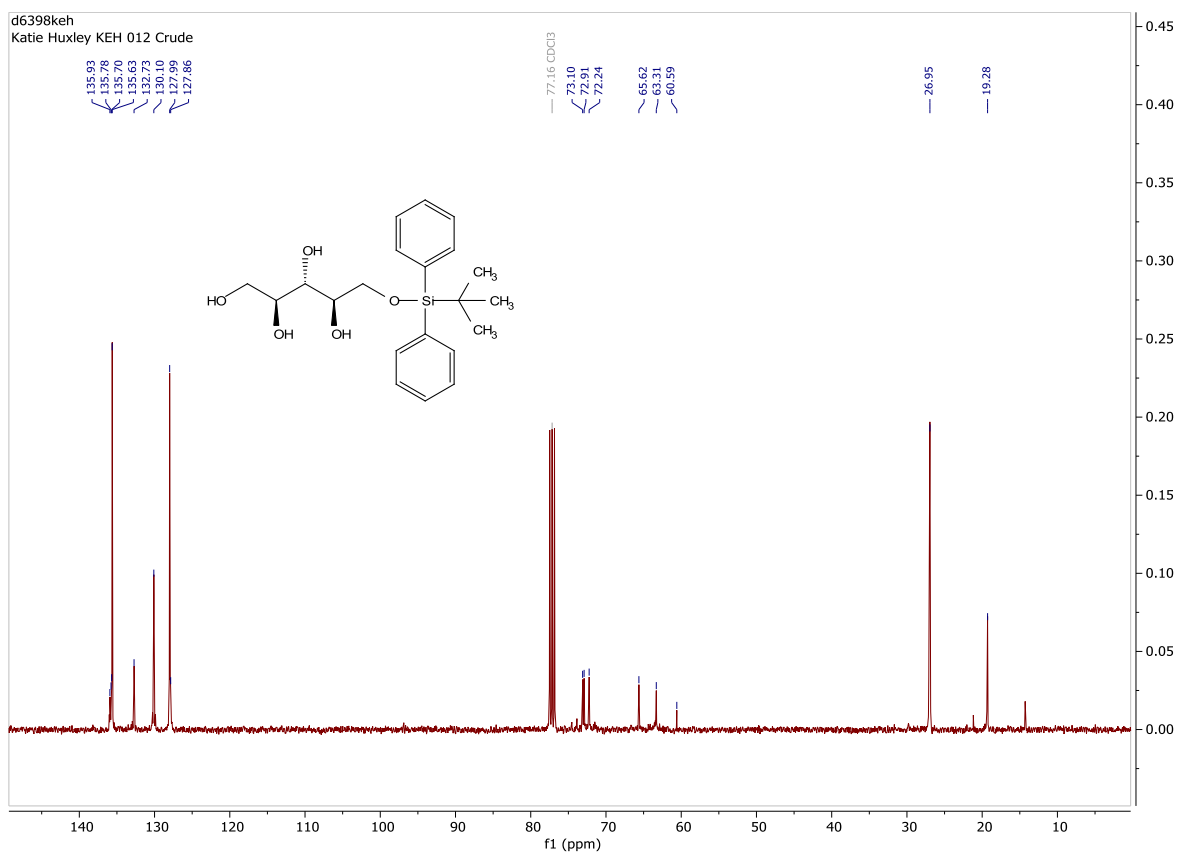
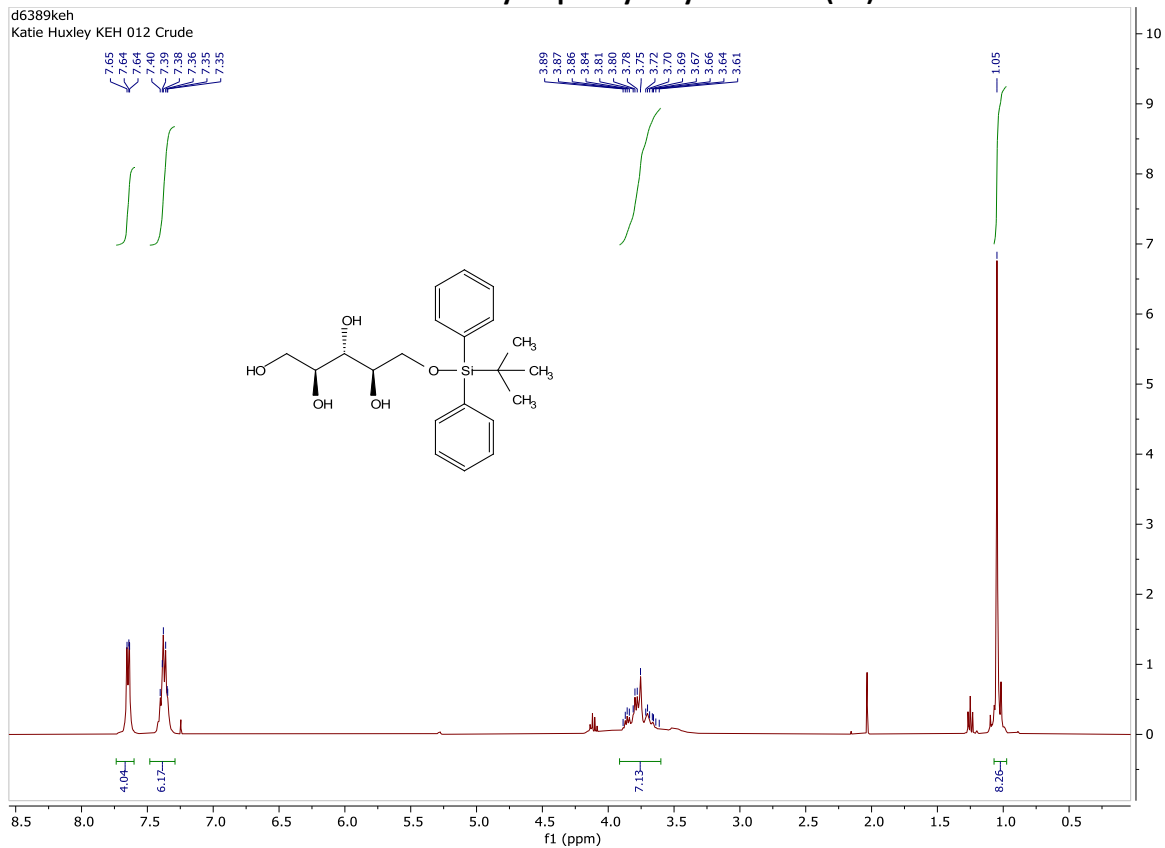
Methyl-2,3-di-O-benzyl-D-ribose (8)



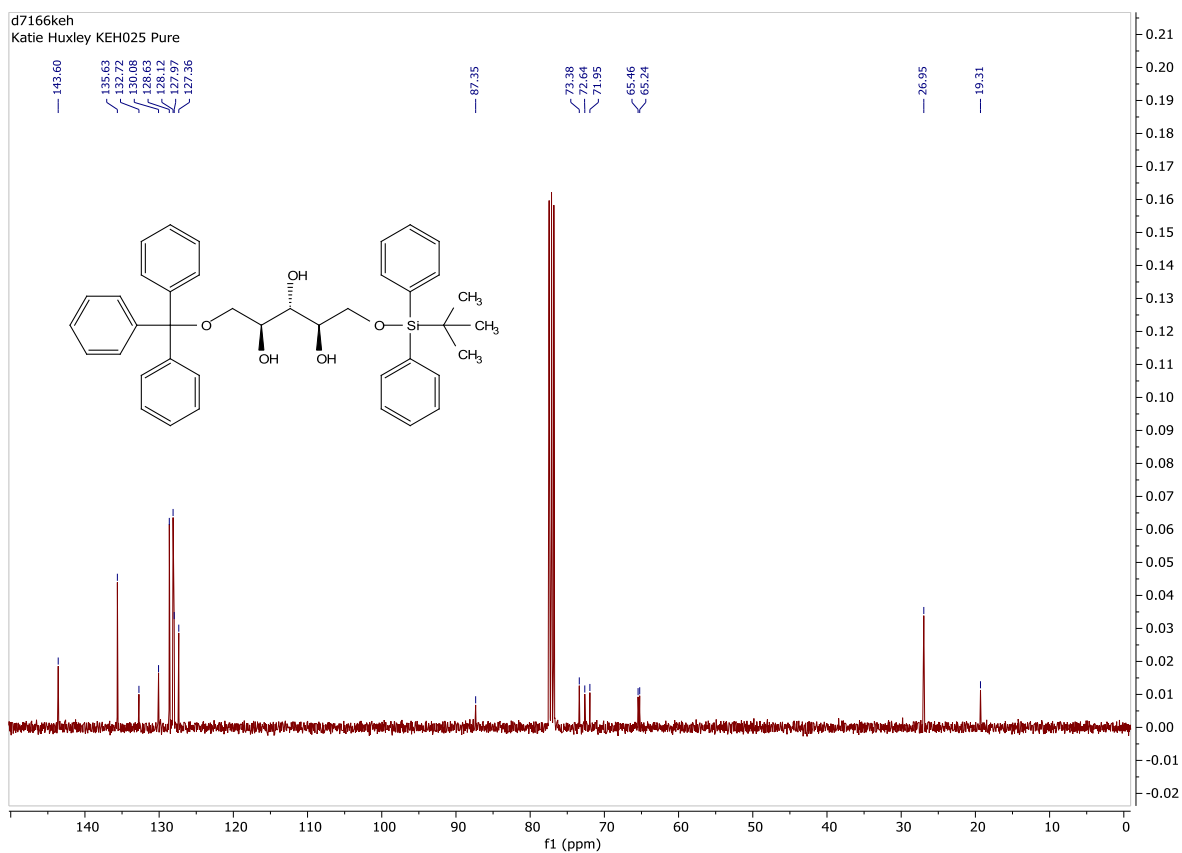
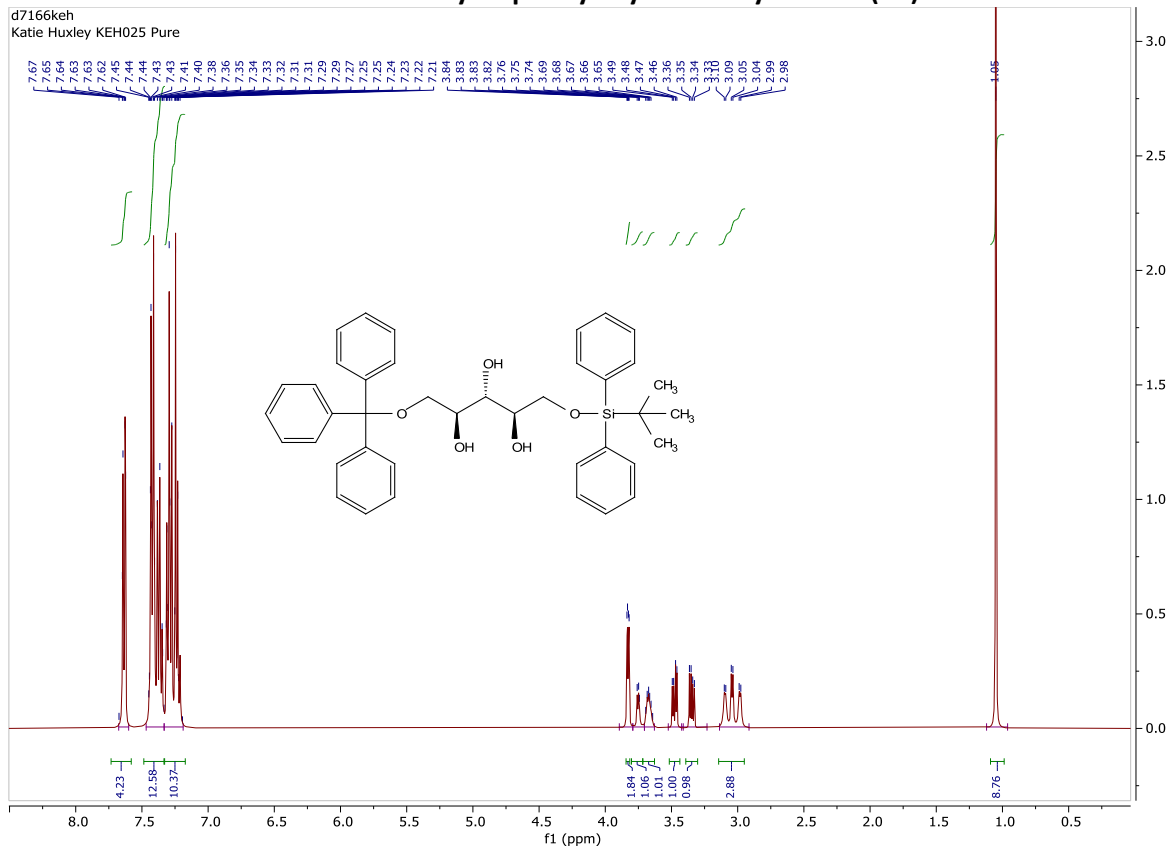
Methyl-2,3-di-O-benzyl- α,β -L-ribofuranoside (9)



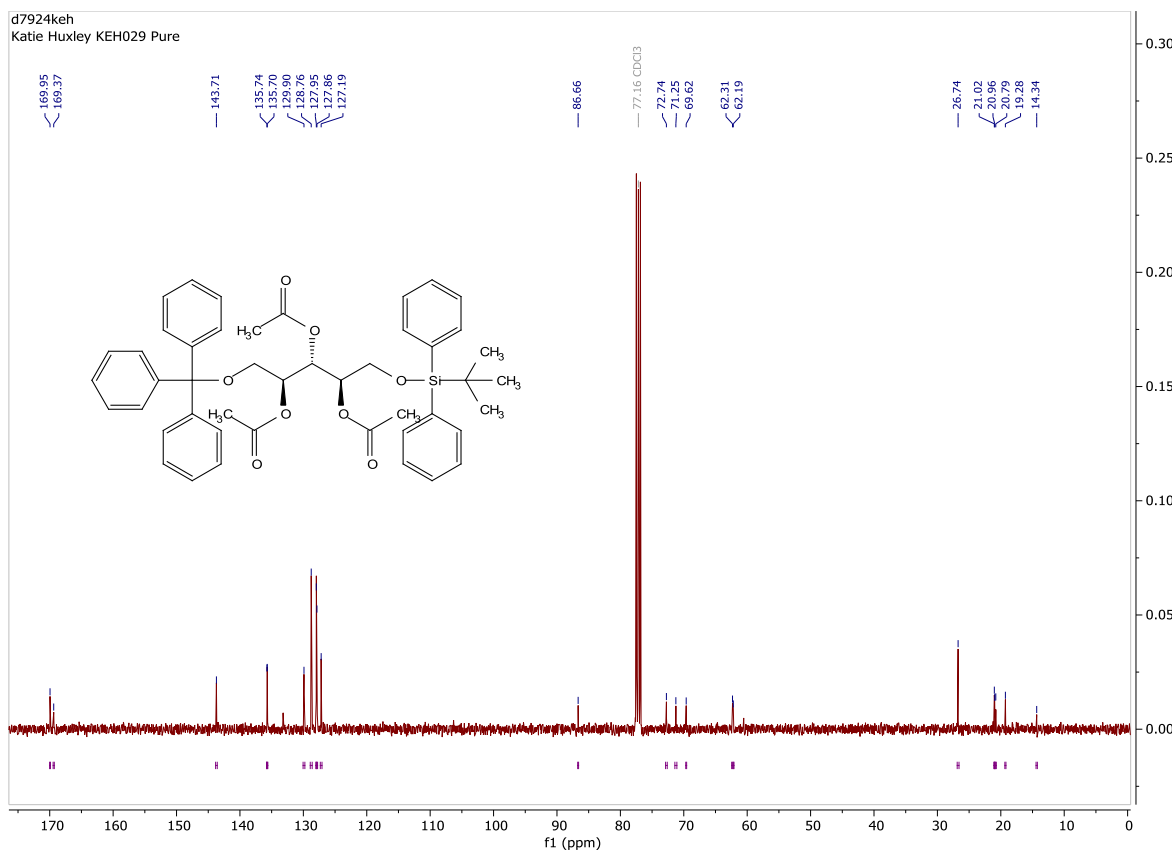
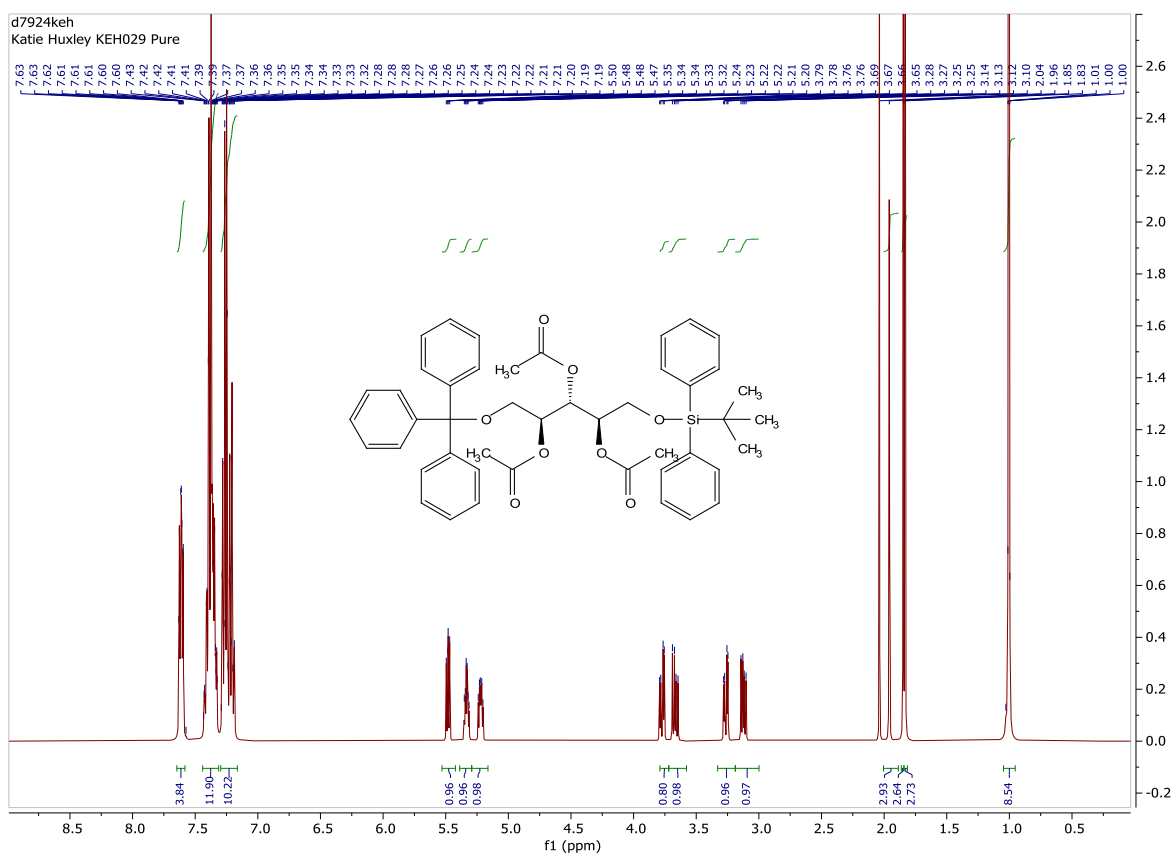
5-O-tert-butyl-diphenyl-silyl-D-ribose (22)



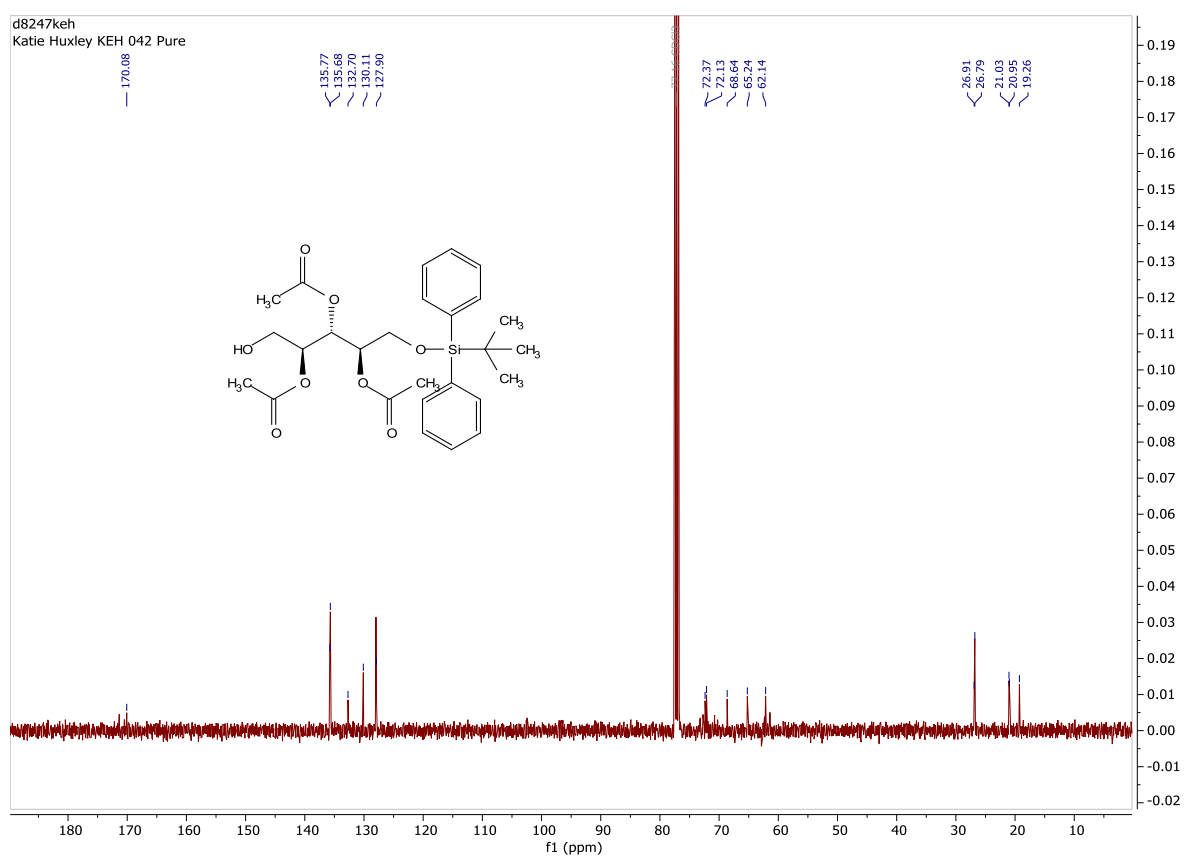
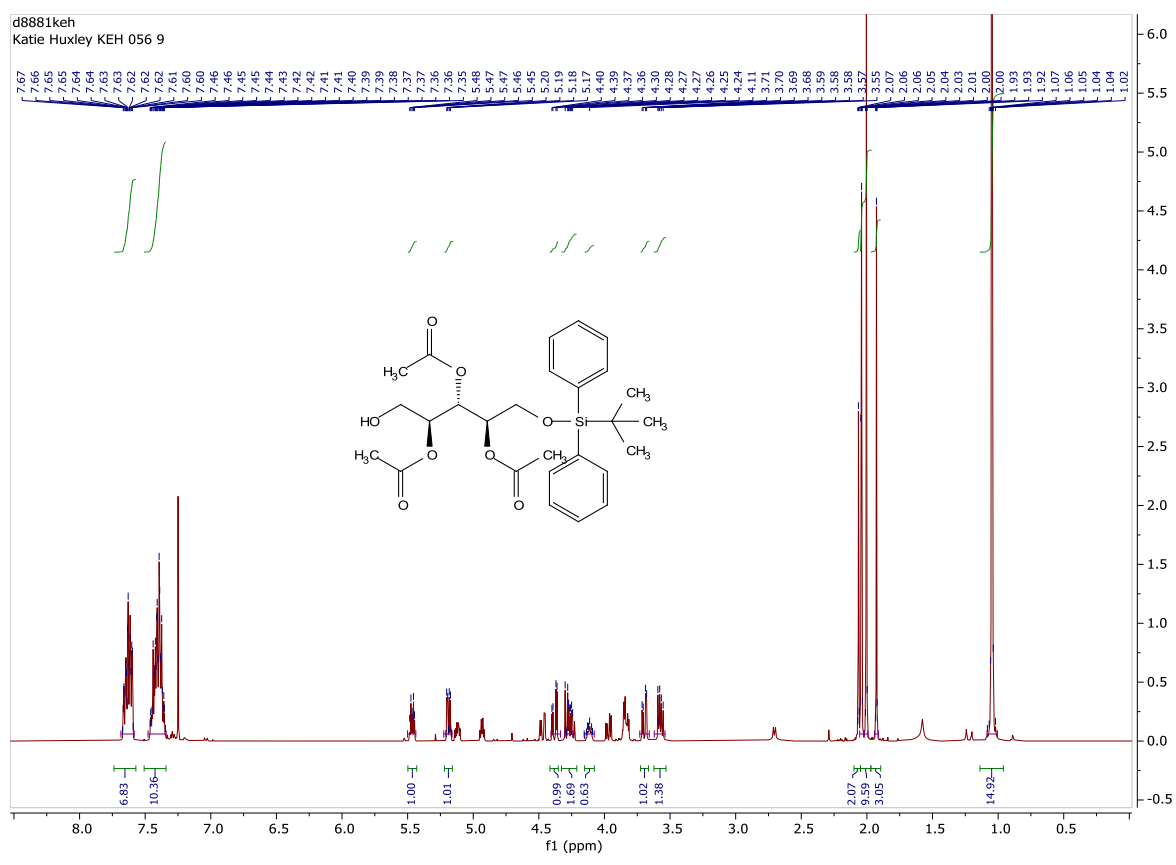
5-O-tert-butyl-diphenylsilyl-1-O-trityl-ribose (12)



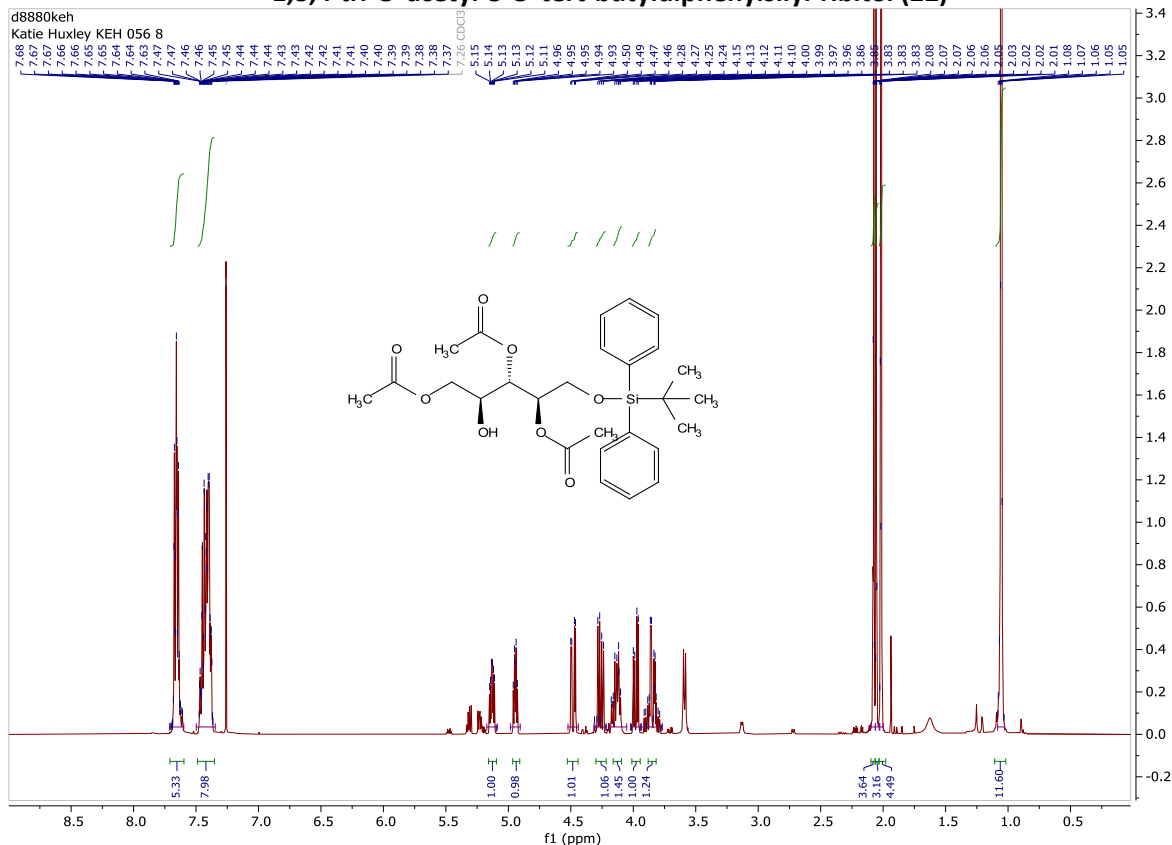
2,3,4-tri-O-acetyl-5-O-tert-butyl-diphenylsilyl-1-O-trityl-ribose (17)



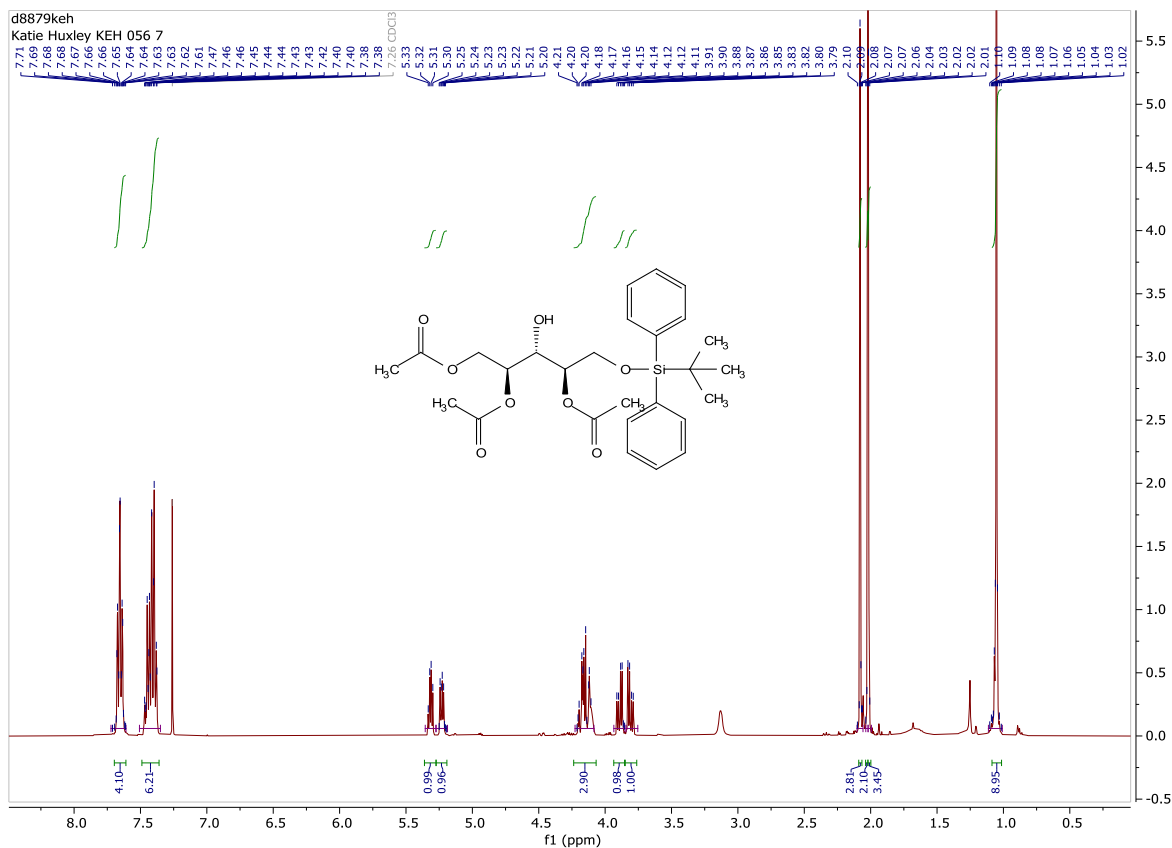
2,3,4-tri-O-acetyl-5-O-tert-butylidiphenylsilyl-ribose (18)



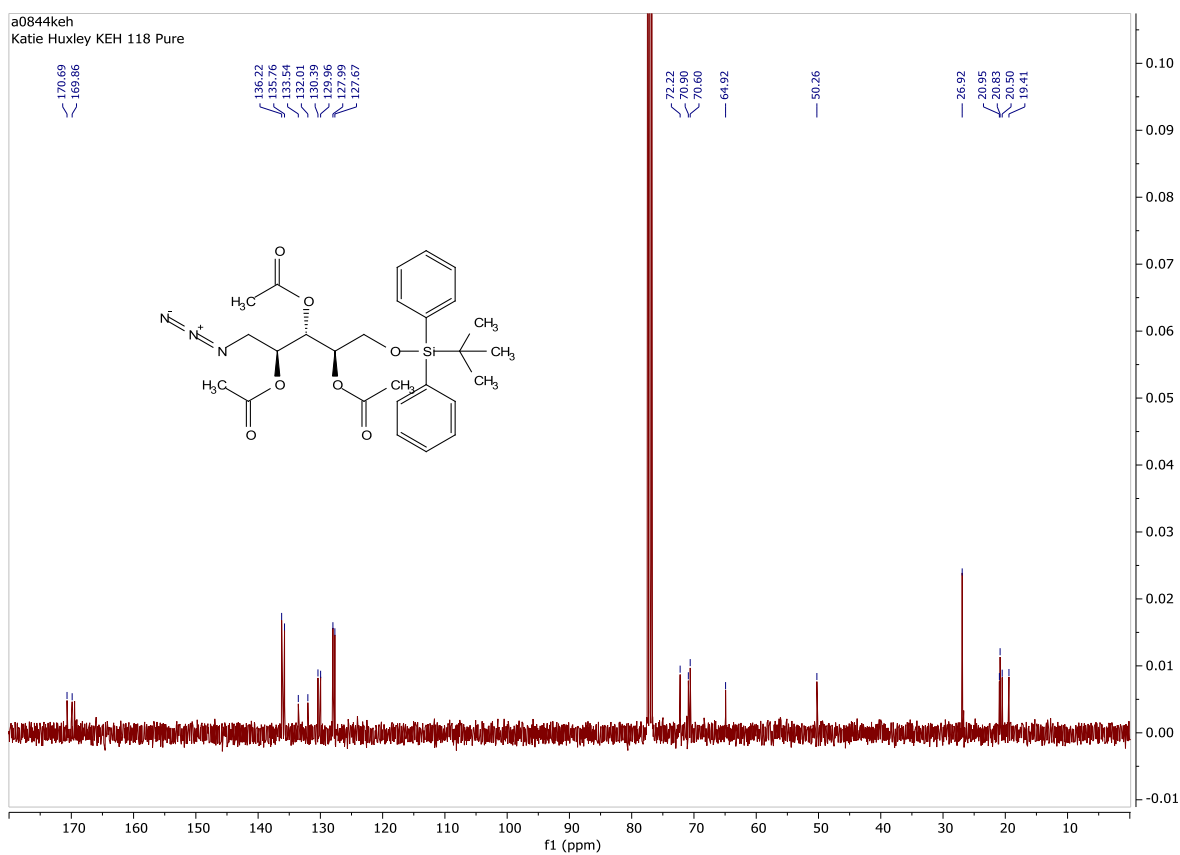
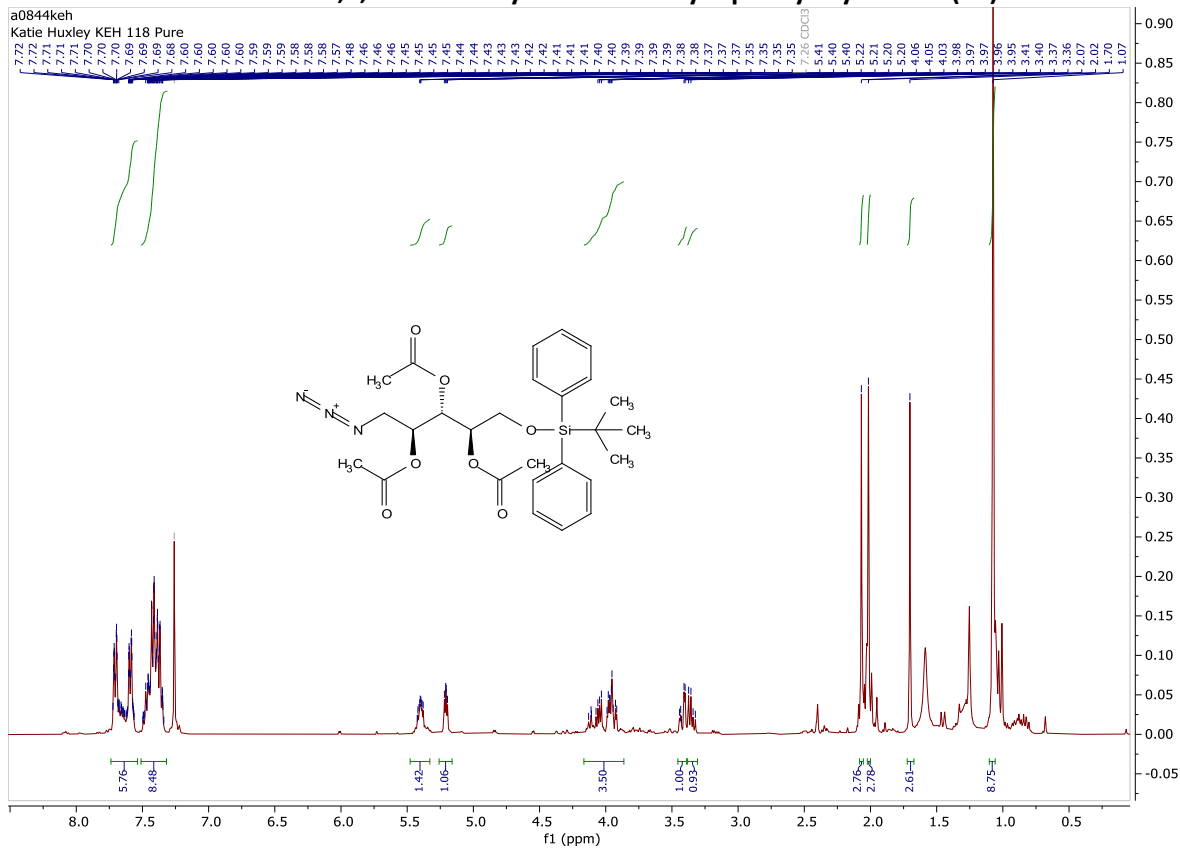
1,3,4-tri-O-acetyl-5-O-tert-butyl-diphenylsilyl-ribose (22)



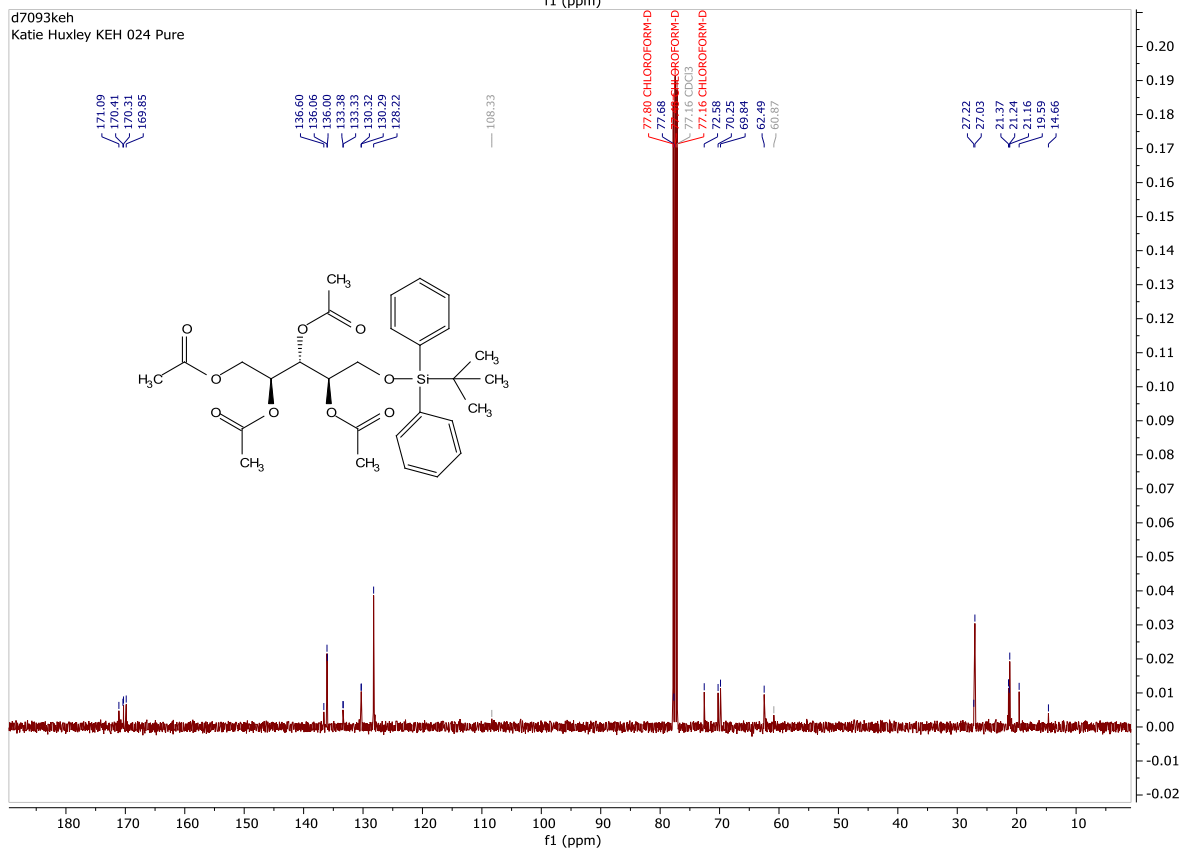
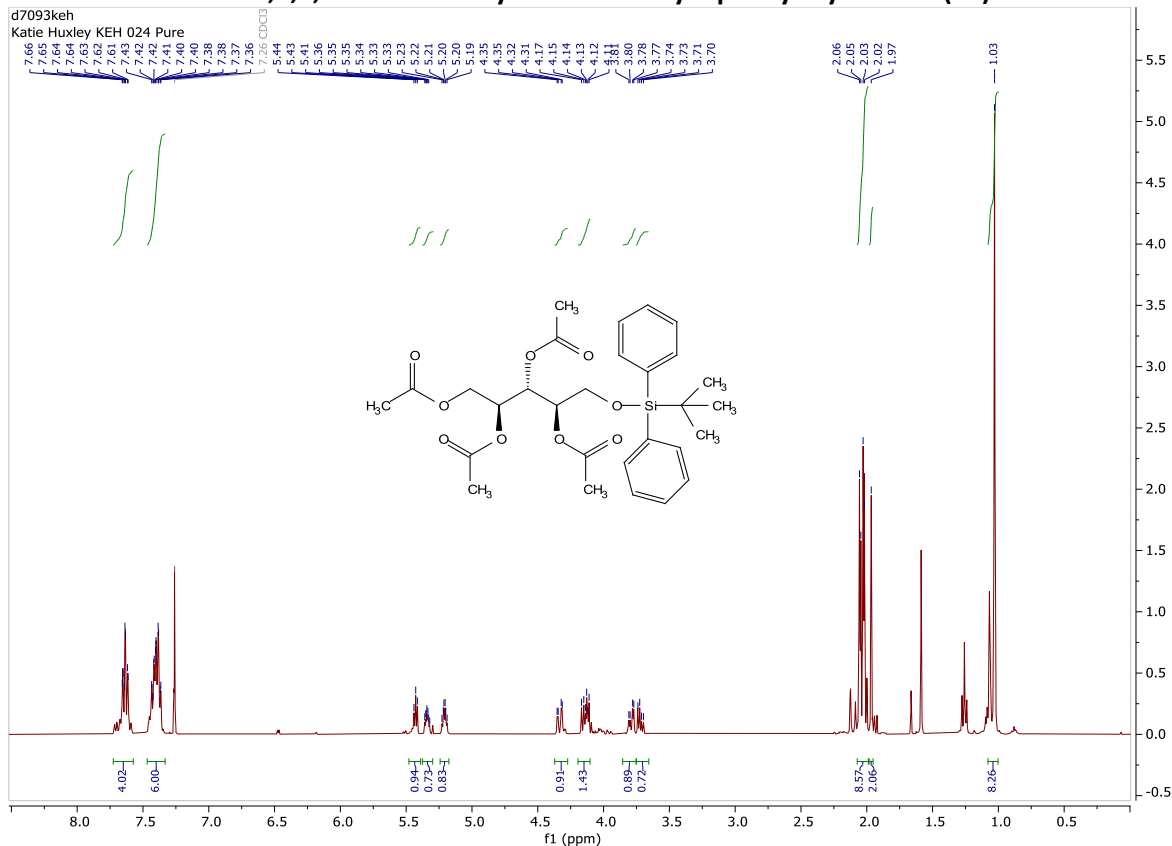
1,3,4-tri-O-acetyl-5-O-tert-butyl-diphenylsilyl-ribose (23)



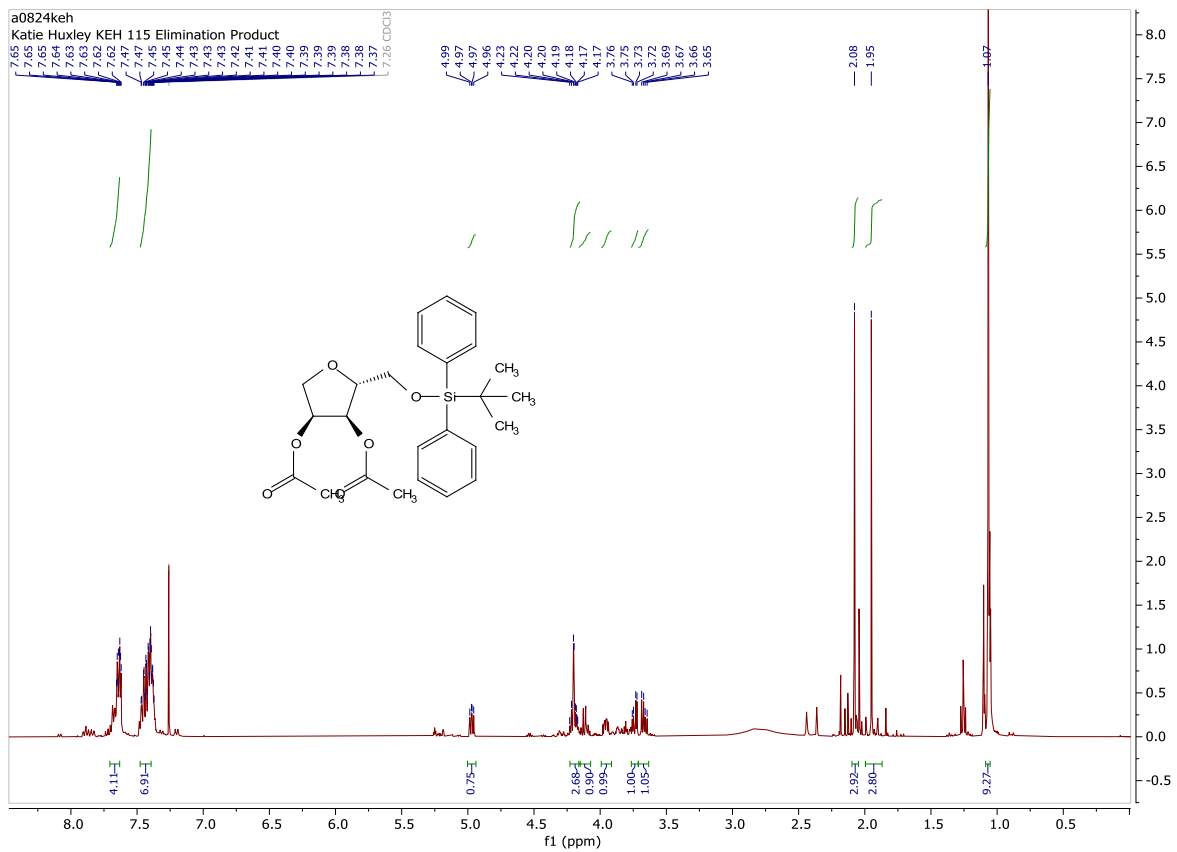
1-Azido-2,3,4-tri-O-acetyl-5-O-tert-butylidiphenylsilyl-ribose (19)



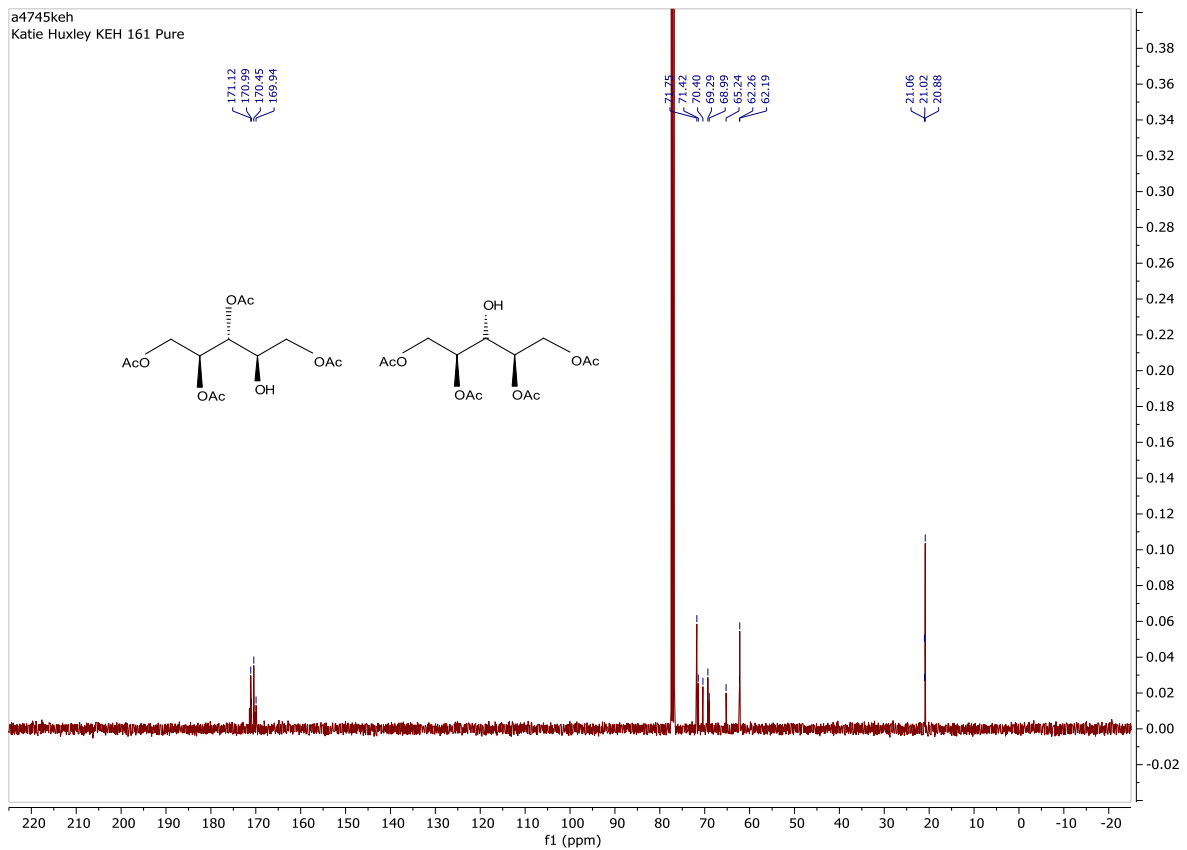
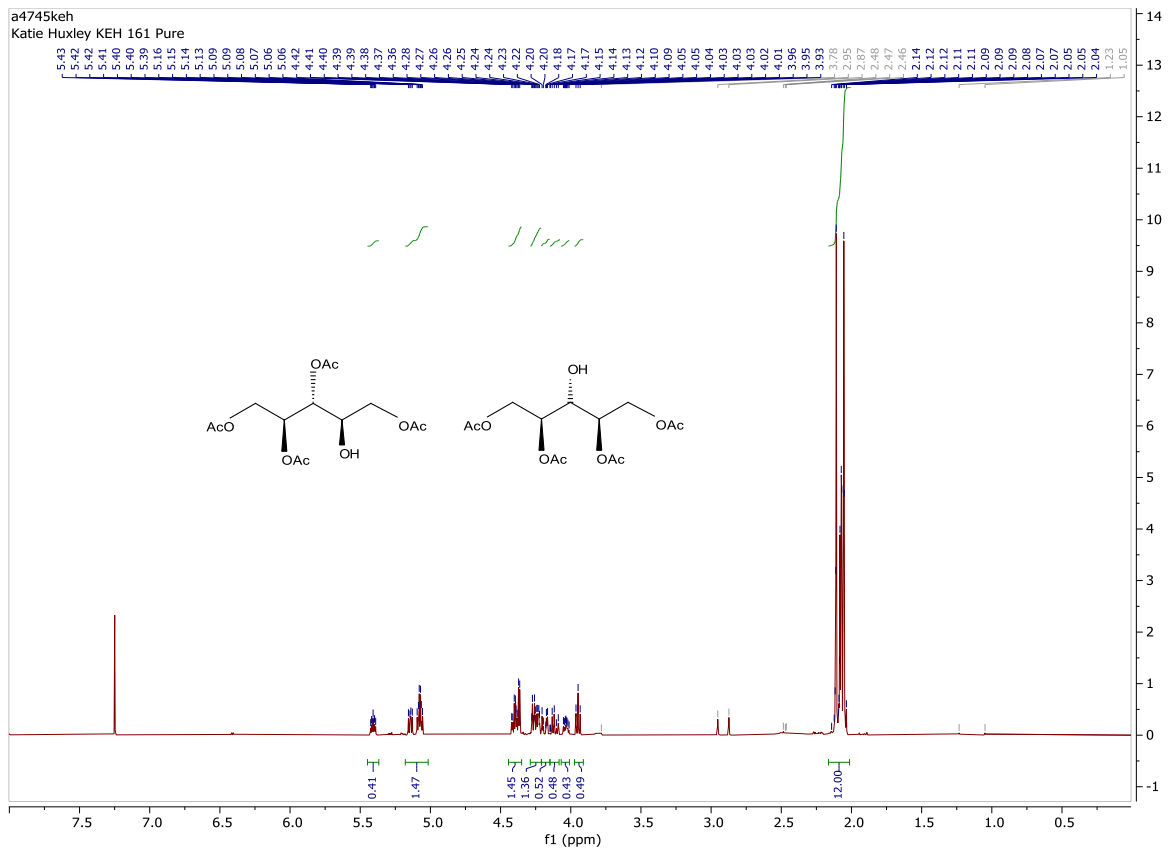
1-2,3,4,5-tetra-O-acetyl-5-O-tert-butylidiphenylsilyl-ribose (25)



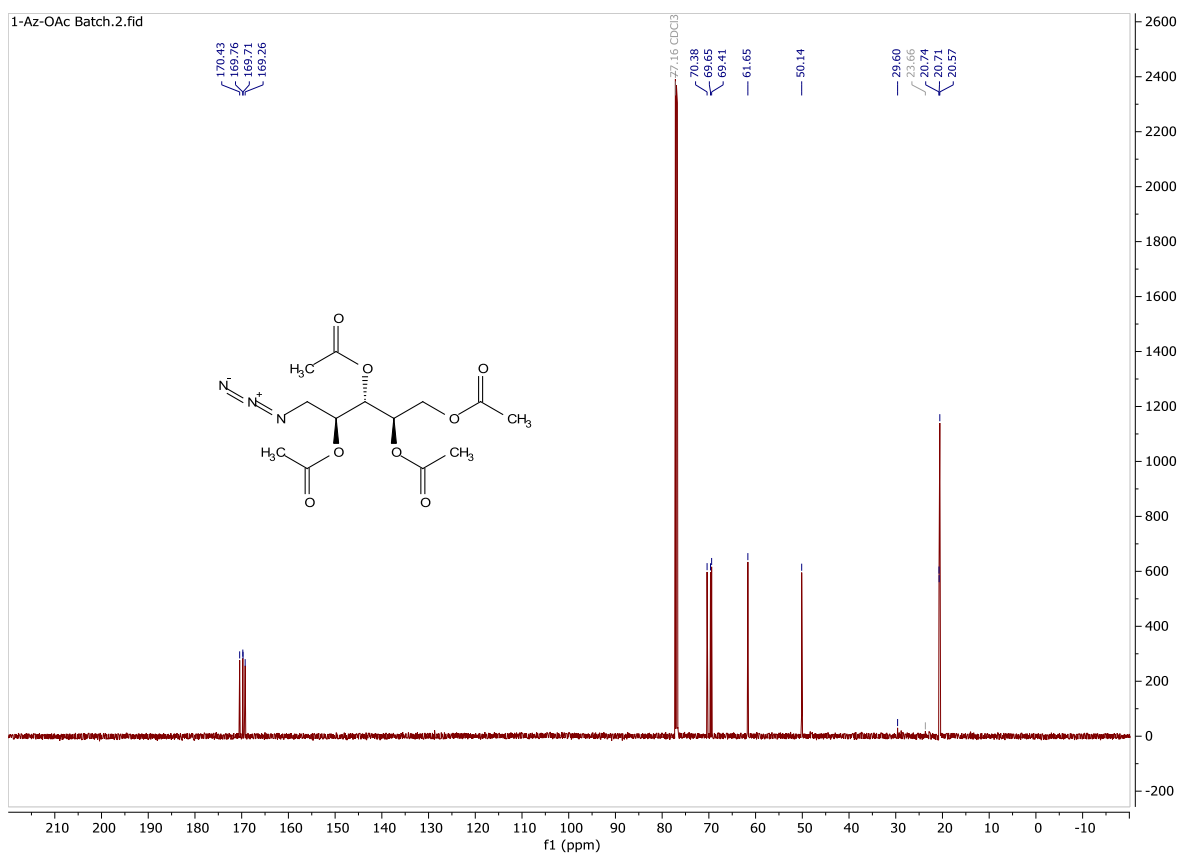
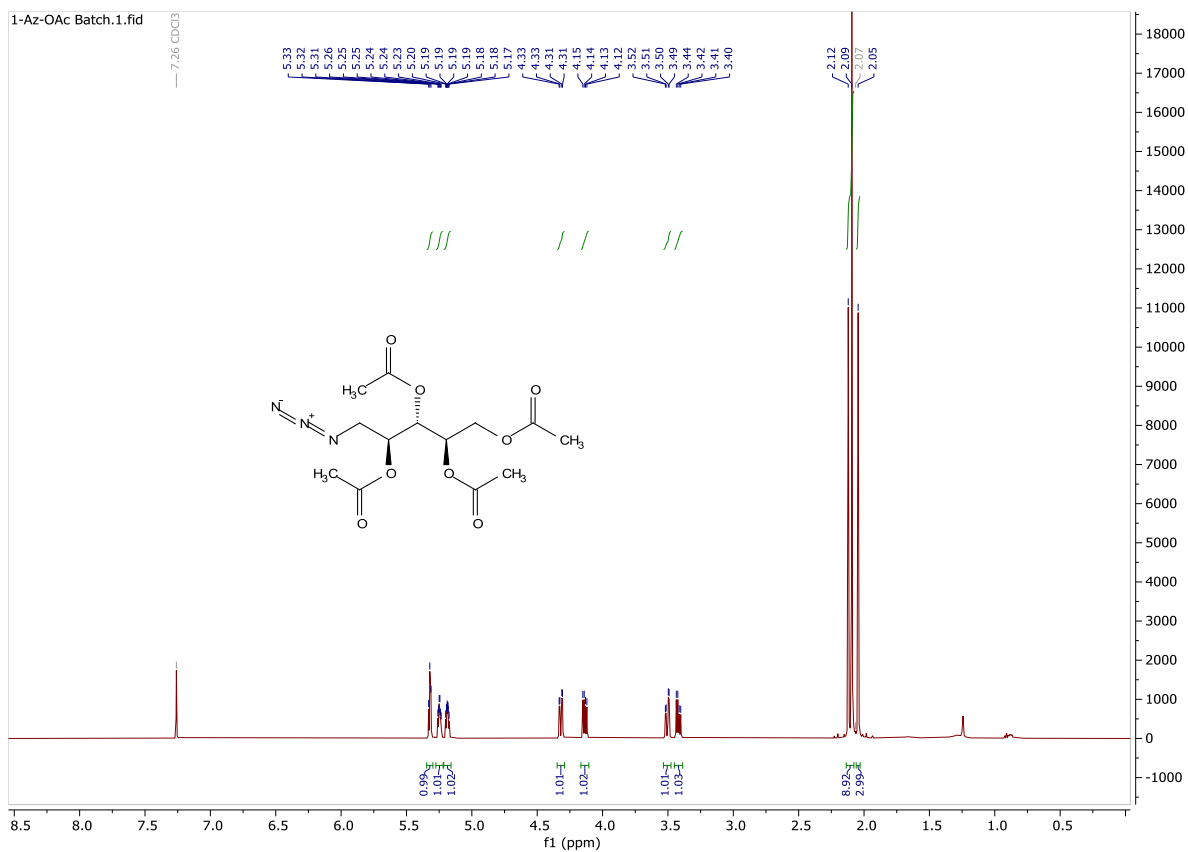
1,4-anhydro-2,3-di-O-acetyl-5-tert-butylidiphenylsilyl-deoxy-D,L-ribose (26)



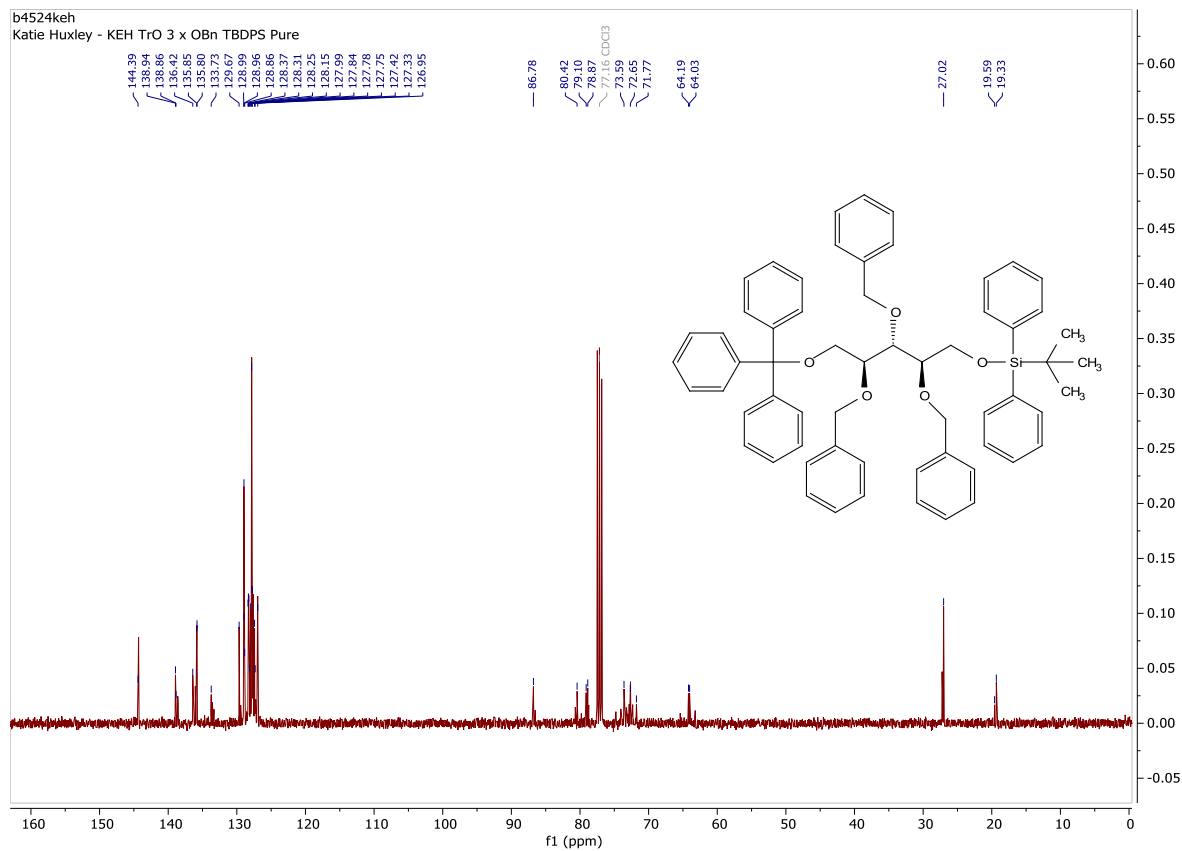
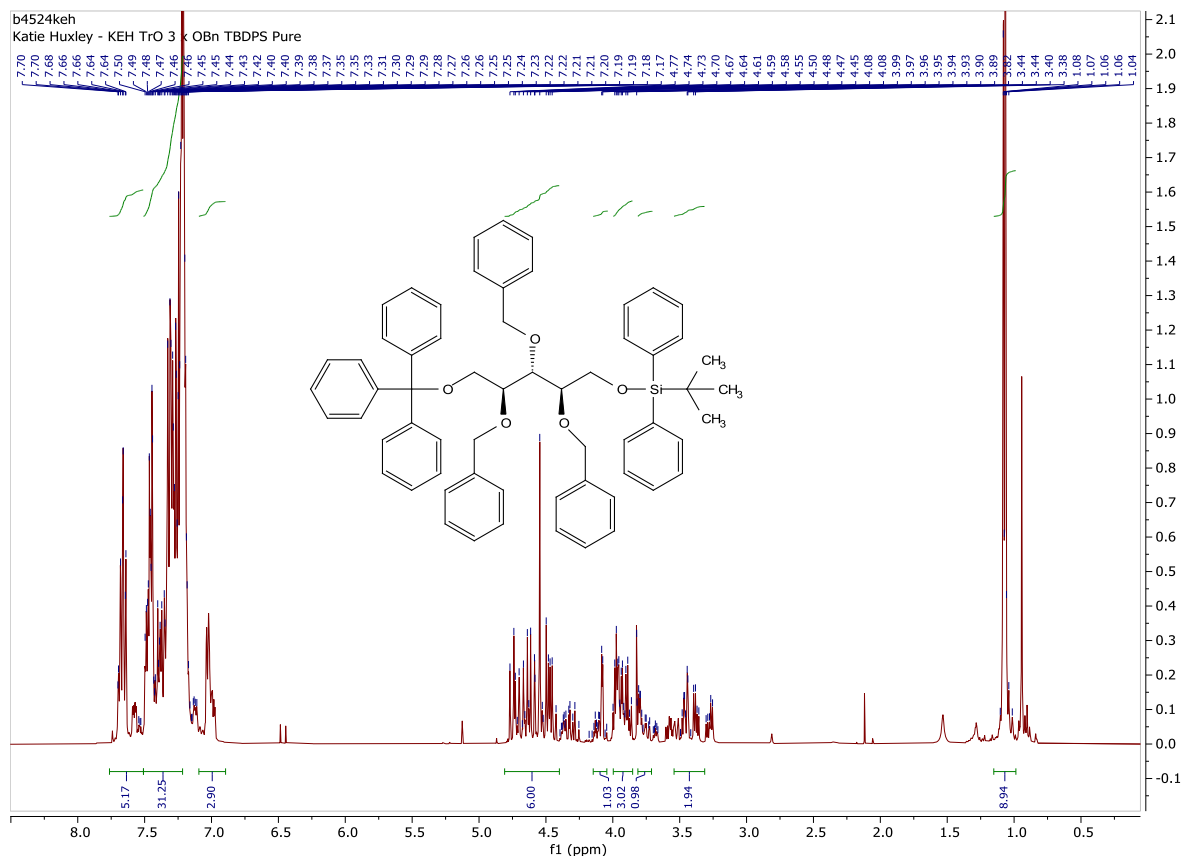
1,2,3,5-tetra-O-acetyl-D-ribose and 1,2,4,5-tetra-O-acetyl-D-ribose



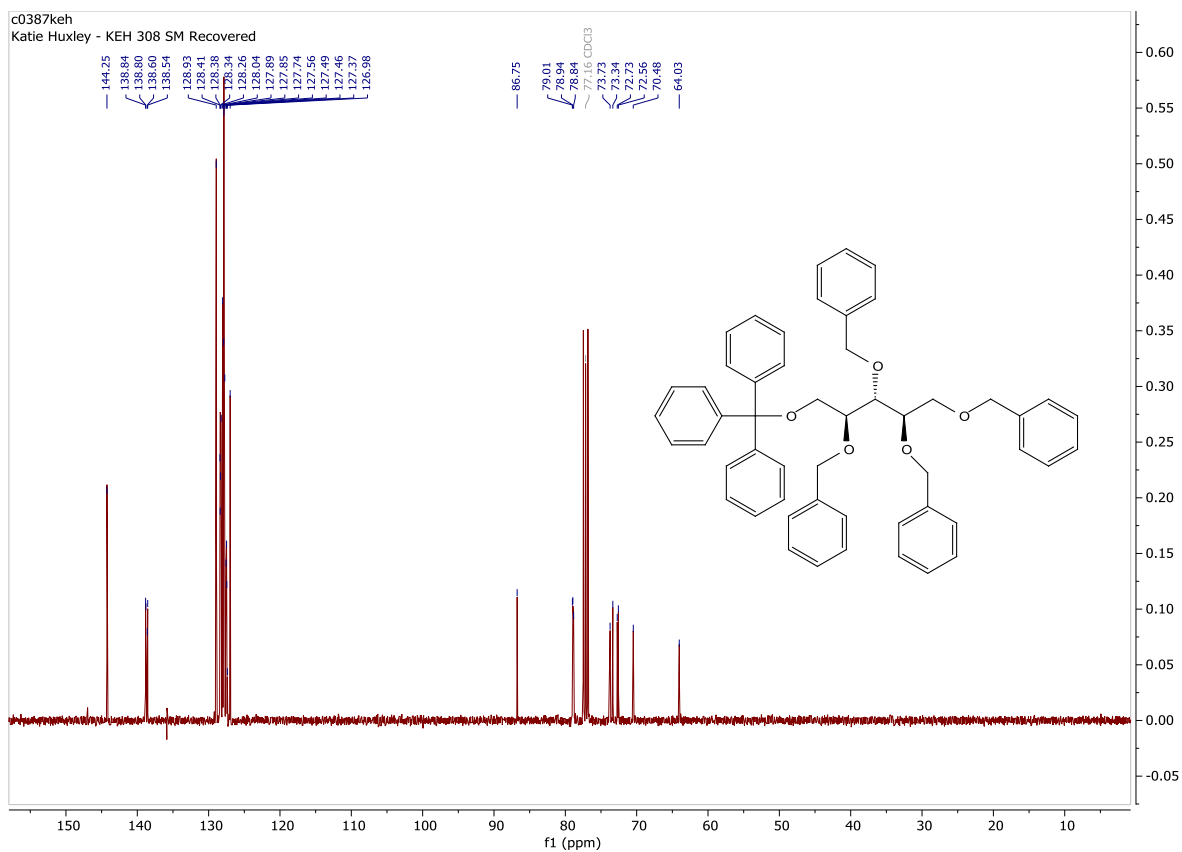
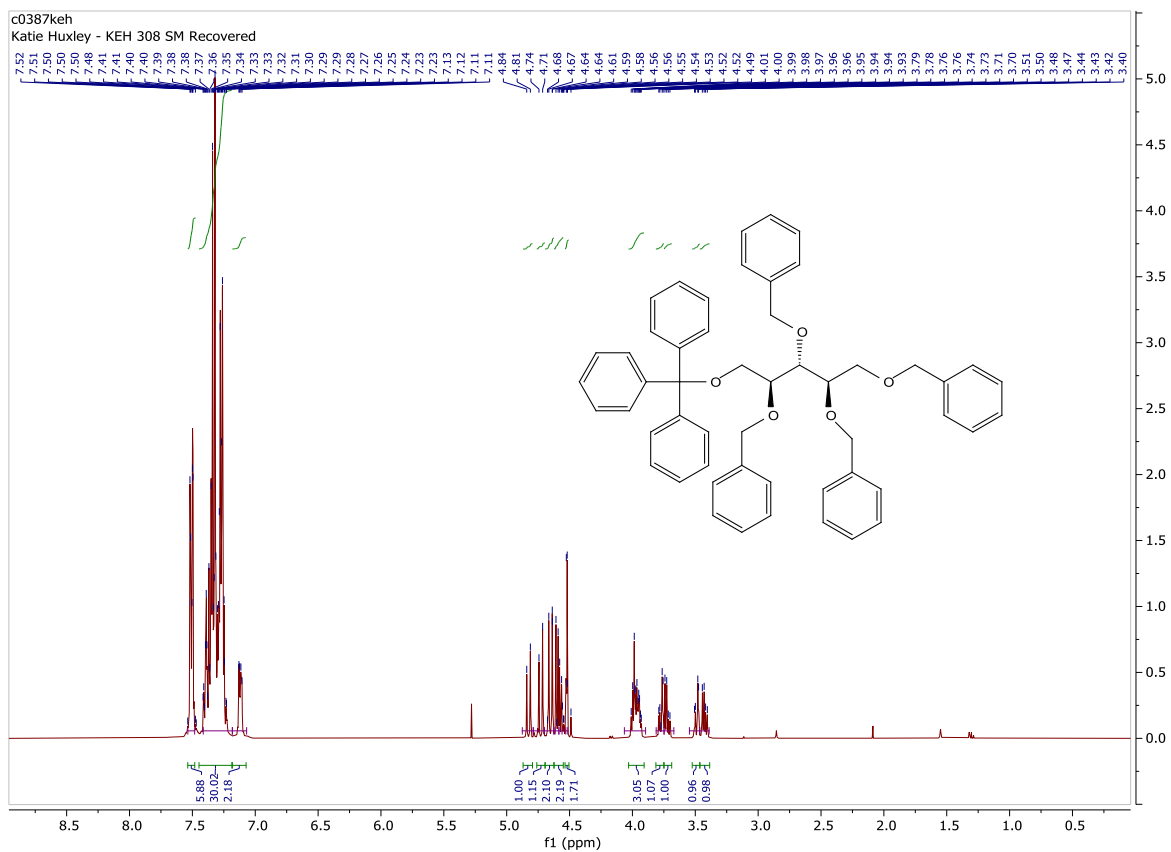
2,3,4,5-tetra-O-acetyl-1-azido-D-ribitol (1-Az-OAc Probe)



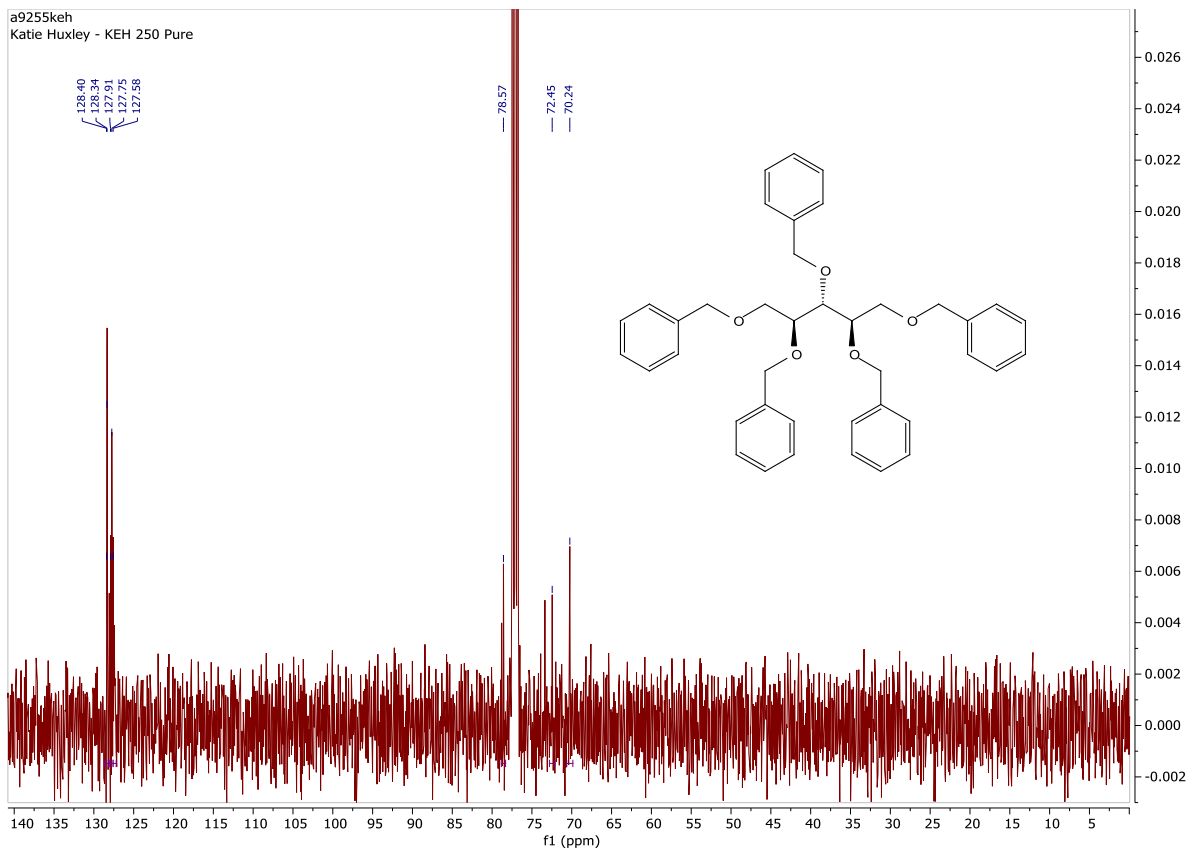
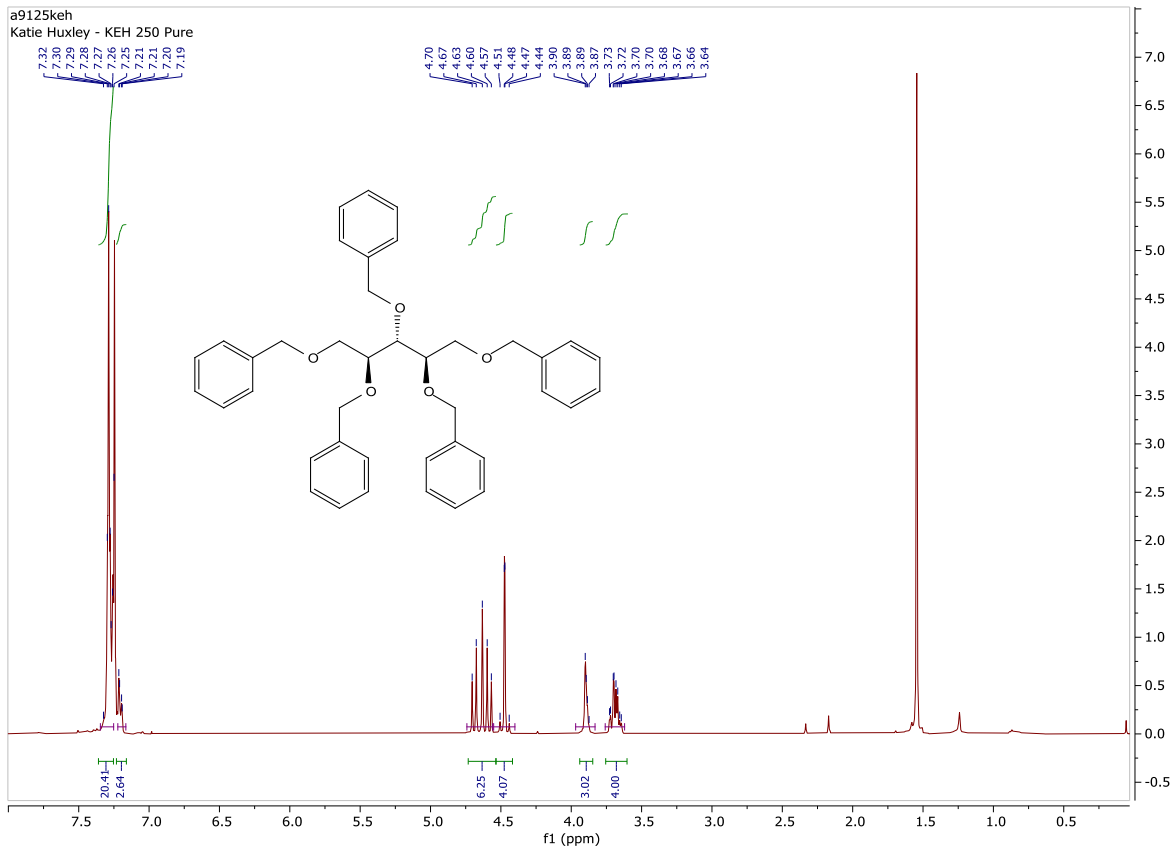
2,3,4-tri-O-benzyl-5-O-tert-butylidiphenylsilyl-1-O-trityl-D-ribose (13)



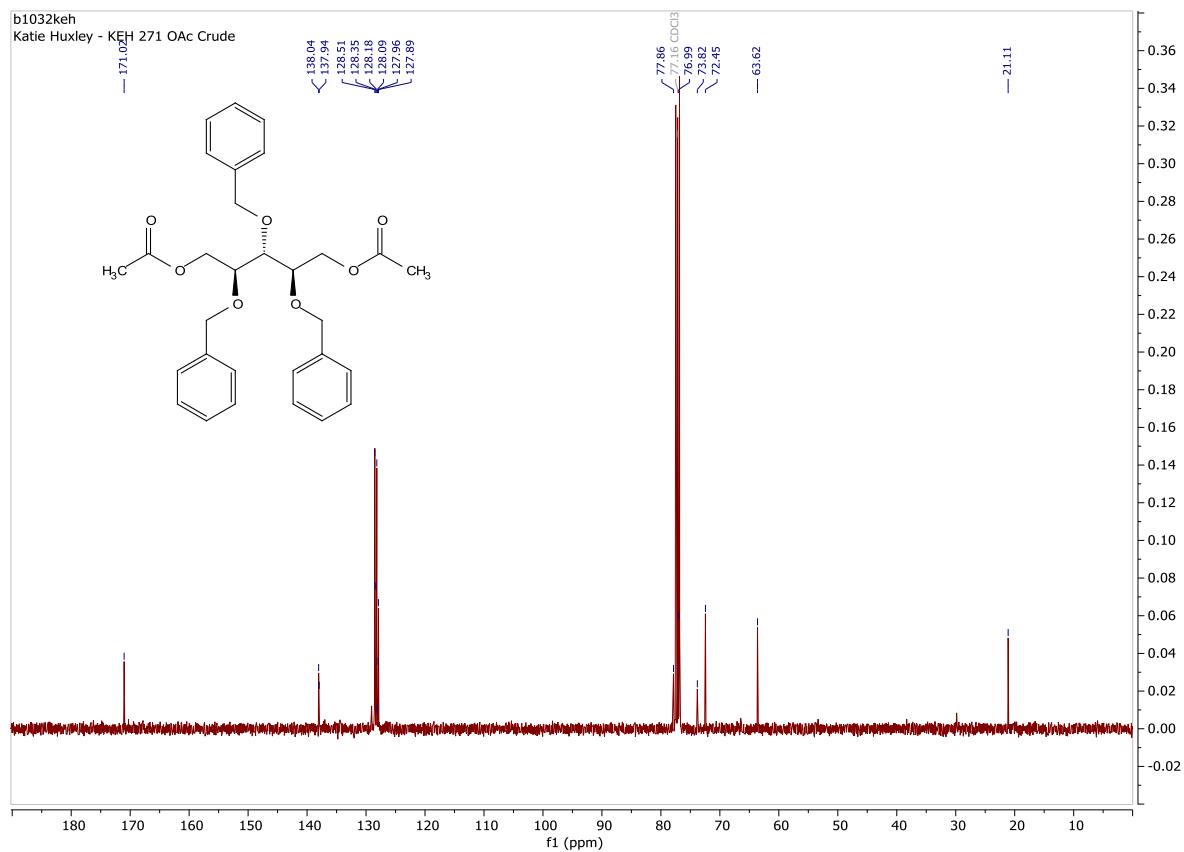
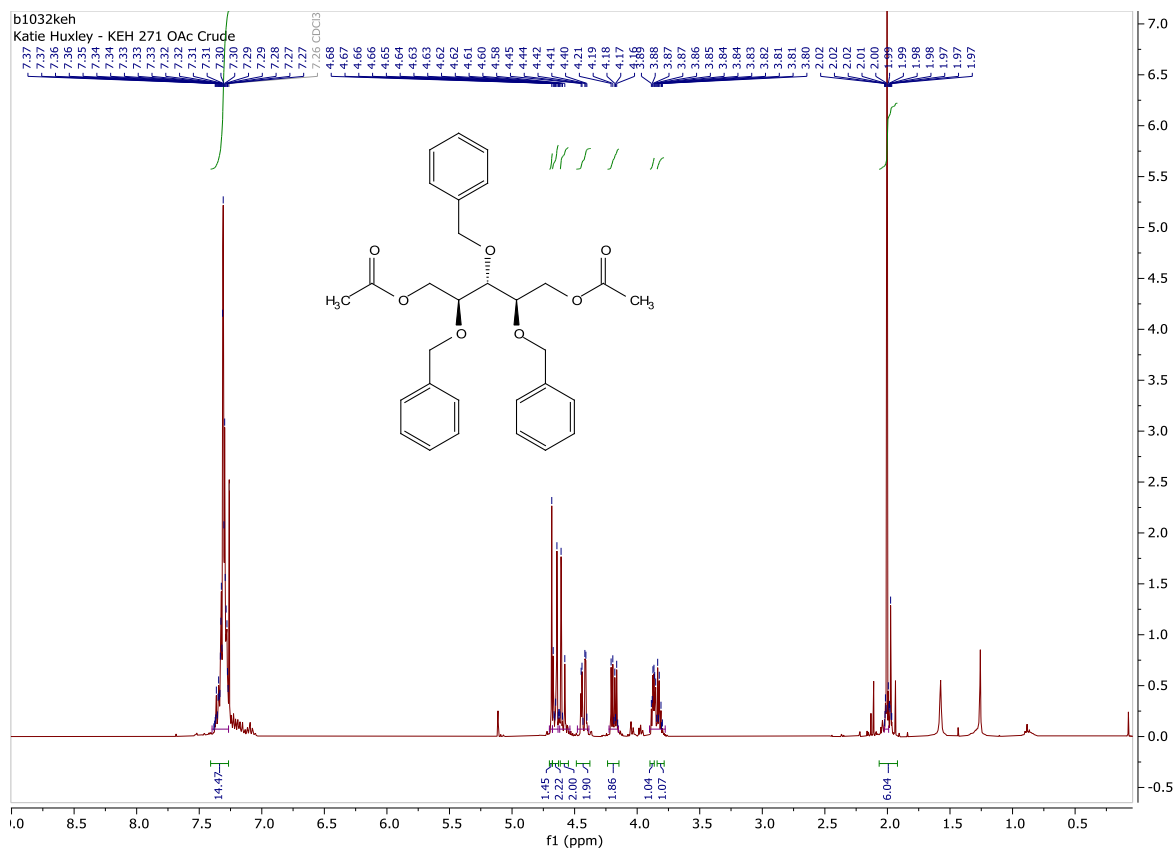
2,3,4,5-tetra-O-benzyl-1-O-trityl-D-ribose (32)



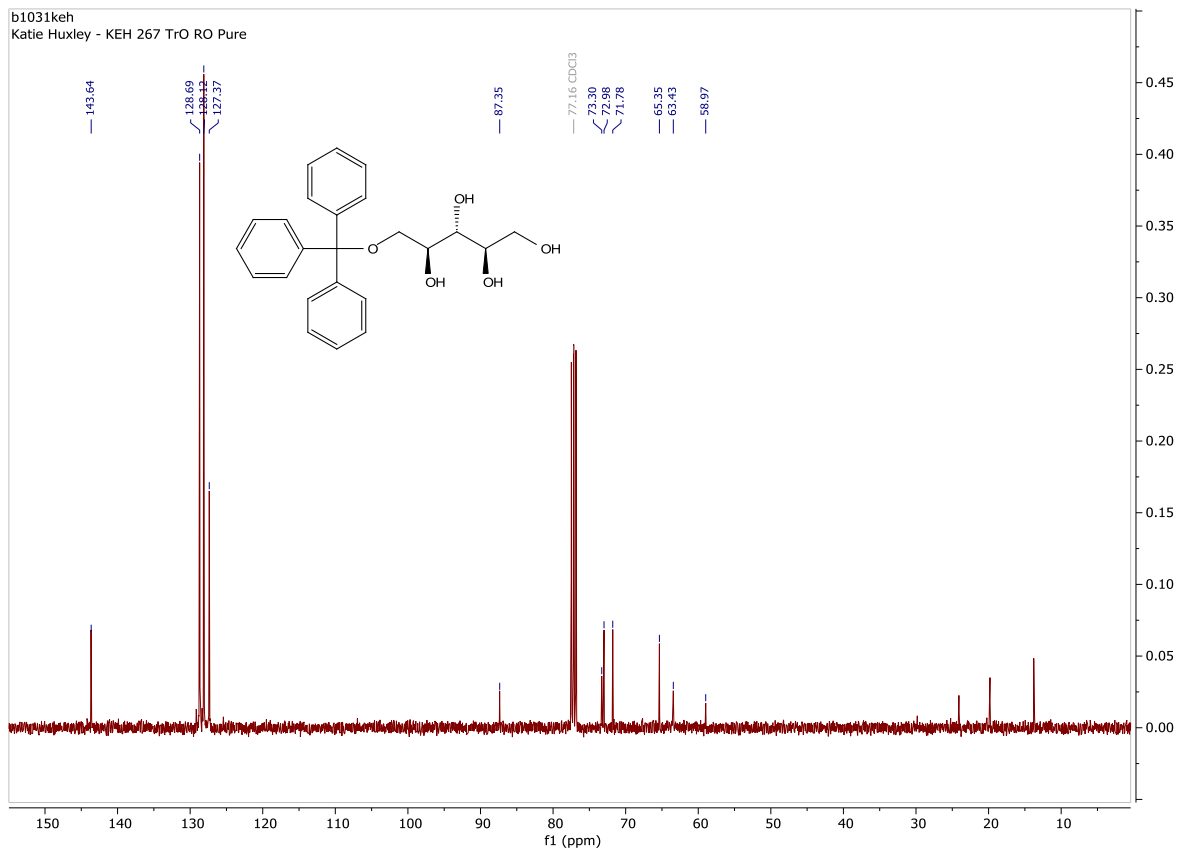
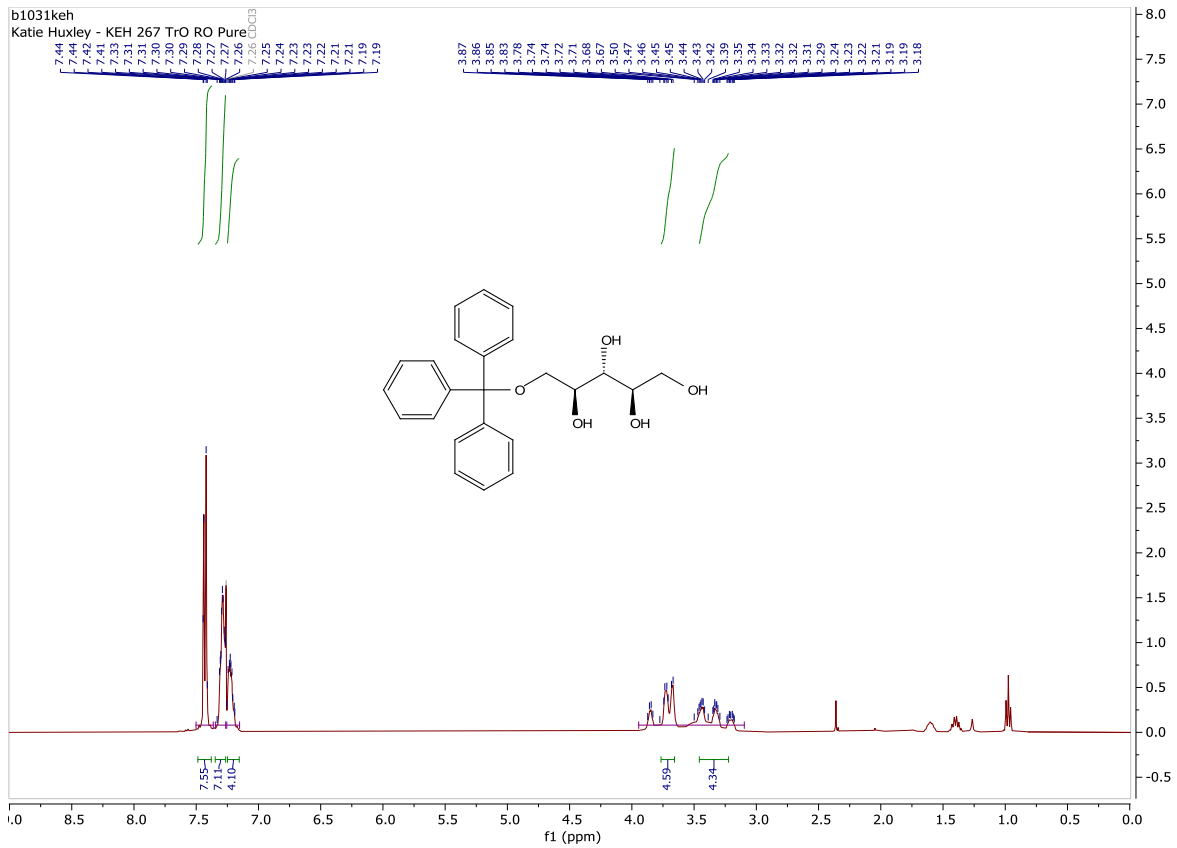
1,2,3,4,5-penta-O-benzyl-ribose (33)



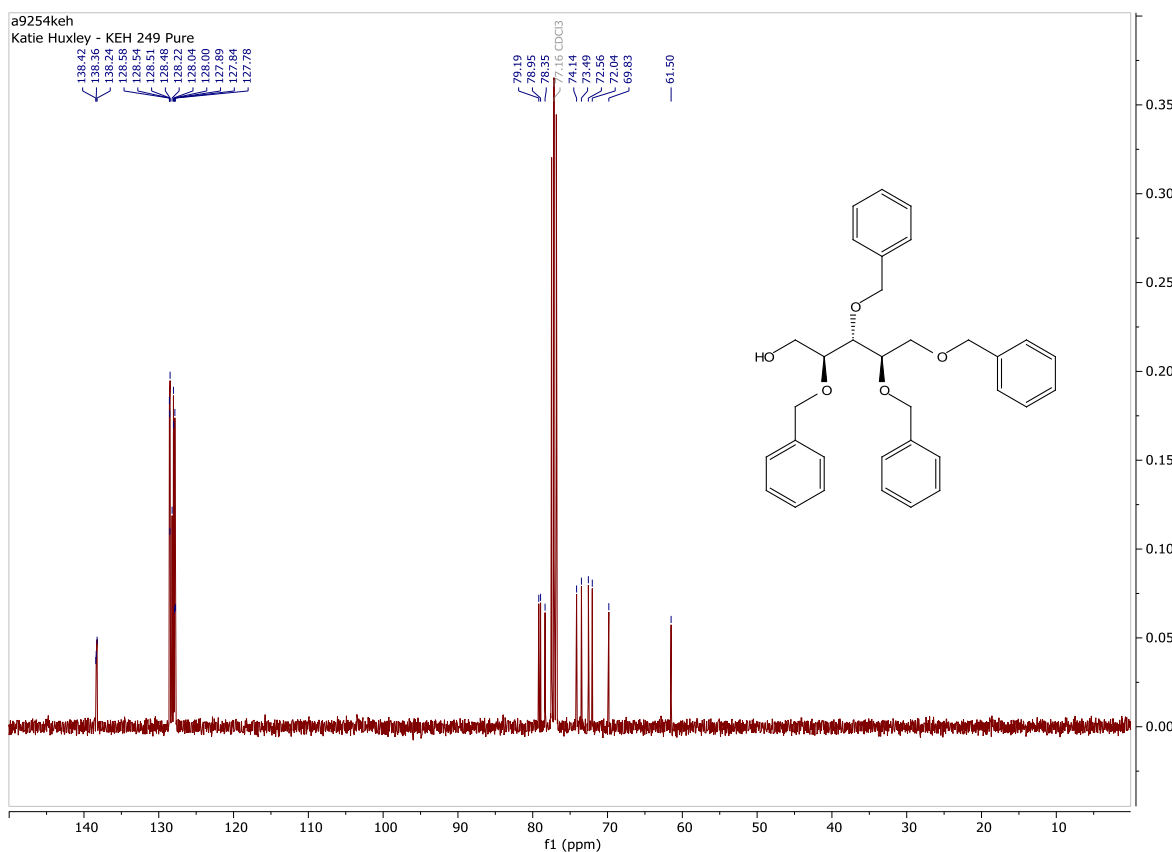
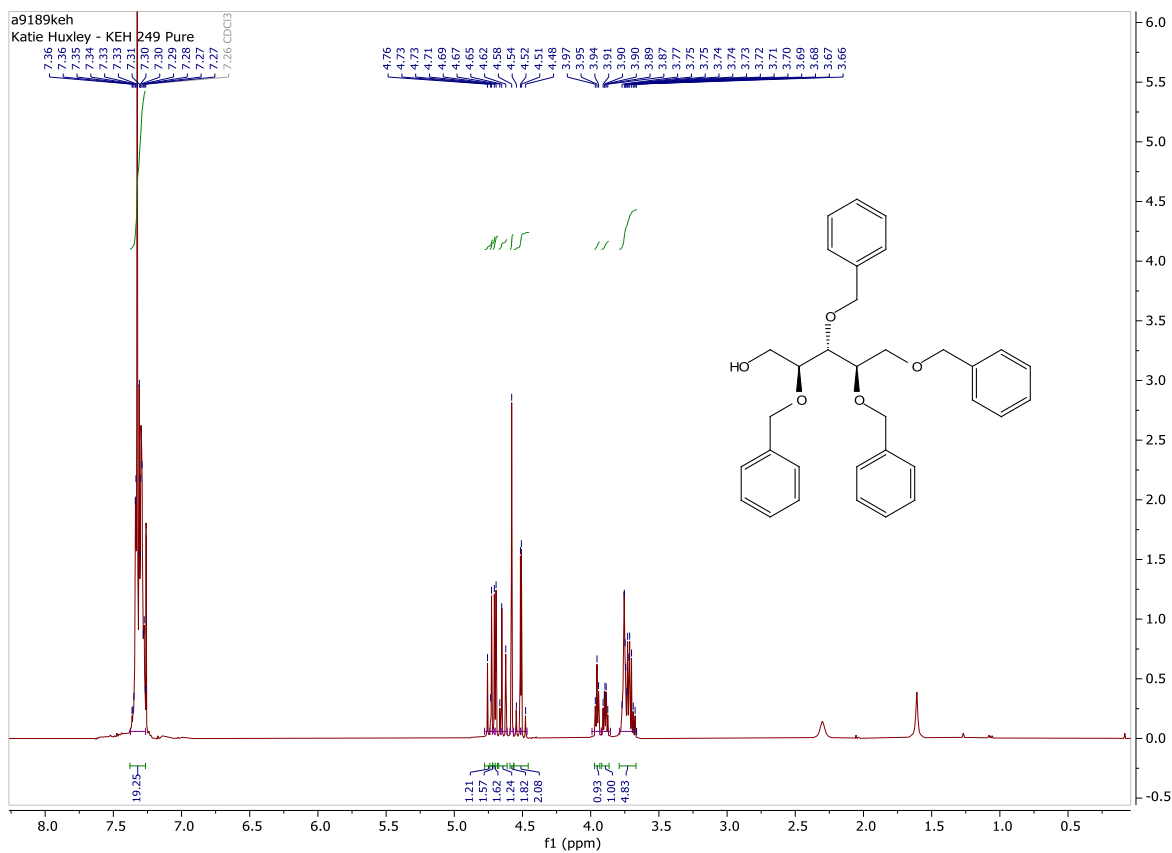
1,5-di-O-acetyl-2,3,4-tetra-O-benzyl-D-ribose (34)



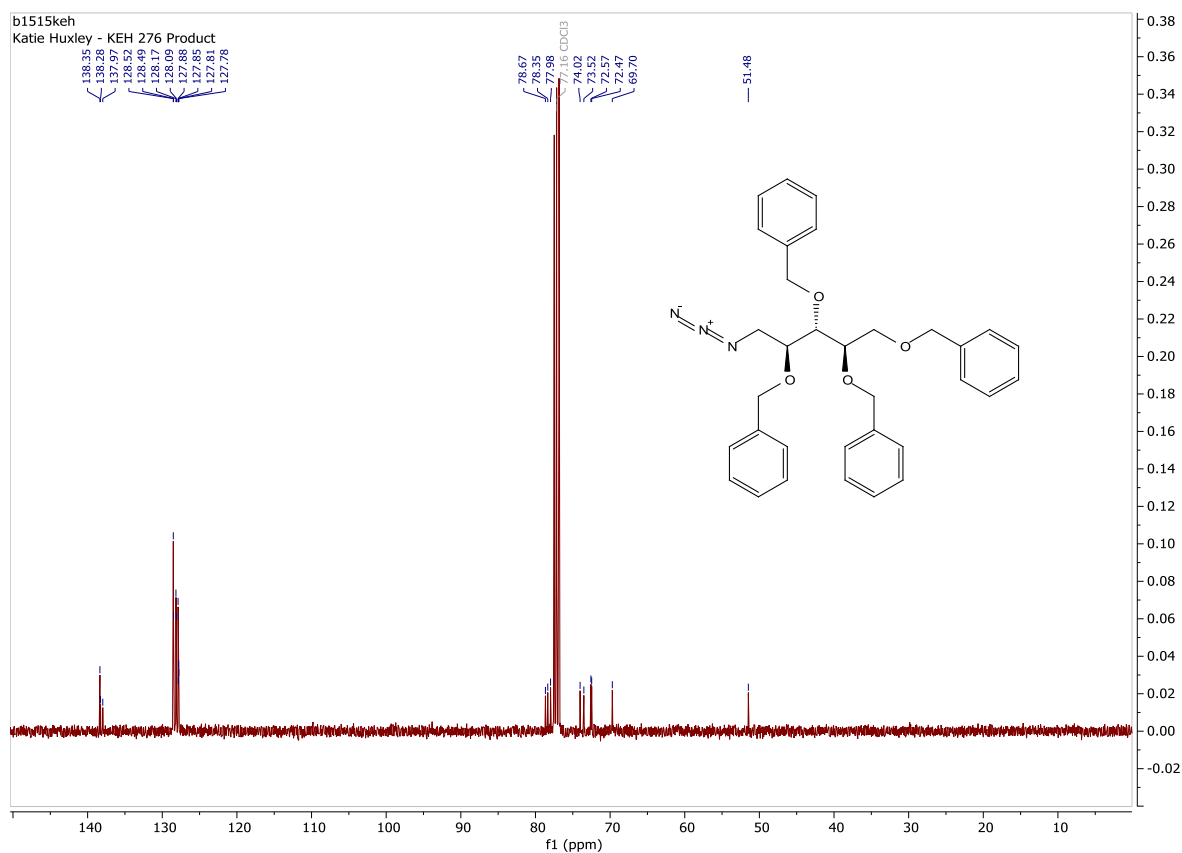
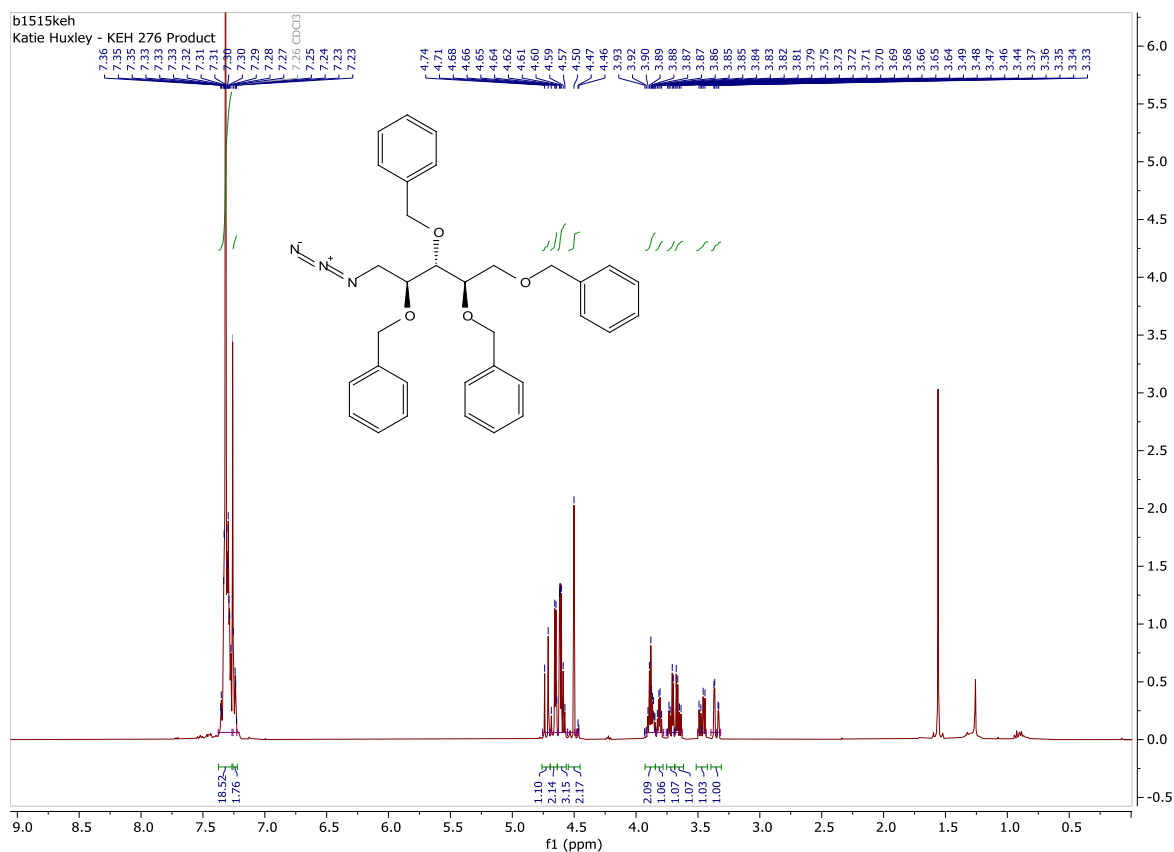
1-O-trityl-D-ribitol (11)



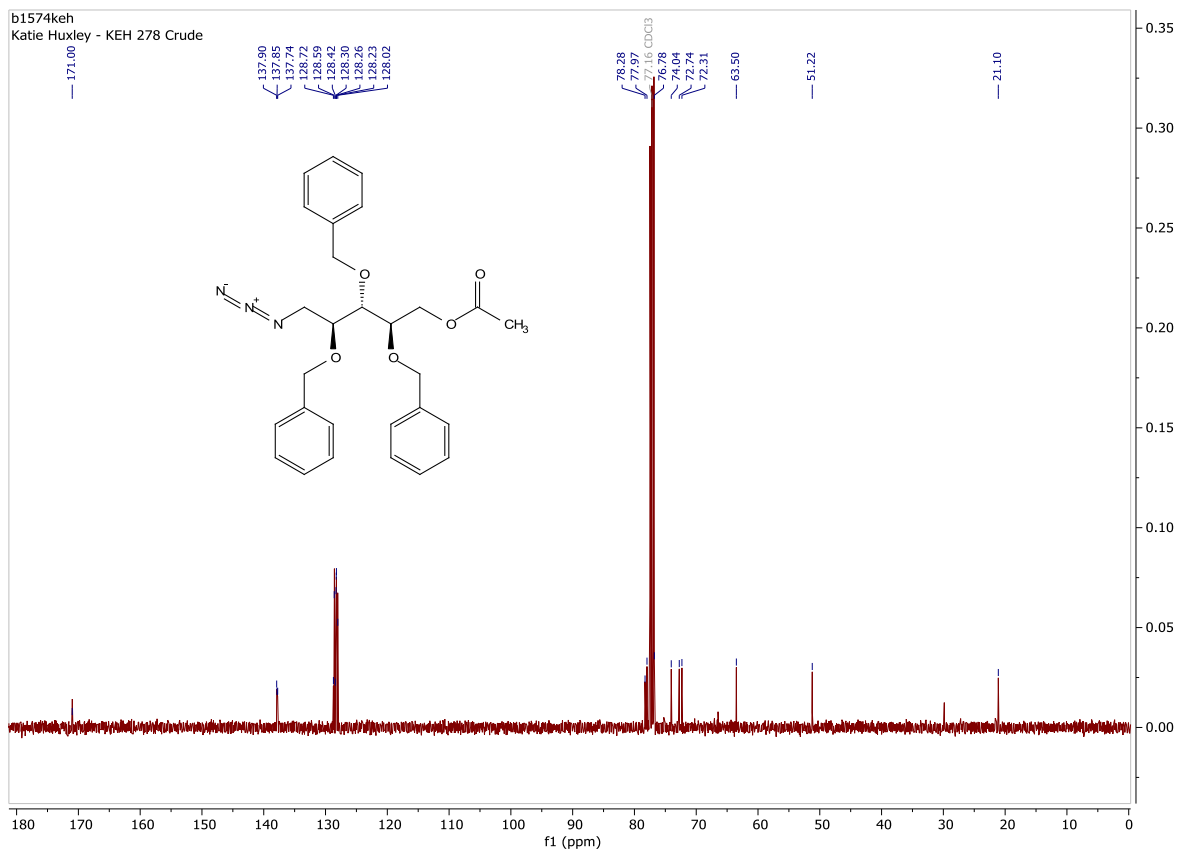
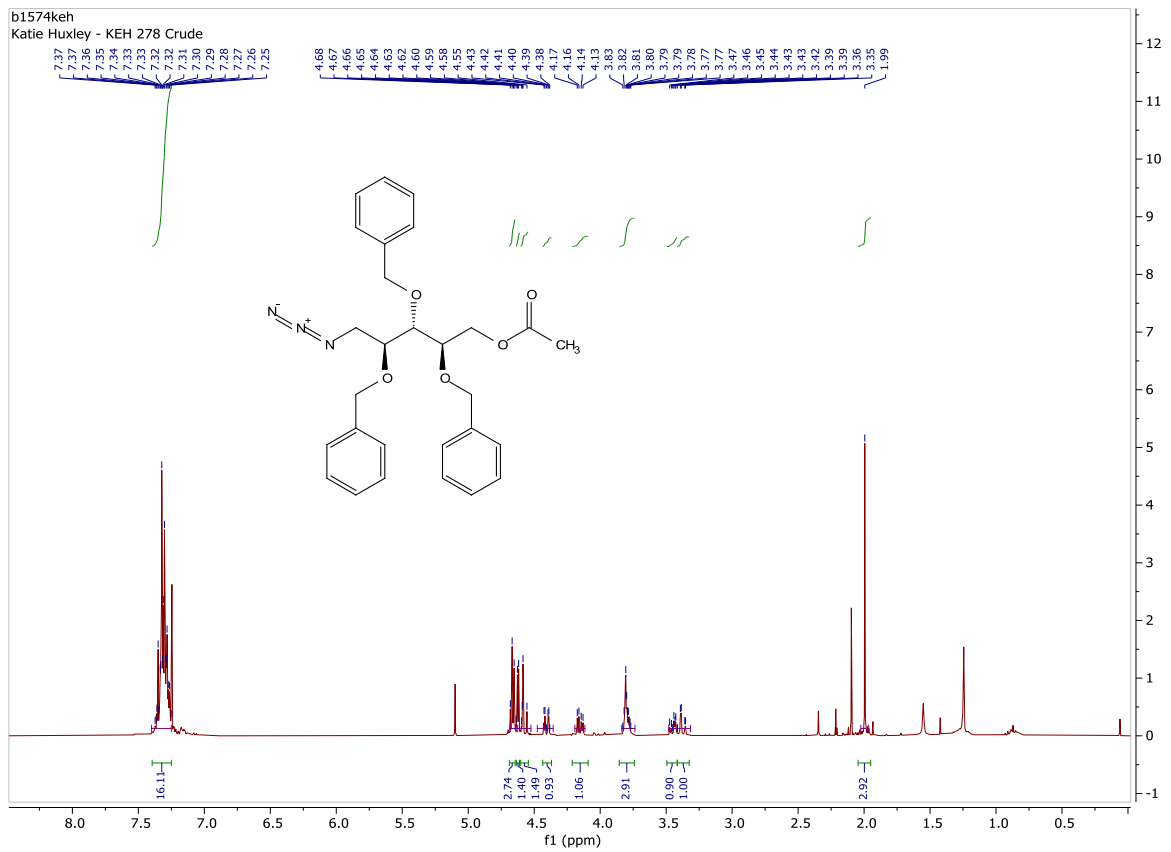
2,3,4,5-tetra-O-benzyl-D-ribose (35)



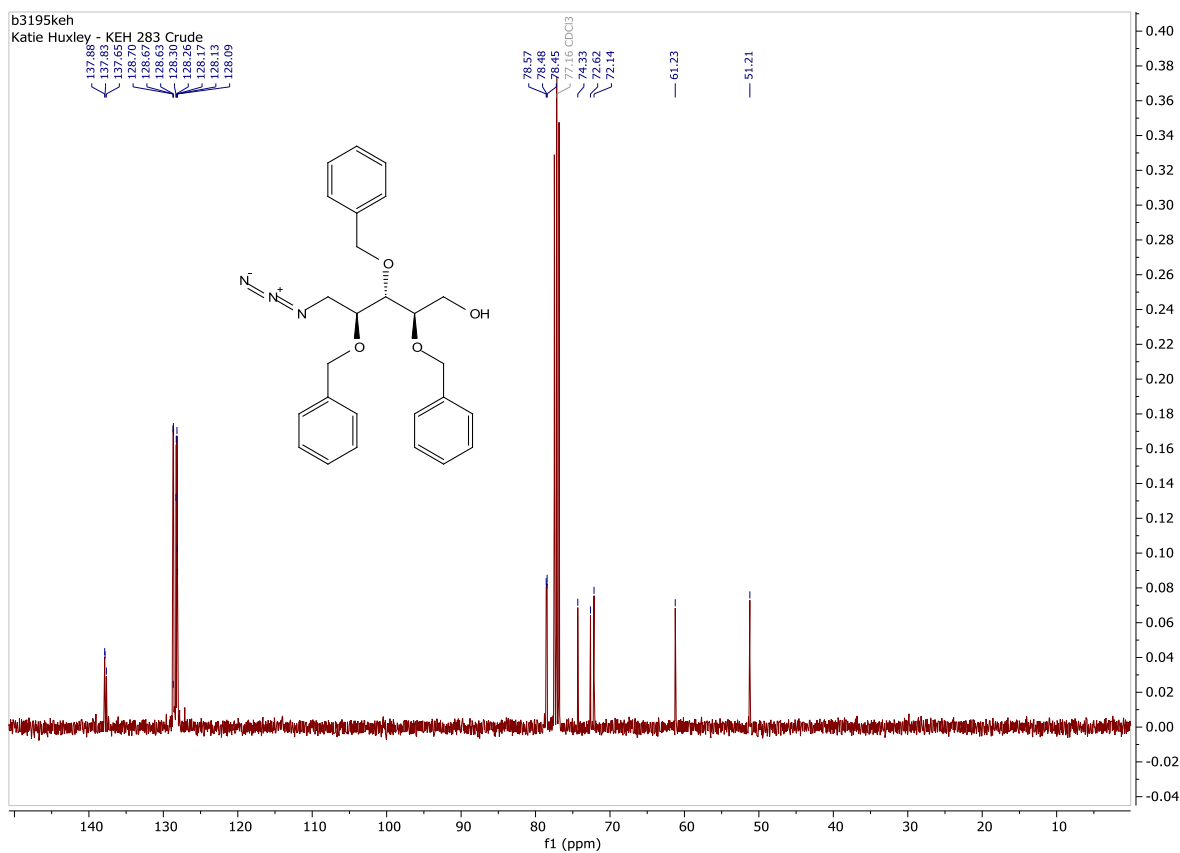
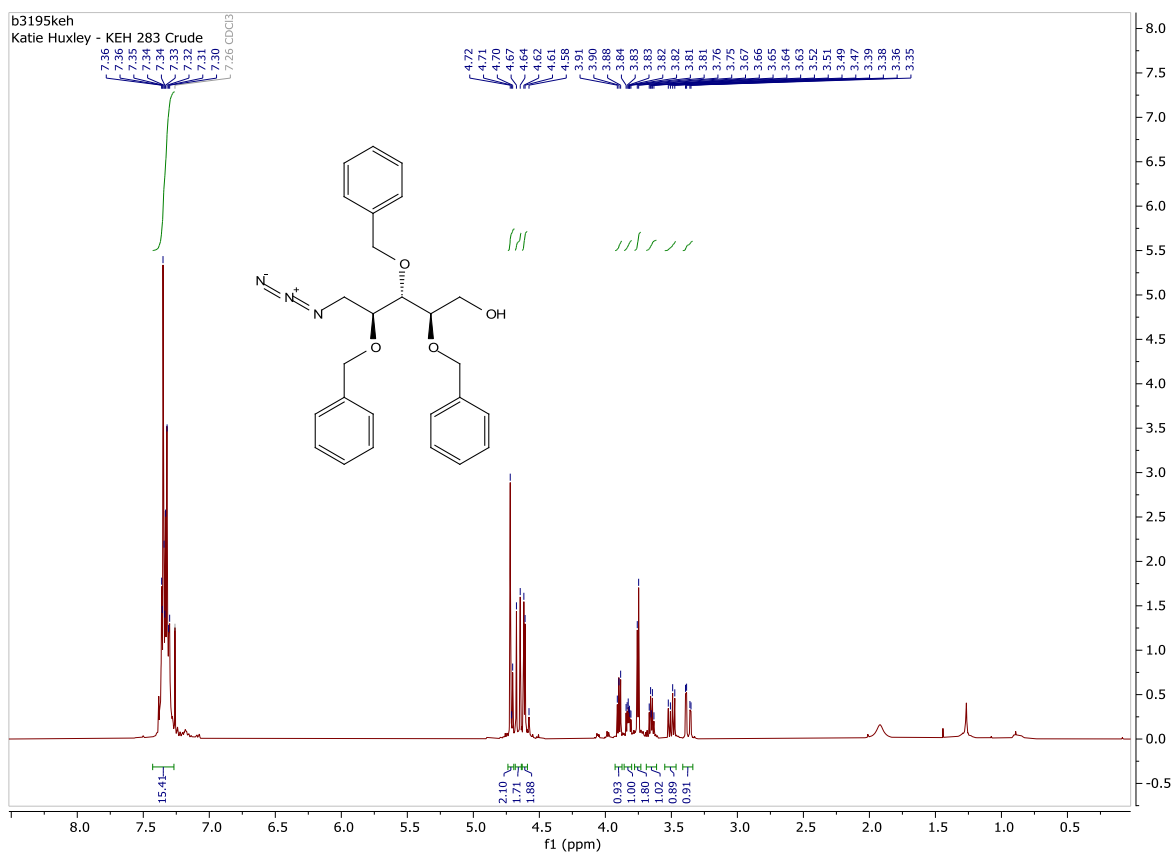
1-azido-2,3,4,5-tetra-O-benzyl-D-ribose (36)



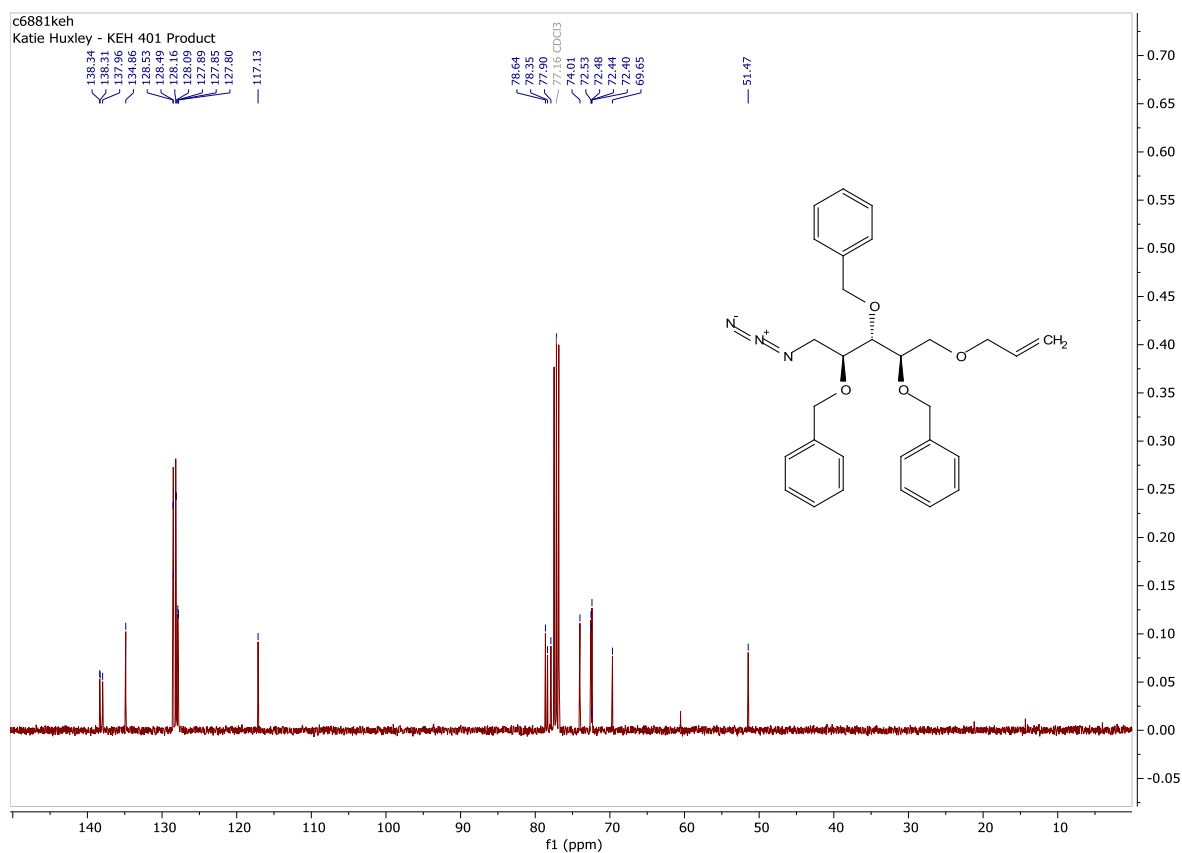
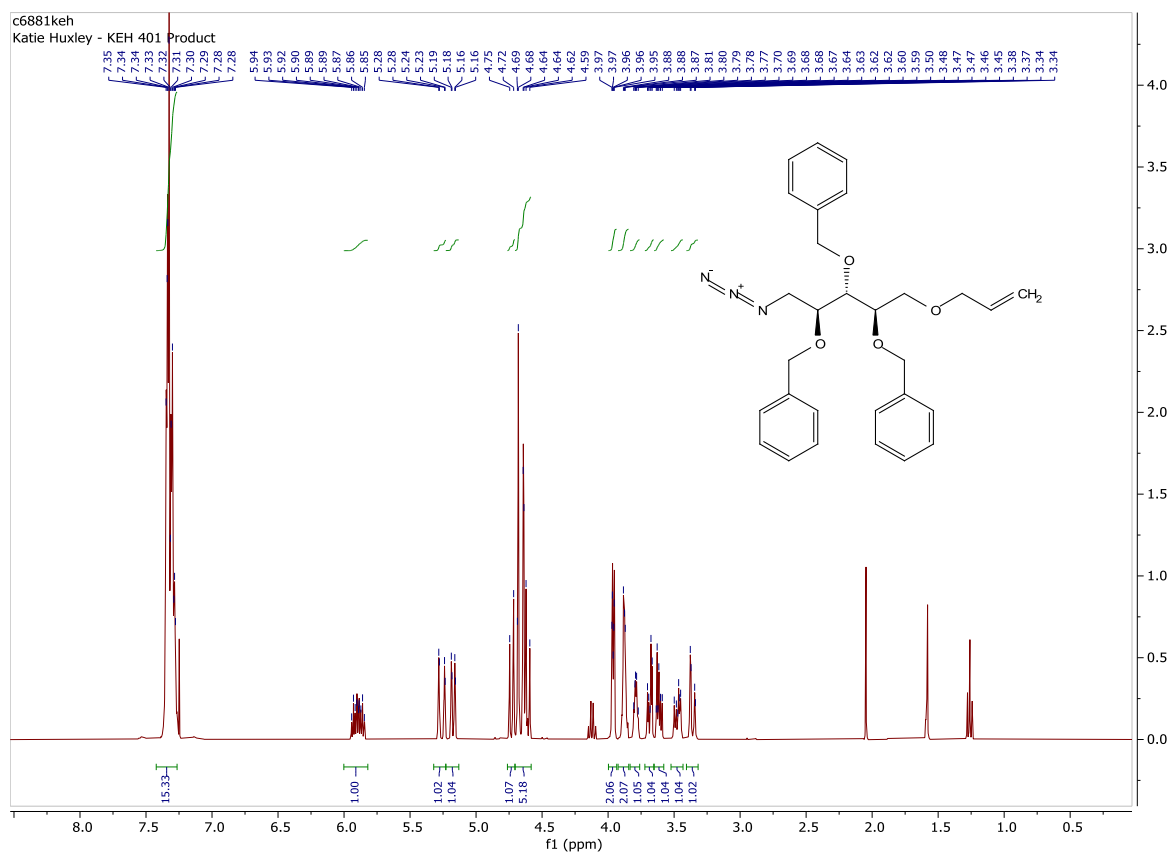
5-O-acetyl-1-azido-2,3,4-tri-O-benzyl-D-ribose (39)

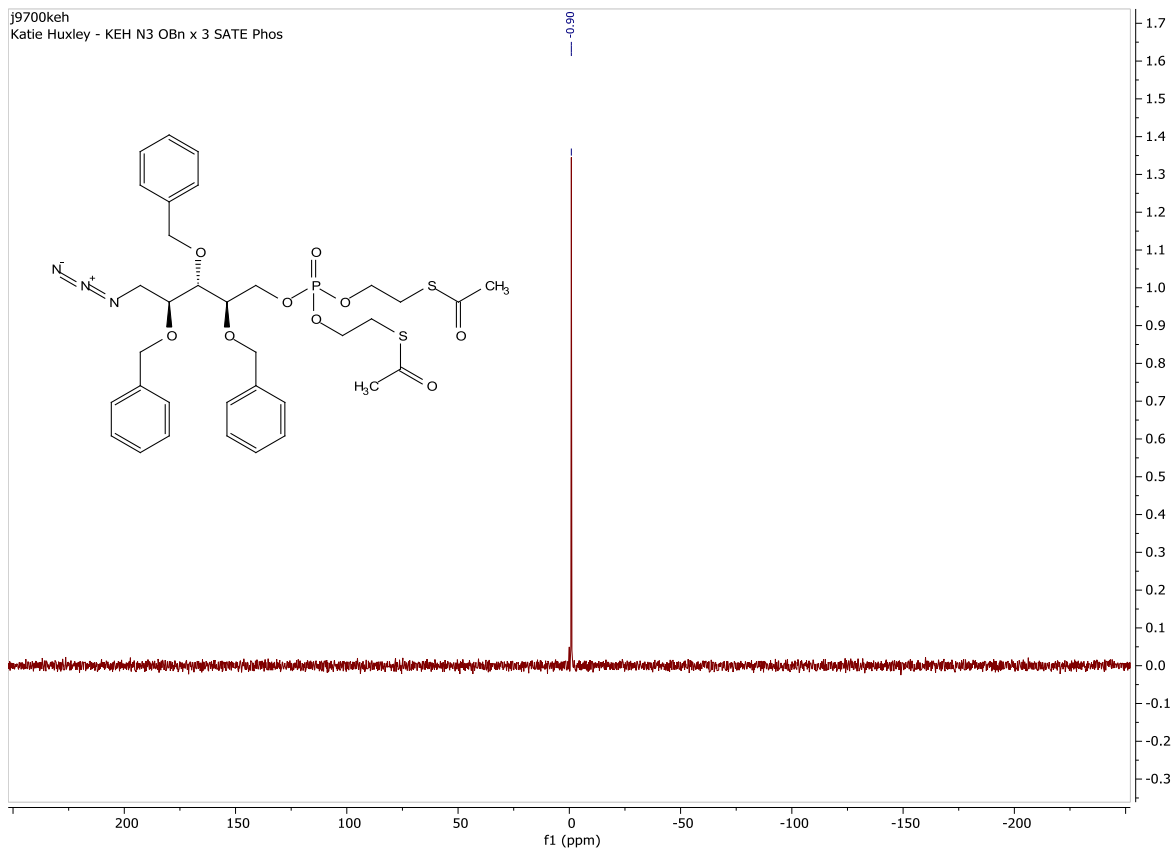


1-azido-2,3,4-tri-O-benzyl-D-ribose (6)

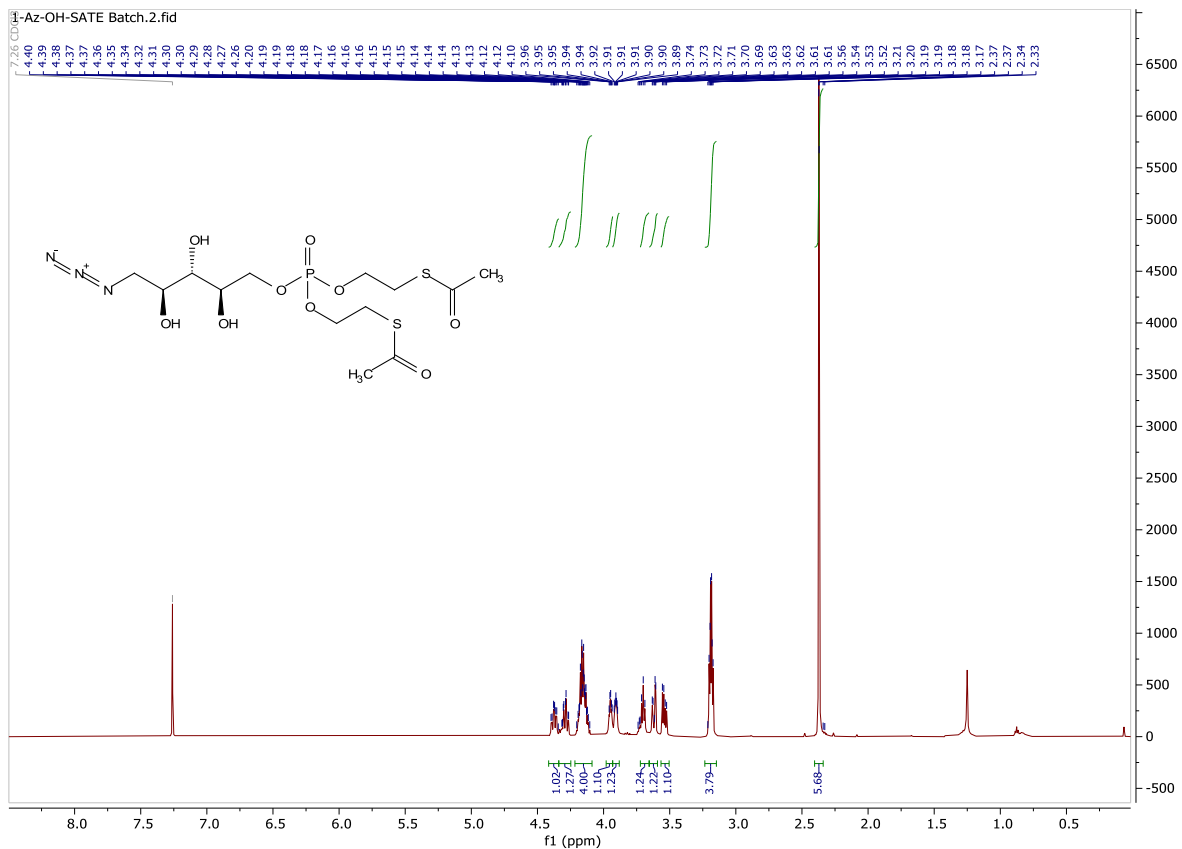


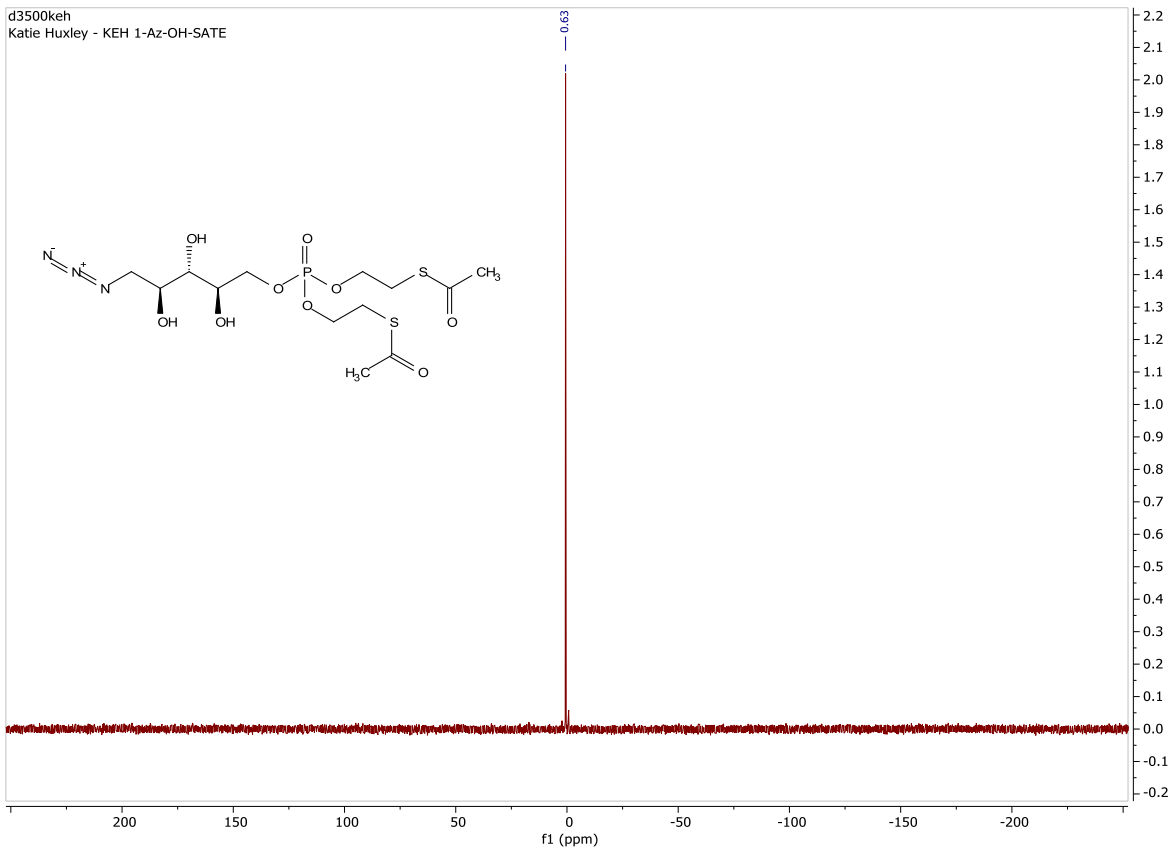
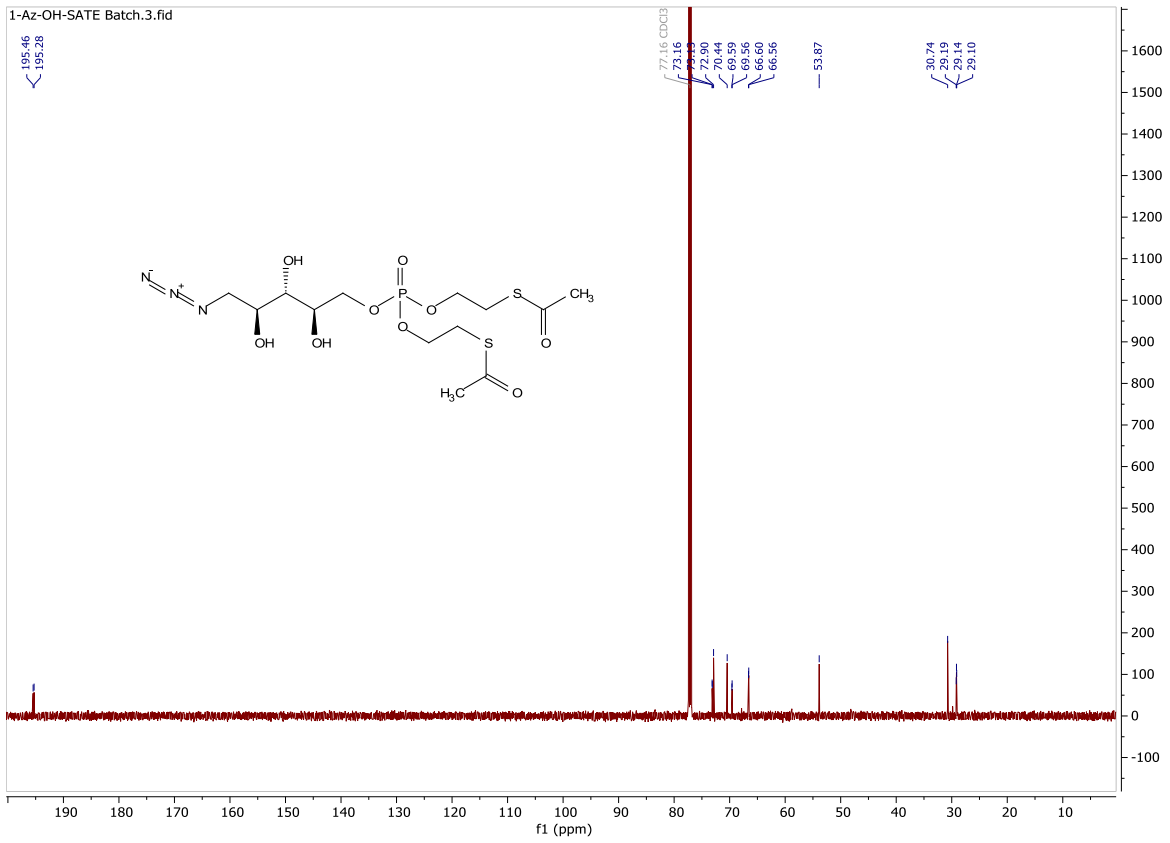
5-O-allyl-1-azido-2,3,4-tri-O-benzyl-D-ribose (47)



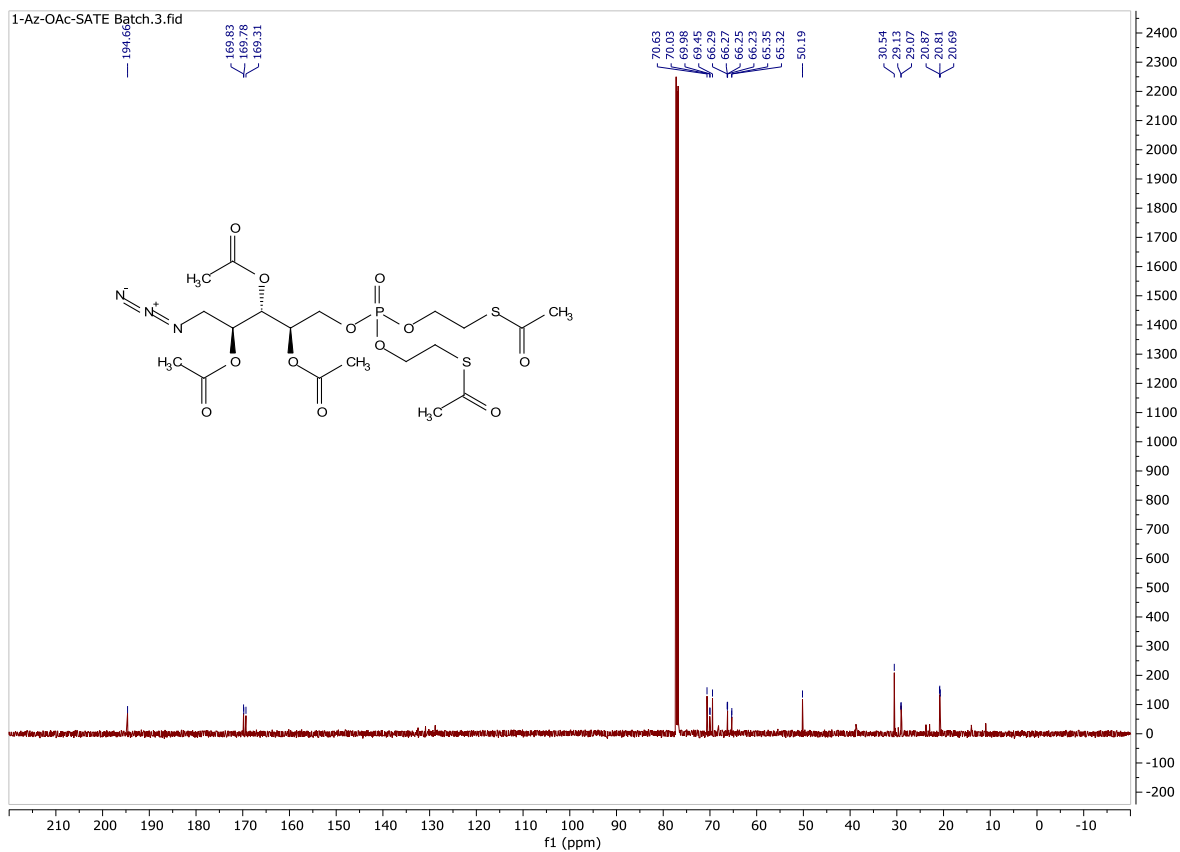
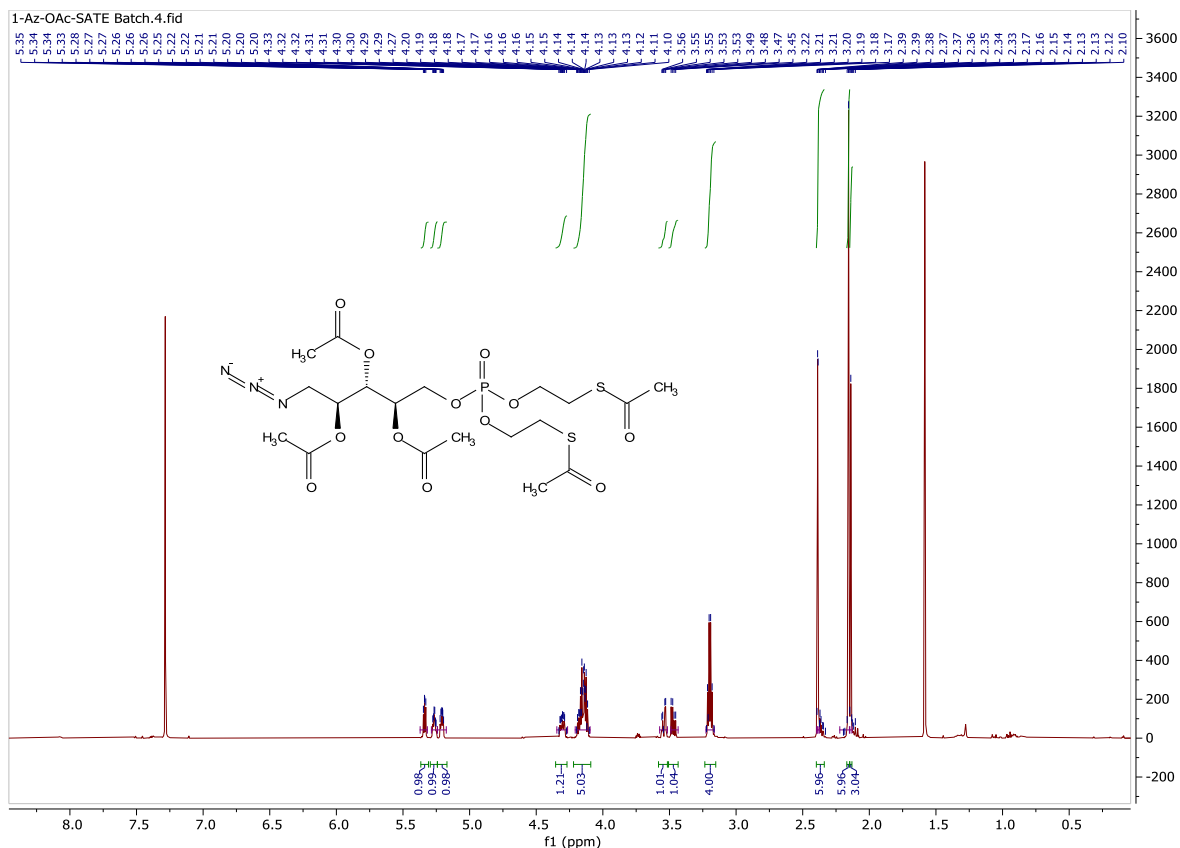


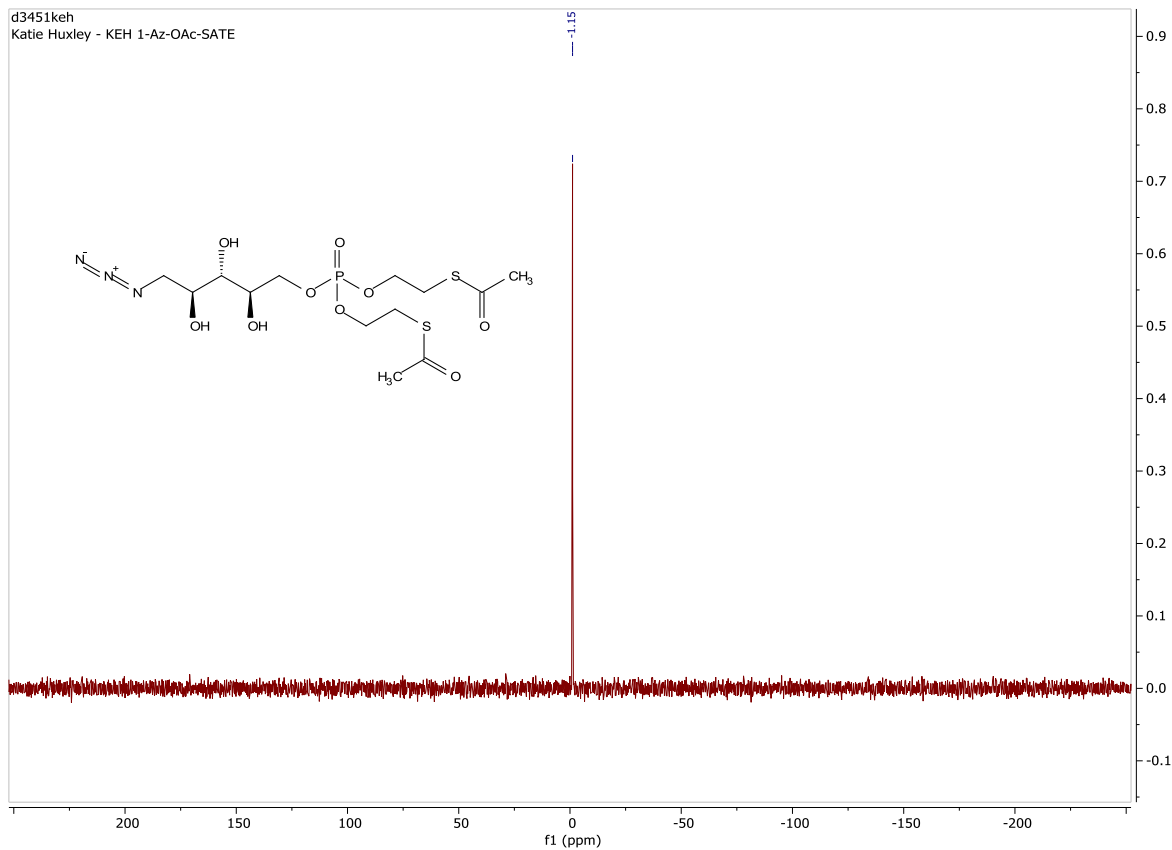
1-azido-D-ribose-5-(bis-S-acetyl-2-thioethyl-phosphate) (1-Az-OH-SATE Probe)



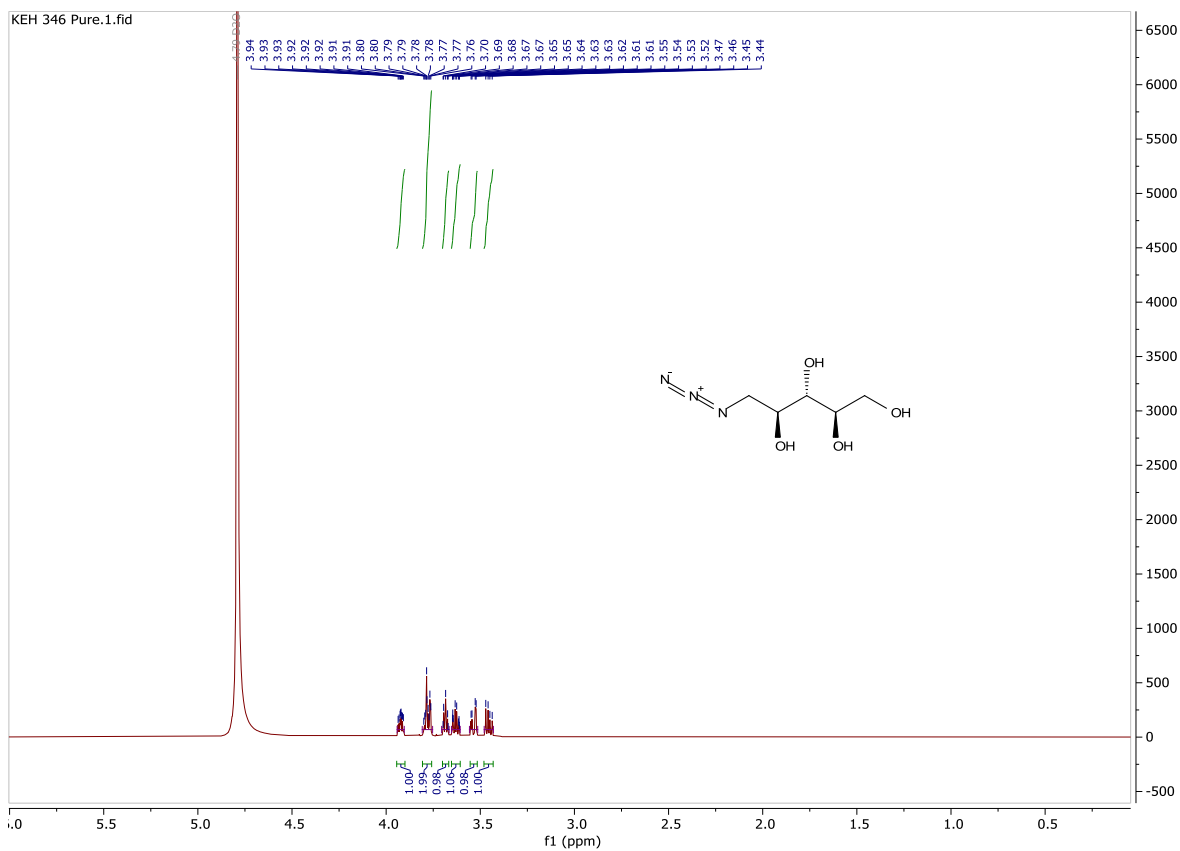


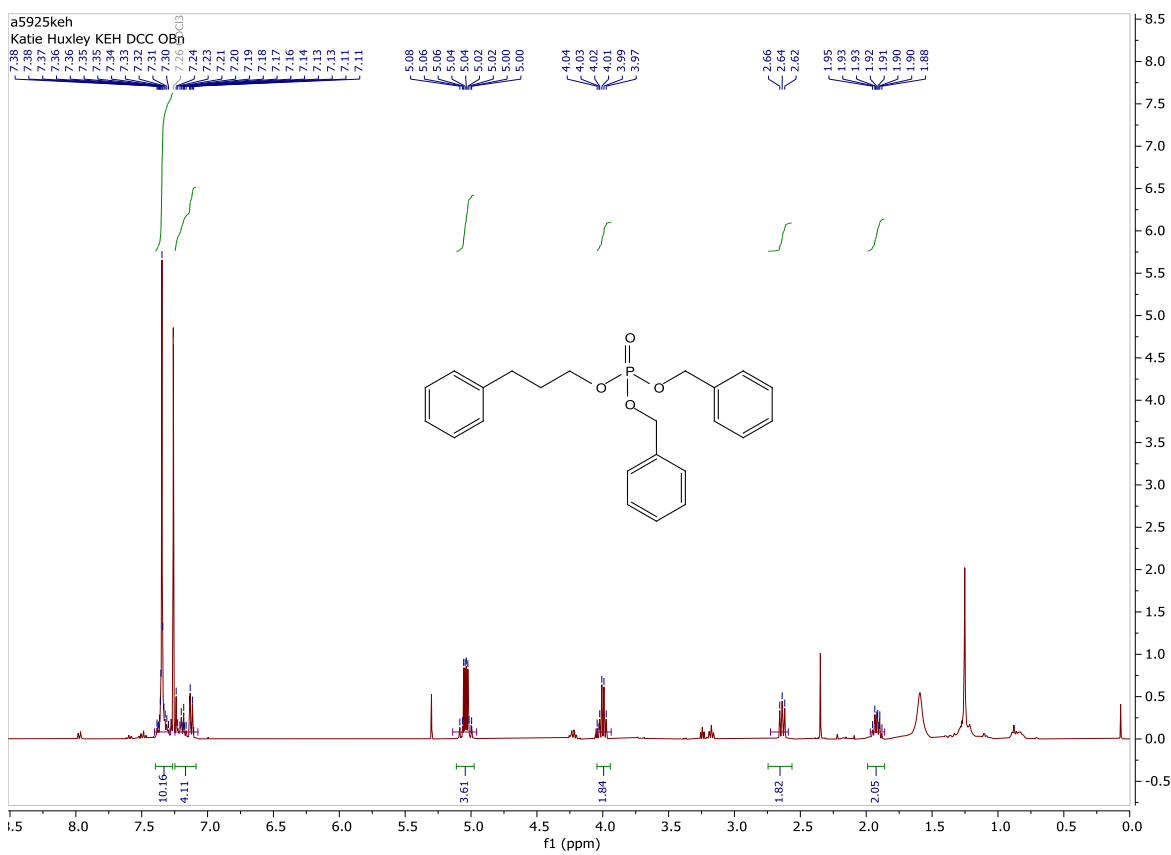
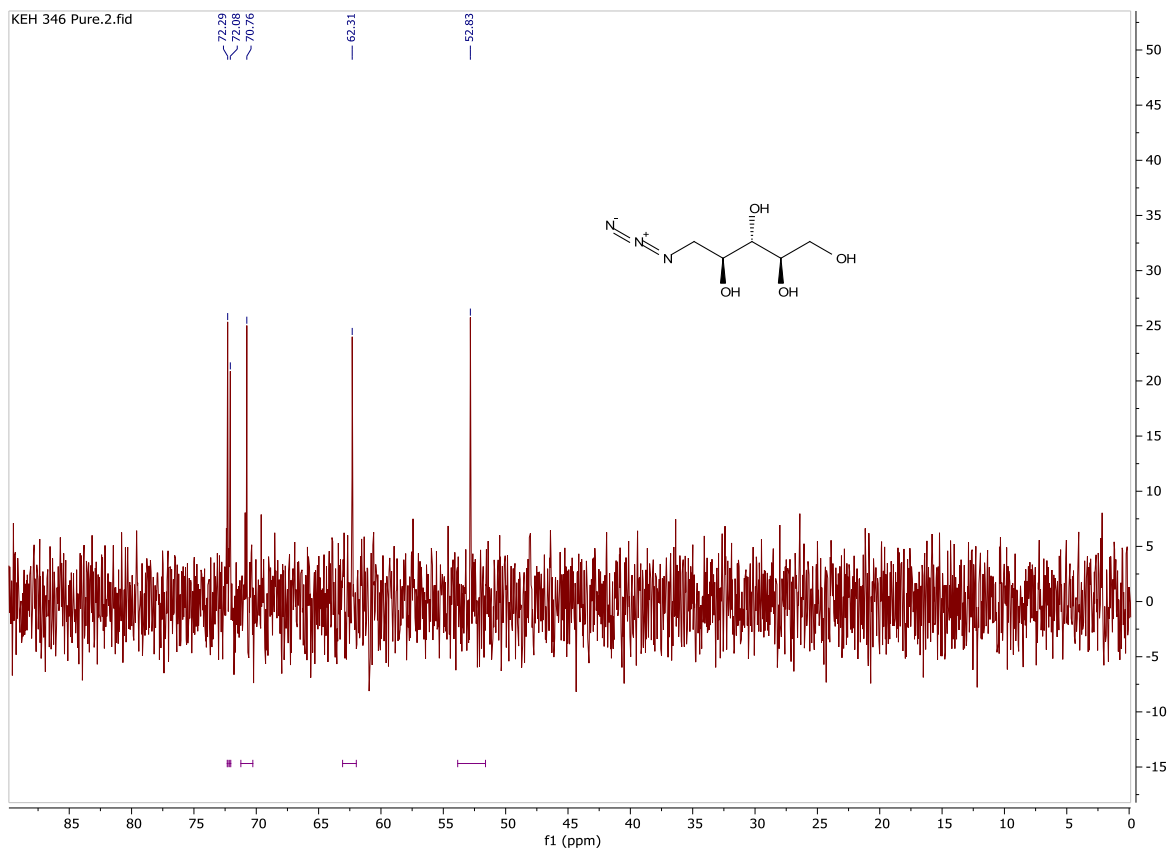
2,3,4-*tri-O*-acetyl-1-azido-D-ribose-5-(bis(*S*-acetyl-2-thioethyl)phosphate) (1-Az-OAc-SATE Probe)

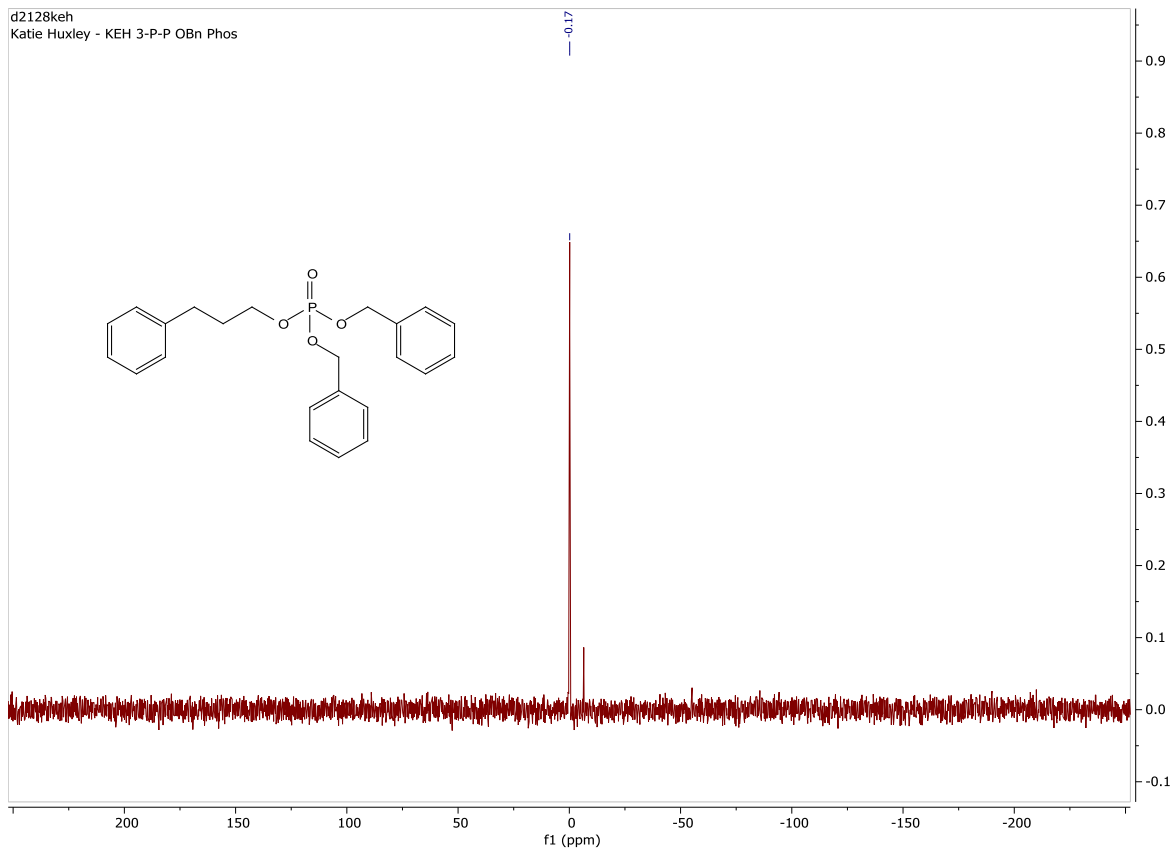
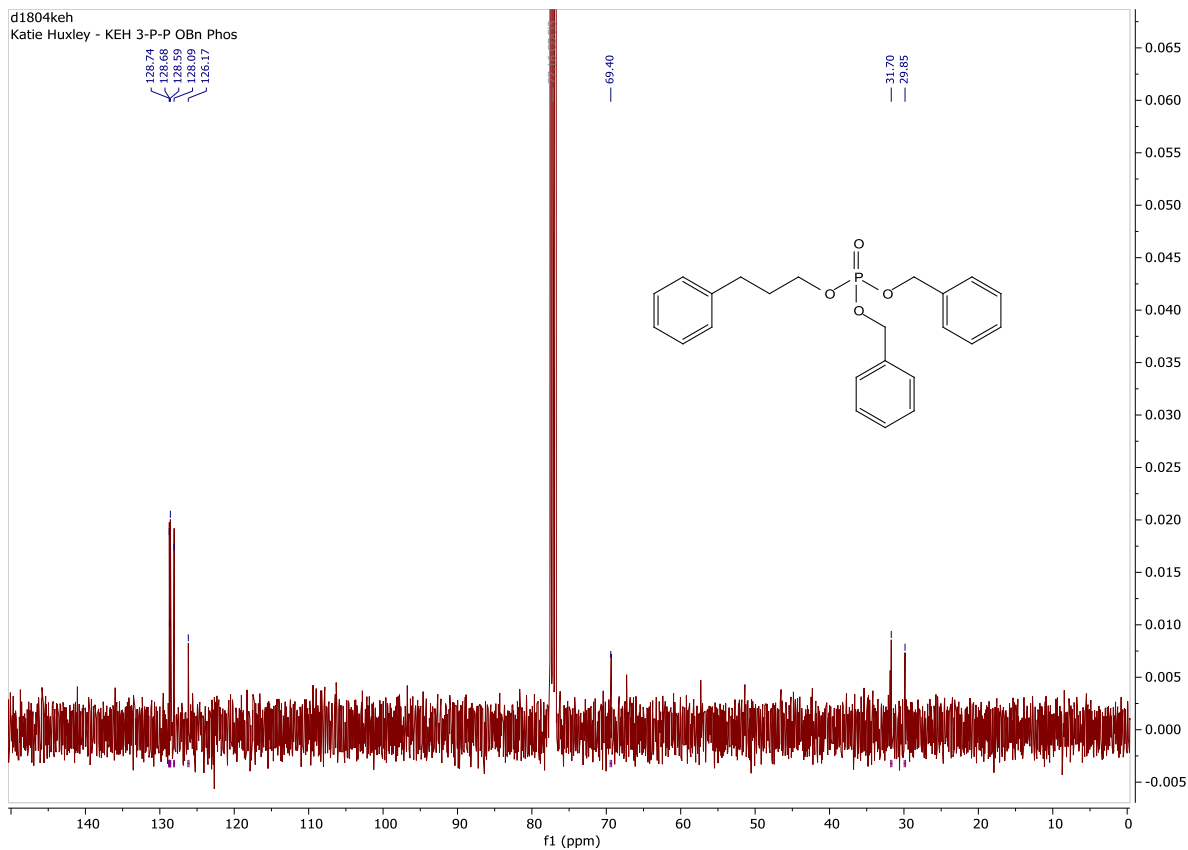




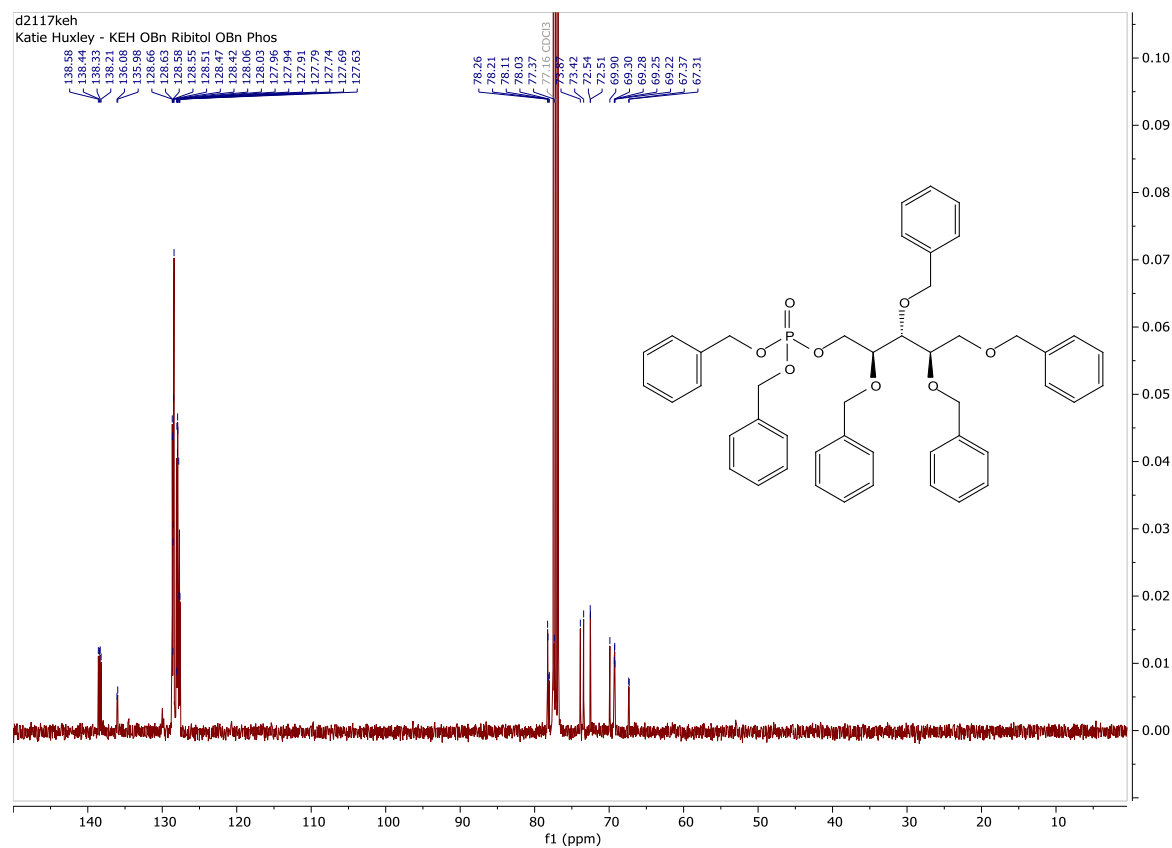
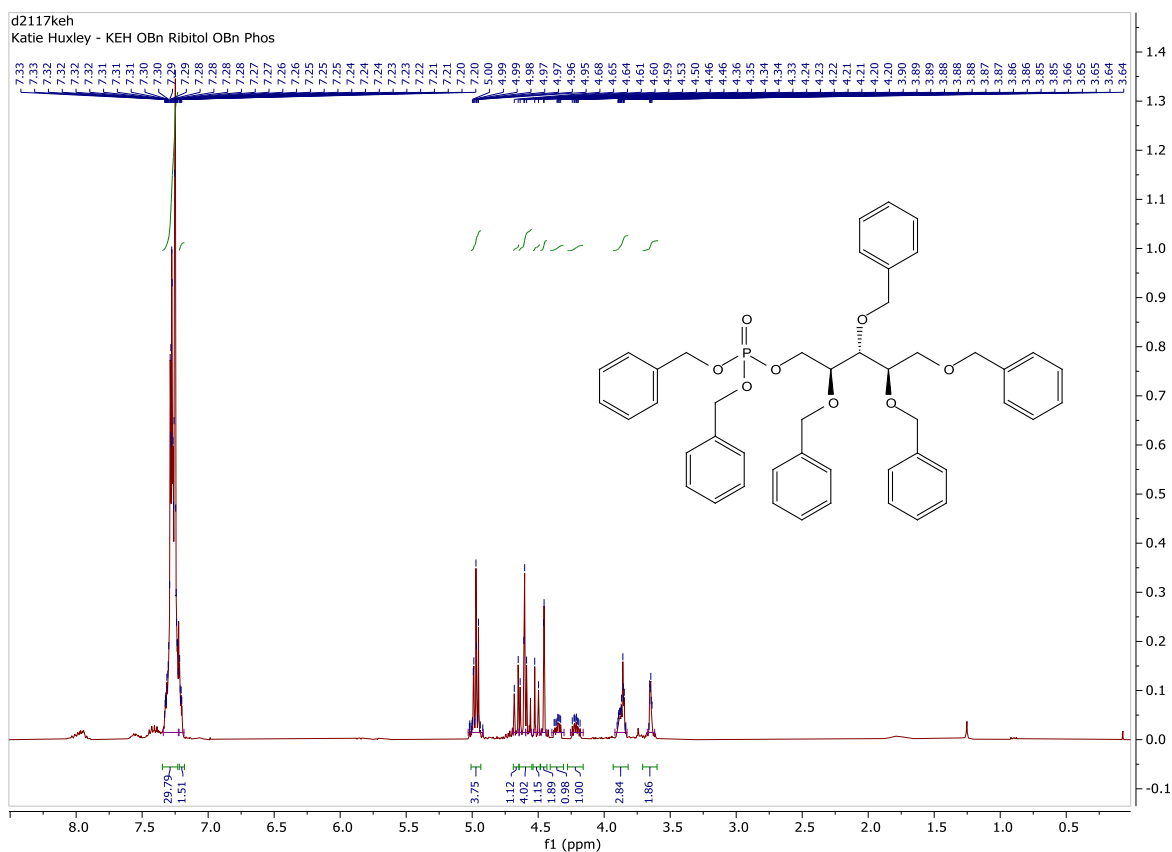
1-azido-ribitol (1-Az-OH Probe)

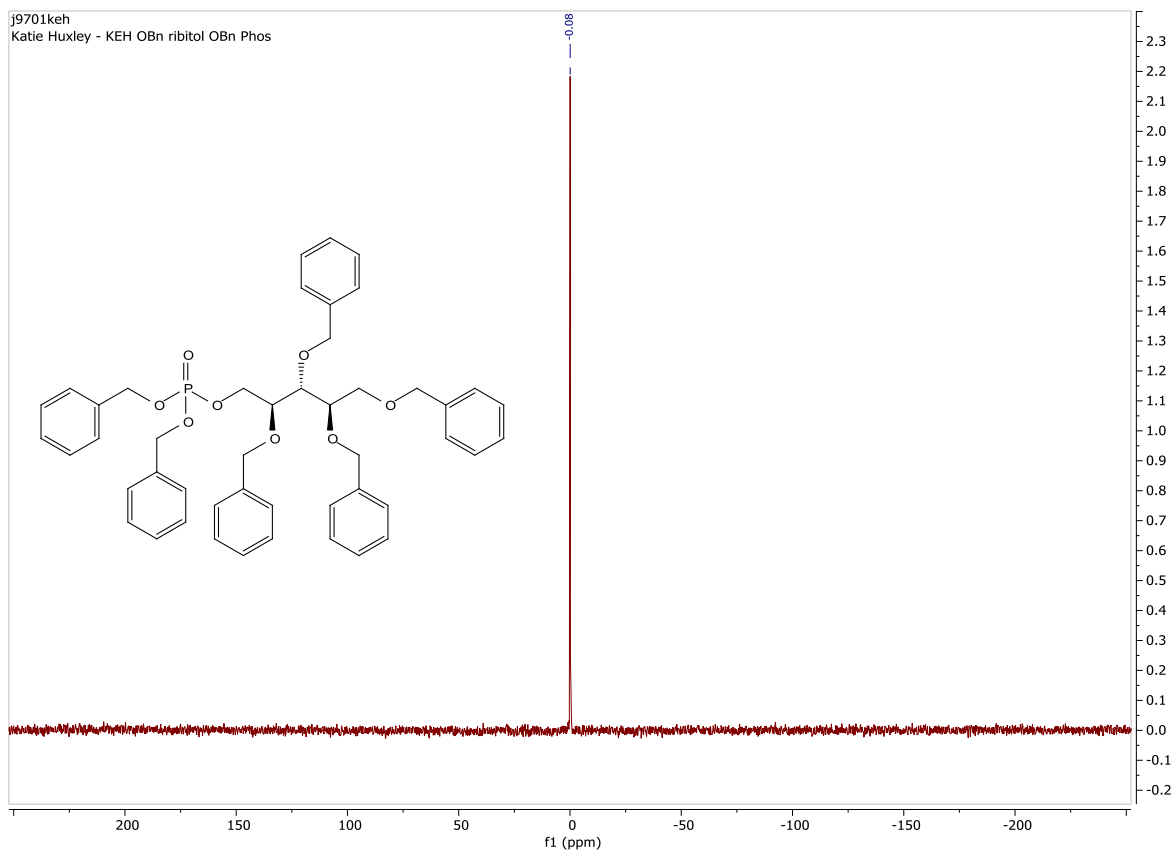




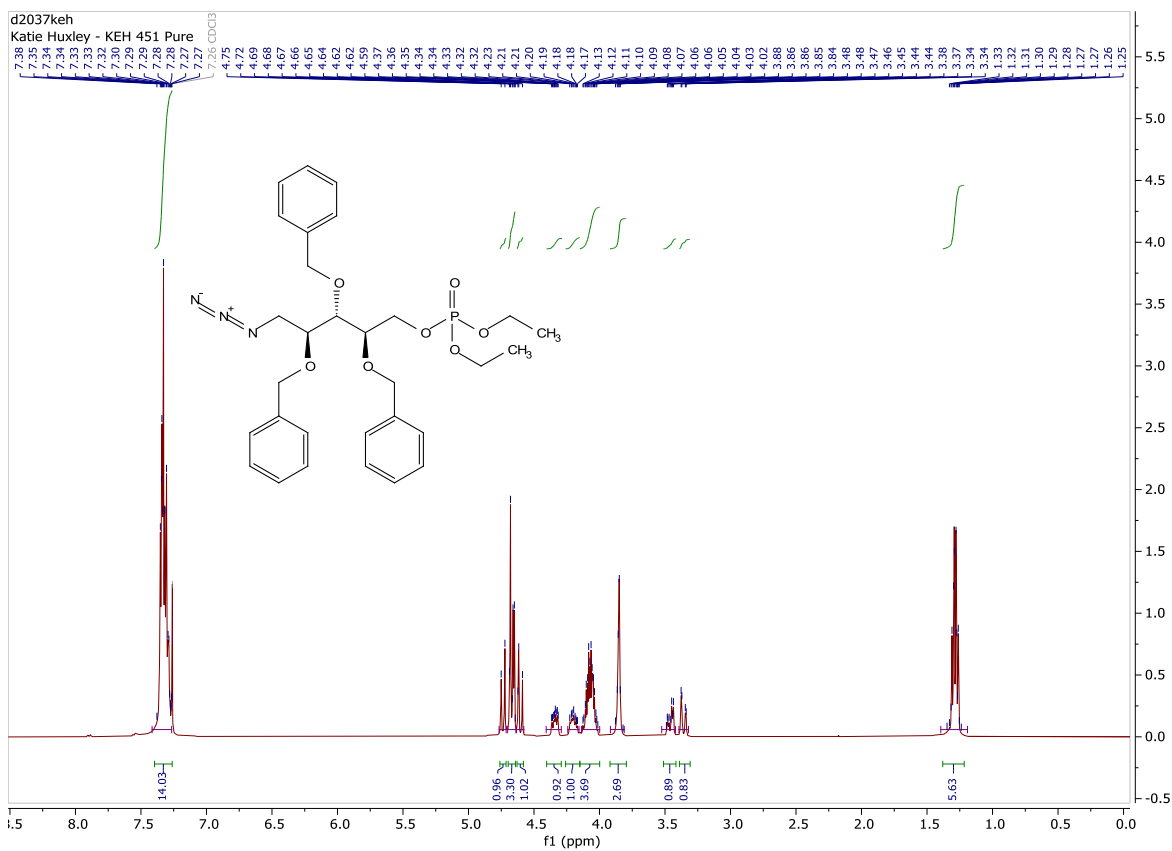


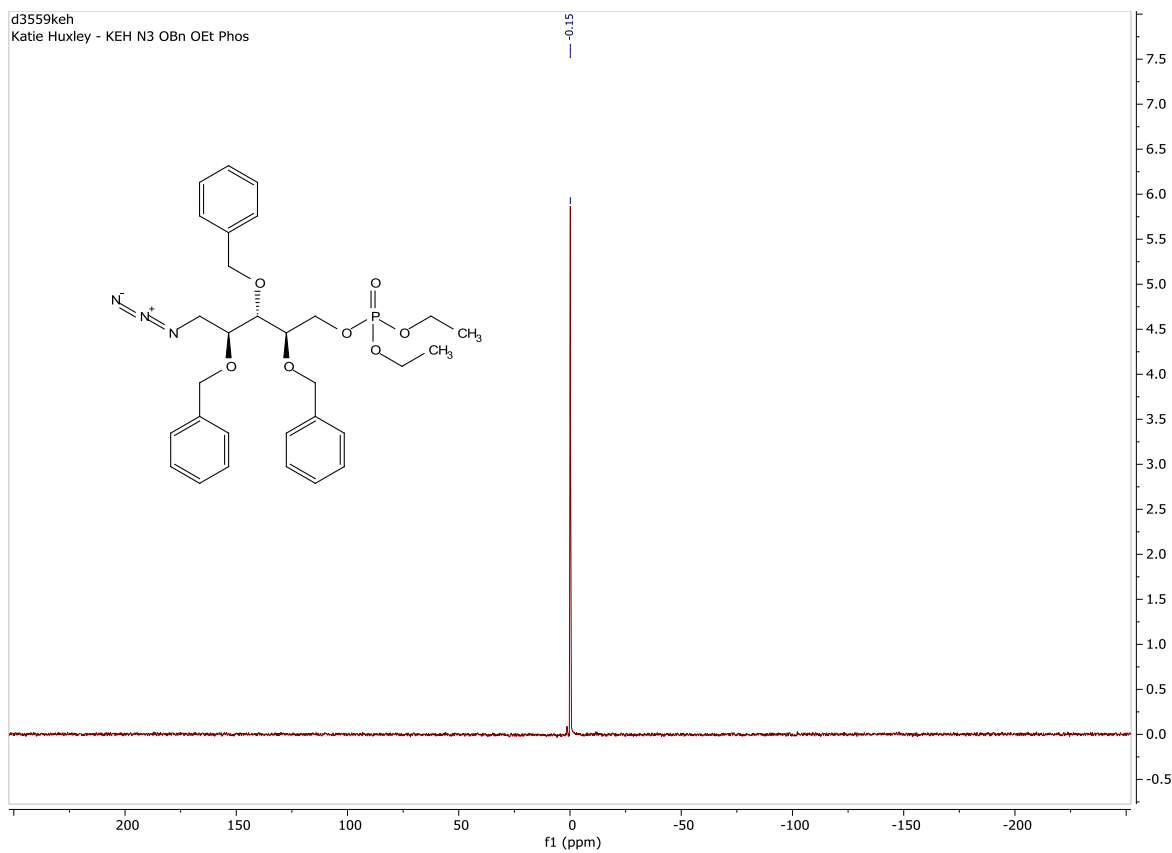
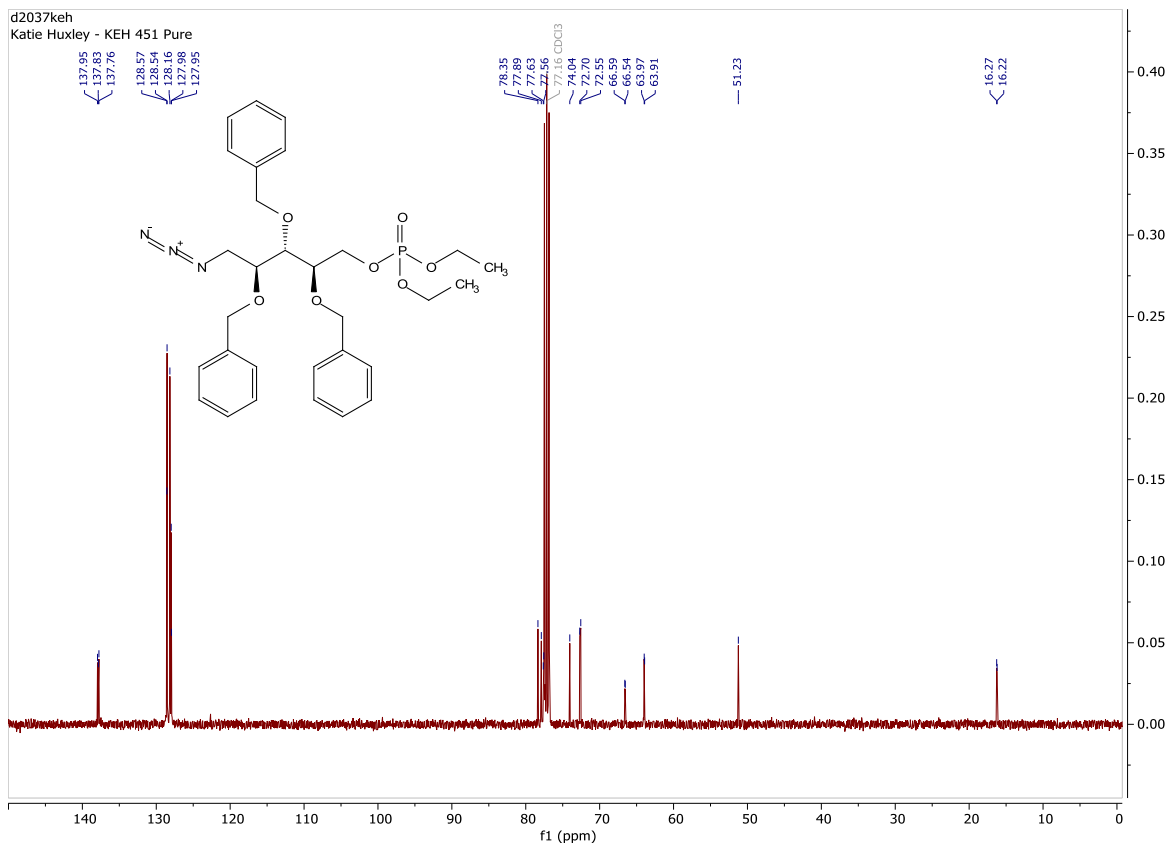
2,3,4,5-tetra-O-benzyl-ribose-1-(bis-benzylphosphate)



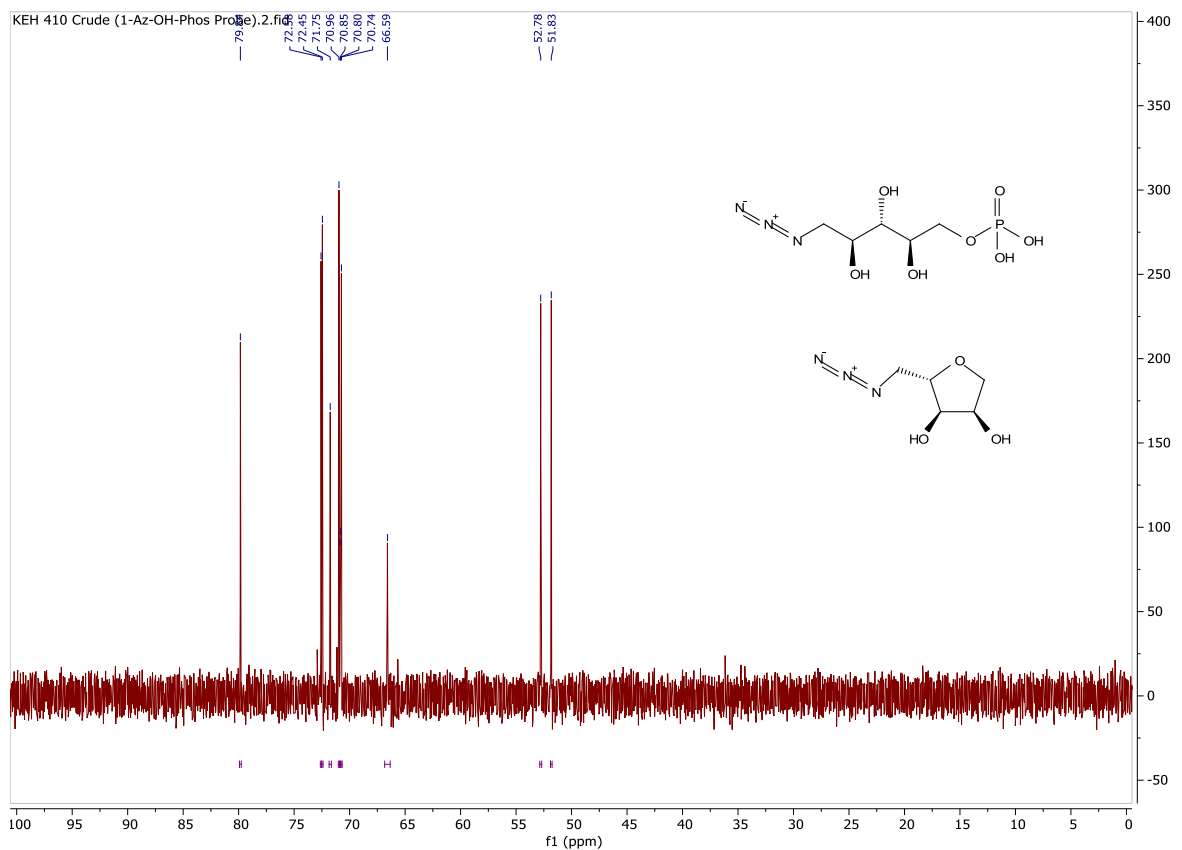
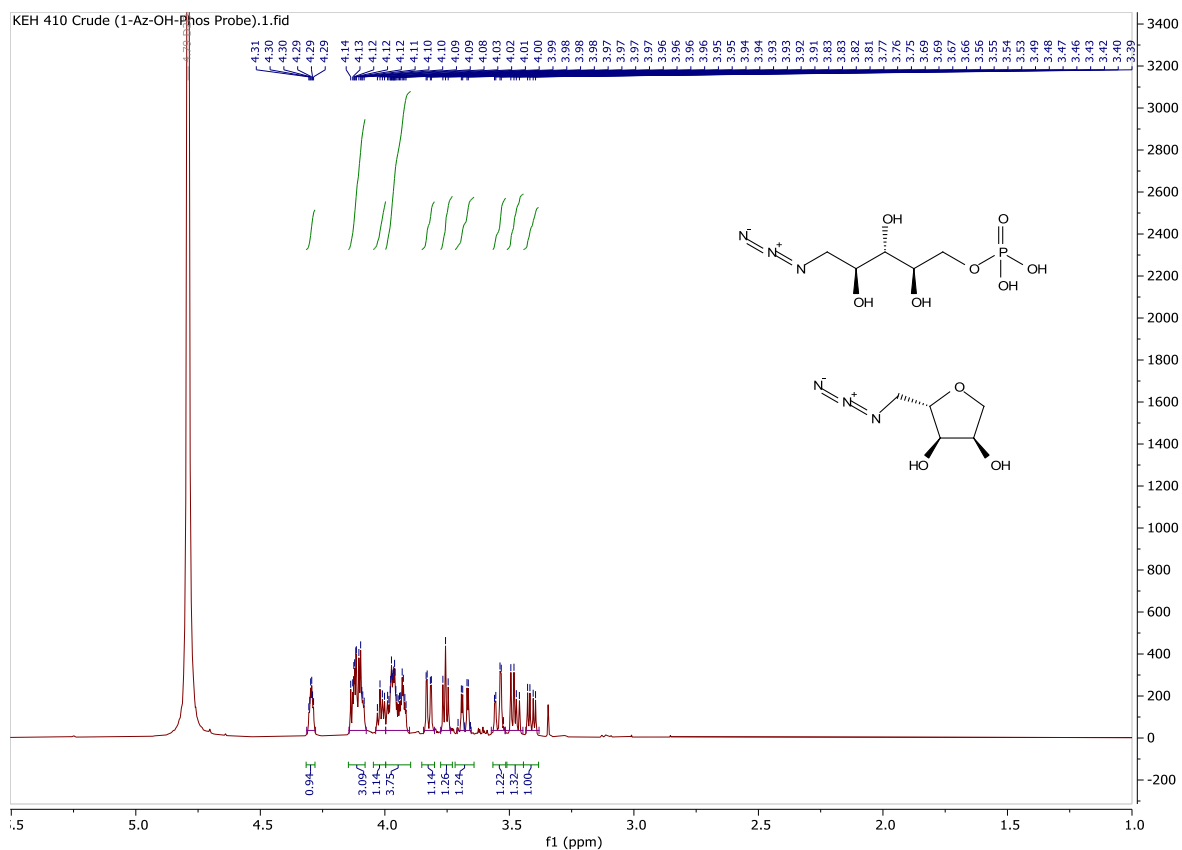


1-azido-2,3,4-tri-O-benzyl-D-ribose-5-(diethyl-phosphate) (43)

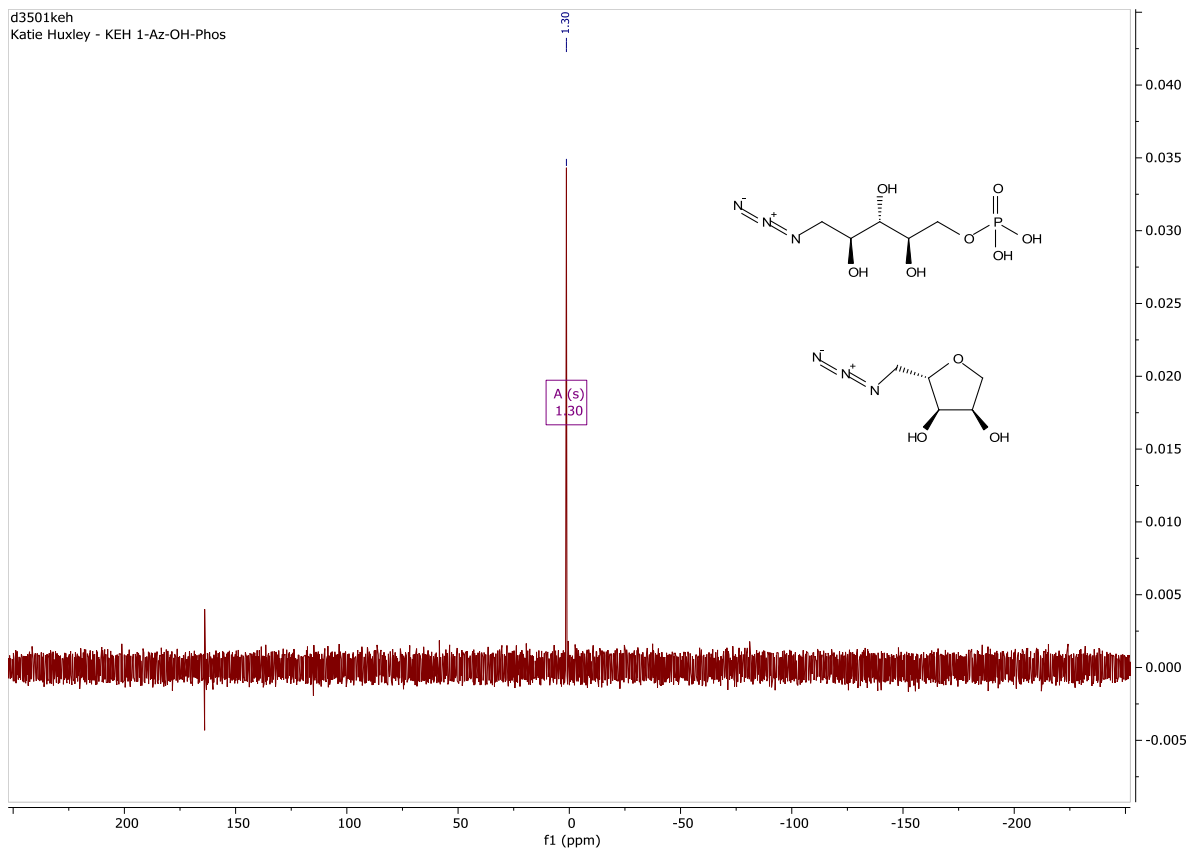




1-azido-D-ribose-5-phosphate (1-Az OH Phos Probe)

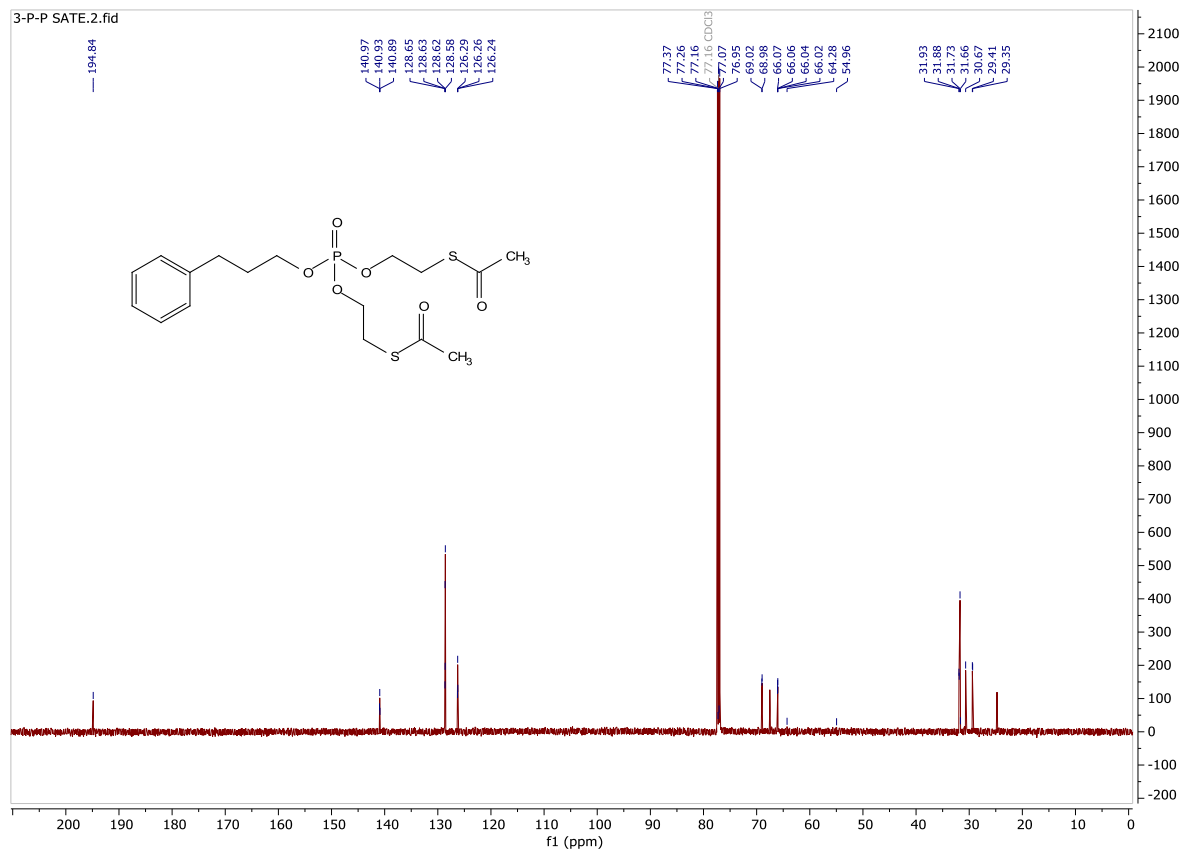
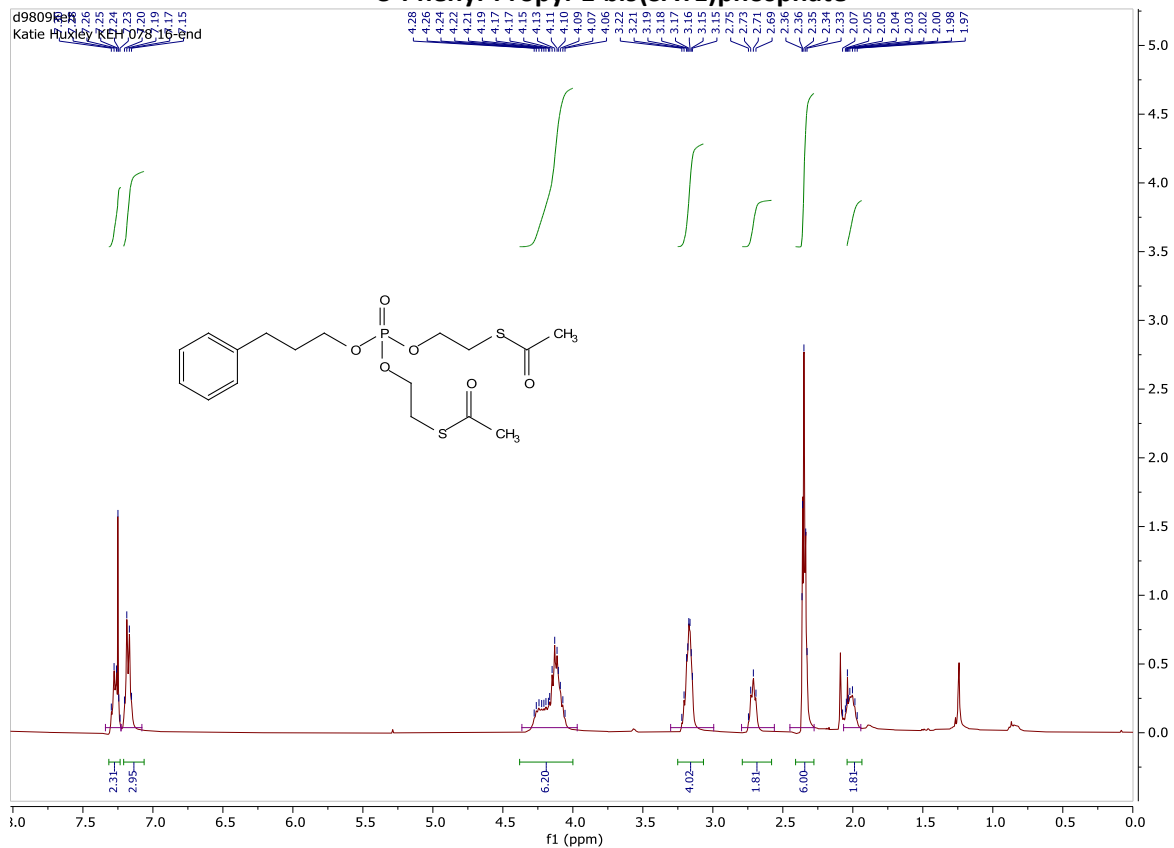


d3501keh
Katie Huxley - KEH 1-Az-OH-Phos

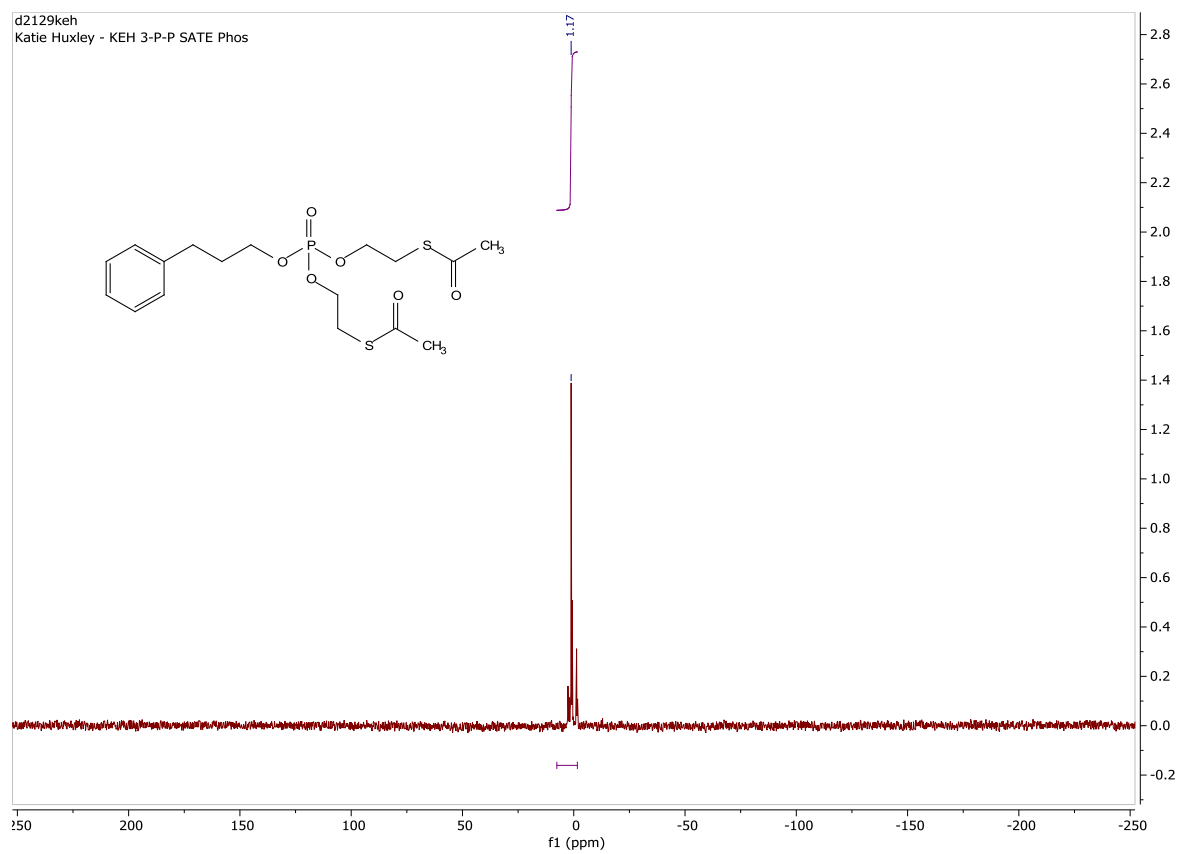


Chapter 4

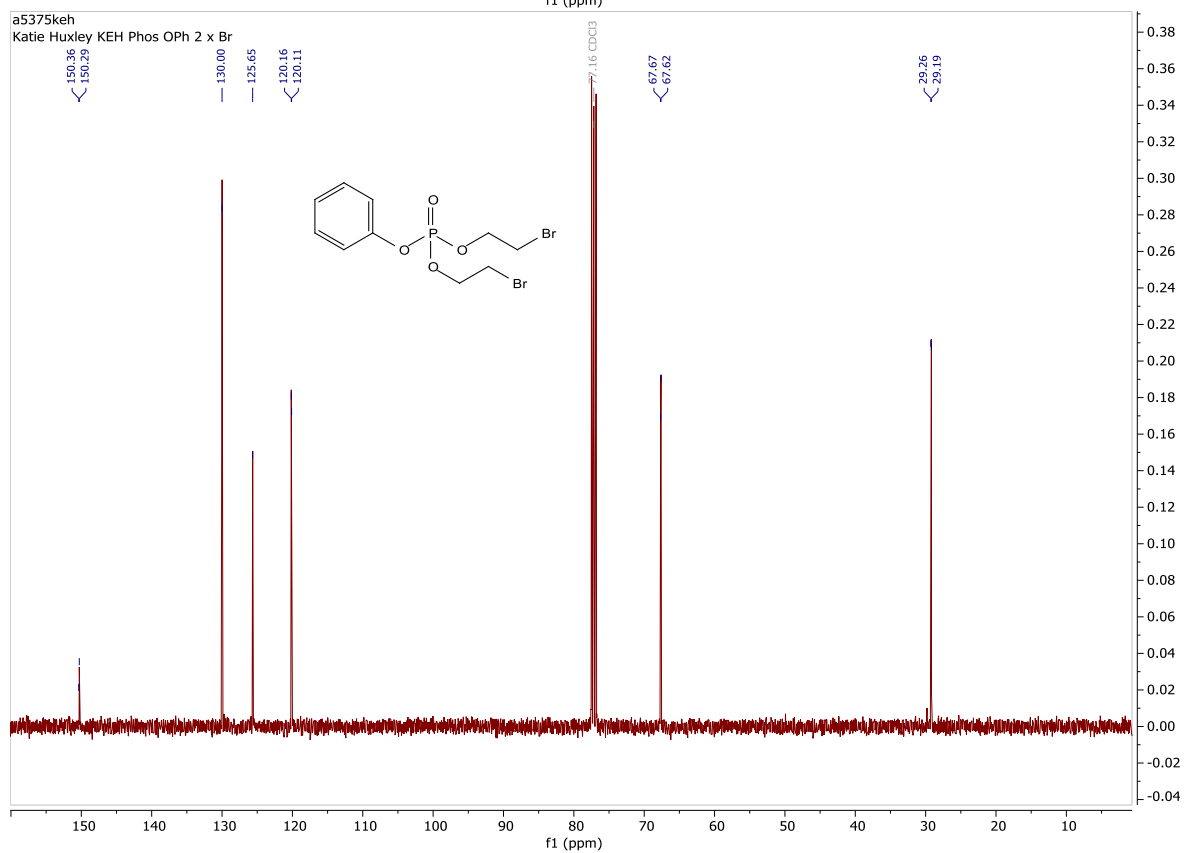
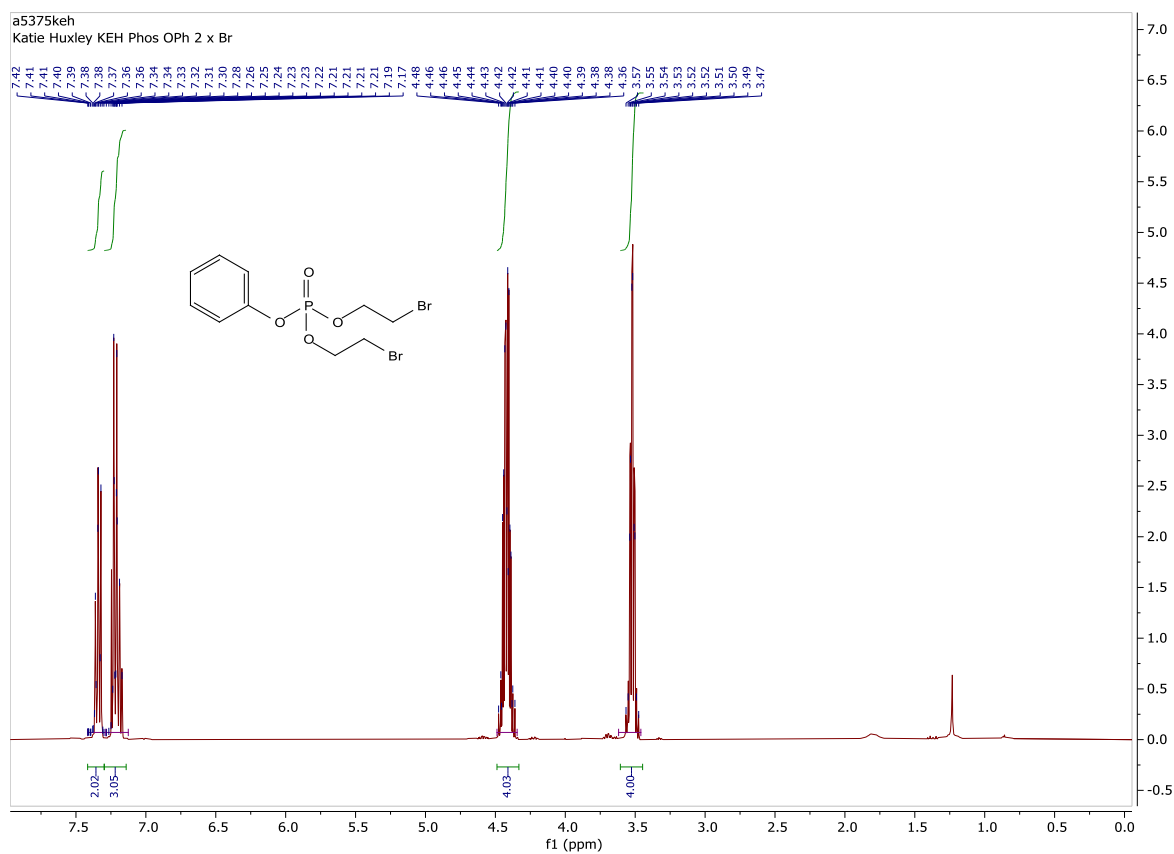
3-Phenyl-Propyl-1-bis(SATE)phosphate

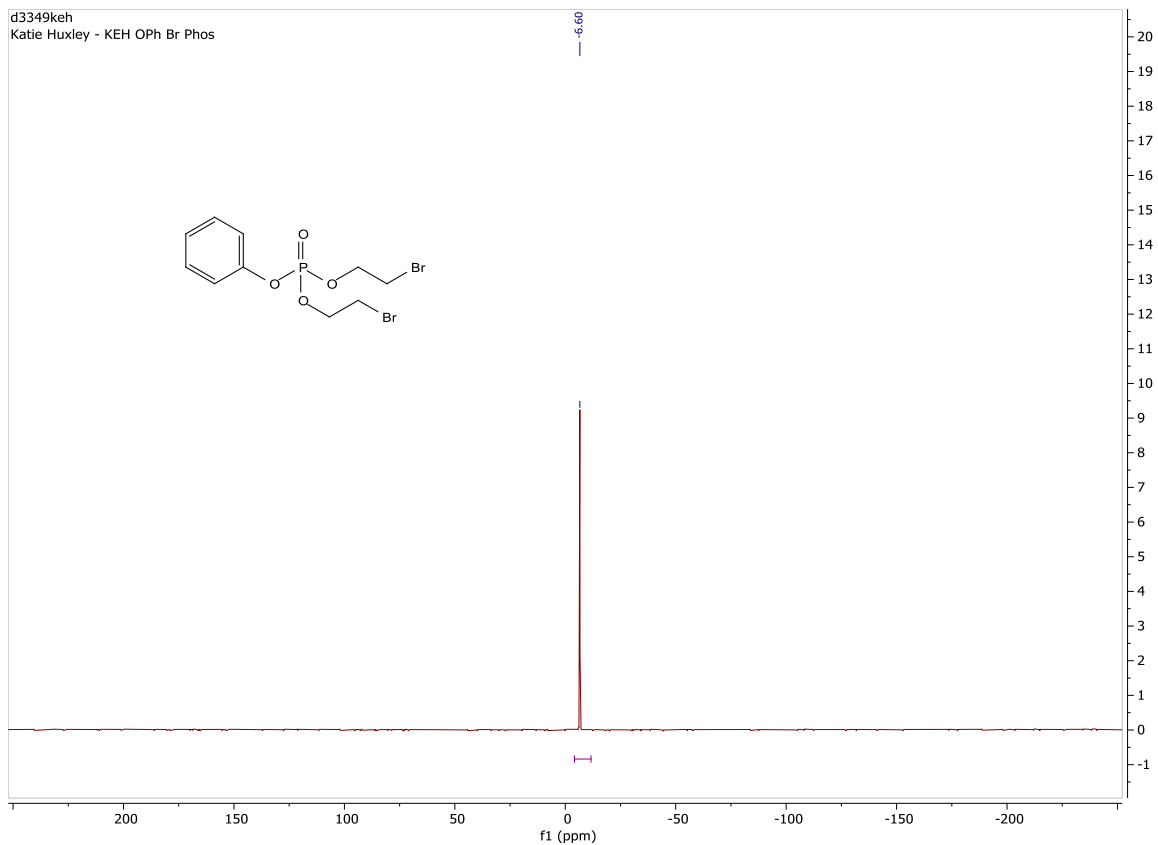


d2129keh
Katie Huxley - KEH 3-P-P SATE Phos

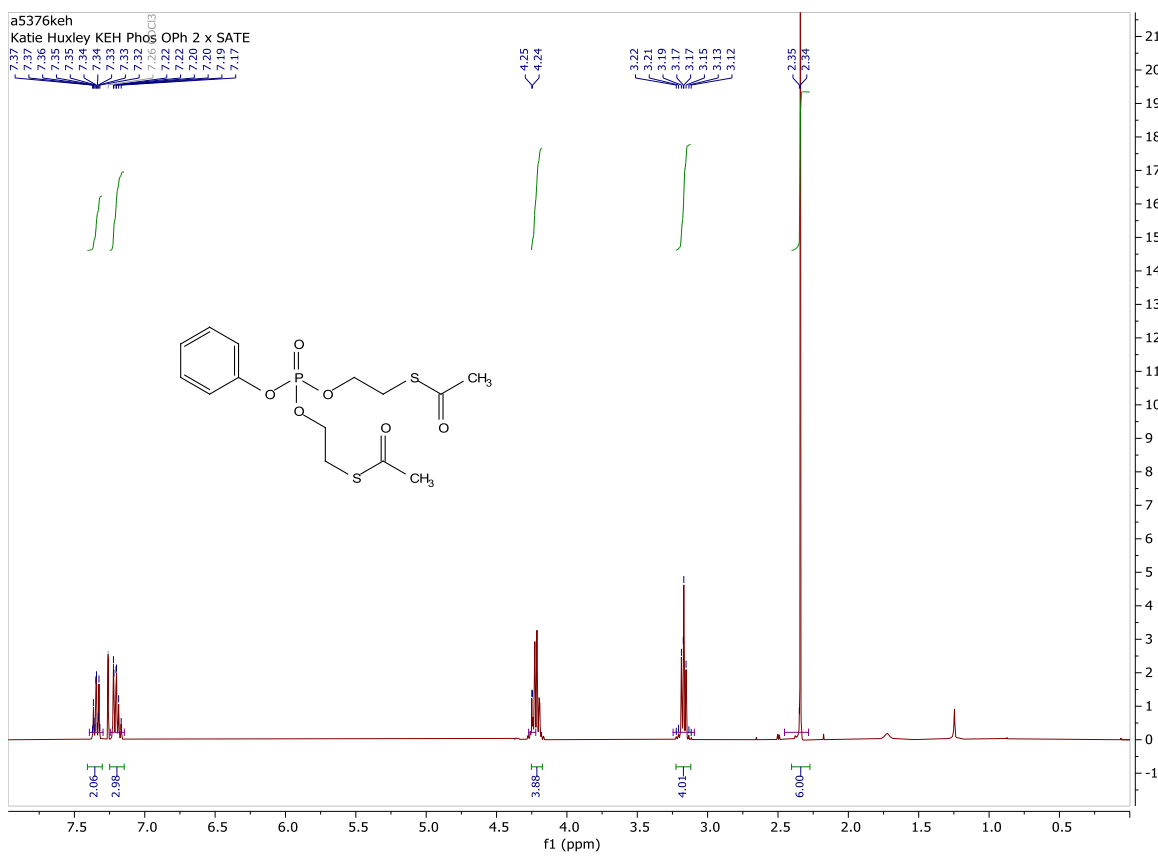


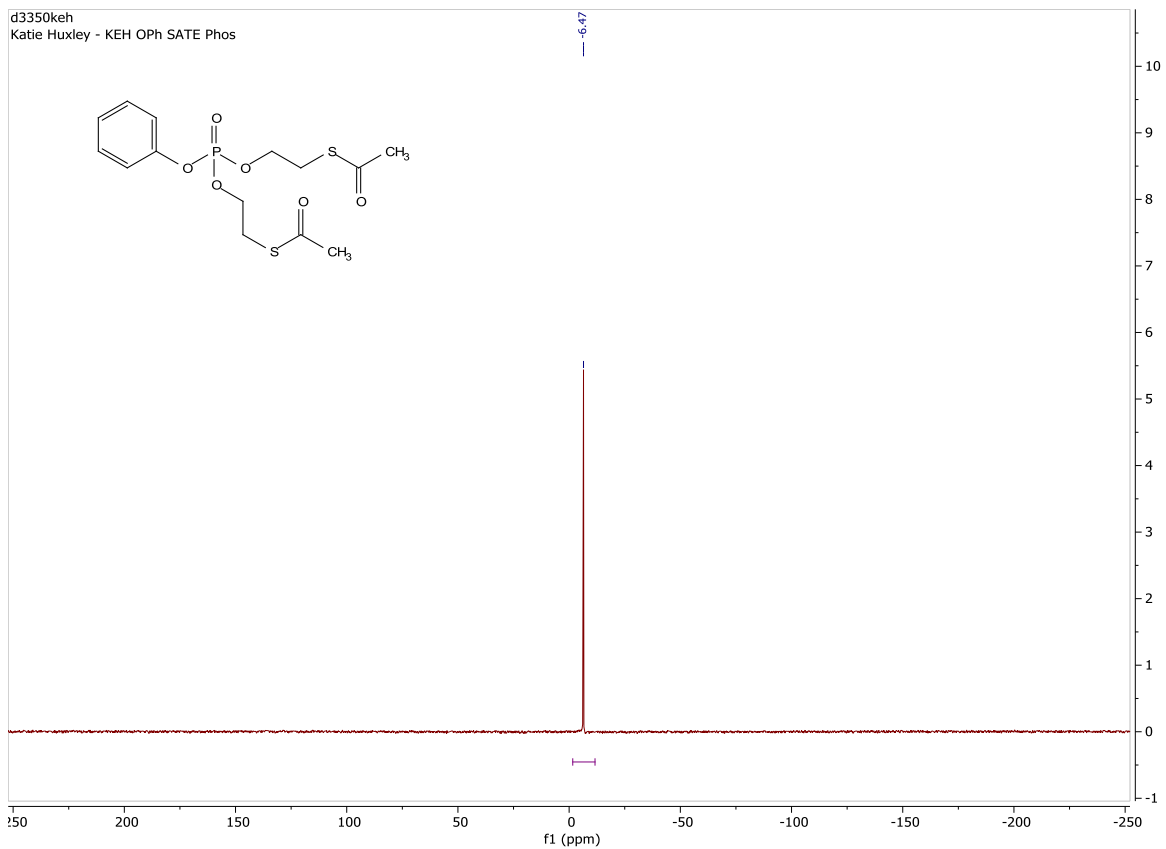
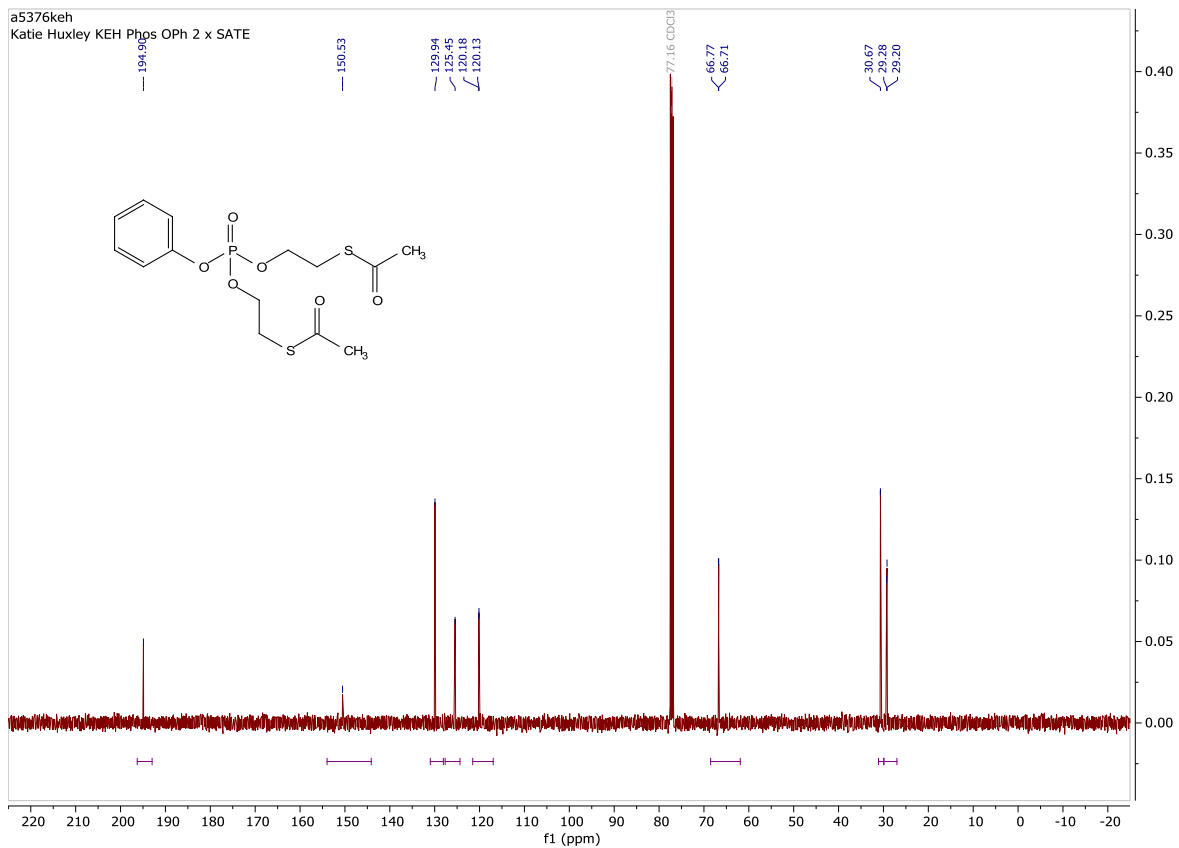
Phenyl-bis(2-bromoethyl)phosphate (62)



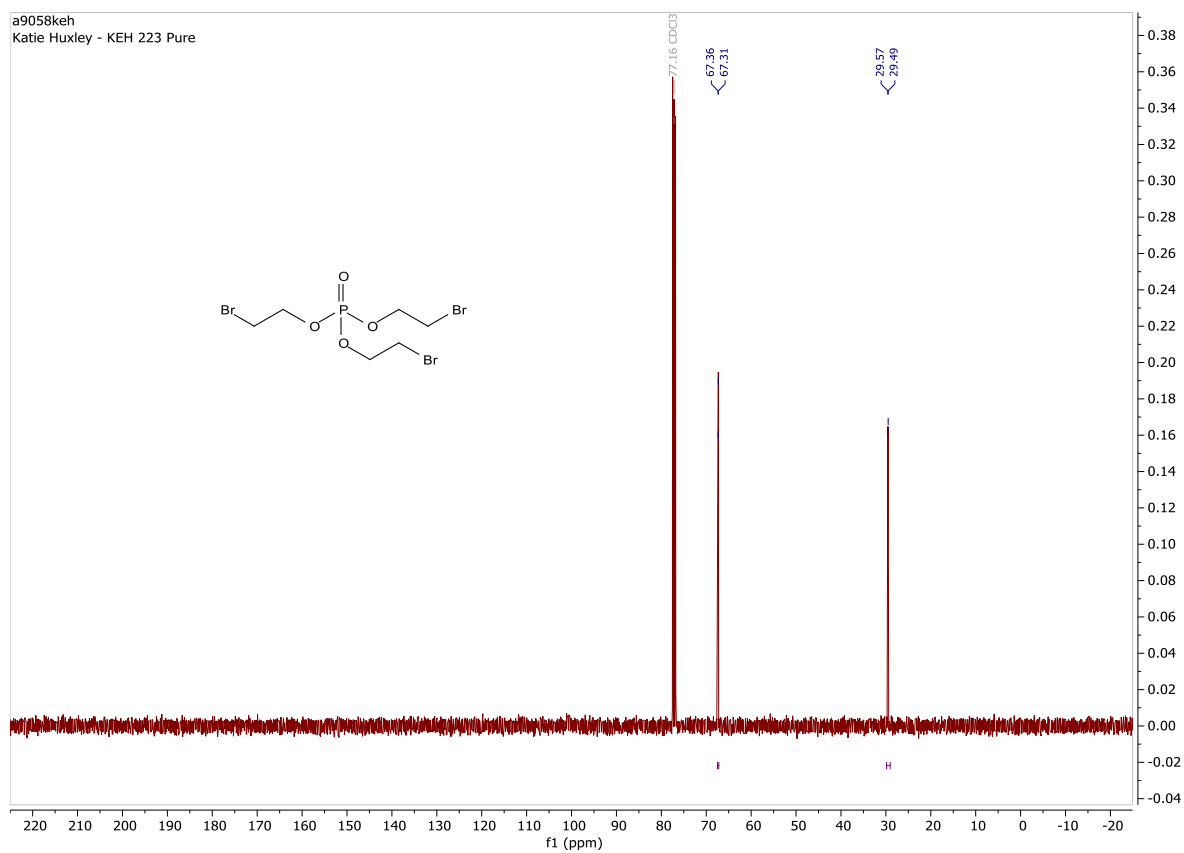
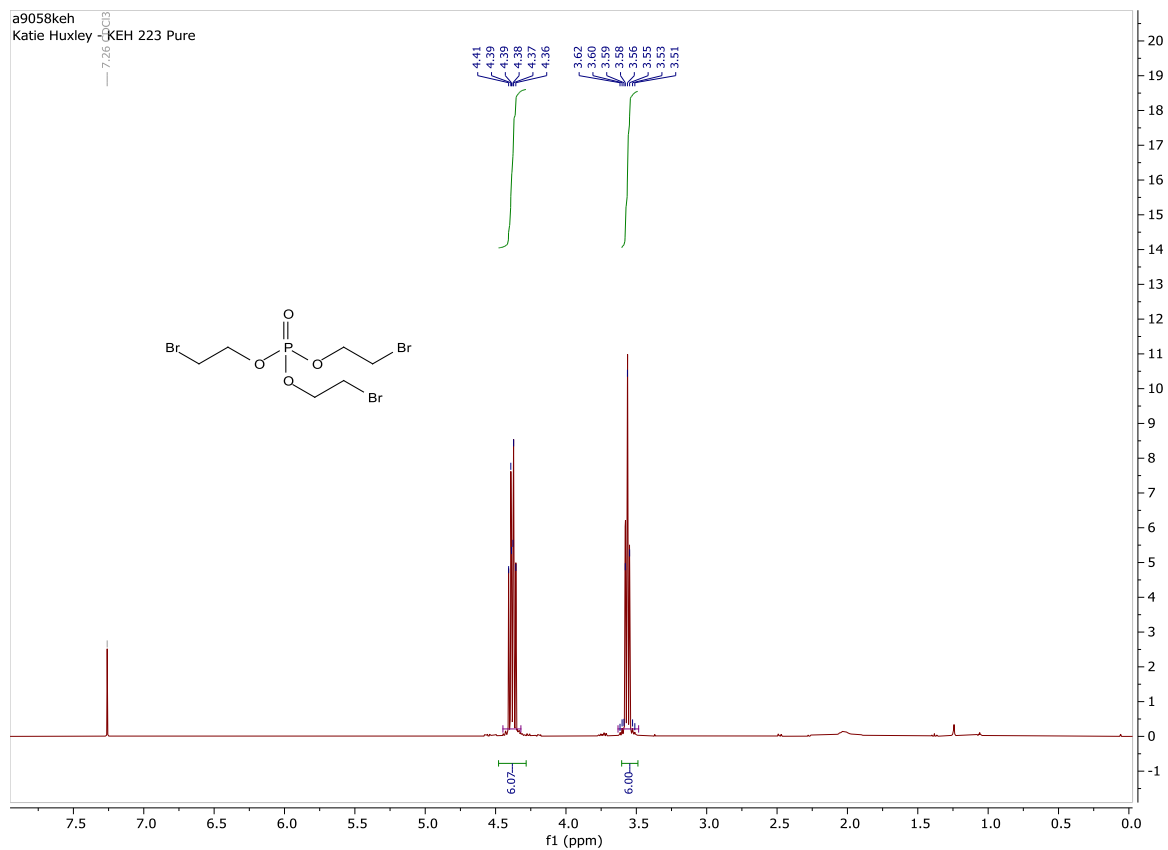


Phenyl-*bis*(SATE)phosphate (60)

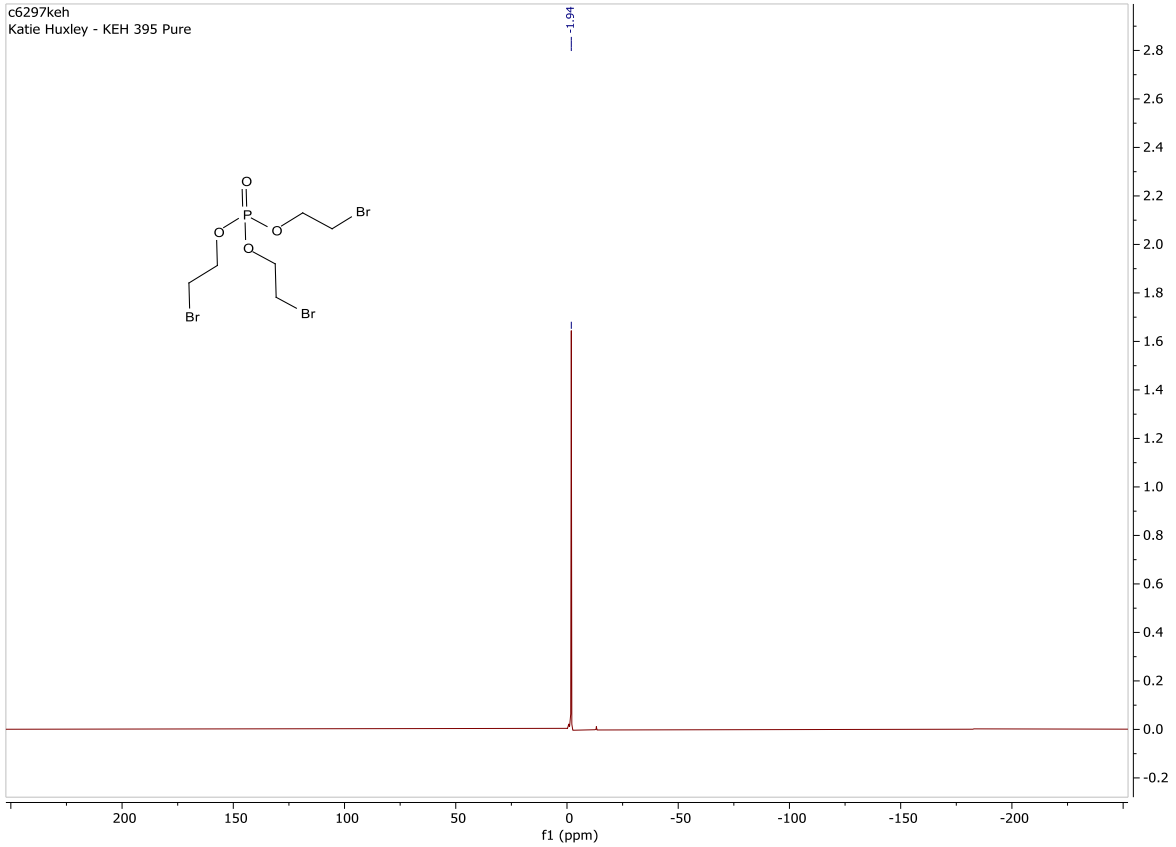




tris(2-bromoethyl)phosphate (66)

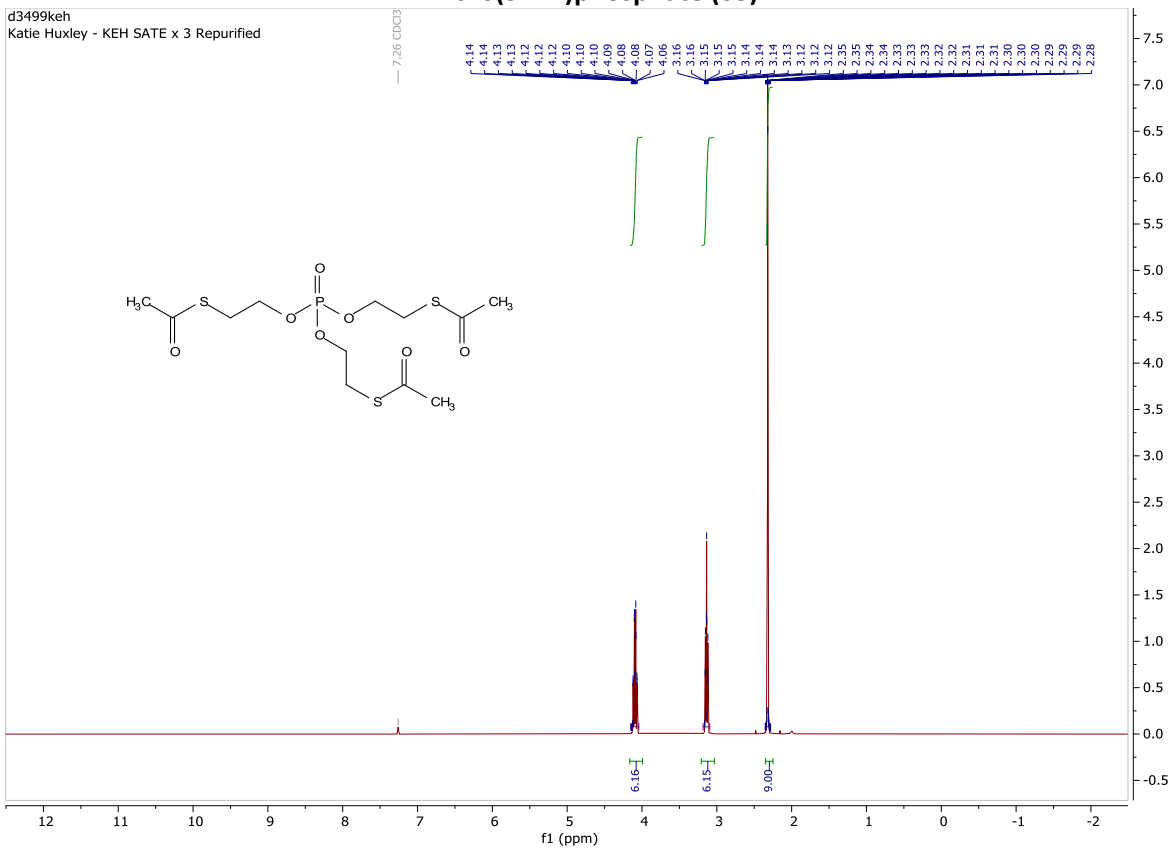


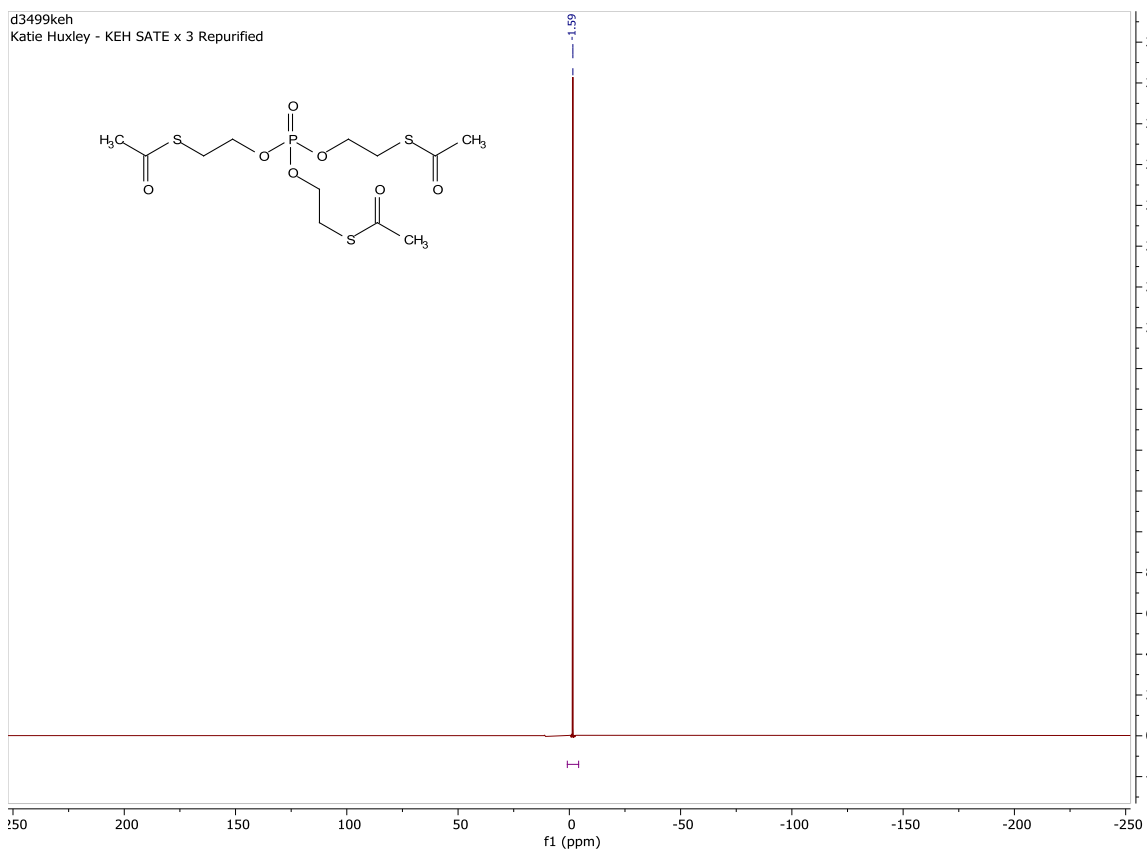
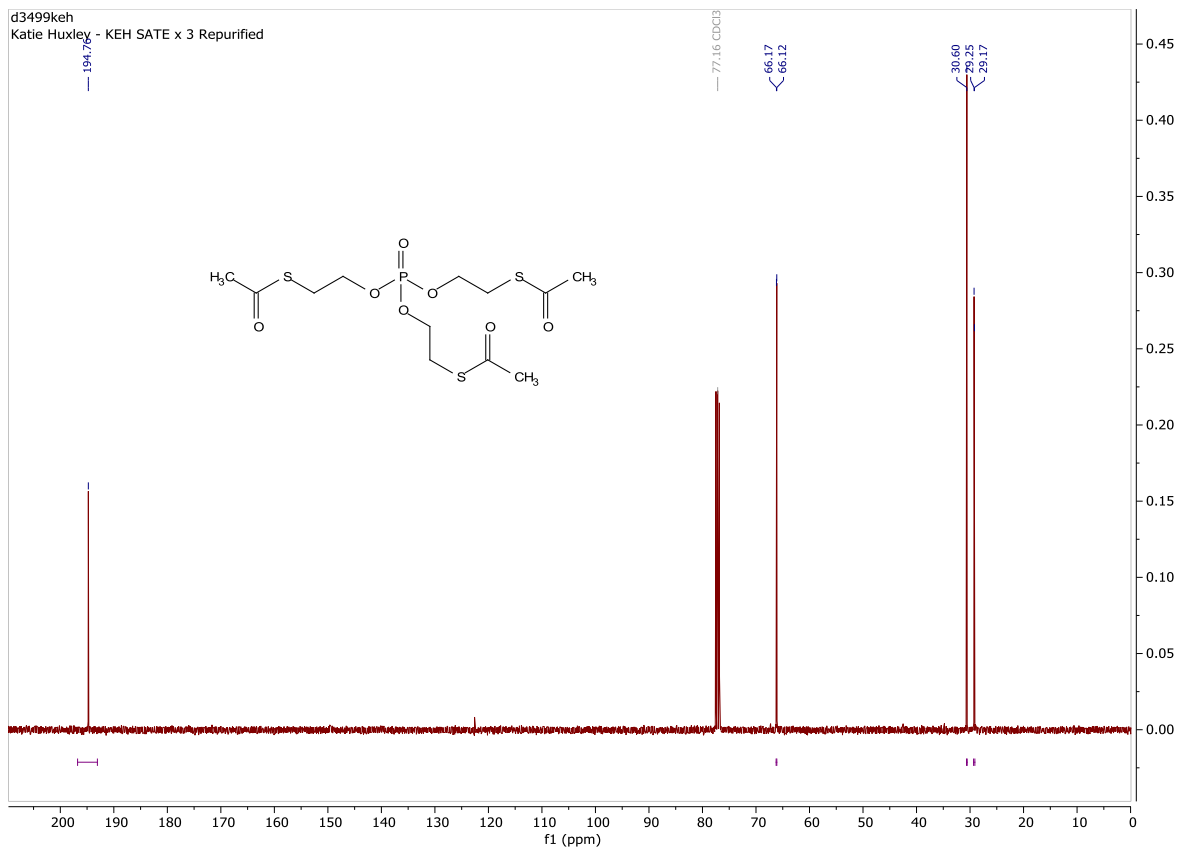
c6297keh
Katie Huxley - KEH 395 Pure



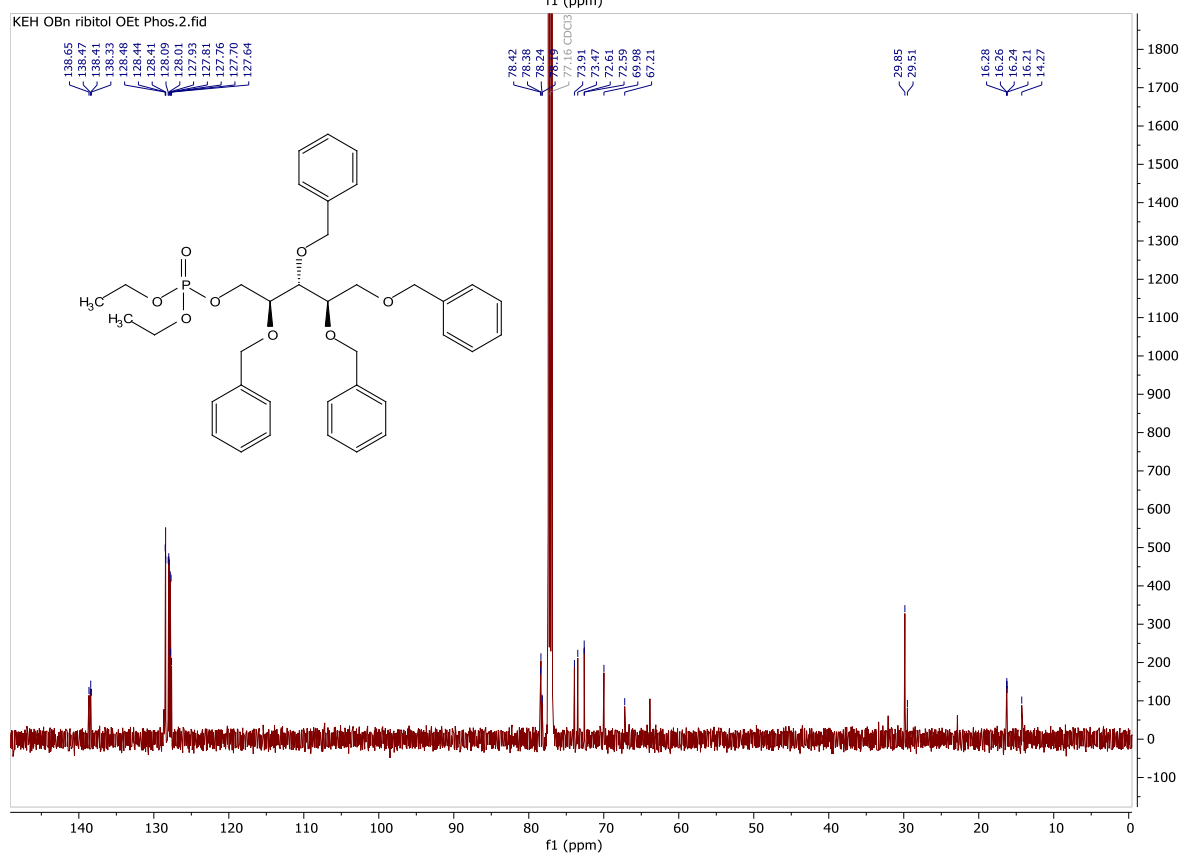
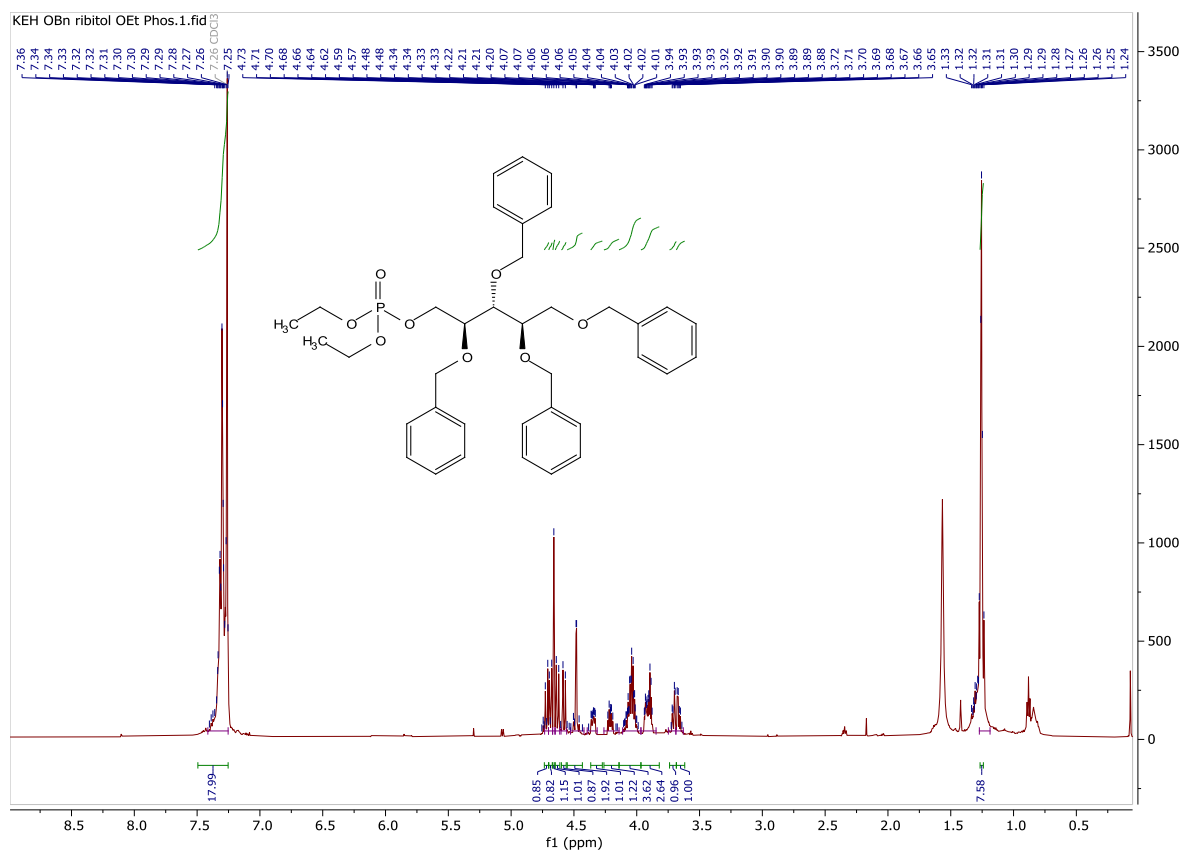
tris(SATE)phosphate (65)

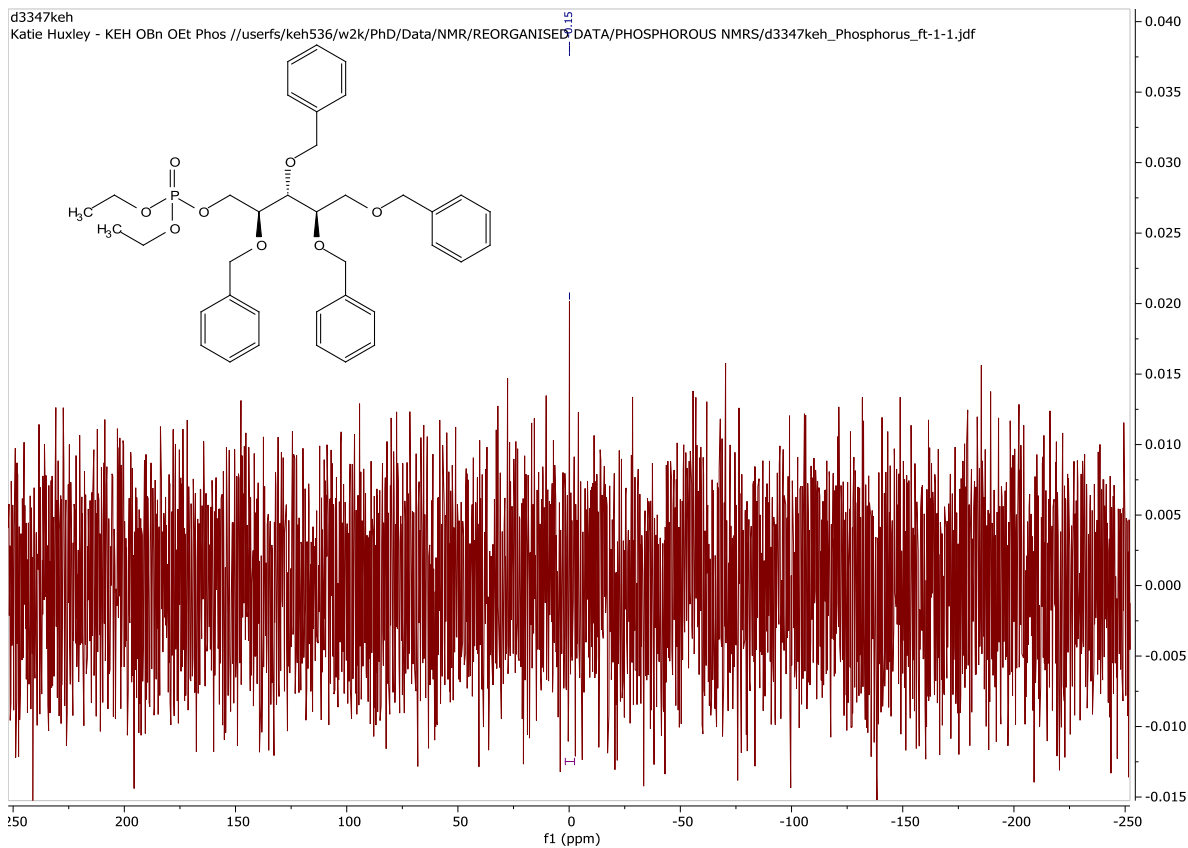
d3499keh
Katie Huxley - KEH SATE x 3 Repurified



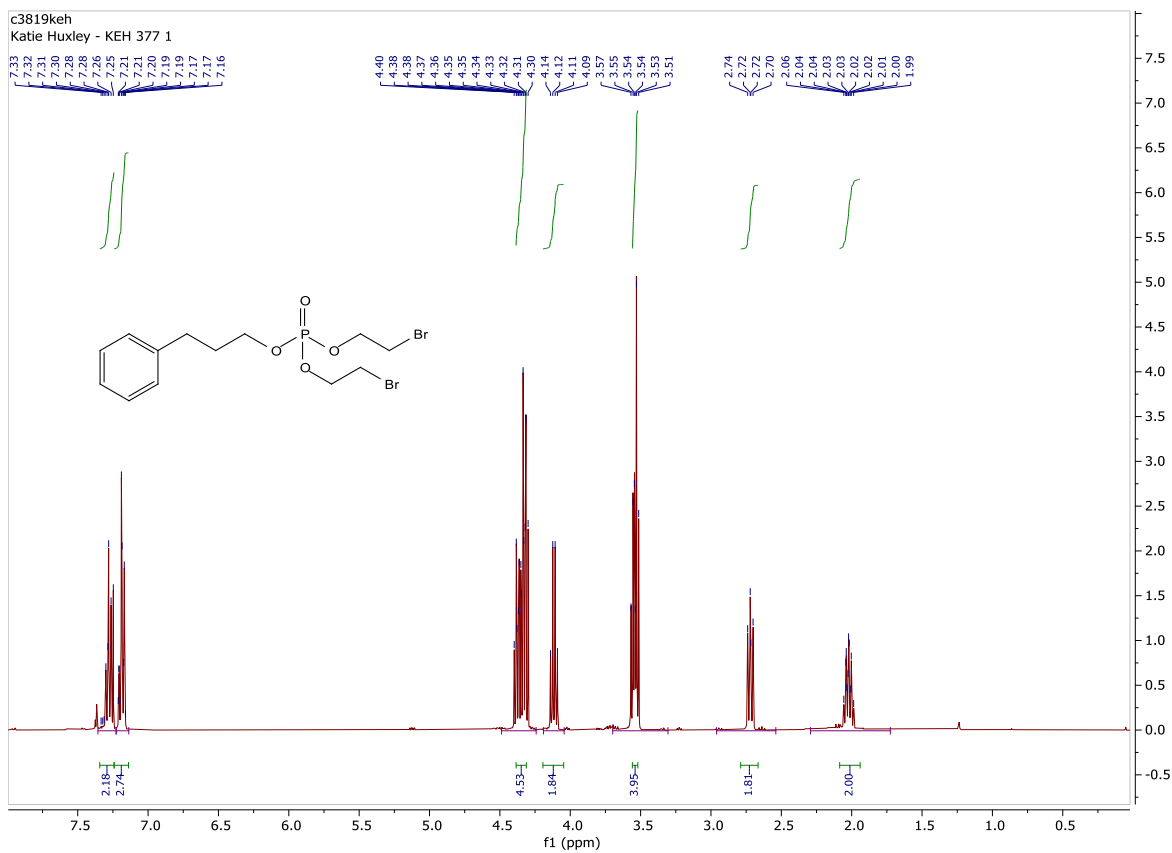


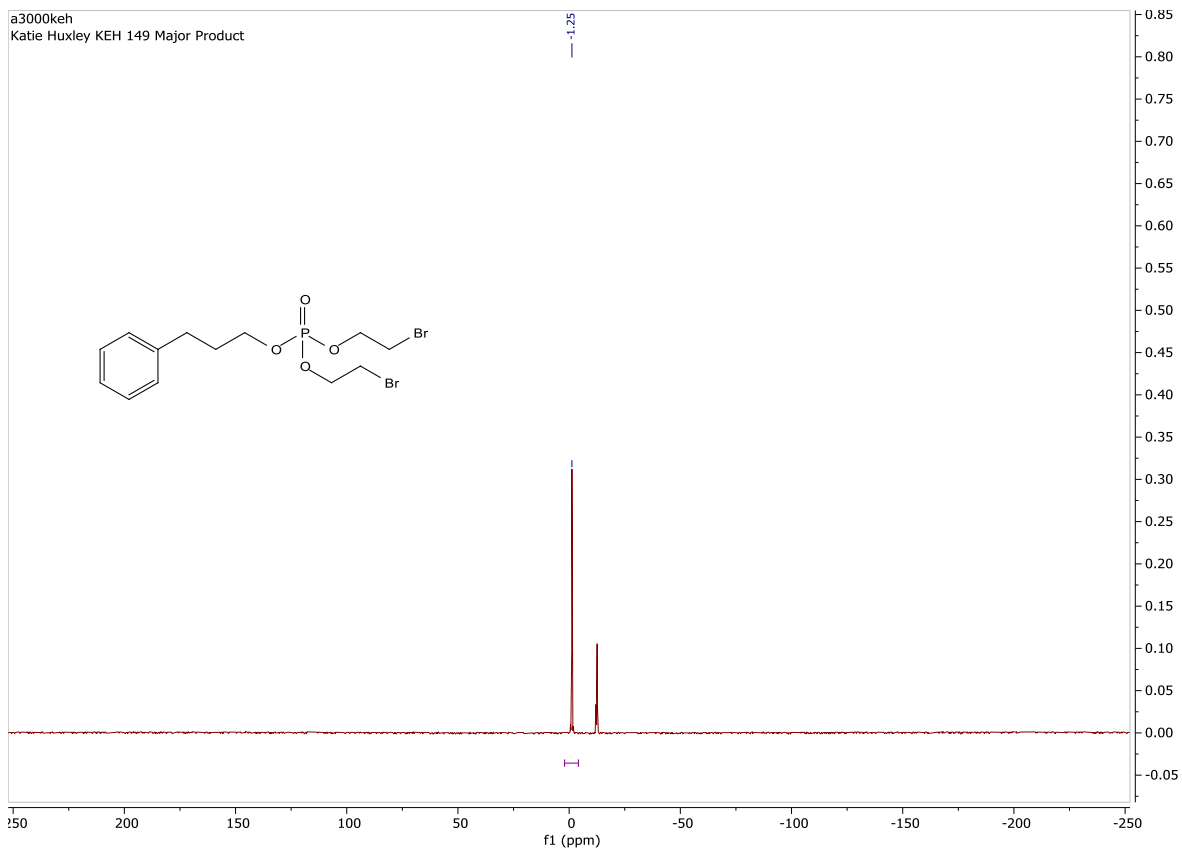
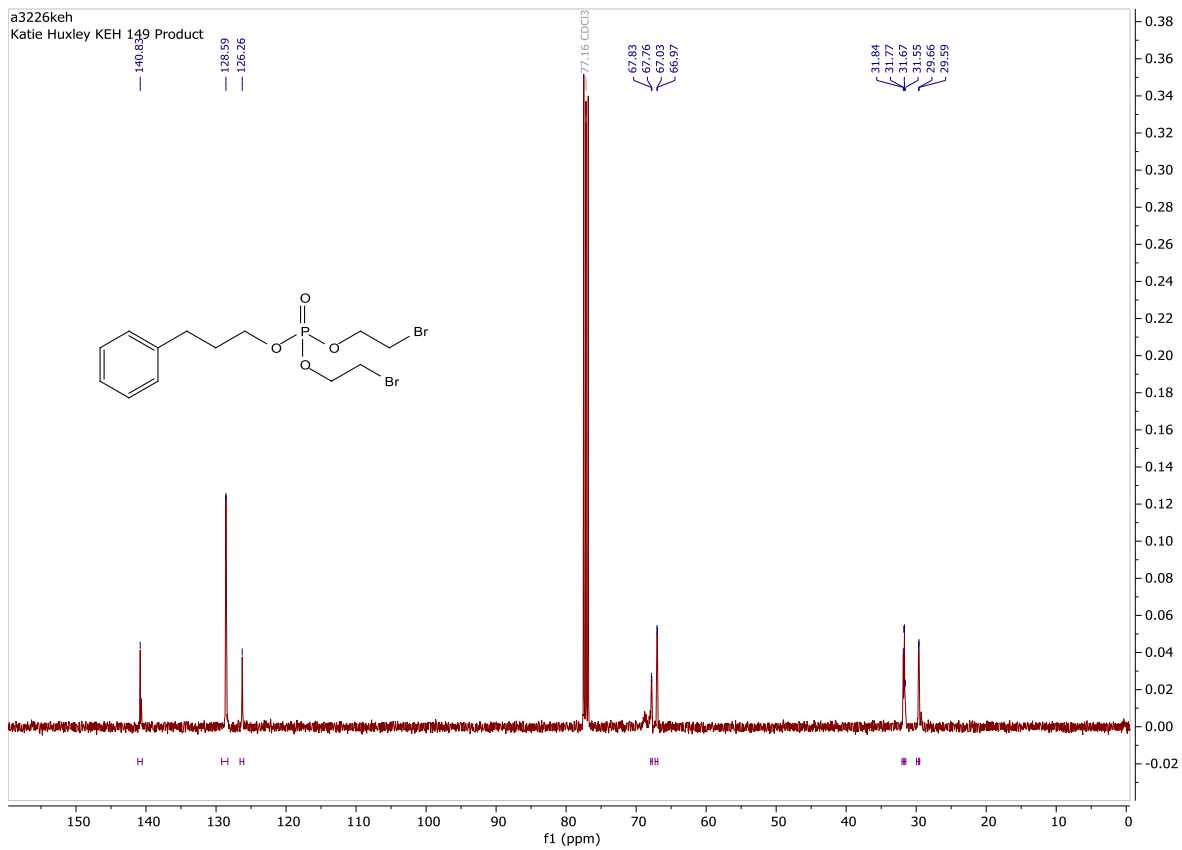
2,3,4,5-tetra-O-benzyl-ribose-5-(bis-ethyl-phosphate) (69)

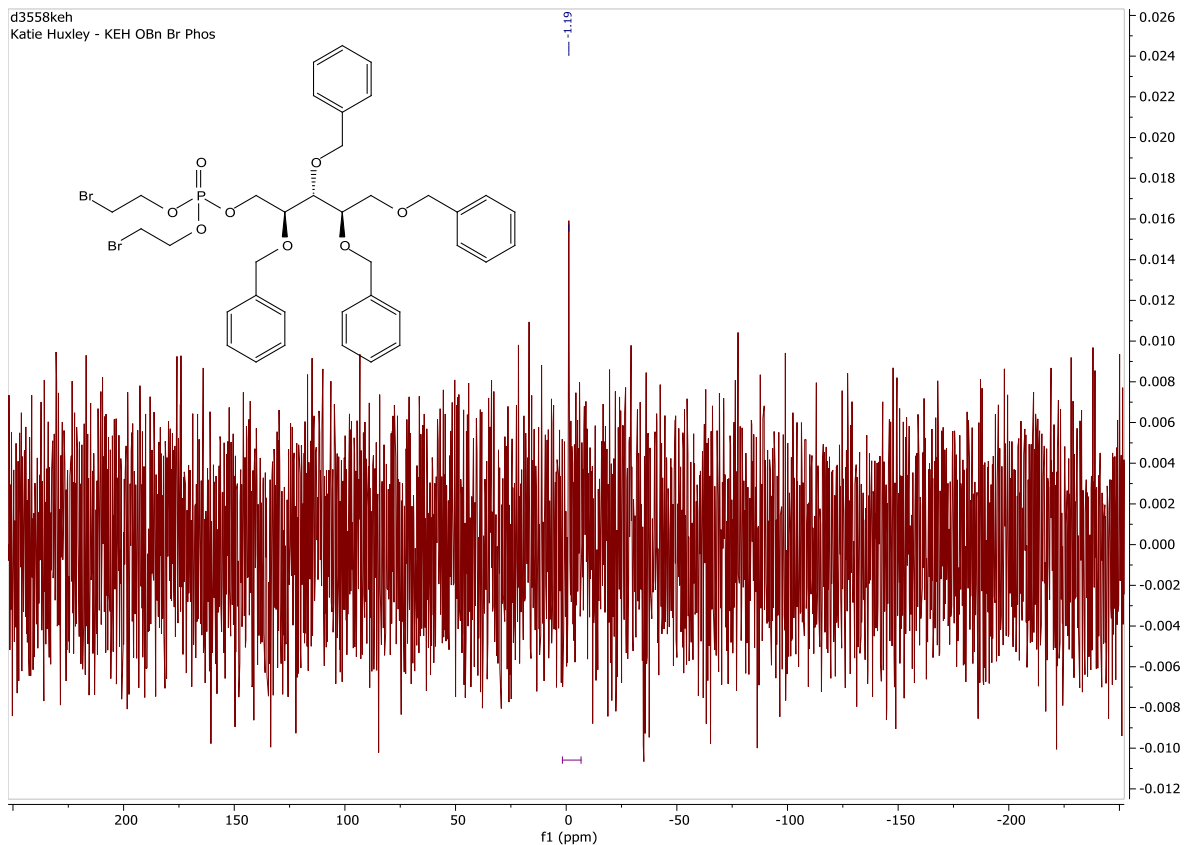




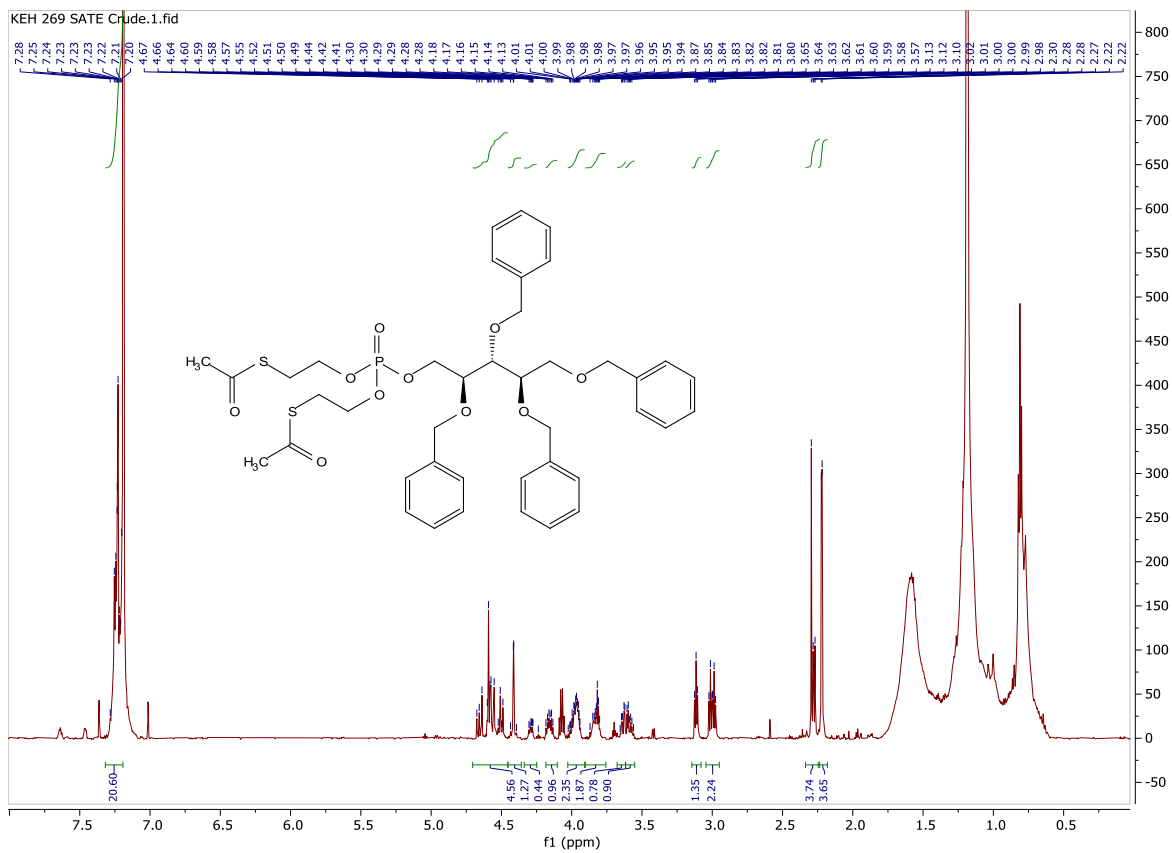
3-Phenyl-Propyl-1-bis(2-bromo-ethyl)phosphate (70)

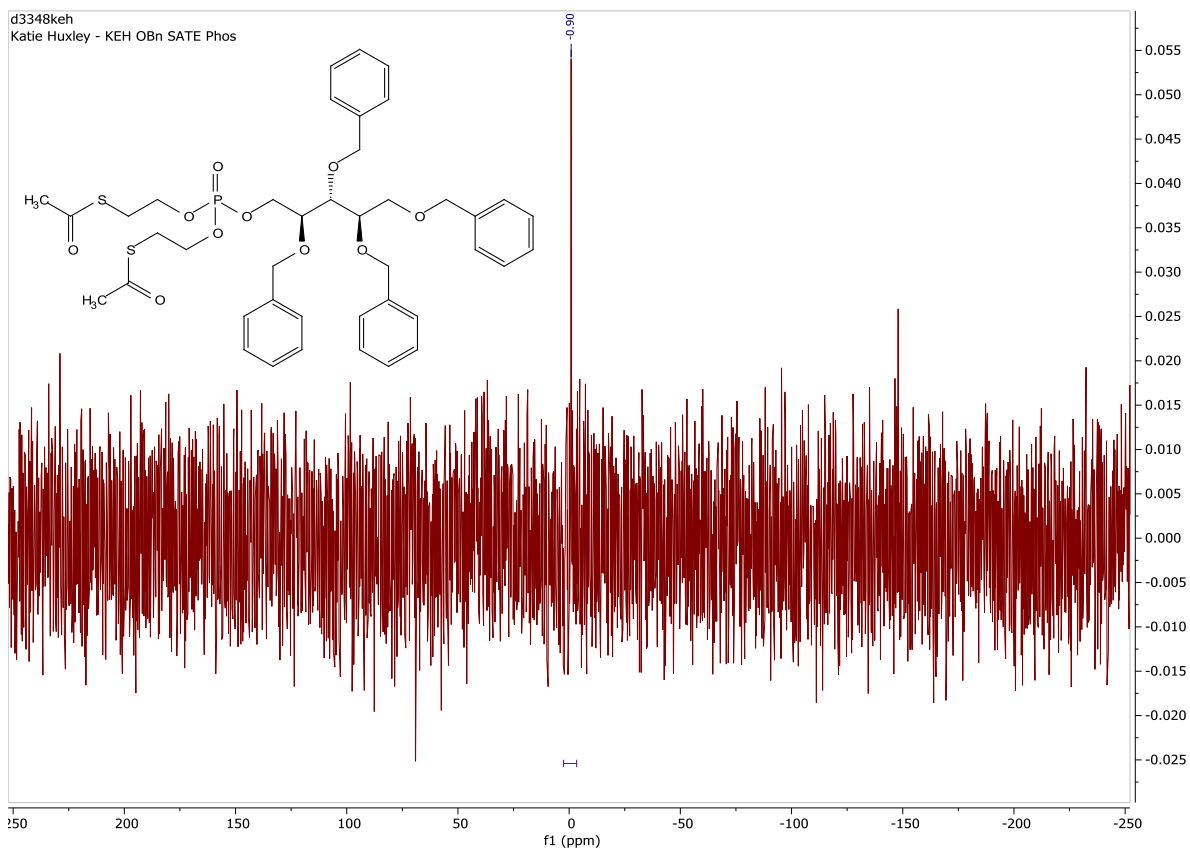
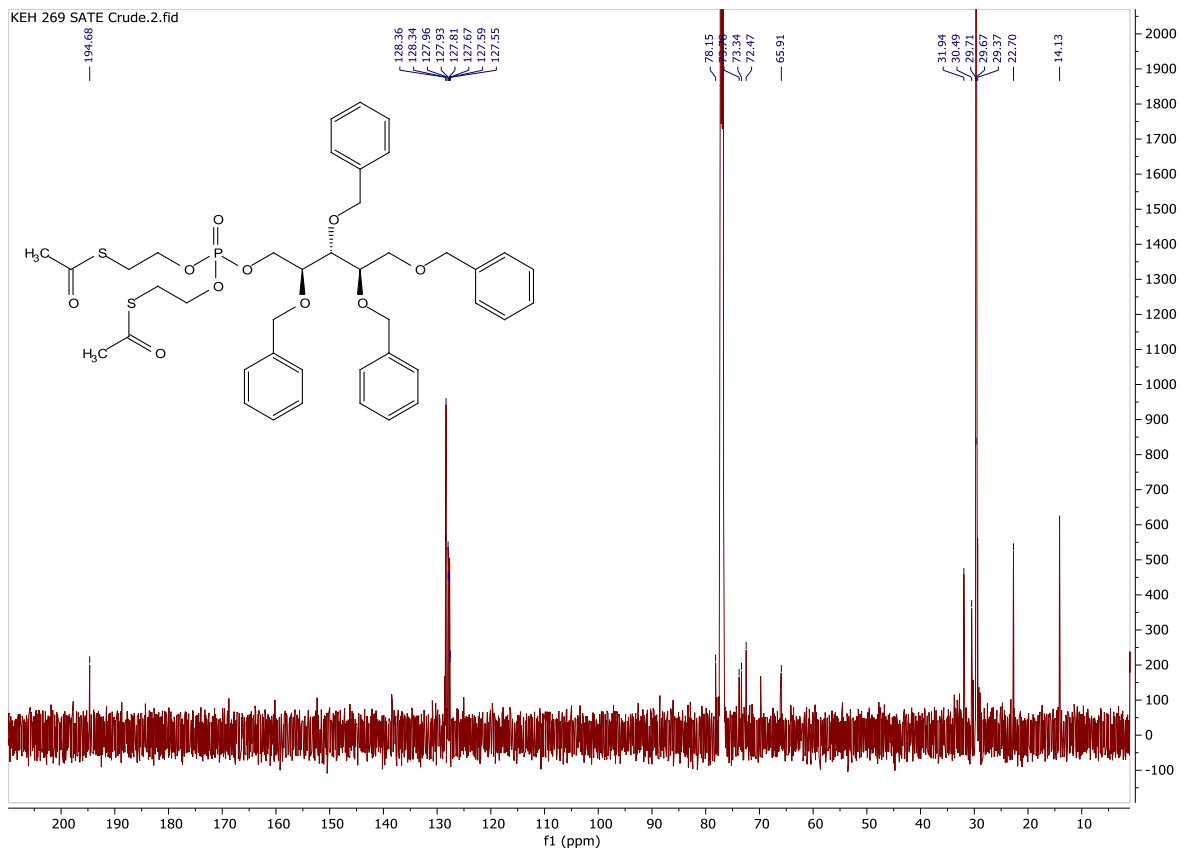






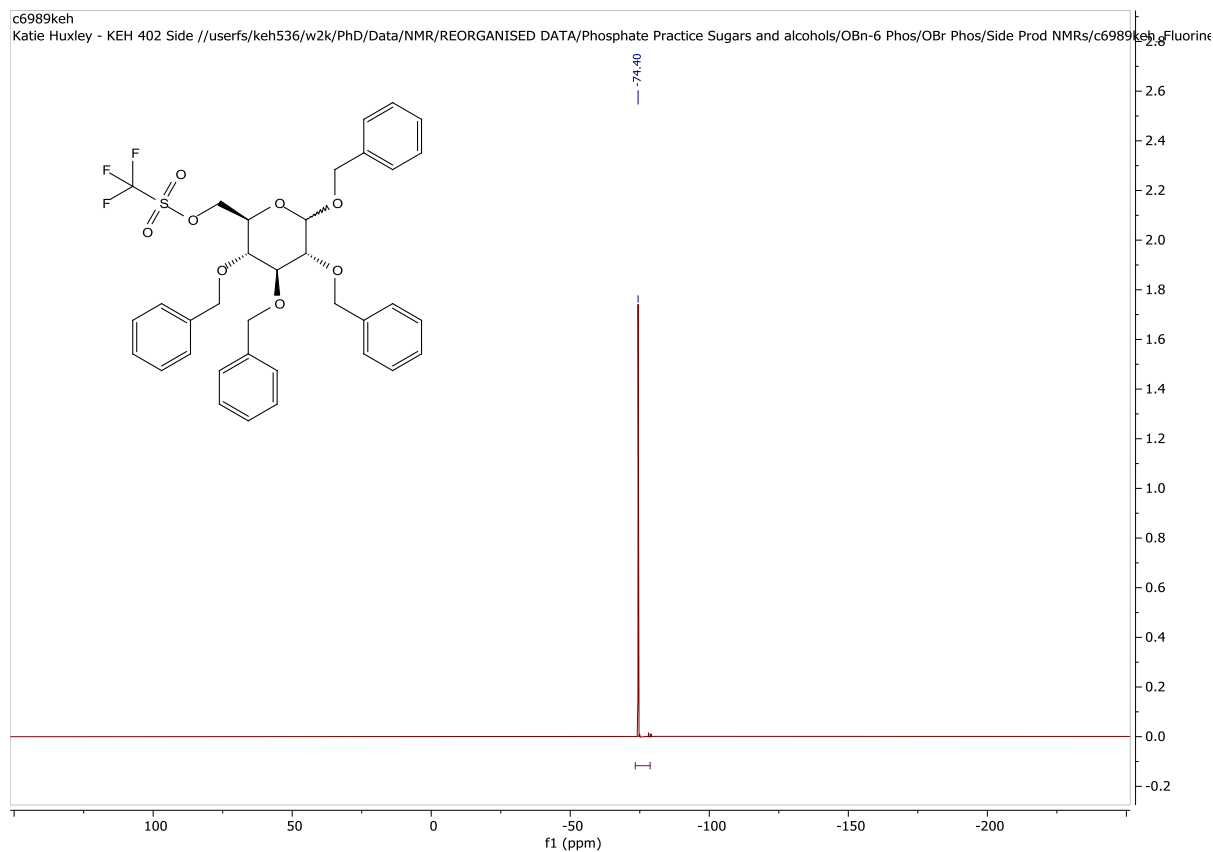
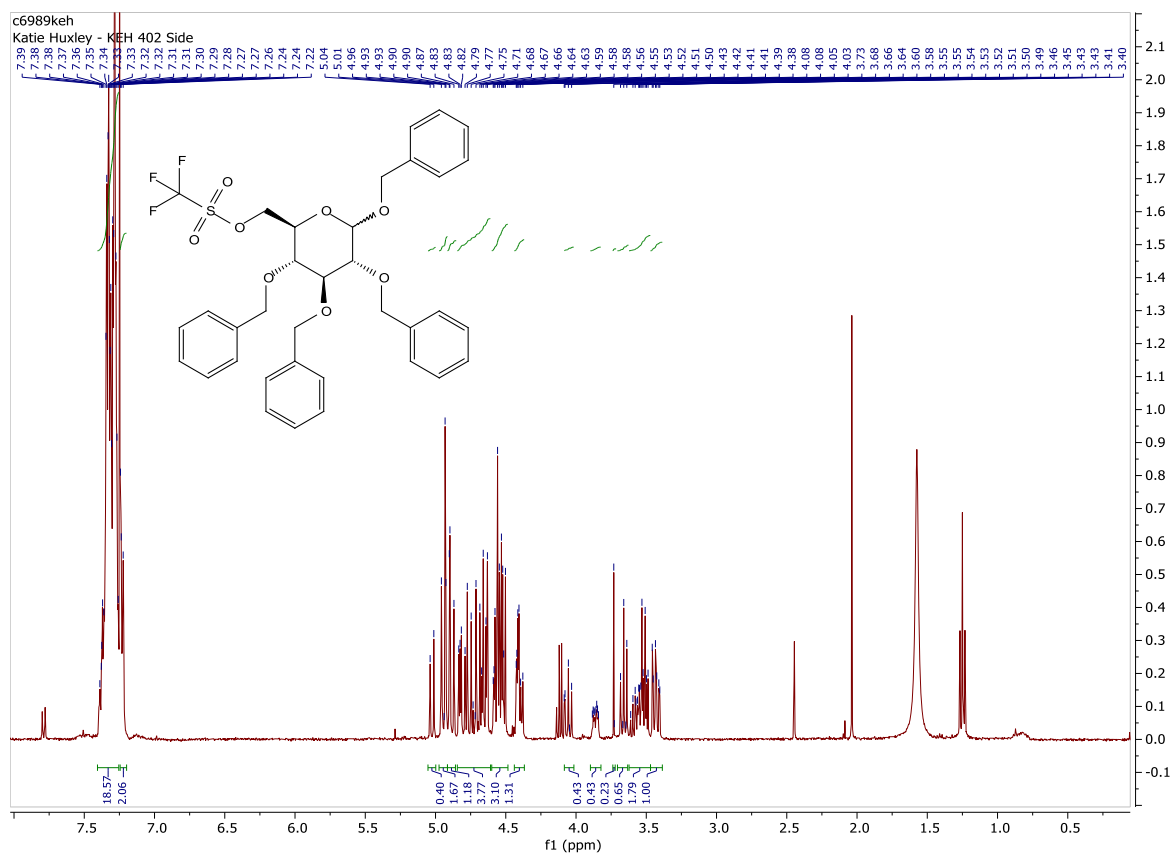
2,3,4,5-tetra-O-benzyl-ribose-5-bis(SATE)phosphate



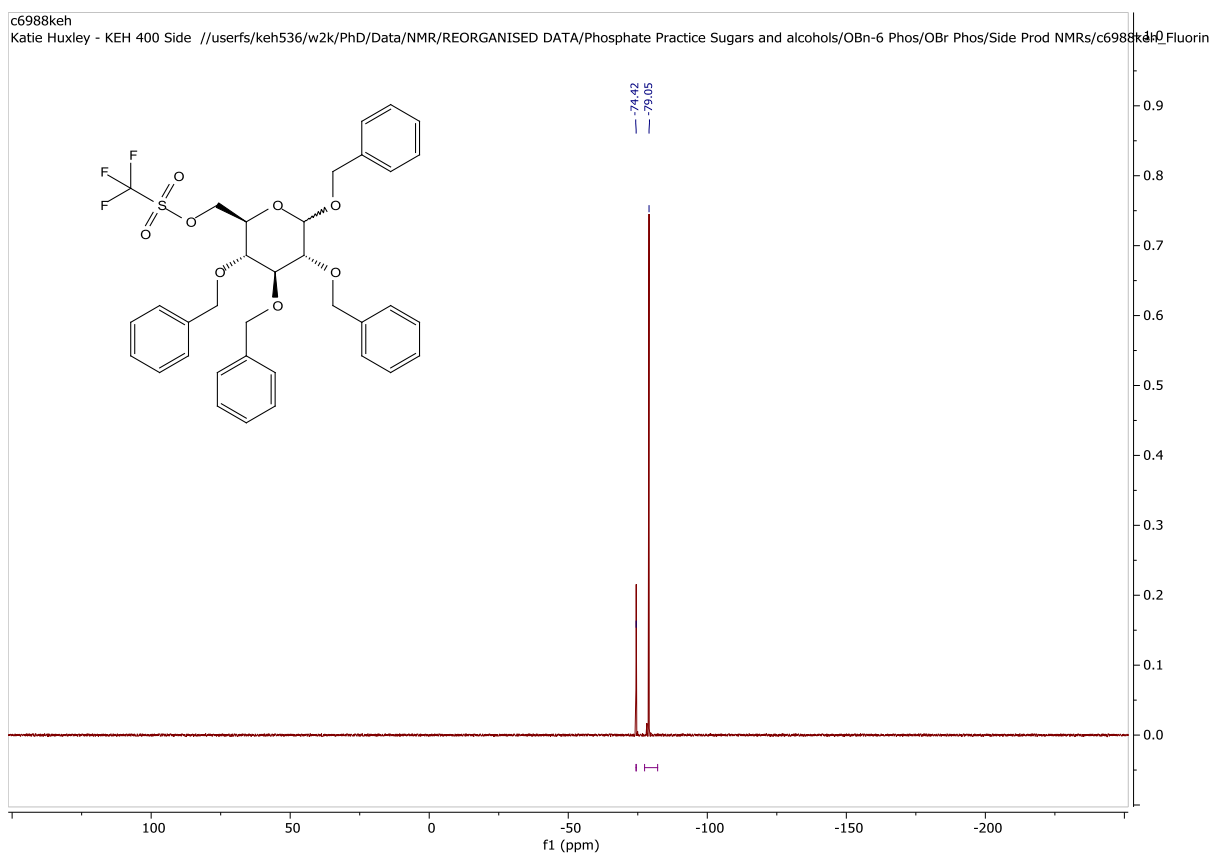


Chapter 5

OBn-glucose triflate side-product

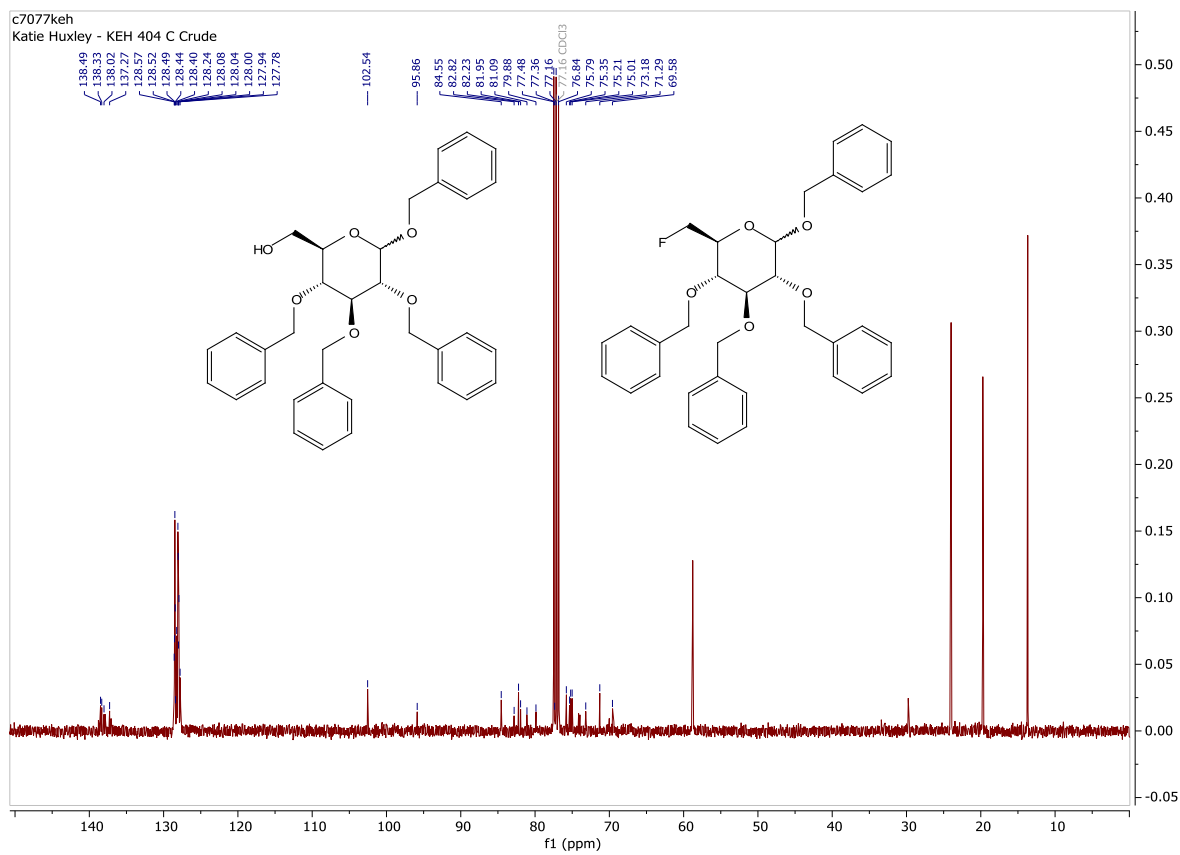
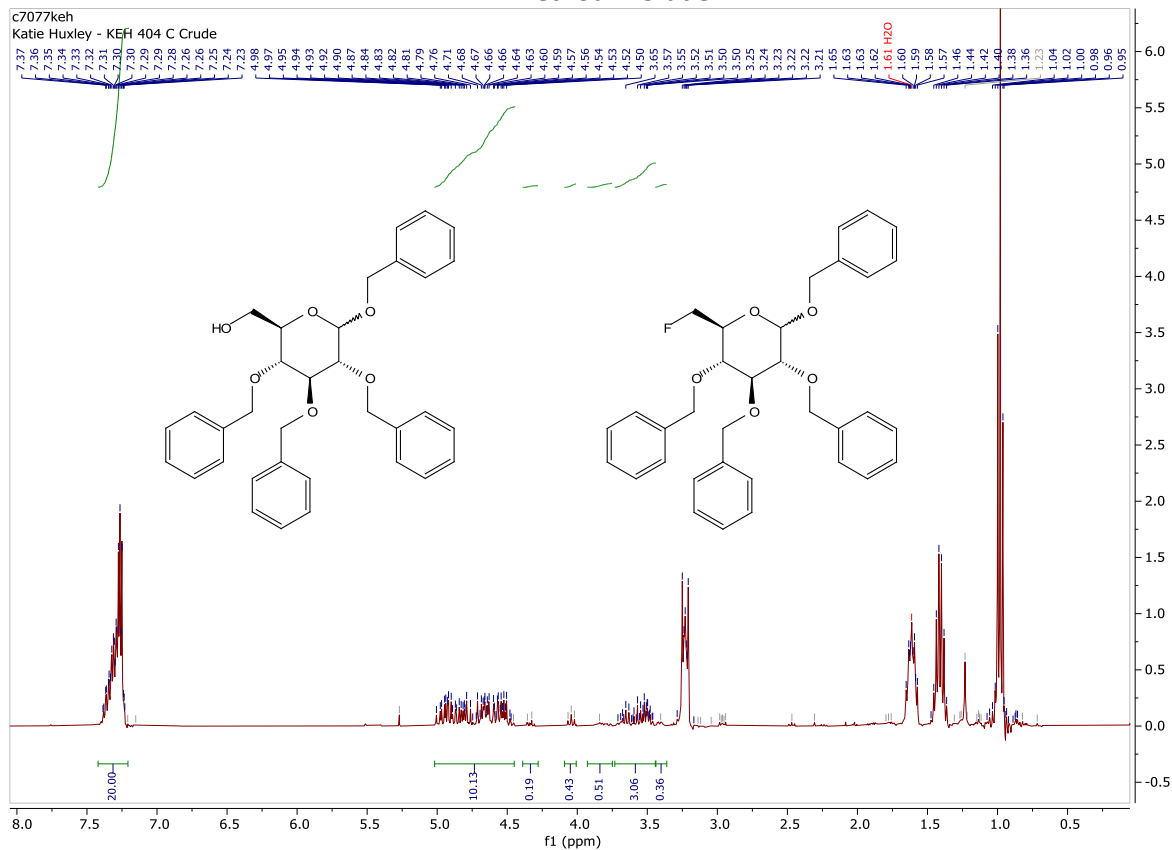


³¹P NMR after standing at RT – Decomposition to free triflate ion seen

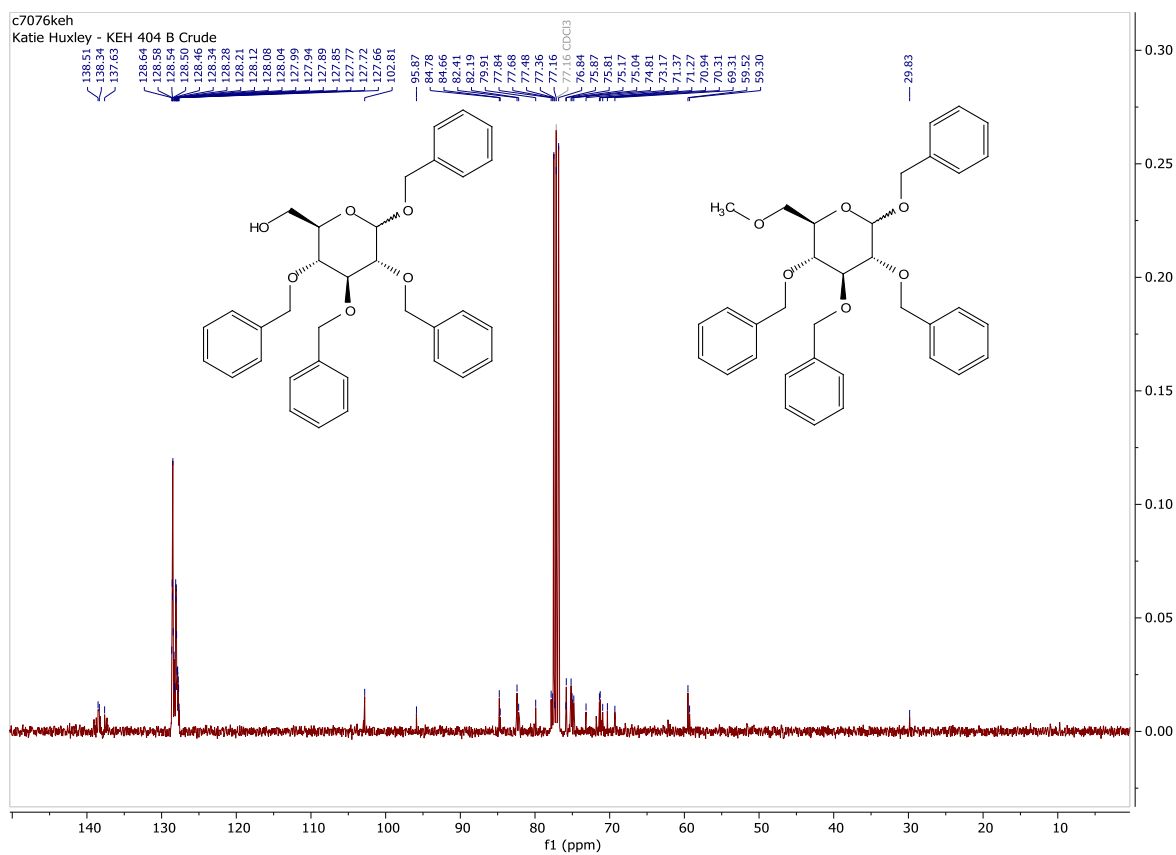
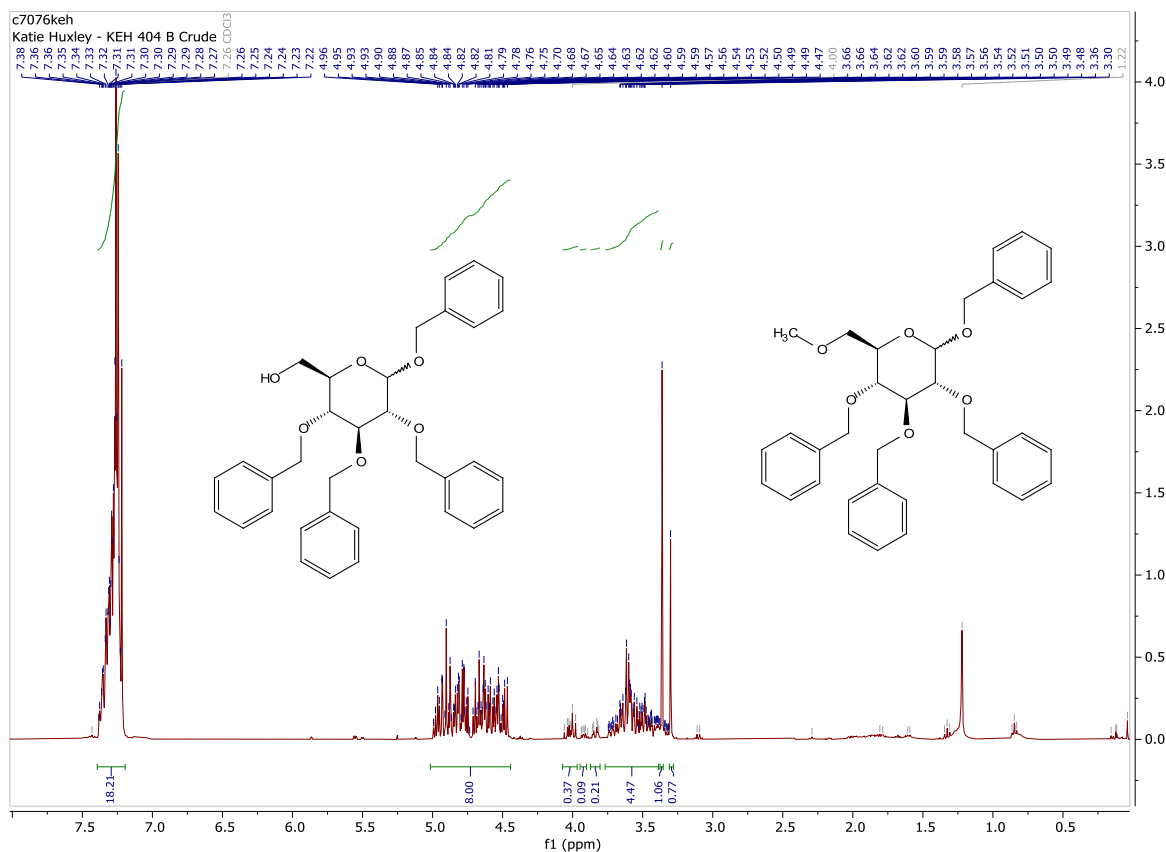


Recovery of Starting Sugar from Triflated Side-product

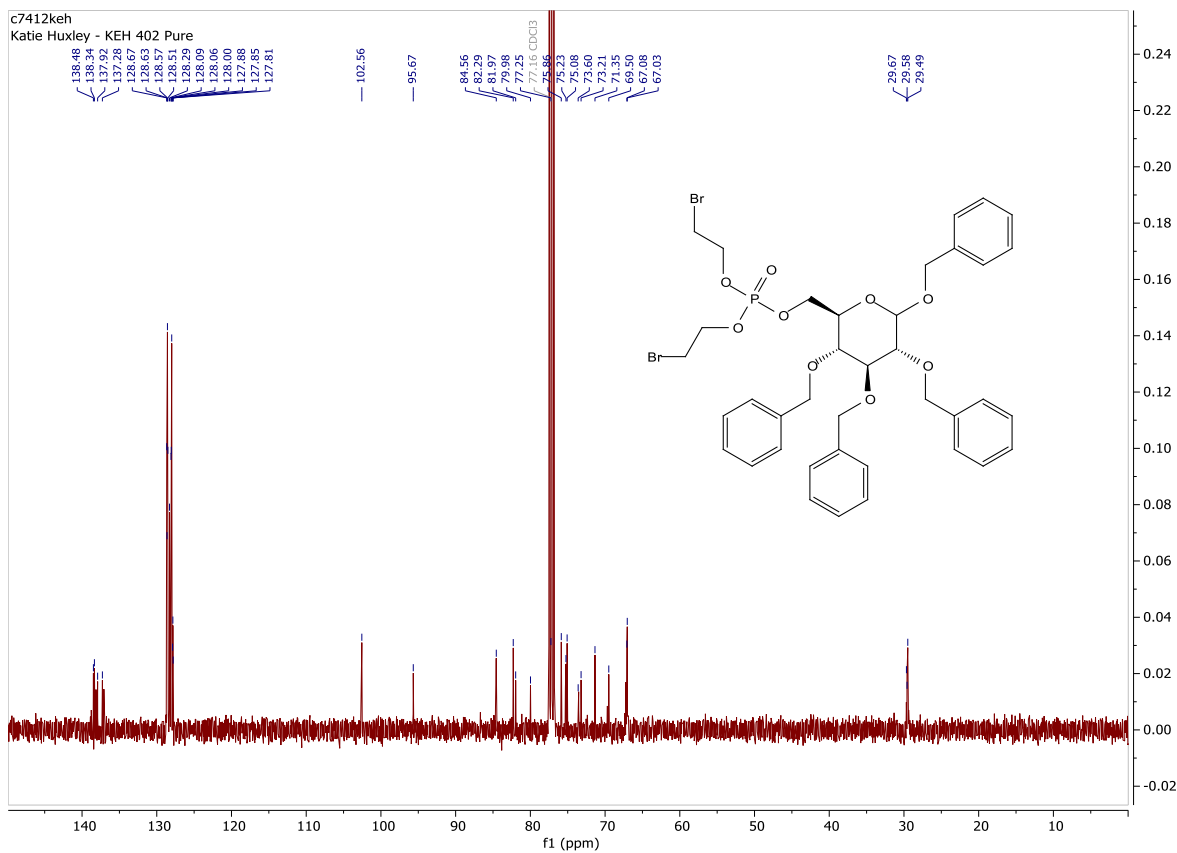
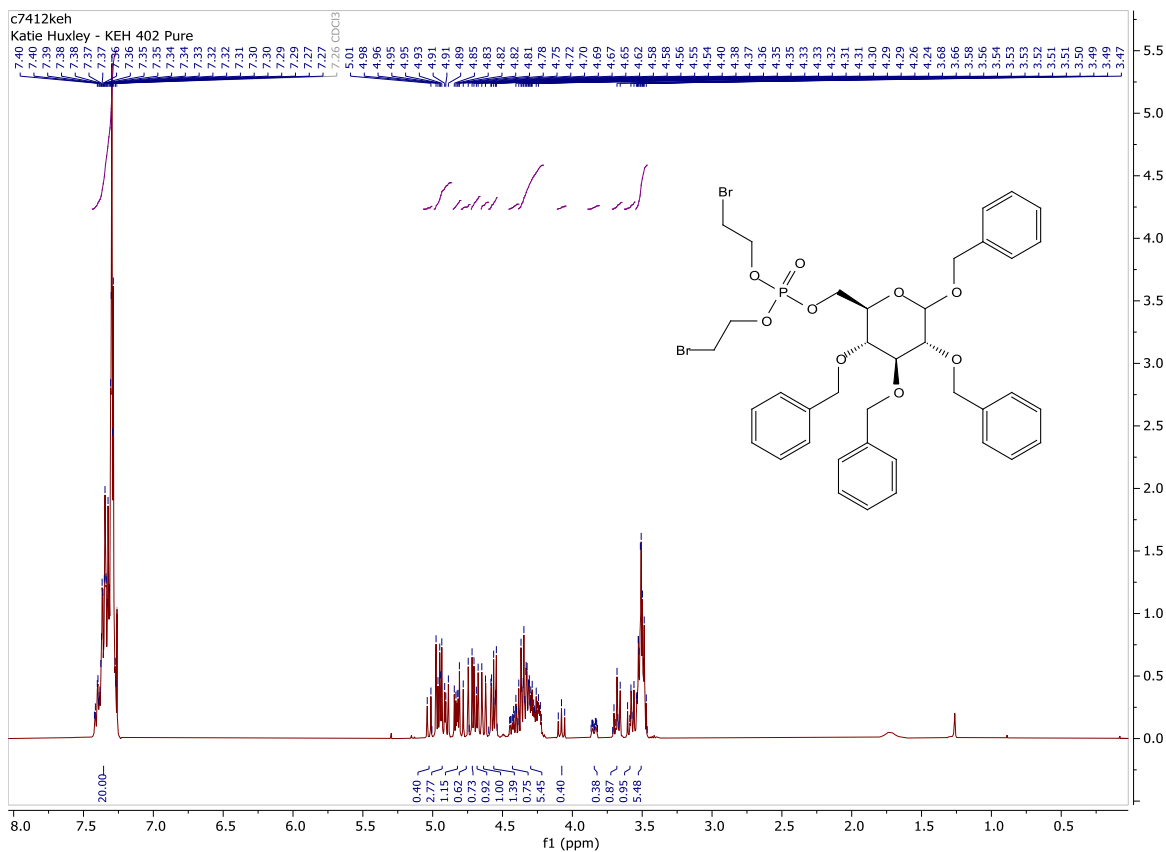
Method A Crude

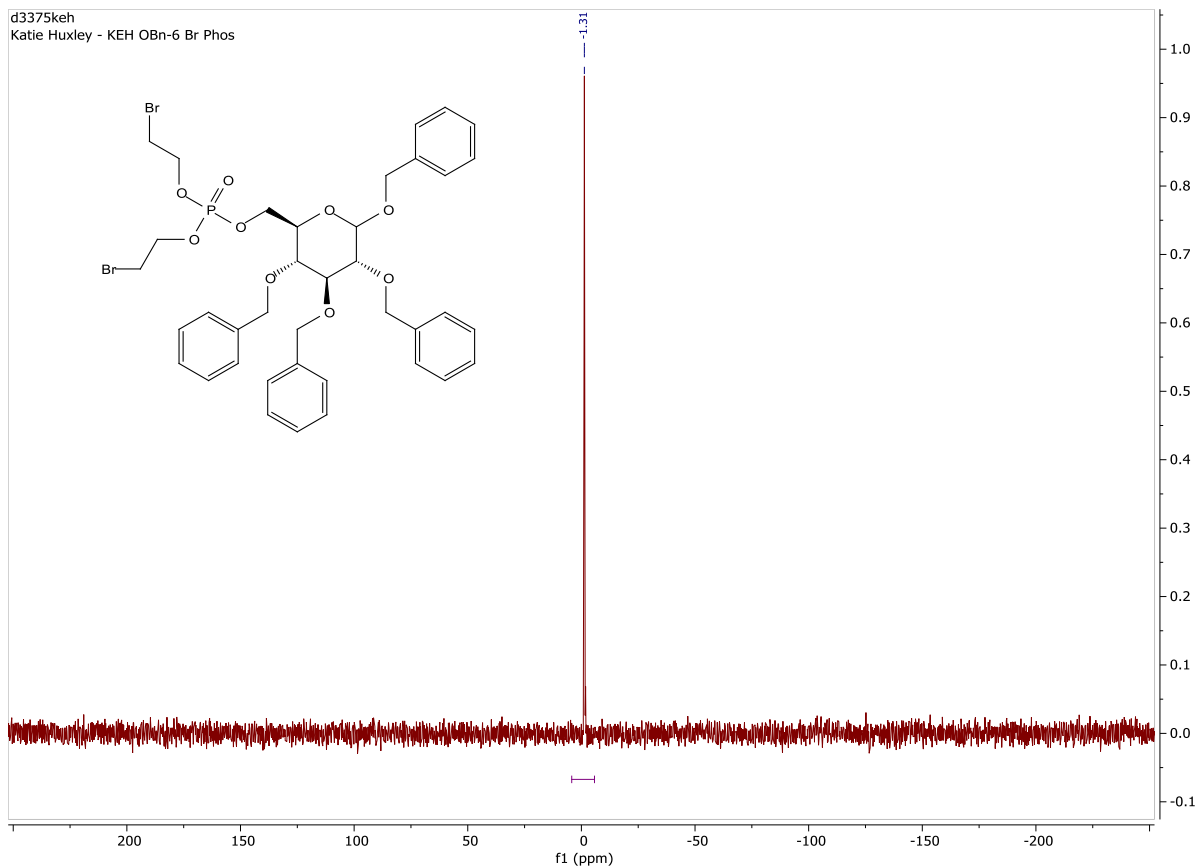


Method B Crude

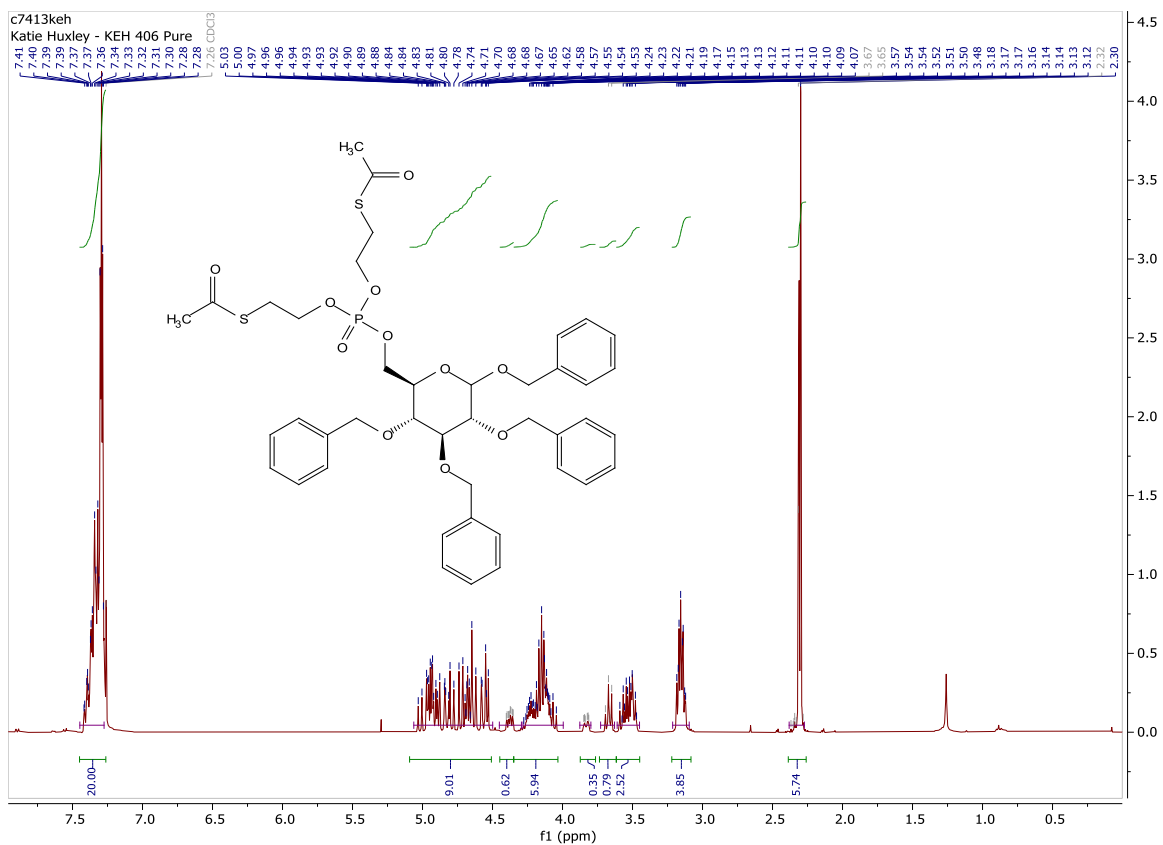


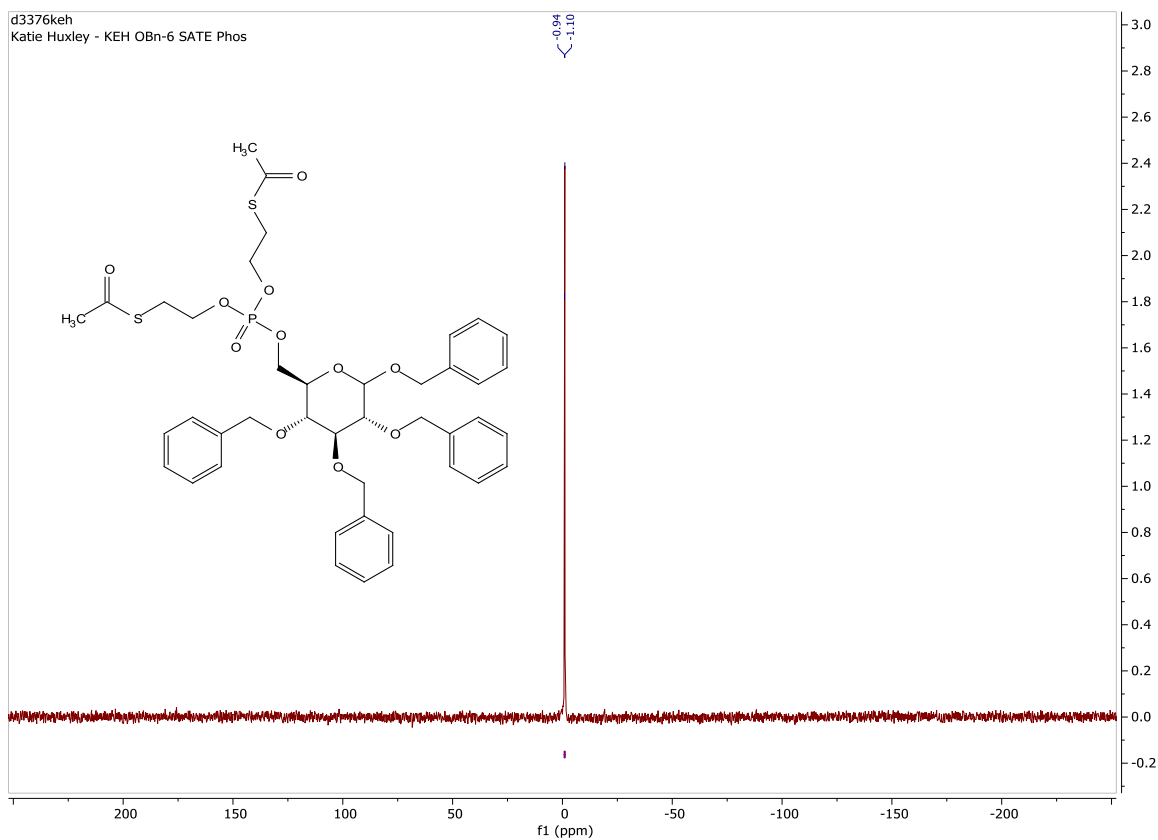
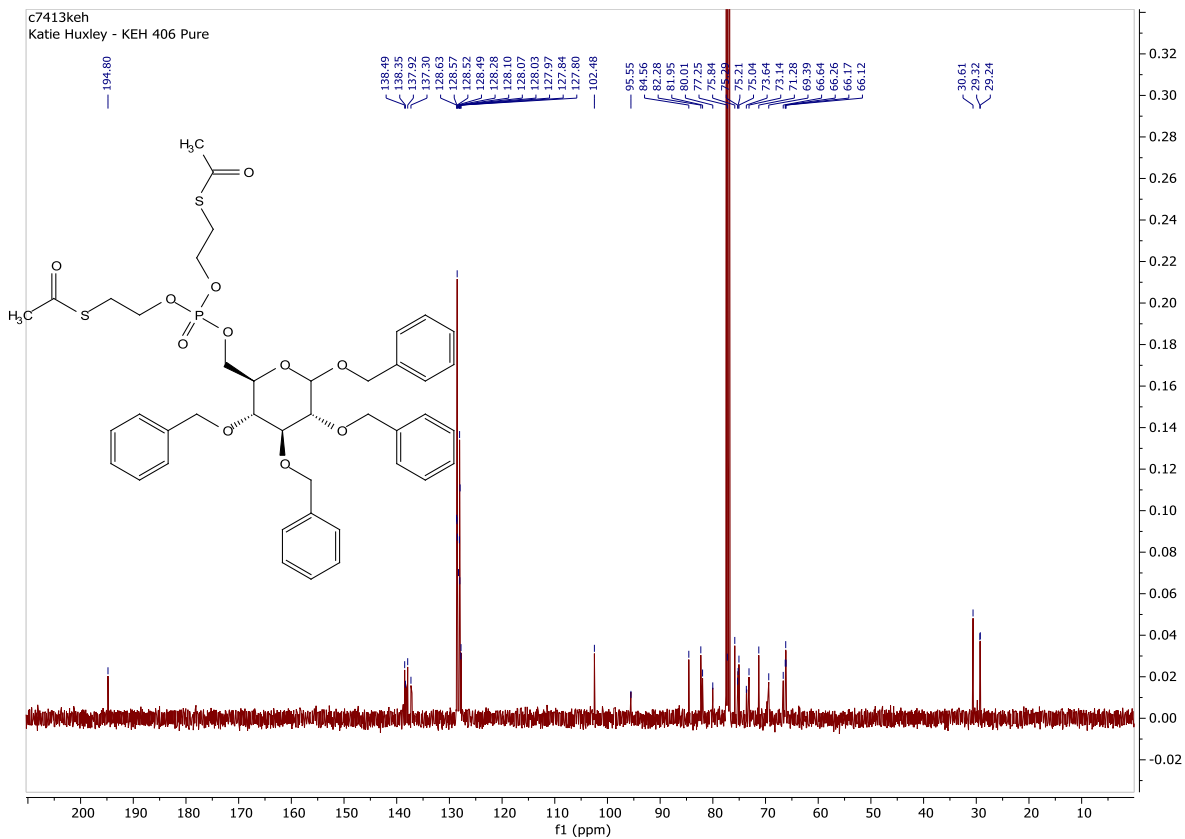
1,2,3,4-tetra-O-benzyl-6-bis(2-bromoethyl)phosphate- α,β -D-glucose



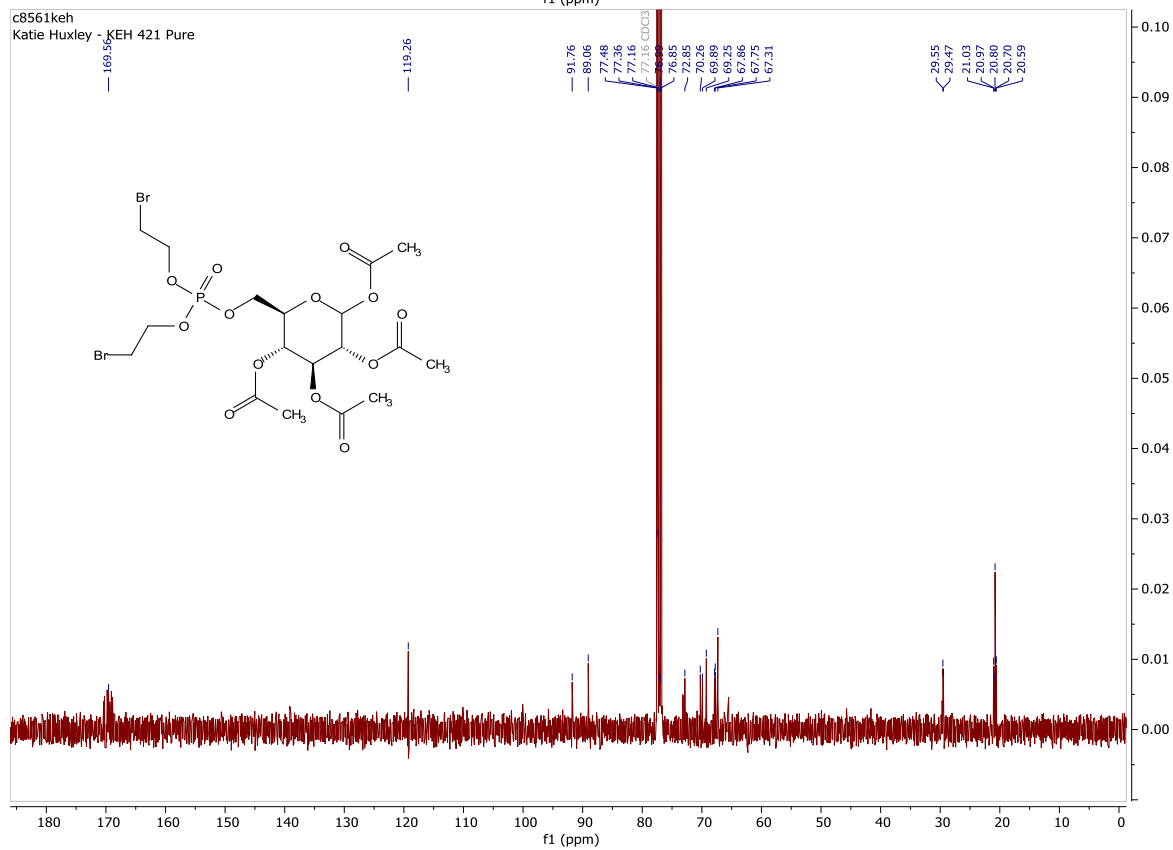
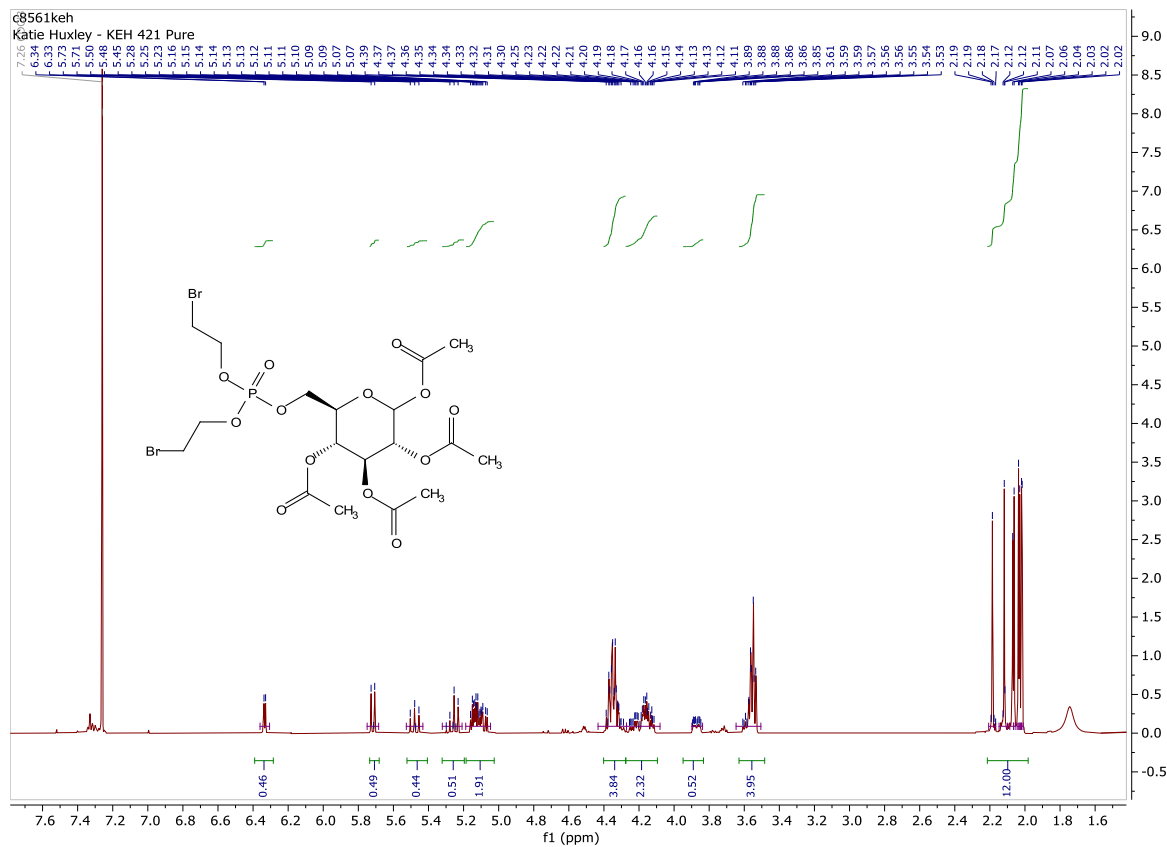


1,2,3,4,-tetra-O-benzyl-6-bis(SATE)phosphate-α,β-D-glucose

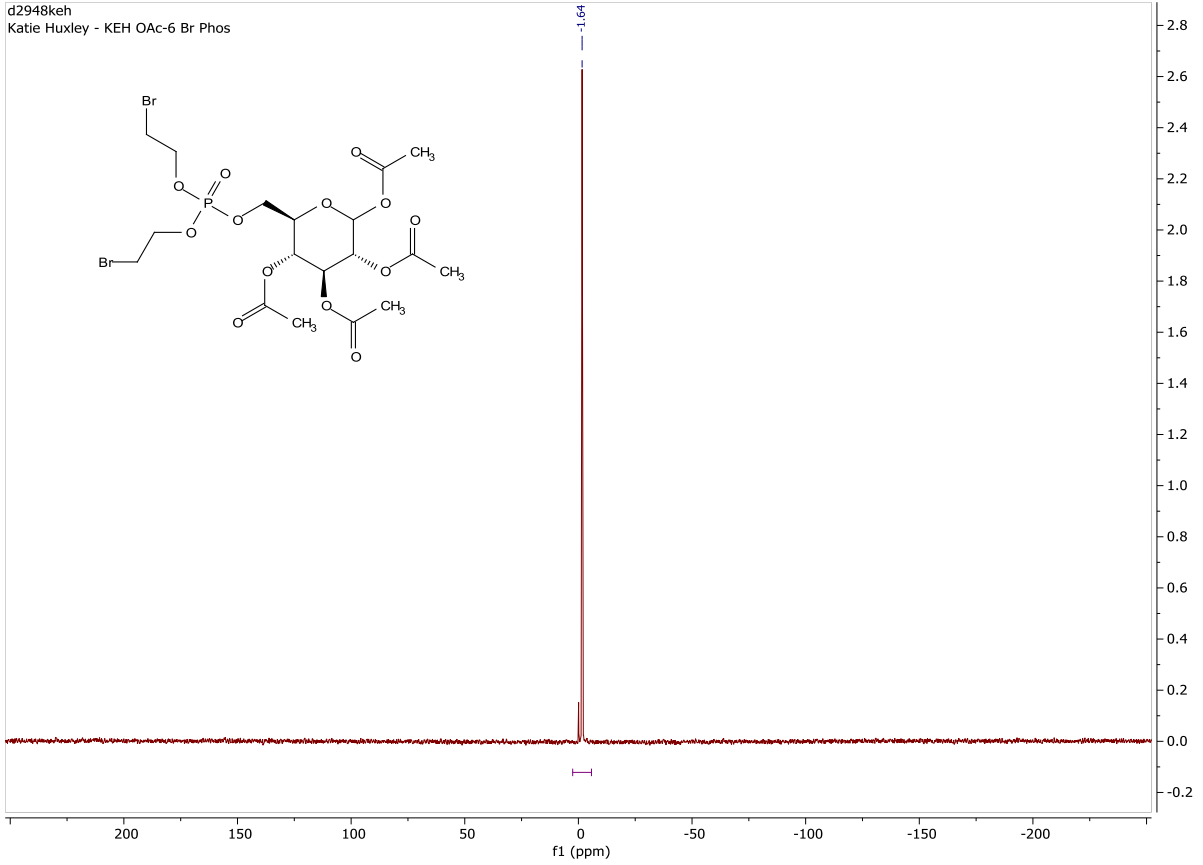




1,2,3,4-tetra-O-acetyl-6-bis-(2-bromoethyl)phosphate- α,β -D-glucose

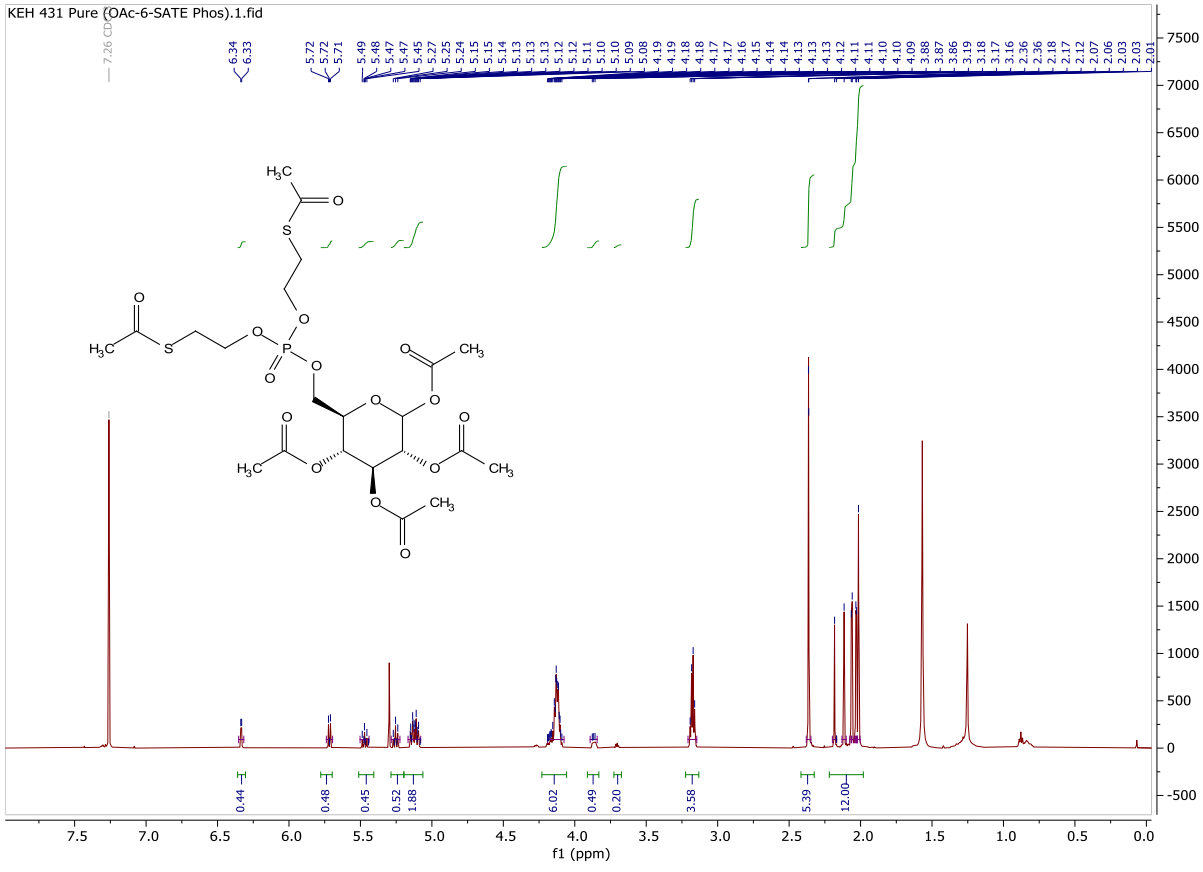


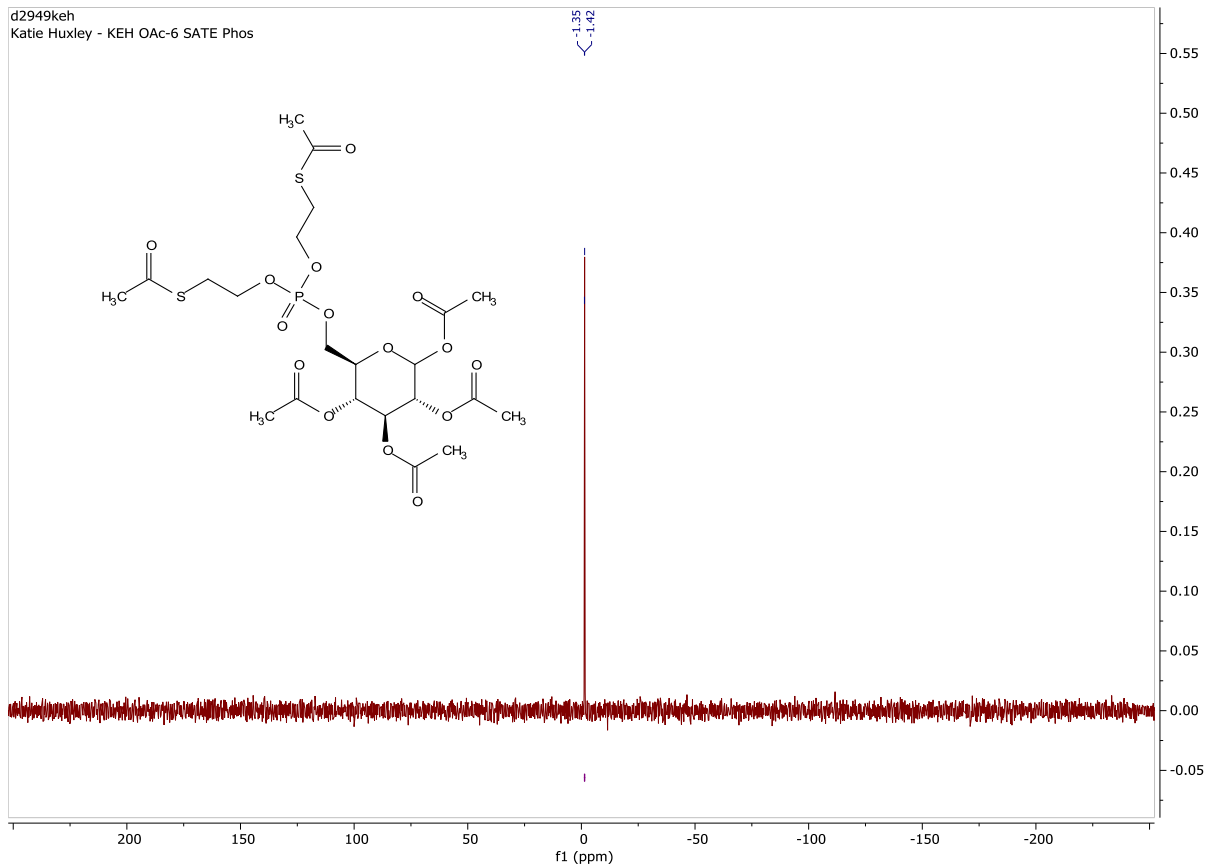
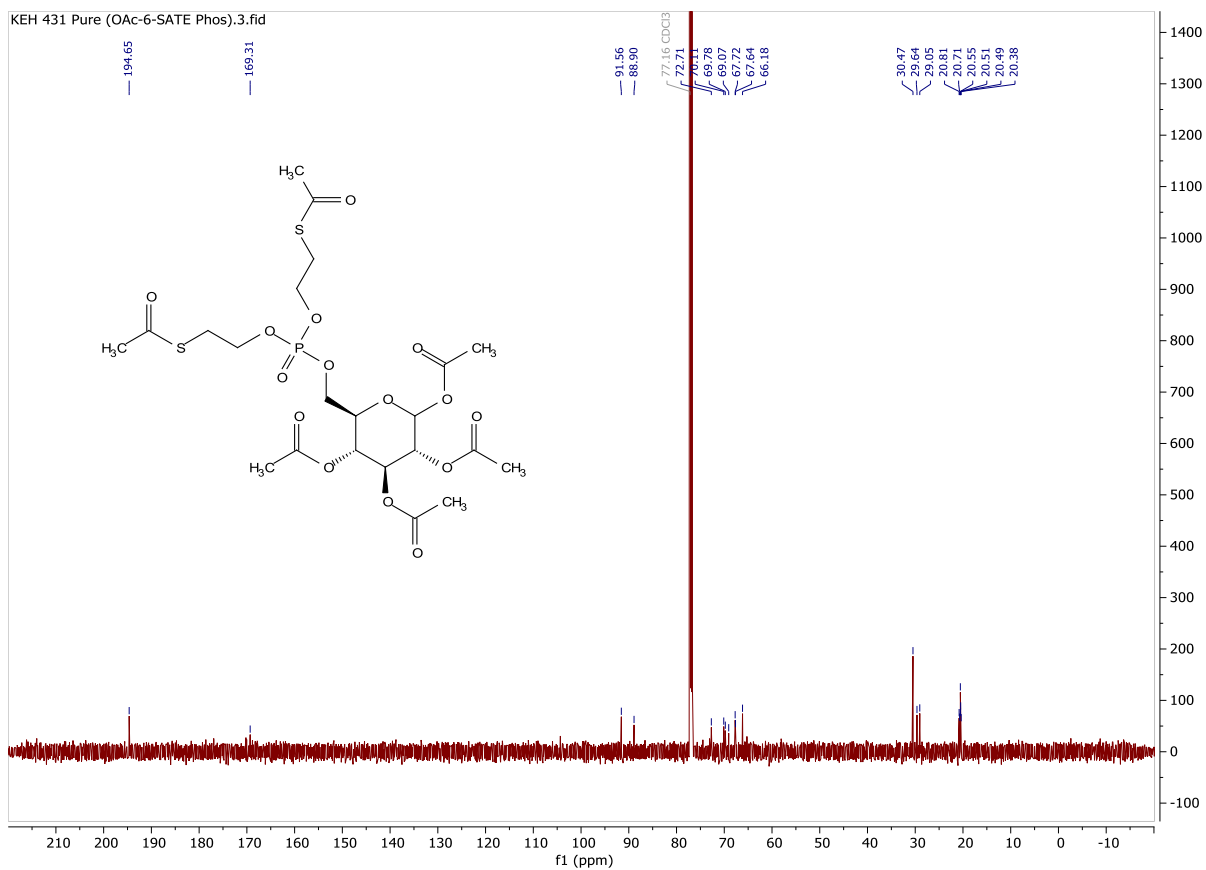
d2948keh
Katie Huxley - KEH OAc-6 Br Phos



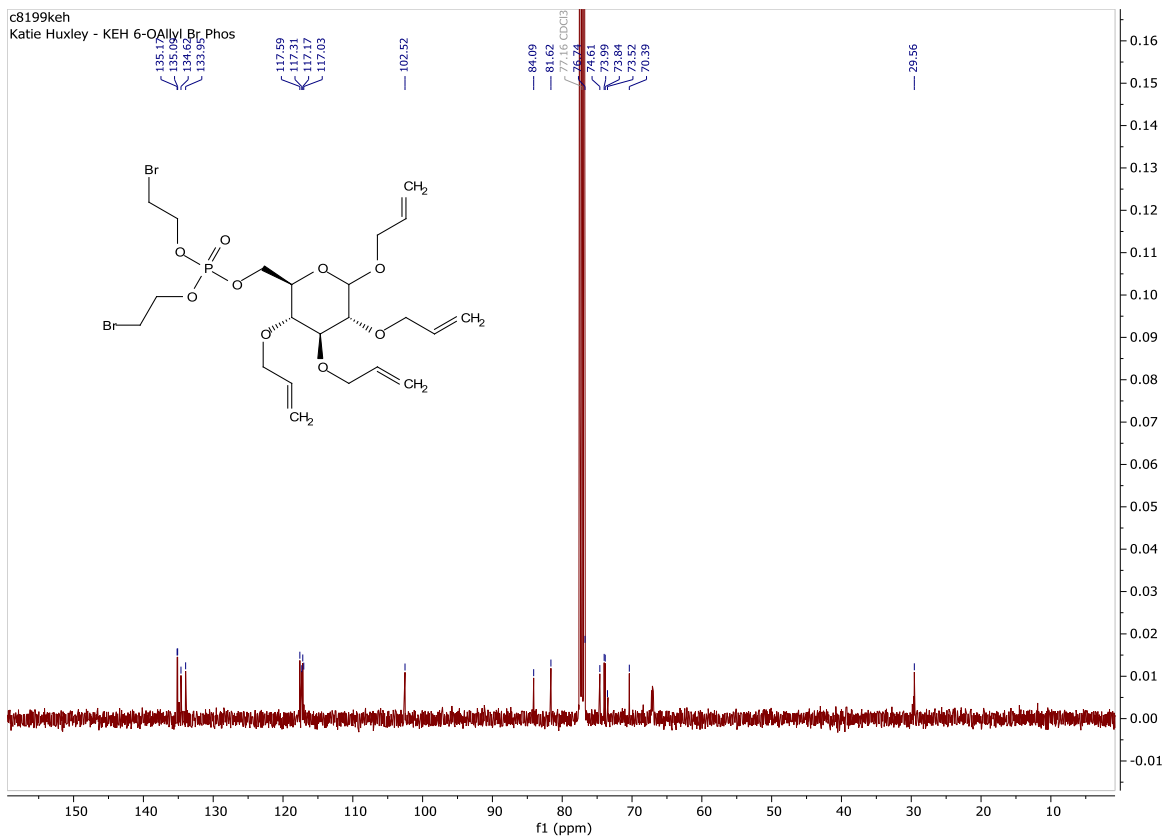
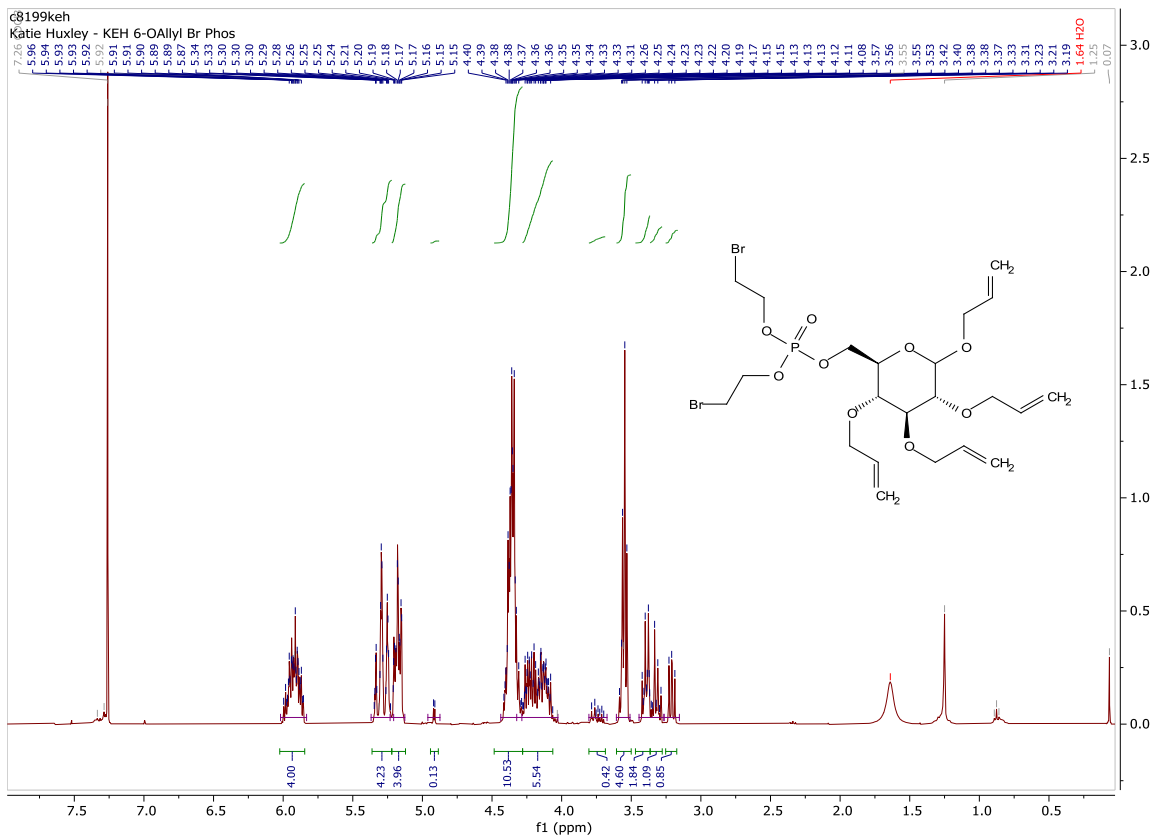
1,2,3,4,-tetra-O-acetyl-6-bis(SATE)phosphate-α,β-D-glucose

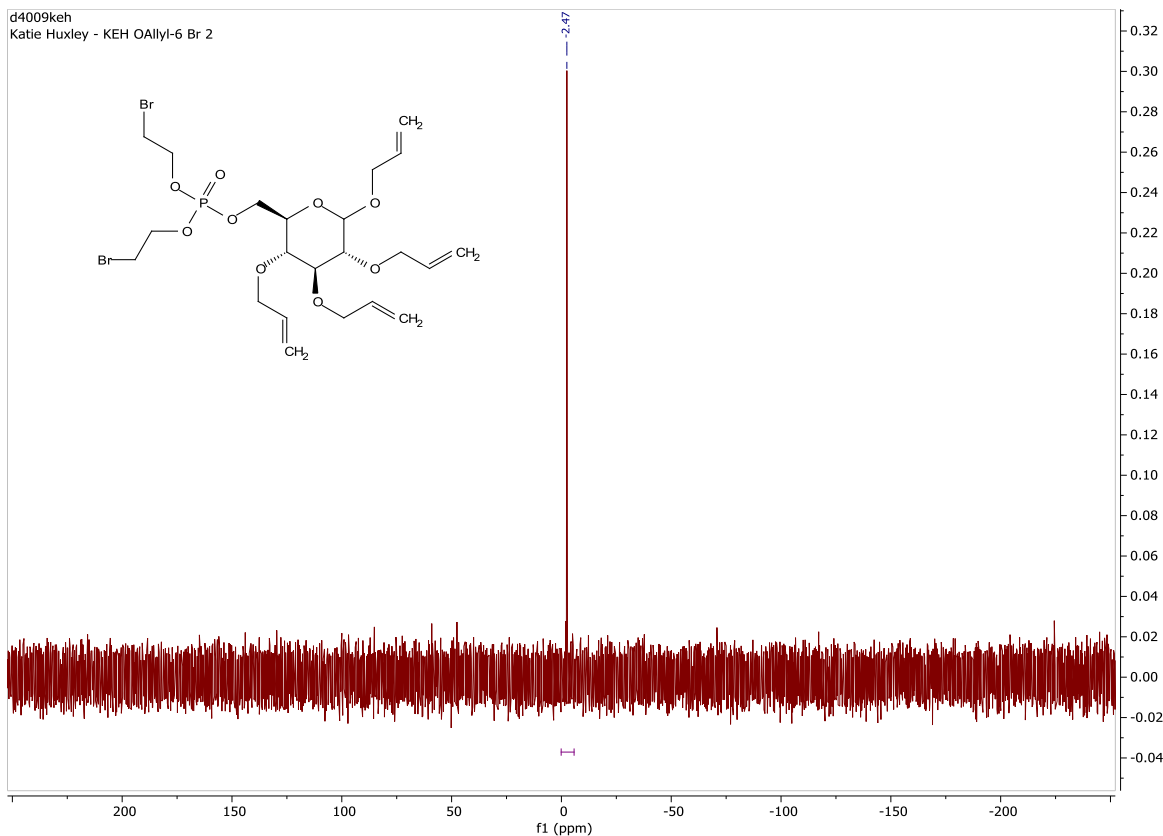
KEH 431 Pure (OAc-6-SATE Phos).1.fid



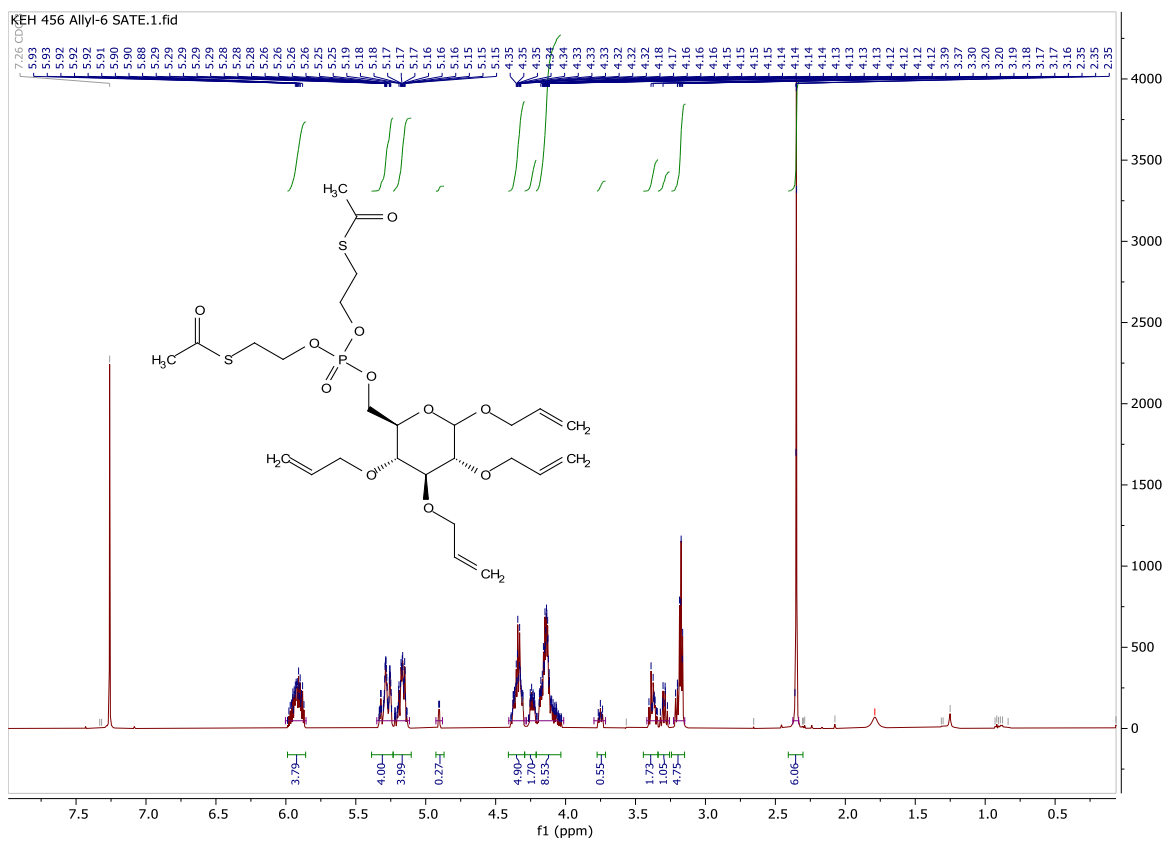


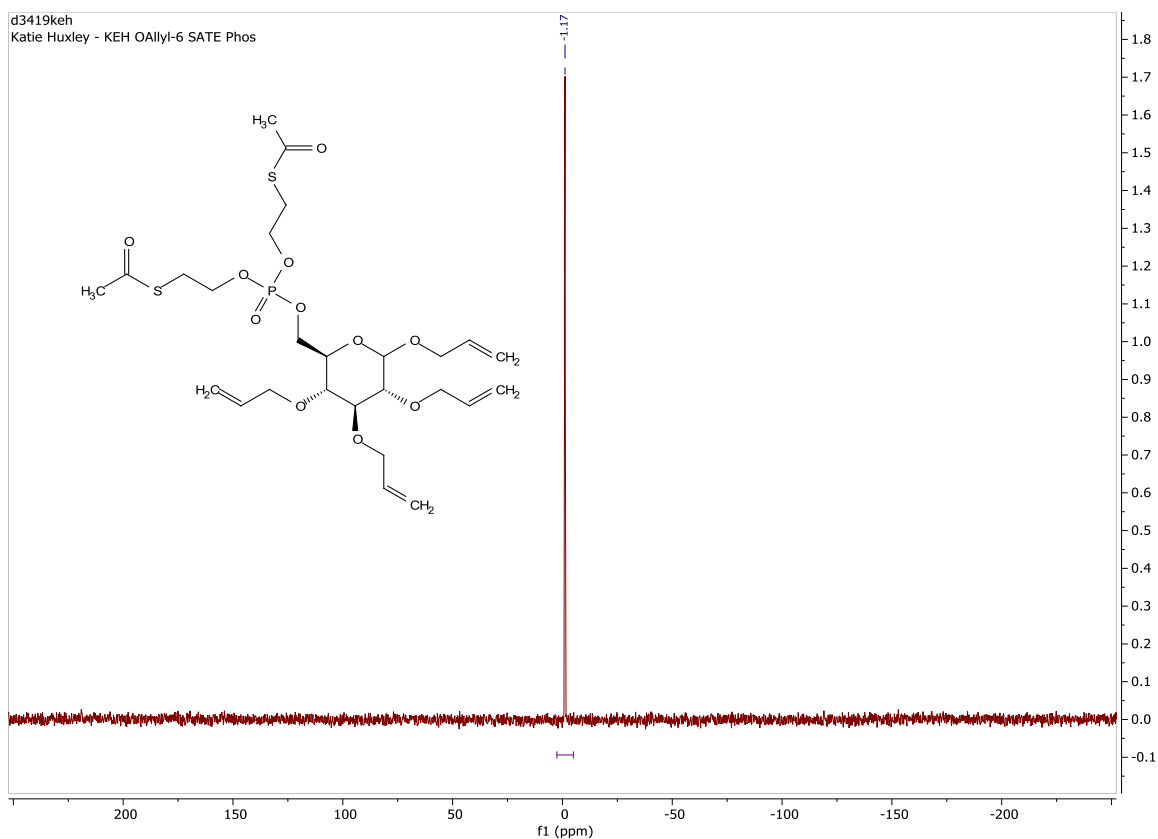
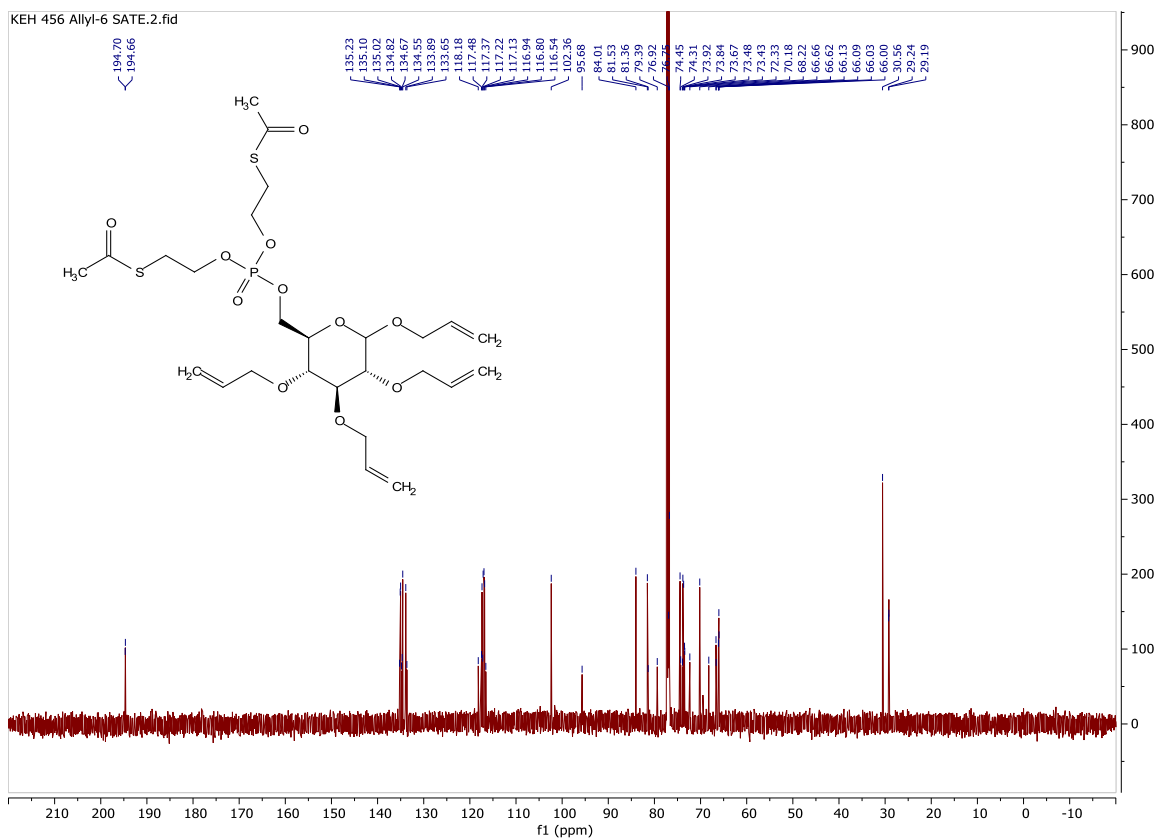
1,2,3,4,-tetra-O-allyl-6-bis(2-bromoethyl)phosphate- α,β -D-glucose

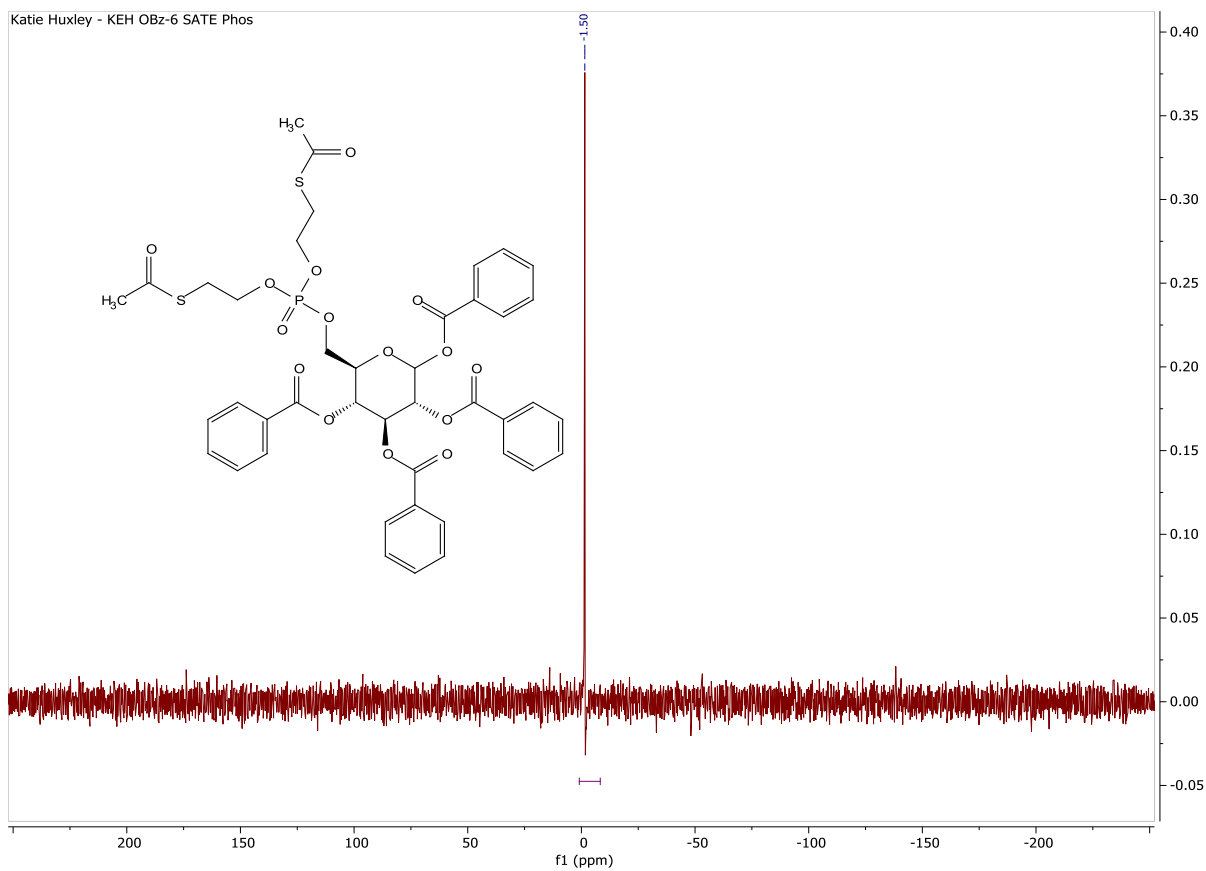
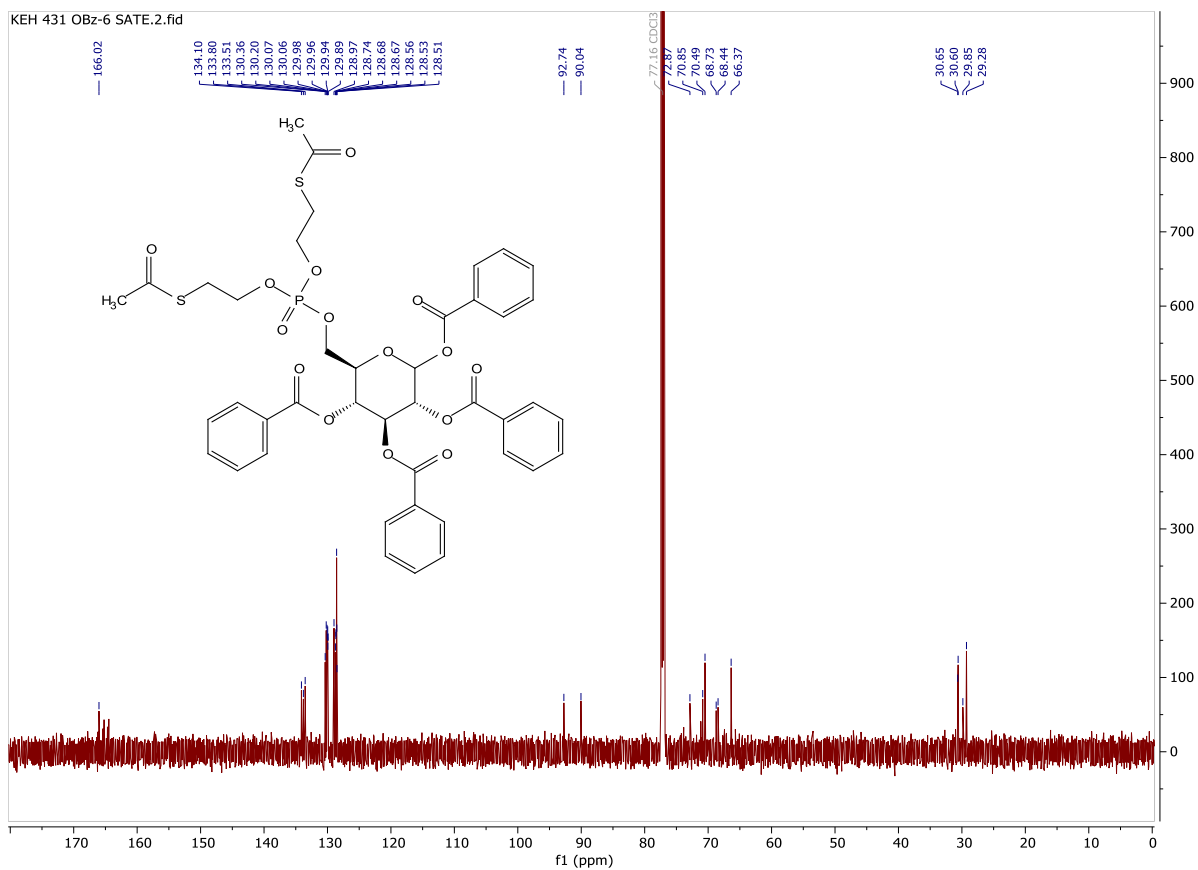




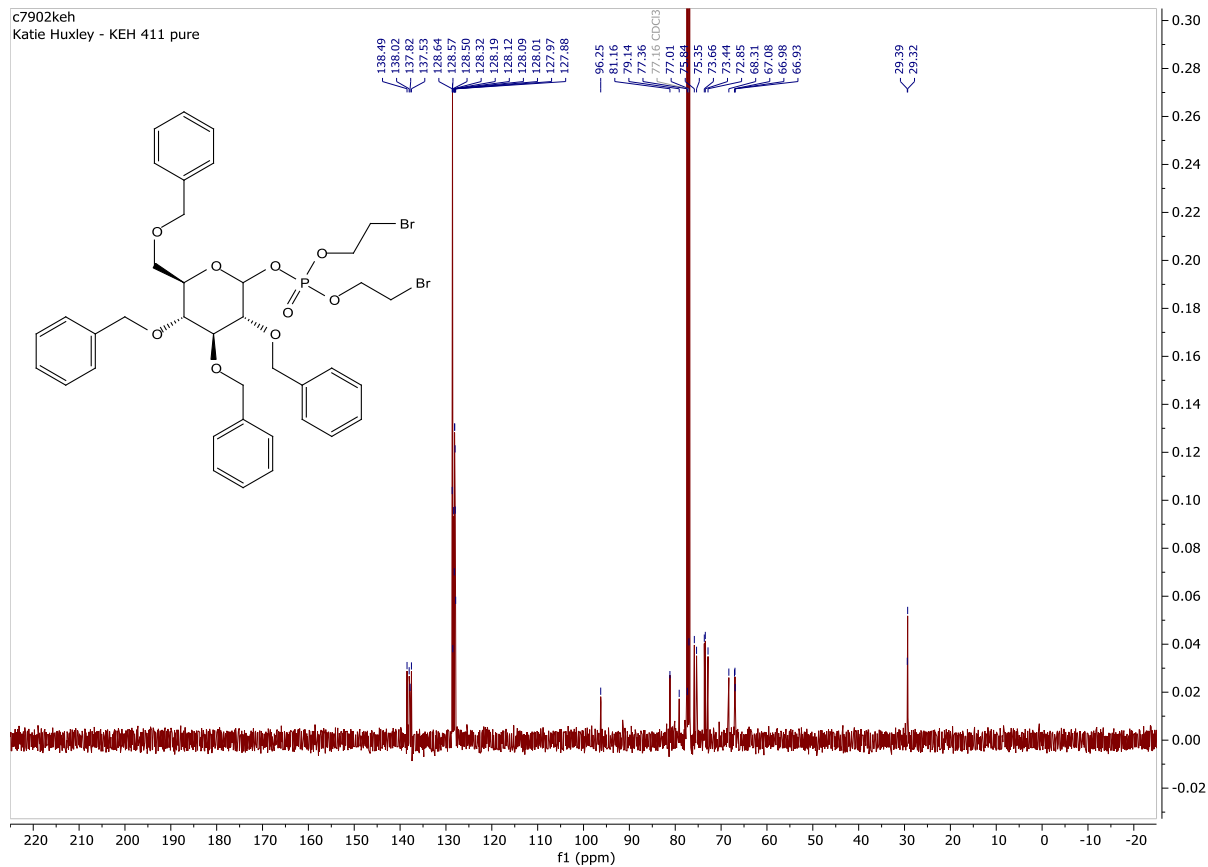
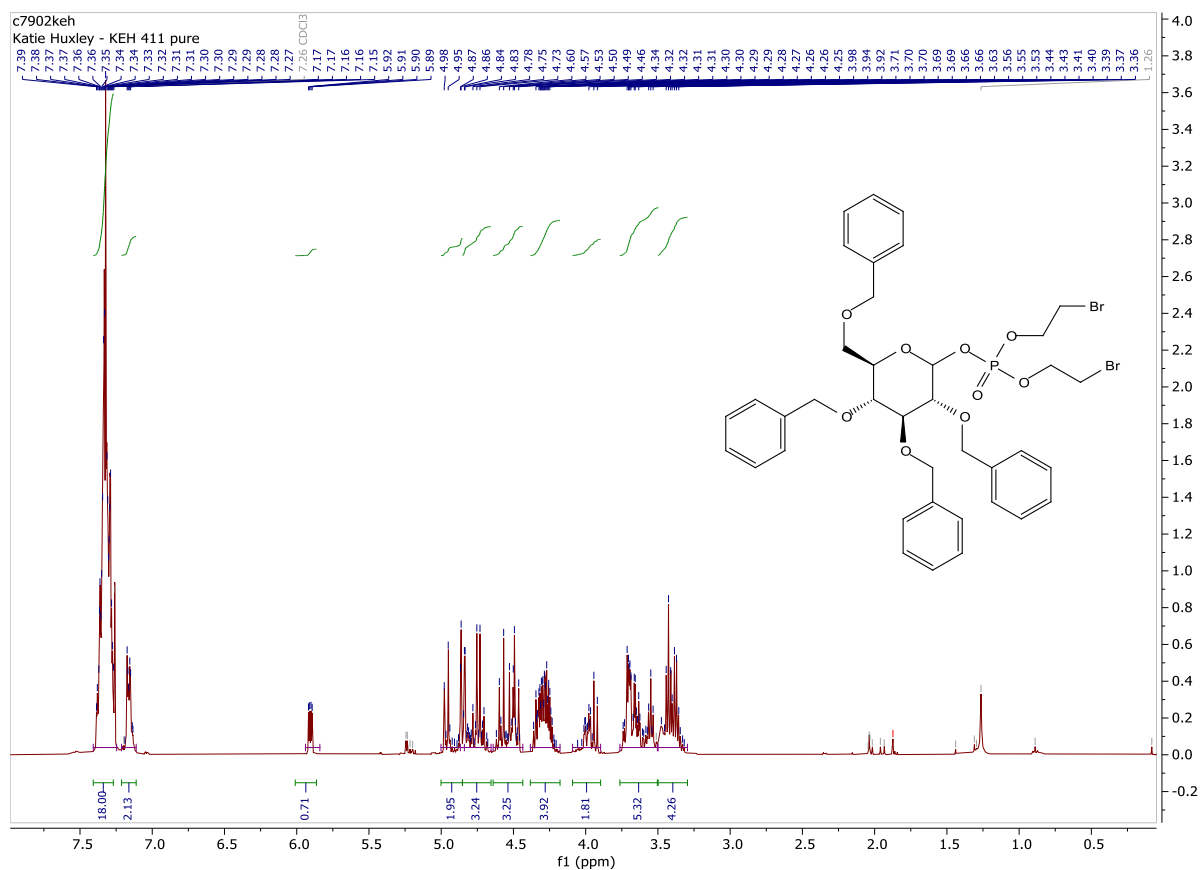
1,2,3,4,-tetra-O-allyl-6-bis(SATE)phosphate- α,β -D-glucose



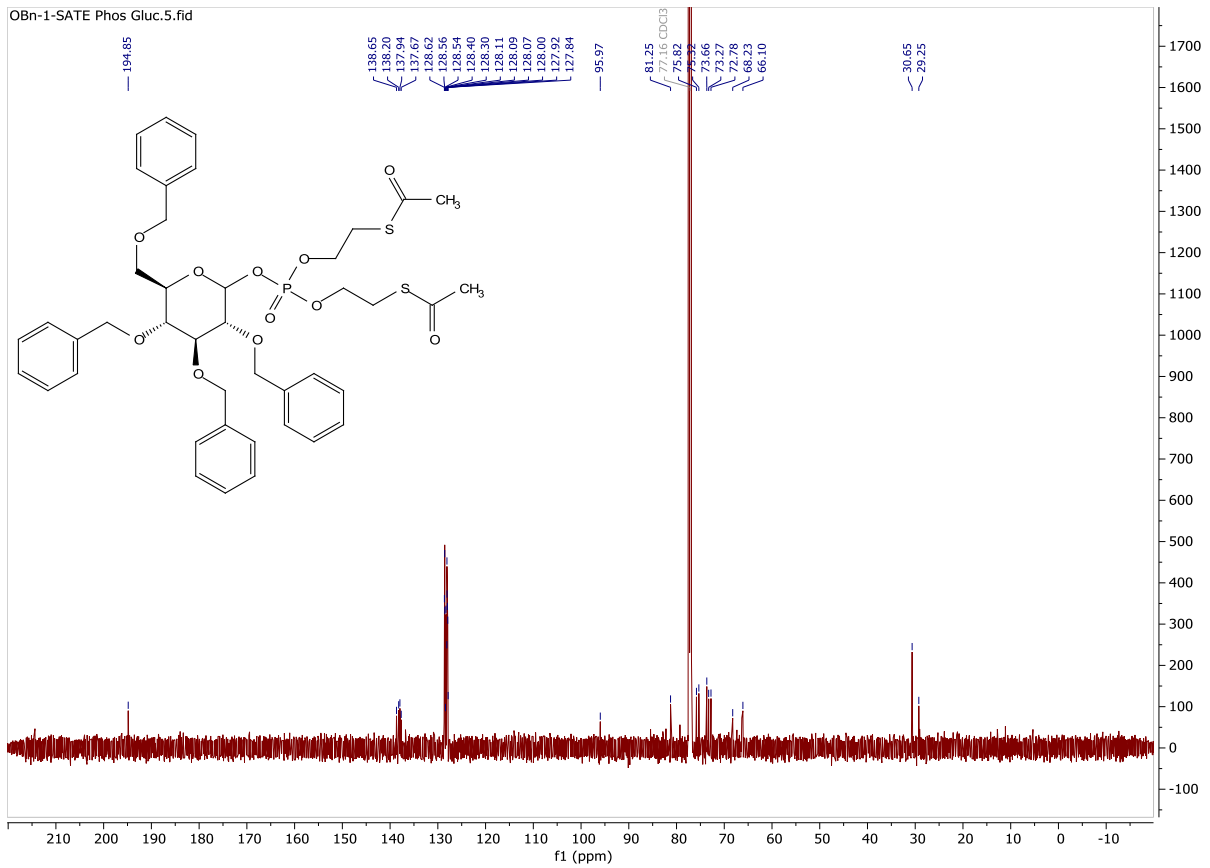
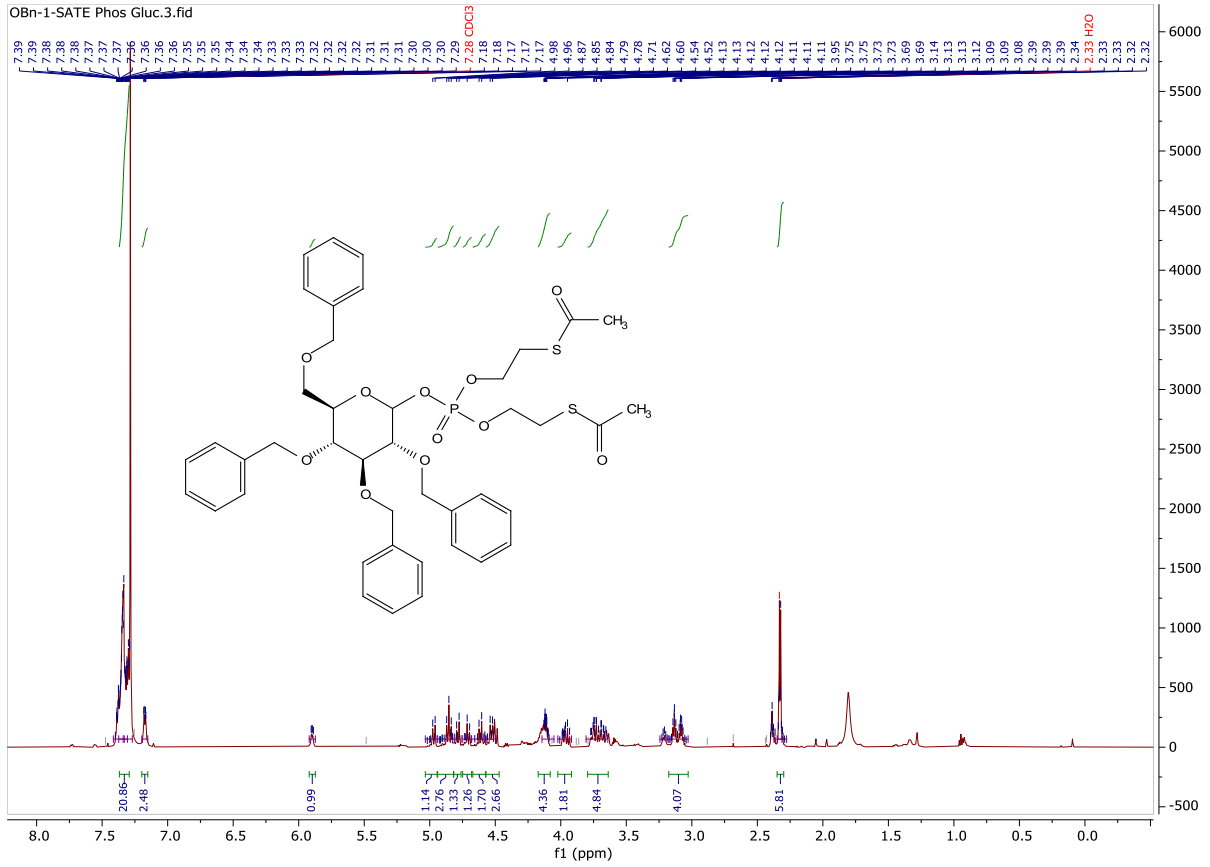


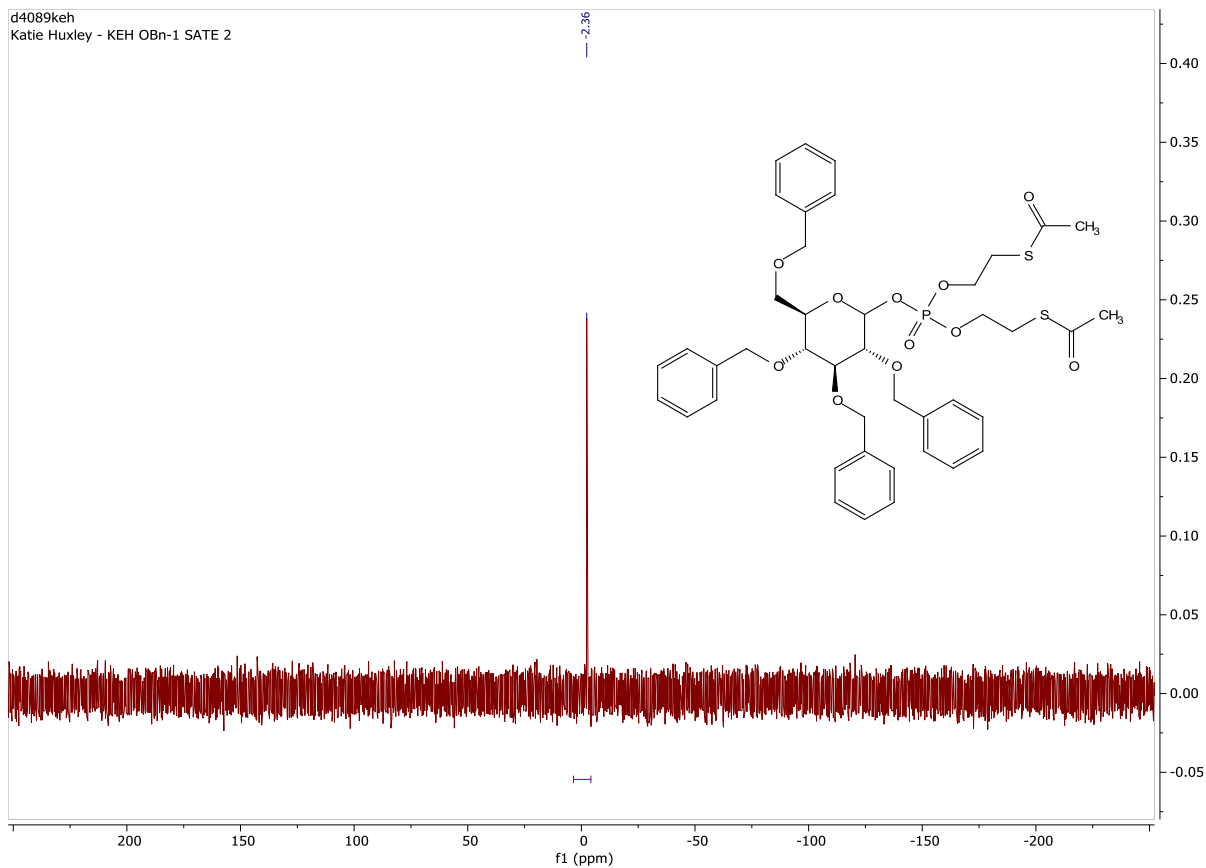


2,3,4,6-tetra-O-benzyl-1-bis(2-bromoethyl)phosphate- α,β -D-glucose

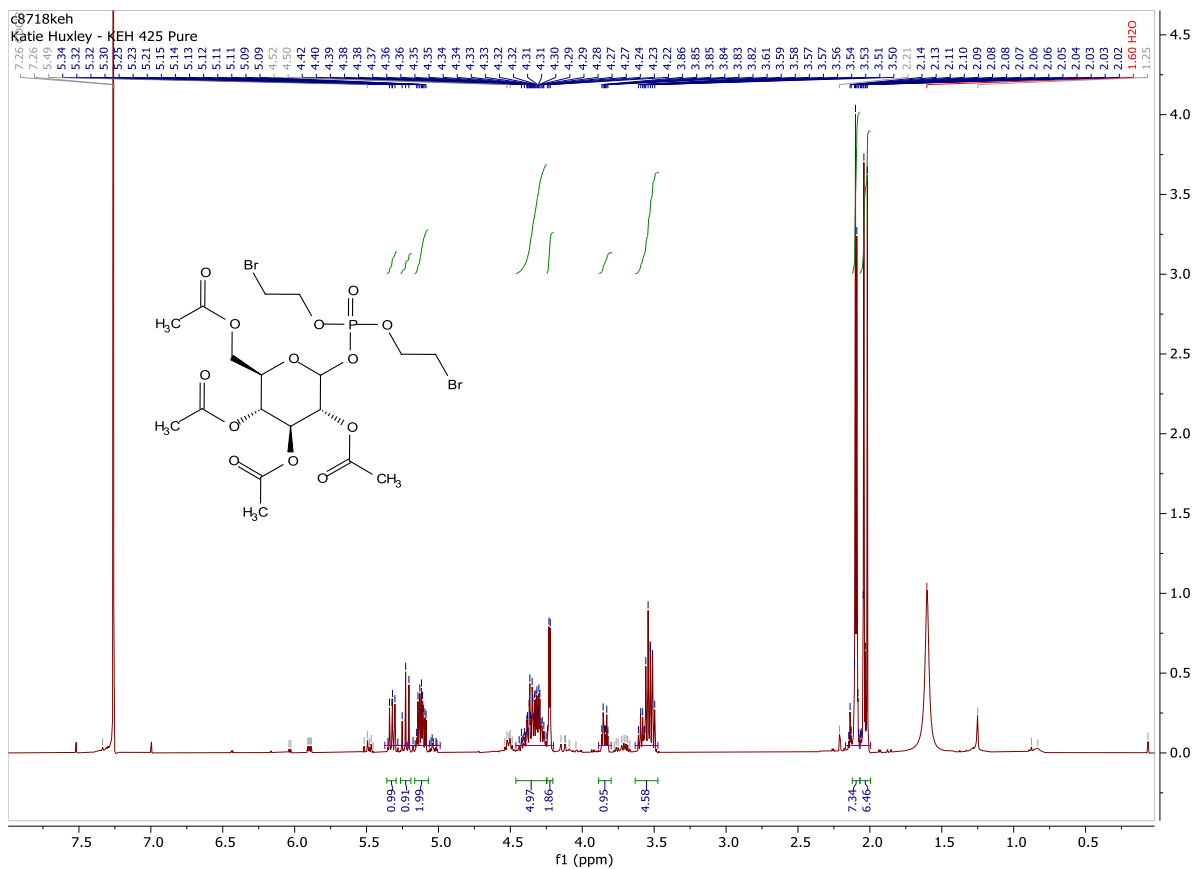


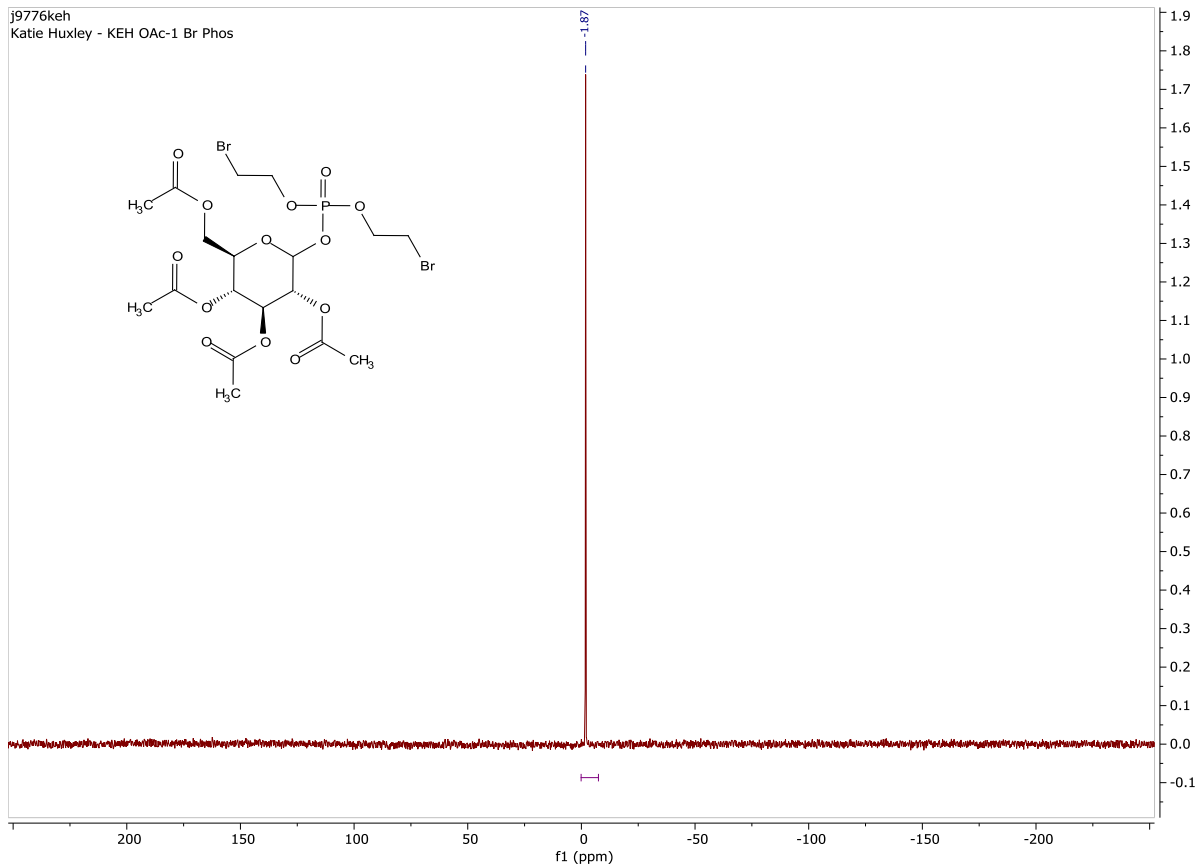
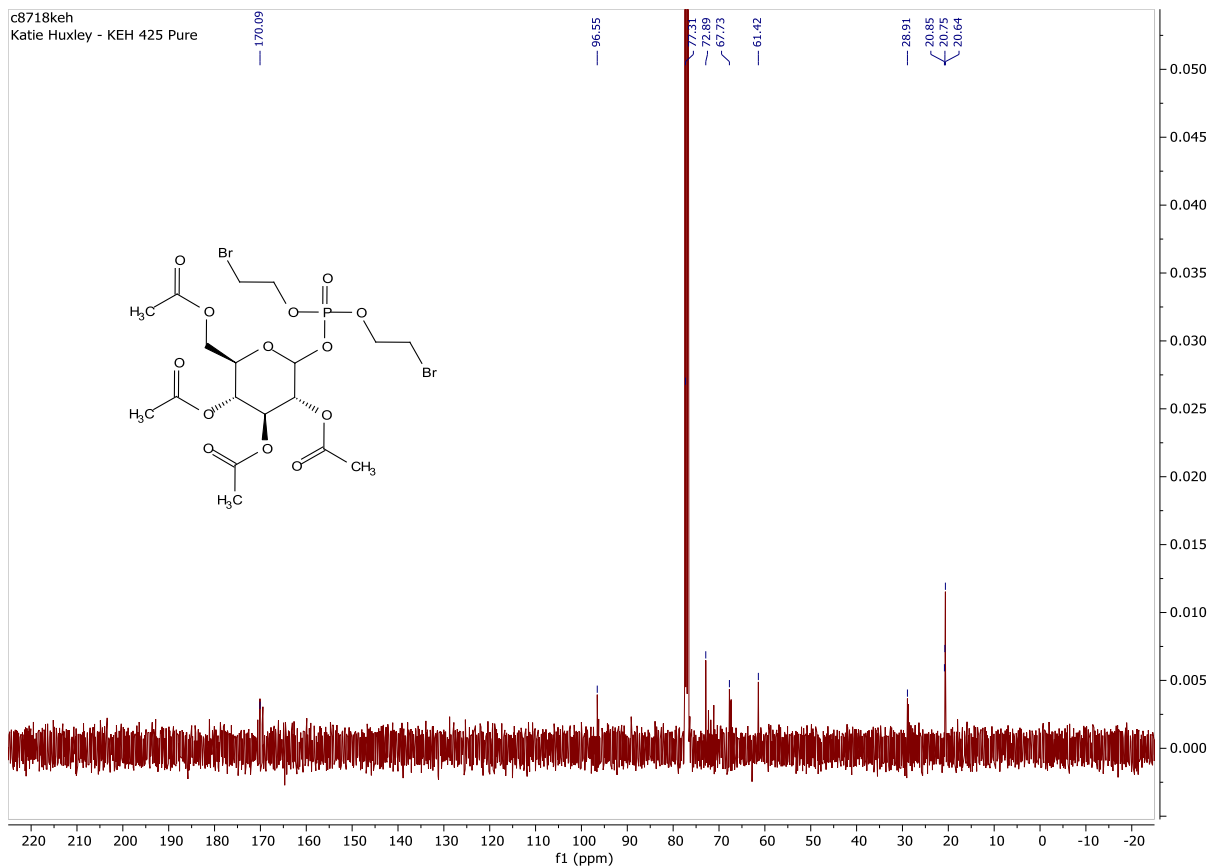
2,3,4,6-tetra-O-benzyl-1-bis(SATE)phosphate- α,β -D-glucose



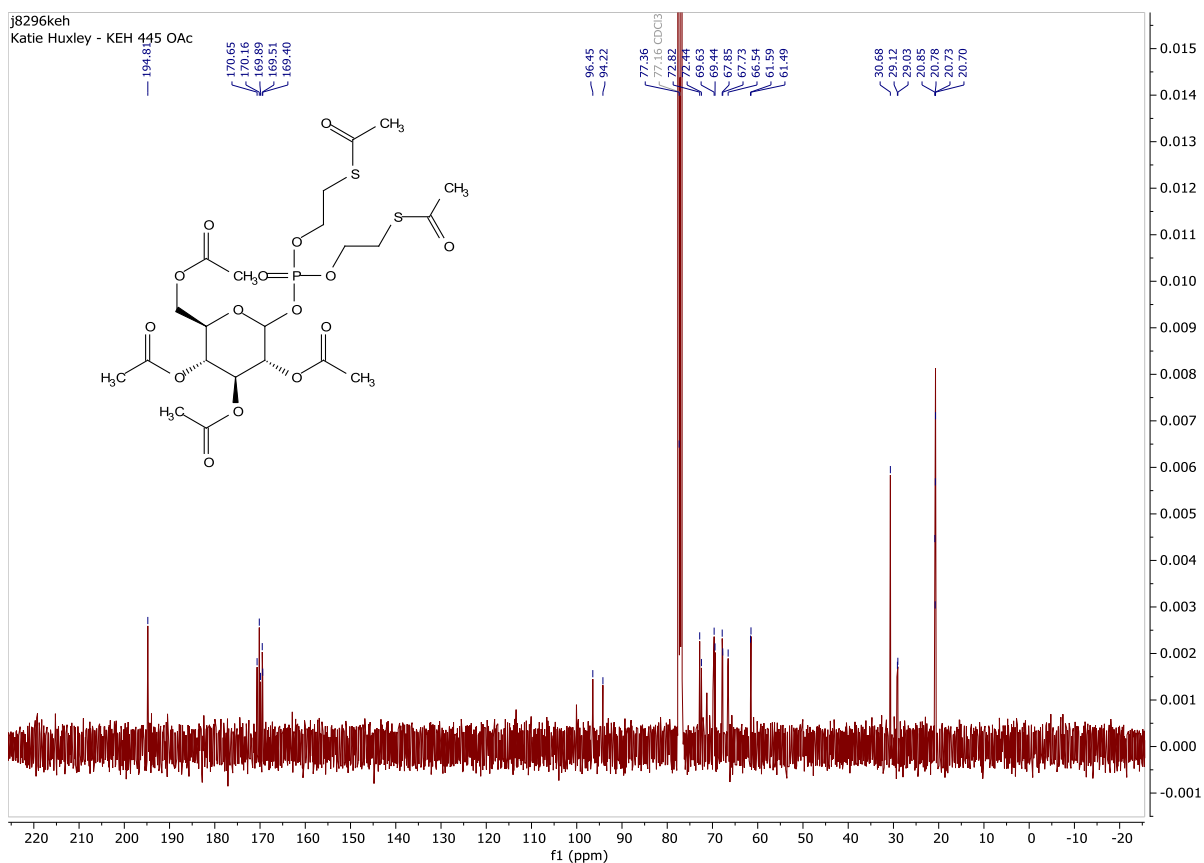
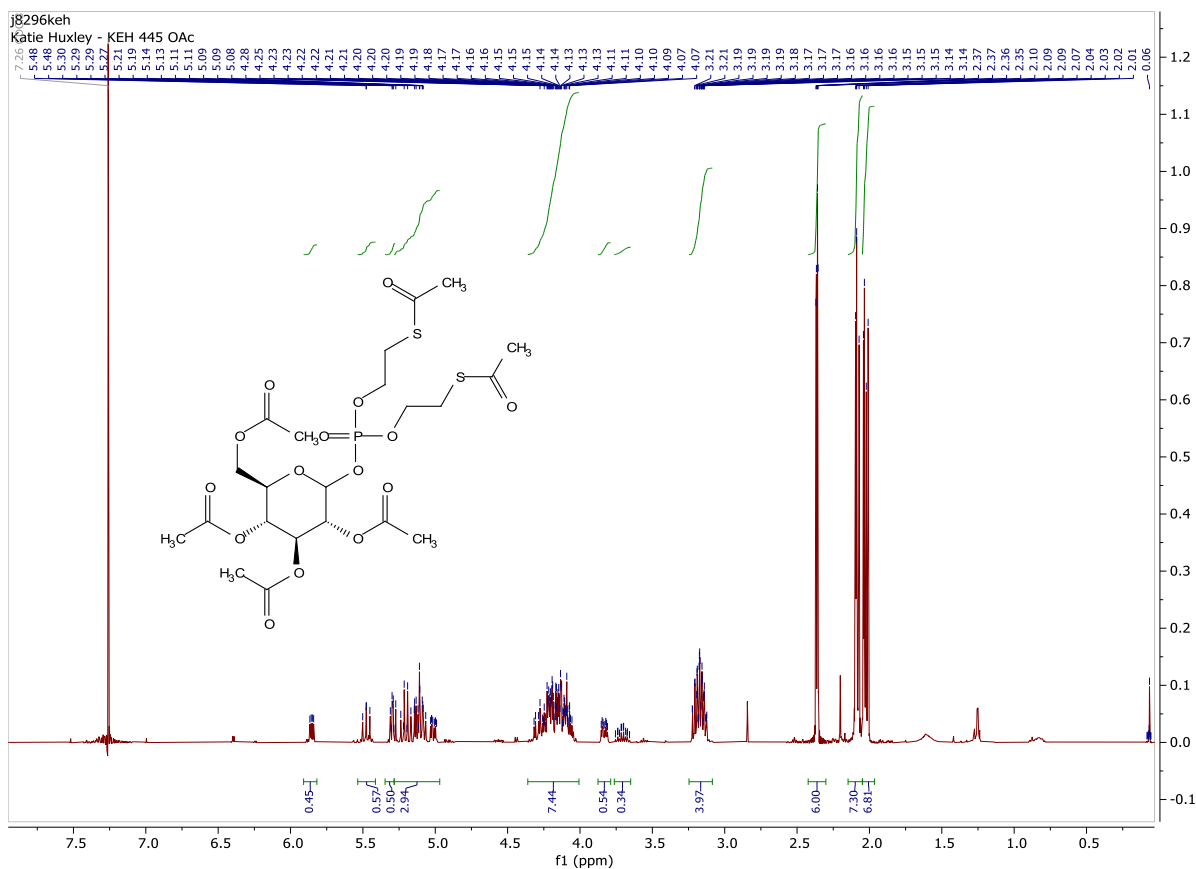


2,3,4,6-tetra-O-acetyl-1-bis(2-bromoethyl)phosphate- α,β -D-glucose

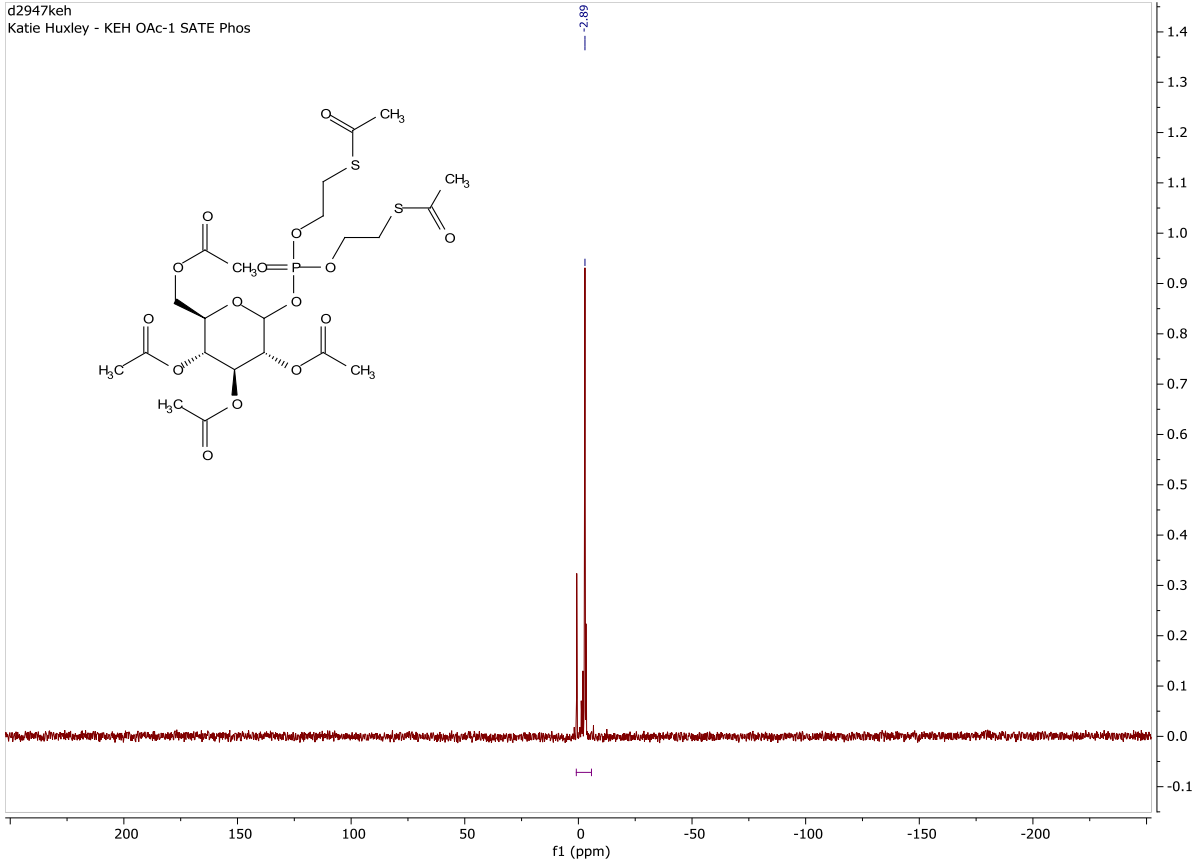




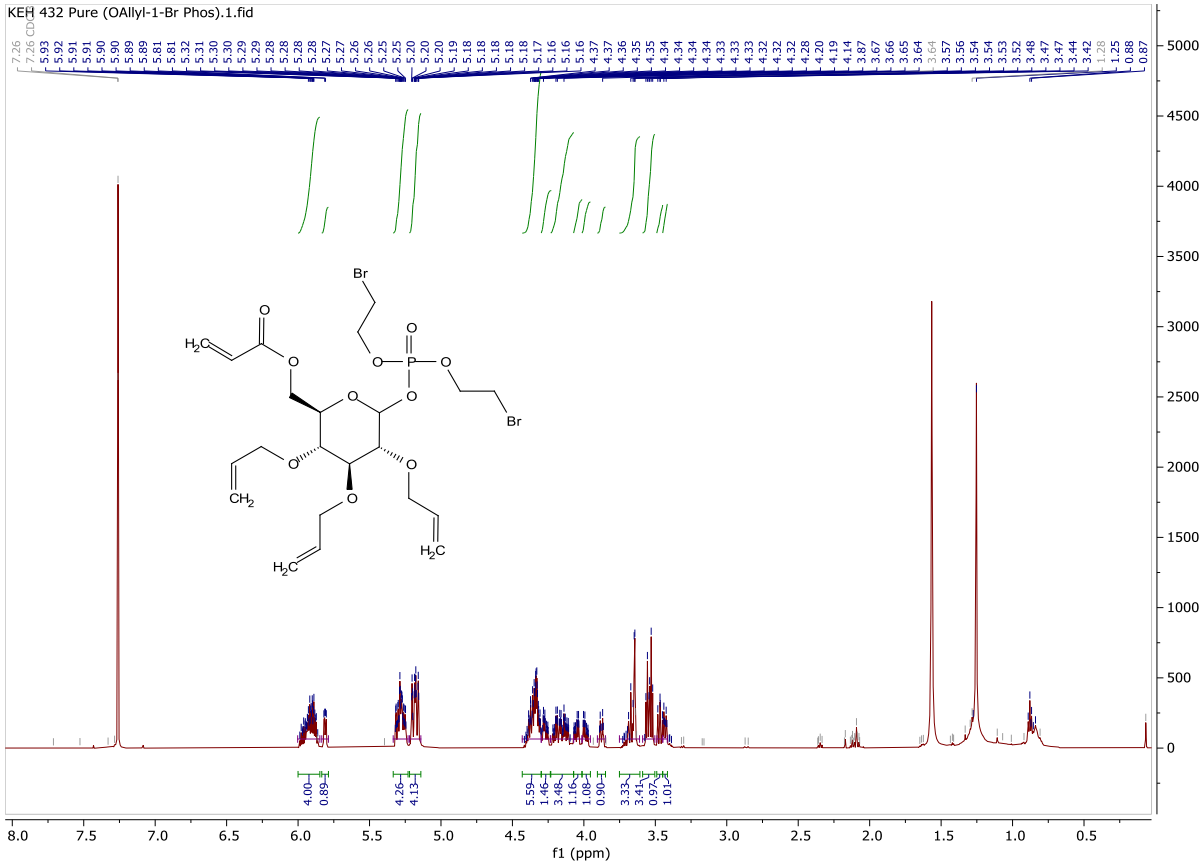
2,3,4,6-tetra-O-acetyl-1-bis(SATE)phosphate- α,β -D-glucose

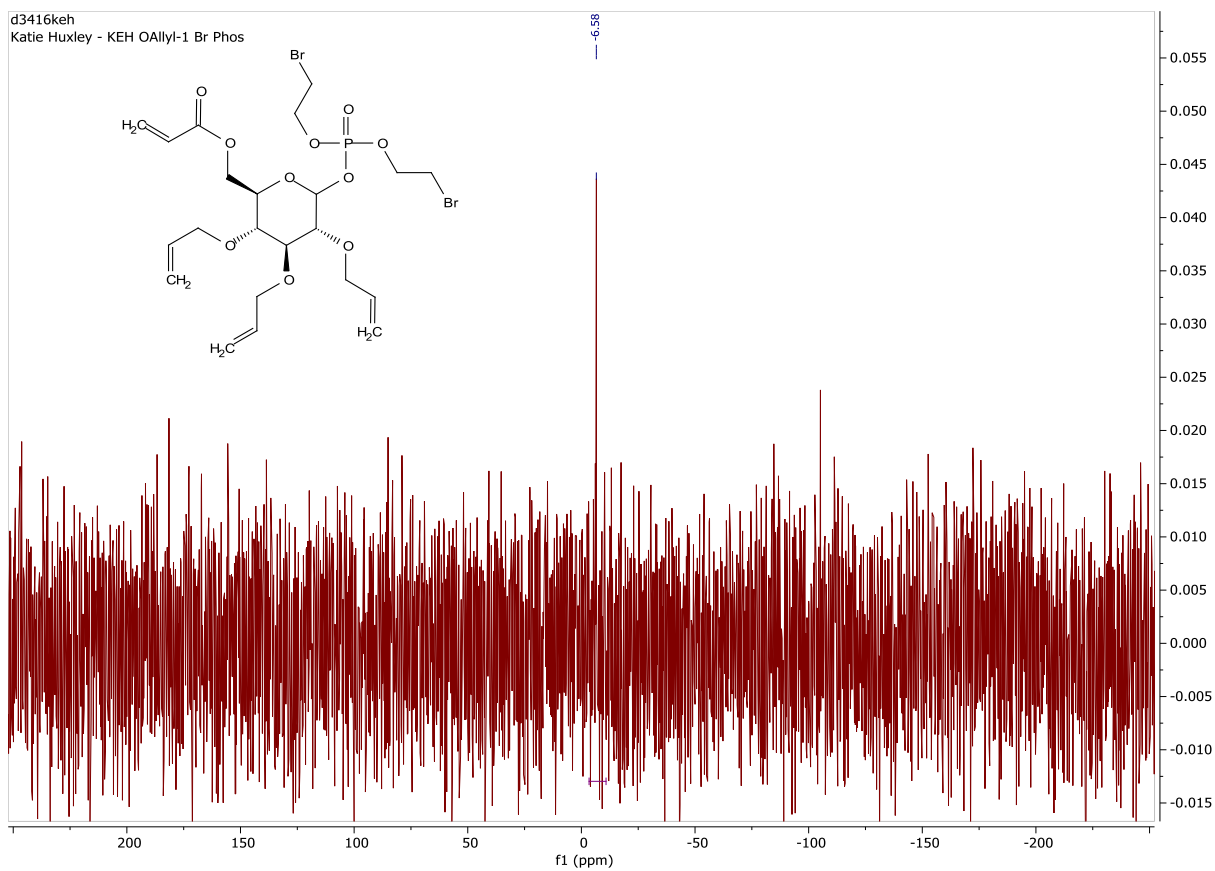
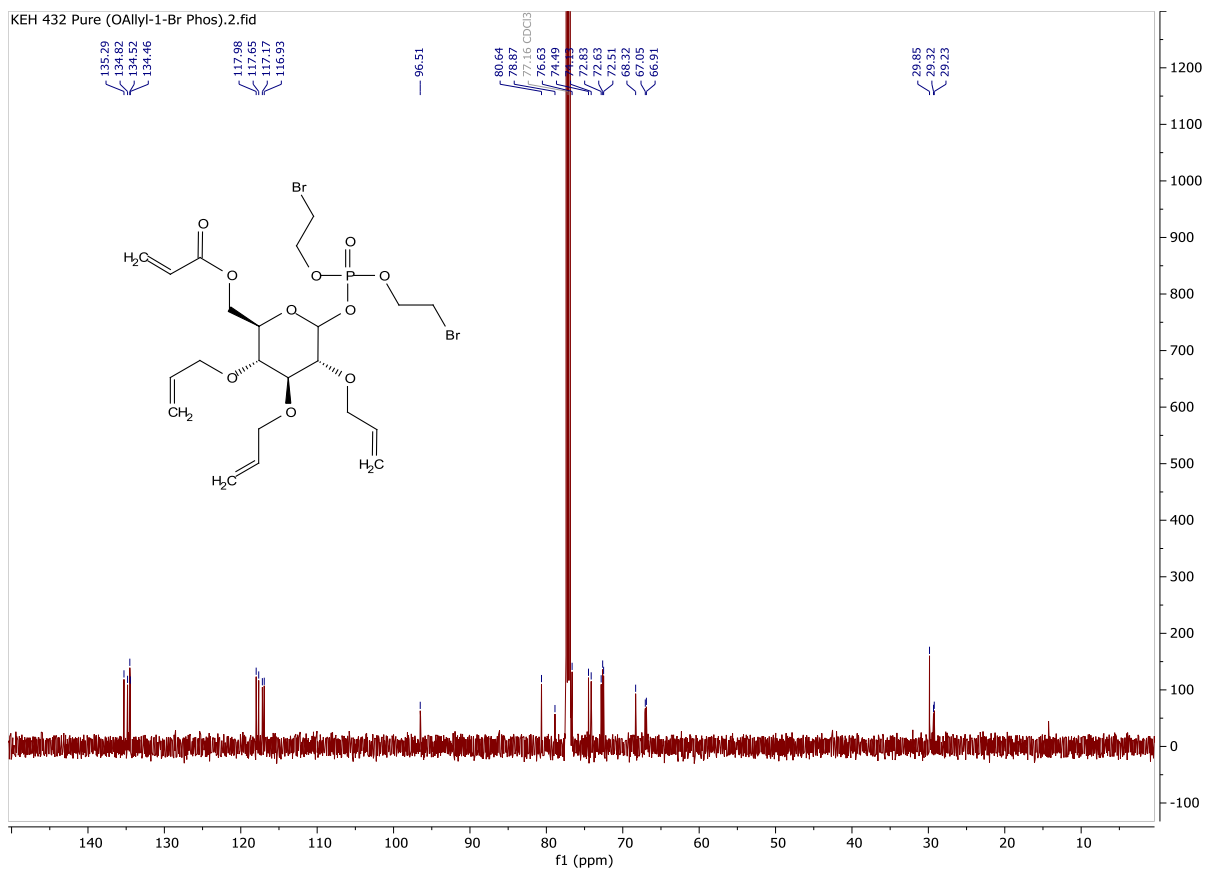


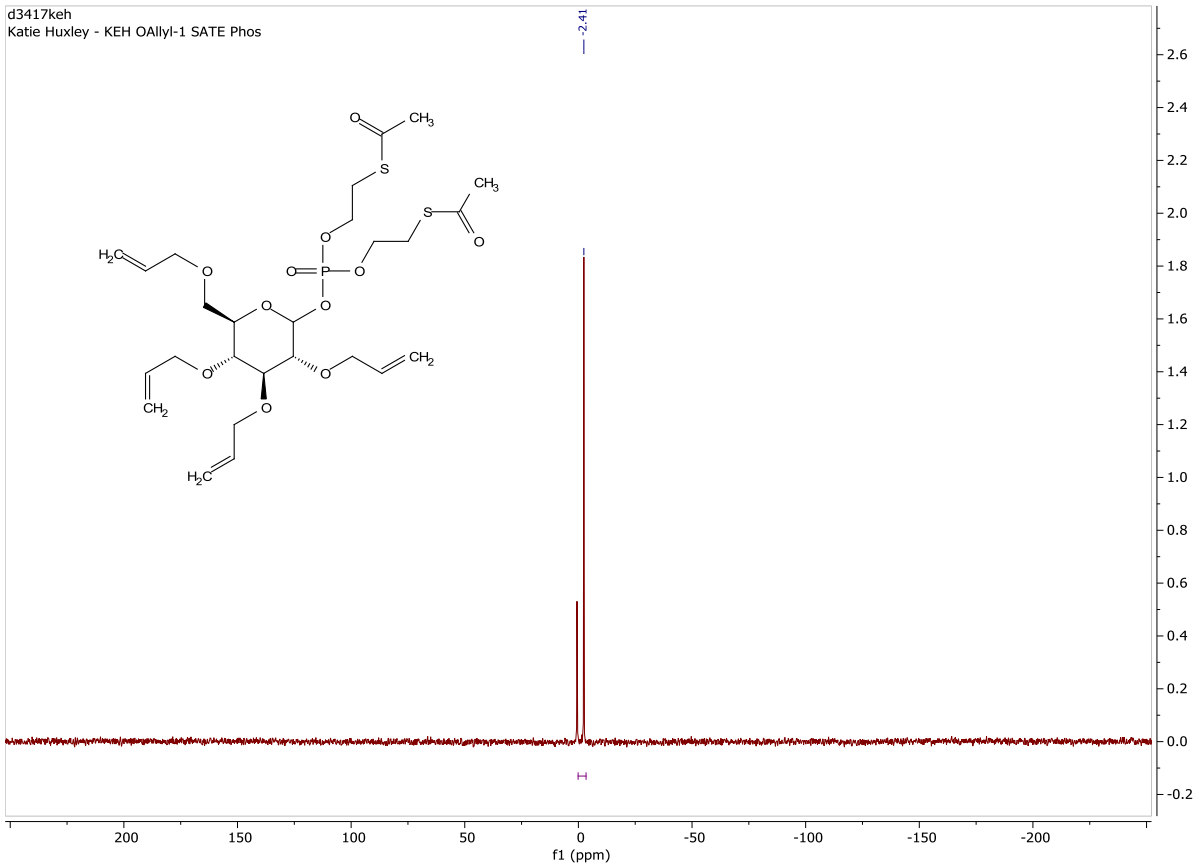
d2947keh
Katie Huxley - KEH OAc-1 SATE Phos



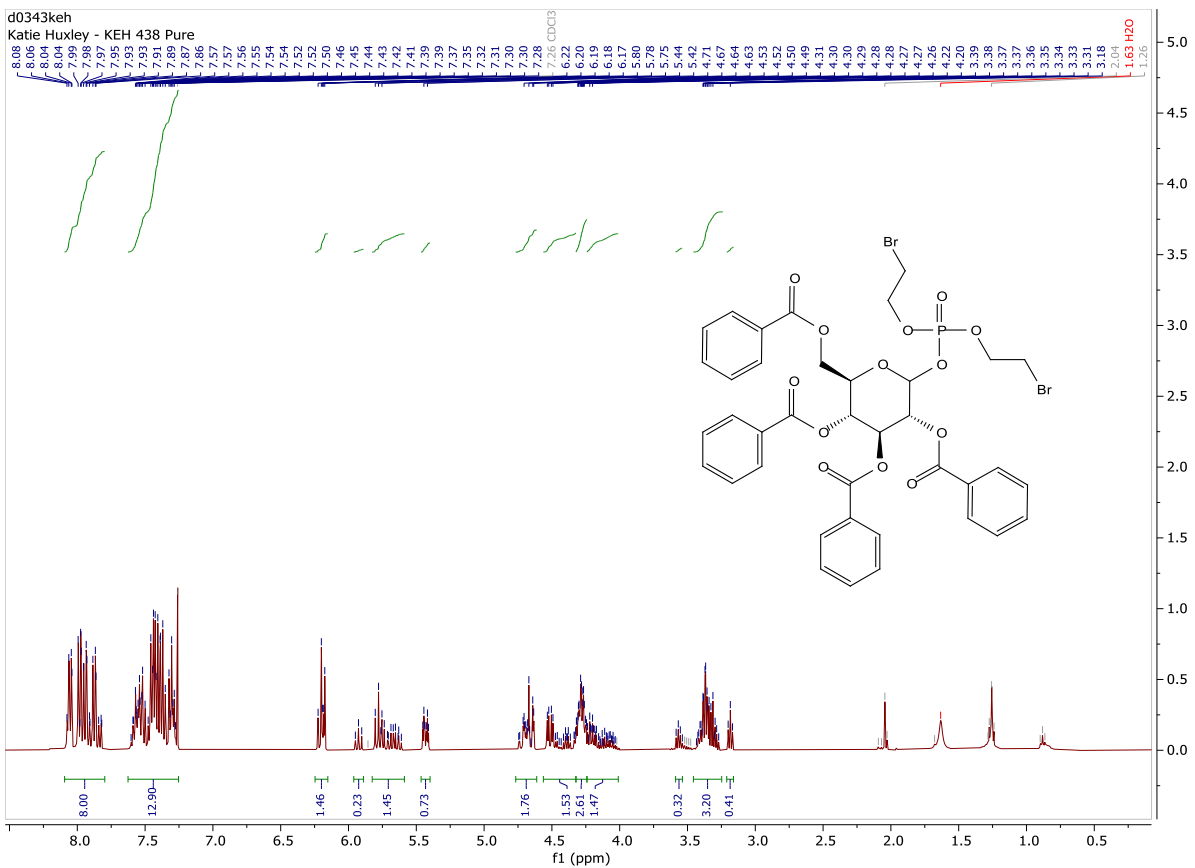
2,3,4,6-tetra-O-allyl-1-bis(2-bromoethyl)phosphate- α,β -D-glucose

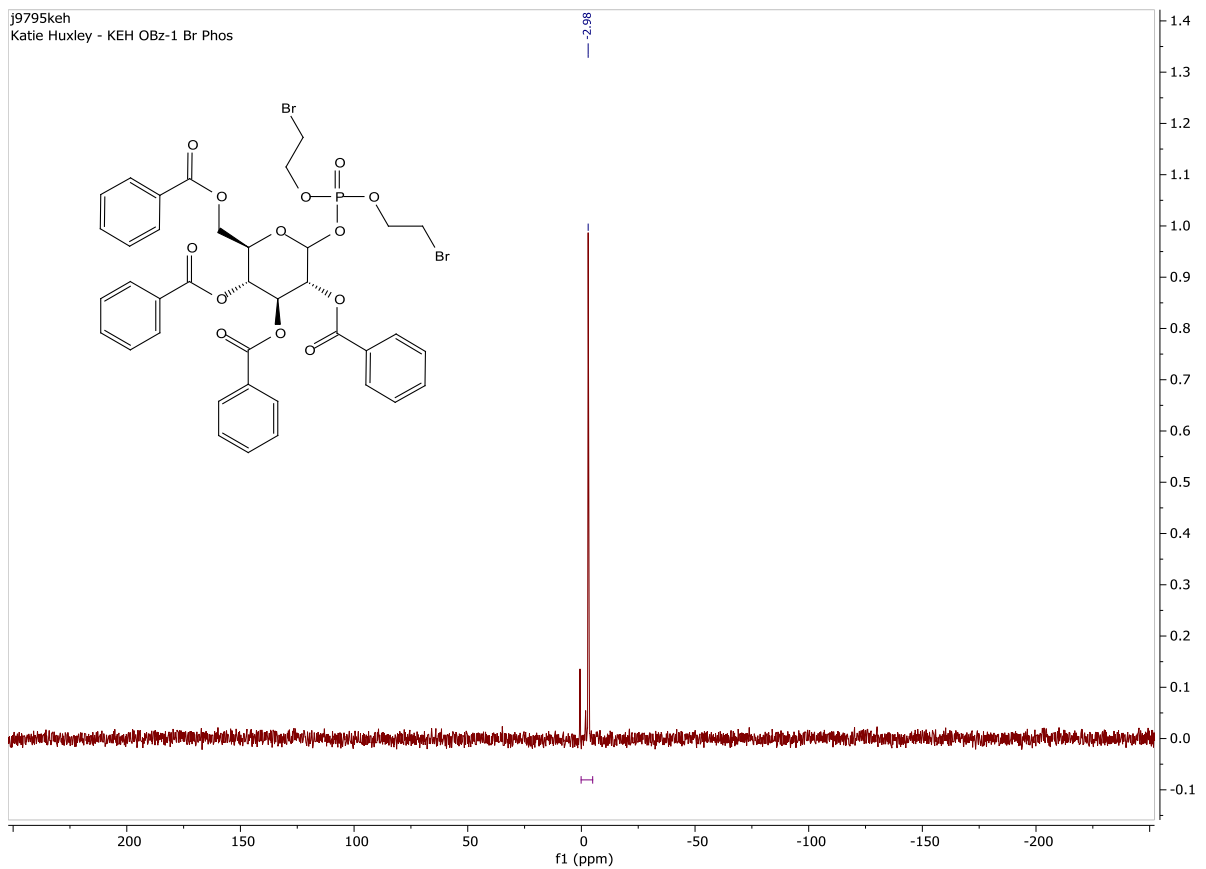
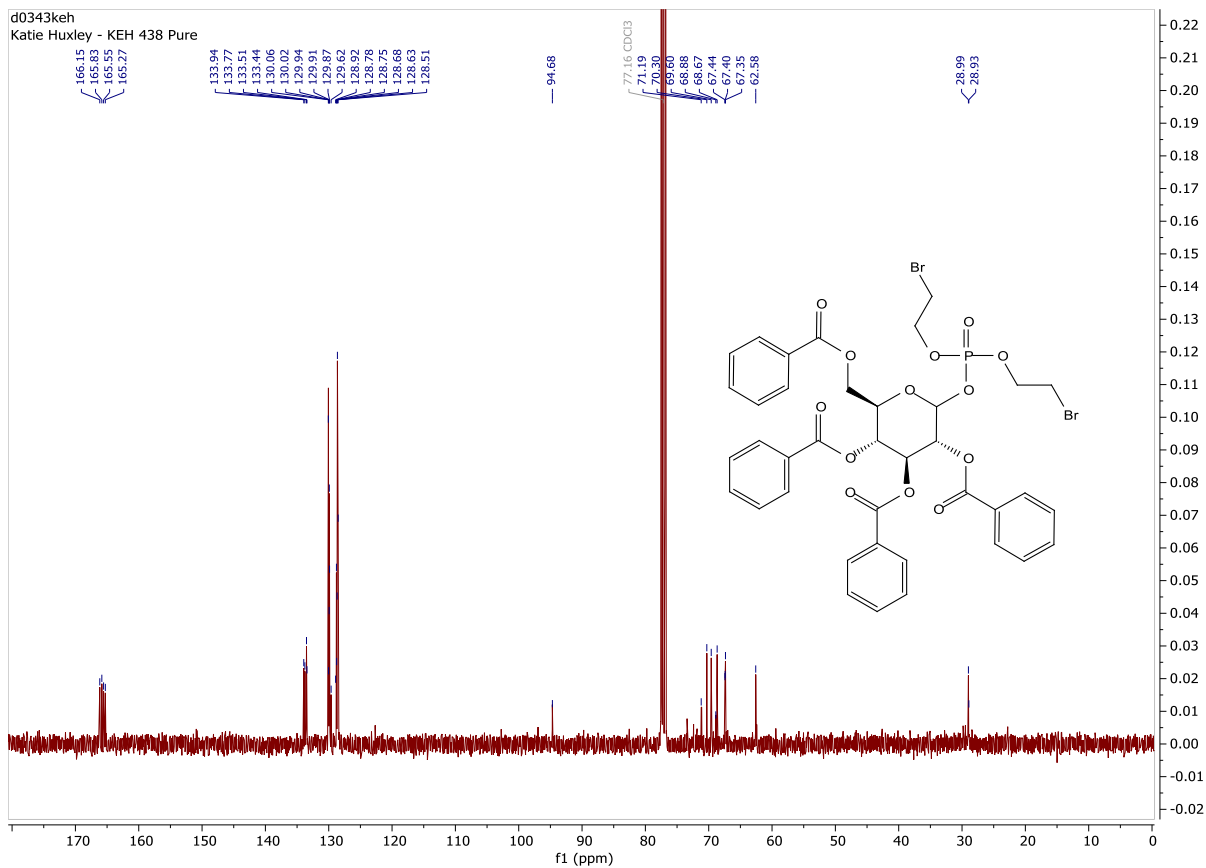




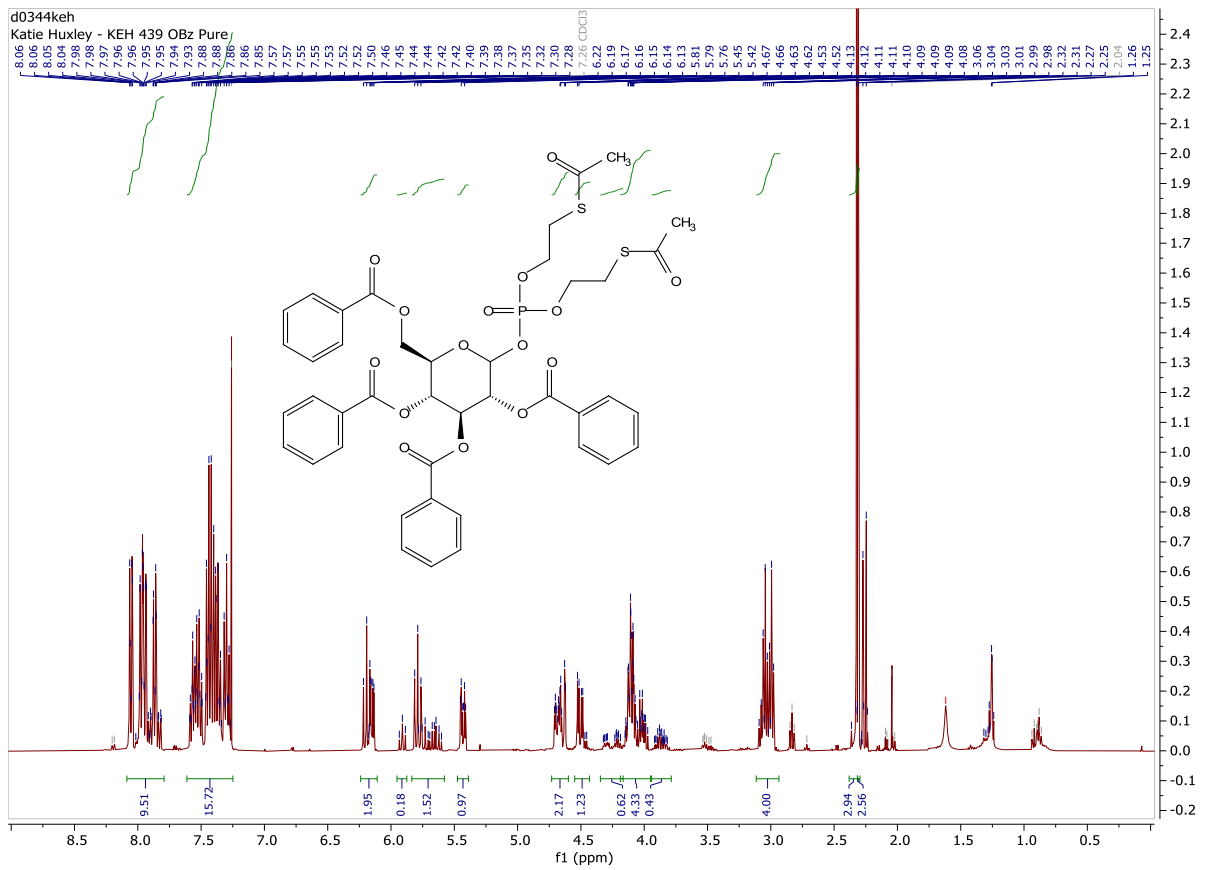


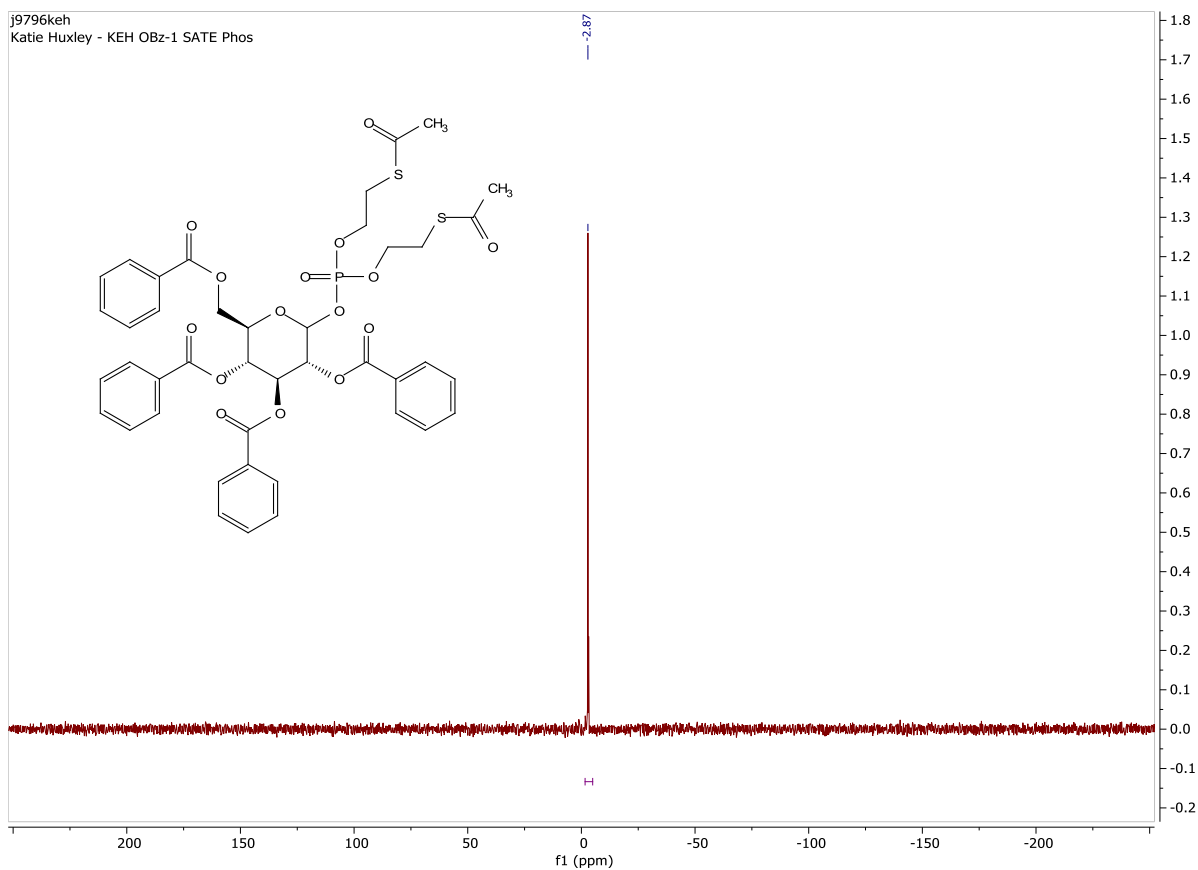
2,3,4,6-tetra-O-benzoyl-1-bis(2-bromoethyl)phosphate- α,β -D-glucose



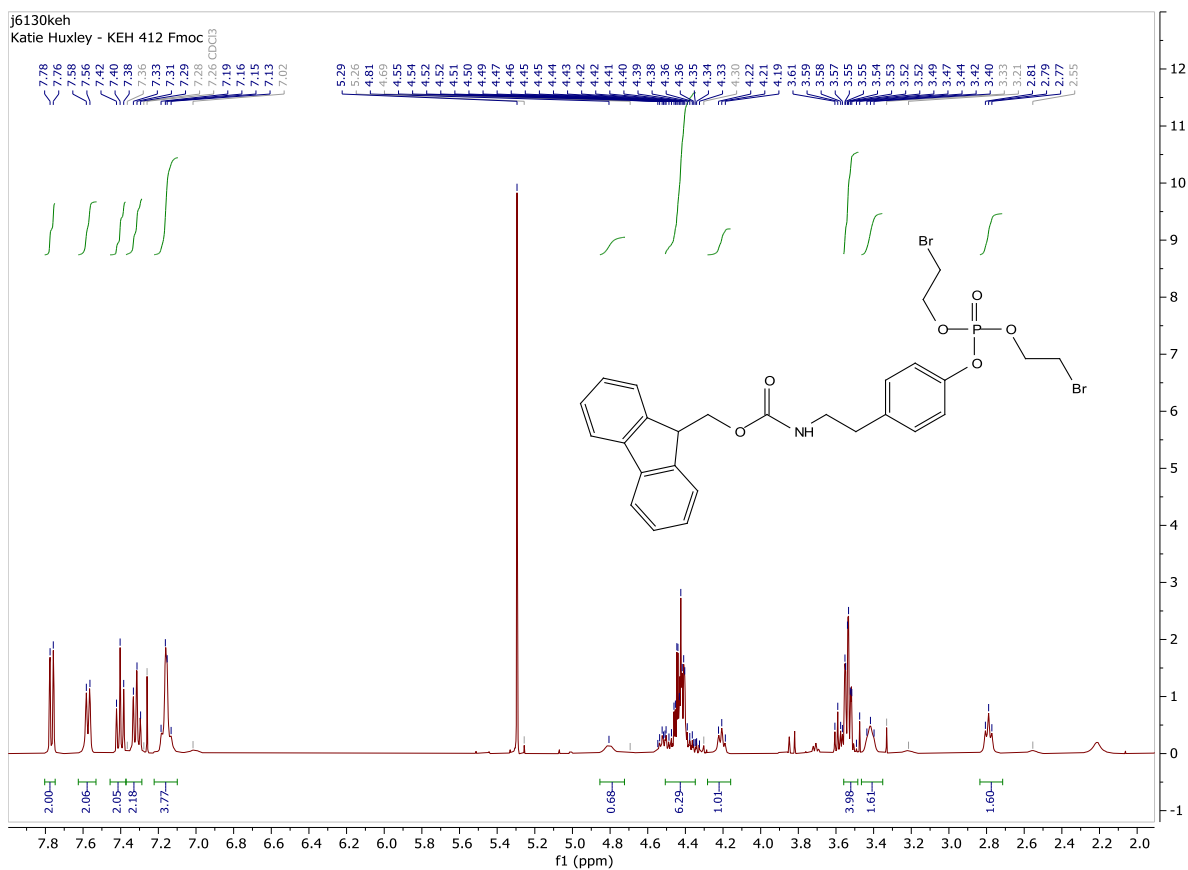


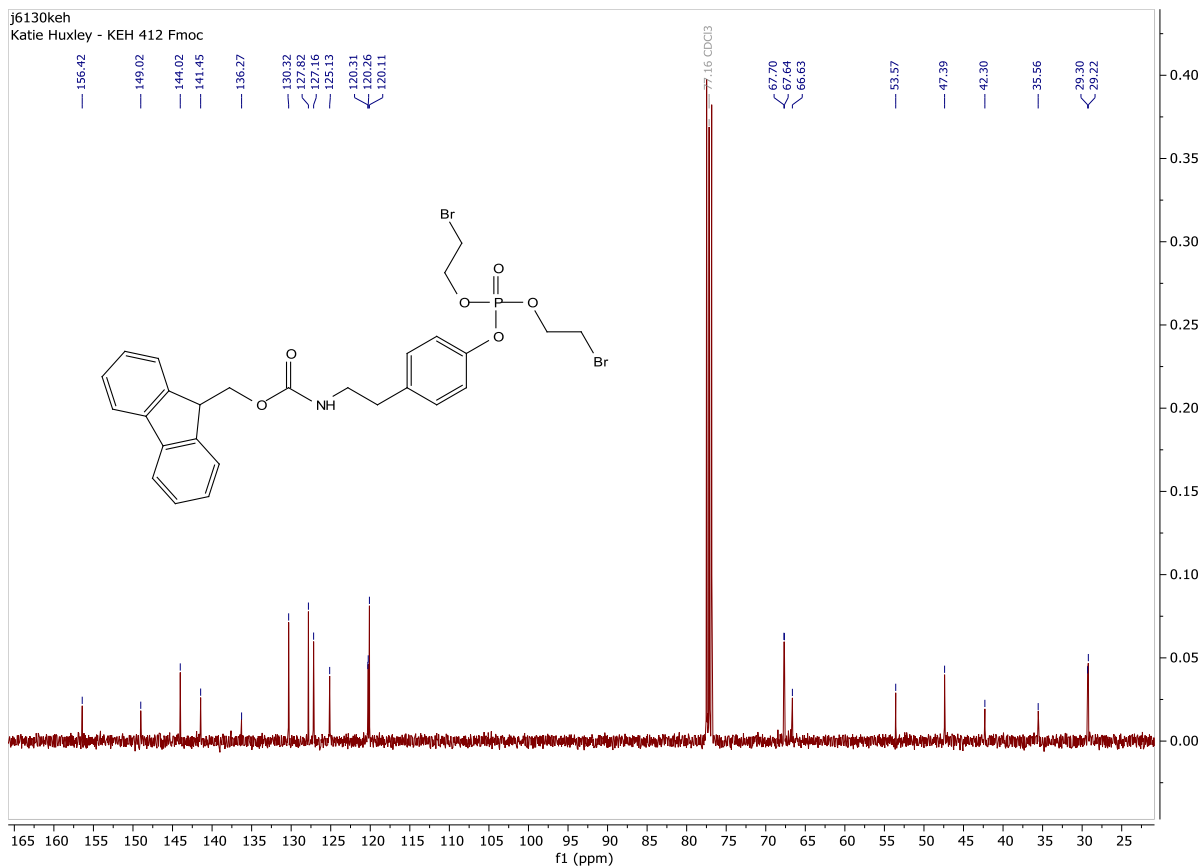
2,3,4,6-tetra-O-benzoyl-1-bis(SATE)phosphate- α,β -D-glucose



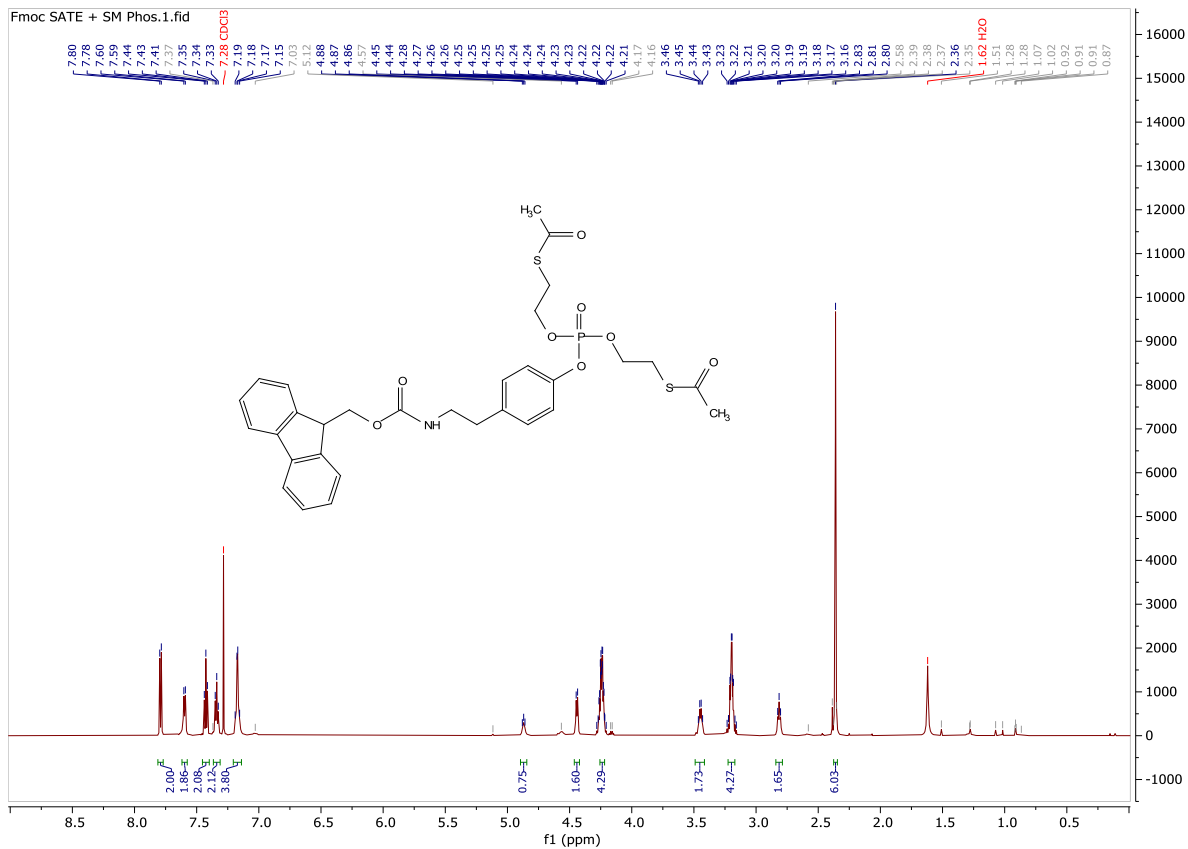


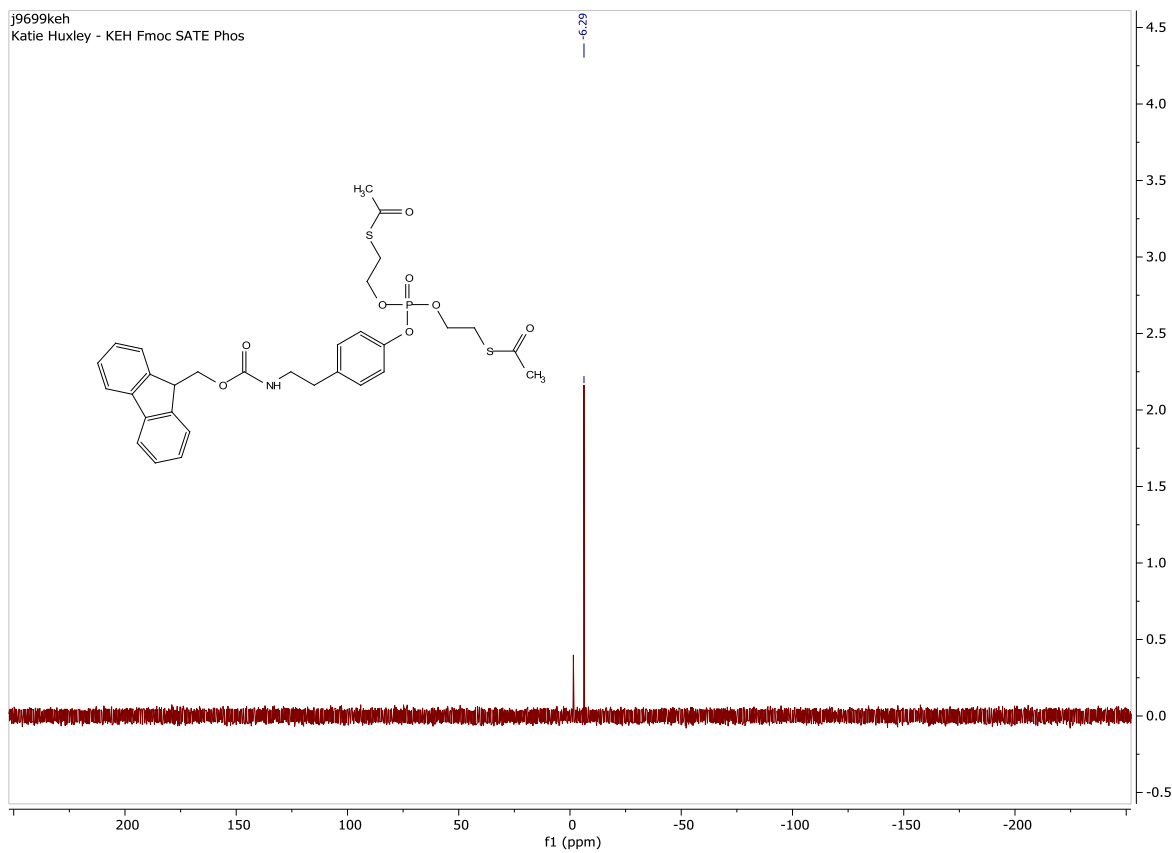
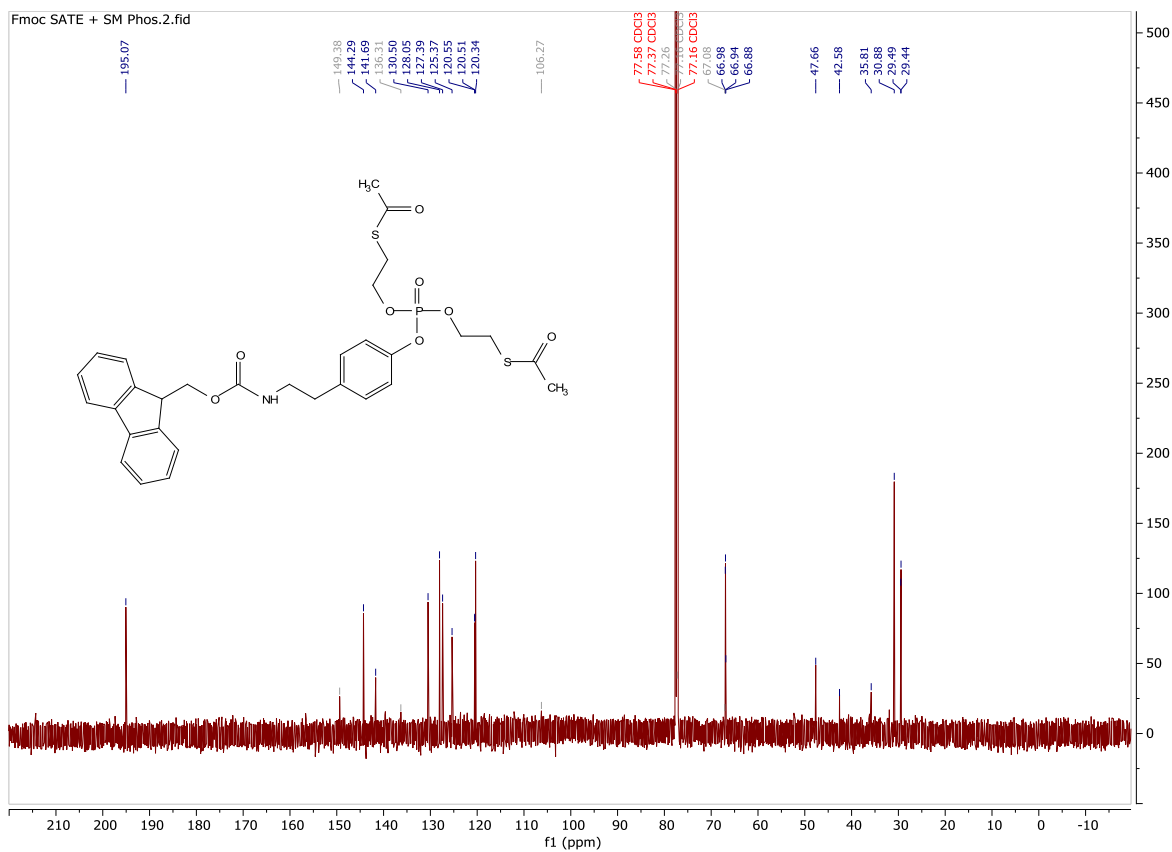
***N*-Fmoc-3-(bis(2-bromoethyl)phosphate)-tyramine**



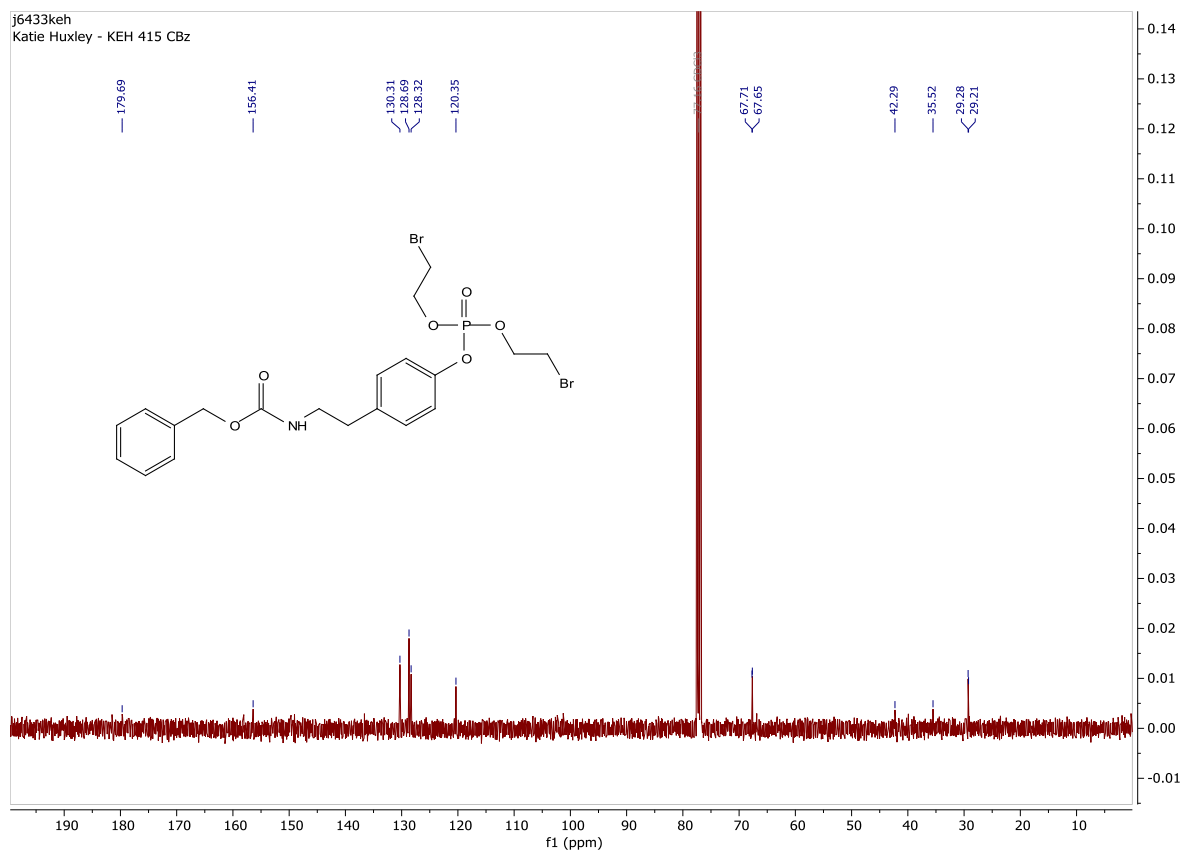
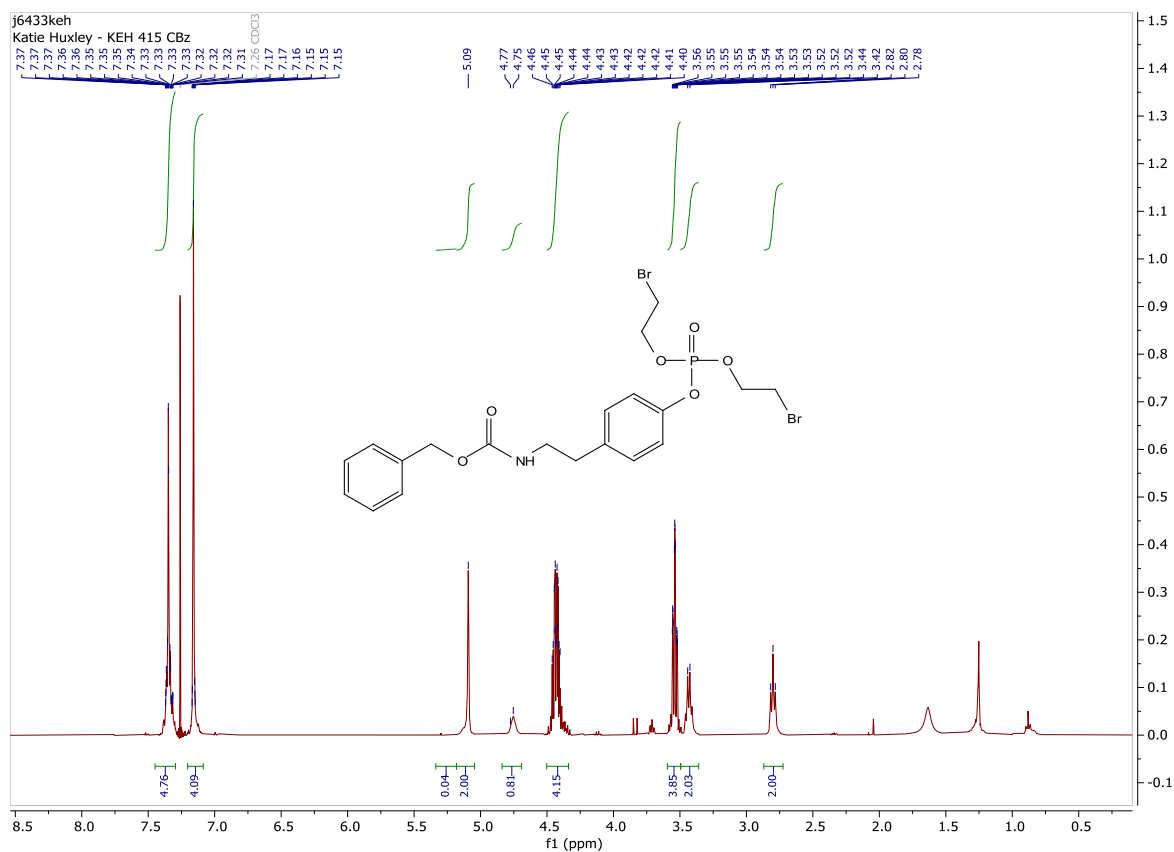


N-Fmoc-3-(bis(SATE)phosphate)-tyramine

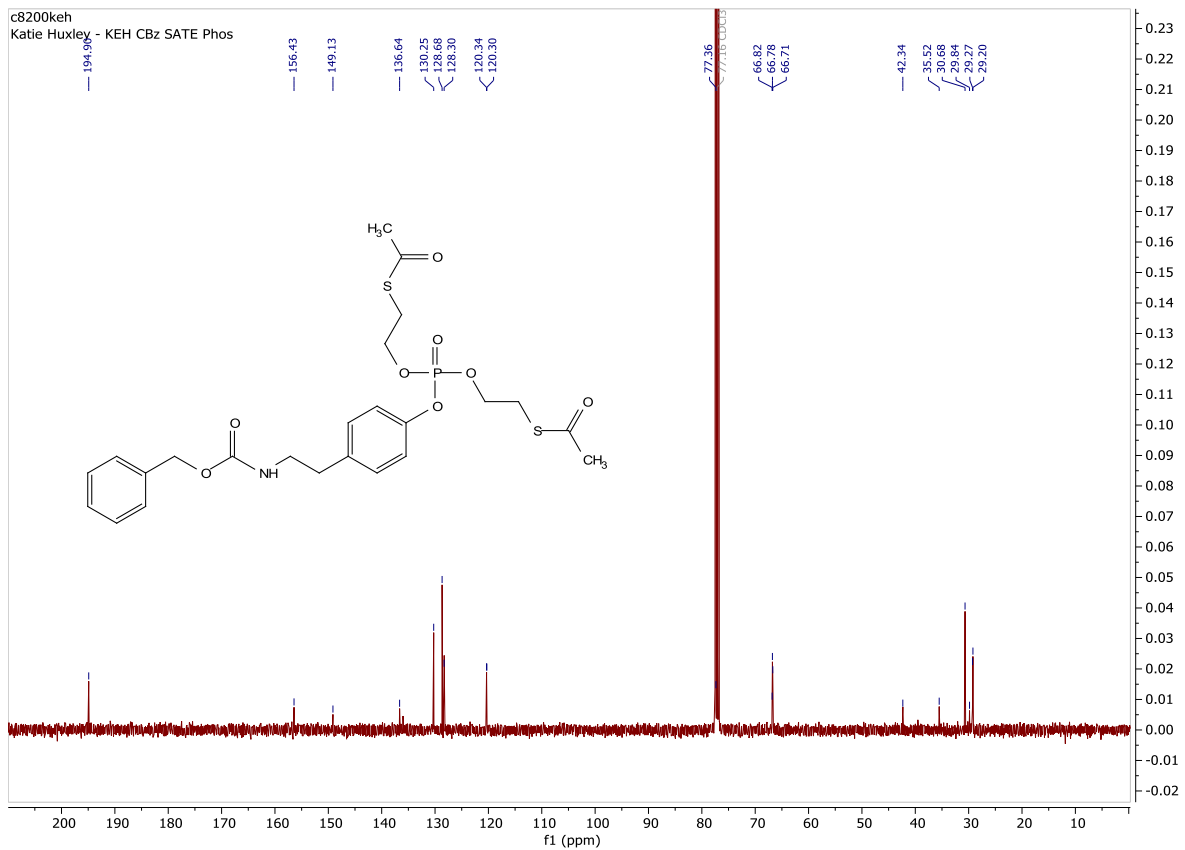
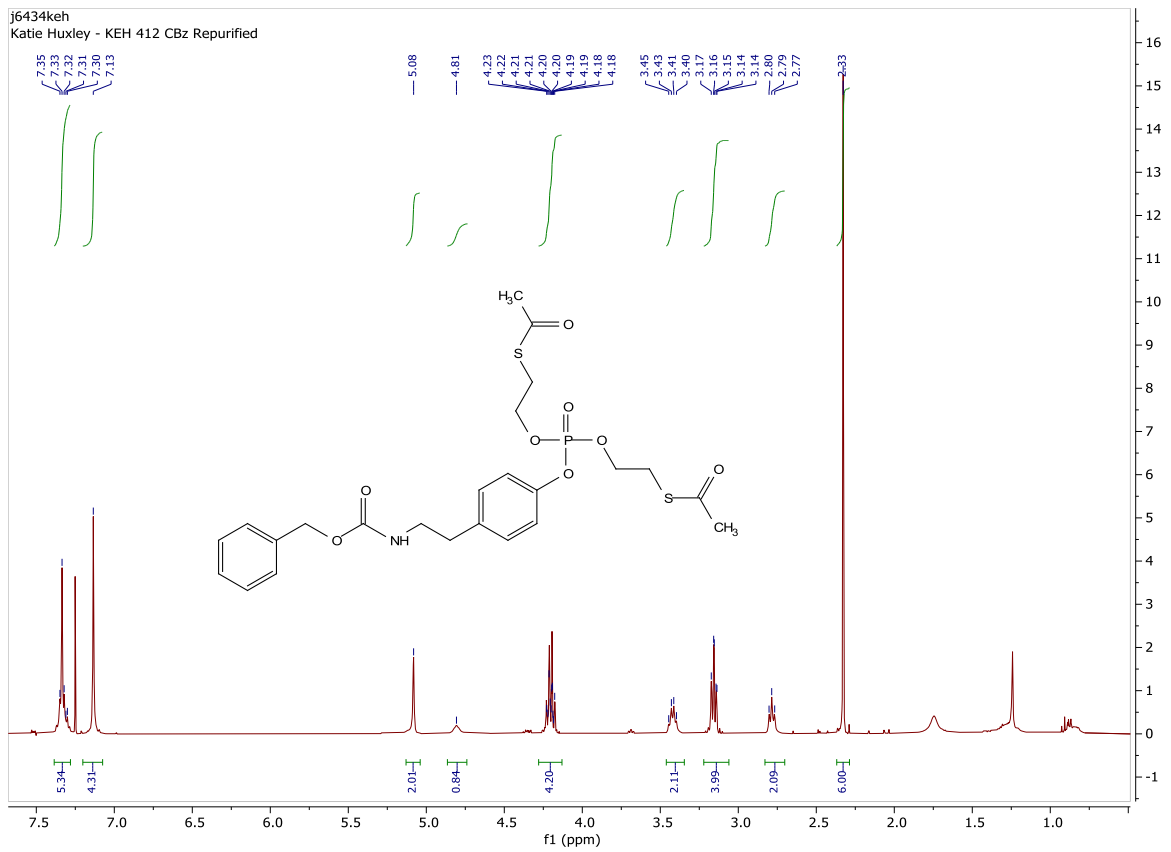


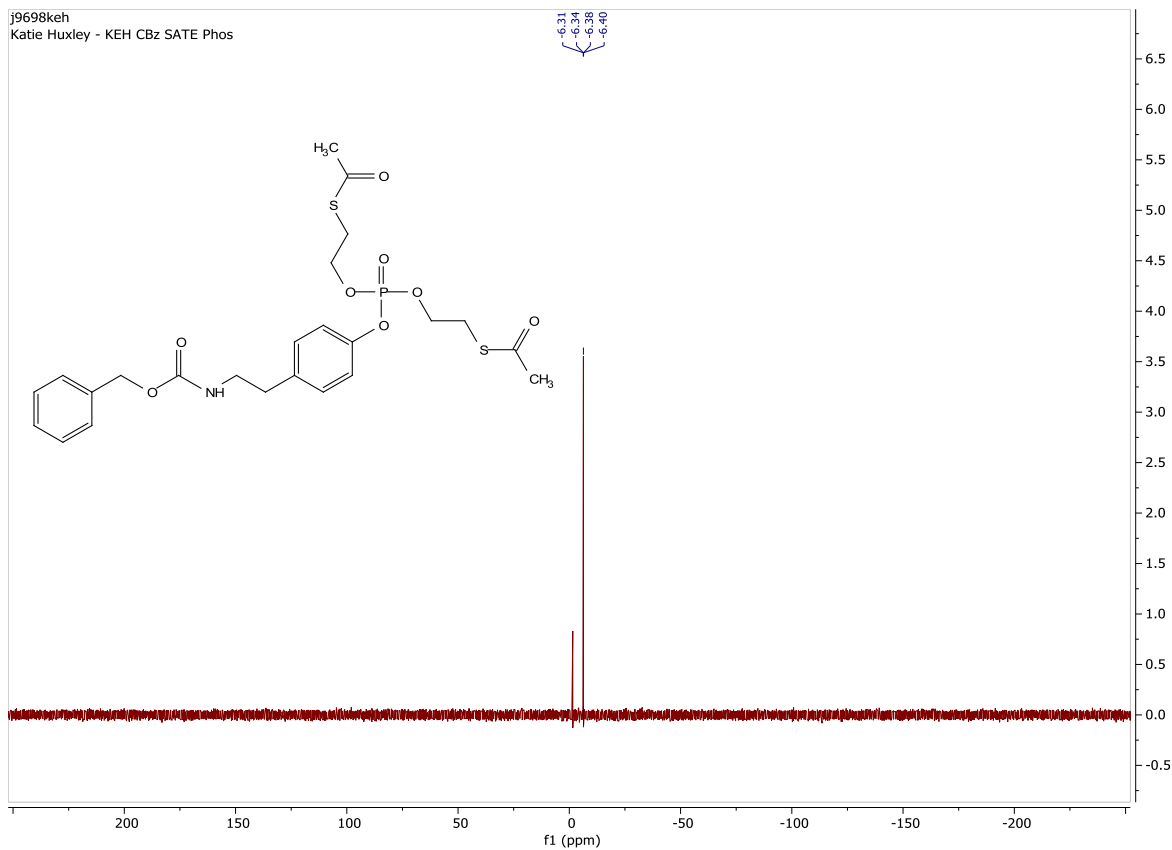


N-Cbz-3-(bis(2-bromoethyl)phosphate)-tyramine

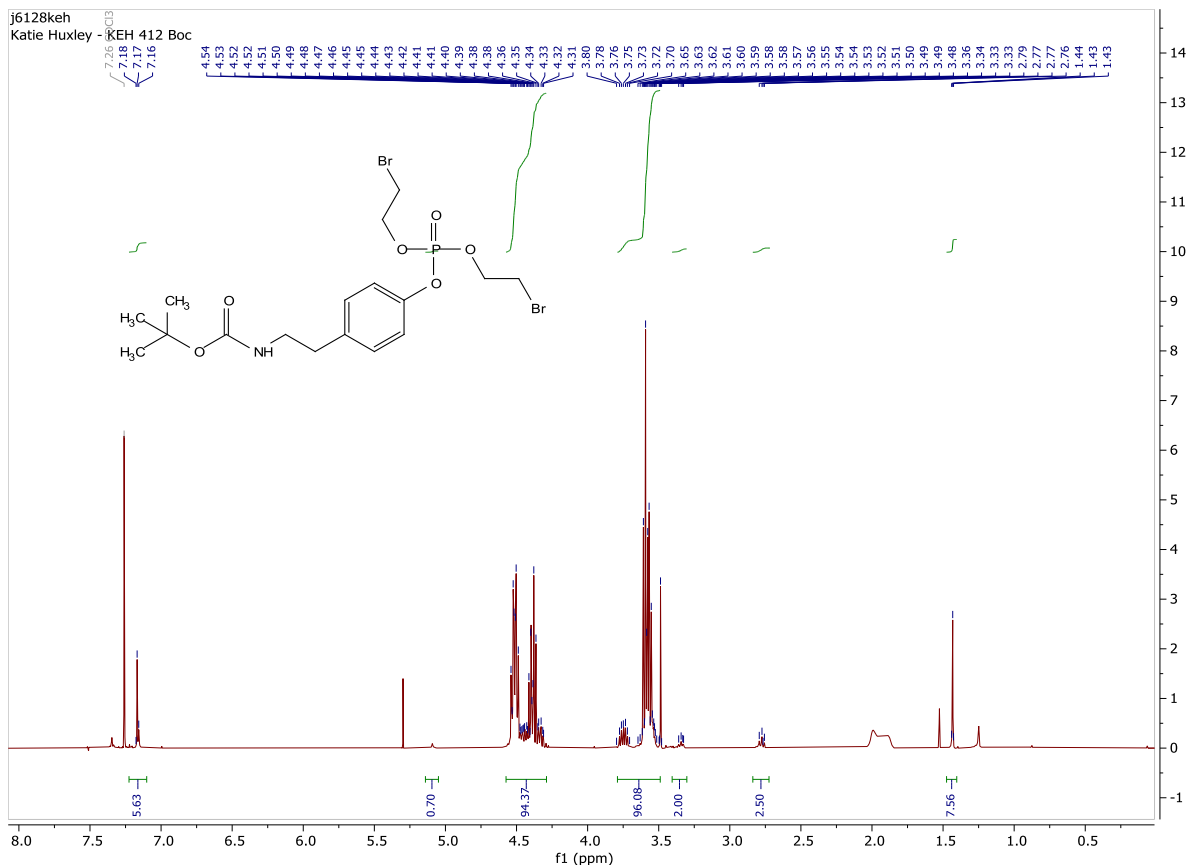


N-CBz-3-(bis(SATE)phosphate)-tyramine

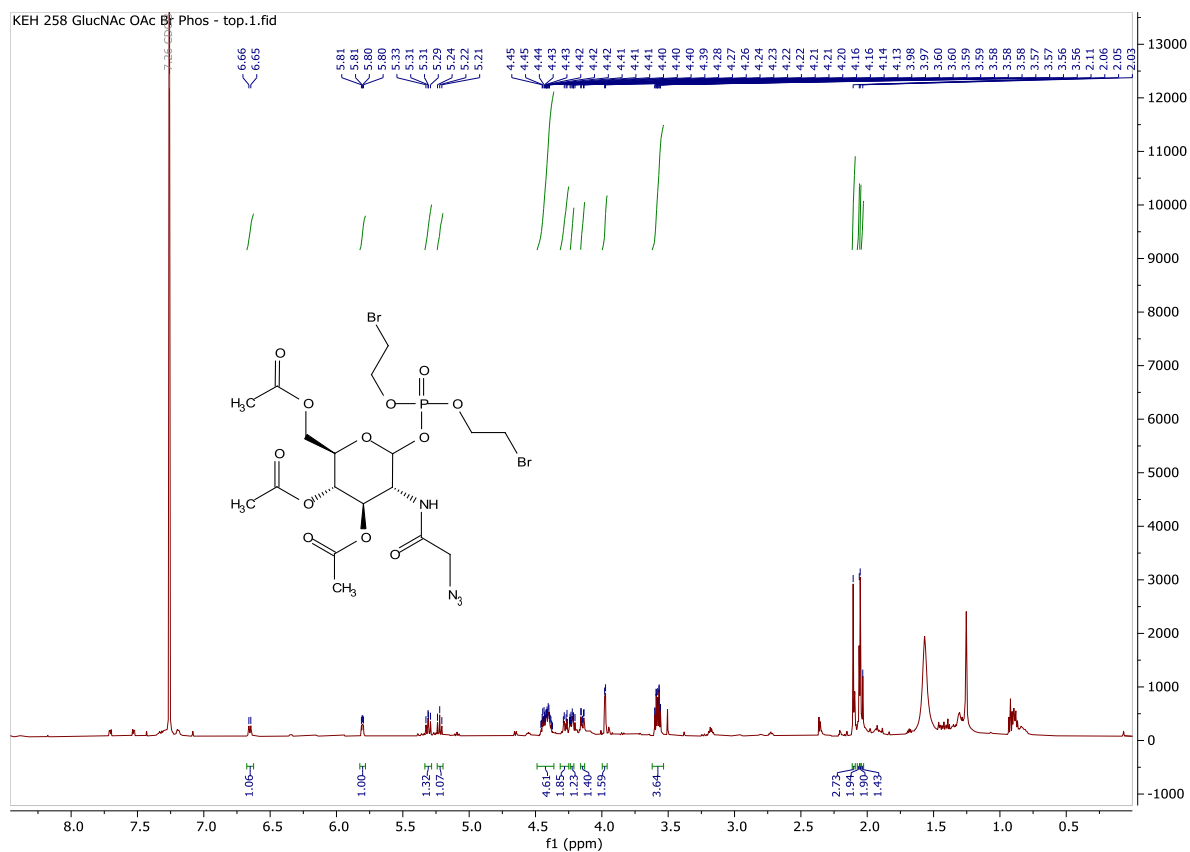




***N*-Boc-3-(bis(2-bromoethyl)phosphate)-tyramine**



3,4,6-tri-O-acetyl-2-N-azido-acetimido-1-bis(2-bromoethyl)phosphate- α -D-glucosamine



List of Abbreviations

2,2-DMP	2,2-dimethoxy propane
2-Br-OEt	2-bromo-ethanol
Ac ₂ O	acetic anhydride
AcOH	acetic acid
B4GAT1	beta-1,4-glucuronyltransferase 1
BCl ₃	boron trichloride
Bcs1	mitochondrial chaperone BCS1
BnBr	benzyl bromide
BnOH	benzyl alcohol
BODIPY	4,4-difluoro-4-bora-3a,4a-diaza-s-indacene
DFGL	direct fluorescent glycan labelling
CeGL	chemoenzymatic glycan labelling
CMDs	congenital muscular dystrophies
CMP	cytidine monophosphate
CSA	camphor sulphonic acid
CTP	cytidine-tri-phosphate
DAG1	dystroglycan 1
DCM	dichloromethane
DGC	dystrophin-glycoprotein complex
DiPEA	diisopropylethylamine
DMF	dimethylformaldehyde
ER	endoplasmic reticulum
EtOAc	ethyl acetate
EtOH	ethanol
FKRP	fukutin related protein
FKTN	fukutin
Fuc	fucose
Gal	galactose
GalNAc	<i>N</i> -acetylgalactosamine
GC-MS	gass chromatography-mass spectroscopy

GlcA	glucuronic acid
GlcNAc	glucosamine
GlcNAz	<i>N</i> -azidoacetylglucosamine
Gluc	glucose
GnT-IX	α -1,6-monnaosylglycoprotein 6- β - <i>N</i> -acetylglucosaminyltransferase B
H ₂ O	water
HCl	hydrochloric acid
HF	hydrofluoric acid
HNK1	human natural killer-1
IMAC	immobilised metal affinity chromatography
ISPD	2-C-methyl-D-erythritol-4-phosphate cytidyltransferase
KBr	potassium bromide
KSAc	potassium thioacetate
LacNAc	<i>N</i> -acetylglucosamine
LARGE	LARGE xylosyl-and glucuronyltransferase 1
Man	Mannose
ManNAc	<i>N</i> -acetylmannosamine
ManNAz	<i>N</i> -azidoacetylmannosamine
MEB	muscle eye brain disease
MeOH	methanol
MEP	non-mevalonate pathway
MgSO ₄	magnesium sulphate
MOE	metabolic oligosaccharide engineering
MP-Neu5Ac9N ₃	C9-azide tagged CMP-neuraminic acid
MS	mass Spectrometry
MsCl	mesyl chloride
N ₃	azide
NADH	nicotinamide adenine dinucleotide
NADPH	nicotinamide adenine dinucleotide phosphate hydrogen
NaH	sodium hydride

NaHCO ₃	sodium bicarbonate
NaN ₃	sodium azide
NaOMe	sodium methoxide
NEt ₃	triethylamine
NEt ₃ .HCl	triethylamine hydrochloride
Neu5Gc	<i>N</i> -glycolylneuraminic acid
NeuAc	<i>N</i> -acetylneuraminic acid
NH ₄ Cl	ammonium chloride
OAc	acetate protecting group
OAllyl	allyl protecting group
OBn	benzyl protecting group
OBz	benzoyl protecting group
OMe	methyl protecting group
OTr	trityl protecting group
PAL	periodate oxidation and aniline catalysed oxime ligation
PCl ₃	phosphorus trichloride
PdCl ₂	palladium dichloride
PO(OEt) ₃	triethyl phosphate
POCl ₃	phosphorus oxychloride
POMGnT1	protein <i>O</i> -mannose β-1,2- <i>N</i> -acetylglucosamineyltransferase
POMT1	protein <i>O</i> -mannosyltransferase 1
POMT2	protein <i>O</i> -mannosyltransferase 2
PPi	pyrophosphate
p-TsOH	p-toluene sulphonic acid
RboP	ribitol-5-phosphate
RT	room temperature
SATE	<i>S</i> -acetyl-2-thioethyl
Ser	serine
TAA	thioacetic acid
TarI	ribitol-5-phosphate cytidyltransferase
TarJ	ribulose-5-phosphate reductase
TBDPS	<i>tert</i> -butyldiphenyl silyl protecting group

Tf ₂ O	triflic anhydride
THF	tetrahydrofuran
Thr	threonine
TMEM5	ribitol xylosyltransferase 1
TsCl	tosyl chloride
UDP	uridine diphosphate.
Xyl	xylose
ZnCl	zinc chloride
α-DG	α-dystroglycan

References

1. M. Kanagawa and T. Toda, *J. Neuromuscul. Dis.*, 2017, **4**, 259-267.
2. L. Wells, *J. Biol. Chem.*, 2013, **288**, 6930-6935.
3. H. Manya and T. Endo, *Biochim. Biophys. Acta Gen. Subj.*, 2017, **1861**, 2462-2472.
4. A. Varki and P. Gagneux, *Glycobiology*, 2017, **27**, 77-88.
5. R. G. Spiro, *Glycobiology*, 2002, **12**, 43R-56R.
6. C. Reily, T. J. Stewart, M. B. Renfrow and J. Novak, *Nat. Rev. Nephrol.*, 2019, **15**, 346-366.
7. E. Bieberich, *Adv. Neurobiol.*, 2014, **9**, 47-70.
8. N. Lannoo and E. J. Van Damme, *Plant Sci.*, 2015, **239**, 67-83.
9. S. Esmail and M. F. Manolson, *Eur. J. Cell. Biol.*, 2021, **100**, 151186.
10. M. Riemersma, D. S. Froese, W. van Tol, U. F. Engelke, J. Kopec, M. van Scherpenzeel, A. Ashikov, T. Krojer, F. von Delft, M. Tessari, A. Buczkowska, E. Swiezewska, L. T. Jae, T. R. Brummelkamp, H. Manya, T. Endo, H. van Bokhoven, W. W. Yue and D. J. Lefeber, *Chem. Biol.*, 2015, **22**, 1643-1652.
11. R. Sentandreu and D. H. Northcote, *Biochem. J.*, 1968, **109**, 419-432.
12. M. Loibl and S. Strahl, *Biochim. Biophys. Acta*, 2013, **1833**, 2438-2446.
13. S. H. Stalnaker, R. Stuart and L. Wells, *Curr. Opin. Struct. Biol.*, 2011, **21**, 603-609.
14. J. L. Praissman and L. Wells, *Biochemistry*, 2014, **53**, 3066-3078.
15. T. Yoshida-Moriguchi and K. P. Campbell, *Glycobiology*, 2015, **25**, 702-713.
16. K.-I. Inamori, Y. Hara, T. Willer, M. E. Anderson, Z. Zhu, T. Yoshida-Moriguchi and K. P. Campbell, *Glycobiology*, 2013, **23**, 295-302.
17. H. Xiong, K. Kobayashi, M. Tachikawa, H. Manya, S. Takeda, T. Chiyonobu, N. Fujikake, F. Wang, A. Nishimoto, G. E. Morris, Y. Nagai, M. Kanagawa, T. Endo and T. Toda, *Biochem. Biophys. Res. Commun.*, 2006, **350**, 935-941.
18. M. Taniguchi-Ikeda, I. Morioka, K. Iijima and T. Toda, *Mol. Aspects Med.*, 2016, **51**, 115-124.
19. K. H. Holt, R. H. Crosbie, D. P. Venzke and K. P. Campbell, *FEBS Lett.*, 2000, **468**, 79-83.
20. C. M. Dobson, S. J. Hempel, S. H. Stalnaker, R. Stuart and L. Wells, *Cell. Mol. Life Sci.*, 2013, **70**, 2849-2857.
21. Y. Zhang, C. Meng, L. Jin, X. Chen, F. Wang and H. Cao, *Chem. Commun.*, 2015, **51**, 11654-11657.
22. S. H. Gee, F. Montanaro, M. H. Lindenbaum and S. Carbonetto, *Cell*, 1994, **77**, 675-686.
23. H. B. Peng, A. A. Ali, D. F. Daggett, H. Rauvala, J. R. Hassell and N. R. Smalheiser, *Cell Adhes. Commun.*, 1998, **5**, 475-489.
24. S. Sugita, F. Saito, J. Tang, J. Satz, K. Campbell and T. C. Südhof, *J. Cell Biol.*, 2001, **154**, 435-445.
25. S. Sato, Y. Omori, K. Katoh, M. Kondo, M. Kanagawa, K. Miyata, K. Funabiki, T. Koyasu, N. Kajimura, T. Miyoshi, H. Sawai, K. Kobayashi, A. Tani, T. Toda, J. Usukura, Y. Tano, T. Fujikado and T. Furukawa, *Nat. Neurosci.*, 2008, **11**, 923-931.
26. K. M. Wright, K. A. Lyon, H. Leung, D. J. Leahy, L. Ma and D. D. Ginty, *Neuron*, 2012, **76**, 931-944.
27. A. Chiba, K. Matsumura, H. Yamada, T. Inazu, T. Shimizu, S. Kusunoki, I. Kanazawa, A. Kobata and T. Endo, *J. Biol. Chem.*, 1997, **272**, 2156-2162.
28. M. Kanagawa and T. Toda, *J. Biochem.*, 2018, **163**, 359-369.
29. H. Manya, A. Chiba, A. Yoshida, X. Wang, Y. Chiba, Y. Jigami, R. U. Margolis and T. Endo, *Proc. Natl. Acad. Sci. U. S. A.*, 2004, **101**, 500-505.
30. K. Akasaka-Manya, H. Manya and T. Endo, *Biochem. Biophys. Res. Commun.*, 2004, **325**, 75-79.
31. A. Yoshida, K. Kobayashi, H. Manya, K. Taniguchi, H. Kano, M. Mizuno, T. Inazu, H. Mitsuhashi, S. Takahashi, M. Takeuchi, R. Herrmann, V. Straub, B. Talim, T. Voit, H. Topaloglu, T. Toda and T. Endo, *Dev. Cell*, 2001, **1**, 717-724.

32. K.-I. Inamori, T. Endo, Y. Ide, S. Fujii, J. Gu, K. Honke and N. Taniguchi, *J. Biol. Chem.*, 2003, **278**, 43102-43109.
33. M. Kaneko, G. Alvarez-Manilla, M. Kamar, I. Lee, J.-K. Lee, K. Troupe, W.-J. Zhang, M. Osawa and M. Pierce, *FEBS Lett.*, 2003, **554**, 515-519.
34. R. Barresi, D. E. Michele, M. Kanagawa, H. A. Harper, S. A. Dovico, J. S. Satz, S. A. Moore, W. Zhang, H. Schachter, J. P. Dumanski, R. D. Cohn, I. Nishino and K. P. Campbell, *Nat. Med.*, 2004, **10**, 696-703.
35. T. Endo, *J. Biochem.*, 2015, **157**, 1-12.
36. K.-I. Inamori, T. Yoshida-Moriguchi, Y. Hara, M. E. Anderson, L. Yu and K. P. Campbell, *Science*, 2012, **335**, 93-96.
37. M. O. Sheikh, D. Venzke, M. E. Anderson, T. Yoshida-Moriguchi, J. N. Glushka, A. V. Nairn, M. Galizzi, K. W. Moremen, K. P. Campbell and L. Wells, *Glycobiology*, 2020, **30**, 817-829.
38. M. M. Goddeeris, B. Wu, D. Venzke, T. Yoshida-Moriguchi, F. Saito, K. Matsumura, S. A. Moore and K. P. Campbell, *Nature*, 2013, **503**, 136-140.
39. J. L. Praissman, T. Willer, M. O. Sheikh, A. Toi, D. Chitayat, Y.-Y. Lin, H. Lee, S. H. Stalnaker, S. Wang, P. K. Prabhakar, S. F. Nelson, D. L. Stemple, S. A. Moore, K. W. Moremen, K. P. Campbell and L. Wells, *Elife*, 2016, **5**, 1-18.
40. S. Vuillaumier-Barrot, C. Bouchet-Séraphin, M. Chelbi, L. Devisme, S. Quentin, S. Gazal, A. Laquerrière, C. Fallet-Bianco, P. Loget, S. Odent, D. Carles, A. Bazin, J. Aziza, A. Clemenson, F. Guimiot, M. Bonnière, S. Monnot, C. Bole-Feysot, J.-P. Bernard, L. Loeuillet, M. Gonzales, K. Socha, B. Grandchamp, T. Attié-Bitach, F. Encha-Razavi and N. Seta, *Am. J. Hum. Genet.*, 2012, **91**, 1135-1143.
41. L. T. Jae, M. Raaben, M. Riemersma, E. van Beusekom, V. A. Blomen, A. Velds, R. M. Kerkhoven, J. E. Carette, H. Topaloglu, P. Meinecke, M. W. Wessels, D. J. Lefeber, S. P. Whelan, H. van Bokhoven and T. R. Brummelkamp, *Science*, 2013, **340**, 479-483.
42. T. Willer, K.-I. Inamori, D. Venzke, C. Harvey, G. Morgensen, Y. Hara, D. Beltrán Valero de Bernabé, L. Yu, K. M. Wright and K. P. Campbell, *Elife*, 2014, **3**, 1-24.
43. T. Yoshida-Moriguchi, L. Yu, S. H. Stalnaker, S. Davis, S. Kunz, M. Madson, M. B. A. Oldstone, H. Schachter, L. Wells and K. P. Campbell, *Science*, 2010, **327**, 88-92.
44. M. Kanagawa, K. Kobayashi, M. Tajiri, H. Manya, A. Kuga, Y. Yamaguchi, K. Akasaka-Manya, J.-I. Furukawa, M. Mizuno, H. Kawakami, Y. Shinohara, Y. Wada, T. Endo and T. Toda, *Cell Rep.*, 2016, **14**, 2209-2223.
45. I. Gerin, B. Ury, I. Breloy, C. Bouchet-Seraphin, J. Bolsée, M. Halbout, J. Graff, D. Vertommen, G. G. Muccioli, N. Seta, J.-M. Cuisset, I. Dabaj, S. Quijano-Roy, A. Grahn, E. Van Schaftingen and G. T. Bommer, *Nat. Commun.*, 2016, **7**, 11534.
46. H. Manya, Y. Yamaguchi, M. Kanagawa, K. Kobayashi, M. Tajiri, K. Akasaka-Manya, H. Kawakami, M. Mizuno, Y. Wada, T. Toda and T. Endo, *J. Biol. Chem.*, 2016, **291**, 24618-24627.
47. N. Kuwabara, H. Manya, T. Yamada, H. Tateno, M. Kanagawa, K. Kobayashi, K. Akasaka-Manya, Y. Hirose, M. Mizuno, M. Ikeguchi, T. Toda, J. Hirabayashi, T. Senda, T. Endo and R. Kato, *Proc. Natl. Acad. Sci. U. S. A.*, 2016, **113**, 9280-9285.
48. S. B. Richard, M. E. Bowman, W. Kwiatkowski, I. Kang, C. Chow, A. M. Lillo, D. E. Cane and J. P. Noel, *Nat. Struct. Biol.*, 2001, **8**, 641-648.
49. W. N. Hunter, *J. Biol. Chem.*, 2007, **282**, 21573-21577.
50. T. Willer, H. Lee, M. Lommel, T. Yoshida-Moriguchi, D. B. V. de Bernabe, D. Venzke, S. Cirak, H. Schachter, J. Vajsar, T. Voit, F. Muntoni, A. S. Loder, W. B. Dobyns, T. L. Winder, S. Strahl, K. D. Mathews, S. F. Nelson, S. A. Moore and K. P. Campbell, *Nat. Genet.*, 2012, **44**, 575-580.
51. T. Roscioli, E.-J. Kamsteeg, K. Buysse, I. Maystadt, J. van Reeuwijk, C. van den Elzen, E. van Beusekom, M. Riemersma, R. Pfundt, L. E. L. M. Vissers, M. Schraders, U. Altunoglu, M. F. Buckley, H. G. Brunner, B. Grisart, H. Zhou, J. A. Veltman, C. Gilissen, G. M. S. Mancini, P. Delrée, M. A. Willemsen, D. P. Ramadža, D. Chitayat, C. Bennett, E. Sheridan, E. A. J. Peeters, G. M. B. Tan-Sindhunata, C. E. de Die-Smulders, K. Devriendt, H. Kayserili, O. A. E.-F. El-

- Hashash, D. L. Stemple, D. J. Lefeber, Y.-Y. Lin and H. van Bokhoven, *Nat. Genet.*, 2012, **44**, 581-585.
52. H. Tokuoka, R. Imae, H. Nakashima, H. Many, C. Masuda, S. Hoshino, K. Kobayashi, D. J. Lefeber, R. Matsumoto, T. Okada, T. Endo, M. Kanagawa and T. Toda, *Nat. Commun.*, 2022, **13**, 1847.
 53. M. P. Pereira and E. D. Brown, *Biochemistry*, 2004, **43**, 11802-11812.
 54. M. Zolli, D. J. Kobric and E. D. Brown, *Biochemistry*, 2001, **40**, 5041-5048.
 55. A. Follens, M. Veiga-da-Cunha, R. Merckx, E. van Schaftingen and J. van Eldere, *J. Bacteriol.*, 1999, **181**, 2001-2007.
 56. S. Baur, J. Maries-Wright, S. Buckenmaier, R. J. Lewis and W. Vollmer, *J. Bacteriol.*, 2009, **191**, 1200-1210.
 57. C. Singh, E. Glaab and C. L. Linster, *J. Biol. Chem.*, 2017, **292**, 1005-1028.
 58. K. Kobayashi, Y. Nakahori, M. Miyake, K. Matsumura, E. Kondo-Iida, Y. Nomura, M. Segawa, M. Yoshioka, K. Saito, M. Osawa, K. Hamano, Y. Sakakihara, I. Nonaka, Y. Nakagome, I. Kanazawa, Y. Nakamura, K. Tokunaga and T. Toda, *Nature*, 1998, **394**, 388-392.
 59. M. Brockington, D. J. Blake, P. Prandini, S. C. Brown, S. Torelli, M. A. Benson, C. P. Ponting, B. Estournet, N. B. Romero, E. Mercuri, T. Voit, C. A. Sewry, P. Guicheney and F. Muntoni, *Am. J. Hum. Genet.*, 2001, **69**, 1198-1209.
 60. L. Aravind and E. V. Koonin, *Curr. Biol.*, 1999, **9**, R836-837.
 61. K. Kuchta, L. Knizewski, L. S. Wyrwicz, L. Rychlewski and K. Ginalski, *Nucleic Acids Res.*, 2009, **37**, 7701-7714.
 62. T. A. Lynch, L. T. Lam, N. T. Man, K. Kobayashi, T. Toda and G. E. Morris, *Biochem. Biophys. Res. Commun.*, 2012, **424**, 354-357.
 63. T. Yamamoto, M. Kawaguchi, N. Sakayori, F. Muramatsu, S. Morikawa, Y. Kato, N. Shibata and M. Kobayashi, *Neurosci. Res.*, 2006, **56**, 391-399.
 64. J. N. Weiser, M. Shchepetov and S. T. Chong, *Infect. Immun.*, 1997, **65**, 943-950.
 65. J. R. Zhang, I. Idanpaan-Heikkila, W. Fischer and E. I. Tuomanen, *Mol. Microbiol.*, 1999, **31**, 1477-1488.
 66. J. I. Tamura, T. Tamura, S. Hoshino, R. Imae, R. Kato, M. Yokono, M. Nagase, S. Ohno, N. Manabe, Y. Yamaguchi, H. Many and T. Endo, *ACS Chem. Biol.*, 2022, **17**, 1513-1523.
 67. N. Kuwabara, R. Imae, H. Many, T. Tanaka, M. Mizuno, H. Tsumoto, M. Kanagawa, K. Kobayashi, T. Toda, T. Senda, T. Endo and R. Kato, *Nat. Commun.*, 2020, **11**, 303.
 68. M. Alhamidi, E. Kjeldsen Buvang, T. Fagerheim, V. Brox, S. Lindal, M. Van Ghelue and Ø. Nilssen, *PLoS One*, 2011, **6**, e22968.
 69. K. Johnson, M. Bertoli, L. Phillips, A. Topf, P. Van den Bergh, J. Vissing, N. Witting, S. Nafissi, S. Jamal-Omidi, A. Lusakowska, A. Kostera-Pruszczyk, A. Potulska-Chromik, N. Deconinck, C. Wallgren-Pettersson, S. Strang-Karlsson, J. Colomer, K. G. Claeys, W. De Ridder, J. Baets, M. von der Hagen, R. Fernandez-Torron, M. Zulaica Ijurco, J. B. Espinal Valencia, A. Hahn, H. Durmus, T. Willis, L. Xu, E. Valkanas, T. E. Mullen, M. Lek, D. G. MacArthur and V. Straub, *Skelet. Muscle*, 2018, **8**, 23.
 70. K. M. Fumiaki Saito, *Skelet. Muscle*, 2011, **1**, 22.
 71. S. H. Stalnaker, K. Aoki, J.-M. Lim, M. Porterfield, M. Liu, J. S. Satz, S. Buskirk, Y. Xiong, P. Zhang, K. P. Campbell, H. Hu, D. Live, M. Tiemeyer and L. Wells, *J. Biol. Chem.*, 2011, **286**, 21180-21190.
 72. H. Topaloğlu and B. Talim, *Handb. Clin. Neurol.*, 2008, **87**, 219-234.
 73. J. Sasaki, K. Ishikawa, K. Kobayashi, E. Kondo-Iida, M. Fukayama, H. Mizusawa, S. Takashima, Y. Sakakihara, Y. Nakamura and T. Toda, *Hum. Mol. Genet.*, 2000, **9**, 3083-3090.
 74. Muscular Dystrophies U. K. Charity The limb girdle muscular dystrophies (LGMDs) Factsheet, <https://www.muscular dystrophyuk.org/wp-content/uploads/2015/09/LGMD-general.pdf> (accessed 13/04/2022).

75. Genetics Home Walker-Warburg syndrome, <https://ghr.nlm.nih.gov/condition/walker-warburg-syndrome>, (accessed 25/07/2019).
76. National Institute of Health - MedlinePlus, Walker-Warburg syndrome, <https://medlineplus.gov/genetics/condition/walker-warburg-syndrome/#causes>, (accessed 10/9/2022).
77. A. Varki, *Glycobiology*, 2017, **27**, 3-49.
78. K. T. Schjoldager, Y. Narimatsu, H. J. Joshi and H. Clausen, *Nat. Rev. Mol. Cell Biol.*, 2020, **21**, 729-749.
79. B. Lin, X. Qing, J. Liao and K. Zhuo, *Cells*, 2020, **9**, 1022.
80. H. Haukedal and K. K. Freude, *Front. Neurosci*, 2021, **14**, 1432.
81. S. Mereiter, M. Balmaña, D. Campos, J. Gomes and C. A. Reis, *Cancer Cell*, 2019, **36**, 6-16.
82. H. C. Hang and C. R. Bertozzi, *Bioorg. Med. Chem.*, 2005, **13**, 5021-5034.
83. X. Yang and K. Qian, *Nat. Rev. Mol. Cell Biol.*, 2017, **18**, 452-465.
84. M. L. W. J. Smeenk, L. W. Mike, J. Agramunt and K. M. Bongers, *Curr. Opin. Chem. Bio.*, 2021, **60**, 79-88.
85. D. M. Patterson, L. A. Nazarova and J. A. Prescher, *ACS Chem. Biol.*, 2014, **9**, 592-605.
86. Q. Wang, T. R. Chan, R. Hilgraf, V. V. Fokin, K. B. Sharpless and M. G. Finn, *J. Am. Chem. Soc.*, 2003, **125**, 3192-3193.
87. A. E. Speers, G. C. Adam and B. F. Cravatt, *J. Am. Chem. Soc.*, 2003, **125**, 4686-4687.
88. C. G. Gahmberg and L. C. Andersson, *J. Biol. Chem.*, 1977, **252**, 5888-5894.
89. C. G. Gahmberg and S. Hakomori, *J. Biol. Chem.*, 1973, **248**, 4311-4317.
90. M. Critcher, T. O'Leary and M. L. Huang, *Biochem. J*, 2021, **478**, 703-719.
91. N. Nischan and J. J. Kohler, *Glycobiology*, 2016, **26**, 1-8.
92. P.-A. Gilormini, A. R. Batt, M. R. Pratt and C. Biot, *Chem. Sci.*, 2018, **9**, 7585-7595.
93. T. J. Sminia, H. Zuilhof and T. Wennekes, *Carbohydr. Res.*, 2016, **435**, 121-141.
94. A. Lopez Aguilar, J. G. Briard, L. Yang, B. Ovaryn, M. S. Macauley and P. Wu, *ACS Chem. Biol.*, 2017, **12**, 611-621.
95. N. J. Pedowitz and M. R. Pratt, *RSC Chem. Bio.*, 2021, **2**, 306-321.
96. N. K. Devaraj, *ACS Cent. Sci.*, 2018, **4**, 952-959.
97. Y. Zeng, T. N. C. Ramya, A. Dirksen, P. E. Dawson and J. C. Paulson, *Nat. Methods*, 2009, **6**, 207-209.
98. J. Nilsson, U. Rüetschi, A. Halim, C. Hesse, E. Carlsohn, G. Brinkmalm and G. Larson, *Nat. Methods*, 2009, **6**, 809-811.
99. E. Klement, Z. Lipinski, Z. Kupihár, A. Udvardy and K. F. Medzihradzsky, *J. Proteome Res.*, 2010, **9**, 2200-2206.
100. T. N. C. Ramya, E. Weerapana, B. F. Cravatt and J. C. Paulson, *Glycobiology*, 2013, **23**, 211-221.
101. A. P. Matthey, W. R. Birmingham, P. Both, N. Kress, K. Huang, J. M. Van Munster, G. S. Bulmer, F. Parmeggiani, J. Voglmeir, J. E. R. Martinez, N. J. Turner and S. L. Flitsch, *ACS Catal.*, 2019, **9**, 8208-8212.
102. J. Huang, H. Qin, Z. Sun, G. Huang, J. Mao, K. Cheng, Z. Zhang, H. Wan, Y. Yao, J. Dong, J. Zhu, F. Wang, M. Ye and H. Zou, *Sci. Rep.*, 2015, **5**, 10164.
103. F. Sun, S. Suttapitugsakul and R. Wu, *Anal. Chem.*, 2019, **91**, 4195-4203.
104. J. E. McCombs and J. J. Kohler, *Bioconjug. Chem.*, 2016, **27**, 1013-1022.
105. H. Kayser, R. Zeitler, C. Kannicht, D. Grunow, R. Nuck and W. Reutter, *J. Biol. Chem.*, 1992, **267**, 16934-16938.
106. L. K. Mahal, K. J. Yarema and C. R. Bertozzi, *Science*, 1997, **276**, 1125-1128.
107. E. Saxon and C. R. Bertozzi, *Science*, 2000, **287**, 2007-2010.
108. M. Sawa, T. L. Hsu, T. Itoh, M. Sugiyama, S. R. Hanson, P. K. Vogt and C. H. Wong, *Proc. Natl. Acad. Sci. U. S. A.*, 2006, **103**, 12371-12376.
109. S. T. Laughlin, J. M. Baskin, S. L. Amacher and C. R. Bertozzi, *Science*, 2008, **320**, 664-667.

110. D. J. Voadlo, H. C. Hang, E. J. Kim, J. A. Hanover and C. R. Bertozzi, *Proc. Natl. Acad. Sci. U. S. A.*, 2003, **100**, 9116-9121.
111. B. W. Zaro, Y. Y. Yang, H. C. Hang and M. R. Pratt, *Proc. Natl. Acad. Sci. U. S. A.*, 2011, **108**, 8146-8151.
112. A. R. Batt, B. W. Zaro, M. X. Navarro and M. R. Pratt, *Chembiochem*, 2017, **18**, 1177-1182.
113. M. Boyce, I. S. Carrico, A. S. Ganguli, S. H. Yu, M. J. Hangauer, S. C. Hubbard, J. J. Kohler and C. R. Bertozzi, *Proc. Natl. Acad. Sci. U. S. A.*, 2011, **108**, 3141-3146.
114. C. M. Whitman, F. Yang and J. J. Kohler, *Bioorg. Med. Chem. Lett.*, 2011, **21**, 5006-5010.
115. C. Büll, T. Heise, D. M. H. Beurskens, M. Riemersma, A. Ashikov, F. P. J. T. Rutjes, T. H. Van Kuppevelt, D. J. Lefeber, M. H. Den Brok, G. J. Adema and T. J. Boltje, *ACS Chem. Biol.*, 2015, **10**, 2353-2363.
116. K. N. Chuh, B. W. Zaro, F. Piller, V. Piller and M. R. Pratt, *J. Am. Chem. Soc.*, 2014, **136**, 12283-12295.
117. R. Xie, L. Dong, Y. Du, Y. Zhu, R. Hua, C. Zhang and X. Chen, *Proc. Natl. Acad. Sci. U. S. A.*, 2016, **113**, 5173-5178.
118. Z. S. Chinoy, C. Bodineau, C. Favre, K. W. Moremen, R. V. Durán and F. Friscourt, *Angew. Chem. Int. Ed. Engl.*, 2019, **58**, 4281-4285.
119. A. Kitowski and G. J. L. Bernardes, *Chembiochem*, 2020, **21**, 2696-2700.
120. J. L. Daughtry, W. Cao, J. Ye and J. M. Baskin, *ACS Chem. Biol.*, 2020, **15**, 318-324.
121. B. W. Zaro, A. R. Batt, K. N. Chuh, M. X. Navarro and M. R. Pratt, *ACS Chem. Biol.*, 2017, **12**, 787-794.
122. J. E. G. A. Dold, J. Pfozter, A. K. Späte and V. Wittmann, *Chembiochem*, 2017, **18**, 1242-1250.
123. J. E. G. A. Dold and V. Wittmann, *Chembiochem*, 2021, **22**, 1243-1251.
124. A. K. Späte, J. E. G. A. Dold, E. Batroff, V. F. Schart, D. E. Wieland, O. R. Baudendistel and V. Wittmann, *Chembiochem*, 2016, **17**, 1374-1383.
125. A. K. Späte, V. F. Schart, S. Schöllkopf, A. Niederwieser and V. Wittmann, *Eur. J. Chem.*, 2014, **20**, 16502-16508.
126. N. D. Pham, C. S. Fermaintt, A. C. Rodriguez, J. E. McCombs, N. Nischan and J. J. Kohler, *Glycoconj. J.*, 2015, **32**, 515-529.
127. C. Ma, H. Takeuchi, H. Hao, C. Yonekawa, K. Nakajima, M. Nagae, T. Okajima, R. S. Haltiwanger and Y. Kizuka, *Int. J. Mol. Sci.*, 2020, **21**, 1-18.
128. W. Qin, K. Qin, X. Fan, L. Peng, W. Hong, Y. Zhu, P. Lv, Y. Du, R. Huang, M. Han, B. Cheng, Y. Liu, W. Zhou, C. Wang and X. Chen, *Angew. Chem. Int. Ed. Engl.*, 2018, **57**, 1817-1820.
129. N. Darabedian, B. Yang, R. Ding, G. Cutolo, B. W. Zaro, C. M. Woo and M. R. Pratt, *Front. Chem.*, 2020, **8**, 1-14.
130. Y. Hao, X. Fan, Y. Shi, C. Zhang, D. e. Sun, K. Qin, W. Qin, W. Zhou and X. Chen, *Nat. Commun.*, 2019, **10**, 4065.
131. R. T. Almaraz, U. Aich, H. S. Khanna, E. Tan, R. Bhattacharya, S. Shah and K. J. Yarema, *Biotechnol. Bioeng.*, 2012, **109**, 992-1006.
132. A. K. Späte, H. Bußkamp, A. Niederwieser, V. F. Schart, A. Marx and V. Wittmann, *Bioconjug. Chem.*, 2014, **25**, 147-154.
133. P. A. Gilormini, C. Lion, D. Vicogne, T. Levade, S. Potelle, C. Mariller, Y. Guérardel, C. Biot and F. Foulquier, *Chem. Commun.*, 2016, **52**, 2318-2321.
134. A. Niederwieser, A. K. Späte, L. D. Nguyen, C. Jüngst, W. Reutter and V. Wittmann, *Angew. Chem. Int. Ed. Engl.*, 2013, **52**, 4265-4268.
135. V. F. Schart, J. Hassenrück, A. K. Späte, J. E. G. A. Dold, R. Fahrner and V. Wittmann, *Chembiochem*, 2019, **20**, 166-171.
136. Y. Zhu, L. I. Willems, D. Salas, S. Cecioni, W. B. Wu, L. J. Foster and D. J. Voadlo, *J. Am. Chem. Soc.*, 2020, **142**, 15729-15739.
137. F. Doll, A. Buntz, A. K. Späte, V. F. Schart, A. Timper, W. Schrimpf, C. R. Hauck, A. Zumbusch and V. Wittmann, *Angew. Chem. Int. Ed. Engl.*, 2016, **55**, 2262-2266.

138. H. Y. Tan, R. Eskandari, D. Shen, Y. Zhu, T. W. Liu, L. I. Willems, M. G. Alteen, Z. Madden and D. J. Vocadlo, *J. Am. Chem. Soc.*, 2018, **140**, 15300-15308.
139. K. K. Palaniappan and C. R. Bertozzi, *Chem. Rev.*, 2016, **116**, 14277-14306.
140. M. E. Griffin and L. C. Hsieh-Wilson, *Cell Chem. Biol.*, 2016, **23**, 108-121.
141. L. A. Walter, A. R. Batt, N. Darabedian, B. W. Zaro and M. R. Pratt, *Chembiochem*, 2018, **19**, 1918-1921.
142. D. Soares da Costa, J. C. Sousa, S. D. Mesquita, N. I. Petkova-Yankova, F. Marques, R. L. Reis, N. Sousa and I. Pashkuleva, *Molecules*, 2020, **25**, 795.
143. R. Xie, S. Hong, L. Feng, J. Rong and X. Chen, *J. Am. Chem. Soc.*, 2012, **134**, 9914-9917.
144. H. Wang, R. Wang, K. Cai, H. He, Y. Liu, J. Yen, Z. Wang, M. Xu, Y. Sun, X. Zhou, Q. Yin, L. Tang, I. T. Dobrucki, L. W. Dobrucki, E. J. Chaney, S. A. Boppart, T. M. Fan, S. Lezmi, X. Chen, L. Yin and J. Cheng, *Nat. Chem. Biol.*, 2017, **13**, 415-424.
145. A. Lamoot, A. Uvyn, S. Kasmi and B. G. De Geest, *Angew. Chem. Int. Ed. Engl.*, 2021, **60**, 6320-6325.
146. S. Lim, W. Kim, S. Song, M. K. Shim, H. Y. Yoon, B. S. Kim, I. C. Kwon and K. Kim, *Bioconjug. Chem.*, 2021, **32**, 199-214.
147. J. C. Paulson, J. E. Sadler and R. L. Hill, *J. Biol. Chem.*, 1979, **254**, 2120-2124.
148. Q. Chao, Y. Ding, Z. H. Chen, M. H. Xiang, N. Wang and X. D. Gao, *Front. Chem.*, 2020, **8**, 513.
149. E. Kim, *Molecules*, 2018, **23**.
150. F. Tang, M. Zhou, K. Qin, W. Shi, A. Yashinov, Y. Yang, L. Yang, D. Guan, L. Zhao, Y. Tang, Y. Chang, L. Zhao, H. Yang, H. Zhou, R. Huang and W. Huang, *Nat. Chem. Biol.*, 2020, **16**, 766-775.
151. M. Noel, P.-A. Gilormini, V. Coge, N. Yamakawa, D. Vicogne, C. Lion, C. Biot, Y. Guérardel and A. Harduin-Lepers, *Chembiochem*, 2017, **18**, 1251-1259.
152. S. H. Yu, P. Zhao, T. Sun, Z. Gao, K. W. Moremen, G. J. Boons, L. Wells and R. Steet, *J. Biol. Chem.*, 2016, **291**, 3982-3989.
153. A. Lopez Aguilar, L. Meng, X. Hou, W. Li, K. W. Moremen and P. Wu, *Bioconjug. Chem.*, 2018, **29**, 1231-1239.
154. N. E. Mbua, X. Li, H. R. Flanagan-Steet, L. Meng, K. Aoki, K. W. Moremen, M. A. Wolfert, R. Steet and G. J. Boons, *Angew. Chem. Int. Ed. Engl.*, 2013, **52**, 13012-13015.
155. T. Zheng, H. Jiang, M. Gros, D. S. del Amo, S. Sundaram, G. Lauvau, F. Marlow, Y. Liu, P. Stanley and P. Wu, *Angew. Chem. Int. Ed. Engl.*, 2011, **50**, 4113-4118.
156. Q. Li, Z. Li, X. Duan and W. Yi, *J. Am. Chem. Soc.*, 2014, **136**, 12536-12539.
157. J.-L. Chaubard, C. Krishnamurthy, W. Yi, D. F. Smith and L. C. Hsieh-Wilson, *J. Am. Chem. Soc.*, 2012, **134**, 4489-4492.
158. L. Wen, Y. Zheng, K. Jiang, M. Zhang, S. M. Kondengaden, S. Li, K. Huang, J. Li, J. Song and P. G. Wang, *J. Am. Chem. Soc.*, 2016, **138**, 11473-11476.
159. H. Zhu, S. Wang, D. Liu, L. Ding, C. Chen, Y. Liu, Z. Wu, R. Bollag, K. Liu, W. M. Alexander, J. Yin, C. Ma, L. Li and P. G. Wang, *Anal. Chem.*, 2020, **92**, 6297-6303.
160. T. Sun, S.-H. Yu, P. Zhao, L. Meng, K. W. Moremen, L. Wells, R. Steet and G.-J. Boons, *J. Am. Chem. Soc.*, 2016, **138**, 11575-11582.
161. Z. L. Wu, M. Whittaker, J. M. Ertelt, A. D. Person and V. Kalabokis, *Glycobiology*, 2020, **30**, 970-980.
162. Z. L. Wu, A. Luo, A. Grill, T. Lao, Y. Zou and Y. Chen, *Bioconjug. Chem.*, 2020, **31**, 2098-2102.
163. T. Abukar, S. Rahmani, N. K. Thompson, C. N. Antonescu and W. W. Wakarchuk, *Carbohydr. Res.*, 2021, **500**, 108249.
164. L. Wen, M. R. Gadi, Y. Zheng, C. Gibbons, S. M. Kondengaden, J. Zhang and P. G. Wang, *ACS Catal.*, 2018, **8**, 7659-7666.
165. S. Hong, Y. Shi, N. C. Wu, G. Grande, L. Douthit, H. Wang, W. Zhou, K. B. Sharpless, I. A. Wilson, J. Xie and P. Wu, *Nat. Commun.*, 2019, **10**, 1799.

166. S. H. Yu, M. Boyce, A. M. Wands, M. R. Bond, C. R. Bertozzi and J. J. Kohler, *Proc. Natl. Acad. Sci. U. S. A.*, 2012, **109**, 4834-4839.
167. B. Ramakrishnan and P. K. Qasba, *J. Biol. Chem.*, 2002, **277**, 20833-20839.
168. J. Choi, L. J. S. Wagner, S. B. P. E. Timmermans, S. A. Malaker, B. Schumann, M. A. Gray, M. F. Debets, M. Takashima, J. Gehring and C. R. Bertozzi, *J. Am. Chem. Soc.*, 2019, **141**, 13442-13453.
169. B. Schumann, S. A. Malaker, S. P. Wisnovsky, M. F. Debets, A. J. Agbay, D. Fernandez, L. J. S. Wagner, L. Lin, Z. Li, J. Choi, D. M. Fox, J. Peh, M. A. Gray, K. Pedram, J. J. Kohler, M. Mrksich and C. R. Bertozzi, *Mol. Cell*, 2020, **78**, 824-834.e815.
170. M. F. Debets, O. Y. Tastan, S. P. Wisnovsky, S. A. Malaker, N. Angelis, L. K. R. Moeckl, J. Choi, H. Flynn, L. J. S. Wagner, G. Bineva-Todd, A. Antonopoulos, A. Cioce, W. M. Browne, Z. Li, D. C. Briggs, H. L. Douglas, G. T. Hess, A. J. Agbay, C. Roustan, S. Kjaer, S. M. Haslam, A. P. Snijders, M. C. Bassik, W. E. Moerner, V. S. W. Li, C. R. Bertozzi and B. Schumann, *Proc. Natl. Acad. Sci. U S A*, 2020, **117**, 25293-25301.
171. K. Islam, *Cell Chem. Biol.*, 2018, **25**, 1171-1184.
172. A. Cioce, S. A. Malaker and B. Schumann, *Curr. Opin. Chem. Bio.*, 2021, **60**, 66-78.
173. U. Pradere, E. C. Garnier-Amblard, S. J. Coats, F. Amblard and R. F. Schinazi, *Chem. Rev.*, 2014, **114**, 9154-9218.
174. A. R. Van Rompay, M. Johansson and A. Karlsson, *Pharmacol. Ther.*, 2000, **87**, 189-198.
175. Y. Ding, J.-L. Girardet, Z. Hong, V. C. H. Lai, H. An, Y.-H. Koh, S. Z. Shaw and W. Zhong, *Bioorg. Med. Chem. Lett.*, 2005, **15**, 709-713.
176. M. P. Cataldi, P. Lu, A. Blaeser and Q. L. Lu, *Nat. Commun.*, 2018, **9**, 3448.
177. H. C. Hang, C. Yu, D. L. Kato and C. R. Bertozzi, *Proc. Natl. Acad. Sci. U. S. A.*, 2003, **100**, 14846-14851.
178. E. M. Sletten and C. R. Bertozzi, *Acc. Chem. Res.*, 2011, **44**, 666-676.
179. A. K. Sarkar, T. A. Fritz, W. H. Taylor and J. D. Esko, *Proc. Natl. Acad. Sci. U. S. A.*, 1995, **92**, 3323-3327.
180. A. J. Wiemer and D. F. Wiemer, *Top. Curr. Chem.*, 2015, **360**, 115-160.
181. M. Komabayashi, T. Stiller and S. Jopp, *J. Mol. Liq.*, 2021, **325**, 115167.
182. T. Kamkhachorn, A. R. Parameswar and A. V. Demchenko, *Org. Lett.*, 2010, **12**, 3078-3081.
183. S. Ohkawabata, M. Kanemaru, S.-y. Kuawahara, K. Yamamoto and J.-i. Kadokawa, *J. Carbohydr. Chem.*, 2012, **31**, 659-672.
184. K. Takashima, M. Sakano, E. Kinouchi, S. Nakamura, S. Marumoto, F. Ishikawa, K. Ninomiya, I. Nakanishi, T. Morikawa and G. Tanabe, *Bioorg. Med. Chem. Lett.*, 2021, **33**, 127751.
185. T. Lasek, J. Dobias, M. Budesinsky, J. Kozak, B. Lapunikova, I. Rosenberg, G. Birkus and O. Pav, *Tetrahedron*, 2021, **89**, 132159.
186. G. Zhao, W. Yao, J. N. Mauro and M. Y. Ngai, *J. Am. Chem. Soc.*, 2021, **143**, 1728-1734.
187. S. Valverde, M. García, A. M. Gómez and J. C. López, *Chem. Commun.*, 2000, DOI: 10.1039/b000771o, 813-814.
188. A. Shaw, P. Das and S. Ajay, *Synthesis*, 2016, **48**, 3753-3762.
189. A. Chronowska, E. Gallienne, C. Nicolas, A. Kato, I. Adachi and O. R. Martin, *Tetrahedron Lett.*, 2011, **52**, 6399-6402.
190. M. U. Roslund, O. Aitio, J. Wärnä, H. Maaheimo, D. Y. Murzin and R. Leino, *J. Am. Chem. Soc.*, 2008, **130**, 8769-8772.
191. O. P. Chevallier and M. E. Migaud, *Beilstein J. Org. Chem.*, 2006, **2**, 14.
192. G. Zhang, M. Fu and J. Ning, *Carbohydr. Res.*, 2005, **340**, 155-159.
193. M. Islam, G. P. Shinde and S. Hotha, *Chem. Sci.*, 2017, **8**, 2033-2038.
194. M. Fusari, S. Fallarini, G. Lombardi and L. Lay, *Bioorg Med Chem*, 2015, **23**, 7439-7447.
195. L. Cattiaux, A. Mee, M. Pourcelot, G. Sfihi-Loualia, T. Hurtaux, E. Maes, C. Fradin, B. Sendid, D. Poulain, E. Fabre, F. Delplace, Y. Guerardel and J. M. Mallet, *Bioorg. Med. Chem.*, 2016, **24**, 1362-1368.

196. E. Zhang, S. Wang, L. L. Li, Y. G. Hua, J. F. Yue, J. F. Li and C. Y. Jin, *Bioorg. Med. Chem. Lett.*, 2018, **28**, 497-502.
197. C. Jia, Y. Zhang, L.-H. Zhang, P. Sinaÿ and M. Sollogoub, *Carbohydr. Res.*, 2006, **341**, 2135-2144.
198. C. Chbib, A. J. Sobczak, M. Mudgal, C. Gonzalez, D. Lumpuy, J. Nagaj, K. Stokowa-Soltys and S. F. Wnuk, *J. Sulphur Chem.*, 2016, **37**, 307-327.
199. P. Das, S. Ajay and A. K. Shaw, *Synthesis*, 2016, **48**, 3753-3762.
200. G. W. J. Fleet and P. W. Smith, *Tetrahedron*, 1986, **42**, 5685-5692.
201. Y. S. Shin, D. B. Jarhad, M. H. Jang, K. Kovacikova, G. Kim, J.-S. Yoon, H.-R. Kim, Y. E. Hyun, A. S. Tipnis, T.-S. Chang, M. J. van Hemert and L. S. Jeong, *Eur. J. Med. Chem.*, 2020, **187**, 111956.
202. M. Fouché, L. Rooney and A. G. M. Barrett, *J. Org. Chem.*, 2012, **77**, 3060-3070.
203. A. Venkanna, E. Sreedhar, B. Siva, K. S. Babu, K. R. Prasad and J. M. Rao, *Tetrahedron Asymmetry*, 2013, **24**, 1010-1022.
204. S. Šesták, M. Bella, T. Klunda, S. Gurská, P. Džubák, F. Wöls, I. B. H. Wilson, V. Sladek, M. Hajdúch, M. Poláková and J. Kóňa, *ChemMedChem*, 2018, **13**, 373-383.
205. G. Chandra, Y. W. Moon, Y. Lee, J. Y. Jang, J. Song, A. Nayak, K. Oh, V. A. Mulamoottil, P. K. Sahu, G. Kim, T.-S. Chang, M. Noh, S. K. Lee, S. Choi and L. S. Jeong, *J. Med. Chem.*, 2015, **58**, 5108-5120.
206. P. J. Garegg, R. Johansson, I. Lindh and B. Samuelsson, *Carbohydr. Res.*, 1986, **150**, 285-289.
207. K. Napora, T. M. Wrodnigg, P. Kosmus, M. Thonhofer, K. Robins and M. Winkler, *Bioorg. Med. Chem. Lett.*, 2013, **23**, 3393-3395.
208. M. Miyazawa, T. Takahashi, I. Horibe and R. Ishikawa, *Tetrahedron*, 2012, **68**, 2007-2010.
209. B. Ren, M. Wang, J. Liu, J. Ge, X. Zhang and H. Dong, *Green Chem.*, 2015, **17**, 1390-1394.
210. J.-F. Longevial, K. El Cheikh, D. Aggad, A. Lebrun, A. van der Lee, F. Tielens, S. Clément, A. Morère, M. Garcia, M. Gary-Bobo and S. Richeter, *Eur. J. Chem.*, 2017, **23**, 14017-14026.
211. S. A. Svarovsky, Z. Szekely and J. J. Barchi, *Tetrahedron Asymmetry*, 2005, **16**, 587-598.
212. C. G. Casinovi, M. Framondino, G. Randazzo and F. Siani, *Carbohydr. Res.*, 1974, **36**, 67-73.
213. A. E. Christina, D. v. d. Es, J. Dinkelaar, H. S. Overkleeft, G. A. v. d. Marel and J. D. C. Codée, *Chem. Commun.*, 2012, **48**, 2686.
214. M. Tortosa, N. A. Yakelis and W. R. Roush, *J. Am. Chem. Soc.*, 2008, **130**, 2722-2723.
215. F. Kleinbeck and E. M. Carreira, *Angew. Chem. Int. Ed.*, 2009, **48**, 578-581.
216. A. S. Sofian and C. Kuan Lee, *J. Carbohydr. Chem.*, 2003, **22**, 185-206.
217. K. R. Prasad and P. Gutala, *Tetrahedron*, 2011, **67**, 4514-4520.
218. S. Mouné, G. Niel, M. Busquet, I. Eggleston and P. Jouin, *J. Org. Chem.*, 1997, **62**, 3332-3339.
219. J. Hao, X. Zhang, P. Zhang, J. Liu, L. Zhang and H. Sun, *Tetrahedron*, 2009, **65**, 7975-7984.
220. I. Raji, F. Yadudu, E. Janeira, S. Fathi, L. Szymczak, J. R. Kornacki, K. Komatsu, J.-D. Li, M. Mrksich and A. K. Oyelere, *Bioorg. Med. Chem.*, 2017, **25**, 1202-1218.
221. pKa Values for Organic and Inorganic Bronsted Acids at 25°C,
<https://owl.oit.umass.edu/departments/OrganicChemistry/appendix/pKaTable.html>,
(accessed 12/4/2020).
222. pKa Table,
https://edisciplinas.usp.br/pluginfile.php/1885601/mod_resource/content/1/pKa%20table_organic.pdf, (accessed 12/4/2020).
223. Approximate pKa chart of the functional groups: values to know,
<https://www.chem.indiana.edu/wp-content/uploads/2018/03/pka-chart.pdf>, (accessed 12/4/2020).
224. A. E. Wróblewski and I. I. B ak-Sypień, *Tetrahedron Asymmetry*, 2007, **18**, 2218-2226.
225. A. Nagy, B. Csordás, V. Zsoldos-Mády, I. Pintér, V. Farkas and A. Perczel, *Amino Acids*, 2017, **49**, 223-240.

226. A. S. Figueredo, L. O. B. Zamoner, M. Rejzek, R. A. Field and I. Carvalho, *Tetrahedron Lett.*, 2018, **59**, 4405-4409.
227. C. Pasti, E. Rinaldi, C. Cervellati, F. Dallochio, R. Hardré, L. Salmon and S. Hanau, *Bioorg. Med. Chem.*, 2003, **11**, 1207-1214.
228. C. Wiles, P. Watts and S. J. Haswell, *Tetrahedron Lett.*, 2006, **47**, 5261-5264.
229. Y. Koga, S. Sakamaki, M. Hongu, E. Kawanishi, T. Sakamoto, Y. Yamamoto, H. Kimata, K. Nakayama, C. Kuriyama, Y. Matsushita, K. Ueta, M. Tsuda-Tsukimoto and S. Nomura, *Bioorg. Med. Chem.*, 2013, **21**, 5561-5572.
230. W. Ndugire, B. Wu and M. Yan, *Molecules*, 2019, **24**.
231. C. M. Liu, C. D. Warren and R. W. Jeanloz, *Carbohydr. Res.*, 1985, **136**, 273-284.
232. R. C. Pinto, M. M. Andrade and M. T. Barros, *Tetrahedron Lett.*, 2012, **53**, 6633-6636.
233. D. Alvarez-Dorta, E. I. Leon, A. R. Kennedy, A. Martin, I. Perez-Martin, C. Riesco-Fagundo and E. Suarez, *Chemistry*, 2013, **19**, 10312-10333.
234. W. Lu, L. Navidpour and S. D. Taylor, *Carbohydr. Res.*, 2005, **340**, 1213-1217.
235. H. Che, Y. Fang, S. K. Gurung, J. Luo, D. H. Yoon, G.-H. Sung, T. W. Kim and H. Park, *Bull. Korean. Chem. Soc.*, 2014, **35**, 2038-2042.
236. T. S. Rasmussen, H. Koldso, S. Nakagawa, A. Kato, B. Schiott and H. H. Jensen, *Org. Biomol. Chem.*, 2011, **9**, 7807-7813.
237. H. Huang, J. Ash and J. Y. Kang, *Org. Lett.*, 2018, **20**, 4938-4941.
238. H. Huang, J. Denne, C.-H. Yang, H. Wang and J. Y. Kang, *Angew. Chem. Int. Ed. Engl.*, 2018, **57**, 6624-6628.
239. C. D. Spicer, M. Pujari-Palmer, H. Autefage, G. Insley, P. Procter, H. Engqvist and M. M. Stevens, *ACS Cent. Sci.*, 2020, **6**, 226-231.
240. L. Liang, T. Y. Wade Wei, P. Y. Wu, W. Herrebout, M. D. Tsai and S. P. Vincent, *ChemBioChem*, 2020, **21**, 2982-2990.
241. K. M. Sureshan, M. Trusselle, S. C. Tovey, C. W. Taylor and B. V. L. Potter, *J. Org. Chem.*, 2008, **73**, 1682-1692.
242. R. G. Bhat, N. S. Kumar and B. M. Pinto, *Carbohydr. Res.*, 2007, **342**, 1934-1942.
243. A. Borio, A. Hofinger, P. Kosma and A. Zamyatina, *Tetrahedron Lett.*, 2017, **58**, 2826-2829.
244. B. Xiong, G. Wang, C. Zhou, Y. Liu, J. Li, P. Zhang and K. Tang, *Phosphorus Sulfur Silicon Relat. Elem.*, 2018, **193**, 239-244.
245. S. P. Vincent and L. N. Gastinel, *Carbohydr. Res.*, 2002, **337**, 1039-1042.
246. H. Miyazawa, H. Yokokura, Y. Ohkubo, Y. Kondo and N. Yoshino, *J. Fluor. Chem.*, 2004, **125**, 1485-1490.
247. M. Barbier, E. Grand and J. Kovensky, *Carbohydr. Res.*, 2007, **342**, 2635-2640.
248. M. Nagaraju, A. Krishnaiah and H. B. Mereyala, *Synth. Commun.*, 2007, **37**, 2467-2472.
249. K. Burgess, D. A. Chaplin, I. Henderson, Y. T. Pan and A. D. Elbein, *J. Org. Chem.*, 1992, **57**, 1103-1109.
250. S. Benzaria, H. Pelicano, R. Johnson, G. Maury, J. L. Imbach, A. M. Aubertin, G. Obert and G. Gosselin, *J. Med. Chem.*, 1996, **39**, 4958-4965.
251. C. Périgaud, J. L. Girardet, I. Lefebvre, M. Y. Xie, A. M. Aubertin, A. Kirn, G. Gosselin, J. L. Imbach and J. P. Sommadossi, *Antivir. Chem. Chemother.*, 1996, **7**, 338-345.
252. S. Peyrottes, D. Egron, I. Lefebvre, G. Gosselin, J. L. Imbach and C. Périgaud, *Mini Rev. Med. Chem.*, 2004, **4**, 395-408.
253. C. Schultz, *Bioorg. Med. Chem.*, 2003, **11**, 885-898.
254. I. Lefebvre, C. Périgaud, A. Pompon, A. M. Aubertin, J. L. Girardet, A. Kirn, G. Gosselin and J. L. Imbach, *J. Med. Chem.*, 1995, **38**, 3941-3950.
255. H. Y. Tan, R. Eskandari, D. Shen, Y. Zhu, T.-W. Liu, L. I. Willems, M. G. Alteen, Z. Madden and D. J. Vocadlo, *J. Am. Chem. Soc.*, 2018, **140**, 15300-15308.
256. W.-Q. Liu, M. Vidal, C. Olszowy, E. Million, C. Lenoir, H. Dhôtel and C. Garbay, *J. Med. Chem.*, 2004, **47**, 1223-1233.

257. J. F. A. Pijnenborg, E. A. Visser, M. Noga, E. Rossing, R. Veizaj, D. J. Lefeber, C. Büll and T. J. Boltje, *Chemistry*, 2021, **27**, 4022-4027.
258. J. F. A. Pijnenborg, E. Rossing, J. Merx, M. J. Noga, W. H. C. Titulaer, N. Eerden, R. Veizaj, P. B. White, D. J. Lefeber and T. J. Boltje, *Nat. Commun.*, 2021, **12**, 7024.
259. B. N. Kakde, E. Capota, J. J. Kohler and U. K. Tambar, *J. Org. Chem.*, 2021, **86**, 18257-18264.
260. H. Huang and J. Y. Kang, *Synlett*, 2019, **30**, 635-641.
261. Diisopropylphosphoramidous dichloride,
<https://www.sigmaaldrich.com/GB/en/sds/aldrich/307254>, (accessed 13/2/22).
262. *US Pat. Pat.*, 183373 A1, 2017.
263. Y.-H. Koh, J. H. Shim, J. Z. Wu, W. Zhong, Z. Hong and J.-L. Girardet, *J. Med. Chem.*, 2005, **48**, 2867-2875.
264. H. Li, J.-C. Yoo, Y.-C. Baik, W.-J. Lee and J.-H. Hong, *Bull. Korean. Chem. Soc.*, 2010, **31**, 2514-2518.
265. M. K. Patel and B. G. Davis, *Org. Biomol. Chem.*, 2010, **8**, 4232-4235.
266. M. T. Liu, N. N. Nagre and K. Ryan, *Bioorg. Med. Chem.*, 2014, **22**, 834-841.
267. B. R. Sculimbrene, Y. Xu and S. J. Miller, *J. Am. Chem. Soc.*, 2004, **126**, 13182-13183.
268. J. Schulz, M. W. Beaton and D. Gani, *J. Chem. Soc., Perkin Trans. 1*, 2000, , 943-954.
269. L. Linderoth, P. Fristrup, M. Hansen, F. Melander, R. Madsen, T. L. Andresen and G. H. Peters, *J. Am. Chem. Soc.*, 2009, **131**, 12193-12200.
270. M. T. Cook, S. A. Schmidt, E. Lee, W. Samprasit, P. Opanasopit and V. V. Khutoryanskiy, *J. Mater. Chem. B.*, 2015, **3**, 6599-6604.
271. P. Adler, A. Pons, J. Li, J. Heider, B. R. Brutiu and N. Maulide, *Angew. Chem. Int. Ed. Engl.*, 2018, **57**, 13330-13334.
272. B. J. Foust, J. Li, C.-H. C. Hsiao, D. F. Wiemer and A. J. Wiemer, *ChemMedChem*, 2019, **14**, 1597-1603.
273. D. J. Anderson, R. McDonald and M. Cowie, *Angew. Chem. Int. Ed. Engl.*, 2007, **46**, 3741-3744.
274. D. Gasperini, S. E. Neale, M. F. Mahon, S. A. Macgregor and R. L. Webster, *ACS Catal.*, 2021, **11**, 5452-5462.
275. S. Singh, Z. Su, M. Grossutti and F. I. Auzanneau, *Carbohydr Res*, 2014, **390**, 50-58.
276. G. T. Giuffredi, L. E. Jennings, B. Bernet and V. Gouverneur, *J. Fluor. Chem.*, 2011, **132**, 772-778.
277. N. Santschi, N. Aiguabella, V. Lewe and R. Gilmour, *J. Fluor. Chem.*, 2015, **179**, 96-101.
278. T. Hamada, A. Chieffi, J. Ahman and S. L. Buchwald, *J. Am. Chem. Soc.*, 2002, **124**, 1261-1268.
279. Z. Khedri, M. M. Muthana, Y. Li, S. M. Muthana, H. Yu, H. Cao and X. Chen, *Chem. Commun. (Camb)*, 2012, **48**, 3357-3359.
280. N. Darabedian, J. Gao, K. N. Chuh, C. M. Woo and M. R. Pratt, *J. Am. Chem. Soc.*, 2018, **140**, 7092-7100.
281. F. Rajas, A. Gautier-Stein and G. Mithieux, *Metabolites*, 2019, **9**.
282. J. Fettke, T. Albrecht, M. Hejazi, S. Mahlow, Y. Nakamura and M. Steup, *New Phytol*, 2010, **185**, 663-675.
283. S. N. Jager, E. O. J. Porta and G. R. Labadie, *Steroids*, 2019, **141**, 41-45.
284. J. C. Lee, S. W. Chang, C. C. Liao, F. C. Chi, C. S. Chen, Y. S. Wen, C. C. Wang, S. S. Kulkarni, R. Puranik, Y. H. Liu and S. C. Hung, *Chemistry*, 2004, **10**, 399-415.
285. S. Mohamed, Q. Q. He, R. J. Lepage, E. H. Krenske and V. Ferro, *Eur. J. Org. Chem.*, 2018, **2018**, 2214-2227.
286. B. Fraser-Reid, Z. Wu, U. E. Udodong and H. Ottosson, *J. Org. Chem.*, 1990, **55**, 6068-6070.
287. T. Utamura, K. Kuromatsu, K. Suwa, K. Koizumi and T. Shingu, *Chem. Pharm. Bull.*, 1986, **34**, 2341-2353.
288. K. Hiruma-Shimizu, A. P. Kalverda, P. J. Henderson, S. W. Homans and S. G. Patching, *J. Labelled Comp. Radiopharm.*, 2014, **57**, 737-743.

289. E. Kaji, T. Komori, M. Yokoyama, T. Kato, T. Nishino and T. Shirahata, *Tetrahedron*, 2010, **66**, 4089-4100.
290. Y. Konda, T. Toida, E. Kaji, K. Takeda and Y. Harigaya, *Carbohydr. Res.*, 1997, **301**, 123-143.
291. S. Hackbusch, A. Watson and A. H. Franz, *Carbohydr. Res.*, 2018, **458-459**, 1-12.
292. V. Kumar, N. Yadav and K. P. R. Kartha, *Carbohydr. Res.*, 2014, **397**, 18-26.
293. L. M. Doyle, S. O'Sullivan, C. Di Salvo, M. McKinney, P. McArdle and P. V. Murphy, *Org. Lett.*, 2017, **19**, 5802-5805.
294. J. Dinkelaar, M. D. Witte, L. J. van den Bos, H. S. Overkleeft and G. A. van der Marel, *Carbohydr. Res.*, 2006, **341**, 1723-1729.
295. L. Kerins, S. Byrne, A. Gabba and P. V. Murphy, *J. Org. Chem.*, 2018, **83**, 7714-7729.
296. S. Ghorai, R. Mukhopadhyay, A. P. Kundu and A. Bhattacharjya, *Tetrahedron*, 2005, **61**, 2999-3012.
297. M. A. Fernández-Herrera, S. Mohan, H. López-Muñoz, J. M. V. Hernández-Vázquez, E. Pérez-Cervantes, M. L. Escobar-Sánchez, L. Sánchez-Sánchez, I. Regla, B. M. Pinto and J. Sandoval-Ramírez, *Eur. J. Med. Chem.*, 2010, **45**, 4827-4837.
298. T. Nokami, A. Shibuya, H. Tsuyama, S. Suga, A. A. Bowers, D. Crich and J. Yoshida, *J. Am. Chem. Soc.*, 2007, **129**, 10922-10928.
299. K. Gulbe, J. Luginina, E. Jansons, A. Kinens and M. Turks, *Beilstein J. Org. Chem.*, 2021, **17**, 964-976.
300. W. Ouyang, H. Huang, R. Yang, H. Ding and Q. Xiao, *Mar. Drugs*, 2020, **18**.
301. C. Cassani, G. Bergonzini and C. J. Wallentin, *Org. Lett.*, 2014, **16**, 4228-4231.
302. Z.-G. Gao, H. T. Duong, T. Sonina, S.-K. Kim, P. Van Rompaey, S. Van Calenbergh, L. Mamedova, H. O. Kim, M. J. Kim, A. Y. Kim, B. T. Liang, L. S. Jeong and K. A. Jacobson, *J. Med. Chem.*, 2006, **49**, 2689-2702.
303. B. Cheng, L. Dong, Y. Zhu, R. Huang, Y. Sun, Q. You, Q. Song, J. C. Paton, A. W. Paton and X. Chen, *ACS Chem. Biol.*, 2019, **14**, 2141-2147.
304. C. Y. Jao, M. Roth, R. Welti and A. Salic, *Proc. Natl. Acad. Sci. U S A*, 2009, **106**, 15332-15337.
305. A. Dixit, G. P. Jose, C. Shanbhag, N. Tagad and J. Kalia, 2022, DOI: bioRxiv doi:10.1101/2022.03.31.486572.
306. Y. Li, S. Kinting, S. Hoppner, M. E. Forstner, O. Uhl, B. Koletzko and M. Griese, *Biochim. Biophys. Acta. Mol. Cell. Biol. Lipids*, 2019, **1864**, 158516.
307. E. R. van Rijssel, T. P. M. Goumans, G. Lodder, H. S. Overkleeft, G. A. van der Marel and J. D. C. Codée, *Org. Lett.*, 2013, **15**, 3026-3029.
308. A. H. Viuff and H. H. Jensen, *Org. Biomol. Chem.*, 2016, **14**, 8545-8556.
309. T. Wennekes, K. M. Bongers, K. Vogel, R. J. B. H. N. van den Berg, A. Strijland, W. E. Donker-Koopman, J. M. F. G. Aerts, G. A. van der Marel and H. S. Overkleeft, *Eur. J. Org. Chem.*, 2012, **2012**, 6420-6454.
310. S. K. Maurya and R. Rana, *Beilstein J. Org. Chem.*, 2017, **13**, 1106-1118.
311. E. Raluy, O. Pàmies and M. Diéguez, *Adv. Synth. Catal.*, 2009, **351**, 1648-1670.
312. F. John and V. Wittmann, *J. Org. Chem.*, 2015, **80**, 7477-7485.
313. S. Li, J. Jaszczyk, X. Pannecoucke, T. Poisson, O. R. Martin and C. Nicolas, *Adv. Synth. Catal.*, 2020, **363**, 470-483.
314. S. N. Dhawan, T. L. Chick and W. J. Goux, *Carbohydr. Res.*, 1988, **172**, 297-307.
315. O. Baszczyński, J. M. Watt, M. D. Rozewitz, A. H. Guse, R. Fliegert and B. V. L. Potter, *J. Org. Chem.*, 2019, **84**, 6143-6157.
316. C. M. Dojahn, M. Hesse and C. Arenz, *Chem. Commun.*, 2013, **49**, 3128-3130.
317. H. Fang, B. Peng, S. Y. Ong, Q. Wu, L. Li and S. Q. Yao, *Chem. Sci.*, 2021, **12**, 8288-8310.
318. D. Kubacka, M. Kozarski, M. R. Baranowski, R. Wojcik, J. Panecka-Hofman, D. Strzelecka, J. Basquin, J. Jemielity and J. Kowalska, *Pharmaceuticals (Basel)*, 2022, **15**.
319. S. Liu, B. Zhou, H. Yang, Y. He, Z. X. Jiang, S. Kumar, L. Wu and Z. Y. Zhang, *J. Am. Chem. Soc.*, 2008, **130**, 8251-8260.

320. S. Pan, S. Y. Jang, S. S. Liew, J. Fu, D. Wang, J. S. Lee and S. Q. Yao, *Angew. Chem. Int. Ed. Engl.*, 2018, **57**, 579-583.